Investigating the host-microbe dialogue in aging

A thesis presented to the National University of Ireland, Cork for the degree of Doctor of Philosophy

by

Christina Killian, B.Sc.

School of Biochemistry and Cell Biology,

School of Microbiology,

College of SEFS,

University College Cork, Cork, Ireland

Research supervisors:
Dr Susan Joyce
Dr David Clarke

Head of School of Biochemistry and Cell Biology: Professor Justin V. McCarthy
Head of School of Microbiology: Dr David Clarke

December 2022

DECLARATION OF INPUT FROM OTHER RESEARCHERS

Results Chapter 3: The BTBR Autism murine study was designed by Dr Susan Joyce, Prof. John Cryan, Dr Sarah Louise Long, Dr Sofia Cussotto, Dr Anna Golubeva and Dr Eoin Sherwin. Animal handling and behavioural studies and analysis were conducted by Dr Sofia Cussotto, Dr Anna Golubeva and Dr Eoin Sherwin (Cryan Lab, UCC), APC Microbiome Ireland, UCC, following prior approval from the University College Cork Animal Experimentation Ethics Committee, *Figure 3.17*. *Bifidobacterium adolescentis* strain APC 2715 came from the APC Microbiome Institute (APC, Cork, Ireland) and *Lactobacillus salivarius* strain P0003 was isolated by Dr Sarah L Long, daily doses were prepared and monitored by myself, Dr Sarah L Long, Elaine O'Shea (Joyce Lab, UCC) and Dr Anna Golubeva and Dr Eoin Sherwin (Cryan Lab, UCC). Materials collected and dissections were carried out by Dr Anna Golubeva, Dr Eoin Sherwin, Dr Sofia Cussotto, myself and Dr Sarah L Long.

Results Chapter 3: Controls for Parkinson's Disease metabolites study, stool samples from healthy, age-matched control subjects were from pre-existing collected ELDERMET Study (https://link.springer.com/referenceworkentry/10.1007/978-1-4614-6418-1_94-1?noAccess=true) in University College Cork (Claesson *et al.* 2012), with the permission of Prof. Paul O'Toole. Parkinson's Disease plasma and stool samples were collected (2015) as part of Prof. Cora O'Neills Lab (Parkinson's Disease and the Microbiome study). Ellen Joyce (MSc student, thesis submitted 2016) analysed bile acid metabolites present in plasma samples, post extraction and quantification by Dr Susan Joyce, data not shown. Medical Student Mr. Arnav Mahajan determined stool fatty acid levels using TargetLynx^{TM} software. Independently collected plasma samples were examined as part of another unpublished study.

Results Chapter 4 and 5: RNA sequencing was conducted by Genewiz Europe (Leipzig, Germany). Ribomaps conducted Bioanalyser analysis. Dr Darren Fenton provided raw, unnormalized gene counts for analysis.

Results Chapter 5: Mr. Sam Walsh (MSc student, 2019) determined that adherent invasive *Escherichia coli* (AIEC) HM605, reduced *Caenorhabditis elegans* (*C. elegans*) lifespan, data not shown. He uncovered that HM605, and a subset of HM605 genes, could influence *C. elegans* lifespan, development and gut colonisation, data not shown. Ms. Zoe Walsh, as part of her final year project (2020), subsequently examined 24 deletion mutations in *E.coli* HM605 *Table 5.1*, data not shown.

DECLARATION

This is to certify that the thesis work I am submitting, for the degree Doctor of Philosophy, is my own and has not been submitted for another degree, except where otherwise stated, either at University College Cork or elsewhere. All external references and sources are clearly acknowledged and identified within the contents by reference to the researchers to their publications. I have read and understood the regulations of University College Cork concerning plagiarism.

Signature: Christina Killian

Student Number: 112306981

Date: 16/12/2022

Acknowledgements

I would like to thank my supervisors Dr Susan Joyce and Dr David Clarke. I would like to thank Eli Lilly Kinsale Ltd., for their sponsorship funding and giving me the opportunity to undertake this PhD.

I also would like to thank all the members of the Joyce lab, both past and present. Particularly, Dr Sarah Long, Katie Wall and Alvaro Lopez-Gallardo, thank you for all your continuous support and advice throughout this project.

I am very grateful to everyone in the School of Biochemistry and Cell Biology, who helped me over these past few years. Thank you to the past and present members of the ROC lab, for all your help and advice. Thank you Gavin Kinsley, Susan Barry and Olive Cosgrave for always helping me with my orders and administration. Thank you to Ribomaps, Aoife O'Connell and Dr Gary Loughran for all your advice and help with my RNA extraction and analysis. A special thank you to Dr Darren Fenton, without whom, the RNAseq analysis would not have been possible. Thank you Dr Andrew Lindsay, Dr Kellie Dean and Professor Justin McCarthy. Thank you all for your encouragement, suggestions and your constant availability to help, I really appreciate it.

Lastly, thank you to my friends and family. Thank you Patrycja, Louise and Seema, for lending an ear, keeping me motivated and encouraging me to stay positive. Thank you to my Aunt Anne, for all your guidance. A special thank you to my family. I am eternally grateful to my wonderful Mum, Dad, brothers Michael and Andrew, and my boyfriend Mike, for their love and constant support. You all provided me with continuous help, support, advice, encouragement and confidence not only in my work, but also in myself. You kept me motivated and encouraged me to persevere and remain resilient throughout. Also, a special thank you to Mike's family, Ashley, Helen, Rosie and Paul, for all your warm encouragements and continuous help, support and advice. I could not have completed this PhD without you all.

Table of Contents

DECLARATION OF INPUT FROM OTHER RESEARCHERS ..... ***I***

DECLARATION ..... ***II***

Acknowledgements ..... ***III***

List of Figures ..... ***VIII***

List of Tables ..... ***XII***

Abstract ..... ***XIII***

Abbreviations ..... ***XIV***

Chapter 1 – General Introduction ***1***

1.1 Aging and longevity **2**

1.2 The environment and aging **5**

1.3 Immunosenescence and Inflammaging **6**

1.4 Diet and the role of gut microbiota in aging and longevity **7**

1.4.1 Bacterial metabolism of Bile acids (BAs) 10

1.4.1.1 Farnesoid X Receptor (FXR) signalling 14

1.4.1.2 The G protein-coupled receptor TGR5, a bile acid signalling receptor 15

1.4.1.3 Other bile acid mediated receptor signalling 16

1.4.2 Fatty acids are dietary derived and microbially produced, as well as cellularly synthesised 17

1.5 The Gut Microbiota and Disease **20**

1.5.1 Crohn's Disease 20

1.5.2 Gut-brain axis in disease 21

1.5.2.1 Autism Spectrum Disorder 23

1.5.2.2 Parkinson's Disease 29

1.6 Models of aging **31**

1.7 *Caenorhabditis elegans* **32**

1.7.1 The *Caenorhabditis elegans* Life cycle 33

1.7.2 The *Caenorhabditis elegans* – The nematode model of aging 35

1.7.3 *Caenorhabditis elegans* longevity systems 36

1.7.3.1 age-1 and daf-2 37

1.7.3.2 eat-2 37

1.7.3.3 clk-1 39

1.7.3.4 ife-2 40

1.7.3.5 Metformin 40

1.7.3.6 Resveratrol 41

1.7.3.7 Rapamycin 42

1.7.3.8 β-Hydroxybutyrate 42

1.7.4 The gut microbiota in *Caenorhabditis elegans* 43

1.7.4.1 Dafachronic acids and Bile acids are cholesterol derivatives that may feed into similar pathways 44

1.7.4.2 DAF-12 receptor signalling is similar to the bile acid nuclear receptors in humans 47

1.8 Project aims and objectives **48**

Chapter 2 – Materials and Methods ***50***

2.1 Bacterial 51
2.1.1 Bacterial strains 51
2.1.2 Bacterial Culture 51
2.1.3 Bacterial Growth Assessment 55

2.2 *Caenorhabditis elegans* manipulation 55
2.2.1 Growth and Maintenance of nematode *Caenorhabditis elegans* 55
2.2.2 *Caenorhabditis elegans* Stage Synchronisation 57
2.2.3 *Caenorhabditis elegans* Lifespan Assessment Assay 59
2.2.4 *Caenorhabditis elegans* Development Assay 59
2.2.5 Bacterial Colonisation Assessment Assay in *Caenorhabditis elegans* 60
2.2.6 Gene expression detected by Fluorescence Microscopy in *Caenorhabditis elegans* 61
2.2.7 RNA Extraction from *Caenorhabditis elegans* 62
2.2.8 *Caenorhabditis elegans* RNA Quality Assessment and Sequence Alignment 64

2.3 Ultra Performance Liquid Chromatography Tandem Mass Spectrometer (UPLC-TMS) of Bile Acids and Fatty Acids 64
2.3.1 Clinical study of metabolites in Parkinson's Disease 64
2.3.2 Animal study of metabolites in Autism Spectrum Disorder 72
2.3.3 Design of Autism Microbial Interference study 72
2.3.4 Clinical study of metabolites in Bacterial and *Caenorhabditis elegans* 76
2.3.5 Bile Acid and Fatty Acid Extraction 77
2.3.6 Ultra Performance Liquid Chromatography Tandem Mass Spectrometry Chemicals 82
2.3.7 Ultra Performance Liquid Chromatography Tandem Mass Spectrometry 82

2.4 Statistical Analysis 83

Chapter 3 – Functionality of the gut microbiome is altered in neurological associated disorders 84

3.0 Abstract 85

3.1 Introduction 86

3.2 Results 89
Part I: Autism Spectrum Disorder - Can bacterial intervention reverse the gut associated deficits in bile acid metabolism to influence behaviour? 89
3.2.1.1 Autism Spectrum Disorder - the follow-on Study 90
3.2.1.2 Circulating bile acids were altered following microbial treatments of BTBR mice 96
3.2.1.3 Faecal bile acids were altered following microbial treatments of BTBR mice 102
3.2.1.4 Lactobacillus salivarius strain P0003 and Bifidobacterium adolescentis strain 2715 interventions improved BTBR mouse behaviour symptomatically. 118
Part II: Parkinson's Disease - Are bile acid and fatty acid levels altered in circulation and in the gut of Parkinson's Disease patients? 121
3.2.2.0 Microbial metabolic functions are altered in Parkinson's Disease. 122
3.2.2.1 Quality controls for Bile Acids 123
3.2.2.2 Specific microbially altered circulating bile acids are enriched in Parkinson's Disease patients 124
3.2.2.3 Female Parkinson's Disease patients have higher circulating bile acid concentrations compared to male Parkinson's Disease patients. 128
3.2.2.4 Total and conjugated circulating bile acid concentrations correlate with age in Parkinson's Disease patients 131
3.2.2.5 Bile acid agonists for nuclear receptors FXR and VDR are elevated in circulation of treated Parkinson's Disease patients. 135
3.2.2.6 Specific microbially altered faecal bile acids are enriched in Parkinson's Disease patients 136
3.2.2.7 Total and conjugated faecal bile acid concentrations negatively correlate with age in Parkinson's Disease patients 141

3.2.2.8 Specific faecal bile acid concentrations correlate with disease severity in Parkinson's Disease patients. 144
3.2.2.9 Sinemet-Treated Parkinson's Disease patients have lower concentrations of faecal bile acids compared to Non-Sinemet-Treated patients. 145
3.2.2.10 Specific circulating fatty acids are enriched in Parkinson's Disease patients. 150
3.2.2.11 Circulating fatty acids alter with age, in Parkinson's Disease patients. 154
3.2.2.12 Specific circulating fatty acid concentrations correlate with disease severity in Parkinson's Disease patients. 156
3.2.2.13 Specific faecal fatty acids are reduced in Parkinson's Disease patients. 158
3.2.2.14 Faecal fatty acids alter with age, in Parkinson's Disease patients. 161
3.2.2.15 Specific faecal fatty acid concentrations correlate with disease severity in Parkinson's Disease patients. 163
3.2.2.16 Sinemet-Treated Parkinson's Disease patients have higher concentrations of faecal fatty acids compared to Non-Sinemet-Treated patients. 168

3.3 Discussion 171

Chapter 4 – Examining bile acids to determine if their activation influences lifespan in the model of aging Caenorhabditis elegans 182

4.0 Abstract 183

4.1 Introduction 183

4.2 Results 188

4.2.1 Assessment of *Escherichia coli* OP50 bacterial growth in the presence of individual primary and secondary bile acids. 188
4.2.2 Primary and secondary bile acids were detected in *Escherichia coli* OP50 and gut of *Caenorhabditis elegans*, and their concentrations increased in a dose-dependent manner 191
4.2.3 The primary bile acid Chenodeoxycholic Acid and the secondary bile acid Deoxycholic Acid reduce *Caenorhabditis elegans* lifespan 196
4.2.4 Specific bile acids can alter *Caenorhabditis elegans* larvae developmental timing 205
4.2.5 Specific concentrations of the primary bile acid Chenodeoxycholic Acid and the secondary bile acid Deoxycholic Acid induce nuclear translocation of *Caenorhabditis elegans* transcription factor DAF-16 210
4.2.6 Ultra Performance Liquid Chromatography Tandem Mass Spectrometry (UPLC-TMS) assessment of Δ^4-Dafachronic Acid and Δ^7-Dafachronic Acid levels in *Caenorhabditis elegans* strain SS104 treated with individual primary and secondary bile acids. 214
4.2.7 Bile acids influence the *Caenorhabditis elegans* transcriptome towards different outcomes 219
4.2.8 The *Caenorhabditis elegans* transcriptome was similar following treatment with bile acids Ursodeoxycholic Acid compared to Chenodeoxycholic Acid, and Lithocholic Acid compared to Ursodeoxycholic Acid 222
4.2.9 The microbially produced secondary bile acid, Lithocholic Acid, induced changes in the *Caenorhabditis elegans* transcriptome, compared to the parent primary bile acid, Chenodeoxycholic Acid 227
4.2.10 Alterations in *Caenorhabditis elegans* transcription of genes involved in longevity and immune response, when treated with bile acid Lithocholic Acid compared to Chenodeoxycholic Acid 229

4.3 Discussion 235

Chapter 5 – Exploring gut microbial interactions that can alter lifespan in the model of aging Caenorhabditis elegans 243

5.0 Abstract 244

5.1 Introduction 244

5.2 Results 247

5.2.1 *Escherichia coli* HM605 and its deletion mutations affect *Caenorhabditis elegans* strain SS104 L1 larvae lifespan....247
5.2.2 *Escherichia coli* HM605 and its deletion mutations affect *Caenorhabditis elegans* L4 larvae lifespan....249
5.2.3 Assessment of the rate of growth of *Escherichia coli* HM605 and its deletion mutants....251
5.2.4 The effect of *Escherichia coli* HM605 and its deletion mutants: Δ*fim*H and Δ*dsb*A, on *Caenorhabditis elegans* developmental timing is strain dependent....253
5.2.5 *Escherichia coli* HM605 is capable of colonising the gut of *Caenorhabditis elegans*....255
5.2.6 RNA extraction and sequencing to determine whether *Escherichia coli* HM605 and its deletion mutations effect *Caenorhabditis elegans* transcriptome....257
5.2.7 *Escherichia coli* HM605 induced changes in the *Caenorhabditis elegans* transcriptome, compared to the *Escherichia coli* OP50 control....260
5.2.8 *Escherichia coli* HM605 deletion mutant, Δ*dsb*A, induced changes in the *Caenorhabditis elegans* transcriptome, compared to *Escherichia coli* HM605....263
5.2.9 The transcription of *Caenorhabditis elegans* genes involved in immune response and longevity, were altered by *Escherichia coli* strains....266

5.3 Discussion....272

Chapter 6 – General Discussion....278

Chapter 7 – References....292

Appendix I – Chapter 1 – Introduction....354

Appendix II – Chapter 2 – Materials and Methods....354

Appendix III – Chapter 3 – Supplementary Information....354

Appendix IV – Chapter 4 – Supplementary Information....397

Appendix V – Chapter 5 – Supplementary Information....461

List of Figures

Figure 1.1: The nine hallmarks of aging. 3

Figure 1.2: The dominant microbial taxa of the elderly. 10

Figure 1.3: The liver produces bile acids (BAs), however gut microbes are responsible for BA diversity.. ……13

Figure 1.4: Different BAs can act as molecules for nuclear receptor, and G protein-coupled receptor, signalling……15

Figure 1.5: Fatty acids from the diet influence processes locally in the gut and systemically……19

Figure 1.6: Summary of reported alterations to bacterial representation of individuals with ASD……28

Figure 1.7 The nematode Caenorhabditis elegans life cycle at 22^{o}C.....34

Figure 1.8: Factors affecting Caenorhabditis elegans lifespan and longevity.....38

Figure 1.9: Dafachronic acid and bile acid signalling pathways show cholesterol processing conservation between C. elegans and humans respectively.....45

Figure 2.1: Schematic representation outlining main steps of synchronisation of C. elegans. 58

Figure 2.2: Schematic representation of the Parkinson's Disease (a) plasma and (b) faecal study and analysis.....68

Figure 2.3: Schematic representation of the Autism Spectrum Disorder (ASD) murine study design...76

Figure 2.4: Schematic representation of Bile Acid and Fatty Acid extraction process.....79

Figure 3.1: Viable bacteria delivered to the murine BTBR model of ASD.....91

Figure 3.2: Assessment of bile acid extraction efficiency from biological material from WT and ASD murine model. 92

Figure 3.3: Principal component analysis (PCA) examining relative distance, on the basis of bile acids, in WT C57BL/6 J and ASD model BTBR animals. 95

Figure 3.4: Assessment of circulating bile acids in WT C57BL/6 J and ASD model BTBR mice. 98

Figure 3.5: Assessment of total and free circulating bile acids in WT C57BL/6 J and ASD model BTBR mice.....99

Figure 3.6: Assessment of circulating tauro conjugated bile acids in WT C57BL/6 J and ASD model BTBR mice.....100

Figure 3.7: Assessment of the potential to activate signalling bile acid receptors in circulation for WT C57BL/6 J and ASD model BTBR mice.....102

Figure 3.8: Principal component analysis (PCA) to represent all faecal bile acids detected from WT C57BL/6 J and BTBR ASD murine model. 104

Figure 3.9: Relative assessment of faecal bile acids in WT C57BL/6 J and BTBR ASD murine model. 106

Figure 3.10: Assessment of total and free faecal bile acids in WT C57BL/6 J and BTBR ASD murine model, at baseline week 0. 109

Figure 3.11: Assessment of total and free faecal bile acids in WT C57BL/6 J and BTBR ASD murine model, week 2.....110

Figure 3.12: Assessment of total and free faecal bile acids in WT C57BL/6 J and BTBR ASD murine model, at endpoint week 9. ..... *111*
Figure 3.13: Assessment of total tauro conjugated and free tauro conjugated faecal bile acids in WT C57BL/6 J and BTBR ASD murine model, at baseline week 0. ..... *113*
Figure 3.14: Assessment of total tauro conjugated and free tauro conjugated faecal bile acids in WT C57BL/6 J and BTBR ASD murine model, at week 2. ..... *114*
Figure 3.15 Assessment of total tauro conjugated and free tauro conjugated faecal bile acids in WT C57BL/6 J and BTBR ASD murine model, at endpoint week 9. ..... *115*
Figure 3.16: Assessment of potential signalling bile acids in WT C57BL/6 J and ASD BTBR mice. *118*
Figure 3.17: Assessment of gut motility, permeability, and ASD behavioural phenotypes in WT C57BL/6 J and ASD model BTBR mice. *119*
Figure 3.18: Assessment of extraction efficiency from control volunteers (C) and Parkinson's Disease patients (PD) human biological material. *123*
Figure 3.19: Principal component analysis (PCA) of all detected bile acids for plasma material. *124*
Figure 3.20: Assessment of circulating bile acids in Parkinson's Disease patients compared to Control Volunteers. *127*
Figure 3.21: Assessment of circulating bile acids, with respect to gender, in Parkinson's Disease patients compared to Control Volunteers. *130*
Figure 3.22: Assessment of circulating bile acids correlation with age in Parkinson's Disease patients relative to healthy individuals. *131*
Figure 3.23: Assessment of circulating bile acids correlation with age from Parkinson's Disease patients treated with medication, and in healthy humans. *134*
Figure 3.24: Assessment of potential signalling bile acids from Parkinson's Disease patients, relative to healthy individuals. *136*
Figure 3.25: Principal component analysis (PCA) of all detected bile acids for faecal material. *137*
Figure 3.26: Assessment of faecal bile acids from Parkinson's Disease patients, compared to healthy individuals. *138*
Figure 3.27: Assessment of faecal bile acid moieties by gender from Parkinson's Disease patients, compared to healthy control volunteers. *140*
Figure 3.28: Assessment of faecal bile acids correlation with age from Parkinson's Disease patients, relative to healthy individuals. *144*
Figure 3.29: Assessment of faecal bile acids correlation with UPDRS score from Parkinson's Disease patients. *145*
Figure 3.30: Assessment of faecal bile acids from Parkinson's Disease patients receiving Sinemet medication. *149*
Figure 3.31: Principal component analysis (PCA) of all detected fatty acids for plasma material. *150*
Figure 3.32: Assessment of plasma fatty acids from Parkinson's Disease patients, compared to healthy control individuals. *153*

Figure 3.33: Assessment of circulating fatty acids correlation with age from Parkinson's Disease patients, relative to healthy control volunteers. *155*
Figure 3.34: Assessment of circulating fatty acids correlated with disease severity in Parkinson's Disease patients. *157*
Figure 3.35: Principal component analysis (PCA) of all detected fatty acids for faecal material. *158*
Figure 3.36: Assessment of faecal fatty acids from Parkinson's Disease patients, compared to healthy control volunteers. *161*
Figure 3.37: Assessment of faecal fatty acids correlated with age in Parkinson's Disease patients, relative to healthy control volunteers. *162*
Figure 3.38: Assessment of faecal fatty acids correlated with disease severity in Parkinson's Disease patients. *165*
Figure 3.39: Assessment of faecal fatty acid correlation to cognitive function in Parkinson's Disease patients. *167*
Figure 3.40: Assessment of faecal fatty acids from Parkinson's Disease patients receiving Sinemet medication, compared to those treated with other Parkinson's Disease medications. *170*
Figure 4.1: Chemical structure of primary and secondary bile acids. *186*
Figure 4.2: Assessment of Escherichia coli OP50 bacterial growth in the absence and presence of individual primary and secondary bile acids. *191*
Figure 4.3: Ultra Performance liquid Chromatography Tandem Mass spectrometry (UPLC-TMS) assessment of bile acid uptake into Escherichia coli OP50. ..... *193*
Figure 4.4: Ultra Performance Liquid Chromatography Tandem Mass Spectrometry (UPLC-TMS) assessment of bile acid levels in Caenorhabditis elegans SS104 strain. *195*
Figure 4.5: Lifespan and longevity assessment of Caenorhabditis elegans strain SS104 in the presence and absence of primary and secondary bile acids. *197*
Figure 4.6: Lifespan and longevity assessment of Caenorhabditis elegans wild-type (WT) Bristol strain N2 in the presence and absence of primary and secondary bile acids. *199*
Figure 4.7: Lifespan and longevity assessment of reproductive adulthood Caenorhabditis elegans temperature sensitive strain SS104 in the presence and absence of primary and secondary bile acids. *201*
Figure 4.8: Lifespan and longevity assessment of Caenorhabditis elegans wild-type (WT) Bristol strain N2 in adulthood, in the presence and absence of primary and secondary bile acids. *203*
Figure 4.9: Assessment of development of Caenorhabditis elegans strain SS104 in the presence and absence of primary and secondary bile acids. *206*
Figure 4.10: Assessment of development of Caenorhabditis elegans wild-type (WT) Bristol strain N2 in the presence and absence of primary and secondary bile acids. *208*
Figure 4.11: Fluorescence microscopy assessment of bile acid-induced DAF-16:GFP expression in Caenorhabditis elegans CF1139 strain. *213*

Figure 4.12: Measurement of green fluorescence intensity representing bile acid-induced DAF-16:GFP expression in Caenorhabditis elegans CF1139 strain. 213
Figure 4.13: Potential longevity pathways in Caenorhabditis elegans and mammals. 214
Figure 4.14: Detection of Δ^4-Dafachronic Acid and Δ^7-Dafachronic Acid by Ultra Performance Liquid Chromatography Tandem Mass Spectrometry (UPLC-TMS). 215
Figure 4.15: Detection of Δ^4-Dafachronic Acid in nematode extracts with and without BA feeding..216
Figure 4.16: Assessement of detection of Δ^4-Dafachronic Acid in Caenorhabditis elegans strain SS104 and Escherichia coli OP50. 218
Figure 4.17: Correlation between paired RNA sample replicates showing Spearman's rank correlation coefficient R values. 222
Figure 4.18: Volcano plot of Caenorhabditis elegans SS104 strain top transcribed genes, when treated with bile acid UDCA compared to CDCA. 223
Figure 4.19: Volcano plot of top five transcribed genes, and clec-4, in Caenorhabditis elegans strain SS104 treated with bile acid LCA compared to UDCA. 225
Figure 4.20: Alterations in Caenorhabditis elegans SS104 strain transcriptome treated with bile acid LCA, compared to CDCA 229
Figure 4.21: Caenorhabditis elegans longevity and immune response signalling pathways in bile acid LCA treated nematodes, compared to CDCA. 234
Figure 4.22: Potential bile acid longevity pathway in Caenorhabditis elegans. 235
Figure 5.1: Assessment of Escherichia coli HM605 and its deletion mutations on Caenorhabditis elegans strain SS104 L1 lifespan. 249
Figure 5.2: Assessment of Escherichia coli HM605 and its deletion mutations on Caenorhabditis elegans strain SS104 and Caenorhabditis elegans wild-type strain N2 L4 lifespan. 251
Figure 5.3: Assessment of the rate of growth of Escherichia coli HM605 and its deletion mutations, compared to control Escherichia coli OP50. 252
Figure 5.4: Assessment of Escherichia coli HM605 and its deletion mutations on Caenorhabditis elegans strain SS104 and Caenorhabditis elegans wild-type strain N2 L1 development. 254
Figure 5.5: Colonisation of the Caenorhabditis elegans gut by Escherichia coli strains. 256
Figure 5.6: Correlation between RNA sample replicates showing Spearman's rank correlation coefficient R values. 260
Figure 5.7: Caenorhabditis elegans strain SS104 transcriptome when cultured with Escherichia coli HM605, compared to Escherichia coli OP50. 262
Figure 5.8: Caenorhabditis elegans strain SS104 transcriptome when cultured with Escherichia coli HM605 deletion mutants: ΔdsbA and ΔfimH, compared to Escherichia coli HM605. 266
Figure 5.9: Caenorhabditis elegans longevity and immune response signalling pathways. 271

List of Tables

Table 1.1: Summary of recent investigations of gut microbiome alterations in older populations..... 9

Table 1.2: Summary of C. elegans daf genes examined in this study.....35

Table 2.1: Bacterial strains applied to this thesis.....52

Table 2.2: Caenorhabditis elegans strains applied to this study.....56

Table 2.3: Clinical demographics of Parkinson's Disease patients where plasma was obtained. 70

Table 2.4: Clinical demographics of faecal samples obtained from ELDERMET control volunteers and Parkinson's Disease patients included in this study. 71

Table 2.5: Cage, Litter and Cohort information on control groups C57BL/6 J and BTBR T^{+} $Itpr3^{tf}$/J mice.....73

Table 2.6: Cage, Litter and Cohort information on BTBR mice of treatment groups Bifidobacterium adolescentis strain APC2715 and Lactobacillus salivarius P0003. 74

Table 2.9: Bile Acids analysed in this study.....80

Table 2.10: Fatty Acids analysed in this study. 81

Table 4.1: Summary of Caenorhabditis elegans lifespan assays in the presence of individual bile acids 204

Table 4.2: Summary of the effect of each bile acid on Caenorhabditis elegans lifespan and development.....209

Table 4.3: Caenorhabditis elegans SS104 RNA samples and their quality assessed post extraction..220

Table 4.4: Caenorhabditis elegans strain SS104 RNA samples and their quality assessed post by Genewiz Europe. 221

Table 4.5: FastQC and STAR alignment report on RNA sequencing. 222

Table 4.6: Differential transcriptome analysis for C. elegans strain SS104 strain in the presence of bile acids UDCA compared to CDCA. 224

Table 4.7: Differentially transcribed genes in Caenorhabditis elegans strain SS104 cultured with bile acid 1 mM LCA, compared to 1 mM UDCA. 226

Table 5.1: Name and function of the Escherichia coli HM605 mutants screened in this study.....248

Table 5.2: Caenorhabditis elegans strain SS104 RNA samples and their quality assessed post extraction. 258

Table 5.3: FastQC and STAR alignment report on RNA sequencing. 259

Abstract

This thesis aimed to investigate the role of the gut microbiota and their associated functionality in the context of aging and life stage related diseases. The focus was maintained on key inter-kingdom signalling molecules, host produced but bacterially modified Bile acids (BAs) and on dietary microbially derived Fatty acids (FAs) as key elements to indicate gut microbial potential impactful roles. In the context of Chapter 3, this thesis examined the levels of BAs and FAs, to identify convergence on specific microbially produced, or modified, metabolites in the two neurological disease states representing (1) early life (murine model of Autism Spectrum Disorder (ASD)) and (2) later life (human Parkinson's Disease(PD)). It further established the potential to redress the balance through microbial intervention, as a cause or consequence in the case of ASD. BAs converged during the healthy aging process, in Chapter 4, to determine the nature of these specific interactions, based on nuclear receptor conservation. The *Caenorhabditis elegans* nematode model of aging was employed to determine and genetically decipher potential individual BA influences. Chapter 5 built on recognising that gut microbes and the pathobiont *Escherichia coli* HM605 induced inflammation. This chapter also focused on the mechanisms by which *Escherichia coli* HM605 could influence the aging process.

Abbreviations

C. elegans	*Caenorhabditis elegans*
°C	Degrees Celsius
16S	16s subunit ribosomal RNA gene sequencing
3βHSD	3-β-hydroxysteroid dehydrogenase
4EP	4-ethylphenol
4EPS	4-ethylphenyl sulfate
5AV	5-aminovaleric acid
600nm	Wavelength 600 nanometer
7KLCA	7-ketolithocholic acid
AA	Arachidonic acid
ACh	Acetylcholine
AD	Alzheimer's disease
ADI-R	Autism Diagnostic Interview-Revised
ADP	Adenosine diphosphate
AIEC	Adherent-invasive *E. coli*
Akt	Protein kinase B (PKB)
AMP	Adenosine monophosphate (5'-adenylic acid)
AMPK	AMP-activated protein kinase
APC	APC Microbiome Ireland, UCC
ApoE	Apolipoprotein E
ApoEε2	Apolipoprotein E ε2
ApoEε4	Apolipoprotein E ε4
ASD	Autism spectrum disorder
ATP	Adenosine triphosphate
BA	Bile acid
BAC	Bile acid cholyl-CoA synthetase
BAI	Bile acid-inducible
BAT	Bile acid-CoA:amino acid N-acyltransferase
BDNF	Neurotrophic factor

BLSA	Baltimore Longitudinal Study of Aging
BSH	Bile salt hydrolase
BTBR	Black and Tan BRachyury *T+Itpr3tf*/J
BTBR_2715	BTBR treated *Bifidobacterium adolescentis* strain 2715
BTBR_P0003	BTBR treated *Lactobacillus salivarius* strain P0003
BTBR_Veh	BTBR control
C57	C57BL/6 J
C57_Veh	C57 control
CA	Cholic Acid
Ca^{2+}	Calcium ion
$CaCl_2$	Calcium chloride
CAd4	Deuterated cholic acid
cAMP	Cyclic adenosine monophosphate
CAR	Constitutive androstane receptor
CCR2	C–C motif chemokine receptor 2
CD	Crohn's disease
CDCA	Chenodeoxycholic Acid
CDCAd4	Deuterated chenodeoxycholic acid
cDNA	Complementary deoxyribonucleic acid
CF	Female control
cf-mt-DNA	Cell free mitochondrial DNA
CFU	Colony Forming Unit
CFU/ml	Colony Forming Units per mililitre
CHD	Coronary heart disease
CINC-2α/β	Cytokine-induced neutrophil chemoattractant-2 alpha/beta
cm	centimeter
CM	Male control
CNS	Central nervous system
CO	Carbon monoxide
COMT	Catechol-O-methyltransferase
COX	Cyclooxygenase

CpG	5’-Cytosine-phosphate-Guanine-3’
CREC	Clinical Research Ethics Committee
CVD	Cardiovascular disease
CYP	cytochrome P450
Δ^4DA	Δ^4-Dafachronic acid
Δ^7DA	Δ^7-Dafachronic acid
DA	Dafachronic acid
daf	dauer formation
daf-c	dauer constitutive
daf-d	dauer defective
DAMPs	Damage-associated molecular patterns
DB	Database
DCA	Deoxycholic Acid
DCAd4	Deuterated deoxycholic acid
dH_2O	deionised water
DHA	cis-4,7,10,13,16,19-Docosahexaenoic Acid
DHCA	Dehydrocholic acid
DHCA	Dehydrocholic acid
diHETE	Dihydroxyeicosatetraenoic acid
DNA	Deoxyribonucleic acid
E. coli	*Escherichia coli*
EA	cis-11-Eicosenoic Acid
EET	Epoxyeicosatrienoic acids
EGFR	Epidermal growth factor receptor
eIF4E	Eukaryotic translation initiation factor 4E
EPA	cis-5,8,11,14,17-Eicosapentaenoic Acid
ER	Endoplasmic reticulum
ERK1/2	Extracellular signal-regulated kinases
ETE	Eicosatetraenoic acid
FA	Fatty acid
FDA	Food and Drug Administration (US)

FDR	False discovery rate
FGF15/19	Fibroblast growth factor 15/19
FGF21	Fibroblast growth factor-21
FGFR4	Fibroblast growth factor receptor 4
FITC Flux	Fluorescein isothiocyanate dextran paracellular flux
FMT	Faecal microbial transplant
FOXO	Forkhead family of transcription factors
FOXO3A	Forkhead box class O 3a
FXR	Farnesoid X receptor
g	grams
g/L	gram per litre
GAAC	General amino acid control
GABA	Gamma-Aminobutyric acid
GABAA	Gamma-Aminobutyric acid type A
$GABA_{B1b}$	Gamma-Aminobutyric acid type B, 1b isoform
GCA	Glycocholic acid
GCDCA	Glycochenodeoxycholic acid
GDCA	Glucodeoxycholic acid
GDF11	Growth Differentiation Factor 11
GDF15	Growth/differentiation factor 15
GF	Germ Free
GHCA	Glycohyocholic acid
GHDCA	Glycohyodeoxycholic acid
Ghrhr	Long-lived growth hormone-releasing hormone
GI	Gastro intestinal
GIT	Gastrointestinal tract
GLCA	Glycolithocholic acid
GLP-1	Glucagon-like peptide 1
GPCRs	G-protein–coupled receptors
GPR40	G-protein-coupled receptor 40
GUDCA	Glycoursocholic acid

GWAS	Genome-wide association studies
HBOT	Hyperbaric oxygen therapy
HCA	Hyocholic acid
HDAC	Histone deacetylase
HDAC1/2	Histone deacetylase protein 1/2
HDCA	Hyodeoxycholic acid
HFD	High fat diet
HHP	Hyperoxic-Hypoxic Paradox
HIF	Hypoxia induced factor
HITChip	Human Intestinal Tract Chip
HNF-4	Hepatocyte nuclear factor 4
HPHPA	3-(3-hydroxy phenyl)-3-hydroxypropionic acid
HPLC	High performance liquid chromatography
HS	High sensitivity
HSD-1	Hydroxysteroid dehydrogenase 1
HSDH	Hydroxysteroid dehydrogenases
HSP	Heat-shock protein
IAA	Indoleacetic acid
Iald	Indolealdehyde
IBD	Inflammatory bowel disease
IDF	Invention Disclosure Form
IGF-1	Insulin-like growth factor 1
IGFR	Insulin growth factor receptor
IL	Interleukin
ILA	Indolelactic acid
INFγ	Interferon gamma
InsR	Insulin receptor
IS	Internal standard
ITS	Internal transcribed spacer
JNK	c-Jun N-terminal kinase
K_2HPO_4	Potassium Phosphate dibasic

KH_2PO_4	Potassium phosphate monobasic
Km^R	kanamycin-resistant
KO	Knock-out
KPO_4	Potassium phosphate buffer
L	litre
L-dopa	levodopa (l-3,4-dihydroxyphenylalanine)
L1	larval stage 1
L2	larval stage 2
L2d	pre-dauer L2
L3	larval stage 3
L4	larval stage 4
LB	Luria Broth
LCA	Lithocholic acid
LCFA	Long chain fatty acids
LDL	Low-density lipoprotein
LKB1	Liver Kinase B1
LOX	Lipoxygenase
LPS	Lipopolysaccharide
LT	Leukotriene
LTB_4	Leukotriene B_4
LX	Lipoxin
LXR	Liver X receptor
M	Molar
m/z	Mass-to-charge ratio
MafG	Musculoaponeurotic Fibrosarcoma Oncogene Homolog G
MAOB	Monoamine oxidase-B
MAP	Mitogen-activated protein
MAPK	Mitogen-activated protein kinase
MAPT	Microtubule-associated protein tau
MCA	Muricholic acid
MCFA	Medium chain fatty acids

MeOH	Methanol
metr-1	Methionine synthase
mg	milligram
mg/ml	milligram per millilitre
$MgSO_4$	Magnesium sulfate
MHC	Major histocompatibility complex
MIA	Maternal immune activation
MIF	Macrophage migration inhibition factor
MIP-3α	Macrophage Inflammatory Protein-3 alpha
miRNA	MicroRibonucleic acid
ml	millilitre
ml/L	millilitre per litre
mM	millimolar
mm	millimeter
MoCA	Montreal Cognitive Assessment
MPP+	1-methyl-4-phenylpyridinium
MPTP	1-methyl-4-phenyl-1,2,3,6-tetrahydropyridine
mRNA	Messenger Ribonucleic acid
MRS	De Man, Rogosa and Sharpe
MS	Multiple sclerosis
MT2	Melatonin 2 receptor
mTOR	Mammalian target of rapamycin
MTT	Microbiota Transfer Therapy
MUFA	Monounsaturated fatty acid
MW	Molecular weight
N	4 moles per litre
n-3	omega-3
n-6	omega-6
N/A	Not applicable
N2	WT Bristol strain
Na_2HPO_4	Sodium phosphate dibasic

nAChR	Nicotinic acetyl-choline receptor
NaCl	Sodium chloride
NAD^+	Nicotinamide adenine dinucleotide
NAFLD	Non-alcoholic fatty liver disease
NaN_3	Sodium azide
NaOH	Sodium hydroxide
NF-κB	Nuclear factor kappa-light-chain-enhancer of activated B cells
ng/g	nanogram per gram
ng/ml	nanogram per millilitre
NGM	Nematode Growth Media
NHR	Nuclear hormone receptor
NO_2	Nitrogen dioxide
NR	Nuclear receptor
Nrf	Nuclear respiratory factor
O^-	Superoxide
O/N	Overnight
O_3	Ozone
OD	Optical density
OD_{600}	Optical density at wavelength 600 nanometer
OD_{600} per ml	Optical density at wavelength 600 nanometer per millilitre
OSM-9	Osmotic avoidance abnormal-9
PBS	Phosphate buffered saline
PCA	Principal components analysis
PCR	Polymerase chain reaction
PD	Parkinson’s Disease
PDF	Female Parkinson's disease
PDL3	post-dauer L3 stage
PDL4	post-dauer L4 stage
PDM	Male Parkinson's disease
PGC1	Proliferator-activated receptor-gamma coactivator-1alpha
PI3K	Phosphatidylinositol-3-OH kinase

PM	Particulate matter
PM10	Particulate matter less than 10 µm in diameter
PM2.5	Particulate matter less than 2.5 µm in diameter
POMC	pro-opiomelanocortin
PPAR	Peroxisome proliferator- activated receptor
PPARA	Peroxisome proliferator activated receptor alpha and delta
PPARD	Peroxisome proliferator activated receptor alpha and delta
PPAR	Peroxisome proliferator- activated receptor gamma
PSA	Polysaccharide
PUFA	Polyunsaturated fatty acid
PXR	Pregnane X receptor
qPCR	Quantitative polymerase chain reaction
qRT-PCR	Quantitative reverse transcription PCR
QTOF	Quadrupole time-of-flight
RA	Reproductive Adult
RIN	RNA integrity number
RNA	Ribonucleic acid
RNAseq	RNA-sequencing
ROS	Reactive oxygen species
rpm	Revolutions per minute
rRNA	Ribosomal Ribonucleic acid
RT	Room Temperature
RT	Retention time
S/N	supernatant
SAAR	Sulfur amino acid restriction
SAMP8	Senescence Accelerated Mouse-Prone 8
sams-1	S-adenosylmethionine synthase
SCD	Stearoyl-CoA-desaturase
SCFA	Short chain fatty acids
SD	Standard deviation
SERPINs	Serine protease inhibitors

SFA	Saturated fatty acid
SHP	Small heterodimer partner
SIRT	Sirtuin
SNP	Single-nucleotide polymorphism
SO_2	Sulfur dioxide
Spp.	Species
SS104	Temperature-sensitive, *glp-4*(*bn2*) mutation
STAR	Spliced Transcripts Alignment to a Reference
STC1	Stanniocalcin 1
SXR	Xenobiotic receptor
T_0	Time zero
T_{24}	24 hour timepoint
T3	Thyroid hormone
T4	Thyroxine
TCA	Taurocholic acid
TCA	Tricarboxylic acid
TCDCA	Taurochenodeoxycholic acid
TCPOBOP	1,4-bis[2-(3,5 dichloropyridyloxy)] benzene
TDCA	Taurodeoxycholic acid
tdo-2	tryptophan 2,3-dioxygenase
TFEB	Transcription factor EB
TGF-β	Transforming growth factor beta
TGR5	Tanaka G receptor 5
TGR5	Takeda-G-protein-receptor-5
Th1	T helper type 1
Th2	T helper type 2
THCA	Taurohyocholic acid
THDCA	Taurohyodeoxycholic acid
THRA	Thyroid hormone receptor alpha
TLCA	Taurolithocholic acid
TMAO	Trimethylamine-N-oxide

TMCA	Tauromuricholic acid
TNF	Tumor necrosis factor
TNF-α	Tumor necrosis factor alpha
TOR1/2	Target of rapamycin protein 1/2
TRI Reagent	TRIzol
tRNA	Total Ribonucleic acid
TUDCA	Tauroursodeoxycholic acid
UCC	University College Cork
UDCA	Ursodeoxycholic acid
UPDRS	Unified Parkinson's Disease Rating Scale
UPLC	Ultra performance liquid chromatography
UPLC-MS	Ultra performance liquid chromatography - mass spectrometry
UPLC-TMS	Ultra Performance Liquid Chromatography Tandem Mass Spectrometry
v/v	volume per volume
VDR	Vitamin D receptor
VEGF	Vascular endothelial growth factor
VEGF-α	Vascular endothelial growth factor alpha
VLCFA	Very long-chain fatty acid
w/v	weight per volume
WHO	World Health Organisation
WT	wild-type
α-MCA	Alpha-muricholic acid
α-syn	α-synuclein
β-MCA	Beta-muricholic acid
βHB	β-Hydroxybutyrate
µg	microgram
µg/ml	Microgram per millilitre
µl	microlitre
µl/min	microlitre per minute
µM	micromolar
ω-MCA	Omega-muricholic acid

Chapter 1 – General Introduction

1.1 Aging and longevity

The process of aging represents a huge, multifactorial biological question. This thesis is focused on elucidating associations and possible effects of microbial processes and metabolites on aging, and in age-related diseases. This is of importance since the aging demographic (proportion of people >60 years of age) is increasing in the modern world due to better medicines and treatments. Indeed, life expectancy in the Republic of Ireland is 84 years of age for women and 80.4 years of age for men. Furthermore, it is projected that 1.56 million Irish people will represent the age of 65 and beyond by 2051 (Health, 2020). Similarly, the World Health Organisation (WHO) expect that the aged (65 years and over) world's population will increase from 12% to 22% by 2050 (https://www.who.int/news-room/fact-sheets/detail/ageing-and-health). Therefore, while lifespan is extending, considerable efforts are being made to understand the aging process, and also to similarly extend health-span, in order to close the gap between healthy years and life expectancy.

At the biochemical level, it is speculated that aging is a consequence not only of active gene programming, but of evolved limitations in somatic maintenance and a accumulation of damage (Kirkwood, 2005). The potential for genes to evolve and evade aging, therefore, is difficult, as natural selection may not experience their benefit and value. Most recently, López-Otín *et al.*, (2013) defined aging as "a progressive loss of physiological integrity, leading to impaired function and increased vulnerability to death". The authors identified nine biochemical hallmarks of aging, to include genomic instability, telomere attrition, epigenetic alterations, loss of proteostasis, deregulated nutrient sensing, mitochondrial dysfunction, cellular senescence, stem cell exhaustion and altered intercellular communication (*Figure 1.1*). The hallmarks are not stand alone, but represent a gradual progression of modification and of process re-programming to elicit global effects.

No one gene or process is responsible for aging. At the genetic level a range of genome-wide association studies (GWAS) have provided insight into allele frequencies of genetic variants associated with a specific trait or disease. Applied to aging, meta-analysis (statistical analysis of the data from independent primary studies focused on the same question) was applied to examine DNA methylation and single-nucleotide polymorphism (SNP), from over 40,000 individuals to identify 137

genome-wide significant loci, of which 113 are novel (McCartney *et al.,* 2021). The authors based aging progression on "epigenetic clocks", where accumulation of CpG modification on specific genes could be taken as a readout of accelerated aging. Of specific interest in this space is that metabolism and immunity had been identified as underpinning these "clocks" in aging (Gibson *et al.,* 2019). The work illustrates that heritable DNA methylation-based biomarkers can provide real insight into biological aging. Interestingly, the lack of DNA methylation systems is a limitation of the model of aging *C. elegans* and this is of concern in translating nematode work to mammals (Corsi *et al.,* 2015). However, other modifications have recently been identified to frame such changes to gene expression in *C. elegans* in the context of aging (Luo *et al.,* 2015). Whether there is correspondence for *C. elegans* gene modifications and mammaliam gene CpG methylation remains to be determined in the context of aging.



Figure 1.1: **The nine hallmarks of aging.** Adapted from (López-Otín *et al.,* 2013). Each is a separate layer contributing to the aging process.

Gibson *et al.,* (2019) showed that epigenetic aging is correlated with lifestyle (including smoking and obesity) and parental longevity. Deelen *et al.*, (2019) studied

European, East Asian and African American ancestry and found apolipoprotein E (ApoE) variant ε4 correlated with shorter lifespan, while variant ε2 significantly associated with better survival (Deelen *et al.,* 2019). ApoE is generally a component of lipid transport particles in circulation to and from different tissues, including the brain (Mahley and Rall, 2000). Indeed, these variants are associated with an increased (ε4) or reduced (ε2) risk for age-related diseases, including Alzheimer's disease (AD) and cardiovascular disease (Mahley and Rall, 2000). More recently, ε4 variant was associated with accumulation of lipid droplets in the brain, increasing the risk for AD (Raulin *et al.,* 2022). Deelen *et al.*, (2019) determined the number of independent signals at the APOE locus using SNPTEST, and MetaXcan, to identify genetically predicted tissue-specific expression associations with longevity. They found increased expression of genes *KANSL1*, *CRHR1, ARL17A*, and *LRRC37A2*, and a reduction in gene expression of *ANKRD31* and *BLOC1S1* were associated with higher survival rates and longevity (Deelen *et al.,* 2019). However, the exact relationship between the expression of these genes and longevity in humans has not been determined, and needs further analysis. Recently, *KANSL1* variants have been associated with the microtubule-associated protein tau (MAPT) gene, an aberrant protein associated with Parkinson's Disease (PD) (Soto-Beasley *et al.,* 2020).

The Baltimore Longitudinal Study of Aging (BLSA), in humans, applied proteomic approaches to identify a senescence associated secretome, pointing to roles for growth/differentiation factor 15 (GDF15), stanniocalcin 1 (STC1), and serine protease inhibitors (SERPINs), as significantly positively correlated with age (Basisty *et al.,* 2020). Taken together, these studies highlight aging as a genetic and progressive condition, with the potential for intervention. Although nutrient sensing is included, the contribution of diet and gut health, including microbes and their processes, have not been highlighted. Emerging evidence point to pivotal roles for these parameters in healthy aging and other age-associated disease states (Connell *et al.,* 2022), as discussed below.

1.2 The environment and aging

Whilst genetics is certainly central to the aging demographic, other factors including the hallmarks above (*Figure 1.1*), can contribute to the aging process. Among them are diet and the environment. Although such combinatorial approaches are in their infancy, the importance of examining environment in terms of stressors (both physical and social) is being recognised (Malecki *et al.,* 2022). López-Otín *et al.*, (2013) explored the hallmarks of aging (*Figure 1.1* above) with environmental effects including epigenetic alterations or "epigenetic clock" and indeed circadian rhythm or body clock to the processes. Indeed, both biotic and abiotic- environmental factors can impact overall health and disease status. Different environments are associated with exposure to potential toxins, accumulation of genetic mutations, availability of resources to include hygenic conditions, water and even medicines, socioeconomic status, sedentary lifestyle and associated diseases. A recent study conducted in China found an association between built environment and lung cancer in women (Xie *et al.,* 2022). Xie *et al.*, (2022) determined that air pollutants (PM2.5, PM10, SO_2, CO, O_3 and NO_2) were at high levels in built environments, leading to an increased risk of women's lung cancer (Xie *et al.,* 2022). Similar to air pollution, climate, particularly heatwaves, have a negative impact on aging. A study in Finland found that heatwaves were significantly associated with increased mortality rates among those aged 65 and over (Kollanus *et al.,* 2021). Socioeconomic status can also impact overall health and aging. Low socioeconomic status is associated with a lower education level and poorer living environment. In Hungary, women with a low socioeconomic status were found to be more prone to obesity, and a positive association was found between X chromosome loss or mosaicism, due to telomere shortening, and increasing age (Annar *et al.,* 2022). Similarly, in Denmark, adults with higher income were associated with early dementia diagnosis, compared to adults with low socioeconomic status (Petersen *et al.,* 2021). There is an association between people with low socioeconomic status and unhealthy lifestyle, such as sedentary behaviour. Sedentary behaviour is associated with mortality due to the increased risk of type 2 diabetes mellitus, obesity, cardiovascular disease, aging-associated frailty and cancer (Bouchard *et al.,* 2015). An increased risk of stroke has also been associated with sedentary behaviour (Lee and Paffenbarger, 1998). Interestingly, MacNeil *et al.*,

(2021) found that older adults who had a history of exercise had lower levels of resting circulating fractalkine, IL-3, IL-6, and TNF-α, compared to older adults with sedentary lifestyles (MacNeil *et al.,* 2021). Environmental influences, including air quality, pollutants, soil quality and urban settings, can all impact aging and longevity in different directions and in association with disease states (Plagg, 2021). An unhealthy lifestyle may contribute to an increase in inflammaging in the older population.

1.3 Immunosenescence and Inflammaging

Aging is associated with susceptibility to low-grade, sterile chronic inflammation, known as "Inflammaging"; a term first coined by (Franceschi *et al.,* 2000). As we age, the immune system undergoes significant change and aging and this is termed "Immunosenescence". These changes were noted as early as 1986, with decreases in T cell responses in elderly with a mean age of 85 years old (Murasko *et al.,* 1986). Later, thymic involution was recorded, whereby the levels of naïve T cells (CD4+ and CD8+) reduce as we age (Qi *et al.,* 2014), and changes in the innate immune response were determined, such as the age-related decrease in the functionality of neutrophils (Fortin *et al.,* 2006). Indeed, the senescence-associated secretory phenotype (SASP) appears induced by IL-1α production and NF-κB activity, leading to increased levels of circulating inflammatory cytokines, TNF-α and IL-8 (Ong *et al.,* 2018). These factors are associated with age-related inflammatory conditions such as osteoarthritis and atherosclerosis (Ong *et al.,* 2018). Circulating mitochondrial DNA is reported to contribute here, by acting as "damage-associated molecular pattern" (DAMP) agents, resulting in elevations of TNF-α and IL-6 (Pinti *et al.,* 2014). Clearing of senescence associated cells (*via* senolytic drugs) may ameliorate inflammaging, by decreasing the release of cell free mitochondrial DNA (cf-mt-DNA) (Iske *et al.,* 2020) and other responses.

Interestingly, specific diets can influence inflammation levels, particularly the Western diet (high salt, lipid and carbohydrates) which is associated with low grade but chronic inflammation, while the Mediterranean diet is anti-inflammatory in nature. The latter is shown to promote anti-inflammatory bacterial species

prevalence in the GI tract of the elderly, determined from faecal samples (van Soest *et al.,* 2020). Indeed, 612 Europeans classified as non-frail or pre-frail individuals were monitored over 12-months following introduction to an elderly tailored, Mediterranean diet. The authors identified microbial taxa that positively correlated with lower frailty and improved cognitive function, altered through dietary intervention (Ghosh *et al.,* 2020). Here, the diet positively influenced inflammation markers (Interleukin-17 and C-reactive protein) and it was noted that, in terms of metabolism, short and branch chained FA production increased while secondary BAs, *p*-Cresols, ethanol and carbon dioxide were reduced. These changes are believed to be a consequence of microbial representation alterations (Ghosh *et al.,* 2020). Interestingly, circulating fractalkine, IL-3, IL-6, and TNF-α, inflammation associated markers were reduced in exercising older adults, relative to matched sedentary individuals (MacNeil *et al.,* 2021).

1.4 Diet and the role of gut microbiota in aging and longevity

Germ-free (GF) animals, born and raised in the absence of microbes, live for longer than their microbial colonized counterparts (Luczynski *et al.,* 2016). Such mice show reduced levels of inflammation, the immune system development and training is impaired and such animals are associated with reduced metabolites to the brain. The influence of the gut microbiota was equated to the level of delayed aging previously associated to exercise (Luczynski *et al.,* 2016). This points to the gut microbiota as influencing the aging process. The gastrointestinal (GI) tract is home to approximately 10^{14} microbes, at a maximum regionally, translating to 100 fold microbial genetic representation over human genetic representation (Luckey, 1972; Gill *et al.,* 2006). The evidence points to regional representation in density and diversity in the GI tract. The representation is specific to the different functionality in each region, to nutrient availability and indeed oxygen levels as well as to regional immune system differences (Frank *et al.,* 2007; Zoetendal *et al.,* 2012). Microbial representation can modulate specific immune functions. Although gut microbial composition is unique for individuals, the gut microbiota converge on their functionality, be it to convert dietary and host produced substances in order to cross

talk to the host, or to aid the host by producing essential vitamins and other factors including co-factors, biogenic amines etc (Joyce and Gahan, 2016). It is now well established that the diet and host factors enrich for different outcomes in health and disease and more recently a link with microbial alterations has been established in the aging process (Badal *et al.,* 2020).

The gut microbiota is unstable in representation from birth until approximately 3 years of age. The subsequent successive colonisations, to reach relative stability, are linked to diet and to feeding milestones, including weaning (Schloss *et al.,* 2012). Changes thereafter, are associated to new diet/s, environment/s, and to insults including exposure to toxins, pathogens and intake of drugs, including antibiotics (Jandhyala *et al.,* 2015) as well as to disease states (Ghosh *et al.,* 2022).

For example, pre-weaning was associated with a higher proportion of bifidobacteria, *Bacteroides* and lactobacilli, in the infant gut, in northern and southern European countries, respectively. Post-weaning was associated with an increased abundance of genus *Bifidobacterium*, *Clostridium coccoides* group and *Bacteroides* (Fallani *et al.,* 2011). In contrast, individuals over the age of 65 appear enriched for *Bacteroides* species while the abundance of species from Faecalibacteria, Proteobacteria and Actinobacteria appears to relate to individual health status (Claesson *et al.,* 2011). More importantly, microbial population changes in the elderly vary according to community variation (residential care, rehabilitation, day-hospital or own residence) and the associated diet. Further influences include degree of exposure to external environments (Claesson *et al.,* 2012). Individuals in long-stay care featured reduced GI microbial diversity, compared to individuals who resided within the community. Interestingly, in a different study, *Bifidobacterium longum* abundance was shown to be inversely correlated with aging (Yatsunenko *et al.,* 2012); members of this genus are normally better represented among infants, pre-weaning (Odamaki *et al.,* 2016). In the same study, individuals over 70 years of age, showed increased relative abundance of Bacteroidetes and Proteobacteria. An Italian study of twenty-four, (105-109 year old) semi-supercentenarians, and fifteen, (22–48 year old) younger adults, reported decreased abundance in Ruminococcaceae, Lachnospiraceae and Bacteroidaceae with increasing age. Specifically, they reported increased *Akkermansia*, *Bifidobacterium*, and *Christensenellaceae* representation among semi-

supercentenarians, again reinforcing the concept of a microbial element to healthy aging (Biagi *et al.,* 2016). Indeed, *Table 1.1* below details human based microbial population investigations in the elderly. It demonstrates good congruency between these independent studies in terms of enrichment and deficits among microbes (Ghosh *et al.*, 2022).

Table 1.1: Summary of recent investigations of gut microbiome alterations in older populations. Adapted from (Ghosh *et al.,* 2022).

Study (cohort size[a])	Country/ region	Molecular technique	Main microbiome alterations in older people
Ruiz-Ruiz et al.[165] (10)	Spain	Proteomics	Tryptophan and indole decreased
Iwauchi et al.[166] (29)	Japan	16S	Pathobionts, *Akkermansia*, Christensenellaceae, *Butyricimonas* increased
Xu et al.[36] (115); Odamaki et al.[37] (77)	Japan[b]	16S	Pathobionts, *Odoribacter*, *Butyricimonas*, Christensenellaceae, *Lactobacillus*, *Oscillospira*, *Oxalobacter*, *Butyrivibrio* increased; core SCFA producers and *Bifidobacterium* decreased
Biagi et al.[38] (54)	Italy[b]	16S	Pathobionts, *Akkermansia*, *Odoribacter*, *Oscillospira*, *Butyricimonas*, Christensenellaceae, Mogibacteriaceae increased; core SCFA producers decreased
Wu et al.[40] (42)	Italy[b]	16S	Pathobionts, *Methanobrevibacter smithii* increased; core SCFA producers decreased
Rampelli et al.[39] (51)	Italy[b]	Shotgun	Core SCFA producers decreased; pathobionts, *Methanobrevibacter smithii*, *Akkermansia muciniphila*, xenobiotic degradation, LPS biosynthesis, phenolic metabolites in serum increased
Wu et al.[40] (46)	Italy[b]	ITS	No significant differences
Collino et al.[167] (233)	Italy[b]	Metabolomics/ HITChip	Para-cresol sulfate and phenylacetic acid increased; butyrate-producing bacteria decreased
Kong et al.[41] (121)	China[b]	16S	Alpha diversity, *Akkermansia* and Christensenellaceae increased
Wang et al.[99] (15)	China[b]	16S	*Akkermansia*, *Parabacteroides*, *Paraprevotella*, pathobionts increased; core SCFA producers decreased
Wang et al.[42] (198)	China	16S	*Butyricimonas*, *Butyricicoccus*, *Odoribacter*, *Alistipes*, *Christensenella*, *Barnesiella*, pathobionts increased; core SCFA producers and *Megamonas* decreased
Bian et al.[100] (284)	China[b]	16S	No significant differences
Zhang et al.[97] (750)	China	Shotgun	Pathobionts, *Lactobacillus salivarius*, *Butyrivibrio crossotus*, *Subdoligranulum variabile*, *Roseburia hominis*, *Coprococcus catus*, *Clostridium sachharolyticum*, *A. muciniphila*, *Victivallis vadensis* increased; *Bifidobacterium* and gender-associated gut microbiome differences decreased
Ke et al.[168] (77)	China	Metabolomics	TMAO increased
Kim et al.[169] (47)	South Korea[b]	16S	Pathobionts, *Akkermansia* and Christensenellaceae increased; core SCFA producers and *Prevotella* decreased
Park et al.[96] (70)	South Korea	16S	*Prevotella copri*, pathobionts, *Roseburia inulinivorans* increased; core SCFA producers, *Megamonas*, *Alistipes*, *Bacteroides uniformis*, *B. vulgatus* decreased
Tuikhar et al.[43] (30)	India[b]	16S	*Akkermansia*, *Butyricimonas*, Ruminococcaceae increased; Prevotellaceae and core SCFA producers decreased
La-Ongkham et al.[95] (47)	Thailand	16S	Pathobionts, *Eubacterium eligens*, *Bacteroides thetaiotamicron*, *B. uniformis*, *B. caccae*, *B. ovatus*, *Parabacteroides distasonis* increased; other core SCFA producers decreased
Rahayu et al.[98] (40)	Indonesia	qPCR	Pathobionts, *Bifidobacterium* decreased; multiple *Lactobacilli* increased
Kashtanova et al.[44] (42)	Russia[b]	16S	*Lactobacillus*, *Roseburia*, *Christensenella* increased; *Dorea*, *Dialister*, *Ruminococcus* decreased
Huang et al.[170]; Cuesta-Zuluaga et al.[101]	Multiple (meta-analysis)	16S	Core gut microbiome members decreased
Galkin et al.[171]	Multiple (meta-analysis)	Shotgun	Pathobionts and *Bifidobacterium bifidum* increased
Wilmanski et al.[103]	United States	16S	Increased gut microbiome uniqueness (or dissimilarity) and decreased *Bacteroides* associated with ageing; faster shift towards uniqueness in healthy ageing cohort

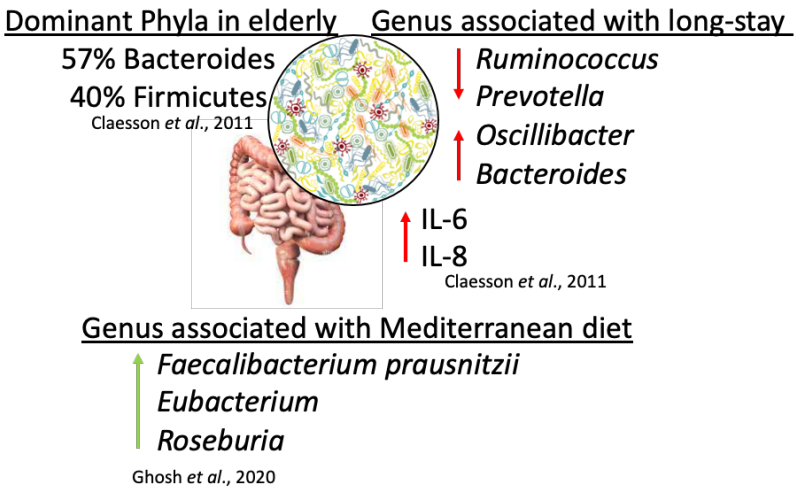


Figure 1.2: **The dominant microbial taxa of the elderly.** Genera associated with increased inflammation and frailty in individuals in long-term residential care are indicated (in red) as increased or decreased (Claesson *et al.,* 2012). Bacterial genera associated with Mediterranean diet which mediated improved cognitive function, decreased inflammation and frailty, are indicated (by the green arrow). Adapted from (Ghosh *et al.,* 2020).

1.4.1 Bacterial metabolism of Bile acids (BAs)

While changes to microbial populations are evident through the different life stages including aging, it is microbial metabolites that are an indicator of actual microbial functionality. The functionally commonly featured microbial and microbially derived metabolites include the amino acid tryptophan and its derivatives, short chain fatty acids (SCFA) and also bile acids (BAs). In this thesis the latter feature in our investigations as a readout of both microbial functions and also as an indicator of interkingdom signalling molecules. The exact roles are discussed below.

BAs are derived from cholesterol in liver hepatocytes by cytochrome P450 enzymes through either the classical pathway, where CYP7A1 (cholesterol 7α-hydroxylase, a cytochrome monooxygenase enzyme) is the rate limiting step regulating the classical BA synthesis pathway, leading to cholic acid (CA) (Li-Hawkins *et al.,* 2000; Norlin *et al.,* 2000). CYP8B1 catalyses 12α-hydroxylation to produce the primary BA cholic acid (CA) (Gåfvels *et al.,* 1999), alternatively, CYP27A1 and CYP7B1 catalyse the conversion to the primary BA chenodeoxycholic acid (CDCA) (Pikuleva *et al.,* 1998)

(*Figure 1.3* below). The less common, mitochondrial-based, alternative BA synthesis pathway only produces CDCA and can occur in all cells. Interestingly, they are both regulated by alternate BA sensing receptors; the farnesoid X receptor (FXR) and Tanaka G protein coupled (TGR5 or GBAR1) receptors. Once produced, BAs are conjugated to the amino acids glycine or taurine to render them soluble for transport to the gall bladder by enzymes BA cholyl-CoA synthetase (BAC) and bile acid-CoA:amino acid N-acyltransferase (BAT) (O'Byrne *et al.,* 2003). They are then postprandially released into the small intestine to aid nutrient and lipid digestion and absorption.

Interestingly, amino acid conjugation ratio differs between organisms, mainly due to diet. For example, glycine conjugates are generally at a 3:1 higher ratio than taurine conjugates in humans and rats, but these conjugates represent <5% in mice (Honda *et al.,* 2020). 95% of secreted BAs are reabsorbed at the terminal ileum and transported back to the liver through enterohepatic circulation while faecal BAs represent the non recycled 5% of total BAs. This cycle repeats itself several times per day and it represents the only mechanism by which cholesterol is released from the body, by humans.

Microbes are equipped to deal with potential toxic effects of soluble BAs (Gopal-Srivastava and Hylemon, 1988). The majority of microbial representatives in the gut carry microbial bile salt hydrolase (BSH) enzymes that hydrolyse or cleave the amide bond from amino conjugated BAs, freeing both amino acids and the BAs in the process. Deconjugated BAs, are now susceptible to further modifications by gut resident bacteria to produce a palate of other BA moieties (Ridlon and Hylemon, 2012). Modifications are through the removal or addition of oxygen and hydroxyl groups, or through epimerization events. Microbes can carry hydroxysteroid dehydrogenases (HSDHs), or the well characterized *bai* operon (restricted to a small number of *Clostridia* species), to mediate these processes and modifications (Long *et al.,* 2017; Heinken *et al.,* 2019).

These modifications, and the resultant BA moiety palate, can impact a number of functions including metabolism, lipid dystrophy, inflammation and indeed circadian rhythm (Joyce *et al.,* 2014; Govindarajan *et al.,* 2016). They also mediate other signalling effects at the cellular level (Degirolamo *et al.,* 2014). Therefore, BAs can be

classified and considered as hormones, to influence processes locally and systemically. Indeed, the diversity of BAs is considered a readout of health and it appears to converge with the microbiota and only under conditions of disease (reviewed by Long *et al.,* 2017).

The nature of the microbial modifications can change the solubility of each moiety so that they can elicit individual and collective effects. Hydrophobic BA, DCA (made from CA) has been associated with negative effects on gut cells, including promoting colonic inflammation and cancer cell development at high levels (Hofmann *et al.,* 1987). However, similarly hydrophobic BA, LCA (from CDCA or UDCA) is associated with promoting apoptotic responses, cell proliferation and indeed Vitamin D receptor activation, all beneficial in the context of the gut (Prete *et al.,* 2020). Interestingly, LCA has been shown to extend lifespan in *Saccharomyces cerevisiae* (yeast) and in *Drosophila melanogaster* (fruit flies) (Goldberg *et al.,* 2010; Staats *et al.,* 2018). A very hydrophilic BA, UDCA, interconvertible to LCA through microbial action, is associated with beneficial effects. It can activate the Akt-dependent survival signalling pathway, to protect cells from DCA-induced apoptosis (Im *et al.,* 2005). In mice, UDCA has been reported to reduce age-associated inflammation and adiposity (Oh *et al.,* 2016). It therefore appears that the microbially produced palate of BAs can influence events at the cellular level to impact health or disease status including cellular health and possibly aging.

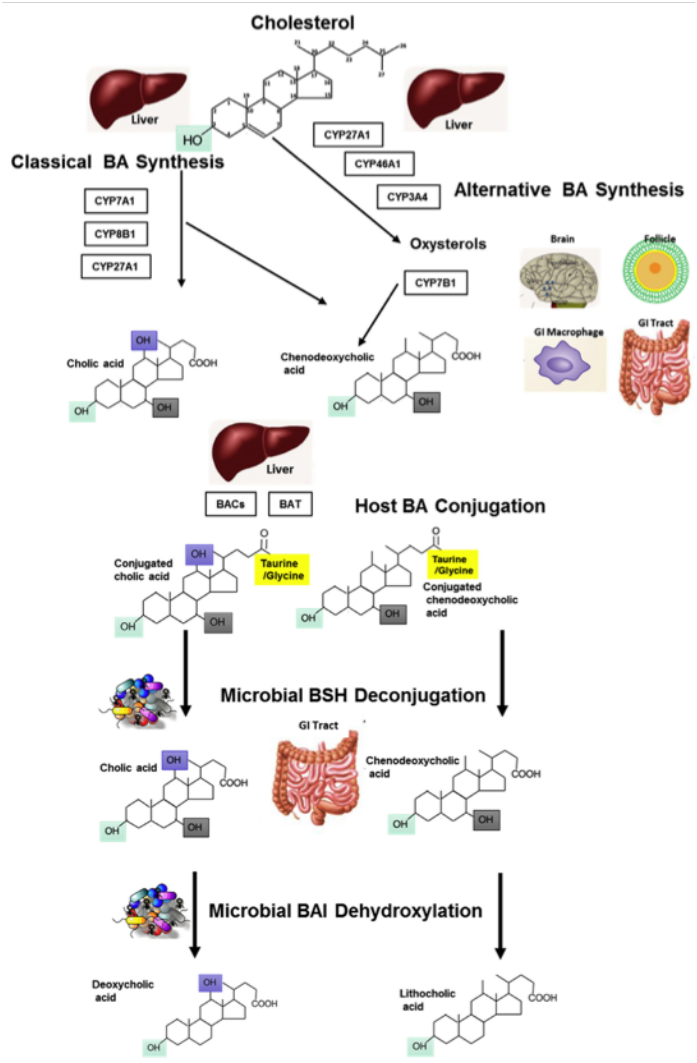


Figure 1.3: **The liver produces bile acids (BAs), however gut microbes are responsible for BA diversity.** Adapted from (Long *et al.,* 2017). BAs are synthesized by cholesterol in the liver by host Cytochrome P450 enzymes (boxed) through the classical and alternative pathways. In the liver, BAs are conjugated to amino acids by the enzymes BA cholyl-CoA synthetase (BAC) and bile acid-CoA:amino acid N-acyltransferase (BAT). Microbial bile salt hydrolase (BSH) enzymes in the gut cleave the amide bond from amino conjugated BAs, freeing BAs for further modifications by gut resident bacteria to produce a palate of other BA moieties, including secondary BA from microbial bile acid-inducible (bai) operon.

1.4.1.1 Farnesoid X Receptor (FXR) signalling

As mentioned above, microbes and their gut representation can produce a palate of different BAs to impact local and systemic signalling. One very important receptor responsive to BAs is the Farnesoid X Receptor (FXR). Indeed, microbially released CDCA is the most potent FXR BA agonist, followed by DCA, CA, αMCA and βMCA whereas UDCA, GUDCA, TUDCA and TMCA behave as FXR antagonists (Chiang, 2013) (*Figure 1.4*). FXR regulates BA homeostasis by inducing fibroblast growth factor 15 (FGF15/19) expression, in mice/human small intestine. FGF15/19 feeds back to the liver to inhibit BA synthesis through a number of strands including *Cyp7a1* directly, and indirectly through FGF receptor 4 (FGFR4) and small heterodimer protein (SHP) (Inagaki *et al.,* 2005). FXR is a major metabolism regulator for glucose, triglyceride, cholesterol metabolism (Sinal *et al.,* 2000; Duran-Sandoval *et al.,* 2004; Zhang *et al.,* 2006) (*Figure 1.4*). FXR targets *MafG* (Musculoaponeurotic Fibrosarcoma Oncogene Homolog G) to also regulate BA synthesis. *MafG* can suppress *Cyp8B1* and weakly suppress *Cyp7B1* (de Aguiar Vallim *et al.,* 2015). FXR modulates inflammatory responses, through NF-κB and IL-1β, and also through MYD88 (Duparc *et al.,* 2017). FXR has been reported to have an anti-inflammatory response, *fxr* inhibits NF-κB through IL-1β, demonstrating that the FXR-SHP pathway may be involved in reducing atherosclerosis progression through decreasing vascular inflammation (Li *et al.,* 2007). FXR is an antagonist of NF-κB-induced hepatic inflammation but maintains NF-κB-stimulation of antiapoptotic genes (Wang *et al.,* 2008). FXR has recently been reported to have a role in fatty acid β-oxidation regulation (Lu *et al.,* 2022). It also mediates transporter functions within the gut and the liver, including those responsible for drug uptake. This receptor is central to many layers of regulation, from different metabolites and from phosphorylation events on serines and threonines to increase or decrease its activity, hence in many studies the protein is not altered in level but in its activity. Indeed, the FXR cross talks with other BA receptors to maintain gut and liver homeostasis. Some of these are discussed below.

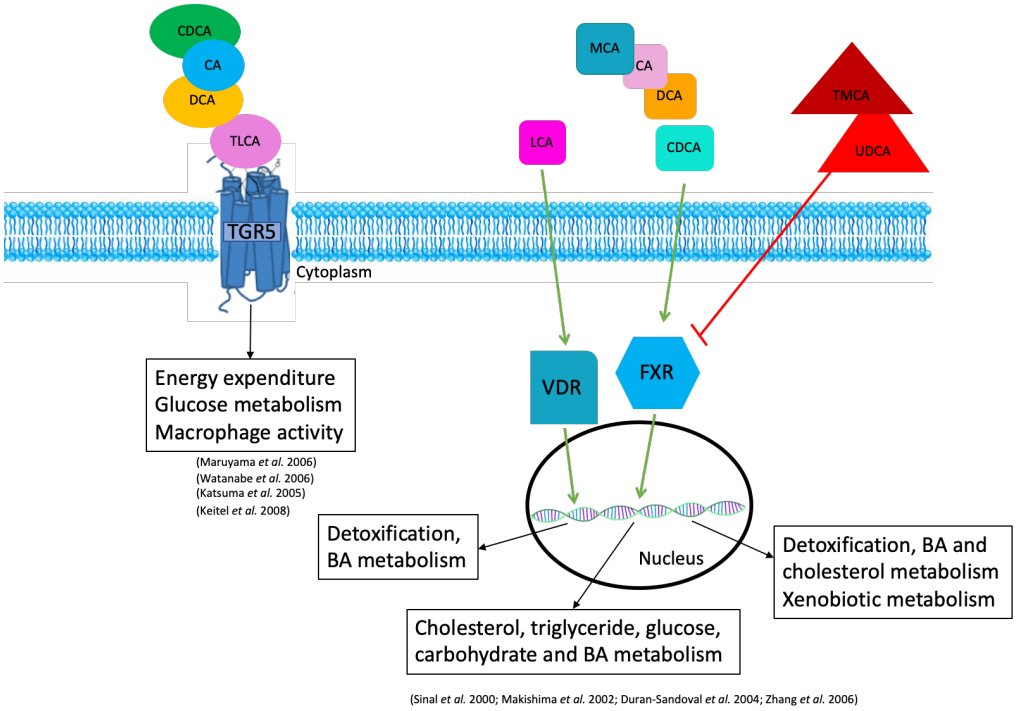


Figure 1.4: **Different BAs can act as molecules for nuclear receptor, and G protein-coupled receptor, signalling.** BA agonists are shown for GPCR TGR5 and NR VDR as well as downstream biological processes, discussed below. BA agonists, CDCA, DCA, CA and MCA, and antagonists, UDCA and TMCA are shown for NR FXR, in addition to downstream biological processes, as discussed above.

1.4.1.2 The G protein-coupled receptor TGR5, a bile acid signalling receptor

It is clear that BAs feed into a range of different signalling receptors involved in metabolism and in immune functions (see *Figure 1.4* above). This suggests that microbial representation and their enzymes can alter all of these processes in different directions, where there is change in diversity and in representation. Microbially derived BA taurolithocholic acid (TLCA) is the most potent activator of a G-protein coupled receptor TGR5. TGR5 can also be activated, in decreasing potency, by LCA, DCA, CDCA and CA (Kawamata *et al.,* 2003) (*Figure 1.4*).

TGR5, expressed in the ileum and the colon and in macrophages, stimulates intracellular cAMP and protein kinase A activation to alter gene expression through second messangers (Maruyama *et al.,* 2002; Kawamata *et al.,* 2003). It influences BA metabolism, in *Tgr5* disrupted mice total BA levels were decreased by 21–25% (Maruyama *et al.,* 2006). TGR5 has a critical role in energy status, through thyroxine

production (thyroid hormone), through browning of white adipose tissue (WAT) and through induction of gut hormones and gut mobility (*Figure 1.4*), (Katsuma *et al.,* 2005). TGR5 has been shown to regulate immune responses (Kawamata *et al.,* 2003; Ichikawa *et al.,* 2012). TGR5 has a role in energy expenditure and glucose metabolism, BA–TGR5–cAMP–D2 signalling pathway is involved in energy expenditure and insulin resistance (Watanabe *et al.,* 2006). In Kupffer cells, LPS-induced cytokine stimulation is through a TGR5-cAMP dependent pathway. TGR5 may play a role in reducing liver injury by preventing overstimulation of cytokine production (Keitel *et al.,* 2008). More recently, increased levels of pro-inflammatory factors and M1 macrophage polarization, through stimulation of NLRP3 inflammasome and caspase-1 cleavage, were reported in *Tgr5*-knockout mice, suggesting that TGR5 may have a role in the regulation of the innate immune response (Shi *et al.,* 2020) (*Figure 1.4*).

1.4.1.3 Other bile acid mediated receptor signalling

A number of different nuclear receptors are responsive to BAs, particularly those BAs produced by microbes. For instance, Vitamin D receptor (VDR), is widely expressed in most tissues and can be activated by microbially produced LCA (Makishima *et al.,* 2002) (*Figure 1.4*). Its main roles include detoxification processes and at the level of the gut and the liver, it is responsible for sulphation effects (Han *et al.,* 2010). The VDR regulates CYP3A4 expression, to result in detox of the liver and of intestinal LCA, labelling it for excretion (Makishima *et al.,* 2002). Hence, VDR is believed to protect the liver from cholestatic injury, VDR also loops with the FXR to regulate BA synthesis in hepatocytes.

LCA is the most potent activator of pregnane X receptor (PXR) or steroid and xenobiotic receptor (SXR) both influence BA metabolism and detoxification (Xie *et al.,* 2001). PXR represses CYP7A1 activity, regulating BA metabolism (Ståhlberg, 1995). PXR also regulates cholesterol homeostasis and atherosclerosis. In wild type mice, PXR induces hypercholesterolemia, and apolipoprotein E deficient ($ApoE^{-/-}$) deficient mice, stimulates progression of atherosclerosis (Zhou *et al.,* 2009).

Constitutive androstane receptor (CAR) also functions to detoxify and metabolise BAs (Guo *et al.,* 2003; Miao *et al.,* 2006). BAs, LCA and CDCA are reported to bind and

activate CAR. In hepatocytes (Moore *et al.,* 2002), CAR regulates BA metabolism by *Cyp7a1* inhibition, and regulates lipid and glucose metabolism through HNF-4 inhibition (Miao *et al.,* 2006). It can also substitute in the absence of FXR induced Shp (small heterodimeric protein) to regulate BA metabolism in the liver. The CAR protects against BA toxicity (Guo *et al.,* 2003) and its agonist 1,4-bis[2-(3,5 dichloropyridyloxy)] benzene (TCPOBOP) could improve insulin sensitivity in a high fat diet (HFD)-induced obesity mouse model, through lipid-lowering effects (Gao *et al.,* 2009). Hence, its activation may prove central to obesity and non-alcoholic liver disease treatments and therapies.

Liver X receptor (LXR), specifically LXRα and LXRβ, are activated by oxysterols 24(S),25-epoxycholesterol and 24(S)-hydroxycholesterol, the precursors for CDCA alternative pathway in the mitochondrion. LXR has an essential role in cholesterol homeostasis (Lehmann *et al.,* 1997). Reportedly, LXR can influence fatty acid metabolism and its regulation (Repa *et al.,* 2000; Horton *et al.,* 2002). *In vitro* glucose uptake in 3T3-L1 adipocytes was also stimulated by LXR activation, suggesting a role for LXR in energy and in glucose metabolism (Laffitte *et al.,* 2003).

1.4.2 Fatty acids are dietary derived and microbially produced, as well as cellularly synthesised.

While BAs are central to metabolism directly and indirectly, other microbial indicators of metabolism and health include fatty acids (FAs). They can be obtained from the diet as well as synthesized *de novo* within the cell. Bacteria can contribute to their compliment by producing FAs from non-digestible fibres (Joyce *et al.,* 2019). FAs are simply a molecule of glycerol to which hydrocarbon chains are added. The size of the carbon chain and position/s of saturation all dictate the type of FA and its potential to signal and to influence inflammation (Calder, 2011). Short-chain FAs (SCFAs; 2-5 carbons), are easily absorbed in the small intestine, they include acetic, propionic, butyric, and valeric acids, they produce energy through their oxidation in the mitochondrion (Schönfeld and Wojtczak, 2016). They are also signalling molecules with central roles in glucose and lipid metabolism and in regulating inflammation processes (He *et al.,* 2020). SCFAs act either directly or through

receptor modulation. Indeed, lactic acid, a product of anaerobic respiration, is a well recognised cell re-programmer, altering local pH and conditions (Garrigues *et al.,* 2001).

Medium-chain FAs (MCFA, 6-12 carbons) hexanoic, heptanoic and octanoic acids are escorted into cells for processing with SCFA at the level of the mitochondrion (Schönfeld and Wojtczak, 2016). Long-chain FAs (LCFA, 14-21 carbons) include myristic, palmitoleic, palmitic, α/βlinolenic, linoleic, oleic acid, stearic, eicosapentaenoic (EPA), arachidonic acid (AA), Cis-11-eicosenoic acids (EA). They are processed in the lysosome and peroxisome, where they are broken down to MCFA or SCFA. The situation is similar for Very-long-chain FAs (VLCFA, 22 carbons) such as docosahexaenoic acid (DHA). Interestingly AA, EPA and DHA have direct and opposing roles to modulate inflammation levels and to induce prostaglandin, thromboxane and leukotrene functions (Calder, 2011). Polyunsaturated FAs (PUFA) have multiple carbon-carbon double bonds and include α/βlinolenic acid and linoleic. These precursors for EPA, AA and DHA are essential FAs (Das, 2006) and they represent monounsaturated and omega-3 or omega-6 FAs.

Linoleic acid can stimulate monocyte differentiation towards inflammation-associated macrophages, by altering CCR2 and CX3CR1 expression (Barlic *et al.,* 2006) to impact cardiovascular disease progression (Barlic *et al.,* 2006). Palmitoleic acid prevents bacterial LPS-induced neutrophil migration and secretion of TNF-α, IL-1β, IL-6, MIP-3α and I-selectin, and regulates CINC-2α/β and VEGF-α, at the wound site and is anti-inflammatory (Weimann *et al.,* 2018). In white adipocytes, palmitoleic acid increases energy expenditure, oxygen consumption, lipolysis, FA esterification and mitochondrial FA oxidation (Cruz *et al.,* 2018). In contrast, palmitic acid can contribute to chronic inflammation by inducing IL-6 production (Staiger *et al.,* 2004) by stimulating other proinflammatory cytokines (Håversen *et al.,* 2009). It can also stimulate macrophages/kupffer cells which can result in disrupted insulin signalling, and elevated total eicosanoids.

AA can undergo cellular metabolism via three different enzymatic pathways: cyclooxygenases (COXs), lipoxygenases (LOXs), and cytochrome P450 (CYP) enzymes (ω-hydroxylases and epoxygenases). These three pathways generate many FA regulators, including prostanoids, leukotrienes (LTs), epoxyeicosatrienoic acids

(EETs), dihydroxyeicosatetraenoic acid (diHETEs), eicosatetraenoic acids (ETEs), and lipoxins (LXs), which have central roles in inflammation and allergenic responses as well as blood clotting and pressure maintenance to influence cardiovascular diseases (CVD), cancers and inflammatory diseases (Wang *et al.,* 2021). DHA and EPA reduce proinflammatory cytokine in circulation (Tan *et al.,* 2018) and help prevent muscle atrophy (Yamaguchi *et al.,* 2021). The influences of FAs on host tissues, cells and organelles are summarized in *Figure 1.5* below.

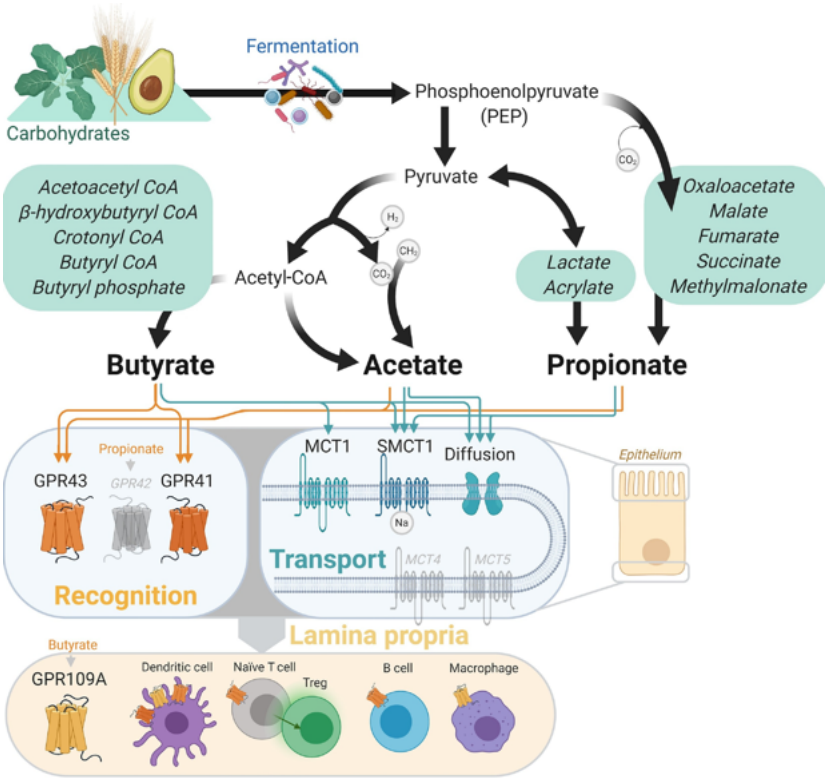


Figure 1.5: **Fatty acids from the diet influence processes locally in the gut and systemically.** Dietary and microbial derived FAs can enter the cells and alter signalling and immune functions in different directions. Adapted from (van der Hee and Wells, 2021).

1.5 The Gut Microbiota and Disease

Hippocrates said that "all disease begins in the gut". Disease, originating from the gut, can result as a function of diet, of metabolites derived from it, and from microbial representation and alterations to both. Some of these are mentioned above (BAs, FAs, amino acid derivatives). Indeed, it is now widely accepted that specific gut microbial communities can have a significant impact on host health, as discussed above. Alterations to gut microbe representation (microbial diversity) and hence their functions, can result in conditions described as gut dysbiosis, an umbrella term. Changes in microbial populations are evident in different diseases including Crohn's disease (CD) (Lennard-Jones, 1989), autism spectrum disorder (ASD) (Mortera *et al.,* 2022) and Parkinson's disease (PD) (Nishiwaki *et al.,* 2020). Perhaps the best representations of Hippocrates statement and a clear role for gut microbial diversity in such processes comes from evidence provided from faecal microbial transplants (FMTs). In the 4th century, a Chinese medicine doctor, Ge Hong, used human faecal suspension to treat severe food poisoning and diarrhea. FMT of rich and diverse pools of microbes (and their metabolites) from healthy donors has been used to treat infections including *Pseudomembranous enterocolitis* (Eiseman *et al.,* 1958; Collins, 1960) and life-threatening *Clostridium difficile* (Schwan *et al.,* 1983) infection. FMT has shown potential to improve each of CD (Fehily *et al.,* 2021), ASD (Li *et al.,* 2021) and PD (Kuai *et al.,* 2021) symptoms.

1.5.1 Crohn's Disease

Crohn's disease (CD) is an inflammatory bowel disease (IBD) resulting from a combination of genetic, environmental, microbial and metabolite factors to create a perfect storm to favour inflammation and damage. A Western world condition, the prevalence of IBD is increasing possibly due to excessive hygiene, leading to a less rich, diverse microbiome, or to the Western diets and its associated enrichments including pathobionts. Diversity of the faecal and mucosal microbiome has been reported to be reduced in CD, and is associated with an increased representation of adherent-invasive *Escherichia coli* (AIEC) species (Giaffer *et al.,* 1992). AIECs are believed to alter inflammation responses in CD, including Interferon γ (IFNγ) levels in

the gut lamina propria (Fais *et al.,* 1991), increasing levels of cytokine IL-12 and T helper type 1 (Th1) cells (Monteleone *et al.,* 1997; Parronchi *et al.,* 1997). Two AIEC strains are of particular interest to us. LF82 is an AIEC that is capable of invading and replicating within epithelial and macrophage cells (Boudeau *et al.,* 1999). Two *fim* mutants were found to allow LF82 to adhere, but prevented host cell membrane elongations. This data showed that type 1 pili are involved in the invasive process of LF82 (Boudeau *et al.,* 2001). Another AIEC strain, HM605 was isolated and sequenced from CD patient colonic biopsy specimen (Clarke *et al.,* 2011) and we have applied it in our studies (Chapter 5) later. Interestingly, a recent study discusses AIEC strains' ability to reduce *Caenorhabditis elegans'* (*C. elegans')* lifespan and the correlation with their virulence levels, indicating that pathogenicity varies between AIEC strains (de Sousa Figueiredo *et al.,* 2021). The connection here, is that persistent pathogens, their metabolites and chronic inflammation can influence the healthy aging process. Other bacterial species are correlated with CD, based on their ability to regulate host gut immune response. *Lactobacillus* spp. are shown to stimulate dendritic cells and may have the potential to inhibit effects induced by other species in the genus (Christensen *et al.,* 2002). Phylum Bacteroidetes and Fusobacteria have been reported as abundant in inflamed CD mucosa (Forbes *et al.,* 2016). *Bacteroides fragilis* polysaccharide (PSA) mediates immune system development by stimulating $CD4^+$ T cells and regulating cytokine production. PSA manages T cell insufficiencies and T_H1/T_H2 imbalances, and controls lymphoid organogenesis (Mazmanian *et al.,* 2005). The gut microbiota can mediates IL-17-producing T-helper cells: $Foxp3^+$ regulatory T cells balance in the lamina propria of the small intestine, regulating immunity and risk of IBD (Ivanov *et al.,* 2008). There is currently no known cure for CD and so the disease is managed by a combination of immune-suppressing medications, including methotrexate or anti-TNF therapy, along with dietary changes and in severe cases surgery.

1.5.2 Gut-brain axis in disease

It is becoming more and more apparent that there is bidirectional communication along what has become accepted as the 'gut–brain axis'. Gut microbes can influence the brain through a number of factors including: FAs, amino acids, peptidoglycans

and tryptophan metabolism; immunological; and neurochemical, such as the vagus nerve and enteric nervous system (Cryan *et al.,* 2019). The gut microbiota can influence the blood-brain barrier. In mice, butyrate-producing *C. tyrobutyricum*, and acetate- and propionate-producing *B. thetaiotaomicron* have been shown to decrease blood-brain barrier permeability (Braniste *et al.,* 2014).

Further evidence for a gut-brain role comes from antibiotic-induced depletion of the gut microbiota. Such treatment in rats was associated with a reduction in spatial memory and reduced visceral sensitivity as well as depressive-like behaviours (Hoban *et al.,* 2016). Biochemically, central nervous system (CNS) serotonin levels, glucocorticoid receptor and corticotrophin releasing hormone receptor 1 mRNA levels, as well as levels of brain derived neurotrophic factor (BDNF) were altered here (Hoban *et al.,* 2017). Indeed, microbial community changes are associated with neurological disorders, autism spectrum disorder (ASD), and neurodegenerative diseases, such as Parkinson's disease (PD). Gut microbiota have been shown to mediate microglia maturation and function in germ-free (GF) mice compared to mice with altered Schaedler flora (Erny *et al.,* 2015), especially in the context of disease, such as PD, indeed, when α-syn-overexpressing mice where orally administered microbiota from PD-affected patients, their physical impairments worsened, compared to those administered microbiota from healthy control individuals, via SCFA signalling and microglia activation (Sampson *et al.,* 2016). Microglia properties are reportedly changed, resulting in defective microglia, in GF mice (Erny *et al.,* 2015). They showed that microglia function was partly restored upon re-colonisation with microbes, including an increase in the presence of SCFAs and microbiota-derived bacterial fermentation products (Erny *et al.,* 2015). SCFAs such as propionate have been shown to act through a CD14-dependent mechanism, to suppress LRP-1 expression and protect the blood brain barrier, through NRF2 (NFE2L2) signalling, from oxidative stress (Hoyles *et al.,* 2018). Interestingly, unconjugated BAs, CA, CDCA and DCA, have been found in brain tissue of rats (Higashi *et al.,* 2017), demonstrating the bidirectional communication of the 'gut–brain axis' and potential impact of microbial derived metabolites on neurological diseases. Human gut microbiota from ASD and PD individuals, transplanted into GF mice demonstrate induction of hallmark

autistic behaviours, and enhanced motor dysfunction, respectively (Sampson *et al.,* 2016; Sharon *et al.,* 2019).

1.5.2.1 Autism Spectrum Disorder

Microbial metabolites and alterations are also associated with Autism spectrum disorder (ASD), a neurodevelopmental disorder which is characterised by social and communication impairments, limited interests and repetitive behaviours (Morgan *et al.,* 2019). ASD has been associated with gastrointestinal abnormalities (Madra *et al.,* 2021). Studies have shown that treatment of offspring, from maternal immune activation (MIA) mouse model, with *Bacteroides fragilis* alters microbial composition, reducing gut permeability and ASD behavioural symptoms, including anxiety-like, stereotypic, communicative and sensorimotor behaviours (Hsiao *et al.,* 2013).

It has been reported that the immune system has a role in ASD. Interestingly, activation of the maternal immune system, such as exposure to viral infection, during pregnancy has been correlated with an increased incidence of ASD in offspring. Studies in mice found that elevation of cytokine interleukin-17a (IL-17a) (Choi *et al.,* 2016) and interleukin-6 (IL-6) (Smith *et al.,* 2007) in the mother may contribute to an abnormal cortical phenotype, mediating transcription and behavioural changes in offspring. Similar studies showed that treatment of offspring, from maternal immune activation (MIA) mouse model, with *Bacteroides fragilis* alters microbial composition, reducing gut permeability and improving ASD behavioural symptoms, including anxiety-like, stereotypic, communicative and sensorimotor behaviours (Hsiao *et al.,* 2013).

Interestingly, the gut microbiome can alter immune response and cognitive function in ASD. *Clostridium* positively correlates with ASD GI symptoms, and with the inflammatory marker, calprotectin (Tomova *et al.,* 2020). Indeed, 3-(3-hydroxy phenyl)-3-hydroxypropionic acid (HPHPA), a metabolic product of the genus *Clostridium*, was found in high concentrations in urine samples from children with autism (Keşli *et al.,* 2014). HPHPA is a metabolite of m-tyrosine (3-hydroxyphenylalanine), which can deplete brain catecholamines causing symptoms of autism behaviour. *Clostridium* species can also induce excess dopamine and reduce norepinephrine, through production of dopamine-beta-hydroxylase

inhibitors, leading to neurotransmitter deficiencies (Shaw, 2010). It has been proposed that ASD behavioural symptoms may result from a dysfunctional midbrain dopaminergic system. It has been speculated that malfunction of mesocorticolimbic and nigrostriatal pathways are contributing to the behavioural characteristics of ASD (Pavăl and Micluția, 2021). It has been demonstrated that β-arrestin2, an arrestin family scaffolding protein, can regulate the dopaminergic system, via the ERK signalling pathway, as overstimulation of dopaminergic receptors can induce ASD-like behaviours in mice (Zhou *et al.,* 2022). Indeed, mice treated with ***p***-Cresol demonstrated ASD-like social behaviour, which was induced by a reduction in the stimulation of central dopamine neurons, as well as exhibiting changes in microbial composition (Bermudez-Martin *et al.,* 2021). In Slovakia, it was reported in children with ASD, a decrease in the ratio of *Bacteroidetes* to *Firmicutes* and an increase in *Lactobacillus* spp. (Tomova *et al.,* 2015). A decrease in the relative abundance of *Bacteroidetes* has led to an increase in the ratio of *Firmicutes* to *Bacteroidetes* in ASD individuals. An abundance of *Lactobacillus* was also reported (Strati *et al.,* 2017). An increase in abundance of Bacteroidetes and Proteobacteria and reduction in abundance of Actinobacteria was reported in 2-4 year old children with ASD (Coretti *et al.,* 2018). *Bifidobacterium longum* abundance was decreased and the abundance of *Faecalibacterium prausnitzii*, a producer of butyrate, was increased (Coretti *et al.,* 2018). *Aerococcus*, *Burkholderia*, *Desulfohalobium*, *Desulfovibrio*, *Oxalobacter*, *Pseudocitrobacter* and *Youngiibacter* are abundant in children with ASD (Tomova *et al.,* 2020). Genera *Constrictibacter*, *Nitriliruptor* and *Dichelobacter* were found abundant in children with ASD. *Youngiibacter*, member of the Clostridiaceae family, and *Nitriliruptor,* member of Actinobacteria family, positively correlated with social interaction. *Youngiibacter* also positively correlated with repetitive score of ADI-R (Autism Diagnostic Interview-Revised) (Tomova *et al.,* 2020). *Oxalobacter* and *Desulfohalobium* correlated with GI score. The positive correlation between S100B, Ca^{2+} binding protein, with communication subscale of ADI-R, shows a potential role in children with ASD (Tomova *et al.,* 2020). Indeed, ASD children have a higher abundance of beta2-toxin gene-producing *C. perfringens* in their gut (Finegold *et al.,* 2017). In a separate study, the *Cpa* and *Cpb2* toxin genes were identified in all *C. perfringens* isolates of ASD (Alshammari *et al.,* 2020). *Cpb2* was associated with gut

dysbiosis, which may have more implications in disease severity (Alshammari *et al.,* 2020).

Children with ASD are also reported to have alterations in levels of oxidative stress, mitochondrial dysfunction, hormone level elevations, lipid profile changes and altered levels of phenolic microbial metabolites, contributing to changes in amino acid, lipid and xenobiotic metabolism, compared to typically developing control individuals (Needham *et al.,* 2021). Faecal samples from children with ASD revealed alterations in glutamate metabolites (Wang *et al.,* 2019). A decrease in 2-keto-glutaramic acid levels in the gut, lower cortisol levels, lower abundance of *Bacteroides vulgatus* and higher abundance of *Eggerthella lenta* and *Clostridium botulinum* were associated with children with ASD (Wang *et al.,* 2019). Taurocholic acid and Chenodeoxycholic acid 3-sulfate were reported to be higher in faecal samples from children with ASD, compared to typical development age-matched volunteers (Wang *et al.,* 2019). It was also determined that those metabolites, including 2-keto-glutaramic acid, L-aspartic acid, and fumaric acid, found to be lower in children with ASD, compared to typical development controls, were associated with altered neurotransmitter metabolism, namely alanine, aspartate, and glutamate metabolism (Wang *et al.,* 2019). Interestingly, glycosphingolipid and lipid related BA pathways were found to be elevated in serum of mothers of children with ASD, compared to population age- and birth-matched controls (Ritz *et al.,* 2020). Alterations in the tricarboxylic acid (TCA) cycle and mitochondrial function, including carnitine shuttle, amino acid, BA, and vitamin A metabolism, aspartate and asparagine metabolism, propanoate metabolism, galactose metabolism, pyruvate metabolism, pentose phosphate pathway, and beta-alanine metabolism, have been associated with ASD (Kim *et al.,* 2021). Specifically, alterations in the leukotriene pathway, metabolism of FAs, metabolism and activation of butanoate, fructose and mannose, and glycolysis and gluconeogenesis were found in serum samples from mothers of children with ASD (Kim *et al.,* 2021). 7α-Hydroxy-3-ox-o-4-cholestenoate (7α–OH–4-CA) was found to be elevated, whereas 7α,25-dihydroxy-4-cholesten-3-one, and 5 β-cholestane-3 α,7α,12α, 27, 27-pentaol were reduced in serum from mothers of children with ASD, compared to controls (Kim *et al.,* 2021). 7α-OHC and 25-OHC have been previously reported to be reduced, and 24-hydroxycholesterol

has been previously reported to be negatively associated with age, in children with ASD compared to healthy controls (Grayaa *et al.,* 2018). Studies investigating ASD, using the maternal immune activation (MIA) C57BL/6 J mice model and controls, revealed elevations in lactate, citrate, urea, purines, dopamine, eicosanoids, microbiome metabolites, oxidized glutathione, niacinamide, thiamine, and pyridoxic acid, and reduced, cholesterol, BAs, vitamin D, amino acids, phospholipids, ceramides, sphingomyelins, short and medium chain acyl-carnitines, and folate-methylation-1-carbon intermediates, as seen in some children with ASD (Zolkipli-Cunningham *et al.,* 2021). Specifically, BAs glycocholic acid, taurocholic acid and taurodeoxycholic acid were decreased in maternal immune activation (MIA) C57BL/6 J mice model, compared to controls (Zolkipli-Cunningham *et al.,* 2021). Similarly, in faecal samples of children with ASD, there were alterations in amino acid, lipid, and xenobiotic metabolism compared to typical development controls, interestingly in the plasma, PUFA and short-chain acylcarnitine levels were increased and saturated FAs and long-chain acylcarnitines were decreased in children with ASD, compared to typical development controls (Needham *et al.,* 2021). Interestingly, hypotaurine and taurine were found at high levels in faecal, but lower levels in the ASD plasma samples. Deficiencies of hypotaurine and taurine can result in cell differentiation defects in the brain, and ultimately neuronal signalling dysregulation (Needham *et al.,* 2021). Indeed, transplantation of human-derived ASD microbiota is sufficient to induce ASD behaviours in germ-free mice. Interestingly, treatment with 5-aminovaleric acid (5AV), a weak GABAA receptor agonist, and taurine, which can act as an inhibitory neuromodulator in the brain, improved social and repetitive behaviours in the BTBR mouse model of ASD (Sharon *et al.,* 2019). *L. rhamnosus* (*JB-1*) induces $GABA_{B1b}$ alterations in mouse brain that are region specific, including decreasing expression in the prefrontal cortex and amygdala and increasing expression in the hippocampus (Bravo *et al.,* 2011). Anxiety- and depression-related behaviour and stress-induced corticosterone were decreased in *L. rhamnosus* (*JB-1*) treated mice while it was found that these effects were mediated by the vagus nerve (Bravo *et al.,* 2011). Children with ASD were reported to have a decrease in abundance of Bacteroidetes and increased abundance of Betaproteobacteria and in the ratio of Firmicutes to Bacteroidetes. The levels of expression of disaccharidases

and transporters were in agreement with these bacterial phylotypes (Williams *et al.,* 2011). Carbohydrate-degrading and fermenting bacteria *Prevotella*, *Coprococcus*, and unclassified *Veillonellaceae* were found in low abundance in children with ASD, and were associated with behaviours of ASD (Kang *et al.,* 2013).

In relation to diet, it was demonstrated that BTBR, ASD model, mice preferred a fat-rich diet (vegetable shortening containing protein (casein)), compared to a carbohydrate-rich diet (sucrose-cornstarch containing protein (casein)) (Tordoff *et al.,* 2014). Indeed, a ketogenic diet, associated with a dopamine D2 receptor antagonist, has been shown to reduce repetitive motor behaviour in a circling phenotype mouse (Brady *et al.,* 2022). Propionic acid intraventricular infusions were found to increase locomotor activity in rodents, perhaps through changes in lipid metabolism (Thomas *et al.,* 2012). Oral administration of *Blautia stercoris* MRx0006 was found to improve ASD-like behaviours in BTBR, ASD model, mice, decreasing the abundance of *Alistipes putredinis*, modulating the faecal microbial metabolite profile, and increasing oxytocin and hypothalamic arginine vasopressin gene expression (Sen *et al.,* 2022). It has also been reported that females with ASD have significantly lower levels of oxytocin, an endogenous neuropeptide hormone regulating bonding and social behaviour in mammals, suggesting that it may contribute to the differences in social ASD behaviours seen in females with autism (Frehner *et al.,* 2022). Conversely, Berendzen *et al.*, (2022) generated three *Oxtr*-null mutant prairie vole lines and found that social attachment, parturition and parental behaviour remained unchanged (Berendzen *et al.* 2022). This study reveals that there may be other hormones, such as vasopressin, inlvoved in bonding and social behaviour. Berendzen *et al.*, (2022) have highlighted that low levels of oxytocin may not contribute to social impairment in children with ASD.

Interestingly, a Microbiota Transfer Therapy (MTT) two-year follow-up study reported that children showed improvements in ASD symptoms, GI symptoms and gut microbiota, noting a significant increase in *Bifidobacteria* and bacterial diversity (Kang *et al.,* 2019). However, caution must be taken with MTT, as contribution of gut microbiota to risk of chronic disease development needs to be elucidated (Walter *et al.,* 2020). A recent study proposed that the differences in the ASD gut microbiome are due to dietary preferences, rather than ASD (Yap *et al.,* 2021). Yap *et al.*, (2021)

reported the only taxa associated with ASD was *Romboutsia timonensis*, that behavioural traits of ASD are due to a less-diverse diet, resulting in a reduced microbiome alpha-diversity (Yap *et al.,* 2021).

4-ethylphenyl sulfate (4EPS), a microbial metabolite, has been shown to be increased in a mouse model of ASD, elevating anxiety-like behaviours (Hsiao *et al.,* 2013). More recently, using a mouse model, it was determined that 4EPS alters region-specific activity and connectivity in the brain, impairing oligodendrocyte maturation and reducing oligodendrocyte–neuron interactions (Needham *et al.,* 2022). Targeting the conversion of dietary tyrosine to 4-ethylphenol (4EP) in the gut may be a potential target for ASD (Needham *et al.,* 2022). Subsequently, an oral GI-restricted adsorbent, AB-2004, a target for small aromatic or phenolic molecules, has been reported to improve anxiety-like ASD behaviours (Stewart Campbell *et al.,* 2022). AB-2004 has high affinity for gut microbial metabolites, including 4EPS, *p*-cresyl sulfate, 3-indoxyl sulfate and hippurate. AB-2004 can target these molecules by preventing their absorption and circulation, from the gut (Stewart Campbell *et al.,* 2022). A pilot human study of 8 weeks of treatment with AB-2004, improved ASD-like behaviour and overall gut health, demonstrating the safety of direct targeting gut-derived metabolites with an oral adsorbent (Stewart Campbell *et al.,* 2022).

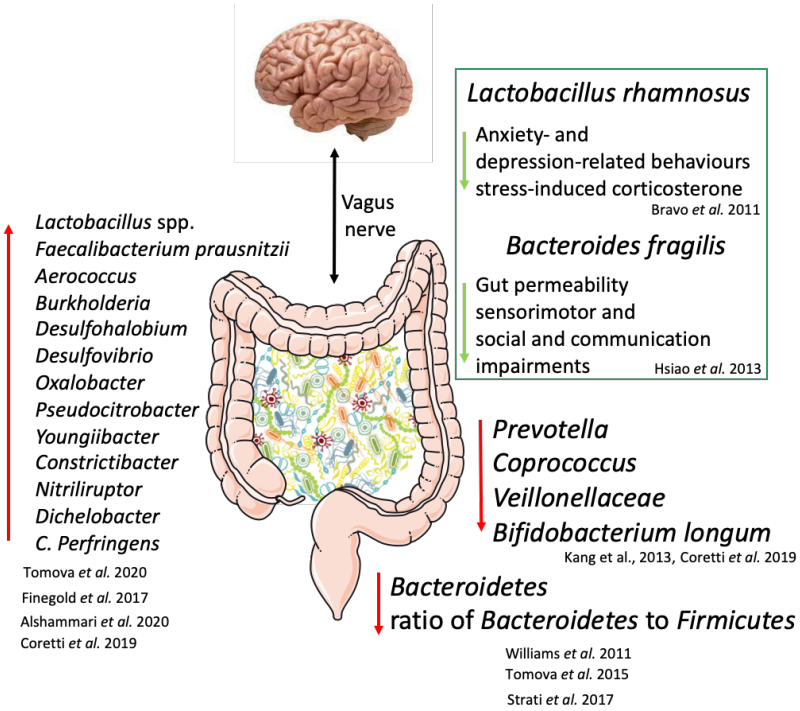


Figure 1.6: **Summary of reported alterations to bacterial representation of individuals with ASD.** Treatment with *L. rhamnosus* (JB-1) (Bravo *et al.,* 2011) and *Bacteroides fragilis* (Hsiao *et al.,* 2013) improved social and communication impairments in mouse models of ASD, demonstrating communication between the gut-brain axis.

1.5.2.2 Parkinson's Disease

Similarly, Parkinson's disease (PD) is also associated with the gut and with microbial population changes. PD is the second most common neurodegenerative disorder and is characterised by the build-up of intraneuronal inclusion bodies, Lewy bodies. Aggregated α-synuclein prions contribute to the formation of Lewy bodies, resulting in the progressive loss of dopaminergic neurons in the substantia nigra (pars compacta) (Braak *et al.,* 2003). Motor symptoms of PD include tremor, bradykinesia and muscle rigidity (Lees *et al.,* 2009). A non-motor symptom, constipation, is recognised as an early symptom of PD, potentially 20 years plus from disease onset. Indeed, appendix removal is associated with a lower risk of PD, as it appears to act as a reservoir or sink for α-synuclein aggregates and truncation products that affect the risk of PD development (Killinger *et al.,* 2018).

Newly diagnosed PD patients demonstrate intestinal permeability (gut leakiness). Mucosal staining showed increased levels α-synuclein (α-syn), nitrotyrosine (oxidative stress), *E. coli* (bacterial translocation) and LPS binding protein (LBP) (serum markers of endotoxin exposure) (Forsyth *et al.,* 2011). Immunostaining identified the presence of α-synuclein in colon tissue of PD patients, at least two years before motor symptoms emerged (Shannon *et al.,* 2012). Relative abundance of *Prevotellaceae* is reduced in faeces of PD patients and severity of motor symptoms were positively associated with abundance of Enterobacteriaceae (Scheperjans *et al.,* 2015). Faecal samples from PD patients showed decreased abundance of *Faecalibacterium* and *Fusicatenibacter* which are correlated with anti-inflammatory and neuroprotective effects in a range of studies (Weis *et al.,* 2019). The authors reported increased calprotectin levels, a marker of inflammation, along with increased representation of *Clostridiales* family XI members within these samples.

They reported that Catechol-O-methyl transferase (COMT) inhibitors directly affect faecal microbiota of PD patients, L-dopa and entacapone medications affected the relative abundance of *Peptoniphilus*, *Finegoldia*, *Faecalibacterium Fusicatenibacter*, *Anaerococcus*, *Bifidobacterium*, *Enterococcus* and *Ruminococcus* (Weis *et al.,* 2019). *Escherichia coli* genetically deleted for *csg*A, encoding the major subunit involved in the production of curli (a microbial α-syn homologue), was associated with reduced α-syn–induced neuronal death and improved neuronal functions with restored mitochondrial health in *Caenorhabditis elegans* (Wang *et al.,* 2021). The classical nematode model of aging, *Caenorhabditis elegans* (*C. elegans*) could be utilized to reflect other disease conditions including interactions with gut microbes. A *C. elegans* model of PD demonstrated symptoms of mitochondrial disruption. *C. elegans* was more sensitive to mitochondrial complex I inhibitors, including fenperoximate, rotenone, pyridaben, or stigmatellin, however, combining D-β-hydroxybutyrate with tauroursodeoxycholic acid (TUDCA) elicited protection in the *C. elegans* model of PD (Ved *et al.,* 2005). TUDCA acts as a mitochondrial stabilizer and anti-apoptotic agent. TUDCA protected against MPTP-induced dopaminergic degeneration by inhibiting JNK phosphorylation and production of reactive oxygen species (ROS), and activating the Akt pro-survival pathway (Castro-Caldas *et al.,* 2012). Ursolic acid, ursodeoxycholic acid (UDCA), ursocholanic acid and dehydro(11,12)ursolic acid lactone were found to rescue mitochondrial function in PD model, parkin-mutant fibroblasts, mainly through glucocorticoid receptor activation and increased Akt phosphorylation (Mortiboys *et al.,* 2013). UDCA was shown to beneficially regulate microbial function in PD models, LRRK2^{G2019S} mutant PD patient tissue (M-LRRK2^{G2019S}), and nonmanifesting LRRK2^{G2019S} mutation carriers (NM-LRRK2^{G2019S}) (Mortiboys *et al.,* 2015). A pilot study of orally administered UDCA to treat human individuals with PD demonstrated small elevations in ATP and reductions in ATPase activity and alterations in Unified Parkinson's Disease Rating Scale (parts I-IV) and Montreal Cognitive Assessment scores, however, gut microbial composition was not examined (Sathe *et al.,* 2020). This shows the potential for BAs to be used for treatment of PD. Taurine is an inhibitory neurotransmitter amino acid and has been shown to have neuroprotective effects. Taurine induces noradrenergic locus coeruleus neuroprotection against microglia-mediated neurotoxicity (Hou *et al.,*

2018). Taurine suppresses paraquat and maneb-induced microglial M1 polarization and gene expression levels of proinflammatory factors, reduces aggregation of α-synuclein and induces protection against dopaminergic neurodegeneration and motor deficits in a PD model (Che *et al.,* 2018). In a rat model of early PD, taurine levels were reduced and levels of N-acetylaspartate were increased (Yang *et al.,* 2020). Oleic acid, diglycerides and triglycerides were increased in α-synuclein-expressing yeast. In *C. elegans*, knock out of the oleic acid-generating enzyme stearoyl-CoA-desaturase (SCD), inhibited the α-synuclein-induced degeneration of dopaminergic neurons. Over-expression of oleic acid in human neural cells stimulated α-synuclein inclusion formation. Inhibition of SCD prevented α-synuclein inclusion formation (Fanning *et al.,* 2019). Heptanoic acid has been reported to be increased in PD patients while butyric acid and caproic acid were at lower levels. Serum propionic acid levels are reduced, which is associated with motor symptoms, cognitive ability and non-depressed state. Propionic acid may have potential as a therapeutic target to reduce symptoms of PD (Wu *et al.,* 2022).

1.6 Models of aging

Investigation of aging and longevity can prove challenging in humans due to their relatively long lifespan and to ethical and other considerations. Therefore, alternative models have been applied to study aging. Among them are non-human primates including New World marmosets (*Callithrix jacchus*) and Old World rhesus macaques (*Macaca mulatta*), which can reach 22 and 40 years of age respectively (Dyke *et al.,* 1986; Tigges *et al.,* 1988). They both demonstrate the onset of human age-related diseases, such as Alzheimer's Disease (Heuer *et al.,* 2012; Arnsten *et al.,* 2019). Here, calorie restriction was shown to benefit healthy aging (Bodkin *et al.,* 2003; Mattison *et al.,* 2012; Colman *et al.,* 2014; Mattison *et al.,* 2017). Also, chemical intervention, including rapamycin, can improve health-span of marmoset monkeys, without side effects other than mild metabolic consequences (Ross *et al.,* 2015). These are effective models, but not readily available as lifespan is still relatively long. Dogs have shorter lifespans, and companion dogs in particular are exposed to many of the same environmental aging factors as humans which makes them a valuable

model of aging (Kaeberlein *et al.,* 2016). Calorie restriction increases lifespan of Labrador retrievers, by approximately two years (Kealy *et al.,* 2002; Lawler *et al.,* 2007; Richards *et al.,* 2013). Rapamycin was also beneficial to dog longevity (Yi *et al.,* 2014). In 2014, the Dog Aging Project (http://www.dogagingproject.com) was launched to investigate the aging process and improve longevity in dogs (Hayden, 2014).

For microbiome experimental questions, vertebrate models such as mice, zebrafish and more recently the African turquoise killifish, have proved effective (Weindruch *et al.,* 1986). Studies using mice and long-lived Ames dwarf mice, have been used to examine the effects of aging and caloric restriction (Wang *et al.,* 2017). Non-vertebrate models of aging include the yeast (*Saccharomyces cerevisiae)*, which can live up to 75 hours, the nematode (*Caenorhabditis elegans*) which survives 3 weeks to 3 months and the fruit fly (*Drosophila melanogaster*), which can live up to 2 months. These models are widely applied to aging investigations due to their relatively short lifespans, low-cost, good genetic characterization and manipulation (Brunet, 2020). *Caenorhabditis elegans* as a model of aging is discussed below and it is relevant to the work reported in this thesis.

1.7 *Caenorhabditis elegans*

Caenorhabditis elegans (*C. elegans)* is the model organism applied to two chapters in this thesis to investigate how BA metabolites and specific bacteria strains might influence aging and lifespan. This soil-dwelling nematode utilizes bacteria and fungi from decaying biomass as a food source. In the 1960s and 70s, Brenner established *C. elegans* as a model system. He and his colleagues performed mutational analysis and determined the regulation of organ development and programmed cell death, producing a seminal paper (Brenner, 1974). *C. elegans* is transparent, it can be a self-reproducing hermaphrodite, reaching up to 1 mm in length (Brenner, 1974). The development of each cell is characterised and it was also the first sequenced multicellular organism (Mitani, 2017). Sulston and Brenner further reported methodologies to determine the basic genetics of *C. elegans,* they described a number of mutations affecting morphology and behaviour (Brenner, 1974; Sulston

and Brenner, 1974). Brenner also used the *C. elegans* model organism to determine nervous system structure (White *et al.,* 1986).

1.7.1 The *Caenorhabditis elegans* Life cycle

Under laboratory conditions, at 22°C, *C. elegans,* fed on *Escherichia coli* (*E. coli*) OP50 strain, develop to reproductive adults (RA), over 44 hours (Brenner, 1974). *The C.elegans* eggs, once produced and fertilized, take *ca*. 9 hours to hatch into larval stage 1 (L1). The L1 larvae continue to develop to larval stage 2 (L2) over a further 9-12 hours. However, L2 stage larvae can then diverge dependent on the presence or absence of food or stress. Under nutrient rich conditions L2 to larval stage 3 (L3) takes 8 hours and another 8 hours are required thereafter, to reach larval stage 4 (L4). It takes a further *ca.* 18 hours to reach RA where hermaphrodites can self-fertilise and the cycle begins again (Olsen and Gill, 2016). If conditions become harsh or sub-optimal, or where nutrients are limited, *C. elegans* have the ability to develop into a state of metabolic dormancy, this state is known as diapause. *C. elegans*, in this state, are called 'dauer' larva. Limited nutrients result from dense worm populations where bacteria (i.e. food) availability is limited. L1 stage produced pheromones, signal to other L1 stage *C. elegans* to develop into pre-dauer L2 (L2d) stage, generally conditions need to be suboptimal even before L1 for pheromone signalling (Golden and Riddle, 1984). After approximately 13 hours, if conditions have not improved, *C. elegans* commit and progress into full dauer stage. The nematode pharynx seals tightly shut, the body is coated with a resistant cuticle and the overall diameter of its body is reduced.

While dauer *C. elegans* use internally stored glycogen and trehalose as energy reserves for survival, relative to the normal mode of development their lifespan can extend, with calorific restriction, up to 3 fold. Once conditions become optimal again, when food is replenished or stress (temperature, population density) is removed, the dauer recovers to a post-dauer L3 stage (PDL3), then moults into post-dauer L4 stage (PDL4), leading to sexually reproductive adult formation. These nematodes continue to reproductive adult stages despite emerging from diapause (*Figure 1.7*).

The genetics controlling entry into dauer are known as *daf* genes (dauer formation genes). Indeed some mutations, called *daf-c* (dauer-forming constitutive) mutations, can lock the nematodes into diapause. On the other hand, *daf-d* (dauer-forming defective) mutants are unable to transition into dauer formation (Riddle *et al.,* 1981; Golden and Riddle, 1984; Schaedel *et al.,* 2012; Olsen and Gill, 2016). *Table 1.2* below describes the *daf* genes examined in this study. The nematodes short lifespan, its life cycle, and the ease of genetic and laboratory manipulation as well as the availability of strains, specific gene knock out strains and those that contain promoter reporter fusions, point to it as an excellent model in which to investigate aging (Klass, 1977). There are known associations with a range of different bacteria, as this worm carries its own diverse gut microbiome in the wild (Johnke *et al.,* 2020), therefore *C. elegans* represents an excellent model in which to study microbe-host interactions.

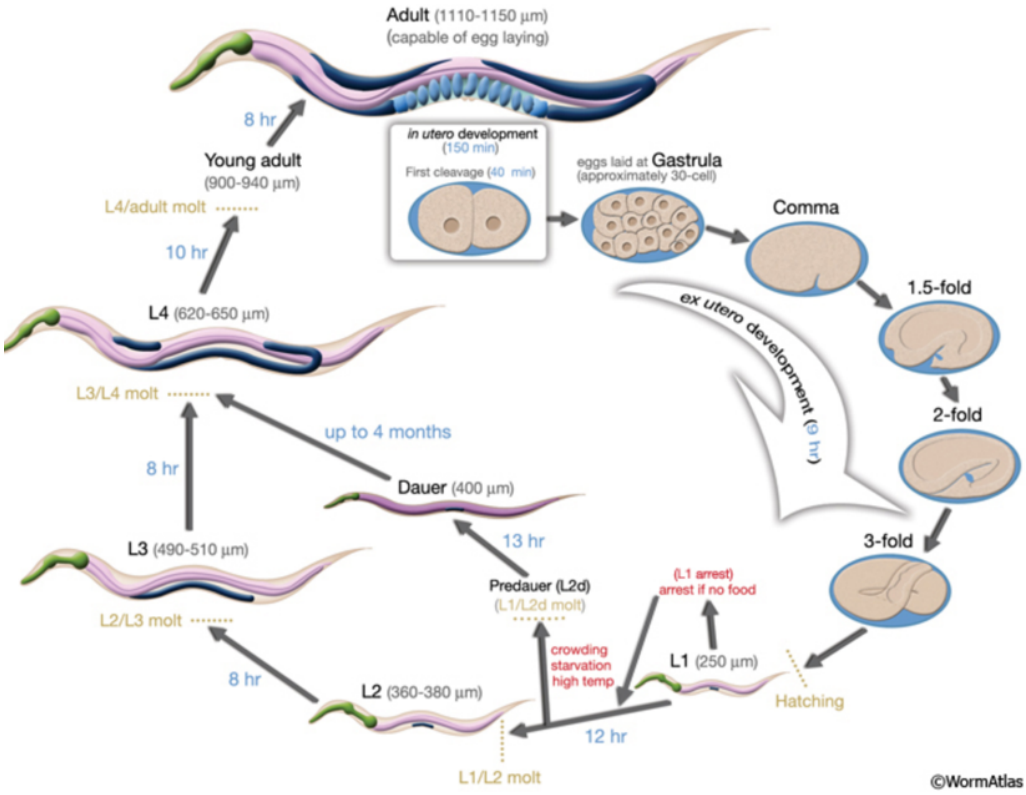


Figure 1.7: **The nematode *Caenorhabditis elegans* life cycle at 22°C.** Reproductive adults lay fertilized eggs which can hatch to larval stage 1 through L2, L3, and L4 and then to reproductive adults (RA). This life cycle can take up to 2-3 days to complete. Under suboptimal conditions larval stage 1 can continue through into pre-dauer L2 to dauer where they can survive up to 3-4 months. Here the time frames, moulting,

points of divergence and and length of each stage are indicated. Taken from Worm Atlas (https://www.wormatlas.org) (Altun and Hall, 2009).

Table 1.2: Summary of *C. elegans daf* genes examined in this study. Adapted from WormBook (http://www.wormbook.org) and Sections 1.7.3, 4.3 and 5.3 of this thesis.

***C. elegans daf* genes**	**Function**	**Mammalian homolog**
daf-2	metabolism, growth, development, longevity, and behaviour	Insulin/IGF-1
daf-3	sensory neurons for dauer formation	SMAD
daf-5	dauer development	Ski
daf-7	normal larval development	TGF-β
daf-9	catalyses the addition of a terminal acid to the side chain of sterol metabolites, involved in dafachronic acid formation	CYP27A1
daf-12	dauer formation, developmental timing, fat metabolism, longevity	FXR
daf-16	downstream of *daf-2*, transcription factor regulating growth, metabolism, stress responses, cell cycle control, and longevity	FOXO
daf-22	Pheromone production	Sterol carrier protein x (SCPx)
daf-28	encodes an insulin/insulin-like peptide agonist for DAF-2 pathway	Insulin/IGF-1 receptor agonist
daf-36	enzyme in Δ^7-Dafachronic Acid biosynthesis	Oxygenase

1.7.2 The *Caenorhabditis elegans* – The nematode model of aging

Klass described the effects of parental age and lifespan, nutrition, temperature and U.V. irradiation on *C. elegans* lifespan (Klass, 1977). *C. elegans* lifespan was 14.5 ± 2.0 days at 20 ± 0.5°C, at high temperatures (25.5°C) *C. elegans* lifespan reduced to 8.9 ± 1.1 days, while low temperatures (10°C) extended *C. elegans* lifespan to 34.7 ± 5.8 days. Percentage egg viability was 95% at 20 ± 0.5 °C, 93% at 25.5°C and 57.7% at 10°C. This study, also described the effect of dietary restriction in extending *C. elegans* lifespan (Klass, 1977). Eight *C. elegans* mutations were described with lifespan extending properties (Klass, 1983). Two of these (mutant clone: 782 and 895)

induced dauer formation, another (mutant clone: 248) decreased food intake, so calorific restriction was induced, due to a chemotaxis-defect. The remaining five mutations showed varying degrees of paralysis severity, mainly affecting pharyngeal pumping, hence calorie restriction resulted from diminished food ingestion (Klass, 1983). Three of these five isolated *C. elegans* mutants were mapped to *age-1* a single genetic locus (originally identified as *daf-23*) (Friedman and Johnson, 1988b). This was the first breakthrough in aging research, it showed that *C. elegans* could be used as a model organism in aging, to identify mutations in individual genes that could extend lifespan (Klass, 1977; Klass, 1983; Friedman and Johnson, 1988b). Others have followed these investigations to identify a range of genetic elements and there are hundreds of genes connected to aging in these nematodes (Mathew *et al.,* 2017). Some of the specific genes and pathways are discussed below, as key elements in lifespan and indeed in aging. Indeed it appears that many different signals (and chemicals) converge to negatively and positively impact the aging process. Many of these pathways are also conserved in humans.

1.7.3 *Caenorhabditis elegans* longevity systems

Many of the signals for nematode development centre on environmental and nutritional stresses. Genetic factors including *age-1*, *daf-2*, *eat-2*, *clk-1* and *ife-2* can influence lifespan in *C. elegans*, and many of these genes converge on one pivotal transcription factor capable of regulating responses either negatively or positively to determine dauer formation, and indeed, lifespan (see *Figure 1.8* below). The cytoplasm to nuclear transcription factor is well conserved in the nematode *C. elegans* (*daf-16*) and in mammals including humans (FOXO *aka* Forkhead box O) (Ogg *et al.,* 1997). Two other key genes and their proteins are associated with the nematode (DAF-2, AGE-1) and human (pathways insulin and Insulin receptor IGF-1) (Barbieri *et al.,* 2003).

However, a range of drugs and other chemicals can also influence *C. elegans* lifespan. For example, ortho-fluoro, Crotamiton (*N*-ethyl-o-crotonotoluidide) derivative, JM03, through osmotic avoidance abnormal-9 (OSM-9), was reported to extend *C. elegans* lifespan (Bao *et al.,* 2022). Polyphenols have also been shown to elicit antiaging effects (Liu *et al.,* 2021) as well as curcumin acetylsalicylate, a compound

that is a combination of aspirin and curcumin, that has been shown to extend *C. elegans* lifespan (Zhou *et al.,* 2021). Some of the key genetic factors: *age-1*, *daf-2*, *eat-2*, *clk-1* and *ife-2*; and drugs: metformin, resveratrol, rapamycin and β-hydroxybutryate; that have been reported to influence *C. elegans* lifespan and contribute to longevity, are discussed below.

1.7.3.1 age-1 and daf-2

A mutation in *age-1*, *age-1(hx546)*, a recessive mutant allele, lowers hermaphrodite self-fertility and extends *C. elegans* lifespan (Friedman and Johnson, 1988a). *age-1* encodes phosphatidylinositol-3-OH kinase (PI3K), specifically, a catalytic (p110α) subunit. Phosphatidylinositol signalling regulates both lifespan and dauer diapause (Morris *et al.,* 1996). *daf-16* is downstream of *daf-2*. *daf-16* mutation, *daf-16(m26)*, inhibits *age-1* lifespan extension (Larsen *et al.,* 1995) (*Figure 1.8*).

Mutations in the *daf-2* gene, specifically *daf-2(e1370)*, induces *C. elegans* lifespan extension up to double the length of the wild-type (Kenyon *et al.,* 1993). *daf-16(m26)* inhibits *daf-2* lifespan extension (Kenyon *et al.,* 1993). *daf-2* encodes a member of the insulin receptor family, namely insulin/IGF-1 receptor (Kimura *et al.,* 1997). Similar to the human insulin/IGF-1 receptor, reduction in DAF-2 signalling leads to developmental and metabolic changes, essentially due to dietary restriction, highlighting the connection between longevity, metabolism and diapause (Kimura *et al.,* 1997). Interestingly, the interaction with DAF-2 induces a signalling cascade that is different in fed and fasted (calorie restricted) states to induce second messengers (SIRT-1, AGE-1 respectively) (*Figure 1.8*). AGE-1 induces a phosphorylation relay that ultimately ends with phosphorylated DAF-16 and prevention of its translocation to the nucleus. SIRT-1 is activated due to dietary restriction and therefore removes inhibition of DAF-16 in the nucleus, allowing transcription of downstream genes. In addition, environmental stresses can activate DAF-16 (*Figure 1.8*).

1.7.3.2 eat-2

Other systems also feed into DAF-16 regulon. For instance, *eat* genes (expressed in the pharyngeal muscle) of *C. elegans* are required for pharyngeal function (Avery,

1993). MC is an excitatory cholinergic neuron that initiates muscle action potential resulting in pharyngeal pumping. Nicotinic acetyl-choline (ACh) receptor (nAChR) is essential for MC transmission, as mutations in an antagonist for nAChR decreased pharyngeal pumping (Raizen *et al.,* 1995). *eat-18* is necessary for pharyngeal nAChR function and there are fourteen recessive mutations in *eat-2* (Raizen *et al.,* 1995). It was concluded that a multisubunit protein complex, involving both *eat-18* and *eat-2*, regulate pharyngeal nAChR function (Raizen *et al.,* 1995). EAT-2 is encoded by *eat-2*, in the pharyngeal muscle of *C. elegans* (McKay *et al.,* 2004). EAT-2 is a non-α-nicotinic acetylcholine receptor subunit, localised to the MC synapse and functions postsynaptically (McKay *et al.,* 2004). Lifespan extension was examined in *eat-2* mutants and it was found that some mutants could extend lifespan to up to 50% longer (Lakowski and Hekimi, 1998). As *eat-2* mutants reduce pharyngeal pumping, *C. elegans* lifespan is extended through caloric restriction (Lakowski and Hekimi, 1998) with a knock-on effect on DAF-16 activity.

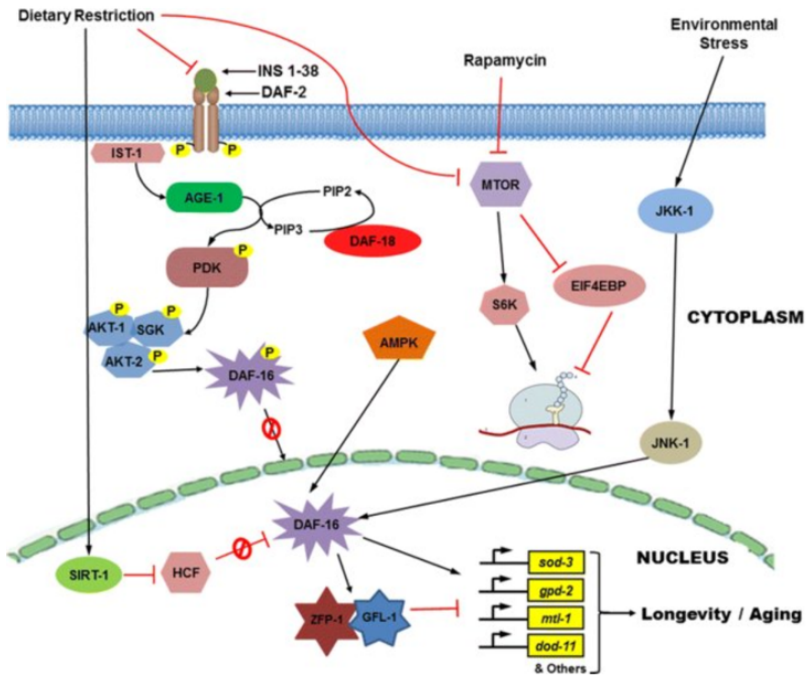


Figure 1.8: **Factors affecting *Caenorhabditis elegans* lifespan and longevity.** Three types of influences are recognised DAF-2 and AGE-1 signalling equivalent to insulin and insulin receptor signalling in humans, chemical signalling e.g. rapamycin to impact protein processing and turnover, and the presence of environmental stresses.

The former and latter converge on transcription factor DAF-16 (FOXO in humans) a highly regulated transcription factor, that can activate *sod-3*, *gpd-2*, *mtl-1* and *dod-11*, involved in inducing longevity in *C. elegans*. Adapted from (Mathew *et al.,* 2017).

1.7.3.3 clk-1

Energy levels are important in longevity and lifespan, enzyme demethoxyubiquinone monooxygenase is encoded by the *C. elegans* gene *clk-1*, this enzyme is involved in ubiquinone biosynthesis and shuttles electrons from complex I and II to complex III during respiration (Jonassen *et al.,* 2001; Bansal *et al.,* 2015). In 1995, mutations in the *clk-1* gene were described as altering *C. elegans* development and behavioural timing (Wong *et al.,* 1995). Mutations in the *clk-1* gene affect *C. elegans* biological clock, specifically: lifespan, swimming, pumping and cell cycles. *clk-1* mutations that effected length of embryonic development, inversely effected the length of *C. elegans* defecation cycle (Wong *et al.,* 1995). It was then proposed that *C. elegans* with *clk-1* mutations are living at a slower pace, and so *clk-1* has a role in the regulation of *C. elegans* metabolism (Lakowski and Hekimi, 1996). CLK-1::GFP fusion was used to show that CLK-1 is present in all somatic cells, specifically in the mitochondria (Felkai *et al.,* 1999). *clk-1* was reported to regulate behavioural rates and mitochondrial activity, demonstrating that mitochondria have a role to play in *C. elegans* longevity (Felkai *et al.,* 1999). *clk-1* was demonstrated to have an essential function in ubiquinone biosynthesis, in *C. elegans* (Miyadera *et al.,* 2001). *clk-1* can modulate cell stress responses in its nuclear form (Monaghan *et al.,* 2015) and more recently Molenaars *et al*., (2018) demonstrated that mutations in the mitochondrial *clk-1* elicit its effects at the level of cytoplasmic mRNA translation, altering polyribosome formation, to confer similar translational defects to *daf-2,* resulting in insulin signalling dampening (Molenaars *et al.,* 2018). The CLK-1 protein was shown to be conserved across eukaryotes (Ewbank *et al.,* 1997). In mice, inactivation of *mclk-1*, an ortholog of *C. elegans clk-1*, extended lifespan as it protected against oxidative stress and DNA damage (Liu *et al.,* 2005).

1.7.3.4 ife-2

The *ife-2* gene is the *C. elegans* isoform of the eukaryotic translation initiation factor 4E (eIF4E). eIF4E binds the 7-monomethyl guanosine cap at the mRNA 5' cap structure of eIF4F, and is a protein complex involved in translational control, recruiting of ribosomes to mRNA (Gingras *et al.,* 1999). Loss of IFE-2 extends *C. elegans* lifespan, in a mechanism independent of DAF-16. This IFE-2 deficiency, further extends *C. elegans* lifespan of mutants *clk-1, eat-2*, *daf-2* and *age-1* (Syntichaki *et al.,* 2007). Lack of IFE-2 protects against oxidative stress and reduces *C. elegans* protein synthesis (Syntichaki *et al.,* 2007). Another study also showed that *ife-2* gene mutation, *ife-2(ok306)*, reduces protein synthesis and extends *C. elegans* lifespan (Hansen *et al.,* 2007).

1.7.3.5 Metformin

Metformin is a widely used biguanide to treat type 2 diabetes, it can reduce glucose levels in the gut, without causing hypoglycaemia or lactic acidosis (Pryor and Cabreiro, 2015). In 1929, glucose-lowering biguanides were first synthesised, consisting of two N-linked guanidines, including dimethyl-biguanide. A physician Jean Sterne singled out dimethyl-biguanide (metformin) to be used clinically in the publication of a successful trial (Sterne, 1957). Although metformin is primarily used as an anti-diabetic drug, it has been shown to extend *C. elegans* healthspan; by extending *C. elegans* mean lifespan, reducing the accumulation of lipofuscin and lastly, extending the ability of youthful locomotory; all through a dietary restriction mechanism, independent of the insulin/IGF-1 signalling pathway (Onken and Driscoll, 2010). Energy sensor AMPK and AMPK-activating kinase, LKB1, are required for metformin-induced positive healthspan effects in *C. elegans*, as in mammals (Onken and Driscoll, 2010). *skn-1* intestinal expression is essential for resistance to oxidative stress, and neurons, and *skn-1* is required for benefits in dietary restriction, for metformin-induced positive healthspan effects in *C. elegans* (Onken and Driscoll, 2010). Metformin modifies microbial folate and methionine metabolism in order to extend *C. elegans* lifespan (Cabreiro *et al.,* 2013). Alteration of S-adenosylmethionine synthase (*sams-1*) and methionine synthase (*metr-1*) in *C. elegans* causes methionine restriction. Metformin induces a dietary restriction longevity effect, through

microbial metabolism, in *C. elegans* (Cabreiro *et al.,* 2013). Microbes coordinate metformin signals that regulate downstream Crp, a transcriptional regulator, through the phosphotransferase signalling pathway (Pryor *et al.,* 2019). Bacterially produced metabolite agmatine, is essential for metformin-induced *C. elegans* lipid metabolism and lifespan effects (Pryor *et al.,* 2019). In humans, metformin-induced gut microbial effects have also been reported (Wu *et al.,* 2017; Chávez-Carbajal *et al.,* 2020). Metformin reduces *Bacteroides fragilis* levels and increases glyco conjugated Ursodeoxycholic Acid (GUDCA) BA concentrations in the human gut (Sun *et al.,* 2018). GUDCA is an FXR receptor antagonist and this decrease in FXR signalling improves metabolic dysfunction (Sun *et al.,* 2018). Although it is difficult to determine lifespan extension in humans, metformin has proven to have other health benefits. A UK 10-year follow-up reported reduced risks for myocardial infarction and death (Holman *et al.,* 2008). Metformin has also been shown to have beneficial effects in relation to cancer, by inhibiting cell migration and acting as a senostatic drug (Yu *et al.,* 2017; Hu *et al.,* 2020) and multiple sclerosis (MS), by improving remyelination (Neumann *et al.,* 2019). Although metformin's mechanisms of action remains elusive, it is clear that there are many health benefits of metformin.

1.7.3.6 Resveratrol

High consumption of saturated fats is positively correlated with coronary heart disease (CHD) mortality, however, in France high consumption of saturated fats isn't associated with high CHD mortality (Renaud and de Lorgeril, 1992). This 'French paradox' is believed to be accredited to wine consumption. Data from Wales revealed that alcohol reduces aggregation of platelets, which in turn decreases the risk of CHD (Renaud and de Lorgeril, 1992). Trans-resveratrol, a trihydroxystilbene in red wine, reduces serum lipids and decreases CHD risk (Siemann, 1992). This led to an interest in the health benefits of resveratrol. Resveratrol was found to induce deacetylation of SIR-2.1, a member of the sirtuin family of NAD^+-dependent deacetylases, and extended *C. elegans* lifespan by up to 14% in a SIR-2.1-dependent manner, that mimicked calorie restriction (Wood *et al.,* 2004). Some studies have reported that resveratrol-induced lifespan extension only occurs under conditions of stress, such as oxidative stress, as resveratrol is a powerful antioxidant (Chen *et al.,*

2013). It is evident that resveratrol has many health benefits, including anticancer (Jang *et al.,* 1997) and anti-inflammatory (Zhou *et al.,* 2018), which may contribute to human lifespan extension.

1.7.3.7 Rapamycin

Rapamycin was approved by the FDA in 1999, as an antirejection drug after organ transplantation, due to its immunosuppressive properties (Rapamune, 1999). Rapamycin also has anticancer properties and was approved in 2011 by the FDA to treat pancreatic cancer. Two genes *TOR1* and *TOR2*, were identified that regulate rapamycin's ability to arrest the G1 phase of *Saccharomyces cerevisiae* cell cycle (Heitman *et al.,* 1991). Deficiency in TOR, or 'target of rapamycin', kinases were found to extend lifespan in *C. elegans* through insulin signalling and nutrient sensing regulation (Vellai *et al.,* 2003). In 2009, it was reported that rapamycin, an inhibitor of the mTOR pathway, extended mouse lifespan when administered later in life, in both genders (Harrison *et al.,* 2009). These results were also seen when compared to other compounds, such as resveratrol, and in higher concentrations of rapamycin (Miller *et al.,* 2011; Miller *et al.,* 2014). It has since been shown that rapamycin treatment, for as little as 3 months, extends lifespan up to 60% and, in the small intestine, induces an increase in the composition of segmented filamentous bacteria (Bitto *et al.,* 2016) which is anti-inflammatory in nature but which elicits its effects by adjusting the gut microbiome and mimicking calorie restriction to extend lifespan (Pearson *et al.*, 2008)

1.7.3.8 β-Hydroxybutyrate

In 1970, "keto acids" β-hydroxybutyrate and acetoacetate were reported in a man in a state of starvation (Cahill, 1970). It was believed that these "keto acids" were to be utilised by the brain, through the breakdown of FAs, as an alternative energy source to spare glucose and protein metabolism (Cahill, 1970). D-β-hydroxybutyrate (βHB) has been shown to protect against neuronal toxicity induced by 1-Methyl-4-phenyl-1,2,3,6-tetrahydropyridine (MPTP) (Tieu *et al.,* 2003). It improves ATP production and mitochondrial respiration through a complex-II mechanism, and it is thought to be a

promising therapy for neurological diseases as it can pass through the blood-brain barrier (Kashiwaya *et al.,* 2000; Tieu *et al.,* 2003). βHB's positive effects on mitochondrial respiration could also be harnessed to treat Alzheimer's disease (Kashiwaya *et al.,* 2000; Zhang *et al.,* 2013). Treatment of mice with ketone body βHB, demonstrated resistance to oxidative stress (Shimazu *et al.,* 2013). This was consistent with reduction in HDAC1 and HDAC2 and enhancement of FOXO3A and MT2 activity (Shimazu *et al.,* 2013). βHB can therefore function as a class I histone deacetylases (HDACs) inhibitor (Shimazu *et al.,* 2013). βHB also has lifespan extension properties (Edwards *et al.,* 2014). In *C. elegans*, βHB increased lifespan by 20%, in a dietary restriction manner (Edwards *et al.,* 2014). DAF-16/FOXO and SKN-1/Nrf longevity pathways are essential for βHB-mediated lifespan extension, this also includes the sirtuin SIR-2.1, and the AMP kinase subunit AAK-2. HDACs HDA-2 and HDA-3, are also required for the lifespan extending ability of βHB (Edwards *et al.,* 2014). βHB enhances *C. elegans* oxygen consumption, thermotolerance, βHB dehydrogenase function and reduces glucose toxicity. βHB also demonstrated beneficial effects on Alzheimer's and Parkinson's disease by reducing amyloid-beta toxicity and alpha-synuclein aggregation, respectively (Edwards *et al.,* 2014). βHB has the potential to be used as a therapy for age-related diseases through its HDAC inhibition-mediated lifespan extension and stress response pathway activation (Edwards *et al.,* 2014).

1.7.4 The gut microbiota in *Caenorhabditis elegans*

Studies examining *C. elegans* in natural habitats indicate the potential for diverse microbial colonization with a clear preference for Proteobacteria, however, an isolate of *Ochrobactrum* was even found to persist in *C. elegans* intestine under conditions of stress (Dirksen *et al.,* 2016). RNAi showed that this enrichment was influenced by *C. elegans* DAF-2/IGFR pathway, through transcription factors DAF-16/FOXO and PQM-1/SALL2 (Zhang *et al.,* 2021). Other colonizing phyla represented in non-lab isolated *C. elegans* are Firmicutes, Actinobacteria, Bacteroidetes and Proteobacteria (Samuel *et al.,* 2016). Although non-proliferating dauer juveniles are correlated with high levels of either pathogens or Bacteroidetes (Samuel *et al.,* 2016). In the laboratory, the *C. elegans* diet is *E.coli* OP50, a uracil auxotrophic strain, that

cannot overgrow the nematode. On intake, *C. elegans* pharyngeal pumping crushes bacteria and as *C. elegans* age, the bacteria can evade crushing to colonise the nematode gut (Klass, 1977; Kumar *et al.,* 2019). Live bacteria are necessary for normal *C. elegans* lifespan, indicating the need for bacterial active metabolism for nutrition, without live bacteria, *C. elegans* development slows and lifespan extends (Lenaerts *et al.,* 2008). A high-throughput screen of 3,983 *Escherichia coli* mutants found five mutants that extended nematode lifespan and these mutants were related to the production of the bacterial polysaccharide colanic acid (Han *et al.,* 2017). Colanic acid altered the nematode mitochondrial dynamics and unfolded protein response (UPR^{mt}) via the transcription factor, ATFS-1 (Han *et al.,* 2017).

E. coli produce a siderophore, enterobactin, that promotes *C. elegans* growth. It sequesters iron and alters ATP synthase functions in the mitochondria (Qi and Han, 2018). Xenobiotic, immune and metabolic signalling pathways are regulated by *C. elegans* to manipulate the composition of various microbiome communities (Zhang *et al.,* 2021). It is clear that bacteria are more than just a source of nutrition to *C. elegans*, specific gut microbiome communities can regulate *C. elegans* health and lifespan through various immune and metabolic signalling pathways.

1.7.4.1 Dafachronic acids and Bile acids are cholesterol derivatives that may feed into similar pathways

Cholesterol is a steroid molecule obtained from the diet by *C. elegans*, but can be synthesised in humans. In *C. elegans*, cholesterol is a precursor of dafachronic acids (DAs), whereas in eukaryotes, it is a precursor for vitamins, steroid hormones, oxysterols and for BAs (Miller, 1988). DA and BA synthesis are very similar between *C. elegans* and humans. DAs act as steroid ligands for the nuclear hormone receptor DAF-12, that controls entry into dauer diapause, reproduction, fat metabolism, and lifespan in *C. elegans*. BAs are steroid molecules that primarily emulsify fats for absorption, but can also undergo microbial modifications, acting as signalling molecules in host metabolism (Long *et al.,* 2017) (*Figure 1.9*).

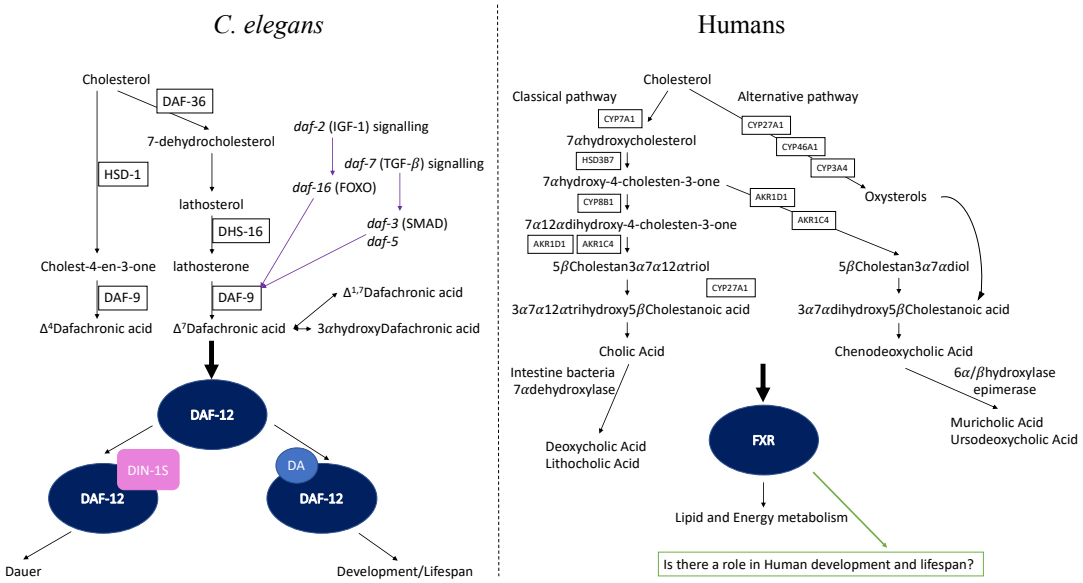


Figure 1.9: **Dafachronic acid and bile acid signalling pathways show cholesterol processing conservation between *C. elegans* and humans, respectively.**

There are two main dafachronic acids (DAs) synthesised from cholesterol, Δ^4-dafachronic acid (Δ^4DA) and Δ^7-dafachronic acid (Δ^7DA), and both are ligands for the DAF-12 receptor (Motola *et al.,* 2006). DAF-12 is suspected to be the equivalent of the human mammalian BA receptor the FXR (discussed above). Two specific 3-keto-cholestenoic acids, metabolites of DAF-9, can bind to DAF-12 and reverse dauer-promoting functions, induced by *C. elegans daf-9* mutants. DAF-9 catalyses the addition of a terminal acid to the side chain of sterol metabolites, similar to CYP27A1, which in mammals, aids the conversion of BA cholic acid (CA) to chenodeoxycholic acid (CDCA) (Motola *et al.,* 2006). These DAs extended lifespan of *daf-9* and *daf-36* knock-out mutants and reduced lifespan in long-lived *daf-9* mutants. This begs the question as to the connection between mammalian and the nematode system and also asks whether FXR could be central to longevity in humans. Noteworthy is that DA production depends on *C. elegans* being in a fed state, the FXR is a metabolic directing BA receptor. As mentioned above, DAs regulate DAF-16/FOXO translocation, to influence longevity int *C. elegans* (Gerisch *et al.,* 2007).

Δ^7DA was shown to be the most potent DAF-12 ligand, and therefore more biologically relevant than Δ^4-dafachronic acid (Sharma *et al.,* 2009). Δ^4DA and Δ^7DA have both independent and overlapping roles in the regulation of *C. elegans*

development and lifespan (Dumas *et al.,* 2010). *C. elegans* development and lifespan are controlled by DAF-12 and the FOXO transcription factor DAF-16, respectively as mentioned above.

3-β-hydroxysteroid dehydrogenase (3βHSD) was identified as a family member, HSD-1 (Dumas *et al.,* 2010). DAF-16/FOXO is inhibited by HSD-1, shown as essential for *C. elegans daf-2* mutant lifespan extension (Dumas *et al.,* 2010). HSD-1 has a role in the biosynthesis of Δ^4DA, but in contrast to DAF-36, an enzyme in Δ^7DA biosynthesis, it is dispensable for proper larval development and lifespan extension (Dumas *et al.,* 2010). DHS-16, a novel 3-hydroxysteroid dehydrogenase, was identified using metabolic genetics, mass spectrometry, and biochemical approaches. DHS-16 was shown to control DAF-12 longevity, through DA biosynthesis (Wollam *et al.,* 2012).

A homolog of vertebrate liver X and vitamin D receptors, *C. elegans* NHR-8 nuclear receptor, regulates apolipoprotein production, FA desaturation and cholesterol balance. DA concentrations were reduced in *C. elegans nhr-8* knock-out mutants, and *nhr-8* was shown to regulate cholesterol levels through *daf-16/FOXO* (Magner *et al.,* 2013). Comparative metabolomics revealed the presence of small amounts of Δ^7DA and 3α-OH-Δ^7DA, and $\Delta^{1,7}$DA as the most abundant DA in *C. elegans* (Mahanti *et al.,* 2014). 3α-OH-Δ^7DA is similar to mammalian BAs with 3α configuration. Interestingly, HSD-1 was previously reported to regulate Δ^4DA biosynthesis, however this study reported that DAF-36 as well as HSD-1 are involved in Δ^7DA and $\Delta^{1,7}$DA biosynthesis (Mahanti *et al.,* 2014). DAs were demonstrated to have partially separate biosynthetic pathways as *dhs-16* and *strm-1* mutants effected Δ^7DA and increased Δ^7DA concentration, respectively, more than $\Delta^{1,7}$DA, however, DA biosynthetic enzymes still need to be determined (Mahanti *et al.,* 2014). In adult hermaphrodites, DAs inhibit proliferation of wild-type germ stem cell development, in a DAF-12-dependent manner. Cytochrome P450 DAF-9 suppression, reverses inhibition of germ cell proliferation (Mukherjee *et al.,* 2017).

1.7.4.2 DAF-12 receptor signalling is similar to the bile acid nuclear receptors in humans

DAF-12 regulates the expression of genes mainly involved in stage-specific developmental programming, showing that DAF-12 predominately functions in *C. elegans* dauer formation and reproductive development (Shostak *et al.,* 2004) (*Figure 1.9*). Transcription of certain let-7-family miRNAs was demonstrated to be regulated by DAF-12, resulting in a complex negative feedback loop to coordinate cell fate decisions and reproductive development (Hammell *et al.,* 2009). DAs increase lifespan in germline-deficient *C. elegans*, lacking somatic reproductive tissues, through DAF-12 signalling and expression of downstream longevity genes, demonstrating an alternative DAF-12 function (Yamawaki *et al.,* 2010). *dbl-1*/TGF-β, *daf-12*/NHR and *daf-36*/oxygenase are inhibited by *daf-16*/FOXO. In fed *C. elegans* larvae, L1 development was repressed due to this pathway interruption by *daf-16*/FOXO. *daf-16*/FOXO induce developmental arrest through *dbl-1*/TGF-β, *daf-12*/NHR and *daf-36*/oxygenase pathway (Kaplan *et al.,* 2015). DAF-16/FOXO transcription factor, TGFβ-responsive DAF-3/SMAD transcription factor and DAF-12 are essential to maintain dauer diapause in *C. elegans*. DAF-3/SMAD functions in sensory neurons, and DAF-16/FOXO and DAF-12 were reported to function in the nervous system, suggesting the presence of interorgan signalling axes, dependent on *daf-2*/IGF-1 signalling (Aghayeva *et al.,* 2021). Most recently, *sup-37* was reported to function as a positive regulator of *daf-12*, *pha-4* and *daf-18*. *sup-37* may act as a link to connect and regulate *C. elegans* longevity pathway (Suriyalaksh *et al.,* 2022)

DAs are ligands for the DAF-12 nuclear receptor, which is a homolog of the mammalian FXR receptor. When *daf-12* alleles were examined a role was determined for progressing the cell cycle at L3 stage. *daf-12* was placed between *lin-14* and *lin-28* in the *C. elegans* pathway and was reported to function in the regulation of stage specific development (Antebi *et al.,* 1998). A follow-up study showed that DAF-12 regulates dauer diapause, cell cycle development and longevity in *C. elegans*. Human NHR-8 and NHR-48 are most similar to DAF-12, and DAF-12 is also a homolog of both mammalian pregnane-X receptors (PXRs) and vitamin D receptor (VDR). DAF-12 is expressed in the somatic gonad and nervous system, from egg to reproductive adult,

but its expression is increased at mid-larval stages (Antebi *et al.,* 2000). Similar larval defects occur in *C. elegans daf-9* and *daf-12* mutants. Both *daf-9* and *daf-12* are involved in *daf-2*/IGF-1 and gonadal signalling. *daf-9* encodes a cytochrome P450 and is involved in the synthesis of DAs, working upstream of DAF-12 (Gerisch *et al.,* 2001).

1.8 Project aims and objectives

At the time of commencement of this project, the gut microbiome and its emerging properties in determining health and influencing disease status were well established. Microbial alterations were also associated with aging. Convergence on microbial functions to produce metabolites were being unravelled and recognised. Indeed functional convergence on specific microbially produced metabolites are a feature of both disease and of the aging process. We hypothesised that host and dietary produced factors e.g. BAs and FAs, are central to human aging and age-related disease processes, because these outputs will be altered as the gut microbiota change. The overall aim of the studies presented here is to investigate whether this is the case. We therefore aimed to establish the base line and potential roles of microbially derived signalling molecules (BAs and FAs) in these processes. Central to the hypothesis was whether diet or bacterial intervention might alter the host-microbe dialogue in aging and age-related diseases.

In chapter 3, we chose two different disease states that are associated with GI discomfort and examined whether metabolites and microbial function were altered in individuals with Parkinson's Disease (PD), compared to age matched control volunteers. This work further established the relationship between beneficial treatments and microbial metabolic responses in humans. A second neurologically related disease, Autism Spectrum Disorder (ASD), had already been investigated similarilarly with a pre-established role for BAs determined in the murine ASD BTBR *T*$^{+}$ *Itpr3*^{tf}/J (BTBR model) (Golubeva *et al.,* 2017). We hypothesized that specific microbes and microbial activities could re-adjust metabolite balance to impact gut physiology and potentially improve ASD behaviour symptomatically. We aimed to test this hypothesis through bacterial interventions. The intention was to validate reversal of previously characterized BA deficits and tryptophan metabolism, and with

the potential to improve gastrointestinal and behavioural symptomatically in this BTBR mouse model of ASD.

In chapter 4, we connected BA moieties, particular those prominent in the aging spectrum, to the nematode model of aging. The rationale for this work is the clear relationship between steroid molecules (DAs and BAs) and the conservation of signalling pathways, particularly those DA activated systems that equate to BA receptors, between humans and *C. elegans*. We hypothesized that specific BAs, made through microbial modification, may have beneficial lifespan extending effects on *C. elegans,* that may be of importance in higher organisms and in humans.

Finally, diet and calorific input are pivotal factors in aging. The diet for *C. elegans* is bacteria and the laboratory strain of choice is uracil deficient *E.coli* OP50. The role of the gut microbiota as a cause and a consequence of disease is well established. There is considerable evidence in the literature to point to single strain outgrowth in the gut that impact the hallmarks of aging. We hypothesized, in chapter 5, that a disease associated gut pathobiont *E.coli* HM605 may impact *C. elegans* lifespan and development negatively. We therefore aimed to elucidate and understand the phenotypic and genetic nature of the bacteria and the nematode relationship in the context of pathobiont induced specific aging.

Chapter 2 – Materials and Methods

2.1 Bacterial

2.1.1 Bacterial strains

All bacterial strains used in this thesis are listed in *Table 2.1* below. *E. coli* OP50 is a uracil auxotroph that is typically used as a food source for *C. elegans* in the laboratory. Adherent invasive *E. coli* HM605, whose genome has been sequenced (Clarke *et al.,* 2011) and all *E. coli* HM605 deletion mutations were provided by Dr David Clarke (*Table 2.1*). Dr Adam O'Driscoll described HM605 deletion mutations construction using P1 transduction (Silhavy *et al.,* 1976). Mutant alleles, for transduction, were obtained from donor strains of the Keio collection (Baba *et al.,* 2006). The Keio collection included 3985 non-essential single-gene deletion mutations of *E.coli* K-12 strain BW25113, they were selected as kanamycin-resistant (Km^R) colonies (Baba *et al.,* 2006). The introduction of a plasmid containing phage λ Red recombinase and synthetic (PCR-generated) DNA allowed the generation of mutant genes, and a helper plasmid encoding the FLP recombinase was used to eliminate resistant genes (Datsenko and Wanner, 2000; Baba *et al.,* 2006).

2.1.2 Bacterial Culture

All *E. coli* strains were maintained as frozen stocks at -80°C. They were prepared as follows: overnight cultures were obtained by growing a single colony of each *E. coli* in 10 ml of their respective media for 18 hours, at 220 rpm, at 37°C. *E. coli* HM605 was grown and maintained aerobically, with antibiotic supplementation (100 μg/ml Ampicillin). *E. coli* HM605 deletion mutations were grown and maintained with antibiotic supplementation (100 μg/ml Ampicillin and 50 μg/ml Kanamycin) in Lysogeny, or Luria-Bertani (LB), broth (Sigma) with 0.015 g/ml technical agar (Neogen) for solid media where required. 750 μl of overnight cultures were added to the same volume of 40% (v/v) glycerol (Sigma) for storage at -80°C. Every week, a frozen stock was accessed and re-streaked individually onto its relevant solid medium. All media and solutions were same day sterilised by autoclaving for 15 mins at 121°C.

***Table 2.1*: Bacterial strains applied to this thesis.**

Strain name	Genotype/ Deposition of sequence/ Description of KO	Origin	Purpose
E. coli OP50	OP50 *ura*	*Caenorhabditis* Genetics Center (CGC, University of Minnesota), (Brenner 1974) Nematode Associated	Normal Food Source for *C. elegans*
E. coli HM605	CADZ01000154	(Clarke *et al*. 2011) Adherent-Invasive *Escherichia coli* (AIEC) strain, human gut	Potential pathogen to *C. elegans*
E. coli HM605 Δ*arcA::km*	Mutation introduced into a wide variety of aerobic enzymes under anaerobic conditions.	Clarke Lab (unpublished)	*C. elegans* longevity and lifespan
E. coli HM605 Δ*atoC::km*	Mutation introduced into atoDAEB operon, leading to short chain fatty acid catabolism and activation of the poly-(R)-3-hydroxybutyrate (cPHB) biosynthetic pathway. Involved in the regulation of motility and chemotaxis via transcriptional induction of the flagellar regulon.	Clarke Lab (unpublished)	*C. elegans* longevity and lifespan
E. coli HM605 Δ*baeR::km*	Mutation introduced into envelope stress response. Activates expression of periplasmic chaperone spy in response to spheroplast formation. Also, baeR could have a role in the activation of CRISPR-Cas casABCDE-ygbT-ygbF operon.	Clarke Lab (unpublished)	*C. elegans* longevity and lifespan
E. coli HM605 Δ*cheY::km*	Mutation introduced into the transmission of sensory signals from the chemoreceptors to the flagellar motors. In active form - enhanced binding switches component, FliM, at the flagellar motor to induce change from anticlockwise to clockwise flagellar rotation.	Clarke Lab (unpublished)	*C. elegans* longevity and lifespan
E. *coli* HM605 Δ*cpxR::km*	Mutation introduced into the binding of stationary phase cells to hydrophobic surfaces, part of the process of biofilm formation.	Clarke Lab (unpublished)	*C. elegans* longevity and lifespan
E. coli HM605 Δ*creB::km*	Mutation introduced into catabolic regulation.	Clarke Lab (unpublished)	*C. elegans* longevity and lifespan
E. coli HM605 Δ*dcuR::km*	Mutation introduced into the C4-dicarboxylate-stimulated regulation of the genes encoding the anaerobic fumarate respiratory system. Weakly regulates the aerobic C4-dicarboxylate transporter dctA.	Clarke Lab (unpublished)	*C. elegans* longevity and lifespan
E. coli HM605 Δ*dsbA::km*	Mutation introduced into a periplasmic thiol:disulfide oxidoreductase.	Clarke Lab (unpublished)	*C. elegans* longevity and lifespan
E. coli HM605 Δ*evgA::km*	Mutation introduced into the expression of emrKY operon and yfdX. Also involved in the control of the expression of a multidrug efflux operon.	Clarke Lab (unpublished)	*C. elegans* longevity and lifespan
E. coli HM605 Δ*fhiA::km*	Mutation introduced into expression of the formate dehydrogenase H and hydrogenase-3 structural genes. Also activates expression of hyf operon (encodes the silent hydrogenase-4 gene cluster).	Clarke Lab (unpublished)	*C. elegans* longevity and lifespan
E. coli HM605 Δ*fimH::km*	Mutation introduced into a component of fimbriae that allow for cell adhesion.	Clarke Lab (unpublished)	*C. elegans* longevity and lifespan
E. coli HM605 Δ*flgG::km*	Mutation introduced into one of the four proteins that comprise the rod section of the basal-body assembly of the flagellar motor.	Clarke Lab (unpublished)	*C. elegans* longevity and lifespan
E. coli HM605 Δ*icd ::km*	Mutation introduced into Isocitrate dehydrogenase – a TCA enzyme.	Clarke Lab (unpublished)	*C. elegans* longevity and lifespan
E. coli HM605 Δ*narL::km*	Mutation introduced into nitrate reductase and formate dehydrogenase-N operons and represses the transcription of fumarate reductase operon.	Clarke Lab (unpublished)	*C. elegans* longevity and lifespan

E. coli HM605 Δ*narP::km*	Mutation introduced into expression of nitrate reductase and formate dehydrogenase-N operons and represses transcription of fumarate reductase operon in response to nitrate/nitrite induction signal.	Clarke Lab (unpublished)	*C. elegans* longevity and lifespan
E. coli HM605 Δ*ompR::km*	Mutation introduced into N-terminus of the protein required for transcriptional expression of both major outer membrane protein genes ompF and ompC. C-terminus is involved in the multimerization of the ompR protein.	Clarke Lab (unpublished)	*C. elegans* longevity and lifespan
E. coli HM605 Δ*pfkAB::km*	Mutation introduced into 6-phosphofructokinase I (PFK I) + 6-phosphofructokinase II.	Clarke Lab (unpublished)	*C. elegans* longevity and lifespan
E. coli HM605 Δ*phoB::km*	Mutation introduced into the positive regulator of the phosphate regulon.	Clarke Lab (unpublished)	*C. elegans* longevity and lifespan
E. coli HM605 Δ*phoP::km*	Mutation introduced into the adaptation of low Mg^{2+} environments and the control of acid resistant genes. Mediates magnesium influx to the cytosol by activation of MgtA.	Clarke Lab (unpublished)	*C. elegans* longevity and lifespan
E. coli HM605 Δ*qseB::km*	Mutation introduced into the activation of transcription of FIhDC, in doing so activates the flagella regulon.	Clarke Lab (unpublished)	*C. elegans* longevity and lifespan
E. coli HM605 Δ*rcsB::km*	Mutation introduced into a response regulator. Regulates expression of genes such as biofilm formation, cell division, colonic acid capsule synthesis and outer membrane protein synthesis.	Clarke Lab (unpublished)	*C. elegans* longevity and lifespan
E. coli HM605 Δ*rssB::km*	Mutation introduced into turnover of sigma S factor by promoting proteolysis in growing cells. Also regulated mRNA polyadenylation pathway during stationary phase.	Clarke Lab (unpublished)	*C. elegans* longevity and lifespan
E.coli HM605 Δ*rtsA::km*	Mutation introduced into sequence specific DNA binding.	Clarke Lab (unpublished)	*C. elegans* longevity and lifespan
E. coli HM605 Δ*torR::km*	Mutation introduced into anaerobic utilization of trimethylamine-N-oxide (TMAO).	Clarke Lab (unpublished)	*C. elegans* longevity and lifespan
E. coli HM605 Δ*uhpA::km*	Mutation introduced into part of the UhpABC signalling cascade that controls the expression of the hexose phosphate transporter UhpT. Activates the transcription of the uhpT gene.	Clarke Lab (unpublished)	*C. elegans* longevity and lifespan
E. coli HM605 Δ*uvrY::km*	Mutation introduced into carbon metabolism. Activates transcription of untranslated csrB RNA and of barA in an autoregulatory loop.	Clarke Lab (unpublished)	*C. elegans* longevity and lifespan
E. coli HM605 Δ*yehT::km*	Mutation introduced into DNA-binding.	Clarke Lab (unpublished)	*C. elegans* longevity and lifespan
E. coli HM605 Δ*ypdB::km*	Mutation introduced into expression of yhjX by binding to its promoter region.	Clarke Lab (unpublished)	*C. elegans* longevity and lifespan
E. coli HM605 Δ*zraR::km*	Mutation introduced into sigma-54 to regulating the expression of zraP. Also involved in the positive regulation of the expression of zraSR operon.	Clarke Lab (unpublished)	*C. elegans* longevity and lifespan
APC1486 *Lactobacilus salivarius* P0003	Isolated from a porcine model by Sarah L. Long (Joyce Lab, Unpublished). It was isolated and characterized on the basis of bile acid metabolism by bile salt hydrolase enzymes and pyrogen free nature.	Joyce Lab Porcine Faeces (Unpublished)	Bile acid modification in a murine Autism spectrum disorder model (ASD)
APC 2715 *Bifidobacterium adolescentis*	This strain was selected from the APC strain collection housed at Teagasc, Moorepark. It was selected on the basis of bile acid metabolism by bile salt hydrolase enzymes and pyrogen free nature.	APC Strain collection	Bile acid modification in a murine Autism spectrum disorder model (ASD)

All strains are relevant to the different study chapters in this thesis. The source, genotype and information relating to their origin and their purpose are listed. Strains were sourced from the Joyce Lab or the Clarke lab. All mutations were kanamycin linked and they were constructed by

Clarke Lab (Adam O'Driscoll). P0003 was isolated by Dr Sarah L. Long (Joyce Lab). P0003 and APC2715 are under IDF.

Lactobacillus salivarius and *Bifidobacterium adolescentis* were maintained as frozen stocks at -80°C. They were prepared as follows: overnight cultures were obtained by growing a single colony of each in 10 ml De Man, Rogosa and Sharpe (MRS) broth (DIFCO), anaerobically (Aerocult cartridge) with an Aerocult for 18 hours at 37°C. *Bifidobacterium adolescentis* was grown and also maintained anaerobically in MRS but supplemented with 0.05% (w/v) cysteine hydrochloride (Sigma). 750 μl of overnight cultures were added to the same volume of 40% (v/v) glycerol (Sigma) for storage at -80°C. Every week, a frozen stock was accessed and re-streaked individually onto MRS agar, with/without 0.05% (w/v) cysteine hydrochloride (Sigma). MRS (DIFCO) broth and agar were sterilised by autoclaving for 15 mins at 121°C.

For daily inoculum preparation to animals (see Section 2.3.3 below) $7.5x10^8$ CFU/ml of each bacterial treatment *Lactobacillus salivarius* and *Bifidobacterium adolescentis* were prepared as follows: 0.05 OD_{600} per ml from a relevant overnight culture was added to 500 ml conical flask containing 200 ml MRS (DIFCO) broth (for *Lactobacillus salivarius*) and MRS broth with 0.05% (w/v) cysteine hydrochloride (Sigma) (for *Bifidobacterium adolescentis*) and allowed to grow anaerobically for 18 hours at 37°C in anaerobic chamber. Thereafter growth was examined (OD_{600}), calculated and centrifuged, twice at room temperature with resuspension in PBS between centrifugation, before $7.5x10^9$ CFU/ml bacterial suspension was constructed in 50mls of PBS containing 25% (v/v) glycerol (Sigma). Following centrifugation at RT, the pellet was washed with 0.8% (w/v) NaCl and centrifuged again. Finally bacteria were resuspended in fresh, sterile water containing 0.8% NaCl then added to animal drinking solution (450 ml sterile water with 0.8% (w/v) NaCl) at $7.5x10^8$ CFU/ml for each bacterial treatment either *Lactobacillus salivarius* (P0003) or *Bifidobacterium adolescentis* (APC2715), while a similar solution but without bacteria was offered to control animals. Serial dilutions of each overnight culture was performed to quality control and assess CFU and to confirm strain integrity.

2.1.3 Bacterial Growth Assessment

Assessment of comparative normal growth was examined for *E. coli* OP50, *E. coli* HM605 and associated variants (deletion mutations) Δ*fim*H, Δ*dsb*A, Δ*flg*G and Δ*bae*R. Comparative growth was also examined for *E. coli* OP50 treated with and without BAs (Sigma) Cholic Acid (CA), Deoxycholic Acid (DCA), Chenodeoxycholic Acid (CDCA), Ursodeoxycholic Acid (UDCA) and Lithocholic Acid (LCA) each at 1 mM, 5 mM and 10 mM. Three individual colonies (*n*=3) of *E. coli* were inoculated into 50 ml falcon tubes containing 10 ml LB with or without the appropriate antibiotic (*Table 2.1* above). The cultures were allowed to grow aerobically for 18 hours at 37°C. Then 0.1 OD_{600} per ml of each *E. coli* was individually inoculated into individual wells of a 96-well plate (Greiner) containing fresh LB broth, in triplicate, to a total volume of 200 μl. Negative controls (*n*=3) contained LB alone to a total volume of 200 μl. Given the difference in colouration due to BAs, a further set of negative controls (*n*=3) for each BA concentration were applied to act as respective blanks, where no bacteria were inoculated (total volume of 200 μl).

These 96 well plates were sealed with a gas semi-permeable membrane seal (Sigma). A ThermoScientific Multiskan FC photometer with SkanIt software 2.5.1 operated at 37°C to detect absorbance (bacterial growth) at 600nm over 24 hours, commencing at T=0 (25 timepoints in total). Correspondence to growth on solid media was assessed at time zero (T_0) when serial dilution was performed from 20 μl 1 OD_{600} per ml of each culture (*n*=3) into 180 μl of 1X Phosphate buffered saline (PBS) to provide a 1:10 dilution $=10^{-1}$. A subsequent series of dilution by a log fold in PBS was performed until a dilution of 10^{-8} was achieved. 10 μl of each dilution was transferred onto LB agar, and the colony forming units (CFUs) were assessed 18 hours later. The same dilution series and application to solid agar as well as culture conditions was performed following growth of these same cultures to 24 hours (T_{24}).

2.2 *Caenorhabditis elegans* manipulation

2.2.1 Growth and Maintenance of nematode *Caenorhabditis elegans*

All *Caenorhabditis elegans* (*C. elegans*) strains: N2 Bristol (wild isolate), SS104 *glp-4(bn2)* I, CF1139 *daf-16(mu86) I; muIs61 [(pKL78) daf16::GFP + rol-6(su1006)]* and

CB1370 *daf-2(e1370)* III, were purchased from the Caenorhabditis Genetics Center (CGC, University of Minnesota), which is funded by NIH Office of Research Infrastructure Programs (P40 OD010440) (*Table 2.2*).

Table 2.2: *Caenorhabditis elegans* strains applied to this study.

Strain name	Genotype/ Deposition of sequence/ Description of KO	Origin	Purpose
N2 Bristol	Wild-type isolate	Caenorhabditis Genetics Center (CGC, University of Minnesota), (Brenner 1974)	Wild-type *C. elegans* Maintained at 25°C
SS104	*glp-4(bn2)* I	Caenorhabditis Genetics Center (CGC, University of Minnesota)	Temperature-sensitive *C. elegans* mutant. Egg-laying at 16°C, non egg-laying at 25°C resulting in synchronous adult cultures
CF1139	*daf-16(mu86)* I; *muIs61 [(pKL78) daf16::GFP + rol-6(su1006)]*	Caenorhabditis Genetics Center (CGC, University of Minnesota)	DAF-16 GFP fluorescence *C. elegans* mutant. Maintained at 25°C
CB1370	*daf-2(e1370)* III	Caenorhabditis Genetics Center (CGC, University of Minnesota) (Kenyon *et al.*, 1993)	Long-lived *C. elegans daf-2* mutant Maintained at 16°C

C. elegans strains (*Table 2.2*) were grown and maintained on Nematode Growth Media (NGM) agar comprising of 3 g/L NaCl, 17 g/L agar, 2.5 g/L tryptone, 25 ml/L 1 M KPO_4 (pH 6.0 (108.3 g KH_2PO_4, 35.6 g K_2HPO_4, dH_2O to 1 litre). The media was autoclaved for sterility for 15 mins at 121°C, then cooled before addition of sterile 1 ml/L 1 M $CaCl_2$, 1 ml/L 5 mg/ml cholesterol in ethanol, 1 ml/L 1 M $MgSO_4$ (Sigma) and pouring into sterile plastic agar plates or dishes. Solid cooled media was seeded for 24 hours with 100 μl of 1 OD_{600} per ml *E. coli* OP50 at 37°C, unless otherwise stated. *C. elegans* N2 and CF1139 strains were grown at 25°C, while *C. elegans* SS104 was maintained at 16°C to facilitate egg laying (Brenner 1974; Kenyon *et al.* 1993). Strains were maintained by a process called "chunking" whereby a sterile scalpel was applied to remove a piece of agar where dauer juveniles were allowed to develop (approximately two weeks for N2 and CF1139 strain and approximately two weeks for *C. elegans* SS104). Chunking routinely maintained stocks by sterile transfer of a 1 cm slice/chunk of dauer stage enriched agar onto fresh NGM agar pre-seeded with 100 μl 1 OD_{600} per ml *E. coli* OP50 incubated at 37ºC for 18 hours. Frozen stocks were constructed by washing five NGM agar plates containing predominately *C. elegans* L1 and L2 larvae, with sterile 1 ml S Buffer (129 ml 0.05 M K_2HPO_4, 871 ml 0.05 M KH_2PO_4, 5.85 g NaCl (Sigma)) and dispensing 750 μl into a sterile 2 ml cryovial tubes

(Merck (Sigma)), containing the same volume of sterile 30% (v/v) glycerol. The solutions were mixed then stored at -80°C. To revive cultures, frozen stocks were allowed thaw slowly at RT and were plated on 90 X 15 mm NGM agar plates pre-seeded with 100 µl 1 OD_{600} per ml OP50 that were allowed to grow at 37°C for 18 hours (Stiernagle 2006). Nematodes were allowed to recover, grow and develop to different stages at 25°C or at 16°C, depending on the assay type.

2.2.2 *Caenorhabditis elegans* Stage Synchronisation

To obtain age-synchronous cultures of *C. elegans*, approximately 15 NGM agar plates enriched for gravid reproductive adults (RAs) were washed and removed into 10 ml cold sterile M9 buffer (3 g/L KH_2PO_4, 6 g/L Na_2HPO_4, 5 g/L NaCl, 1 ml 1 M $MgSO_4$ (Sigma) (*Figure 2.1*). The suspension was placed on ice for 5 mins to allow the RAs to settle to the bottom of the tube. The RAs were washed with 10 ml M9 buffer and bleached (7.5 ml dH_2O, 1.5 ml Bleach (15% sodium hypochlorite (Sigma)) and 2 ml of 4N NaOH (Sigma)) until 70% of RAs had cracked (approximately 5 mins). The falcon tube was filled with 10X PBS (sterile Sigma) to neutralise the bleach and subjected to centrifugation for 3 mins at 1500 rpm (ThermoScientific Sorvall ST 8R centrifuge). The supernatant (S/N) was aspirated leaving a 5 ml volume, the nematodes were rinsed twice with 45 mls M9 buffer, leaving behind 10% of worm suspension each time, the process was repeated 3 times. Finally, 25 ml of sterile 60% (w/v) sucrose solution (Fisher) was added to the worm suspension and subjected to centrifugation for 3 minutes at 1500 rpm. The eggs were removed from the meniscus, using a glass Pasteur pipette, leaving behind carcass and other debris, the eggs were washed with sterile M9 buffer and subjected to centrifugation for 3 minutes at 1500 rpm, a process that was repeated twice. The supernatant was aspirated to leave 5 ml containing the egg suspension. This was agitated gently overnight at a low velocity, (< 110 rpm), to facilitate viable egg hatching, the temperature of incubation depended on the *C. elegans* strain, therefore 25°C was applied for N2 and for CF1139 strains and 16°C for SS104 strain. After 24 - 48 hours the majority of eggs had hatched to yield viable L1 larvae. All L1s were pipetted onto NGM plates pre-seeded with 100 µl 1 OD_{600} per ml *E. coli* OP50 NGM agar until L4 stage for adulthood assays.

Otherwise, for other assays, (lifespan or development), L1s were counted and 30 were applied to each NGM agar plate, pre-seeded with *E. coli* OP50 with the relevant chemical treatments. The methodology applied sterile conditions and was adapted from the protocol of Henry Ancell, Dr Andre Pires da Silva's lab.

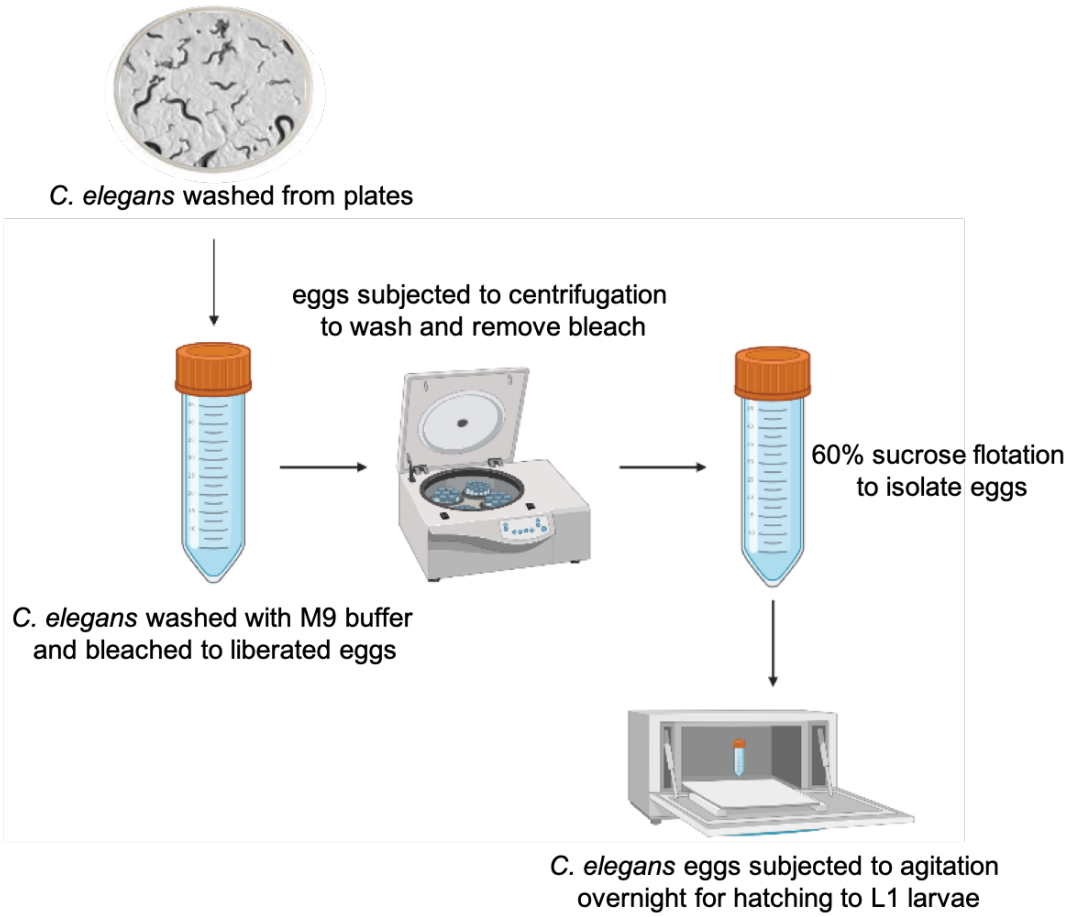


Figure 2.1: **Schematic representation outlining main steps of synchronisation of *C. elegans*.** Created with BioRender.com.

2.2.3 *Caenorhabditis elegans* Lifespan Assessment Assay

To examine *C. elegans* length of life, lifespan assays were performed with either 30 age-synchronised L1 larvae, to investigate early life, or 30 L4 larvae, to examine effects in adulthood. Nematodes were added to control NGM agar plates pre-seeded with 50 µl 1 OD_{600} per ml *E. coli* OP50 for 24 hours at 37°C, unless otherwise stated. Treatment plates were also prepared (*n*=3) using NGM agar plates pre-seeded with 50 µl 1 OD_{600} per ml *E. coli* OP50 for 24 hours at 37°C, containing specific BAs Cholic Acid (CA), Deoxycholic Acid (DCA), Chenodeoxycholic Acid (CDCA), Ursodeoxycholic Acid (UDCA) and Lithocholic Acid (LCA) at concentrations: 1 mM, 5 mM and 10 mM. In investigations of *E. coli* strains, NGM agar plates were pre-seeded with 100 µl 1 OD_{600} per ml of *E. coli* OP50, *E. coli* HM605, and *E. coli* HM605 deletion mutations: Δ*fim*H, Δ*dsb*A, Δ*flg*G and Δ*bae*R, for 24 hours at 37°C. All incubations were maintained at 25°C and *C. elegans* were counted every second day (Olympus SZX16 stereo microscope). Live *C. elegans* were initially determined based on movement, when motility began to slow, *C. elegans* were lightly probed to determine whether live or dead based on reactive movement. *C. elegans* were monitored until 0% survival, indicating length (in days) of life.

2.2.4 *Caenorhabditis elegans* Development Assay

The development of *C. elegans* exposed to WT, different variants of *E. coli*, as well as to different BAs was examined. 30 age-synchronised L1s (prepared as described in section 2.2.2 above) were inoculated onto NGM agar plates (containing chemicals as indicated or not) pre-seeded with either, 100 µl 1 OD_{600} per ml *E. coli* OP50, or a variant *E. coli* strain thereof, for 24 hours at 37°C, unless otherwise stated. Treatment plates were prepared on NGM agar plates containing specific BAs: CA, DCA, CDCA, UDCA and LCA at concentrations: 1 mM, 5 mM and 10 mM, pre-seeded with 100 µl 1 OD_{600} per ml *E. coli* OP50 for 24 hours at 37°C. N2 wild-type *C. elegans* strain were maintained at 25°C and SS104 temperature-sensitive *C. elegans* strain were maintained at 16°C. Eggs through to RA were examined based on size, and consultation with WormAtlas (https://www.wormatlas.org/hermaphrodite/introduction/mainframe.htm).

C. elegans were washed from an NGM agar plates (*n*=3) with 5 ml sterile M9 buffer every 2 days and transferred to a 50 ml falcon. 5 µl of worm suspension was taken onto a microscope slide (*n*=3) and the stages and their number was determined and recorded by microscopy (Olympus SZX16 stereo microscope).

2.2.5 Bacterial Colonisation Assessment Assay in *Caenorhabditis elegans*

To determine the level of colonisation of *E. coli* HM605 WT and variants (Δ*fim*H and Δ*dsb*A) in the *C. elegans* gut, 30 age-synchronised surface sterilized L4s (as described in section 2.2.2 above), were transferred onto control NGM agar (60 X 15 mm plates) again pre-seeded with 50 µl 1 OD_{600} per ml *E. coli* OP50 whilst treatment plates were pre-seeded with 50 µl 1 OD_{600} per ml one of *E. coli* HM605, or deletion mutations Δ*fim*H or Δ*dsb*A, (*n*=3) unless otherwise stated. Plates were maintained at 25°C. *C. elegans* colonisation interrogation was performed on day 2, day 4 and day 6 of *C. elegans* adulthood.

C. elegans colonisation displacement was investigated as follows: 30 hermaphrodite reproductive adult *C. elegans* were hand-picked from 12 NGM solid agar media independently, those pre-seeded with four different *E. coli*: *E. coli* OP50 (*n*=3), *E. coli* HM605 (*n*=3), *E. coli* HM605 Δ*fim*H (*n*=3), and HM605 Δ*dsb*A (*n*=3). Nematodes were allowed to grow for one of 2, 4 or 6 days in the presence of these WT and variant bacterial strains, at 25°C. The nematodes were collected and washed from the plates then added into 1.5 ml Eppendorf tubes containing 1 ml pre-chilled sterile M9 buffer. *C. elegans* were allowed to settled to the bottom of the tube by brief centrifugation for 5 seconds at 3,000 rpm (Eppendorf Centrifuge 5424). Worms were washed three times with sterile M9 buffer - 1 ml. Finally, *C. elegans* were resuspended in 1 ml of M9 buffer containing 1 mM sodium azide (Sigma) for 30 minutes, to inhibit pharyngeal pumping and expulsion of bacteria from the nematode intestine. The mixture was treated with 100 µg/ml gentamicin and incubated at 37°C for 1 hour to kill exterior bacteria. *C. elegans* were washed three times by removing 750 µl of buffer and restoring the volume to 1 ml with sterile M9 buffer. For each treatment 10 individual *C. elegans* were picked and placed into individual Eppendorfs containing 200 µl of sterile M9 buffer. To determine the number of external colony-

forming units (CFU) 10 µl sample was taken from the solution and spread directly to LB agar (with and without antibiotic where relevant). Approximately 400 mg of sterile 1.0-mm silicon carbide particles (Biospec Products) were then added to each tube and the mixture was subject to vortexing for one minute to disrupt the *C. elegans* while leaving the bacteria unaffected. The resulting lysate was plated onto LB agar with and without antibiotic, as relevant at 100 µg/ml Ampicillin and 50 µg/ml Kanamycin. The plates were incubated overnight at 37°C and colonies were counted the following day. Methodology was adapted from (Mellies *et al.,* 2006; Simonsen *et al.,* 2011b).

2.2.6 Gene expression detected by Fluorescence Microscopy in *Caenorhabditis elegans*

Fluorescence microscopy was used to determine gene expression from selected promoters fused to GFP in the nematode. *C. elegans* strain CF1139, *daf-16(mu86) I; muIs61 [(pKL78) daf16::GFP + rol-6(su1006)]* was used in this study to reflect the expression of the DAF-16 protein, associated to longevity, according to the methodology of (Shaham, 2006).

Briefly, *C. elegans* CF1139 L4 larvae were age-synchronised (as described section 2.2.2 above), then mounted for microscopy visualisation. The mounts were prepared first, by addition of a drop of 2% (w/v) agarose onto the centre of a clean microscope slide. To flatten the agarose to a circle of about 0.4 mm, the agarose was pressed down gently with another clean slide. The top slide was removed once the agarose had solidified.

Negative controls were applied with no treatment, bar the normal bacterial exposure to *E. coli* OP50. Positive controls for *C. elegans* CF1139 (*n*=3) were transferred for pre-treatment to 1.5 ml Eppendorf and treated with either 20 mM β-Hydroxybutyrate (Merck) for 1 hour (Edwards *et al.,* 2014) or 20 µM Juglone (Merck) for 1 hour (Abbas and Wink, 2010) then placed at 37°C for 15 minutes (Abbas and Wink, 2010). To stain the nuclei, Hoechst 33342 (1 µg/ml; Merck (Sigma)) was added to all nematodes and allowed to stand for 15 minutes at RT. All worms were then anaesthetised by addition of 2 µl 10 mM sodium azide (NaN_3, Sigma) to each tube

followed by a 20 minutes incubation. 3 worms were added to each mount and images (10X and 40X) were obtained by fluorescent microscope (Leica DM LB2; Leica Co.) Conditions were: Excitation filter BP 470/40, Suppression filter BP 525/50 and Dichromatic mirror 500. ImageJ software was used to analyse the level of fluorescence from each of the images and against the background for each.

2.2.7 RNA Extraction from *Caenorhabditis elegans*

The methodology applied to RNA extraction is adapted from (Pryor *et al.,* 2019), who kindly sent their protocol. RNaseZAP™ (Sigma) was used to wipe all surfaces and equipment to remove RNases before starting. Briefly, ~1000 age-synchronised *C. elegans* SS104 L4 larvae (to determine ~1000 worms, 5 µl of *C. elegans* SS104 L4 larvae suspension was pipetted onto a microscope slide (*n*=3) and the number of worms determined by microscopy (Olympus SZX16 stereo microscope), to determine total worms 5 µl multipled up and ~1000 worms determined) prepared according to section 2.2.2 above, were transferred onto 9 cm NGM plates pre-seeded with 100 µl *E.coli* OP50 (1 OD_{600} per ml *)* for 24 hours at 37°C and, where indicated, NGM plates also contained specific BAs: CA, DCA, CDCA, UDCA and LCA at concentrations of 1 mM, 5 mM and 10 mM.

For investigations on the effects of *E. coli* strains (WT and variants), NGM agar plates were pre-seeded independently with 100 µl of HM605 or the mutants Δ*fim*H and Δ*dsb*A (all grown to a density of 1 OD_{600} per ml) (*n*=3). 1,000 *C. elegans* nematodes were added to each plate and incubated at 25°C to maintain synchronous cultures. After 48 hours, *C. elegans* SS104 adults were collected from plates in 2 ml of sterile nuclease-free water and transferred to 2 ml Eppendorfs. *C. elegans* SS104 were allowed settle to the bottom of the tube and the top solution was carefully decanted without disturbing the settled pellet. 1 ml of RNAse free water was added to wash away the remaining *E. coli* and *C. elegans* SS104 were allowed to re-settle to the bottom, this process was repeated twice. Samples were then prepared for lysis as follows: samples were placed on ice for 3 minutes to allow *C. elegans* SS104 to compact together. RNAse free water was removed on the final wash so that *C. elegans* SS104 were suspended in approximately 100 µl of liquid. Next, 1 µl

Proteinase K (20 mg/ml) was added to each sample (10 µl for every 1 ml DNA/RNA (Zymo research)). In addition 1 µl of Protector RNase Inhibitor (2,000U - Sigma Aldrich) was added to each sample. Sterile lysing beads (Roche™) were added to each Eppendorf and samples were beaten using a MagNA Lyser instrument (Roche™) for four x 30 second rounds of beating at 6000 rpm, with 30 seconds of cooling between each round. Phenol, as 500 µl of TRI Reagent (Merck (Sigma)), was added to each sample, followed by vortexing for 10 seconds. Each sample was then flash frozen in liquid nitrogen and stored at -80°C until RNA extraction.

The frozen samples were transferred to 37°C in a water bath to thaw and this freeze/thaw process was repeated twice more. Then samples were subjected to centrifugation for 2 minutes at 14000 rpm at 4°C (ThermoScientific Sorvall Legend Micro 17R centrifuge). Samples were transferred to RNase-free tubes. Total RNA was extracted, on ice, using a Direct-zol RNA Miniprep kit (Zymo Research). Exactly 1 volume of 100% ethanol was added to each tube. The mixture was transferred into a Zymo-Spin™ IICR Column in a collection tube and subjected to centrifugation (in two steps of 500 µl each). The column was transferred into a new clean, sterile, RNAse free collection tube and the flow-through was safely discarded. 400 µl RNA Wash Buffer was added to the column, then eluted by centrifugation, before the addition of 6 µl of DNase I and 75 µl DNA Digestion Buffer to each tube, then the solutions were mixed by gentle inversion. The mixture was added directly to the column matrix, incubated at RT for 15 minutes, before addition of 400 µl Direct-zol™ RNA PreWash Buffer was added to the column and subjected to centrifugation to ensure complete removal of the wash buffer. The column was carefully transferred into an RNase-free tube. The PreWash Buffer step was repeated. 700 µl Direct-zol™ RNA Wash Buffer was added to the column, and centrifuged, to ensure complete removal of the wash buffer. The column was transferred carefully into an RNase-free Eppendorf tube. The RNA was eluted by adding 30 µl of DNase/RNase free water directly to the column matrix before centrifugation for 1 minute at 14000 rpm at 4°C. 1 µl of Protector RNase Inhibitor (2,000U - Sigma Aldrich) was added into each sample.

2.2.8 *Caenorhabditis elegans* RNA Quality Assessment and Sequence Alignment

To ensure the total RNA extracted was sufficient for sequencing, the quality and quantity of the total RNA was measured. NanoDrop 2000 spectrophotometer (ThermoScientific), Qubit™ RNA HS Assay kit (Biosciences) and 2100 BioAnalyzer (Aligent) were used to examine total RNA quality and quantity. BioAnalyzer analysis was conducted by Ribomaps using Agilent RNA 6000 Nano Kit (5067-1511). Quality samples are expected to return RIN values of 4.6-9.4. Quality assured samples were shipped on dry ice to Genewiz Europe (Leipzig, Germany) for RNA sequencing.

RNA libraries were prepared by Genwiz: Illumina, strand-specific RNA-seq with PolyA selection. Sequencing was performed on Illumina NovaSeq 2x150 bp sequencing, 10M (million) read pairs generated per sample. Dr Darren Fenton checked raw read quality using FastQC; aligned clean reads to the *C. elegans* reference genome WBcel235; Read counts were obtained at gene level using STAR with *C. elegans* WBcel235 Ensembl annotation; Transcription analysis was performed at the gene level using DESeq2; Only genes with counts per million > 1 in all samples in at least one experimental group were considered for analysis. Differential gene expression was considered significant if p value < 0.05 compared to control. Genes were mapped to annotations using their Entrez Gene IDs. Significance of pathways was determined by PANTHER (Ashburner *et al.,* 2000; Mi *et al.,* 2019; Consortium, 2021), with an FDR < 0.05.

2.3 Ultra Performance Liquid Chromatography Tandem Mass Spectrometer (UPLC-TMS) of Bile Acids and Fatty Acids

2.3.1 Clinical study of metabolites in Parkinson's Disease

Plasma samples: 29 Parkinson's Disease (PD) patients and 10 control volunteers, were obtained and stored at -80°C. Stool samples from 40 PD patients and 41 control volunteers were obtained and stored at -80°C. Both the plasma and stool samples from PD patients and the plasma from control volunteers were acquired from the movement disorder clinics at St. Finbarr's Hospital, Cork (Geriatrician led), and Cork University Hospital, Cork (Neurology led). Control volunteers were carers or family members of the PD patients attending these clinics. The stool samples from control

volunteers were acquired from the ELDERMET (https://link.springer.com/referenceworkentry/10.1007/978-1-4614-6418-1_94-1?noAccess=true) project in University College Cork (Claesson *et al.,* 2012). These studies were approved by the Clinical Research Ethics Committee of the Cork Teaching Hospitals (CREC). Staff at the Centre for Gerontology and Rehabilitation, St. Finbarr's Hospital, Cork conducted all participant recruitment, assessments and phlebotomy. Informed consent was acquired from all participants. The plasma samples had already been obtained for a research study investigating a potential biomarker in Parkinson's disease – AKT Activity in Parkinson's disease. The findings of this study, which include these plasma samples, are reported in Sandra Yeomans MSc research thesis (submitted June 2016, data not shown here). Ellen Joyce analysed the levels of BAs present in these plasma samples, which had been extracted and quantified by Dr. Susan Joyce for the purpose of this study and they are reported in her MSc thesis (submitted September 2016, data not shown here). Further interrogation of BAs and added analysis of FAs of these plasma samples were performed and are reported here, see *Table 2.3*.

BAs and FAs were extracted from the stool samples and analysed by Ultra Performance Liquid Chromatography Tandem Mass Spectrometry (UPLC-TMS). 15 µl of deuterated Chenodeoxycholic Acid (CDCAd4) and Cholic Acid (CAd4), as internal standards, were added to 100 mg human stool samples. The stool samples were then transferred to a tube containing 1.4 mm diameter ceramic beads (MagNA Lyser tubes, Roche Diagnostics). 800 µl of ice-cold 50% (v/v) methanol was added to each tube before four 30 second rounds of beating at 6000 rpm were performed by a MagNA Lyser instrument (Roche^{TM}), with 30 seconds of cooling the samples between each round. Samples were incubated at -20°C for 30 minutes, and subjected to centrifugation for 10 minutes at 10,000 rpm. The top layer was transferred to a fresh tube and dried under vacuum. The pellets were then resuspended in 1 ml ice-cold 5% (v/v) formic acid 95% (v/v) acetonitrile solution. The samples were mixed by a vortex for 1 min, followed by agitation for 1 hour at RT. The samples were further subjected to centrifugation for 5 minutes at 10,000 rpm and the top layer was transferred to a fresh tube and dried under vacuum. The pellets were resuspended in 150 µl of 50% (v/v) methanol, let sit in the dark for 10-15 minutes, and were then

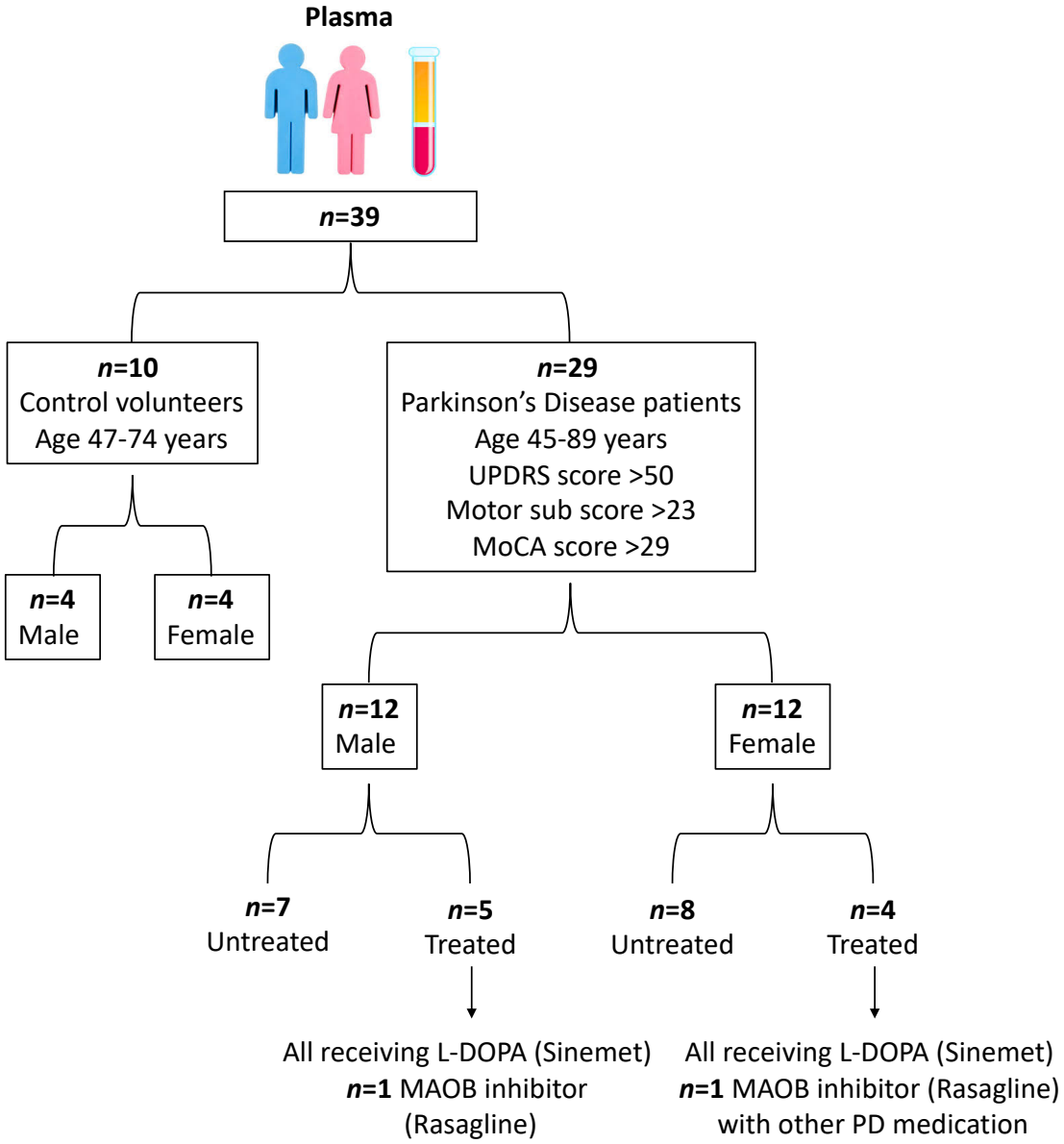
subjected to centrifugation for 5 minutes at 10,000 rpm. The top layer was transferred to a fresh glass vial (Waters Ltd) and 5 µl of each group of samples was transferred into one glass vial labelled "pool". The extracted BAs and FAs were present in the suspension (*Table 2.9 and 2.10*). The suspension was analysed by Ultra Performance Liquid Chromatography Tandem Mass Spectrometry (*Figure 2.2*). All plasma and stool data was analysed using TargetLynx™. Medical Student Arnav Mahajan analysed the FA data by TargetLynx™, see *Table 2.3*.

***Table 2.3*: Persons involved in the clinical study of metabolites in Parkinson's Disease.**

Plasma				
Sample Collection	**Bile acid and Fatty acid Extraction**	**Bile acid TargetLynx™ Analysis**	**Fatty acid TargetLynx™ Analysis**	**Bile acid and Fatty acid Graphing and Analysis**
Prof. Cora O'Neill	Dr Susan Joyce	Christina Killian	Christina Killian	Christina Killian
Faeces				
Sample Collection	**Bile acid and Fatty acid Extraction**	**Bile acid TargetLynx™ Analysis**	**Fatty acid TargetLynx™ Analysis**	**Bile acid and Fatty acid Graphing and Analysis**
Prof. Cora O'Neill (PD samples) Prof. Paul O'Toole (ELDERMET samples)	Christina Killian	Christina Killian	Arnav Mahajan	Christina Killian

Christina Killian conducted BA and FA TargetLynx™ , graphical and overall analysis of all plasma samples. Christina Killian performed BA and FA extractraction from stool samples, BA TargetLynx™ , BA and FA graphical and overall analysis of all stool samples. Prof. Cora O'Neill and Prof. Paul O'Toole undertook sample collection. Dr Susan Joyce extracted BAs and FAs from plasma samples. Mr. Arnav Mahajan conducted FA TargetLynx™ analysis.

a.


Plasma
n=39
n=10
Control volunteers
Age 47-74 years
n=29
Parkinson's Disease patients
Age 45-89 years
UPDRS score >50
Motor sub score >23
MoCA score >29
n=4
Male
n=4
Female
n=12
Male
n=12
Female
n=7
Untreated
n=5
Treated
n=8
Untreated
n=4
Treated
All receiving L-DOPA (Sinemet)
n=1 MAOB inhibitor
(Rasagline)
All receiving L-DOPA (Sinemet)
n=1 MAOB inhibitor (Rasagline)
with other PD medication

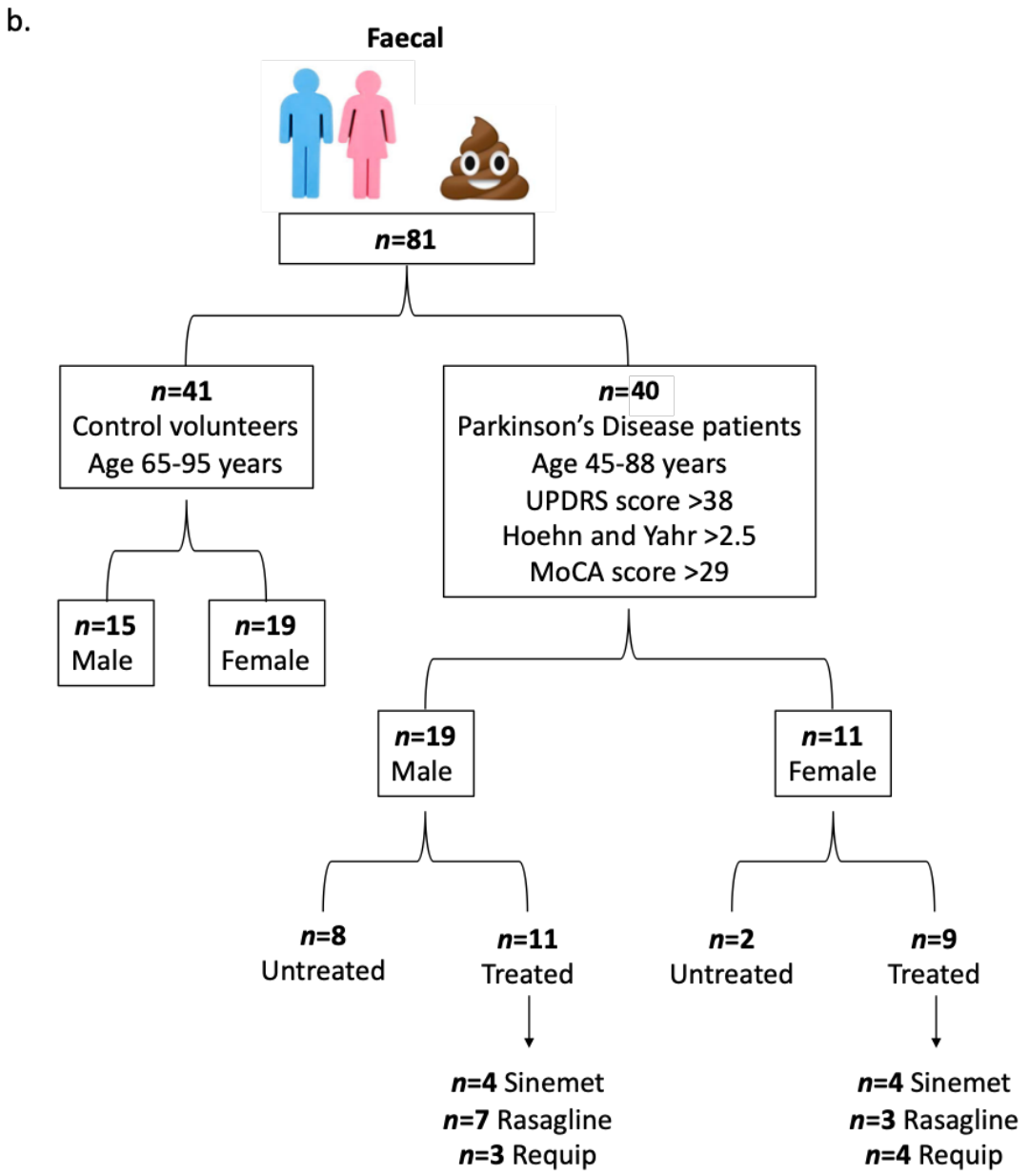


Figure 2.2: **Schematic representation of the Parkinson's Disease (a) plasma and (b) faecal study and analysis.**

Both PD patients and control volunteers were age matched. Plasma PD patients age range 45 – 89 years, control volunteers age range 47 – 74 years. Stool PD patients age range 45 – 88 years, control volunteers age range 65 – 95 years. 29 PD and 10 control plasma samples are included in this analysis. 40 PD patients and 41 control volunteer stool samples were extracted; 30 PD stool samples are included in this analysis as only baseline samples are included - repeated measures were excluded.

34 control stool samples are included in this analysis. 4 samples had no clinical information and so were removed from the analysis. Of the 29 PD patient plasma samples, 11 of these PD patients were receiving PD medication; of the 30 PD patient stool samples, 20 of these PD patients were receiving PD medication; these PD patients are termed 'treated' PD patients. The remaining 18 PD plasma and 10 PD stool patients are termed 'untreated' PD patients and were not receiving PD medication at the time of sample collection. For the stool sample study, only the baseline faecal sample were included in this analysis. Tables *2.4* and *2.5* include assessment of patient disease severity using the Unified Parkinson's Disease Rating Scale (UPDRS). This scale measures disease severity by assessing daily living, scoring from 0-147, measuring best to worst, which comprises of four sub scores: the first score, part I, assesses non-motor experiences; the second scoring, part II, involves motor experiences; the third sub scoring is Part III, which is a motor examination; and finally, part IV assesses motor complications (Society, 2008). Motor sub scoring, was assessed in the plasma samples, with scoring from 1-56, measuring best to worst. Cognitive function was assessed using the Montreal Cognitive Assessment (MoCA) scale with scores from 0-30, no impairment indicated with scores >26 (Nasreddine *et al.,* 2005). The Hoehn and Yahr scale, was also used to determine the level of motor function and overall balance/gait, scoring from stage 1-5 from best-worst (Hoehn and Yahr, 1967) (*Table 2.4* and *Table 2.5*).

***Table 2.4*: Clinical demographics of Parkinson's Disease patients where plasma was obtained.**

ID	Gender	Age	Dopamine modulating therapy	Total daily levodopa dose (or equivalent)	Dopamine modulating medication	Total UPDRS score	UPDRS Motor sub-score	MoCA score
Control								
CON_P1	-	-	-	-	-	-	-	-
CON_P5	M	55	-	-	-	-	-	-
CON_P9	M	74	-	-	-	-	-	-
CON_P14	M	70	-	-	-	-	-	-
CON_P16	M	64	-	-	-	-	-	-
CON_P20	F	70	-	-	-	-	-	-
CON_P41	-	-	-	-	-	-	-	-
CON_P42	F	59	-	-	-	-	-	-
CON_P44	F	47	-	-	-	-	-	-
CON_P45	F	71	-	-	-	-	-	-
Parkinson's Disease								
CON_P3	M	78	L-DOPA	300 mg	Sinemet	13	7	24
CON_P8	M	75	L-DOPA	400 mg	Sinemet	12	8	21
CON_P11	F	88	L-DOPA	300 mg	Sinemet	21		19
CON_P15	-	-	-	-	-	-	-	-
CON_P17	M	75	L-DOPA/ Anticholinergic/ MAOB inhibitor	400 mg	Sinemet/ Procyclidine/ Rasagiline	30	13	19
CON_P19	F	75	L-DOPA	200 mg	Sinemet	2	0	22
CON_P25	F	59	Dopamine agonist/ Anticholinergic/ MAOB inhibitor	700 mg	Requip/ Procyclidine/ Rasagiline	21	8	29
CON_P29	-	-	-	-	-	-	-	-
CON_P34	M	58	MAOB inhibitor	100mg	Rasagiline	-	-	-
CON_P37	M	68	L-DOPA	150 mg	Sinemet	35	15	29
CON_P38	F	84	Dopamine agonist/ L-DOPA/ MAOB inhibitor	250 mg	Requip/ Sinemet/ Rasagiline	40	16	20
CON_P2	F	74	-	-	-	7	5	27
CON_P4	-	-	-	-	-	-	-	-
CON_P7	M	46	-	-	-	8	4	28
CON_P10	F	78	-	-	-	16	10	21
CON_P12	F	89	-	-	-	50	23	15
CON_P13	M	56	-	-	-	38	17	26
CON_P18	-	-	-	-	-	-	-	-
CON_P21	M	75	-	-	-	15	10	26
CON_P22	F	81	-	-	-	-	-	21
CON_P26	M	45	-	-	-	18	10	25
CON_P30	F	80	-	-	-	20	11	17
CON_P31	F	80	-	-	-	25	15	22
CON_P35	M	69	-	-	-	15	11	15
CON_P39	M	64	-	-	-	5	4	17
CON_P40	F	62	-	-	-	22	14	17
CON_P43	M	68	-	-	-	27	12	14
CON_P46	F	71	-	-	-	4	3	25
CON_P48	-	-	-	-	-	-	-	-

Clinical demographics of plasma samples obtained from control volunteers and Parkinson's Disease patients included in this study, including: Gender; Age; Parkinson's Disease medication; Unified Parkinson's Disease Rating Scale (UPDRS) score, ranging from 2, which is very low, to 50 out of a possible 147; Unified Parkinson's Disease Rating Scale (UPDRS) motor sub-score ranging from 0, which is none, to 23 of a possible 56; and Montreal Cognitive Assessment (MoCA) scale score ranging from 14, which is low, to 29 out of a possible 30. A '-' in a cell represents where there is no information applicable/given.

***Table 2.5*: Clinical demographics of faecal samples obtained from ELDERMET control volunteers and Parkinson's Disease patients included in this study.**

ID	Gender	Age	PD Medication	MoCA Score	UPDRS Score	Hoehn & Yahr Staging
Control						
EM803	F	70	-	-	-	-
IEM12	F	72	-	-	-	-
IEM21	M	89	-	-	-	-
IEM23	M	83	-	-	-	-
EM709	F	71	-	-	-	-
IEM29	F	95	-	-	-	-
EM601	M	74	-	-	-	-
EM818	F	70	-	-	-	-
IEM30	F	82	-	-	-	-
EM612	F	75	-	-	-	-
EM603	M	69	-	-	-	-
IEM2	M	72	-	-	-	-
IEM001	F	82	-	-	-	-
EM436	M	78	-	-	-	-
EM707	M	76	-	-	-	-
EM815	F	74	-	-	-	-
IEM4	F	79	-	-	-	-
IEM27	F	93	-	-	-	-
EM604	F	74	-	-	-	-
EM613	M	66	-	-	-	-
EM816	M	75	-	-	-	-
IEM11	F	93	-	-	-	-
IEM26	F	90	-	-	-	-
EM602	M	65	-	-	-	-
EM813	F	71	-	-	-	-
EM606	F	75	-	-	-	-
EM609	F	69	-	-	-	-
EM009	M	71	-	-	-	-
IEM10	M	78	-	-	-	-
IEM3	M	84	-	-	-	-
EM814	M	77	-	-	-	-
EM703	M	92	-	-	-	-
IEM13	F	90	-	-	-	-
EM821	F	68	-	-	-	-
Parkinson's Disease						
ALTP43	F	51	Requip; Rasagiline	-	-	-
AILTP38	F	81	Sinemet	-	-	-
AILTP31	F	62	Requip	17	22	1
AILTI2 (6months)	M	78	Sinemet	-	-	-
AILTP40	M	75	Requip; Rasagiline	-	-	-
AILTI35 (base)	M	55	Requip	28	10	1
AILTI46	F	83	Rasagiline	-	-	-
AILTI10 (base)	F	75	Sinemet 62.5	22	2	1
AILTP49	M	70	Sinemet ; Rasagiline	-	-	-
AILTI7 (base)	M	75	Sinemet; Rasagiline	23 /19	30	2.5
AILTP45	F	61	Requip	-	-	-
AILTI56	F	74	Sinemet and more	-	-	-
AILTP39	M	51	Rasagiline	-	-	-
AILTI53	M	73	Sinemet; Benserazide	-	-	-
AILTI14 (base)	M	63	Requip	-	-	2
AILTI19 (base)	M	58	Rasagiline	-	-	-
AILTP41 41	M	52	Rasagiline	-	-	-
AILTI 11 (base)	F	59	Requip; Rasagiline, Procyclidine	29	21	1
AILTI1 1 year	F	74	Sinemet 25; Biperiden	-	-	-
AILTI51	M	73	Sinemet ; Rasagiline	-	-	-
AILTI8 (base)	M	74	Untreated	-	-	-
AILTP9 (base)	M	75	Untreated	22	20	1.5
AILTI17 (base)	M	56	Untreated	26/23	38	2
ALTI21 (6 months)	M	75	Untreated	26	15	1
AILTI28 (base)	M	69	Untreated	15	15	1
AILTI13 (base)	F	88	Untreated	21	16	1
AILTP20 (base)	F	80	Untreated	26	17	1
AILTI30 (base)	M	64	Untreated	17	5	1
AILTI23 (base)	M	45	Untreated	25	18	1
AILTI12 (6 weeks)	M	46	Untreated	26	8	1

Clinical demographics of faecal samples obtained from ELDERMET control volunteers and Parkinson's Disease patients included in this study, including: Gender; Age; Parkinson's Disease medication; Montreal Cognitive Assessment (MoCA) scale score, ranging from 15, which is low, to 29 out of a possible 30; Unified Parkinson's Disease Rating Scale (UPDRS) score, ranging from 2, which is very low, to 38 out of a possible 147; and Hoehn and Yahr scale score, which are between stages 1 and 2.5 out of a possible 5 stages. A '-' in a cell represents where there is no information applicable/given.

2.3.2 Animal study of metabolites in Autism Spectrum Disorder

This work is a continuation study from (Golubeva *et al.,* 2017). In collaboration with the Joyce Lab, Golubeva *et al*., (2017) found that the relative abundance of bile-metabolizing *Bifidobacterium* and *Blautia* species are reduced in BTBR T^{+} *Itpr3*^{tf}/J mice (BTBR). BTBR (Black and Tan BRachyury) mice are a mouse model of Autism Spectrum Disorder (ASD) and have mutations a^{t} (nonagouti; black and tan), *Itpr3*^{tf} (inositol 1,4,5-triphosphate receptor 3; tufted), and *T* (brachyury) (Golubeva *et al.,* 2017). This continuation study focuses on bacterial interventions, *Lactobacillus salivarius* P0003 and *Bifidobacterium adolescentis* 2715, as strains to target deficiencies central to functions of gut microbiota in BTBR T^{+} *Itpr3*^{tf}/J mice. The intention of this continuation study was to reverse BA deficits and tryptophan metabolism, with the potential to improve gastrointestinal and behavioural symptomatically in the BTBR mouse model of ASD.

2.3.3 Design of Autism Microbial Interference study

Control adult male mice C57BL/6 J (Envigo, UK) and BTBR T^{+} *Itpr3*^{tf}/J (BTBR) (The Jackson Laboratory, US) under a 12 h light-dark cycle, were group housed. Water and standard rodent chow were available to mice *ad libitum*. All experiments were conducted in accordance with European guidelines following approval by University College Cork Animal Ethics Experimentation Committee. The study was conducted for a period of 9 weeks. There were 4 independent treatments and 12 mice per treatment group. In the (1) control group C57BL/6 J mice (C57_Veh), there were 3 mice per cage, with 6 mice per cohort. In the BTBR T^{+} *Itpr3*^{tf}/J groups (BTBR), there were 2 mice per cage, 2-6 mice per litter and 6 mice per cohort. BTBR mice were divided into 3 groups: (2) control group BTBR_Veh, those treated with (3)

Lactobacillus salivarius strain P0003, BTBR_P0003 and those treated with (4) *Bifidobacterium adolescentis* strain 2715, BTBR_2715 (*Table 2.6* and *Table 2.7*).

***Table 2.6*: Cage, Litter and Cohort information on control groups C57BL/6 J and BTBR T^{+} *Itpr3*^{tf}/J mice.**

Animal ID	Cage	Litter	Group	Cohort
1.1	1	Envigo, delivered 04.08.17	C57_Veh	1
1.2			C57_Veh	1
1.3			C57_Veh	1
2.1	2	Envigo, delivered 04.08.17	C57_Veh	1
2.2			C57_Veh	1
2.3			C57_Veh	1
11.1	11	Envigo, delivered 18.08.17	C57_Veh	2
11.2			C57_Veh	2
11.3			C57_Veh	2
12.1	12	Envigo, delivered 18.08.17	C57_Veh	2
12.2			C57_Veh	2
12.3			C57_Veh	2
3.1	3	14.0	BTBR_Veh	1
3.2			BTBR_Veh	1
4.1	4	11.2	BTBR_Veh	1
4.2			BTBR_Veh	1
5.1	5	12.2	BTBR_Veh	1
5.2			BTBR_Veh	1
13.1	13	17.2	BTBR_Veh	2
13.2			BTBR_Veh	2
14.1	14	19.2	BTBR_Veh	2
14.2			BTBR_Veh	2
15.1	15	17.3	BTBR_Veh	2
15.2			BTBR_Veh	2

This bacterial intervention experiment was split across two cohorts, all mice were male aged 6 weeks at baseline week 0, and aged 15 weeks at endpoint week 9. BTBR T^{+} *Itpr3*^{tf}/J mice from each litter were divided into bacterial intervention groups (BTBR_2715 and BTBR_P0003) and control groups (BTBR_Veh). There were a total of 22 cages with 2 BTBR T^{+} *Itpr3*^{tf}/J animals per cage and 3 C57BL/6 J animals per cage. Plasma samples from animal IDs: 2.1, 12.1, and 15.2 were not obtained for this study. Plasma samples from animal IDs: 1.2, and 4.1, and faecal samples, for all weeks, for animal IDs: 11.3, 14.2 and 15.2, were considered outliers and not included in this study.

***Table 2.7*: Cage, Litter and Cohort information on BTBR mice of treatment groups *Bifidobacterium adolescentis* strain APC2715 and *Lactobacillus salivarius* P0003.**

Animal ID	Cage	Litter	Group	Cohort
6.1	6	12.1	BTBR_2715	1
6.2			BTBR_2715	1
7.1	7	14.0	BTBR_2715	1
7.2			BTBR_2715	1
8.1	8	15.0	BTBR_2715	1
8.2			BTBR_2715	1
16.1	16	16.1	BTBR_2715	2
16.2			BTBR_2715	2
17.1	17	17.2	BTBR_2715	2
17.2			BTBR_2715	2
18.1	18	19.2	BTBR_2715	2
18.2			BTBR_2715	2
9.1	9	12.1+14.0	BTBR_P0003	1
9.2			BTBR_P0003	1
10.1	10	11.1	BTBR_P0003	1
10.2			BTBR_P0003	1
19.1	19	16.3	BTBR_P0003	2
19.2			BTBR_P0003	2
20.1	20	19.2	BTBR_P0003	2
20.2			BTBR_P0003	2
21.1	21	18.1	BTBR_P0003	2
21.2			BTBR_P0003	2
22.1	22	16.3+17.3	BTBR_P0003	2
22.2			BTBR_P0003	2

This bacterial intervention experiment was split across two cohorts, all mice were male aged 6 weeks at baseline week 0, and aged 15 weeks at endpoint week 9. BTBR T^{+} *Itpr3*^{tf}/J mice from each litter were divided into bacterial intervention groups (BTBR_2715 and BTBR_P0003) and control groups (BTBR_Veh). There were a total of 22 cages with 2 BTBR T^{+} *Itpr3*^{tf}/J animals per cage and 3 C57BL/6 J animals per cage. Plasma samples from animal IDs: 10.1, 6.2, and 17.1 were not obtained for this study. Plasma samples from animal ID: 18.2, and faecal samples, for all weeks, for animal IDs: 19.2 and 6.1, were considered outliers and not included in this study.

Postdoctoral researcher Sarah Long isolated and screened different strains of *Bifidobacterium* and *Lactobacillus* for BA alterations relevant to different aspects of the BTBR mice model. *Bifidobacterium adolescentis* strain APC 2715 came from the APC Microbiome Institute (APC, Cork, Ireland) and *Lactobacillus salivarius* strain P0003 was isolated by Dr Sarah L. Long. *Bifidobacterium adolescentis* strain APC 2715

and *Lactobacillus salivarius* strain P0003 were chosen based on their antimicrobial and bile-salt hydrolase (BSH) activity. The strains were prepared as described in section 2.1.2 above and presented to animals in drinking water with 0.8% (w/v) NaCl daily and for BTBR_P0003 and BTBR_2715 mice at $7.5x10^8$ CFU/ml (work alternated between Dr Sarah L. Long, Elaine O'Shea and Christina Killian (Joyce Lab, UCC) and Dr Anna Golubeva and Dr Eoin Sherwin (Cryan Lab, UCC)). At week 0, week 2 and week 9, faecal samples from all mice were collected, BAs were extracted as detailed in section 2.3.5 below. At endpoint (week 9) plasma samples were taken, BAs were extracted as detailed in section 2.3.5 below, for UPLC-TMS (*Figure 2.3*). All animal handling was carried out by the Cryan Lab, UCC. Behavioural assessment such as social interaction, intestinal transit and intestinal permeability, were conducted by Dr Golubeva (Cryan Lab, UCC), see *Table 2.8*.

***Table 2.8*: Persons involved in the animal study of metabolites in Autism Spectrum Disorder.**

***Lactobacillus salivarius* strain P0003 *Bifidobacterium adolescentis* strain APC 2715**	**Daily Bacterial Preparation**	**Faecal and Plasma Sample Collection and Storage**	**Bile acid Extraction**	**Bile acid TargetLynx™ Analysis**	**Bile acid Graphing and Analysis**	**Behavioural Assessment**
Isolated and screened by Dr Sarah L. Long	Dr Sarah Long, Elaine O'Shea, Christina Killian (Joyce Lab, UCC) Dr Anna Golubeva, Dr Eoin Sherwin (Cryan Lab, UCC)	Dr Anna Golubeva, Dr Eoin Sherwin (Cryan Lab, UCC) Dr Sarah Long, Christina Killian (Joyce Lab, UCC)	Christina Killian	Christina Killian	Christina Killian	Dr Anna Golubeva, Dr Eoin Sherwin (Cryan Lab, UCC)

Christina Killian conducted BA extraction, TargetLynx™, graphical and overall analysis of all plasma and stool samples. Dr Sarah L. Long isolated and screened *Bifidobacterium* and *Lactobacillus* strains, determining *Lactobacillus salivarius* strain P0003 and *Bifidobacterium adolescentis* strain APC 2715 for this study. Dr Sarah L. Long, Elaine O'Shea, Christina Killian (Joyce Lab, UCC), Dr Anna Golubeva and Dr Eoin Sherwin (Cryan Lab, UCC) prepared *Lactobacillus salivarius* strain P0003 and *Bifidobacterium adolescentis* strain APC 2715 daily. Dr Anna Golubeva and Dr Eoin Sherwin (Cryan Lab, UCC), Dr Sarah L. Long and Christina Killian (Joyce Lab, UCC) collected and stored stool and plasma samples. Dr Anna Golubeva and Dr Eoin Sherwin (Cryan Lab, UCC) conducted all behavioural assessemnts.

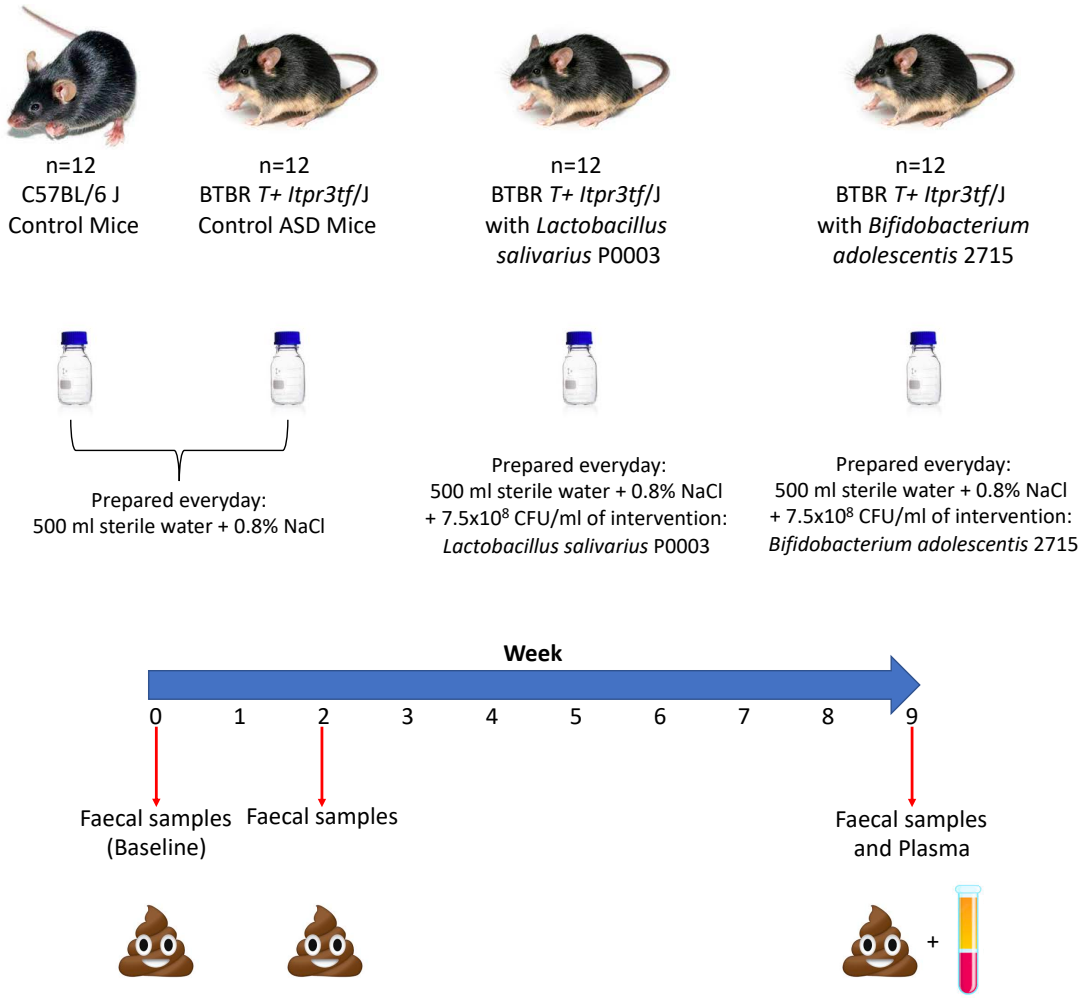


Figure 2.3: **Schematic representation of the Autism Spectrum Disorder (ASD) murine study design.** ASD model mice BTBR T^{+} Itpr3^{tf}/J, were treated everyday with 7.5x10^{8} CFU/ml bacterial interventions either *Lactobacillus salivarius* strain P0003 or *Bifidobacterium adolescentis* strain APC 2715, for 9 weeks. Plasma and faecal BAs were extracted and analysed using UPLC-TMS.

2.3.4 Clinical study of metabolites in Bacterial and *Caenorhabditis elegans*

To investigate the concentration of BA present in *E. coli* OP50 and ingested by *C. elegans* strain SS104, the following experiment was set up: After growth for 48 h, *E. coli* OP50 was scraped off agar plates and resuspended in 1 ml 1X PBS. Each treated *E. coli* OP50 was normalised to 1 OD_{600} per ml, pelleted by centrifuging for 5 minutes at 10,000 rpm, and washed (x2) in 1X PBS. *E. coli* OP50 was resuspended in 200 µl 1X PBS and chilled on ice for 15 minutes. 60 synchronised *C. elegans* SS104 L1s were placed on 100 µl 1 OD_{600} per ml *E. coli* OP50 NGM Agar containing the relevant amino

acid or BA treatment. Plates were incubated at 16°C for 2 weeks. *C. elegans* SS104 were washed off plates with 5 ml 1X PBS and centrifuged at 1500 rpm for 5 minutes. *C. elegans* SS104 were counted under microscope to confirm total number of *C. elegans* SS104 in each treatment. *C. elegans* SS104 were centrifuged 5 minutes 1500 rpm and washed twice in 1X PBS. SS104 were resuspended in 300 μl 1X PBS. Both *E. coli* OP50 and *C. elegans* SS104 were sonicated (AMP=30, CYCLE=0.8) for 3 rounds of 20 second pulses. The samples were on ice at all times.

2.3.5 Bile Acid and Fatty Acid Extraction

In order to extract BAs and FAs for UPLC-MS analysis, two initially different approaches were taken for stool and plasma samples, before the systems then converged. Briefly for stool samples: an internal standard (15 μl (0.5 μg) deuterated Chenodeoxycholic Acid (CDCAd4) and deuterated Cholic Acid (CAd4)) was added to 100 mg human sample and 25 mg mouse sample in an Eppendorf containing 1.4 mm diameter ceramic beads (MagNA Lyser tubes, Roche Diagnostics). The internal standard allows extraction efficiency assessment and normalization between samples for exact quantity determinations relative to a standard curve for each individual BA listed in *Table 2.9* (Joyce *et al.,* 2014). 800 μl of ice-cold 50% (v/v) methanol was added to each tube before four 30 second rounds of beating at 6000 rpm were performed using a MagNA Lyser instrument (Roche™), with 30 seconds of cooling between each bead beating round. For plasma samples, 100 μl was taken and spiked as described above with internal standards (IS) before addition of 500 μl of ice-cold 50% (v/v) methanol and 1 minute of vortexing. Samples irrespective of type, were placed at -20°C for 30 minutes then subjected to centrifugation for 10 minutes at 10,000 rpm at RT. The supernatant was transferred to fresh Eppendorf and dried under vacuum.

Where extractions were performed with bacteria and with nematode material, the internal standard (15 μl of deuterated Chenodeoxycholic Acid (CDCAd4), Cholic Acid (CAd4) and deuterated Deoxycholic Acid (DCAd4)) was added to 1 OD_{600} *E. coli* OP50 in 200 μl LB and to a specific counted number of *C. elegans* SS104 in 200 μl 1xPBS. 200 μl 100% methanol was added to each *E. coli* OP50 and *C. elegans* SS104 sample.

All samples were mixed by vortex for 30 seconds then incubated at -20°C for 1 hour and subjected to centrifugation for 10 minutes at 10,000 rpm. The supernatant was transferred to fresh Eppendorf to dry under vacuum.

The dried pellets for all samples were resuspended in 1 ml ice-cold 5% (v/v) formic acid 95% (v/v) acetonitrile solution. The samples were then mixed by vortex for 1 minute, followed by agitation for 1 hour at RT, then subjected to centrifugation for 5 minutes at 10,000 rpm and the supernatant was transferred to a fresh tube and dried under vacuum. Individual pellets were resuspended in 150 μl of 50% (v/v) methanol, then subjected to centrifugation for 5 minutes at 10,000 rpm. The supernatant was transferred to a glass vial (Waters Ltd) and 5 μl of each samples was transferred into one glass vial labelled “pool”. The extracted BAs and FAs were present are listed in *Table 2.9 and 2.10*. 5 μl of each samples was injected for Ultra Performance Liquid Chromatography Tandem Mass Spectrometry (*Figure 2.4*).

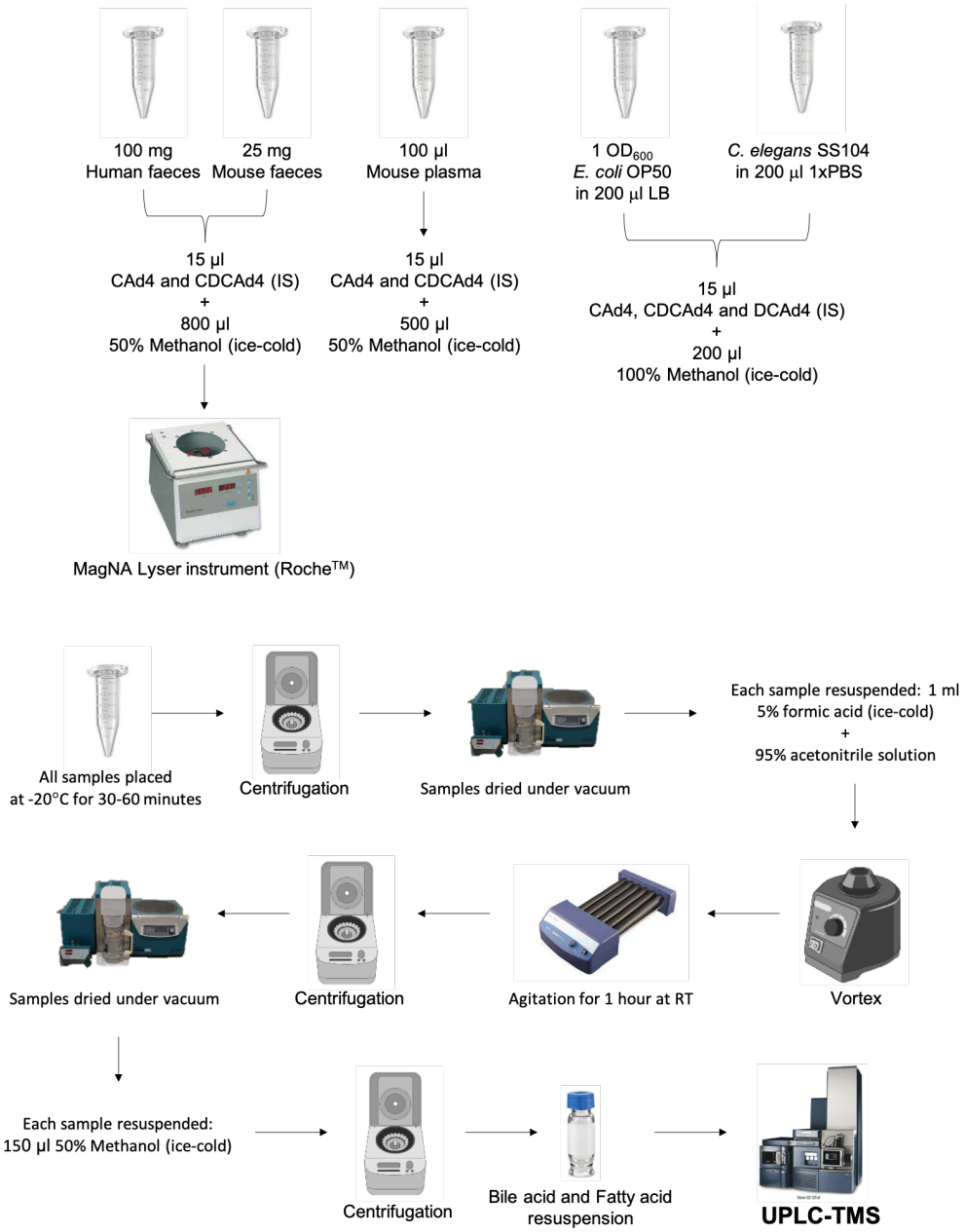


Figure 2.4: **Schematic representation of Bile Acid and Fatty Acid extraction process.**

Created with BioRender.com

***Table 2.9*: Bile Acids analysed in this study.**

	Analyte	Abbreviation	$[MW]^{-H}$	Neutral Formula
	Taurine	Taurine	124.0068	$C_2H_7NO_3S$
1°	Cholic Acid	CA	407.2797	$C_{24}H_{40}O_5$
	Chenodeoxycholic Acid	CDCA	391.2848	$C_{24}H_{40}O_4$
2°	Deoxycholic Acid	DCA	391.2848	$C_{24}H_{40}O_4$
	Ursodeoxycholic Acid	UDCA	391.2848	$C_{24}H_{40}O_4$
	Lithocholic Acid	LCA	375.2899	$C_{24}H_{40}O_3$
Free	Dehydrocholic Acid	DHCA	401.2328	$C_{24}H_{34}O_5$
	Hyodeoxycholic Acid	HDCA	391.2848	$C_{24}H_{40}O_4$
	Hyocholic Acid	HCA	407.2797	$C_{24}H_{40}O_5$
	7-Ketolithocholic Acid	7KLCA	389.2692	$C_{24}H_{38}O_4$
	Murocholic Acid	MurCA	391.2848	$C_{24}H_{40}O_4$
Tauro-conjugated	Taurocholic Acid	TCA	514.2838	$C_{26}H_{45}NO_7S$
	Taurohyocholic Acid	THCA	514.2838	$C_{26}H_{45}NO_7S$
	Taurochenodeoxycholic Acid	TCDCA	498.2889	$C_{26}H_{45}NO_6S$
	Tauroursodeoxycholic Acid	TUDCA	498.2889	$C_{26}H_{45}NO_6S$
	Taurodeoxycholic Acid	TDCA	498.2889	$C_{26}H_{45}NO_6S$
	Taurohyodeoxycholic Acid	THDCA	498.2889	$C_{26}H_{45}NO_6S$
	Taurolithocholic Acid	TLCA	482.294	$C_{26}H_{45}NO_5S$
Glyco-conjugated	Glycocholic Acid	GCA	464.301214	$C_{26}H_{43}NO_6$
	Glycohyocholic Acid	GHCA	464.301214	$C_{26}H_{43}NO_6$
	Glycohyodeoxycholic Acid	GHDCA	448.306298	$C_{26}H_{43}NO_5$
	Glycochenodeoxycholic Acid	GCDCA	448.306298	$C_{26}H_{43}NO_5$
	Glycoursodeoxycholic Acid	GUDCA	448.306298	$C_{26}H_{43}NO_5$
	Glycodeoxycholic Acid	GDCA	448.306298	$C_{26}H_{43}NO_5$
	Glycolithocholic Acid	GLCA	432.311384	$C_{26}H_{43}NO_4$
Muricholics	α-Muricholic Acid	α-MCA	407.2797	$C_{24}H_{40}O_5$
	β-Muricholic Acid	β-MCA	407.2797	$C_{24}H_{40}O_5$
	ω-Muricholic Acid	ω-MCA	407.2797	$C_{24}H_{40}O_5$
	Tauro α-Muricholic Acid	α-TMCA	514.2838	$C_{26}H_{45}NO_7S$
	Tauro β-Muricholic Acid	β-TMCA	514.2838	$C_{26}H_{45}NO_7S$
	Tauro ω-Muricholic Acid	ω-TMCA	514.2838	$C_{26}H_{45}NO_7S$
Internal Standards	Cholic Acid d4	CA d4	411.3049	$C_{24}H_{36}D_4O_5$
	Chenodeoxycholic Acid d4	CDCA d4	395.3099	$C_{24}H_{36}D_4O_4$
	Deoxycholic Acid d4	DCA d4	395.3099	$C_{24}H_{36}D_4O_4$

List of analytes examined showing their molecular weight, neutral formulas and grouped classifications. Deuterated Bile Acids: CAd4, CDCAd4 and DCAd4 were the internal standards used to determine extraction efficiency and normalisation of the analytes detected. Adapted from Dr Sarah Long's thesis (2019).

***Table 2.10*: Fatty Acids analysed in this study.**

	Analyte	Abbreviation	$[MW]^{-H}$	Neutral Formula
	Pyruvic acid	PyrA	87.0082	$C_3H_4O_3$
	Lactic acid	LacA	89.0239	$C_3H_6O_3$
Medium-Chain	Hexanoic Acid	HexA	115.0759	$C_6H_{12}O_2$
	Heptanoic Acid	HepA	129.0916	$C_7H_{14}O_2$
	Octanoic Acid	OctA	143.1072	$C_8H_{16}O_2$
Long-Chain	Myristic Acid	MyrA	227.2011	$C_{14}H_{28}O_2$
	Palmitoleic Acid	PalmitoA	253.2168	$C_{16}H_{30}O_2$
	Palmitic Acid	PalA	255.2324	$C_{16}H_{32}O_2$
	α/γ-Linolelic Acid	α/γ-LinoA	277.2168	$C_{18}H_{30}O_2$
	Linoleic Acid	LinA	279.2324	$C_{18}H_{32}O_2$
	Oleic Acid	OlA	281.2481	$C_{18}H_{34}O_2$
	Stearic Acid	SteA	283.2637	$C_{18}H_{36}O_2$
	cis-5,8,11,14,17-Eicosapentaenoic acid	EPA	301.2168	$C_{20}H_{30}O_2$
	Arachidonic Acid	AA	303.2324	$C_{20}H_{32}O_2$
	Cis-11-Eicosenoic acid	EA	309.2794	$C_{20}H_{38}O_2$
Very-Long Chain	Cis-4,7,10,13,16,19-Docosahexaenoic acid	DHA	327.2324	$C_{22}H_{32}O_2$
Internal Standards	Cholic Acid d4	CA d4	411.3049	$C_{24}H_{36}D_4O_5$
	Chenodeoxycholic Acid d4	CDCA d4	395.3099	$C_{24}H_{36}D_4O_4$

List of fatty acid analytes examined showing their molecular weight, neutral formulas and grouped classifications. Deuterated Bile Acids: CAd4, CDCAd4 and DCAd4 were the internal standards used to

determine extraction efficiency and normalisation of the analytes detected. Adapted from Dr Sarah Long's thesis (2019).

2.3.6 Ultra Performance Liquid Chromatography Tandem Mass Spectrometry Chemicals

All chemicals were purchased from Merck (previously Sigma-Aldrich), unless otherwise stated. Fisher Scientific (Fair Lawn, NJ) supplied the HPLC-grade water, methanol, acetonitrile, ammonium acetate, ammonium formate, ammonium hydroxide, formic acid and acetic acid. Sigma Aldrich and Steraloids, Inc. (Newport, Rhode Island) were suppliers of the standard conjugated and free bile acids and salts. Deuterated cholic acid, deuterated chenodeoxycholic acid and deuterated deoxycholic acid were sourced from Cayman chemicals (Canada). Mr. Alvaro Lopez-Gallardo (Lab technician) constructed 1 mg/ml stock solutions of individual sulfated BAs. These sulfated BAs were prepared in water:MeOH (1:1) and were used as Standards. A stock concentration of 0.00064 - 40 μg/ml was constructed for each BA and this was also prepared by our lab technician. Standard curves were created for each analyte examined and are listed in appendix III S.I.3.1, S.I.3.3, S.I.3.10, S.I.3.13.

2.3.7 Ultra Performance Liquid Chromatography Tandem Mass Spectrometry

UPLC-MS was performed using a modified method of (Joyce *et al.,* 2014). Briefly, in triplicate, 5 μl from each sample was injected onto a C18 Acquity column (Waters Corp.). For analysis, an Acquity UPLC system (Waters Ltd.) coupled online to an LCT Premier mass spectrometer (Waters MS Technologies, Ltd.) was used. Elution of extracts was performed using a 25-minute gradient of 100% Buffer A to 100% Buffer B (A, water, 0.1% (v/v) formic acid; B, acetonitrile, 0.1% (v/v) formic acid) at a flow rate of 500 μl/min and column temperature of 40°C. A negative electrospray mode was used with a scan range of 50–1,000 m/z. Analysis of UPLC-MS data was performed using MassLynx and Targetlynx^{TM} (Waters) software and each analyte was identified using mass and retention time values appendix III S.I.3.2, S.I.3.4, S.I.3.8, S.I.3.9, S.I.3.11, S.I.3.12 and appendix IV S.I.4.2. Standard curves were generated with known BAs or FAs, allowing quantification of each analyte, and each analyte was normalised using the deuterated internal standards.

2.4 Statistical Analysis

Statistical and data analysis was carried out using GraphPad Prism version 6.0 software (https://www.graphpad.com/) and RStudio 2021.09.0. Statistical tests were performed using Wilcoxon test, Kruskal-Wallis, Dunn's Multiple comparison, test one-way ANOVA and two-way ANOVA followed by Tukey's post-hoc test, unless stated otherwise. Spearman's rank correlation co-efficient was used for correlation analysis. For survival analysis log-rank test was carried out. Results were considered statistically significant when $p<0.05$ (ns - no significance, *= $p<0.05$; **=$p<0.01$; ***=$p<0.001$; ****=$p<0.0001$).

Chapter 3 – Functionality of the gut microbiome is altered in neurological associated disorders

3.0 Abstract

Understanding healthy aging is becoming increasingly important. There is evidence to suggest a role for diet, gut microbes and their associated metabolites in aging. A classical indicator of microbial functions are BAs and FAs. Both act as signalling molecules and alterations can reveal modifications to human and dietary produced metabolites, respectively. Indeed, metabolism and signalling are reported as altered in aging. Here, microbial metabolites, BAs and FAs, in the context of neurological disorders, namely Autism Spectrum disorder (ASD) and Parkinson's Disease (PD), are examined representing early and advanced life stages; common to them both are symptoms of gut dysbiosis.

Here we applied an established ASD murine model, and reproduced the deficiencies in BA metabolites already reported in (Golubeva *et al.,* 2017). We advanced the work to investigate targeted BA modification as an interference to restore functionality to deficient BA metabolism and investigated the outcomes. This work identified murine BA alterations that were bacterial intervention strain specific. It further identified restoration of gut health parameters and in behavioural deficits that were strain dependent. Overall this study identified strains of bacteria that could have differential roles in alleviating behavioural and gut effects related to ASD.

Next, we turned our attention to the aging associated PD. Here, we examined BA alterations to determine a convergence in BA moieties in circulation and in both BA and FA moieties in the lower gut (faecal samples). We examined and identified key moieties that were affected by PD prescribed treatments and in particular for Sinemet. Its actions, may be related to transport functions since BAs and FAs appear elevated in the gut. Our tentative analysis suggests a role for BA receptor activation and for detoxification functions in PD. This study identified gender differences with respect to circulating BAs in PD patients. Overall this study identified changes in BA and FA signatures in PD, reflective of microbial functions and enzyme adjustments, suggesting a role for microbes as a contributing cause or a consequence of PD. Both effects could be altered with medication.

3.1 Introduction

This chapter aimed to investigate the link between gut microbes and neurological disorders, at two different stages of life. We also aimed to determine the potential to manipulate gut microbes and their metabolites in a bespoke manner. Neurological disorders are debilitating diseases that encompass a range of conditions from autism spectrum disorder (ASD) to Parkinson's disease (PD), Alzheimer's disease (AD) and multiple sclerosis (MS). They can impact the way in which thoughts and nervous signals are processed (Lima *et al.,* 2022). While the majority of these conditions are associated with mid to later life stages, one condition, ASD, can manifest in very early childhood (Nicholas *et al.,* 2008). Some characteristics of ASD include restrictive repetitive patterns of behaviour with impaired social communication and interaction (Nicholas *et al.,* 2008). On the other hand, PD is a neurological disorder characterised by progressive bradykinesia, muscle rigidity and rest tremor and its incidence is increasing in the aging population (Chapuis *et al.,* 2005). It is estimated that 40% of PD patients suffer from depression (Cummings, 1992). Accelerated progression, in PD, is attributed to progressive degeneration of nigrostriatal dopaminergic neurons, which are fundamental for motor function regulation. Central to this is the accumulation of toxic protein α-synuclein fibrils (Narhi *et al.,* 1999). Although ASD and PD are each associated with different life stages, common to them both are symptoms of gut dysbiosis (Goodwin *et al.,* 1971; Jost and Schimrigk, 1991; Huang *et al.,* 2021; Alharthi *et al.,* 2022). Gut discomfort is associated with ASD as well as altered circadian rhythms (with disrupted sleep cycle) (Tye *et al.,* 2018). In addition, these are also reported as early features of PD, manifesting up to 20 years in advance of full blown PD diagnosis (Postuma *et al.,* 2013; Kumaresan and Khan, 2021). Given that biomarkers for early PD diagnosis are lacking, hence diagnosis is based on altered motor function/movement, or indeed, post mortem analysis, these observations have prompted investigations of the gut-brain axis in both ASD and PD. For instance, the gut microbiota have been shown to influence social development in mice (Desbonnet *et al.,* 2014) and microbiota transfer therapy (MTT) has been shown to alter gut microbial composition and improved behavioural symptoms in children with ASD (Kang *et al.,* 2017). Transfer of the gut microbiota from human PD

patients were shown to induce PD-like symptoms (namely impaired motor function), when transferred into germ-free mice (Sampson *et al.,* 2016).

In the context of PD, α-synuclein protein aggregates are influential in alterations to both gut inflammation and gut permeability, Braak *et al.*, (2003) suggested that the causative agent is either a pathogen or α-synuclein protein aggregates, with the potential to pass through the GIT mucosal barrier (via postganglionic enteric neurons) to enter the central nervous system (CNS), via the vagus nerve, travelling directly to and from the brain (Braak *et al.,* 2003). Mucosal staining confirmed increased gut associated α-synuclein and also oxidative stress (nitrotyrosine staining), bacterial translocation (*E. coli)* and serum endotoxin (LPS) elevation in PD (Forsyth *et al.,* 2011). In addition, two years prior to any motor function related symptoms, immunostaining detected α-synuclein in colonic tissue from PD patients (Shannon *et al.,* 2012). More recently in animal models, this migration gut-brain movement was confirmed as bidirection (Carabotti *et al.,* 2015), solidifying the gut-brain axis as central to PD aetiology.

Evidence to support a role for gut changes and microbes in PD neurological diseases is abundant. Children with ASD demonstrated a decrease in the Bacteroidetes to Firmicutes ratio while *Lactobacillus* spp. were increased (Tomova *et al.,* 2015). This work was supported in a follow up study by (Strati *et al.,* 2017) and by (Coretti *et al.,* 2018; Coretti *et al.,* 2019). The latter also observed decreased *Bifidobacterium longum* abundance while Proteobacteria (LPS producers) representation was increased, as well as *Faecalibacterium prausnitzii*, a producer of butyrate, in 2-4 year old children. In an ASD murine model, gut altered *Blautia* and *Bifidobacterium* species representation were shown to translate to impaired bacteria-mediated BA transformations (Golubeva *et al.,* 2017). Here, faecal primary and secondary tauro-conjugated BAs were significantly increased with concomitant decreased levels in circulation compared to control animals (Golubeva *et al.,* 2017) suggesting a role for BA, potentially as signalling molecules, in ASD.

In the context of PD patients, increased levels of hydrophobic, microbially produced secondary BAs - deoxycholic acid (DCA) and lithocholic acid (LCA) - are reported in the ileum and the appendix of a small cohort of PD patients. These metabolite

changes were accompanied by increased abundance of faecal *Burkholderiales* (it carries BA dehydratase) to promote secondary BA synthesis (Li *et al.,* 2021). The evidence suggests that both microbial populations and their metabolites are altered, differentially, for both ASD and PD. These factors may have a role in disease symptoms and progression or alternatively they may be altered as a cause or consequence of disease. The roles and interactions of microbially modified, dietary derived and host produced factors are detailed in the introduction in sections 1.4 and 1.5. They indicate that altered microbial representation could change inter-kingdom signalling, as a result of diet, lifestyle and genetics.

With this in mind, our group investigated and deciphered gut related deficiencies in microbes and their associated metabolites, with a "knock on" effect on signalling in the BTBR T^{+} *Itpr3*^{tf}/J murine model of ASD (Golubeva *et al.,* 2017). This ASD murine model BTBR (Black and Tan BRachyury) carried the mutations a^{t} (nonagouti; black and tan), *Itpr3*^{tf} (inositol 1,4,5-triphosphate receptor 3; tufted), and *T* (brachyury) (Endo *et al.,* 2019). The mice lack a corpus callosum, they have a reduced hippocampal commissure and exhibit behaviours consistent with ASD (Endo *et al.,* 2019). Using this model, Golubeva *et al.*, (2017) reported a loss of *Blautia* and *Bifidobacterium* species with microbial functional adjustments including faecal BAs, particularly tauro-lithocholic acid (TLCA) and secondary BAs lithocholic acid (LCA). Deoxycholic acid (DCA) and ursodeoxycholic acid (UDCA) were altered in circulation. Observed increases in the level of conjugated BAs, with reduced levels of secondary BAs, may indicate reduction in gateway reaction, microbial bile salt hydrolase (BSH) activity and hence a reduction in substrate for microbial 7α-dehydroxylation to produce secondary BAs in BTBR mice. Alterations in microbial populations, affecting functionality for metabolites could influence signalling functions to impact health and they could be open to manipulation, through strain selection. In the first part of this chapter we explore this intriguing possibility.

Since we and others have associated neurological diseases with gastrointestinal (GI) alterations and discomfort, we further reasoned that microbially produced or altered metabolites could have a role in neurodegenerative diseases where GI discomfort is associated. Therefore, as a second part to this chapter, the human gut metabolites BAs and FAs, both signalling molecules, representing host and dietary aspects,

respectively, were examined independently. Circulating BAs were examined as part of another study to indicate that indeed circulating BAs are altered in the human aetiology towards PD and that medication did influence these metabolite levels (Ellen Joyce MRes, unpublished data 2017, data not shown). This work, with collected and pre-existing faecal samples, was intended as a GI associated study to compliment the circulating BA data.

This chapter investigates the hypothesis that restored microbial functionality could positively impact ASD through BA metabolism. Here in part I, we determined whether targeted restoration of microbial BA modification could pivot BA metabolism beneficially to influence behaviour in the murine ASD model, as a follow up experiment to work performed by the Joyce/Cryan groups (Golubeva *et al.,* 2017). Specific metabolite altering strains were selected based on their potential to re-calibrate BA metabolism. Part II aimed to establish the baseline changes in microbially modified gut, faecal and circulating metabolites for PD sufferers. These changes in BA and FA concentration levels could be an indication of the gut and circulating signalling landscape.

3.2 Results

Part I: Autism Spectrum Disorder - Can bacterial intervention reverse the gut associated deficits in bile acid metabolism to influence behaviour?

3.2.1.1 Autism Spectrum Disorder - the follow-on Study

We replicated the experiment performed by Golubeva *et al.*, (2017) with control animals (C57_Veh) and the ASD murine model were given access to either clean 0.8% (w/v) NaCl in drinking water, or to one of *Lactobacillus salivarius* strain P0003 (BTBR _P0003) ($7.5x10^8$ CFU/ml) or *Bifidobacterium adolescentis* strain 2715 (BTBR _2715) ($7.5x10^8$ CFU/ml), independently over a 9 week period (*Figure 2.3*). The strains were selected to investigate the hypothesis that replenishing the BA status might pivot the gut associated deficits in BA metabolism to influence behaviour. Their bacterial strain properties are described in *Table 2.1*. *Lactobacillus salivarius* strain P0003 and *Bifidobacterium adolescentis* strain 2715 were selected as bacterial interventions on the basis of BA metabolism by bile salt hydrolase enzymes and their pyrogen free nature. *B. adolescentis* strain 2715 is capable of de-conjugation of BAs from taurine, *L. salivarius* strain P0003 is capable of de-conjugation of BAs from taurine and glycine. The solutions were replenished on a daily basis for a period of 9 weeks and viable bacterial CFUs were calculated daily, according to Materials and Methods, Section 2.1.2 and 2.3.3. *Figure 3.1* indicates viable culture delivery of an average of $1x10^7$ CFU/ml on each day for each bacteria strain. Individual animal and cage consumption were not recorded (*Figure 2.3*, Chapter 2). Assessment of BA fold change over weeks 0, 2, 9 was examined, appendix III SI.3.7. No significance was determined in relation to cage effect and cohort effect on each individual BA.

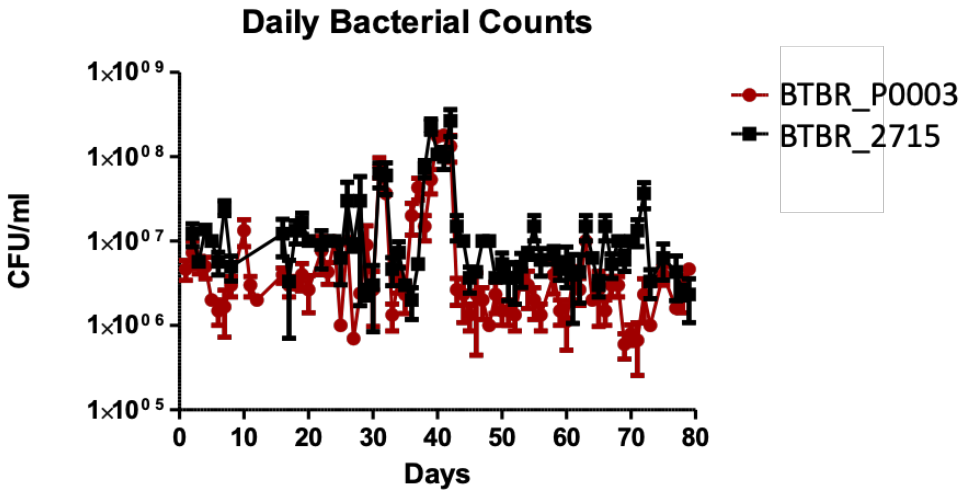


Figure 3.1: **Viable bacteria delivered to the murine BTBR model of ASD.** An average of up to $1x10^7$ CFU/ml of viable cultures was delivered independently, daily, over a 9 week period (n=12/group).

We next wished to establish that the same or similar BA alterations could be detected in the BTBR murine model of ASD relative to control animals. We therefore extracted faecal BAs (at baseline week 0 (in advance of treatment), at week 2 and at endpoint week 9) and circulating BAs (endpoint week 9 only) from individual animals, and subjected them to UPLC-TMS with subsequent analysis according to Materials and Methods, Sections 2.3.5-2.3.7. This work requires endpoint analysis and this will be discussed below.

The quality of the extraction was assessed by the recovery of spiked internal standards (Chenodeoxycholic Acid (CDCAd4) and deuterated Cholic Acid (CAd4)) for each sample and they were of similar levels of recovery, and for each sample type (*Figure 3.2* (a-d)).

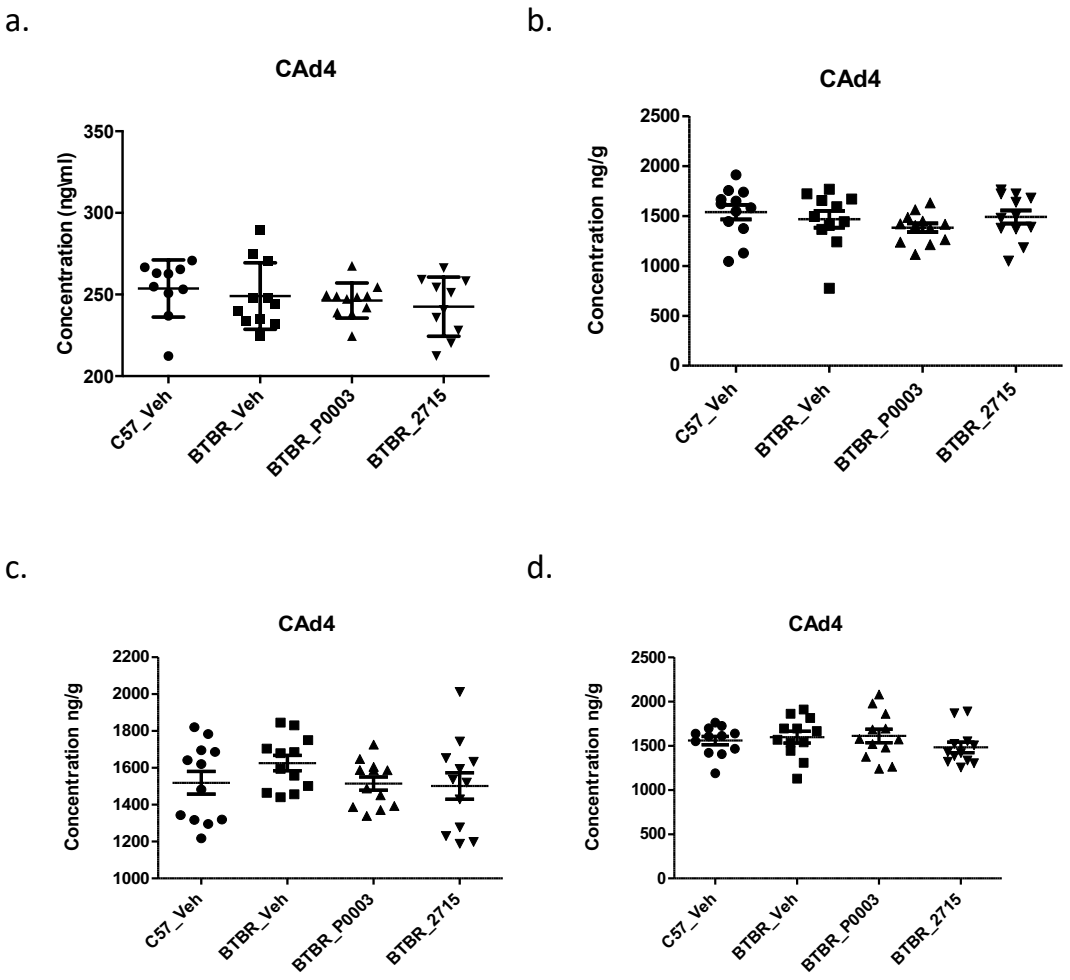
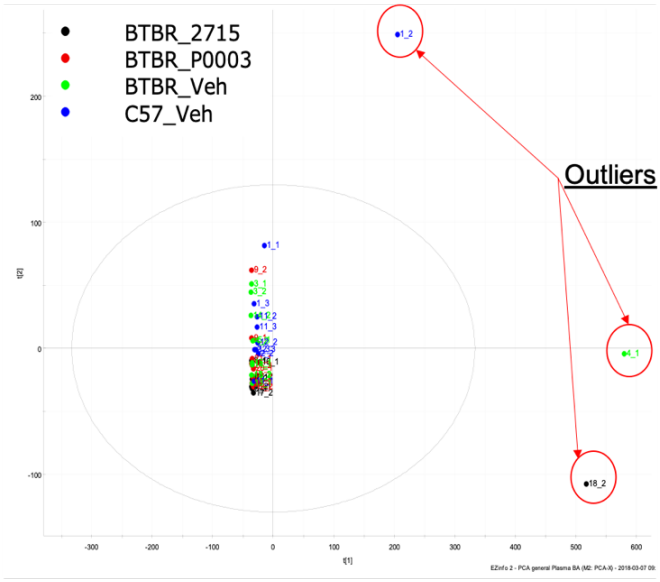


Figure 3.2: **Assessment of bile acid extraction efficiency from biological material from WT and ASD murine model.** Internal standard Cholic Acid d4 was assessed in (a) plasma and (b-d) faeces at week 0, through week 2, to endpoint week 9, from control mice C57BL/6 J (C57_Veh), untreated ASD murine model (BTBR_Veh), and the bacterial treated groups: *L. salivarius* strain P0003 (BTBR_P0003), or *B. adolescentis* strain 2715 (BTBR_2715). In circulation: C57_Veh *n*=10, BTBR_Veh *n*=11, BTBR_P0003 *n*=11 and BTBR_2715 *n*=10. In faeces: C57_Veh *n*=12, BTBR_Veh *n*=12, BTBR_P0003 *n*=12 and BTBR_2715 *n*=12. Statistical significance is indicated and calculated using Kruskal-Wallis and Dunn's Multiple Comparison Test (*= $p<0.05$; **=$p<0.01$; ***=$p<0.001$; ****=$p<0.0001$).

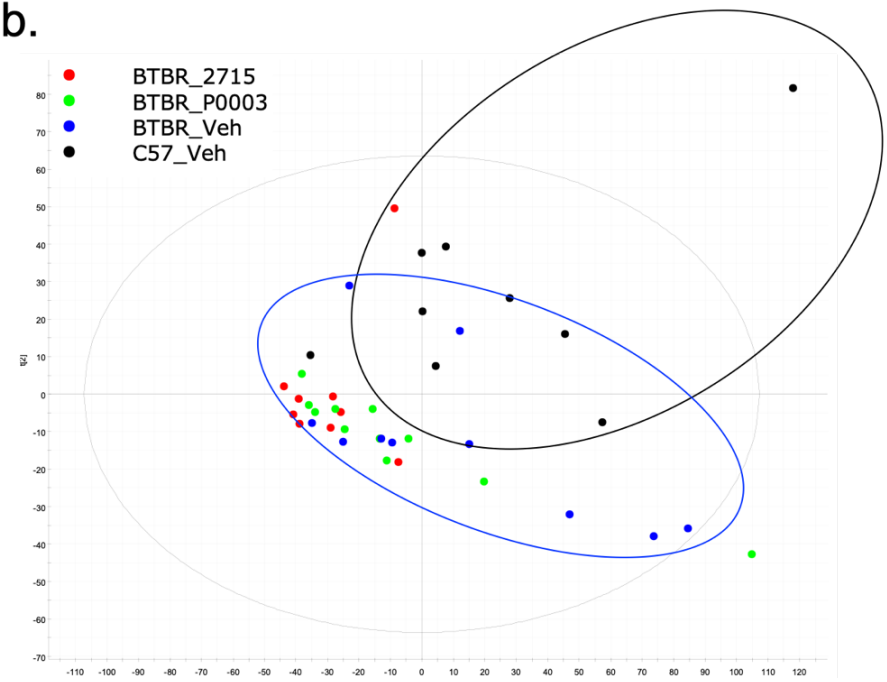
Principal component analysis (PCA) was performed for all detected and derived BA molecules including circulating metabolites (plasma) and those present in faecal

material at endpoint, week 9. These data revealed that endpoint circulating BAs from bacterial treated animals appear to cluster together, while those of the control WT group were more distant but centered between BTBR untreated animals (*Figure 3.3* (a and b)). Two potential outliers were evident, one for the C57_Veh cohort based on all metabolites (animal 1_1) and another for BTBR fed *B. adolescentis* strain APC2715 (animal 9_2), this change did not relate to the IS levels (*Figure 3.2*), however all animals irrespective were included for further analysis. Faecal endpoint sample PCA analysis indicated that WT C57_Veh were distinct for total metabolites relative to BTBR animals by 9 weeks post experiment, confirming that BA metabolite separation is occurring between BTBR and WT animals, the specific BAs altered will be discussed later. However, all BTBR animals were clustered together irrespective of treatment or non-treatment (*Figure 3.3* (c and d)). These data would support different levels of sensitivity in separation for general metabolites in circulation and in excretion or lower gut representation. It was not within the scope of this study to perform untargeted metabolomics. Indeed, the applied methodology would favour lipid molecules over other general metabolites.

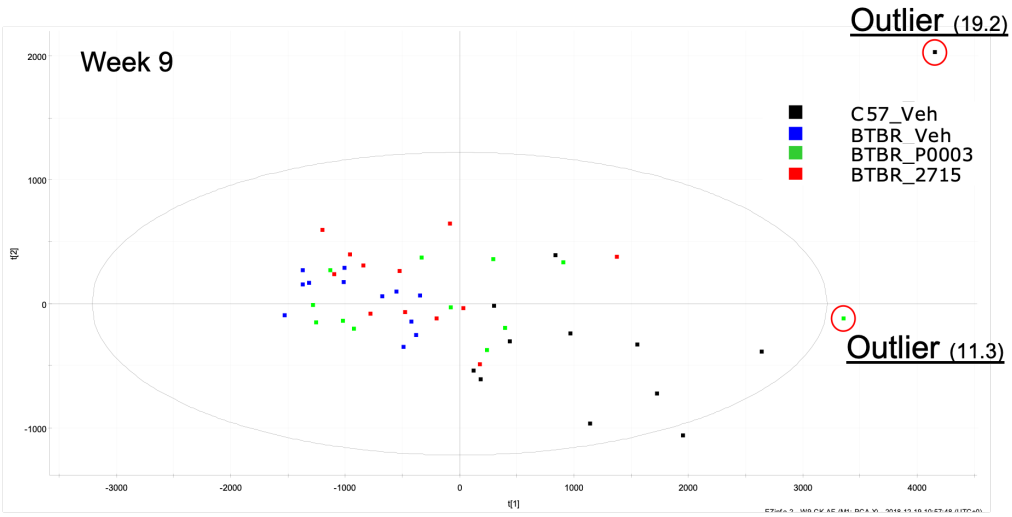
a.


BTBR_2715
BTBR_P0003
BTBR_Veh
C57_Veh
Outliers

b.


BTBR_2715
BTBR_P0003
BTBR_Veh
C57_Veh

c.



d.

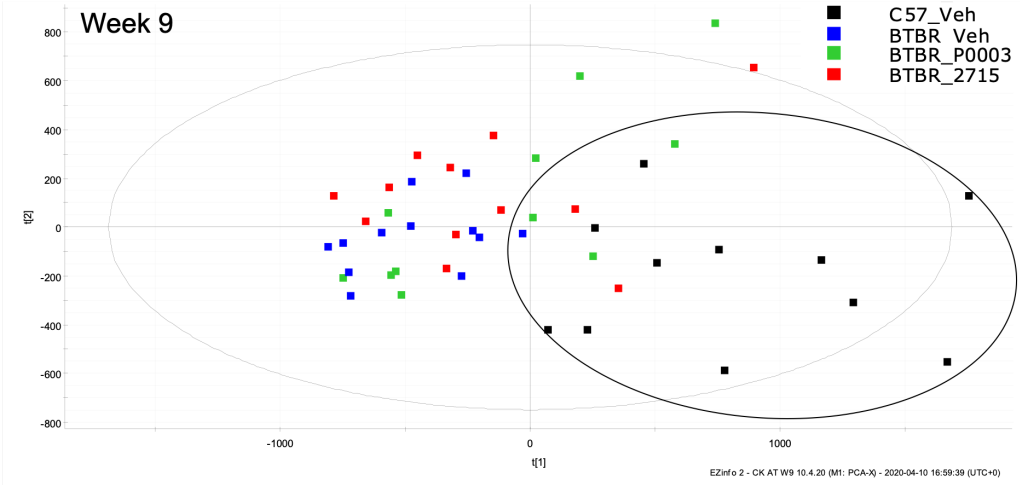


Figure 3.3: **Principal component analysis (PCA) examining relative distance, on the basis of bile acids, in WT C57BL/6 J and ASD model BTBR animals.** Detected BAs are represented for both (a-b) circulating and (c-d) faecal material at endpoint week 9. In circulation (a): C57_Veh *n*=10, BTBR_Veh *n*=11, BTBR_P0003 *n*=11 and BTBR_2715 *n*=10. In circulation (a) one animal from each group C57_Veh (ID 1_2), BTBR_Veh (ID 4_1) and BTBR_2715 (ID 18_2), were outliers and removed, (b) PCA with outliers removed, black circle encompasses C57_Veh animals (black dots), blue circle encompasses BTBR_Veh animals (blue dots), BTBR_P0003 animals (green dots) and BTBR_2715 animals (red dots) also fall into the blue circle. In faeces (c): C57_Veh *n*=12, BTBR_Veh *n*=12, BTBR_P0003 *n*=12 and BTBR_2715 *n*=12. In faeces (c) one animal from each group C57_Veh (ID 19_2) and BTBR_P0003 (ID 11_3), were outliers and removed, (d) PCA with outliers removed, black circle encompasses C57_Veh

animals (black squares); BTBR_Veh animals (blue squares), BTBR_P0003 animals (green squares) and BTBR_2715 animals (red squares) cluster together.

For interference two different bacterial strains were applied to correct for BA deficits based on their antimicrobial and bile-salt hydrolase (BSH), BA altering activity. *L. salivarius* strain P0003 and *B. adolescentis* strain 2715 were isolated from a porcine model and the adult human gut, respectively by Sarah Long (Joyce lab). *B. adolescentis* strain APC 2715 is capable of de-conjugation of BAs from taurine, while *L. salivarius* strain P0003 is capable of de-conjugation of BAs from taurine and glycine (Sarah L. Long unpublished data). The aim was to determine whether the BSH activity of these bacteria could restore deconjugation and primary and secondary BA concentration levels in BTBR mice to levels similar to control, C57BL/6 J mice. Post experimental feeding, over a period of 9 weeks, BA and FA levels were assessed from collected faecal samples (weekly). I have addressed these changes as part one of this chapter below and placed them in frame with independently generated behavioural data (Cryan group).

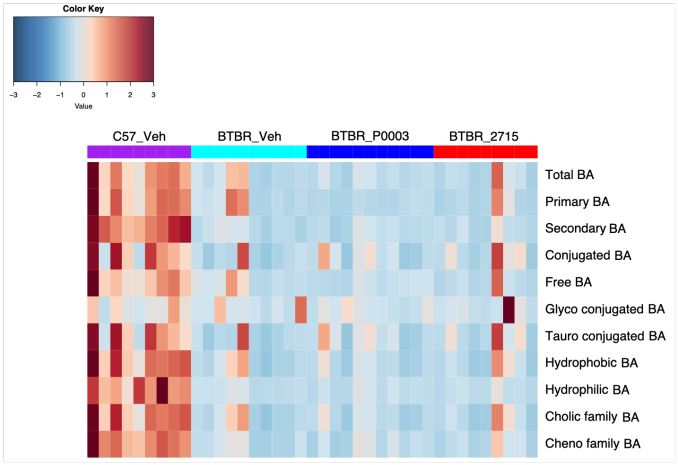
Table appendix III SI.3.2 and 3.4 , indicates that *n*=30 BA moieties were investigated. The retention times (RT), the negative ion mass and formula are indicated for each moiety along with the R^2 value (relating to the integrity of the standard curve) for each (see Material and Methods, Section 2.3.6-2.3.7). A standard curve was generated for each analyte (range: 0.0064-20 ug/ml) reliability was good, R^2 was between 0.94 and 0.99 (appendix III SI.3.1 and 3.3).

3.2.1.2 Circulating bile acids were altered following microbial treatments of BTBR mice

To examine any alterations to BA signatures, endpoint plasma BA were extracted from control groups C57_Veh and BTBR_Veh, and the bacterial treatment groups BTBR_P0003 and BTBR_2715 (Materials and Methods, Section 2.3.5). The endpoint, plasma BAs of the control C57_Veh group was distinct from BTBR treatment groups, with some slight overlap seen with control BTBR_Veh group (*Figure 3.4*). Initial analysis using spearman correlation heatplots show that on the basis of BA classes,

C57_Veh animals appear enriched in circulating BAs of all classes, bar Glyco conjugated BAs relative to BTBR animals, whether they were treated with bacteria or not (*Figure 3.4* (a)). When individual BA moieties were examined, spearman correlation heatplots indicated relative enrichment for all BA moieties except for Glycocholic Acid (GCA), Glycohyocholic Acid (GHCA), Glycodeoxycholic Acid (GDCA) and Lithocholic Acid (LCA) (*Figure 3.2* (b)). Taken together these data indicate that significant quantity differences could be associated to BTBR animals irrespective of treatments in circulation.

a.



b.

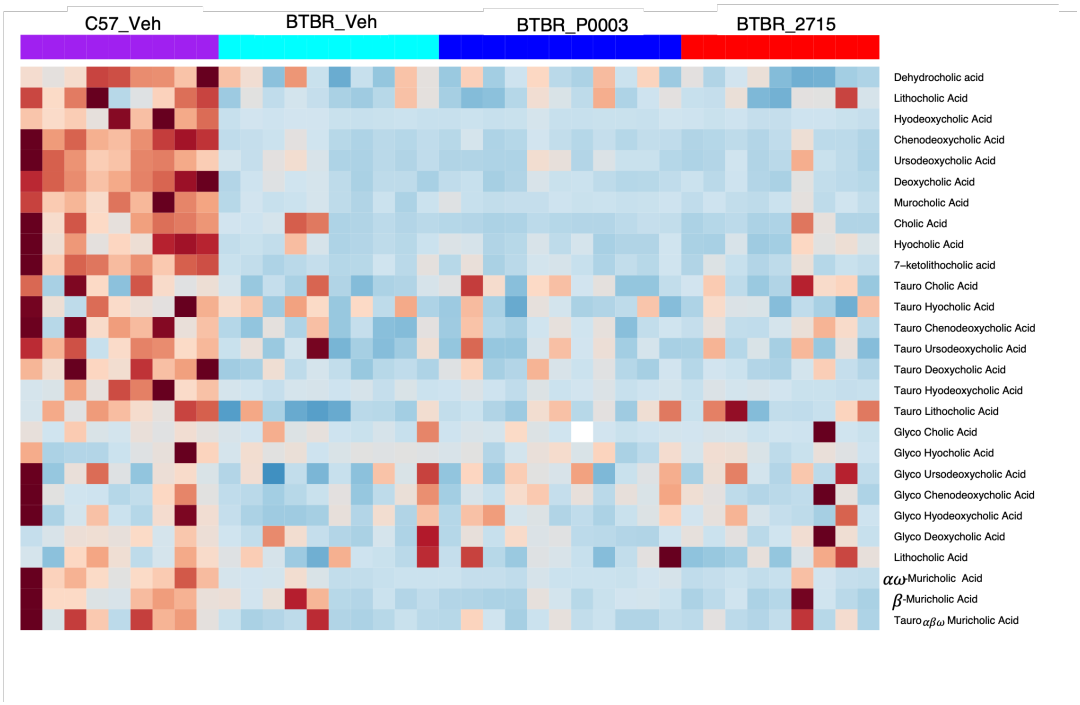


Figure 3.4: **Assessment of circulating bile acids in WT C57BL/6 J and ASD model BTBR mice.** Spearman correlation heatplot of quantities of (a) BA classes and (b) individual BAs, for the different control and treatment groups: C57_Veh *n*=9, BTBR_Veh *n*=10, BTBR_P0003 *n*=11 and BTBR_2715 *n*=9. The degree of correlation of change is indicated, with red as positive and blue as negative. Plots were generated using RStudio software version 2021.09.0.

Next, the specific BAs moieties examined in Golubeva *et al.*, (2017) were examined to determine reproducibility relative to those changes detected in Golubeva *et al.*, (2017). Here, we confirm that BTBR_Veh total BA levels are significantly lower compared to C57_Veh (*Figure 3.5* (a)). Interestingly, the levels of total BAs remain similar across BTBR mice, despite bacterial interventions (*Figure 3.5* (a)). We also confirm that primary BAs: CA, CDCA and βMCA concentrations were lower in BTBR mice compared to control C57_Veh animals, however, they remained unaltered with bacterial treatments (*Figure 3.5* (b-d)). We further confirmed and reproduced the reported secondary BAs: DCA and UDCA, lower levels associated to BTBR mice compared to control C57_Veh, an effect that was not alleviated through bacterial treatments (*Figure 3.5* (e and g)). Interestingly, our data showed that BTBR mice carried lower levels of secondary BA, LCA, compared to control C57_Veh (*Figure 3.5* (f)), however bacterial treatment with *B. adolescentis* strain 2715 (BTBR_2715), appears to increase LCA levels(*Figure 3.5* (f)). Taken together, the data confirms the endpoint effect reported previously, but indicates that introduction of BA metabolizing bacteria did not cause a huge redistribution of BA classes and families as would be expected. Ultimately, bacterial strain introduction did not restore the BA deficit, recorded and reproduced here, for BTBR animals at endpoint.

Golubeva *et al.*, (2017) reported that tauro conjugated circulating BAs are reduced in BTBR mice compared to control C57 animals, with the exception of TLCA. These data were reproducible (*Figure 3.6*). Interestingly, BTBR mice treated with *B. adolescentis* strain 2715, (BTBR_2715), demonstrated higher levels of TLCA, compared to control BTBR_Veh (*Figure 3.6* (f)). Taken together, these animals showed increases in both LCA and TLCA in circulation as a result of *B. adolescentis* intervention.

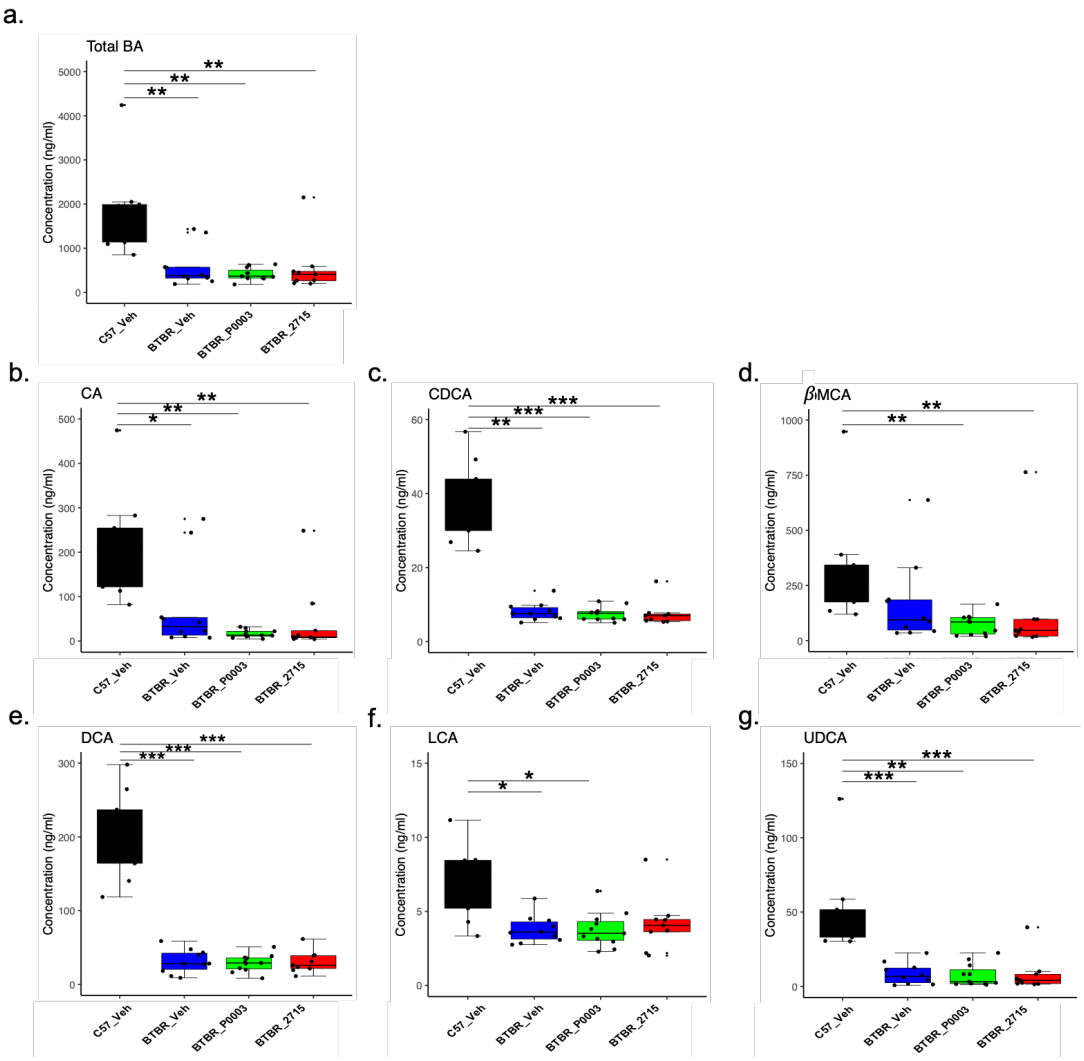


Figure 3.5: **Assessment of total and free circulating bile acids in WT C57BL/6 J and ASD model BTBR mice.** Relative levels of significantly altered (a) total BA, primary BA (b) CA, (c) CDCA (d) β MCA and secondary BAs (e) DCA (f) LCA and (g) UDCA, at endpoint (9 weeks). For controls: C57_Veh (*n*=9) and BTBR_Veh (*n*=10), and where bacterial treatments *L. salivarius* strain P0003 (BTBR_P0003 (*n*=11)) and *B. adolescentis* strain 2715 (BTBR_2715 (*n*=9)) were applied. RStudio software version 2021.09.0 was used for mean ± standard deviation (SD). Statistical significance was calculated using Kruskal-Wallis and Dunn's Multiple Comparison Test (*= p<0.05; **=p<0.01; ***=p<0.001).

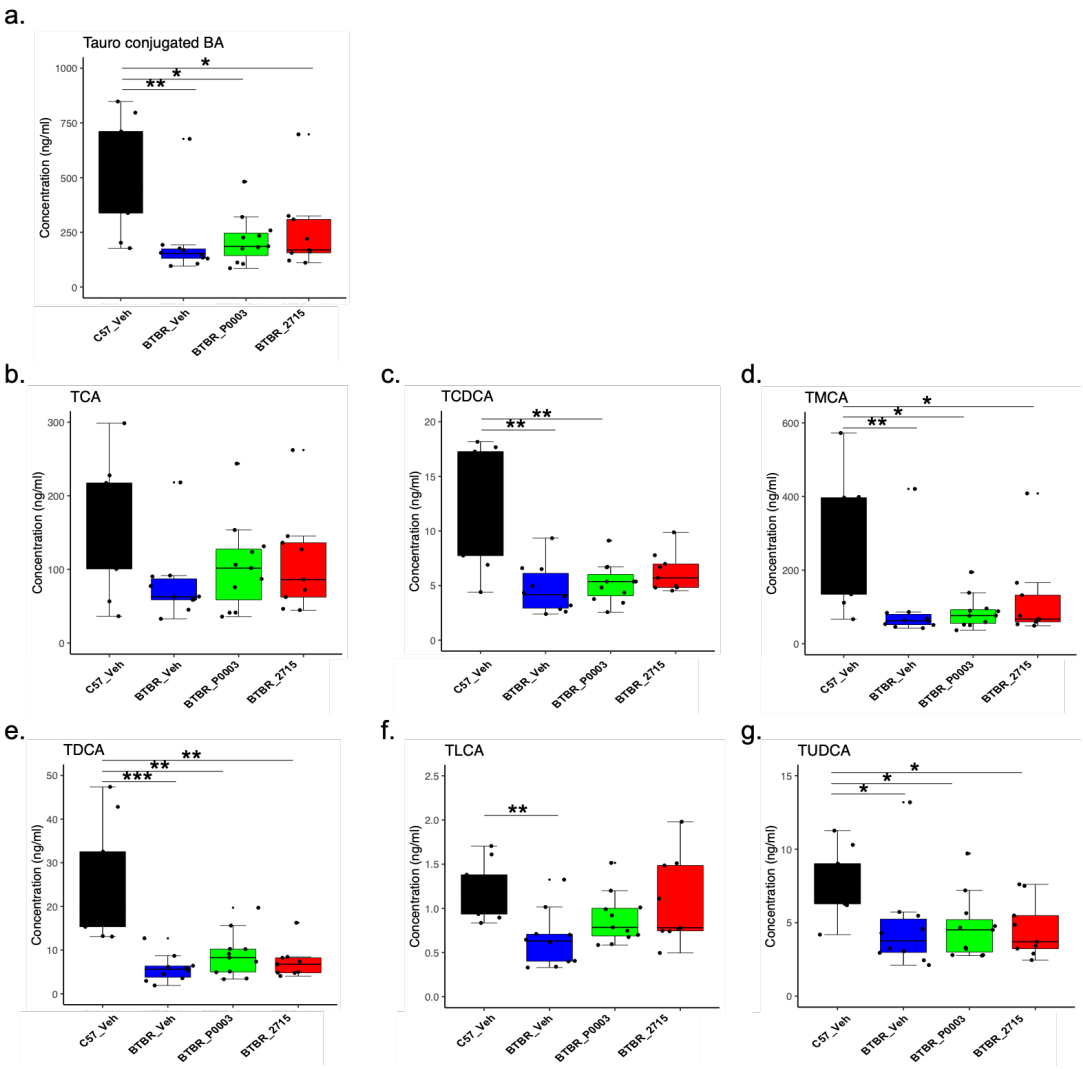


Figure 3.6: **Assessment of circulating tauro conjugated bile acids in WT C57BL/6 J and ASD model BTBR mice.** Relative levels of significantly altered (a) total tauro conjugated BAs, primary tauro conjugated BAs (b) TCA, (c) TCDCA (d) TMCA and secondary tauro conjugated BAs (e) TDCA (f) TLCA and (g) TUDCA, at endpoint (9 weeks). For controls: C57_Veh (*n*=9) and BTBR_Veh (*n*=10), and where bacterial treatments *L. salivarius* strain P0003 (BTBR_P0003 (*n*=11)) and *B. adolescentis* strain 2715 (BTBR_2715 (*n*=9)) were applied. RStudio software version 2021.09.0 was used for mean ± standard deviation (SD). Statistical significance was calculated using Kruskal-Wallis and Dunn's Multiple Comparison Test (*= p<0.05; **=p<0.01; ***=p<0.001). Abbreviations see *Table 2.9*.

Interestingly, despite interference with two different bacterial strains, the concentration of total BA remained unchanged in BTBR mice, but levels were significantly lower relative to control C57 (C57_Veh) group (*Figure 3.5* (a)). Furthermore, across all BTBR treated and untreated groups, all individual BA moieties were of a similar level, with no other significant differences detected across all BTBR groups (*Figure 3.5*). Trends towards increased tauro conjugated moieties were detected in circulation for some bacterial BTBR animals but these small changes did not reach significance (*Figure 3.6*). Taken together the data supports altered BA metabolism in BTBR animals relative to the WT C57_Veh animals, an effect that could be subtly adjusted through bile salt modulating probiotic strains, suggesting a gut physiological effect in these animals that might contribute to lower BA uptake into circulation.

Given the slight, but not significant trend towards elevation of certain BAs, we next examined the potential of the BA signatures to modulate key metabolic and immune function associated BA receptors ((*Figure 3.7*). Specifically, ligands associated to nuclear receptors (NRs), the Farnesoid X Receptor (FXR), Vitamin D receptor (VDR) and G-protein coupled receptor (GPCR), Tanaka G receptor 5 (TGR5), were assessed in circulation. Here, agonist circulating signatures and levels for each receptor were taken as a predictor of their potential activation or repression. The sum of FXR free agonistic BAs are: CA, CDCA, DCA, α-MCA and β-MCA, while antagonists are: UDCA, TUDCA, GUDCA and TMCA; LCA, CDCA, DCA and CA represent VDR agonists while LCA, TLCA, CA, CDCA and DCA are TGR5 agonists. Their respective collective levels were examined to determine any evidence to suggest alterations in BA signalling (*Figure 3.7*). BA agonists for BA receptors, FXR, VDR and TGR5 were significantly lower in all BTBR treated animal groups, compared to C57_Veh control group (*Figure 3.7* (a, c and d)). FXR antagonist BA levels were also significantly lower in all BTBR animals, compared to C57_Veh control group (*Figure 3.7* (b)). This suggests that their respective activation may be reduced in BTBR animals. No significant alterations were detected in BTBR animals treated with either bacteria strain compared to non-treated. Altogether these data confirm the earlier findings of a BA based defect in BTBR animals and they support predictive impacts on NRs and G-Protein coupled receptors to reduce normal gut signalling functions.

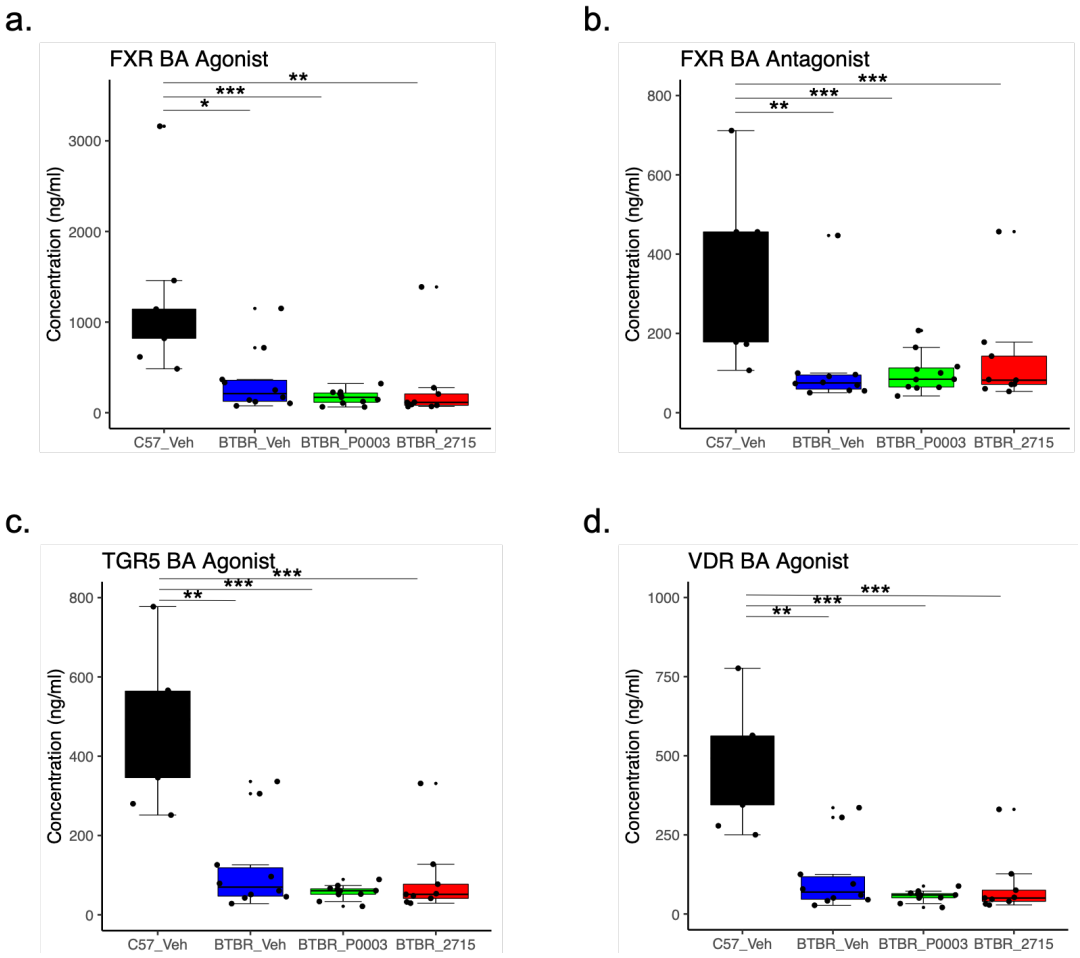


***Figure 3.7:* Assessment of the potential to activate signalling bile acid receptors in circulation for WT C57BL/6 J and ASD model BTBR mice.** Sum of BA (a) Farnesoid X Receptor (FXR) BA Agonists, (b) FXR BA Antagonists, (c) G-protein coupled receptor TGR5 BA Agonists and (d) Vitamin D receptor (VDR) BA Agonists. C57_Veh *n*=9, BTBR_Veh *n*=10, BTBR_P0003 *n*=11 and BTBR_2715 *n*=9. RStudio software version 2021.09.0. Statistical significance was calculated using Kruskal-Wallis and Dunn's Multiple Comparison Test (*= p<0.05; **=p<0.01; ***=p<0.001; ****=p<0.0001).

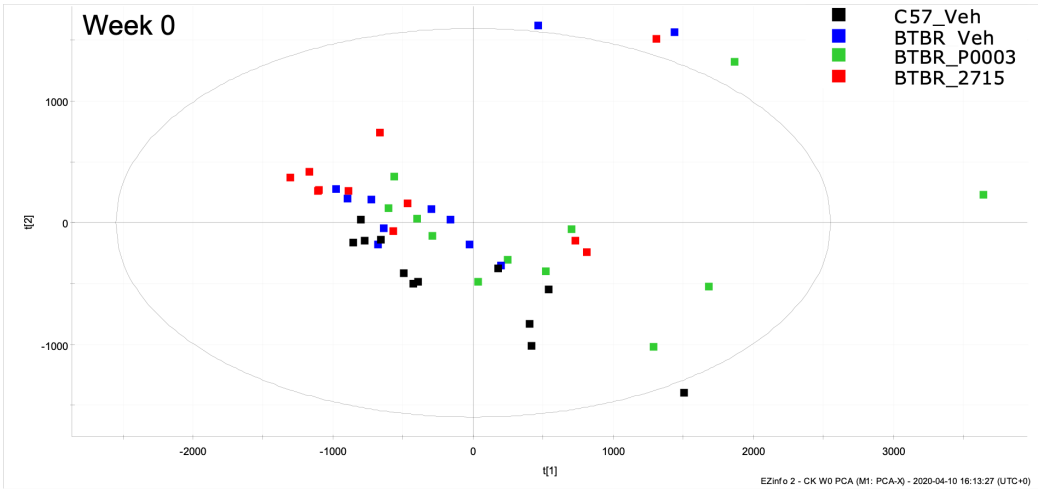
3.2.1.3 Faecal bile acids were altered following microbial treatments of BTBR mice

To determine if gut BA changes are occurring, but not translating to circulation, faecal BAs were examined in WT, control BTBR and bacteria fed BTBR animals. We hypothesize that targeted interference through the introduction of gut bacteria, *B. adolescentis* strain 2715 and *L. salivarius* strain P0003, capable of manipulating BAs, might restore the defects in BA modification, in the gut context, an effect not seen in circulation. Again, UPLC-TMS was applied (Materials and Methods, Section 2.3.5),

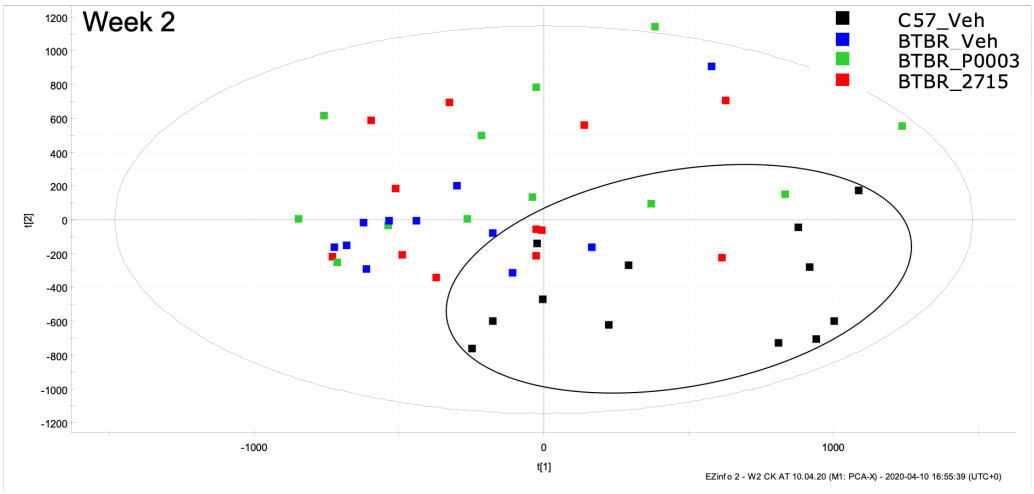
and the repertoire of BAs was examined at times 0, 2 and 9 (endpoint) weeks. Mice were 6 weeks of age at baseline week 0, 8 weeks of age at timepoint week 2, and 15 weeks of age at endpoint week 9.

Principle Component Analysis (PCA) showed that BAs altered over time from baseline (week 0), through week 2, to endpoint week 9 (*Figure 3.8* (a-c)). By week 2, and extending to week 9, all BTBR animals with and without bacterial interventions (*L. salivarius* strain P0003 and *B. adolescentis* strain 2715), appeared to separate distinctly, though not dramatically, from C57_Veh control animals, although they still remained closely clustered with BTBR_Veh animals (black circle *Figure 3.8* (b-c)).

a.



b.



c.

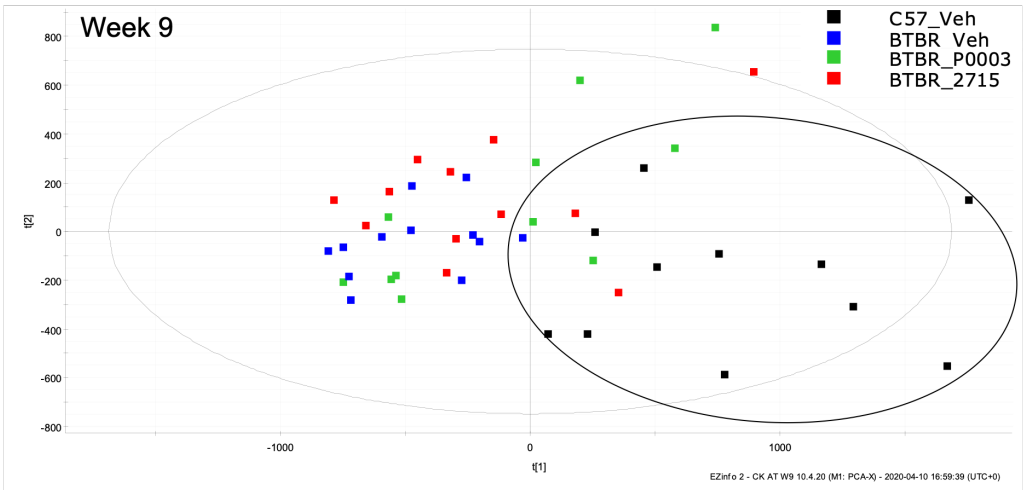


Figure 3.8: **Principal component analysis (PCA) to represent all faecal bile acids detected from WT C57BL/6 J and BTBR ASD murine model.** PCA plots represent relative representation for each animal at (a) baseline week 0, mice aged 6 weeks,

(b) week 2, mice aged 8 weeks and (c) endpoint week 9, mice aged 15 weeks. The black circle in (b) and (c) encompasses C57_Veh animals (black squares). BTBR mice representations (a-c) are blue squares for BTBR_Veh animals, green squares for BTBR_P0003 animals and red squares for BTBR_2715 animals. C57_Veh *n*=11, BTBR_Veh *n*=10, BTBR_P0003 *n*=11 and BTBR_2715 *n*=11.

Spearman correlation heatplots were applied to initially assess relative levels of BA classes and individual moieties over time (weeks 0, 2, 9). Faecal BAs indicate that control group C57_Veh may contain higher relative levels of all classes of BA (*Figure 3.9* (a)), and each individual BA (*Figure 3.9* (b)) an effect that increased over time. Concurrently, all BTBR groups (irrespective of treatment or not) indicated lower levels of all classes of BA (*Figure 3.9* (a)), and of each individual BA (*Figure 3.9* (b)), and this was consistent from baseline week 0 to endpoint week 9. In the lower gut, bacteria treatment groups, (BTBR_P0003 and BTBR_2715) did not show clear distinctions from control BTBR_Veh group from baseline week 0 to endpoint week 9. There was no evidence to suggest modulation by these strains at the collective class or the individual BA levels, confirming the PCA analysis above.

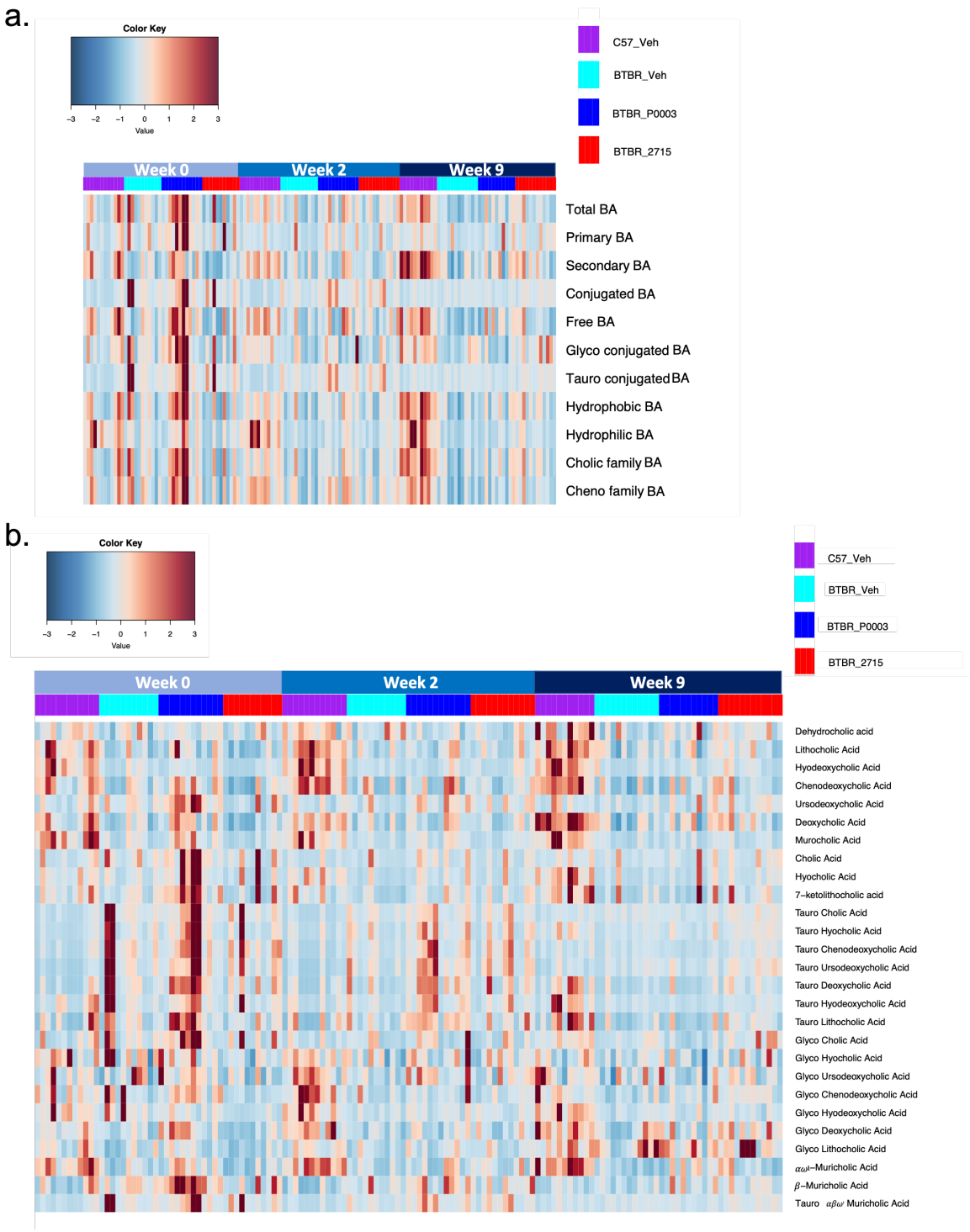


Figure 3.9: **Relative assessment of faecal bile acids in WT C57BL/6 J and BTBR ASD murine model.** Spearman correlation heatplot indicate relative representation of (a) BA classes and (b) individual BAs, for C57_Veh *n*=11, BTBR_Veh *n*=10, BTBR_P0003 *n*=11 and BTBR_2715 *n*=11, over the timeframe from weeks 0, 2 and 9 post treatment. RStudio software version 2021.09.0.

Next, the levels of specific faecal BA moieties were examined (*Figures 3.10*, *3.11* and *3.12*). Here, at baseline week 0, we report no significant differences in levels of total BAs. At baseline, *B. adolescentis* (BTBR_2715) animals had significantly less βMCA, DCA and UDCA, compared to *L. salivarious* (BTBR_P0003) animals, showing variation in BA levels across BTBR groups (*Figure 3.10* (d), (e) and (g)). Individual free BA, secondary BA, LCA were at lower levels across all BTBR mice, compared to C57_Veh mice (*Figure 3.10* (f)). In terms of composition, Golubeva *et al.*, (2017) reported that primary BAs: CA and βMCA, levels were higher in BTBR mice compared to control C57, with CDCA levels lower in BTBR mice compared to control C57_Veh animals. In our study at baseline week 0, there are no differences in the levels of these moieties between BTBR mice and C57_Veh mice (*Figure 3.10* (b-d)). However, BTBR *B. adolescentis* (BTBR_2715) animals showed significantly lower levels of CDCA compared to control C57_Veh (*Figure 3.10* (c)), while BTBR *L. salivarious* (BTBR_P0003) animals showed significantly higher levels of βMCA and for UDCA compared to control C57_Veh (*Figure 3.10* (d) and (g)). Golubeva *et al.*, (2017) reported that secondary BAs: DCA, LCA and UDCA were lower in BTBR mice compared to control C57 animals. Our data confirm these findings, at week 0 (*Figure 3.10* (e-g)).

At week 2, we report no differences in levels of total faecal BAs between BTBR mice (treated or not) and C57_Veh mice (*Figure 3.11*). The levels of CA remained unchanged across the groups (*Figure 3.11* (b)). CDCA remains reduced and DCA and LCA were significantly lower in all BTBR groups compared to control C57_Veh animals (*Figure 3.11* (c), (e) and (f)). βMCA appears higher in BTBR mice, and was significant where animals were treated with *L. salivarious* (BTBR_P0003) relative to control C57_Veh (*Figure 3.11* (d)). BTBR_Veh mice had lower levels of UDCA compared to control C57_Veh, however, BTBR_P0003 were elevated for UDCA compared to control BTBR_Veh and C57_Veh animals (*Figure 3.11* (g)). Indeed BTBR_P0003 may have the potential to increase primary BAs CA, CDCA and βMCA (*Figure 3.11* (b-d)) and secondary BAs DCA, LCA and UDCA (*Figure 3.11* (e-g)), compared to control BTBR_Veh and C57_Veh groups.

At endpoint (week 9), CDCA, DCA and LCA remained significantly elevated in WT animals relative to ASD model BTBR mice (*Figure 3.12* (c), (e) and (f)), while β-MCA levels are elevated in BTBR_Veh animals (*Figure 3.12* (d)). Bacterial interventions, *L. salivarius* strain P0003 (BTBR_P0003) and *B. adolescentis* strain 2715 (BTBR_2715), restored some primary and secondary BA levels to that of control mice C57BL/6 J (C57_Veh) (*Figure 3.12* (a), (c) and (d)). In all, BA concentration levels changed over time from baseline to endpoint at week 9, bacterial interventions BTBR_P0003 and BTBR_2715 demonstrated slight rescuing effects in certain BAs, however, no BA was significantly different compared to BTBR_Veh mice.

In all cases shown below, treatment with *L. salivarious*, BTBR_P0003, showed an enhanced ability to generate key free BAs, the levels were similar in nature to the control C57_Veh, but there were no significantly altered BAs, relative to untreated BTBR. In contrast, significantly lower levels of key free BAs, CDCA, CA, and LCA, relative to WT control animals but not to the BTBR ASD model, were detected where *B. adolescentis* was applied to the BTBR group (*Figure 3.10*), levels became similar to WT C57_Veh control animals by week 9, endpoint (*Figure 3.12*), but were not significant. Taken together, these data indicate a differential effect of genotype on the individual free BAs of the lower gut, specifically focused on strain interference in the BTBR context.

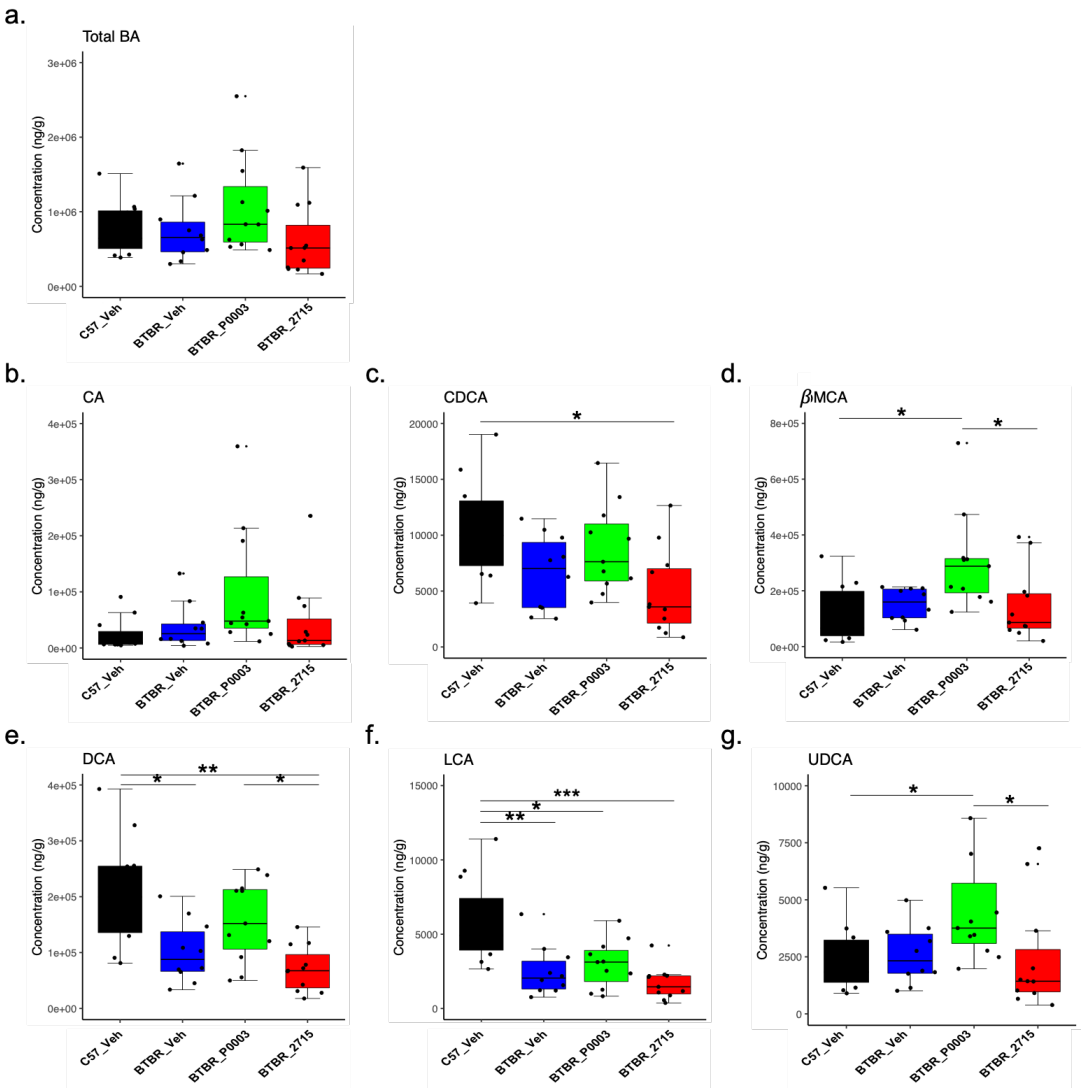


Figure 3.10: **Assessment of total and free faecal bile acids in WT C57BL/6 J and BTBR ASD murine model, at baseline week 0.** Relative levels of significantly altered (a) total BAs, primary BAs (b) CA, (c) CDCA), (d) β-MCA, and secondary BAs (e) DCA, (f) LCA and (g) UDCA, at baseline week 0. For controls: C57_Veh (*n*=11) and BTBR_Veh (*n*=10), and where bacterial treatments *L. salivarius* strain P0003 (BTBR_P0003 (*n*=11)) and *B. adolescentis* strain 2715 (BTBR_2715 (*n*=11)) were applied. RStudio software version 2021.09.0 was used for mean ± standard deviation (SD). Statistical significance was calculated using Kruskal-Wallis and Dunn's Multiple Comparison Test (*= p<0.05; **=p<0.01; ***=p<0.001). Abbreviations see *Table 2.9*.

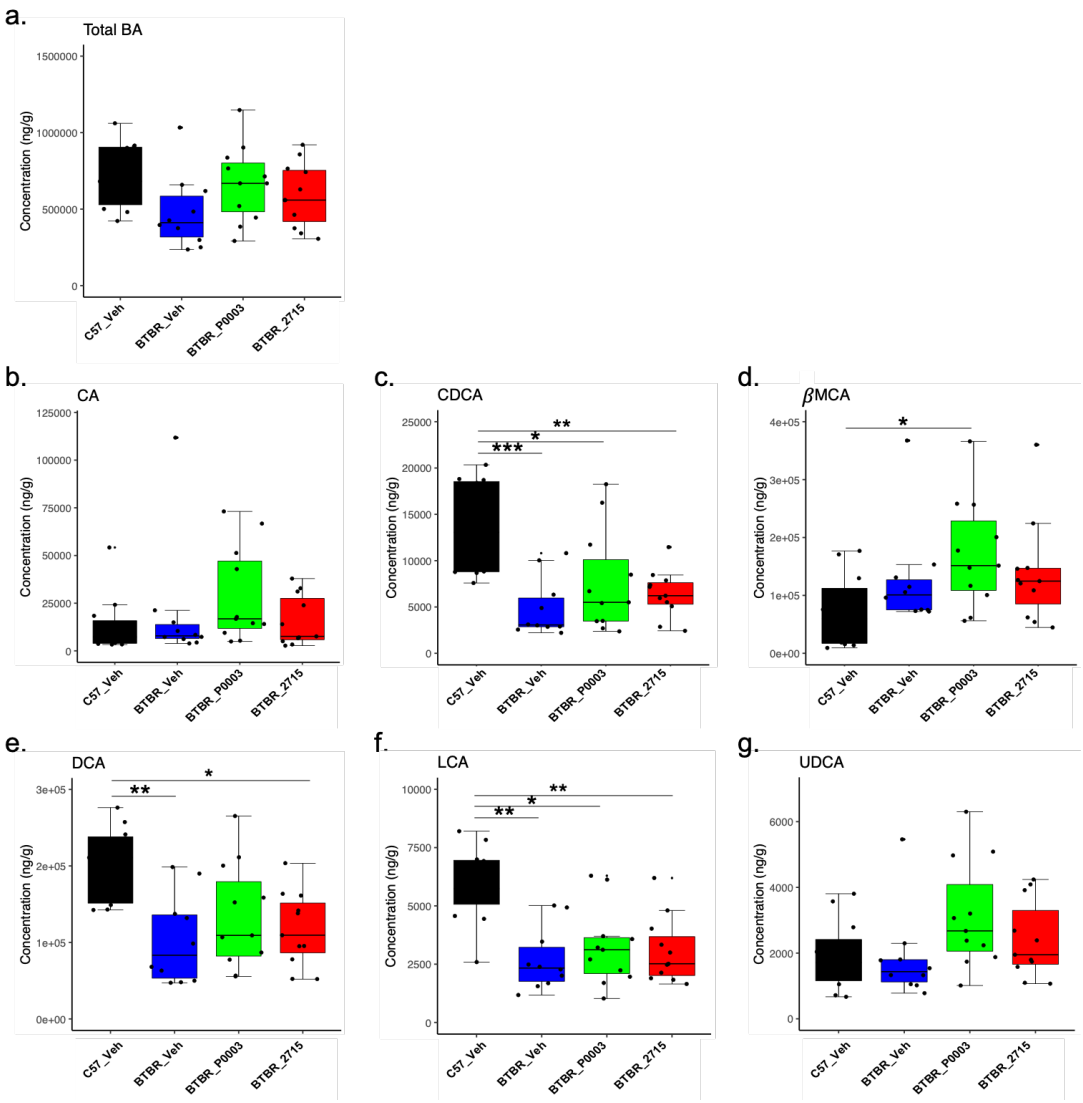


Figure 3.11: **Assessment of total and free faecal bile acids in WT C57BL/6 J and BTBR ASD murine model, week 2.** Relative levels of significantly altered (a) total BAs, primary BAs (b) CA, (c) CDCA), (d) β-MCA, and secondary BAs (e) DCA, (f) LCA and (g) UDCA, at week 2. For controls: C57_Veh (*n*=11) and BTBR_Veh (*n*=10), and where bacterial treatments *L. salivarius* strain P0003 (BTBR_P0003 (n=11)) and *B. adolescentis* strain 2715 (BTBR_2715 (*n*=11)) were applied. RStudio software version 2021.09.0 was used for mean ± standard deviation (SD). Statistical significance was calculated using Kruskal-Wallis and Dunn's Multiple Comparison Test (*= p<0.05; **=p<0.01; ***=p<0.001). Abbreviations see *Table 2.9*.

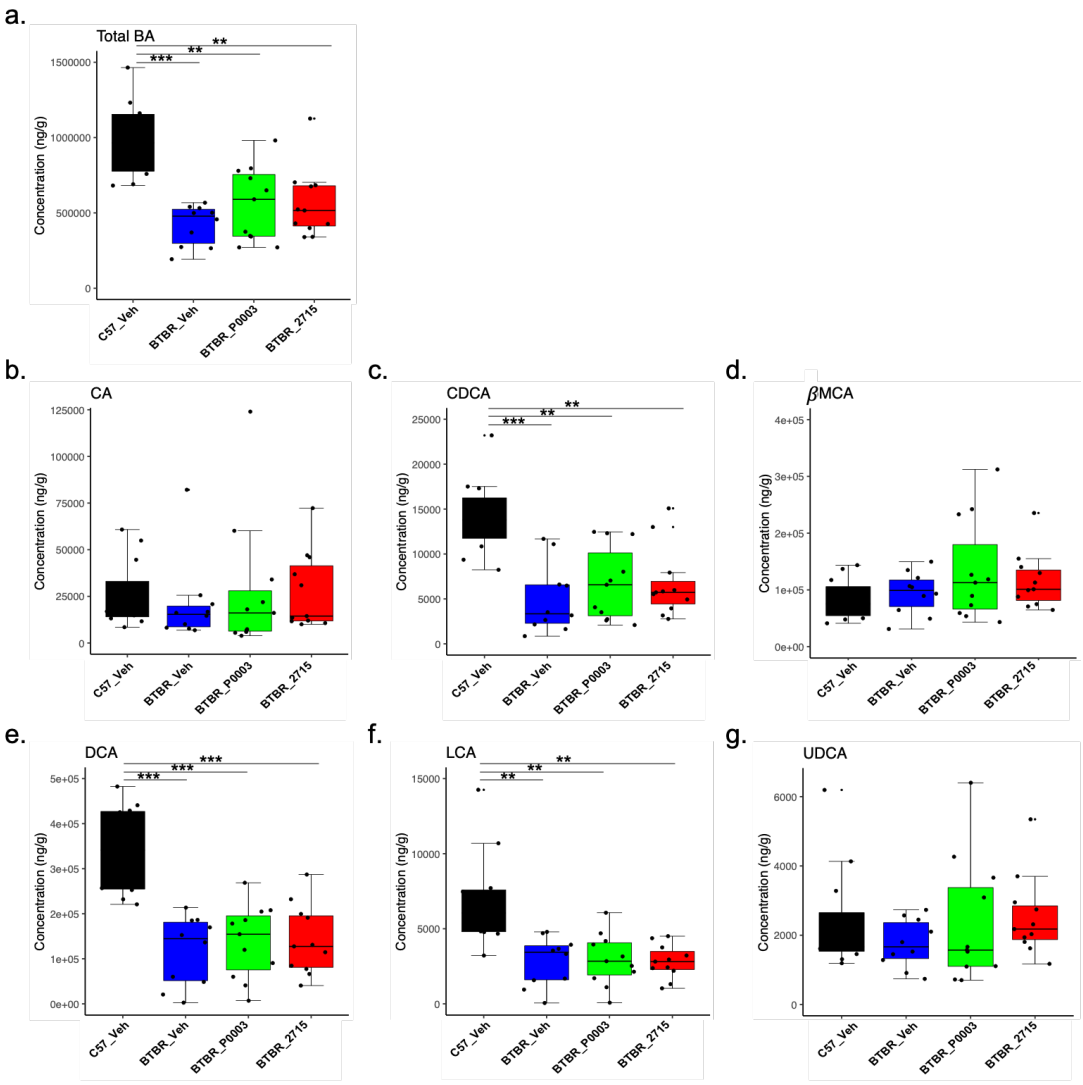


Figure 3.12: **Assessment of total and free faecal bile acids in WT C57BL/6 J and BTBR ASD murine model, at endpoint week 9.** Relative levels of significantly altered (a) total BAs, primary BAs (b) CA, (c) CDCA), (d) β-MCA, and secondary BAs (e) DCA, (f) LCA and (g) UDCA, at endpoint week 9. For controls: C57_Veh (*n*=11) and BTBR_Veh (*n*=10), and where bacterial treatments *L. salivarius* strain P0003 (BTBR_P0003 (*n*=11)) and *B. adolescentis* strain 2715 (BTBR_2715 (*n*=11)) were applied. RStudio software version 2021.09.0 was used for mean ± standard deviation (SD). Statistical significance was calculated using Kruskal-Wallis and Dunn's Multiple Comparison Test (*= p<0.05; **=p<0.01; ***=p<0.001). Abbreviations see *Table 2.9*.

Golubeva *et al.*, (2017) reported that 2 classes of faecal BAs: tauro conjugated primary BAs and tauro secondary BAs, were all reduced in BTBR mice compared to C57 control animals. Here at baseline week 0, such an effect is confirmed in this study (*Figure 3.13* (a)), where TCA (*Figure 3.13* (b)), TMCA (*Figure 3.13* (d)), and TUDCA (*Figure 3.13* (g)) levels are significantly higher in BTBR mice, compared to C57_Veh. Similar to their report, BTBR_Veh concentration levels of TCDCA (*Figure 3.13* (c)), TDCA (*Figure 3.13* (e)) and TLCA (*Figure 3.13* (f)), are higher in BTBR mice relative to C57_Veh control WT mice. Bacterial interventions, particularly *L. salivarius* strain P0003, (BTBR_P0003) demonstrated the highest levels of Tauro conjugated BAs compared to all BTBR mice and C57_Veh (*Figure 3.13*).

At week 2, faecal BAs are similar to that previously reported (Golubeva *et al.,* 2017); untreated ASD animals (BTBR_Veh) showed higher tauro conjugated BA levels compared to C57_Veh WT animals (*Figure 3.14*). BTBR mice treated with bacterial interventions, particularly *L. salivarius* strain P0003 (BTBR_P0003), demonstrated higher levels of Tauro conjugated BAs compared to other BTBR groups, reaching significance compared to C57_Veh (*Figure 3.14*).

Assessment at endpoint (week 9), showed continued reduction of total tauro conjugated BA (*Figure 3.15* (a)), to that of control WT C57_Veh mice. There were no differences between mice groups in TCA (*Figure 3.15* (b)), TCDCA (*Figure 3.15* (c)), TMCA (*Figure 3.15* (d)), and TUDCA (*Figure 3.15* (g)), with the exception of bacterial treated *B. adolescentis* strain 2715 (BTBR_2715), slightly higher in some groups. However, there are no differences in *B. adolescentis* strain 2715 (BTBR_2715) and WT control C57_Veh mice in TDCA (*Figure 3.15* (e)) and TLCA (*Figure 3.15* (f)), while levels were significantly lower in untreated ASD model (BTBR_Veh) and *L. salivarius* strain P0003 (BTBR_P0003) mice compared to WT controls (C57_Veh). Bacterial interventions, *L. salivarius* strain P0003 (BTBR_P0003) and *B. adolescentis* strain 2715 (BTBR_2715), in combination, have the potential to increase total BA concentrations and reduce tauro conjugated BA levels, in BTBR treated mice.

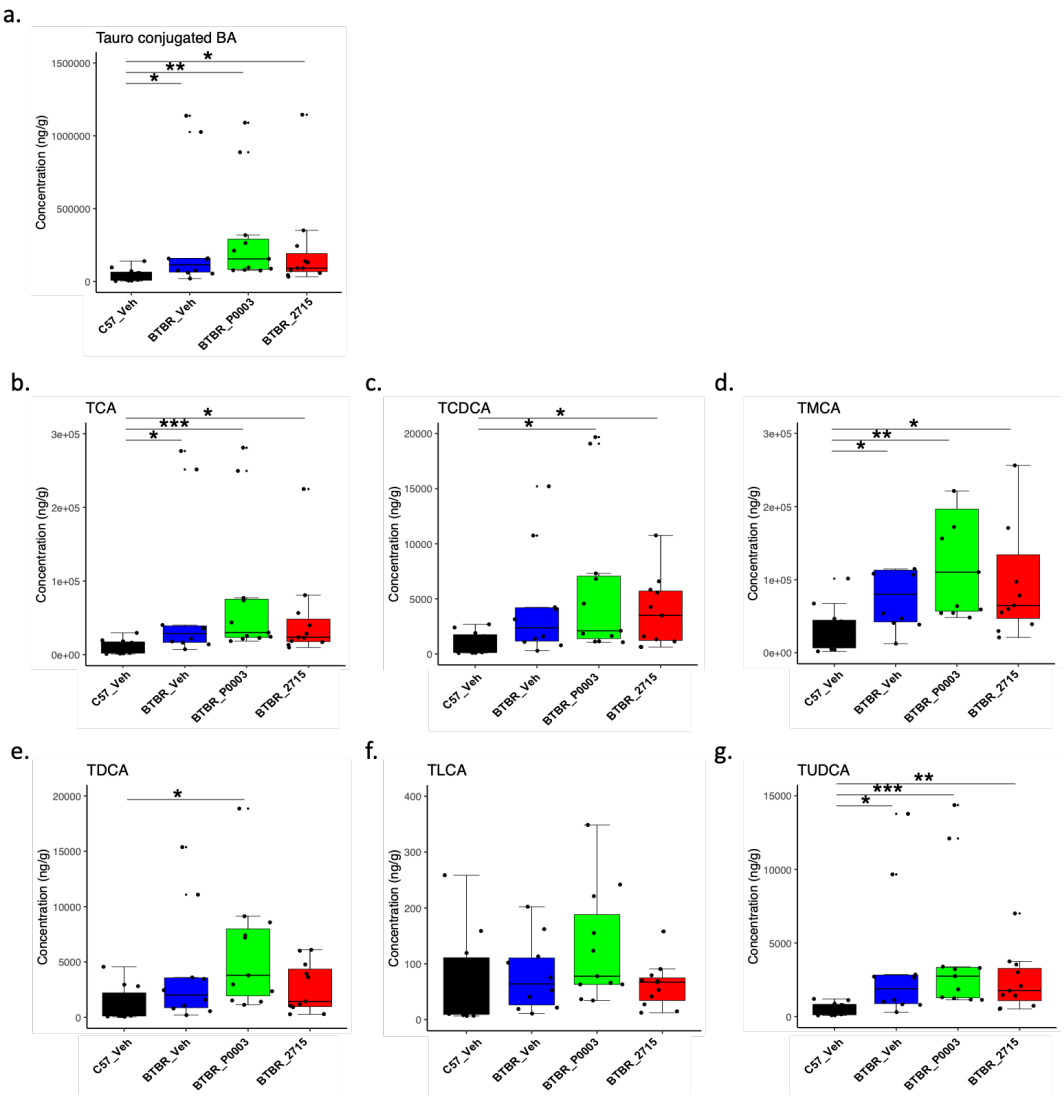


Figure 3.13: **Assessment of total tauro conjugated and free tauro conjugated faecal bile acids in WT C57BL/6 J and BTBR ASD murine model, at baseline week 0.** Relative levels of significantly altered (a) total tauro conjugated BAs, primary tauro conjugated BAs (b) TCA, (c) TCDCA), (d) TMCA, and secondary tauro conjugated BAs (e) TDCA, (f) TLCA and (g) TUDCA, at baseline week 0. For controls: C57_Veh (*n*=11) and BTBR_Veh (*n*=10), and where bacterial treatments *L. salivarius* strain P0003 (BTBR_P0003 (*n*=11)) and *B. adolescentis* strain 2715 (BTBR_2715 (*n*=11)) were applied. RStudio software version 2021.09.0 was used for mean ± standard deviation (SD). Statistical significance was calculated using Kruskal-Wallis and Dunn's Multiple Comparison Test (*= p<0.05; **=p<0.01; ***=p<0.001). Abbreviations see *Table 2.9*.

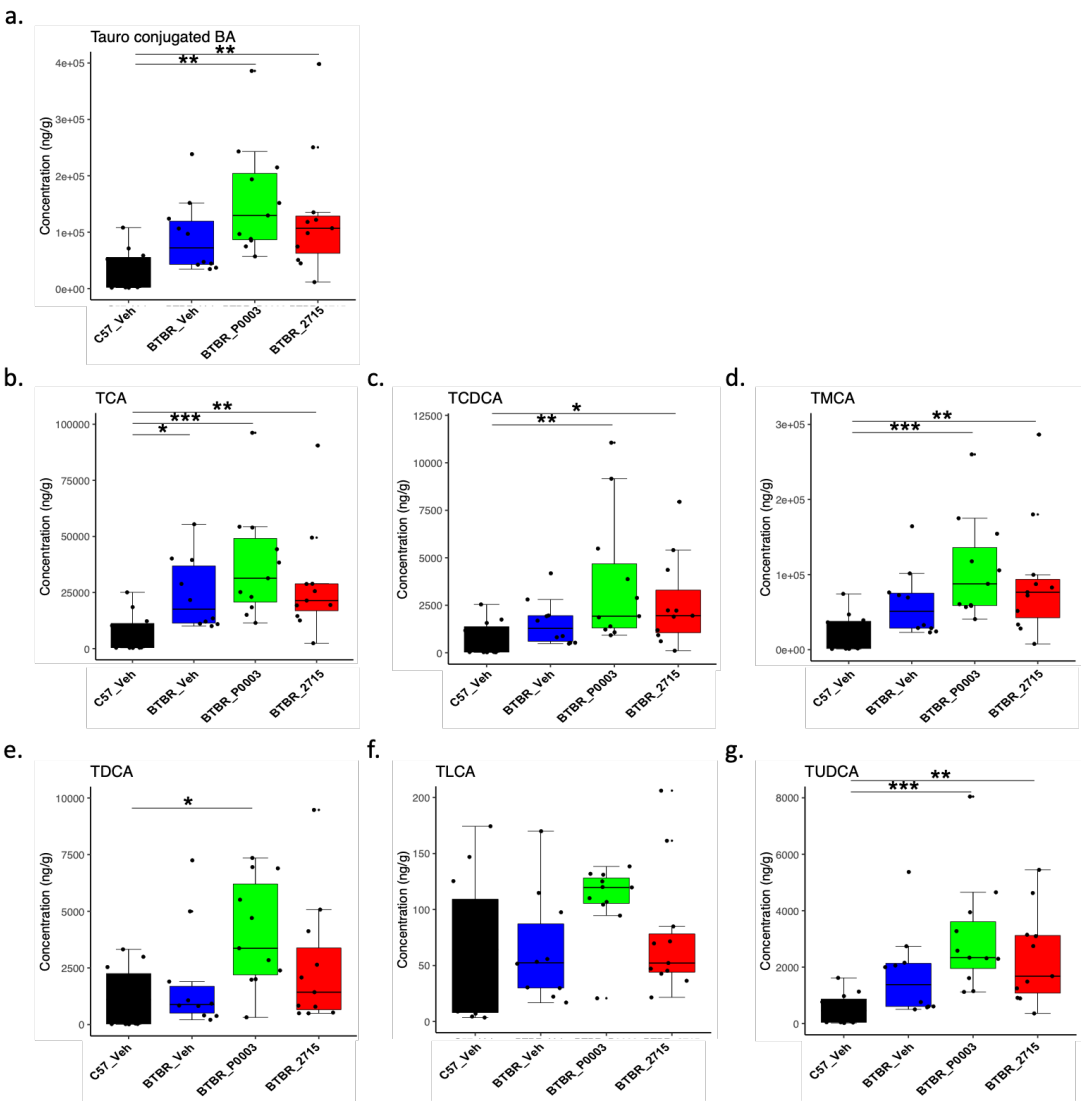


Figure 3.14: **Assessment of total tauro conjugated and free tauro conjugated faecal bile acids in WT C57BL/6 J and BTBR ASD murine model, at week 2.** Relative levels of significantly altered (a) total tauro conjugated BAs, primary tauro conjugated BAs (b) TCA, (c) TCDCA), (d) TMCA, and secondary tauro conjugated BAs (e) TDCA, (f) TLCA and (g) TUDCA, at week 2. For controls: C57_Veh (*n*=11) and BTBR_Veh (*n*=10), and where bacterial treatments *L. salivarius* strain P0003 (BTBR_P0003 (*n*=11)) and *B. adolescentis* strain 2715 (BTBR_2715 (*n*=11)) were applied. RStudio software version 2021.09.0 was used for mean ± standard deviation (SD). Statistical significance was calculated using Kruskal-Wallis and Dunn's Multiple Comparison Test (*= p<0.05; **=p<0.01; ***=p<0.001). Abbreviations see *Table 2.9*.

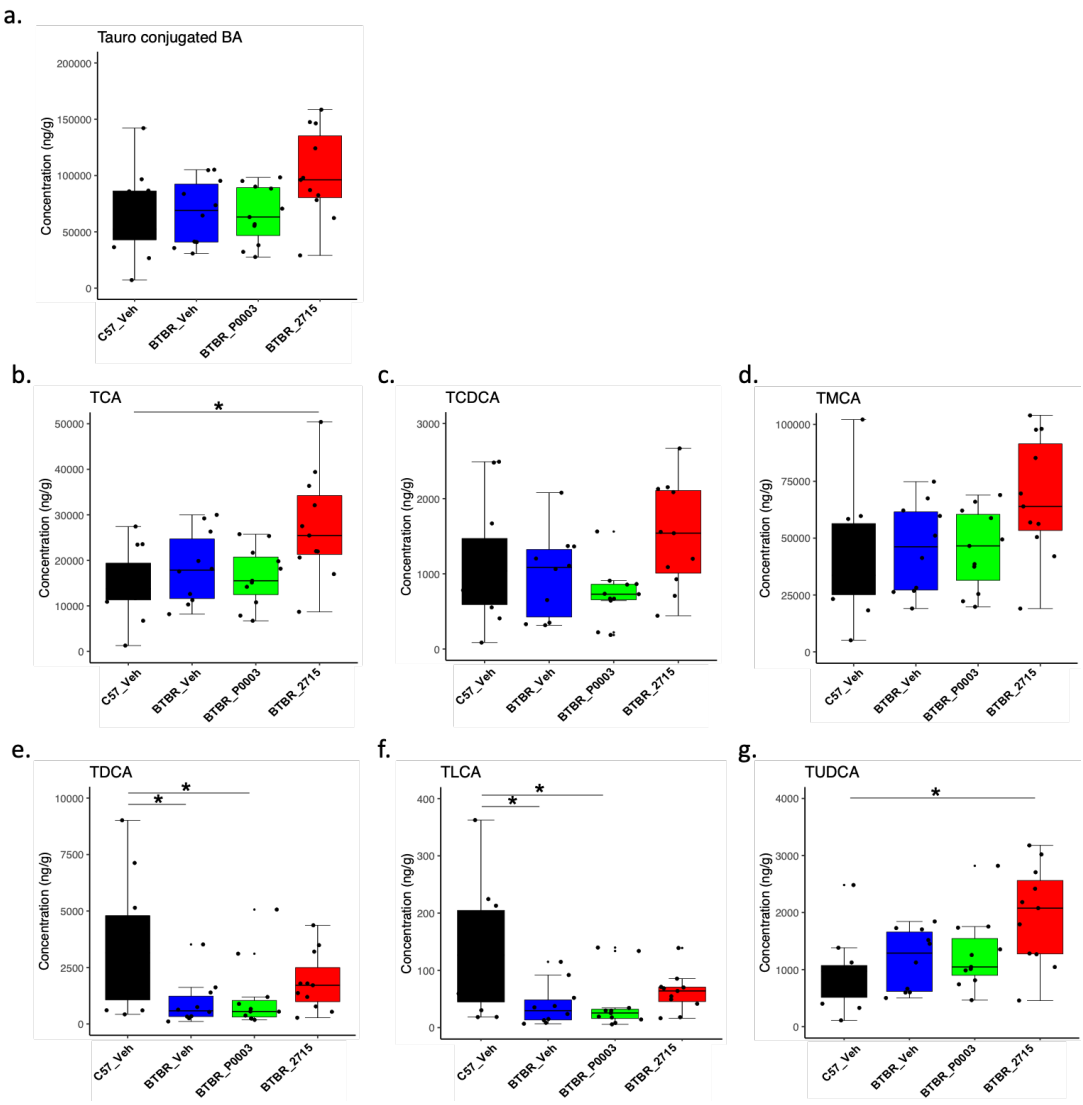
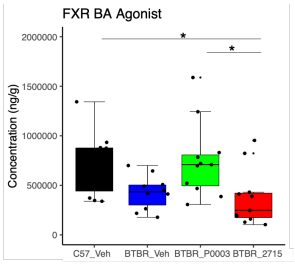


Figure 3.15: **Assessment of total tauro conjugated and free tauro conjugated faecal bile acids in WT C57BL/6 J and BTBR ASD murine model, at endpoint week 9.** Relative levels of significantly altered (a) total tauro conjugated BAs, primary tauro conjugated BAs (b) TCA, (c) TCDCA), (d) TMCA, and secondary tauro conjugated BAs (e) TDCA, (f) TLCA and (g) TUDCA, at endpoint week 9. For controls: C57_Veh (*n*=11) and BTBR_Veh (*n*=10), and where bacterial treatments *L. salivarius* strain P0003 (BTBR_P0003 (*n*=11)) and *B. adolescentis* strain 2715 (BTBR_2715 (*n*=11)) were applied. RStudio software version 2021.09.0 was used for mean ± standard deviation (SD). Statistical significance was calculated using Kruskal-Wallis and Dunn's Multiple Comparison Test (*= p<0.05; **=p<0.01; ***=p<0.001). Abbreviations see *Table 2.9*.

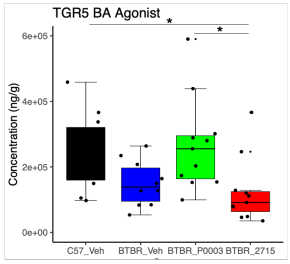
Taken together, similar to that reported by Golubeva *et al.,* (2017) at endpoint (week 9), faecal BAs indicated that the untreated ASD model mice were lower for total, primary and secondary BAs, compared to control WT animals (C57_Veh) (*Figure 3.12*), an effect attributable to tauro conjugated BAs and secondary BAs. We showed that in the lower gut at endpoint, these bacterial interventions, have the potential to increase total BA levels and reduce tauro conjugated BAs. Therefore, BA signature alterations may impact gut-liver axis and local signalling where individual or collective BAs act as ligands for receptor activation and repression. The collective potential of BA ligands (outlined for each receptor above) was assessed to indicate the potential impact on these signalling receptors at the different time points (0, 2, 9 weeks); for FXR, for VDR for TGR5 (*Figure 3.16*).

At start point, baseline week 0, the levels of BAs representing agonist potential were largely the same throughout the groups for the FXR, TGR5 and VDR activation, with most variation between BTBR groups. *L. salivarius* strain P0003 (BTBR_P0003) showed significantly higher levels of these potential BA agonists compared to *B. adolescentis* strain 2715 (BTBR_2715) (*Figure 3.16* (a-c)). Interestingly, at baseline, BTBR groups contained significantly higher levels of potential BA FXR antagonists, compared to WT control C57_Veh mice (*Figure 3.16* (d)). By week 2 these levels were the same for potential activation of the FXR, TGR5 and VDR in bacterial treated *L. salivarius* strain P0003 (BTBR_P0003) animals, though not significant, while BTBR_Veh and *B. adolescentis* strain 2715 (BTBR_2715) animals were significantly lower, compared to C57_Veh control animals (*Figure 3.16* (e-g)). Interestingly, BTBR bacteria treated groups remained significantly higher for potential BA FXR antagonists, compared to WT control C57_Veh mice (*Figure 3.16* (h)). By 9 weeks, potential activation levels for all 3 receptors remained low in the ASD Model BTBR groups relative to control WT animals (*Figure 3.16* (i-k)). Indeed, levels of potential BA FXR antagonists remained similar across all groups, indicating levels restored to that of control WT C57_Veh mice (*Figure 3.16* (l)). The predictions are for possible deficits in the FXR, TGR5 and VDR activation in ASD model BTBR animals over time, effects, partially rectified with bacterial intervention by week 9.

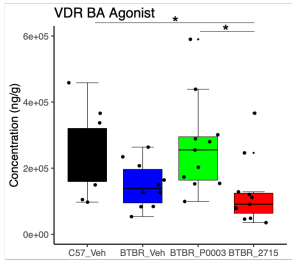
a.



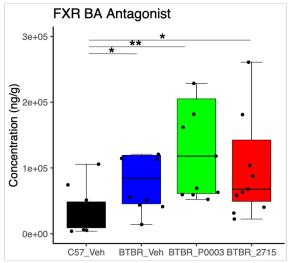
b.



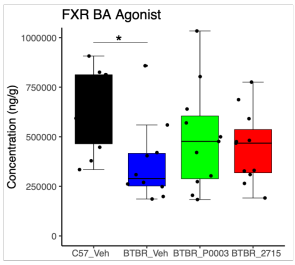
c.



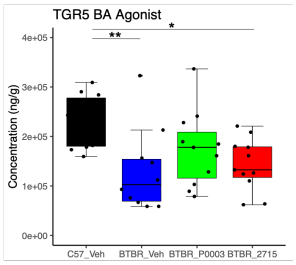
d.



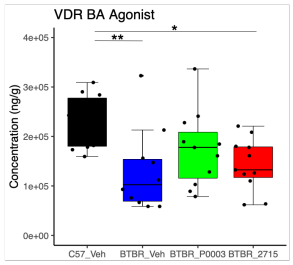
e.



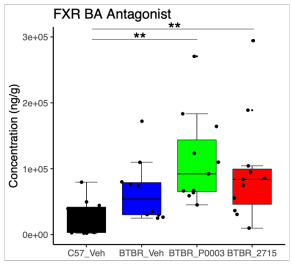
f.



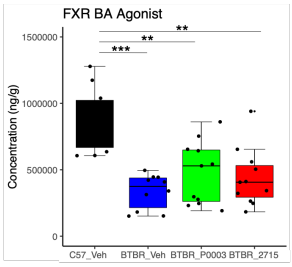
g.



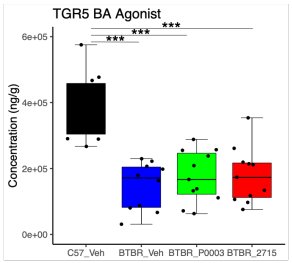
h.



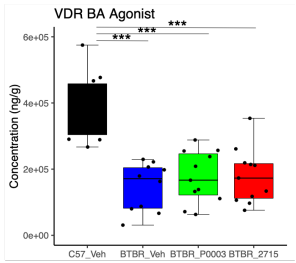
i.



j.



k.



l.

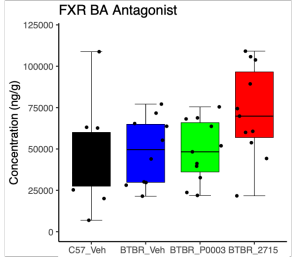


Figure 3.16: **Assessment of potential signalling bile acids in WT C57BL/6 J and ASD BTBR mice.** Specific BA moieties and their potential to act as agonists for nuclear receptors (a), (e), (i) Farnesoid X Receptor (FXR), (b), (f), (j) G-protein coupled receptor TGR5, (c), (g), (k) Vitamin D Receptor (VDR) and potential for (d), (h), (l) FXR antagonist, at baseline week 0 (a-d), week 2 (e-h) and at endpoint week 9 (i-j). C57_Veh *n*=11, BTBR_Veh *n*=10, BTBR_P0003 *n*=11 and BTBR_2715 *n*=11. RStudio software version 2021.09.0 was used with mean ± standard deviation (SD). Statistical significance was calculated using Kruskal-Wallis and Dunn's Multiple Comparison Test (*= p<0.05; **=p<0.01; ***=p<0.001). Abbreviations see *Table 2.9*.

3.2.1.4 Lactobacillus salivarius strain P0003 and Bifidobacterium adolescentis strain 2715 interventions improved BTBR mouse behaviour symptomatically.

Placing this work in context with gut physiology and behaviour, our collaborators (Cryan Lab) conducted a range of assays to determine gut motility and permeability, both defects previously observed in BTBR mice relative to control animals (Golubeva *et al.,* 2017). As previously shown and confirmed here, gut transit was significantly slower in BTBR gut, determined using carmine red-intestinal motility (*Figure 3.17* (a)). Interference by probiotic strains *L. salivarius* strain P0003 (BTBR_P0003) and by *B. adolescentis* strain 2715 (BTBR_2715), indicated significant, small increases in gut transit or mobility (*Figure 3.17* (a)). Furthermore, bacterial interventions could restore gut barrier function regionally, reducing permeability in the gut of BTBR mice to that of control C57 mice (*Figure 3.17* (c)). FITC Flux measurements indicated that small and large intestine permeability were significantly increased in BTBR mice compared to WT C57 control mice (*Figure 3.17* (b-c)). The introduction of either bacteria species could reduce small intestine permeability, though this wasn't significant (*Figure 3.17* (b)), however *L. salivarius* strain P0003 (BTBR_P0003) feeding significantly reduced large intestinal permeability, relative to BTBR untreated mice (BTBR_Veh) (*Figure 3.17* (c)) restoring barrier function to non BTBR, (C57_Veh) levels. Social interactions and anxiety levels, characteristics of the ASD behavioural phenotype and in deficit on the BTBR ASD model, were then examined. Animals were observed in a maze chamber test situation for 1. Curiosity surrounding an open chamber and open space 2. Interaction with familiar and non-familiar objects 3.

Curiosity to explore environment, here, for all 3 tests the delivery of either bacteria strain significantly improved these behaviours (*Figure 3.17* (d)). Interestingly, only *L. salivarius* strain P0003 fed animals proved exploratory in a novel environment (*Figure 3.17* (e)). Interestingly, bacterial interventions did not appear to significantly improve anxiety and depressive-like behaviours in BTBR ASD mice (*Figure 3.17* (f)).

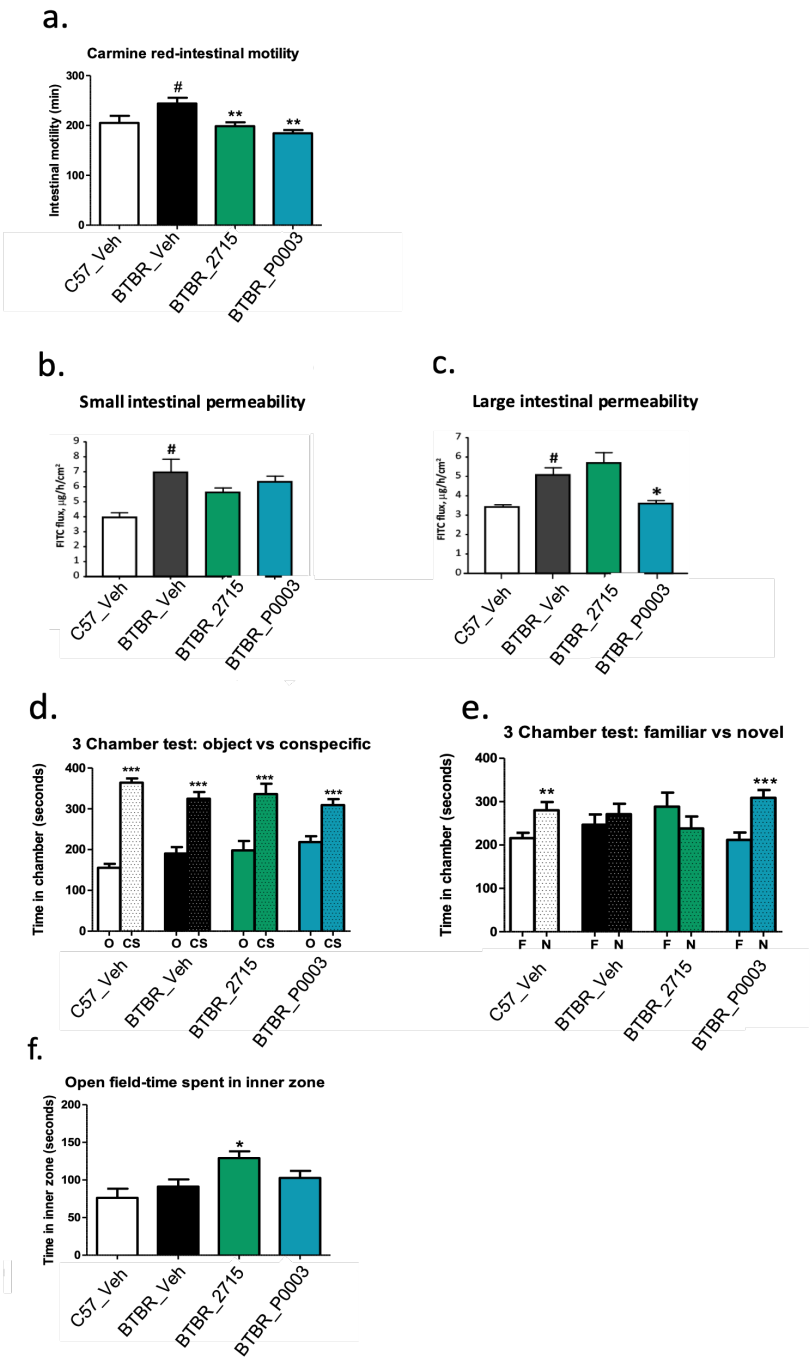


Figure 3.17: **Assessment of gut motility, permeability, and ASD behavioural phenotypes in WT C57BL/6 J and ASD model BTBR mice.** (a) Carmine red-intestinal

motility test. (b) Small intestinal permeability assessment. (c) Large intestinal permeability assessment. (d) Three-chamber test, assessment of social behaviour (object vs. conspecific). (e) Three-chamber test, assessment of social behaviour (familiar vs. non-familiar). (f) Open-field test, assessment of anxiety and depressive-like behaviour. Courtesy of Dr Anna Golubeva (Cryan Lab). *n*=12/group. Statistics: ANOVA and pairwise ANOVA (*= p<0.05; **=p<0.01; ***=p<0.001).

In conclusion, BA alterations in BTBR animals mimicked those reported by our group in 2017 (Golubeva *et al.,* 2017). There were no major circulating BA alterations, with the exception of secondary BAs LCA and TLCA, while its parent BA CDCA was reduced. Interference here, by two different BA modulating representatives of the gut microbiome did not significantly alter BAs to restore them to C57_Veh control WT animal levels, despite elevation in trends towards WT control conjugated BAs and free BAs. Implications are that the master BA regulator the FXR would be agonistically unaltered, at least in circulation.

Faecal BAs were altered over time, by genotype (BTBR) and by treatments with subtle but significant effects. When translated to intestinal physiology, the presence of the strains influenced gut motility and permeability differentially and this could translate to behaviour. The scope of this work did not include hormonal functions and in the discussion below, we will place these data in frame with other literature. Taken together, the age related changes in BA metabolism, the link to behaviour and gut motility as well as barrier function point to potential manipulation of the ASD condition, and gut dysbiosis, through probiotic means, perhaps subtly through targeted BA intervention. The TGR5 and the FXR receptors can mediate these functions -among others- our data showed that in the lower gut, the levels of BA potential agonists for NRs FXR and VDR in all BTBR mice groups was reduced over time suggesting possible lower activation levels of these signalling pathways. We show that microbial feeding has the potential to alter BA receptor signalling both in circulation and in the gut to suggest that these strains may have the potential to be applied to humans as a means to improve behaviour and gastrointestinal traits in ASD.

Part II: Parkinson's Disease - Are bile acid and fatty acid levels altered in circulation and in the gut of Parkinson's Disease patients?

3.2.2.0 Microbial metabolic functions are altered in Parkinson's Disease.

Symptoms of gut dysbiosis have not only been demonstrated in ASD, but also in Parkinson's Disease (PD) (Goodwin *et al.,* 1971; Jost and Schimrigk, 1991; Huang *et al.,* 2021; Alharthi *et al.,* 2022). We reasoned that microbially produced or altered metabolites could also have a role in PD. Above, bacterial intervention appeared to subtly rescue microbial conversions and signalling potential of BAs whilst improving behavioural patterns associated to ASD (in mouse model). We reasoned that the composition and concentrations of human gut metabolites, BAs and FAs, with the potential to influence downstream signalling processes, may be altered in the context of PD. Therefore, as a second part to this chapter, BAs and FAs were extracted and analysed (Materials and Methods, Section 2.3.5), from pre-existing collected (2018) faecal samples (Eldermet), and from those samples garnered by Prof Cora O'Neills Lab (Parkinson's Disease and the Microbiome study). This study was intended as a GI associated study to compliment the circulating BA data for a small cohort of healthy individuals and PD sufferers (Materials and Methods, Section 2.3.1). The associated aetiology of the disease and the relevant demographic details are given (including medications) in Materials and Methods, Section 2.3.1.

Independently circulating BAs were examined as part of another study (Ellen Joyce and Susan Joyce (2017), data not shown) to indicate that indeed circulating BAs are altered in the human aetiology towards PD and that medication did influence these metabolite levels (Ellen Joyce MRes, unpublished data 2017). These circulating BAs were further analysed using Targetlynx^{TM} (Waters) software as we wish to extend the metabolites examined and establish whether the changes seen in the context of PD, are reflected in the gut of PD patients. In this case, human PD patient samples, were compared with age relevant cohorts from the ELDERMET Study (https://link.springer.com/referenceworkentry/10.1007/978-1-4614-6418-1_94-1?noAccess=true), with the permission of Prof P. O'Toole, alterations in BA and FA concentrations were examined to determine the specific changes that could be associated with the gut microbial modification.

3.2.2.1 Quality controls for Bile Acids

As per section 3.2.1.1, tables appendix III SI.3.8-9 indicate that *n*=30 BAs were investigated, and table appendix III SI.3.11-12 indicate that *n*=16 FAs were investigated. The nomenclature, abbreviations, classifications of each, according to microbial or dietary enzyme are indicated in these tables. Each sample was applied (*n*=3 technical replicates) to mass spectrometry (UPLC-TMS) analysis with Internal Standards (IS), deuterated Chenodeoxycholic Acid (CDCAd4) and deuterated Cholic Acid (CAd4) applied to assess the extraction efficiency (Materials and Methods, Section 2.3.5). Extraction was deemed efficient as CAd4 IS levels were equally distributed despite the groupings, for both plasma and faecal samples (*Figure 3.18*). Although recovery was more efficient from plasma than from faecal samples (as expected). A standard curve (range from 0.0064 to 20 μg/ml appendix III SI.3.10 and 3.13) was applied to generate reliable quantities and limit of detection for each BA and FA where reliability was scored R^2 between 0.96 and 0.99 for BA and between 0.5 and 0.99 for FA.

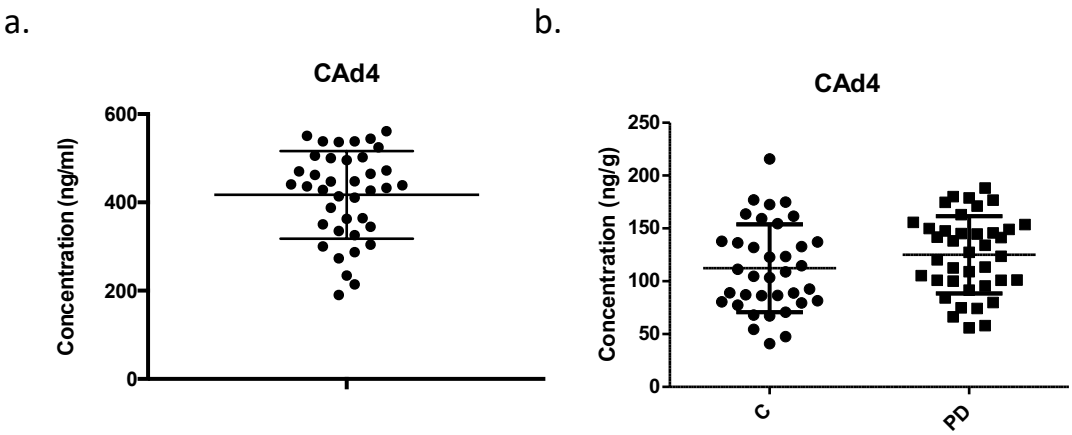


Figure 3.18: **Assessment of extraction efficiency from control volunteers (C) and Parkinson's Disease patients (PD) human biological material.** Internal standard Cholic Acid d4 in (a) plasma of all samples and (b) faeces of control volunteers (C) and Parkinson's Disease patients (PD). In circulation: Control *n*=10, PD *n*=29. In faeces: Control *n*=36, PD *n*=39. GraphPad Prism v6 was used with mean ± standard deviation (SD). Statistical significance is indicated and calculated using Wilcoxon test (*= p<0.05; **=p<0.01; ***=p<0.001; ****=p<0.0001).

3.2.2.2 Specific microbially altered circulating bile acids are enriched in Parkinson's Disease patients.

Circulating BAs (Ellen Joyce and Susan Joyce (2017)) were further analysed using Targetlynx^{TM} (Waters) software to establish whether the changes seen in the context of PD, are reflected in the gut of PD patients. Principle Component Analysis (PCA) showed that BAs remained quite similar across all sample groups (*Figure 3.19*). There was no clear separation between Control volunteers and PD patients, including those PD patients being treated with PD medication (Treated) and those PD patients not being treated with PD medication (Untreated) (see *Table 2.4*) (*Figure 3.19*).

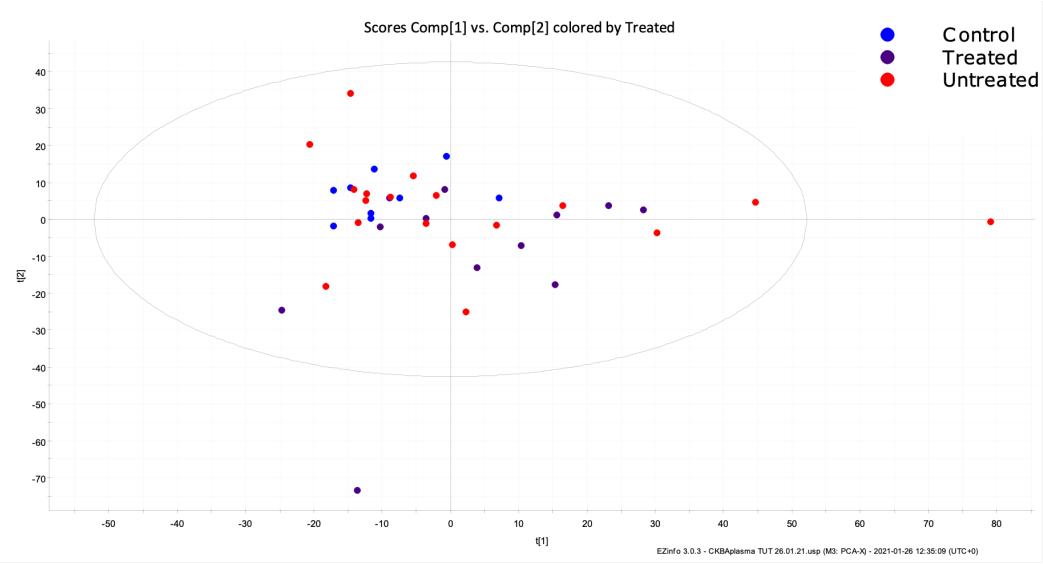
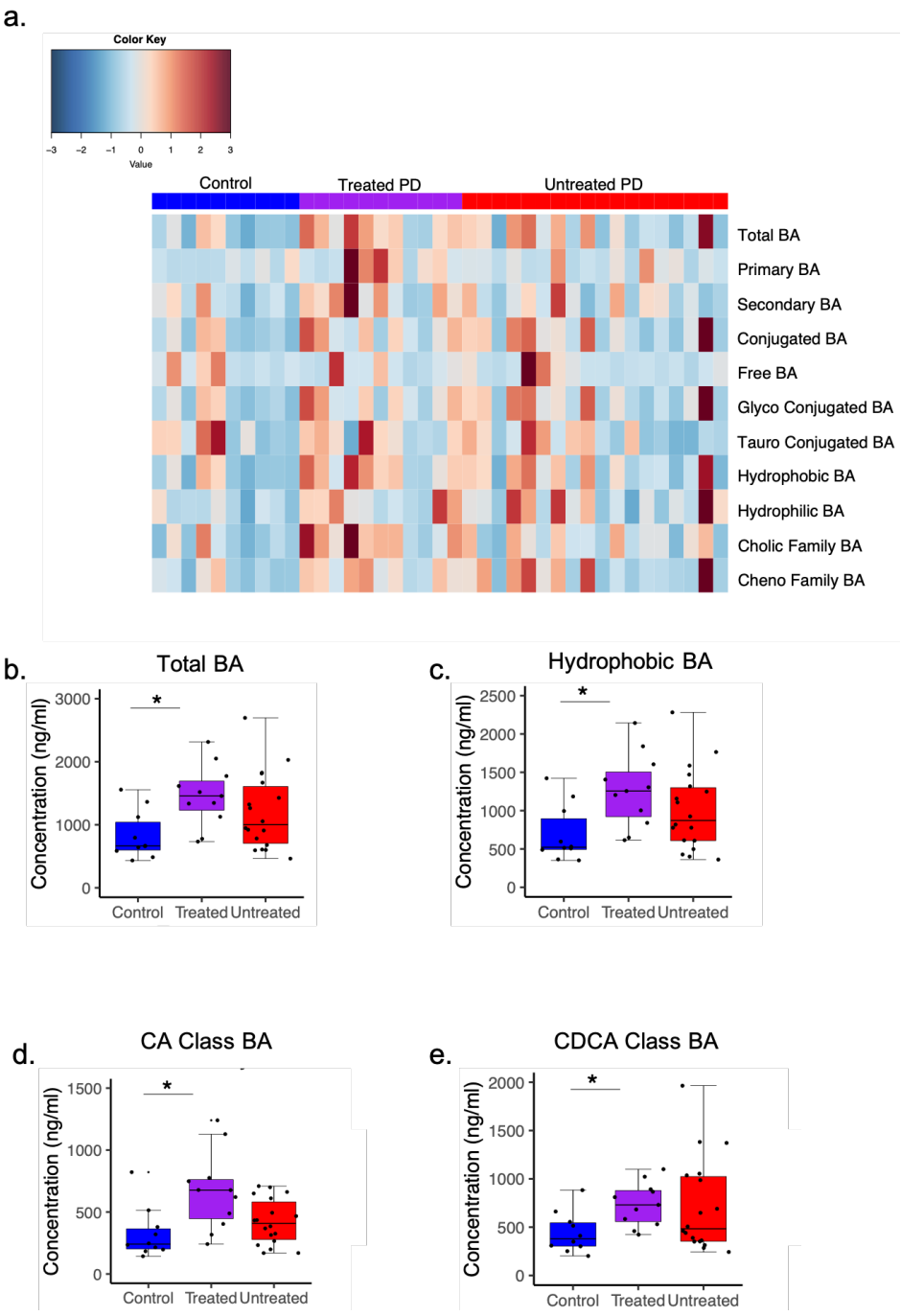


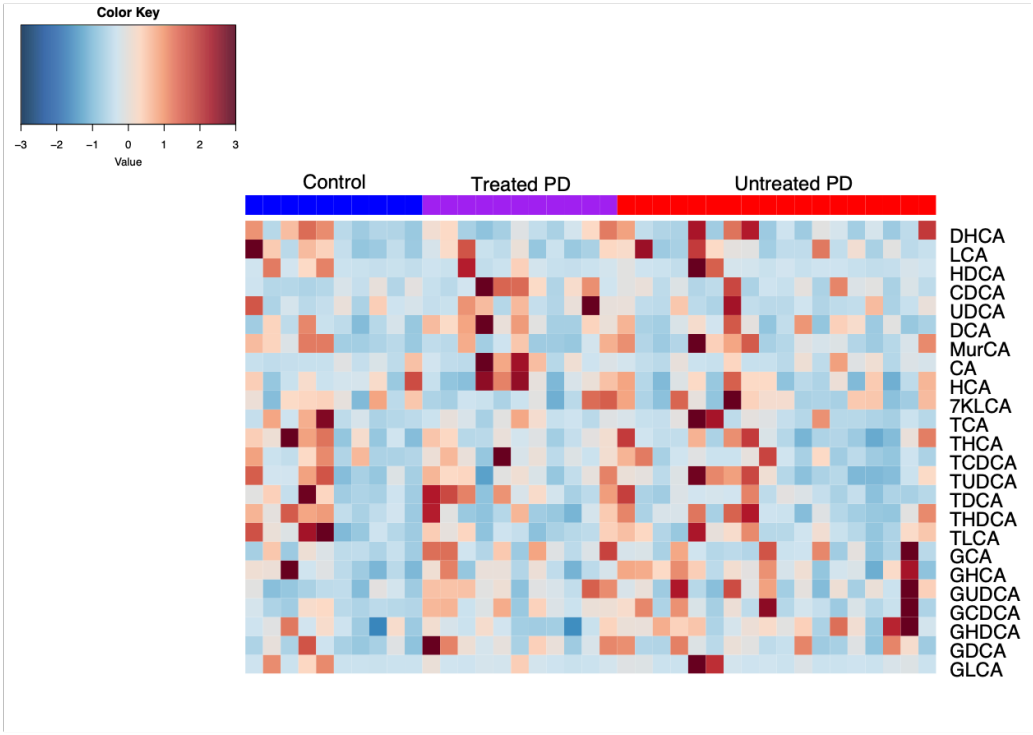
Figure 3.19: **Principal component analysis (PCA) of all detected bile acids for plasma material.** The coloured representations are blue dots for control volunteers (*n*=10), purple dots for PD patients receiving PD medication (Treated *n*=11), and red dots for PD patients not receiving PD medication (Untreated *n*=18).

Initial spearman correlation heatplot analysis indicated that circulating BAs may be increased in PD patients (both those PD patients receiving PD medication (Treated) and those PD patients not receiving PD medication (Untreated) see *Table 2.4*) for all BA classes of (*Figure 3.20* (a)). With respect to each individual BA (*Figure 3.16* (f)), a similar effect was predicted through heatplot analysis compared to control volunteers.

Examining individual circulating BAs more closely, showed that treated PD patients were significantly elevated for the exact levels of total BAs, for hydrophobic BAs (those LCA>DCA>CDCA>CA>UDCA>MCA), cholic acid family of BAs and chenodeoxycholic acid family of mono or dihydroxyl BAs (*Figure 3.20* (b-e)), compared to control volunteers. PD patients displayed significantly higher concentrations of individual circulating conjugated BA GUDCA (*Figure 3.20* (g)), compared to control volunteers. Upon further examination, this elevation of GUDCA was more prevalent in drug treated PD patients (*Figure 3.20* (h)). This data suggests that circulating BAs are indeed altered in PD patients compared to control volunteers, specifically in those PD patients taking PD medications. The levels of secondary BAs (hydrophobic LCA and DCA) and conjugated secondary BA (GUDCA) points to microbial modification enrichment and uptake from the gut, where these moieties are generated.


a.
Color Key
−3 −2 −1 0 1 2 3
Value
Control
Treated PD
Untreated PD
Total BA
Primary BA
Secondary BA
Conjugated BA
Free BA
Glyco Conjugated BA
Tauro Conjugated BA
Hydrophobic BA
Hydrophilic BA
Cholic Family BA
Cheno Family BA
b.
Total BA
Concentration (ng/ml)
3000
2000
1000
0
*
Control
Treated
Untreated
c.
Hydrophobic BA
Concentration (ng/ml)
2500
2000
1500
1000
500
0
*
Control
Treated
Untreated
d.
CA Class BA
Concentration (ng/ml)
1500
1000
500
0
*
Control
Treated
Untreated
e.
CDCA Class BA
Concentration (ng/ml)
2000
1500
1000
500
0
*
Control
Treated
Untreated

f.



g. h.

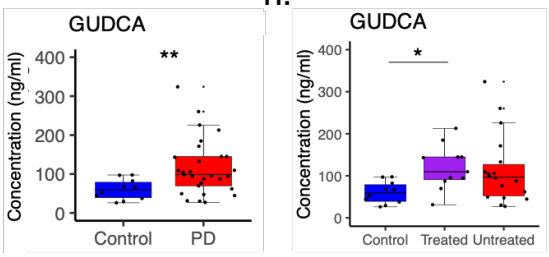
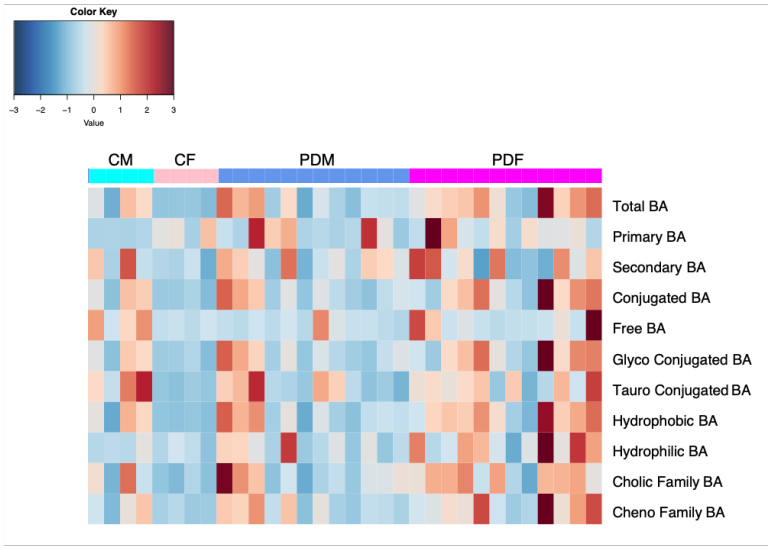


Figure 3.20: **Assessment of circulating bile acids in Parkinson's Disease patients compared to Control Volunteers.** Spearman correlation heatmap of (a) classes and (f) individual BAs; the degree of correlation of change is indicated, with red as positive and blue as negative (RStudio software version 2021.09.0). Significantly altered (b-e) classes and (g-h) individual BAs quantified against standard curves generated for each analyte and normalized according to internal standards (IS), calculated using Targetlynx^{TM} (Waters) software. Control *n*=10, PD *n*=29: Treated PD *n*=11, Untreated PD *n*=18. Statistics was applied using RStudio software version 2021.09.0 and is represented as mean ± standard deviation (SD). Statistical significance is indicated and calculated using Wilcoxon test, and Kruskal-Wallis and Dunn's Multiple Comparison Test (*= p<0.05; **=p<0.01; ***=p<0.001; ****=p<0.0001). Abbreviations see *Table 2.9*.

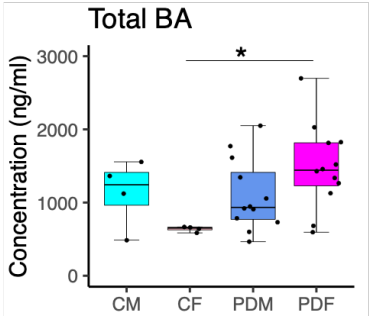
3.2.2.3 Female Parkinson's Disease patients have higher circulating bile acid concentrations compared to male Parkinson's Disease patients.

We next examined whether alterations in circulating BA concentrations are gender specific, particularly as PD is more common in males than in females (~1.5 times more common) (Reekes et al., 2020). Initial analysis using spearman correlation heatplots comparing healthy male (CM) and female (CF) control volunteers, and male (PDM) and female (PDF) PD patients indicated potential higher levels of all classes of BA (*Figure 3.21* (a)) amongst male control volunteers (CM) and female PD patients (PDF) (*Figure 3.21* (a)). This translated to individual BA moiety heatplots (*Figure 3.21* (d)). Examining exact levels of circulating BAs showed that indeed female PD patients (PDF) were significantly increased for total BAs, compared to healthy female control volunteers (CF) (*Figure 3.21* (b)). Interestingly, healthy male control volunteers (CM) showed significantly higher concentrations of total tauro conjugated BAs, compared to their female control counterparts (CF) (*Figure 3.21* (c)). Indeed, male control volunteers (CM) carried significantly higher circulating HDCA, MurCA, TLCA, TCA and THCA, compared to their female counterparts (CF) (*Figure 3.21* (e-i)). This data suggests that circulating BAs are indeed at higher concentrations in male control volunteers (CM) compared to female control volunteers (CF), however, this trend is reversed in PD patients where female PD patients (PDF) trend towards higher concentration levels of circulating BAs compared to male PD patients (PDM).

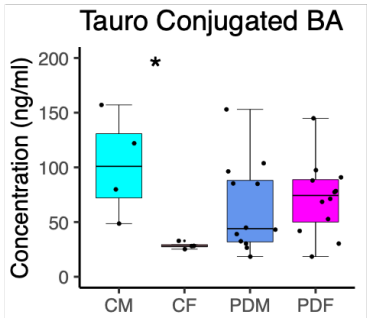
a.


Color Key
−3 −2 −1 0 1 2 3
Value
CM
CF
PDM
PDF
Total BA
Primary BA
Secondary BA
Conjugated BA
Free BA
Glyco Conjugated BA
Tauro Conjugated BA
Hydrophobic BA
Hydrophilic BA
Cholic Family BA
Cheno Family BA

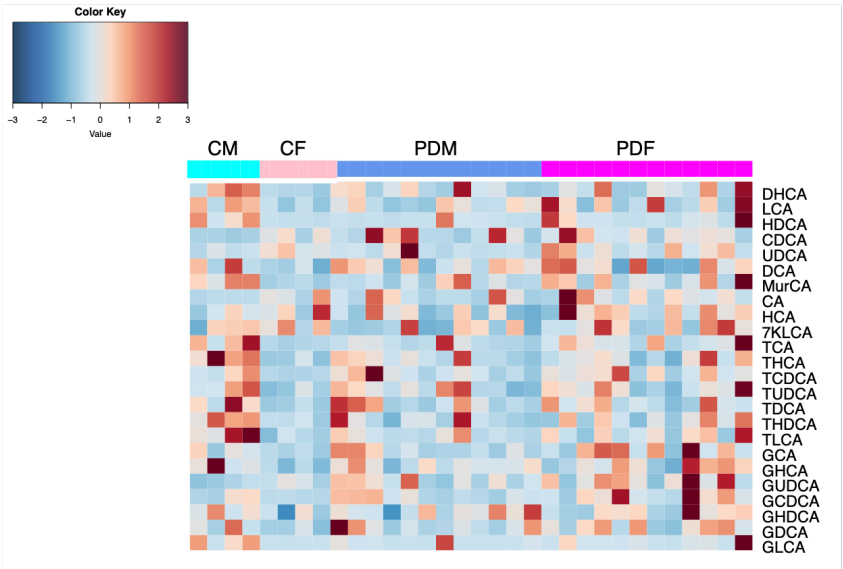
b.


Total BA
Concentration (ng/ml)
3000
2000
1000
0
*
CM
CF
PDM
PDF

c.


Tauro Conjugated BA
Concentration (ng/ml)
200
150
100
50
0
*
CM
CF
PDM
PDF

d.


Color Key
−3 −2 −1 0 1 2 3
Value
CM
CF
PDM
PDF
DHCA
LCA
HDCA
CDCA
UDCA
DCA
MurCA
CA
HCA
7KLCA
TCA
THCA
TCDCA
TUDCA
TDCA
THDCA
TLCA
GCA
GHCA
GUDCA
GCDCA
GHDCA
GDCA
GLCA

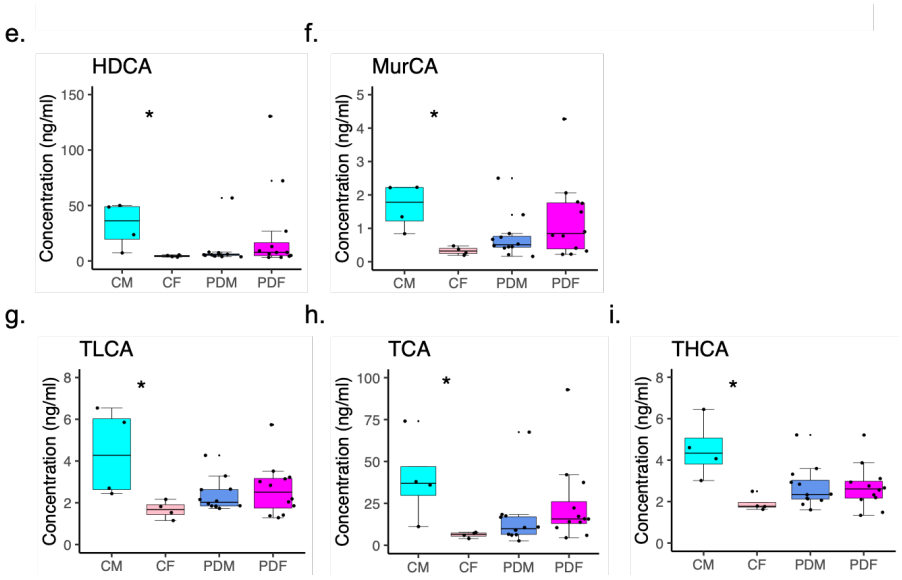


Figure 3.21: **Assessment of circulating bile acids, with respect to gender, in Parkinson's Disease patients compared to Control Volunteers.** Spearman correlation heatmap of (a) classes and (d) individual BAs; the degree of correlation of change is indicated, with red as positive and blue as negative (RStudio software version 2021.09.0). Significantly altered (b) and (c) classes and (e-i) individual BAs quantified against standard curves generated for each analyte and normalized according to internal standards (IS), calculated using Targetlynx™ (Waters) software. Male Control (CM) *n*=4, Female Control (CF) *n*=4, Male PD (PDM) *n*=12, Female PD (PDF) *n*=12. RStudio software version 2021.09.0, represented as mean ± standard deviation (SD). Statistical significance is indicated and calculated using Kruskal-Wallis and Dunn's Multiple Comparison Test (*= p<0.05; **=p<0.01; ***=p<0.001; ****=p<0.0001). Abbreviations *Table 2.9*.

3.2.2.4 Total and conjugated circulating bile acid concentrations correlate with age in Parkinson's Disease patients.

In the literature it has been reported that as we age, our BAs change (Bertolotti *et al.,* 2007; Frommherz *et al.,* 2016; Lee *et al.,* 2016). Indeed, evidence of such changes over time were seen in the ASD BTBR model and WT mice C57_Veh above. We next examined circulating BA concentrations change with respect to age for PD patient's age relative to control individuals. Initial examination of circulating BAs in control volunteers and PD patients revealed that, no BA classes, or individual BAs, that were directionally altered in aging in the healthy cohort. Specific to PD patients, total tauro conjugated BAs, hydrophilic BAs and individual BA, tauro conjugated chenodeoxycholic Acid (TCDCA) (*Figure 3.22* (a-c)), were all significantly positively correlated with age, while control subjects (*n*=8) were not significantly altered for these BAs although a trend towards an increase for both the categories and for TCDCA were evident here (*Figure 3.22* (a-c)). These data suggest differences in gut, bacteria and metabolite functions specific to PD sufferers.

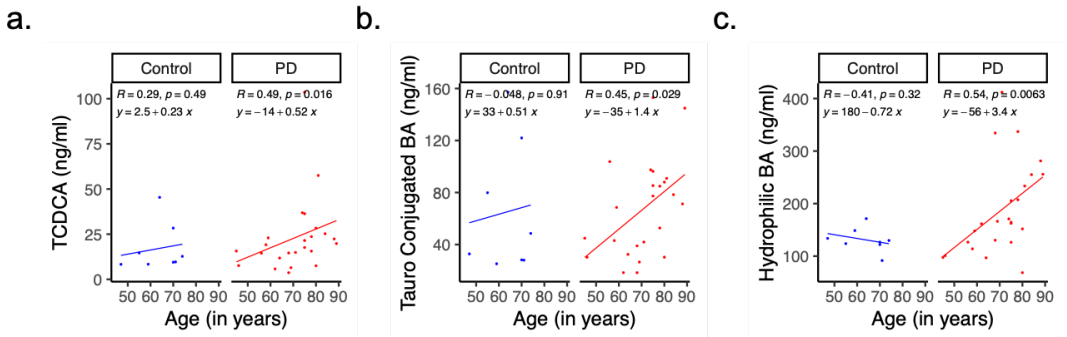


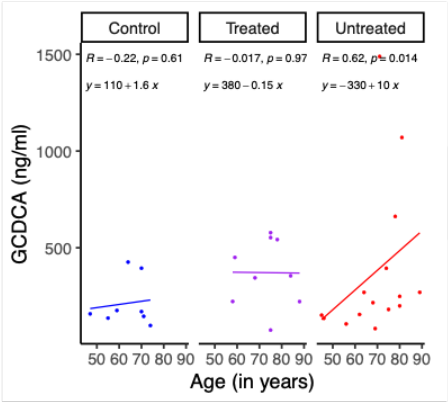
***Figure 3.22:* Assessment of circulating bile acids correlation with age in Parkinson's Disease patients relative to healthy individuals.** (a-c) Spearman correlation assessment, indicates significantly altered (a) individual and (b-c) classes or BA families between Control (healthy individuals) and diagnosed PD sufferers. The age range is from 45-89 years of age, the degree of correlation of change is indicated by R value, and significance is indicated by p value, both values were assessed and calculated using RStudio software version 2021.09.0 mean ± standard deviation (SD). Control *n*=8, PD *n*=24. Spearman correlation (R value) and statistical significance is

indicated (*= p<0.05; **=p<0.01; ***=p<0.001; ****=p<0.0001). Abbreviations see *Table 2.9*.

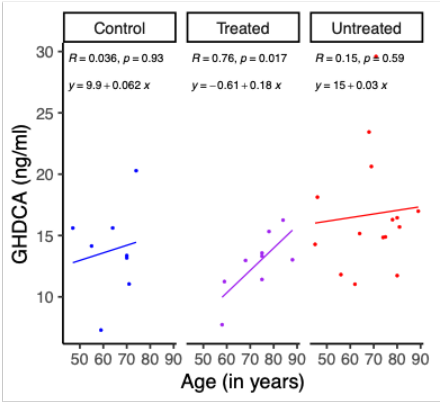
Individuals among the PD cohort (*n*=24) are in receipt of medication (*n*=9) (*Table 2.3*), medications include: Sinemet, Procyclidine, Rasagiline and Requip, further correlation analysis was performed based on medication or not to decipher those alterations that are specific to PD. Here, a number of BAs were significantly elevated with aging and possibly with disease progression, to include total BAs (p=0.013), hydrophobic BAs (p=0.015), conjugated BA (p=0.021). In particular, GCA (p=0.034) and GCDCA (p=0.014) as well as both families of BAs: CA class (p=0.032) and CDCA family class (p=0.038) (*Figure 3.23*).

Interestingly, with treatment, the significant elevation of total BAs, conjugated BAs, both classes and families of BAs and individual moieties GCA and GCDCA were lost, although the levels tended to be elevated, relative to control healthy subjects in the same age range (*Figure 3.23* (a), (e) and (i-n)). Of further interest, treated PD patients now displayed their own significant BAs; Here, GHDCA (p=0.017), two free BAs secondary BA LCA (p=0.00099) and secondary BA MurCA (p=0.013), along with a range of tauro conjugated secondary BA TLCA (p=0.00099); TDCA (p=0.038); TUDCA (p= p=0.00099)), were extremely significantly elevated relative to control individuals (*Figure 3.23* (b-d), (f-h)). It may be that these secondary BAs elevated in Treated PD may confer beneficial effects in circulation, or that treatment either enhances certain gut microbial populations towards BA modification functions or even that efficient but selective transport of conjugated and secondary BAs are occurring, with treatment in the gut. Transport, gut transit and drug/toxin removal are a feature of receptors TGR5, the FXR and VDR and hence the BA ligand potential of agonists and antagonists for these receptors were calculated (see section 3.2.2.5 below) and examined.

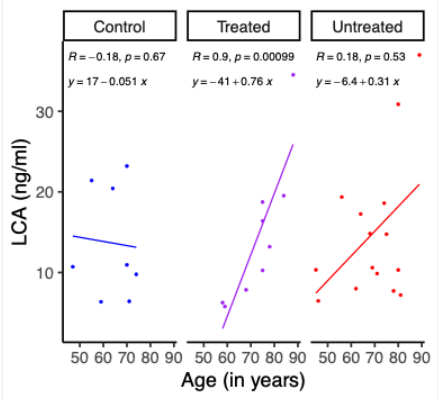
a.


Control
Treated
Untreated
R = −0.22, p = 0.61
y = 110 + 1.6 x
R = −0.017, p = 0.97
y = 380 − 0.15 x
R = 0.62, p = 0.014
y = −330 + 10 x
GCDCA (ng/ml)
1500
1000
500
50 60 70 80 90
Age (in years)

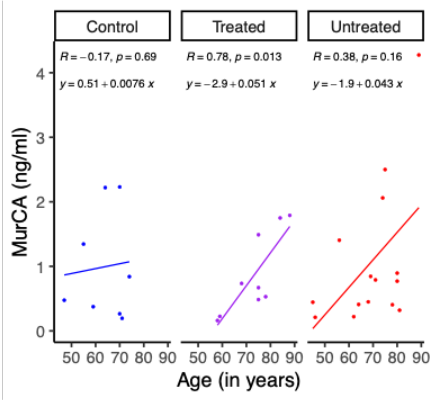
b.


Control
Treated
Untreated
R = 0.036, p = 0.93
y = 9.9 + 0.062 x
R = 0.76, p = 0.017
y = −0.61 + 0.18 x
R = 0.15, p = 0.59
y = 15 + 0.03 x
GHDCA (ng/ml)
30
25
20
15
10
50 60 70 80 90
Age (in years)

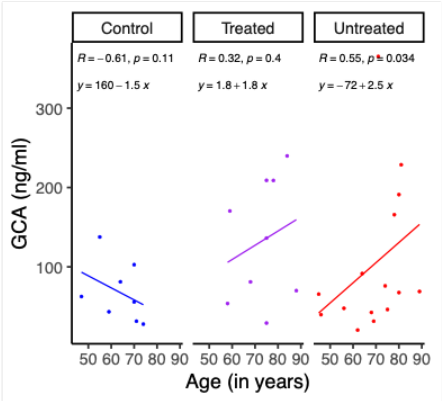
c.


Control
Treated
Untreated
R = −0.18, p = 0.67
y = 17 − 0.051 x
R = 0.9, p = 0.00099
y = −41 + 0.76 x
R = 0.18, p = 0.53
y = −6.4 + 0.31 x
LCA (ng/ml)
30
20
10
50 60 70 80 90
Age (in years)

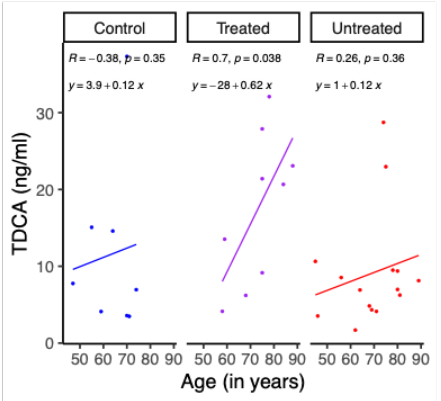
d.


Control
Treated
Untreated
R = −0.17, p = 0.69
y = 0.51 + 0.0076 x
R = 0.78, p = 0.013
y = −2.9 + 0.051 x
R = 0.38, p = 0.16
y = −1.9 + 0.043 x
MurCA (ng/ml)
4
3
2
1
0
50 60 70 80 90
Age (in years)

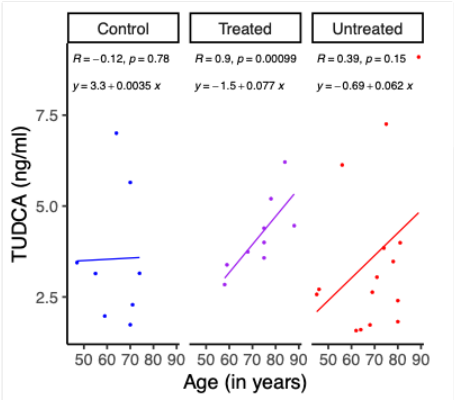
e.


Control
Treated
Untreated
R = −0.61, p = 0.11
y = 160 − 1.5 x
R = 0.32, p = 0.4
y = 1.8 + 1.8 x
R = 0.55, p = 0.034
y = −72 + 2.5 x
GCA (ng/ml)
300
200
100
50 60 70 80 90
Age (in years)

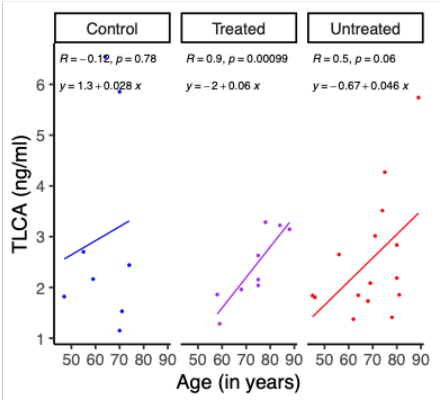
f.


Control
Treated
Untreated
R = −0.38, p = 0.35
y = 3.9 + 0.12 x
R = 0.7, p = 0.038
y = −28 + 0.62 x
R = 0.26, p = 0.36
y = 1 + 0.12 x
TDCA (ng/ml)
30
20
10
0
50 60 70 80 90
Age (in years)

g.


Control
Treated
Untreated
R = −0.12, p = 0.78
y = 3.3 + 0.0035 x
R = 0.9, p = 0.00099
y = −1.5 + 0.077 x
R = 0.39, p = 0.15
y = −0.69 + 0.062 x
TUDCA (ng/ml)
7.5
5.0
2.5
50 60 70 80 90
Age (in years)

h.


Control
Treated
Untreated
R = −0.12, p = 0.78
y = 1.3 + 0.028 x
R = 0.9, p = 0.00099
y = −2 + 0.06 x
R = 0.5, p = 0.06
y = −0.67 + 0.046 x
TLCA (ng/ml)
6
5
4
3
2
1
50 60 70 80 90
Age (in years)

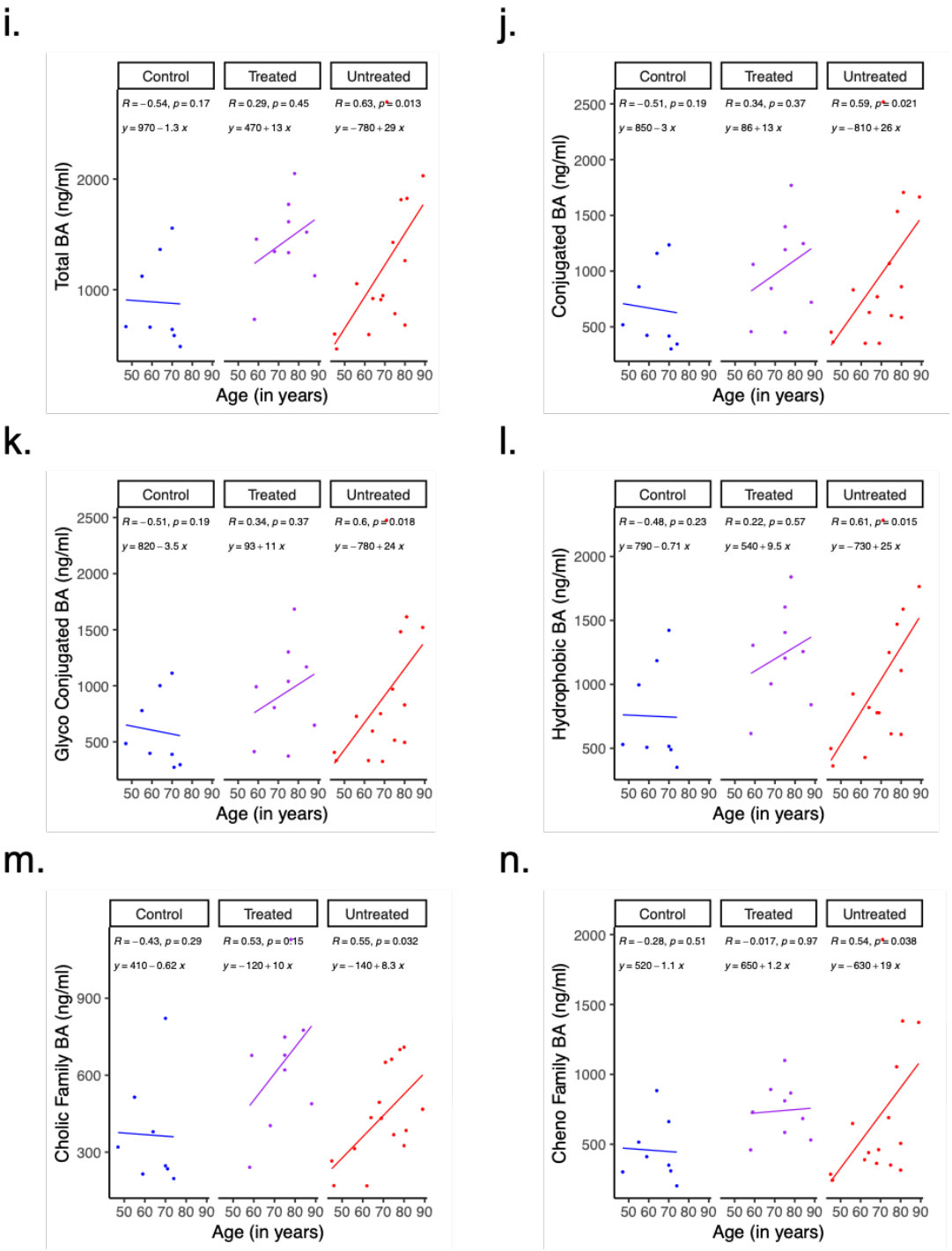


Figure 3.23: **Assessment of circulating bile acids correlation with age from Parkinson's Disease patients treated with medication, and in healthy humans.** (a-n) Spearman correlation assessment, indicates significantly altered (a-h) individual and (i-n) classes or BA families for Control (healthy individuals) and diagnosed PD sufferers divided to two categories, Treated and Untreated, in terms of drug administration. The age range is from 45-89 years of age, the degree of correlation of change is indicated by R value, and significance is indicated by p value, both values

were assessed and calculated using RStudio software version 2021.09.0, mean ± standard deviation (SD). Control *n*=8, PD *n*=24: Treated PD *n*=9, Untreated PD *n*=15. Spearman correlation (R value) and statistical significance is indicated (*= p<0.05; **=p<0.01; ***=p<0.001; ****=p<0.0001). Abbreviations see *Table 2.9*.

3.2.2.5 Bile acid agonists for nuclear receptors FXR and VDR are elevated in circulation of treated Parkinson's Disease patients.

BA agonists and antagonists for nuclear receptors (NR) Farnesoid X Receptor (FXR) and Vitamin D Receptor (VDR), signalling in circulation. The sum of the concentration levels of free BAs: CA, CDCA, DCA, α-MCA and β-MCA represent potential FXR agonists; UDCA, GUDCA, TUDCA and TMCA represent potential FXR antagonists; LCA, CDCA, DCA and CA represent potential VDR agonists; while LCA, TLCA, CA, CDCA and DCA represent potential TGR5 agonists. Their levels were examined to determine any potential alterations in BA signalling.

Concentration levels of circulating potential BA agonists for NRs FXR, TGR5 and VDR were significantly higher in Treated PD patients, compared to untreated patients and control volunteers (*Figure 3.24* (a), (c) and (d)). This suggests potential higher activation of these signalling pathways, perhaps impacting BA synthesis feedback loop and on metabolism. The concentration levels of the FXR antagonist was also significantly higher in Treated PD patients, compared to control volunteers (*Figure 3.24* (b)). Assessment of circulating BAs correlation with UPDRS, motor sub-score and MoCA scale, from Parkinson's Disease patients treated with medication, and without, appendix III SI.3.16-18.

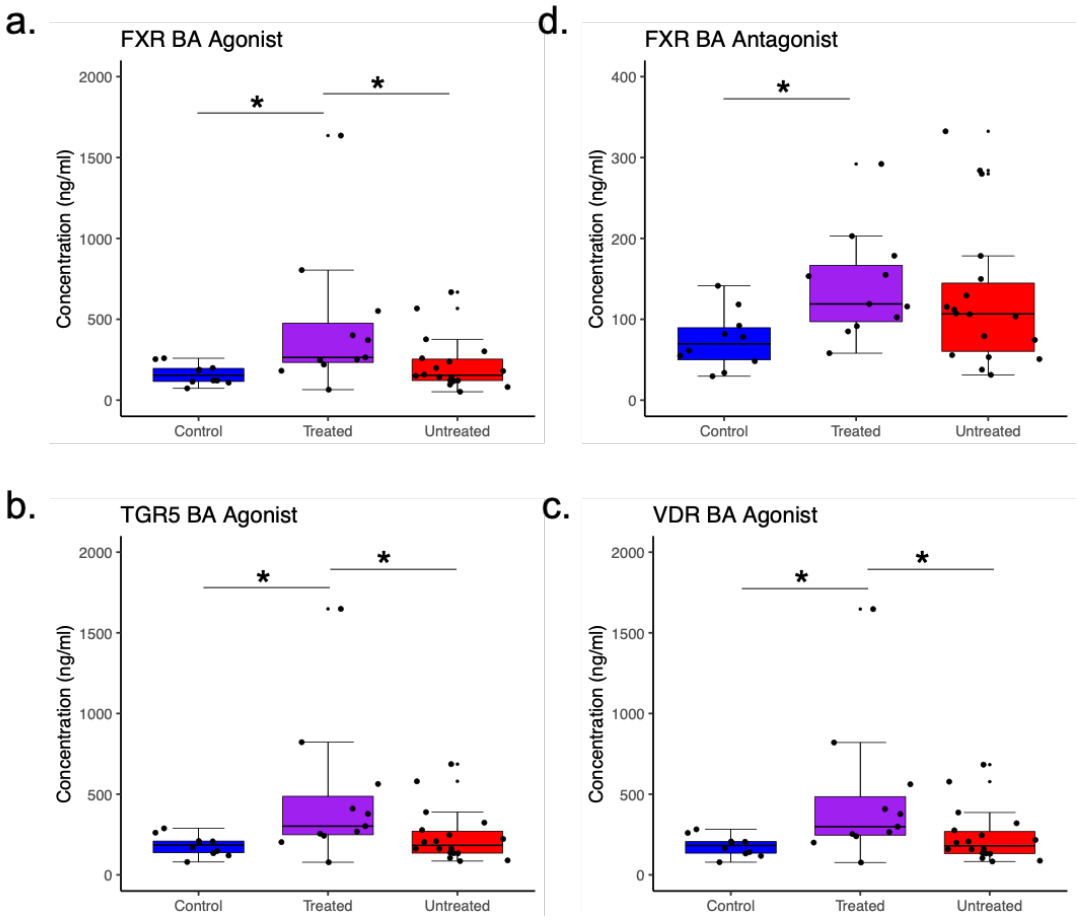


Figure 3.24: **Assessment of potential signalling bile acids from Parkinson's Disease patients, relative to healthy individuals.** Specific BA moieties and their potential to act as agonists for nuclear receptors (a) Farnesoid X Receptor (FXR), (c) G-protein coupled receptor TGR5, (d) Vitamin D Receptor (VDR) and (b) potential FXR BA antagonist. Control *n*=10, Treated PD *n*=11, Untreated PD *n*=18. RStudio software version 2021.09.0, mean ± standard deviation (SD). Statistical significance was calculated using Kruskal-Wallis and Dunn's Multiple Comparison Test (*= p<0.05; **=p<0.01; ***=p<0.001). Abbreviations see *Table 2.9*.

3.2.2.6 Specific microbially altered faecal bile acids are enriched in Parkinson's Disease patients.

Given the enrichment for microbially modified BAs in circulation in PD patients we next examined BA metabolism from a separate cohort of PD patients and from healthy individuals within the same age range, where faecal material, representing the lower gut functions, were collected (ELDERMET study and Parkinson's Disease

and the Microbiome study, Materials and Methods, Section 2.3.1). To examine alterations in faecal BA signatures, faecal BA were extracted from human PD patients and age-matched control volunteers (ELDERMET study), applied to UPLC-TMS and analysed according to Materials and Methods, Section 2.3.5. Principle Component Analysis (PCA) showed that BAs remained quite similar across all sample groups (*Figure 3.25*). There was no clear separation between Control volunteers and Parkinson's Disease patients, including those PD patients being treated with PD medication (Treated) and those PD patients not receiving PD medication (Untreated) (see *Table 2.5*) (*Figure 3.25*).

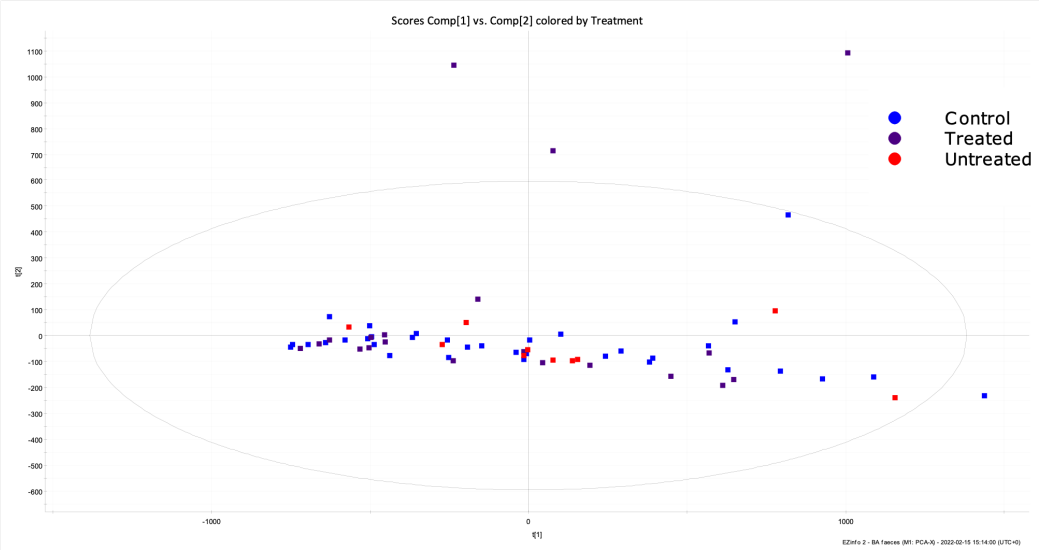


Figure 3.25: **Principal component analysis (PCA) of all detected bile acids for faecal material.** The coloured representations are blue dots for control volunteers (*n*=34), purple dots for PD patients receiving PD medication (Treated *n*=20), and red dots for PD patients not receiving PD medication (Untreated *n*=10).

Initial analysis using spearman correlation heatplots indicated that PD patients (particularly Treated PD patients) showed correlations with higher levels of all classes of BA (*Figure 3.26* (a)), a prediction that remained evident for individual BAs (*Figure 3.26* (b)), relative to control volunteers. When exact quantified levels of each category/class of BA and individual BAs were examined, no significance was detected between PD patients and control volunteers (see appendix III SI.3.19).

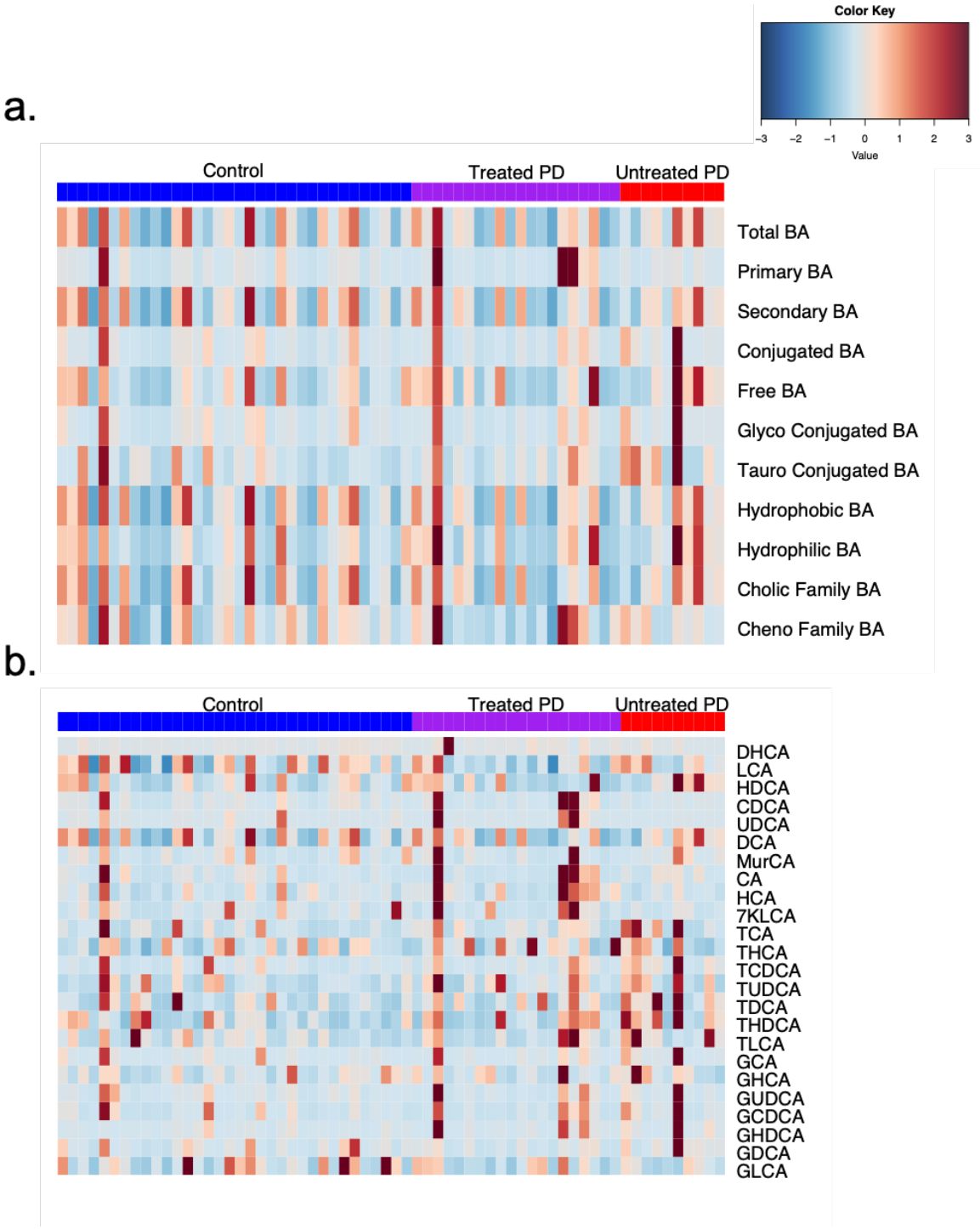


Figure 3.26: **Assessment of faecal bile acids from Parkinson's Disease patients, compared to healthy individuals.** Spearman correlation heatmap of (a) classes and (b) individual BAs; the degree of correlation of change is indicated, with red as positive and blue as negative generated using RStudio software version 2021.09.0. Control *n*=34, PD *n*=30: Treated PD *n*=20, Untreated PD *n*=10. Abbreviations see *Table 2.9*.

Next, we examined whether there were alterations in BA signatures with respect to gender, similar to circulating BAs (section 3.2.2.3). Spearman correlation heatplots comparing control male (CM) and control female (CF) volunteers, and PD male (PDM) and PD female (PDF) patients indicated no differences (*Figure 3.27* (a)), and each individual BA (*Figure 3.27* (b)), compared to male control volunteers (CM) and male PD patients (PDM), respectively. Again, significance between PD patients and control volunteers was not detected in classes or individual BAs (see appendix III SI.3.20).

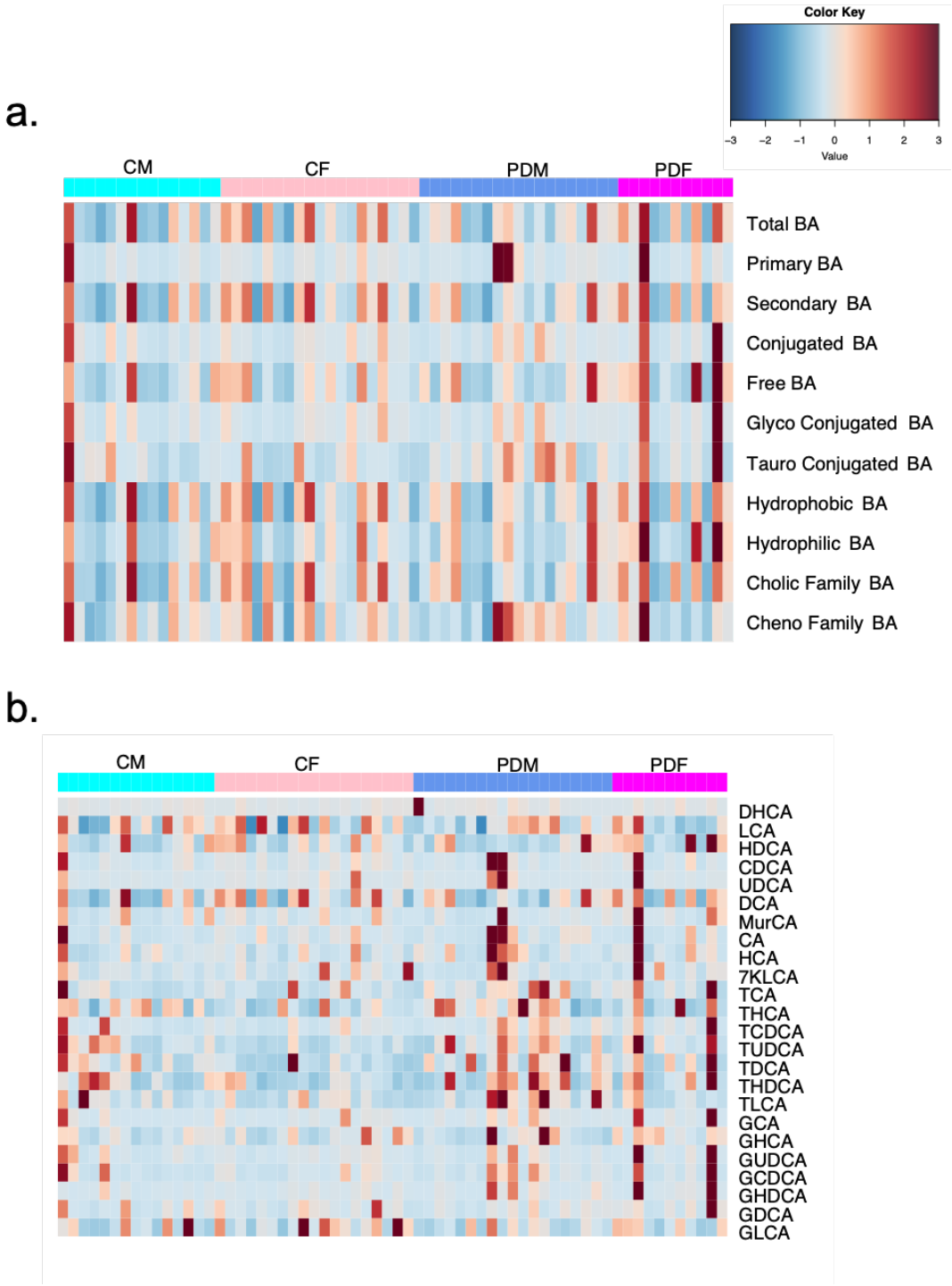
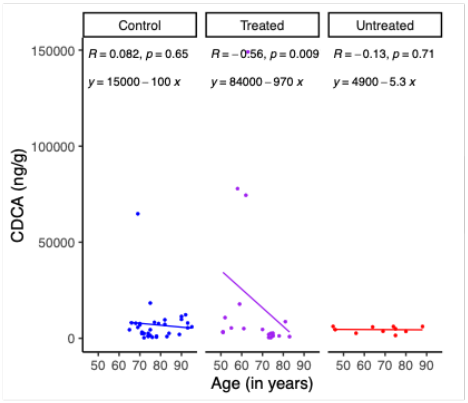


Figure 3.27: **Assessment of faecal bile acid moieties by gender from Parkinson's Disease patients, compared to healthy control volunteers.** Spearman correlation heatmap of (a) classes and (b) individual BAs; the degree of correlation of change is indicated, with red as positive and blue as negative generated using RStudio software version 2021.09.0. Male Control (CM) *n*=15, Female Control (CF) *n*=19, Male PD (PDM) *n*=19, Female PD (PDF) *n*=11. Abbreviations *Table 2.9*.

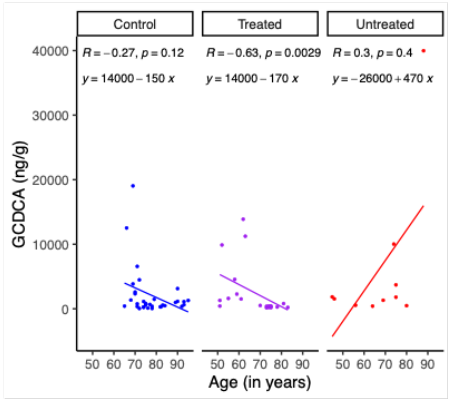
3.2.2.7 Total and conjugated faecal bile acid concentrations negatively correlate with age in Parkinson's Disease patients.

In examining faecal BAs and their categories in aging and in disease, control volunteers showed age related significantly decreased levels of TCDCA (p=0.014) and GCA (p=0.021) (*Figure 3.28* (q) and (r)). PD patients were subdivided into medication treated (Treated) or receiving no medication (Untreated) and examined. Here, while no significant correlation with age was detected for Untreated individuals, Treated PD sufferers showed correlated decreases in total BA (p=0.024), primary BAs (p= 0.037) and secondary BAs (p=0.037) a range of conjugated BA (G/TDCA (p=0.0074,0.014), GLCA (p=0.027), GCDCA (p=0.0029), and the free secondary BAs LCA (p=0.05), and DCA (p=0.044) (*Figure 3.28* (a-p)). This is in stark contrast to the independent study of plasma circulating BAs where treatment is associated with uptake of many of these classes and individual BAs (see section 3.2.2.4 above) and it may therefore reflect transporter and uptake functions, mediated by FXR and other transporters in the gut.

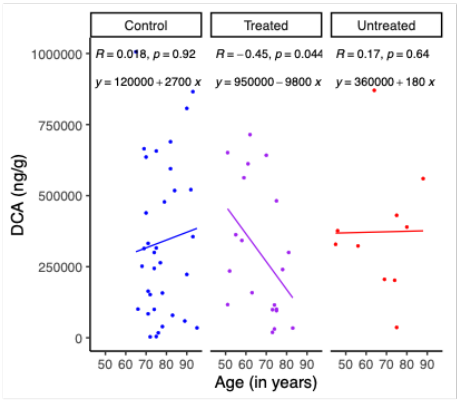
a.


Control
Treated
Untreated
R = 0.082, p = 0.65
y = 15000 − 100 x
R = −0.56, p = 0.009
y = 84000 − 970 x
R = −0.13, p = 0.71
y = 4900 − 5.3 x
CDCA (ng/g)
150000
100000
50000
0
50 60 70 80 90
Age (in years)

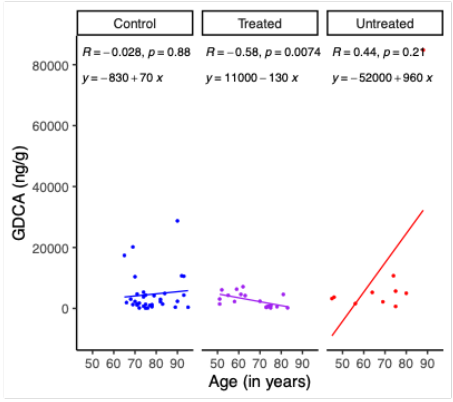
b.


Control
Treated
Untreated
R = −0.27, p = 0.12
y = 14000 − 150 x
R = −0.63, p = 0.0029
y = 14000 − 170 x
R = 0.3, p = 0.4
y = −26000 + 470 x
GCDCA (ng/g)
40000
30000
20000
10000
0
50 60 70 80 90
Age (in years)

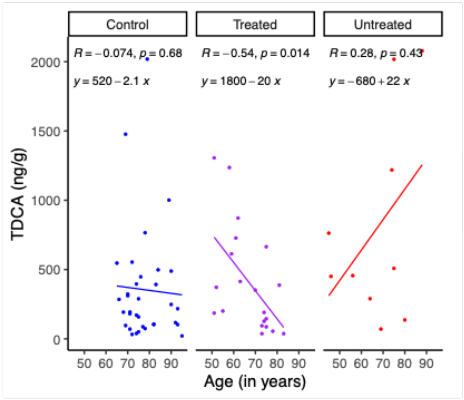
c.


Control
Treated
Untreated
R = 0.018, p = 0.92
y = 120000 + 2700 x
R = −0.45, p = 0.044
y = 950000 − 9800 x
R = 0.17, p = 0.64
y = 360000 + 180 x
DCA (ng/g)
1000000
750000
500000
250000
0
50 60 70 80 90
Age (in years)

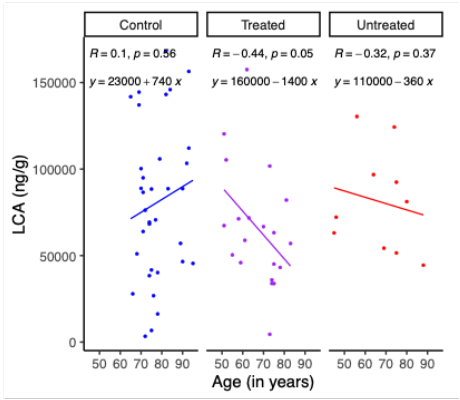
d.


Control
Treated
Untreated
R = −0.028, p = 0.88
y = −830 + 70 x
R = −0.58, p = 0.0074
y = 11000 − 130 x
R = 0.44, p = 0.21
y = −52000 + 960 x
GDCA (ng/g)
80000
60000
40000
20000
0
50 60 70 80 90
Age (in years)

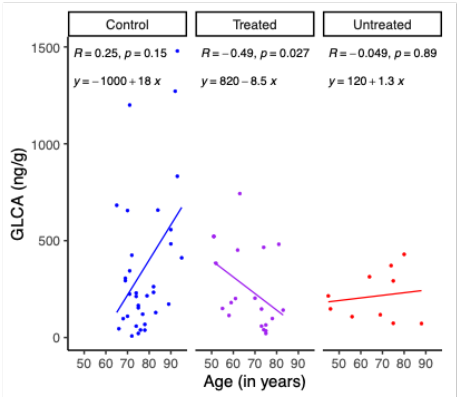
e.


Control
Treated
Untreated
R = −0.074, p = 0.68
y = 520 − 2.1 x
R = −0.54, p = 0.014
y = 1800 − 20 x
R = 0.28, p = 0.43
y = −680 + 22 x
TDCA (ng/g)
2000
1500
1000
500
0
50 60 70 80 90
Age (in years)

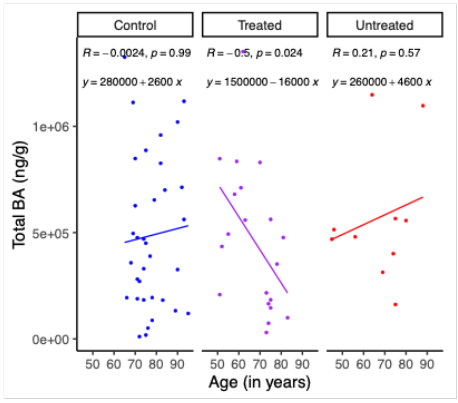
f.


Control
Treated
Untreated
R = 0.1, p = 0.56
y = 23000 + 740 x
R = −0.44, p = 0.05
y = 160000 − 1400 x
R = −0.32, p = 0.37
y = 110000 − 360 x
LCA (ng/g)
150000
100000
50000
0
50 60 70 80 90
Age (in years)

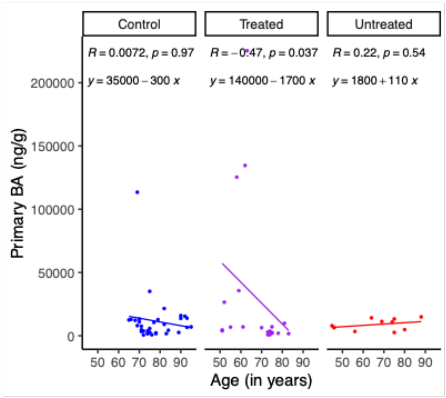
g.


Control
Treated
Untreated
R = 0.25, p = 0.15
y = −1000 + 18 x
R = −0.49, p = 0.027
y = 820 − 8.5 x
R = −0.049, p = 0.89
y = 120 + 1.3 x
GLCA (ng/g)
1500
1000
500
0
50 60 70 80 90
Age (in years)

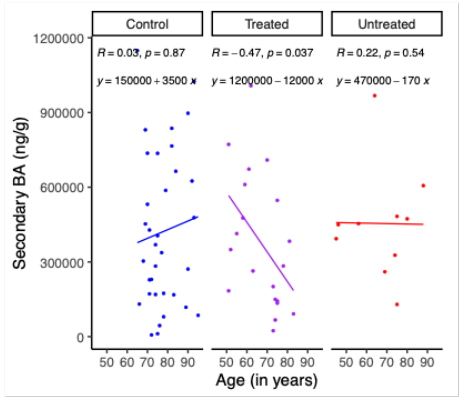
h.


Control
Treated
Untreated
R = −0.0024, p = 0.99
y = 280000 + 2600 x
R = −0.5, p = 0.024
y = 1500000 − 16000 x
R = 0.21, p = 0.57
y = 260000 + 4600 x
Total BA (ng/g)
1e+06
5e+05
0e+00
50 60 70 80 90
Age (in years)

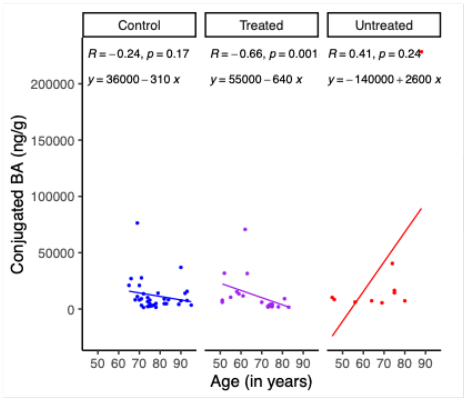
i.


Control
Treated
Untreated
R = 0.0072, p = 0.97
R = −0.47, p = 0.037
R = 0.22, p = 0.54
y = 35000 − 300 x
y = 140000 − 1700 x
y = 1800 + 110 x
Primary BA (ng/g)
Age (in years)

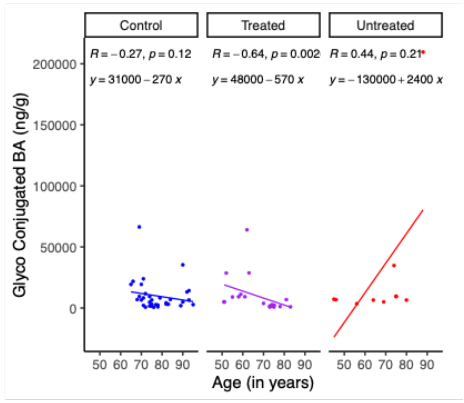
j.


Control
Treated
Untreated
R = 0.03, p = 0.87
R = −0.47, p = 0.037
R = 0.22, p = 0.54
y = 150000 + 3500 x
y = 1200000 − 12000 x
y = 470000 − 170 x
Secondary BA (ng/g)
Age (in years)

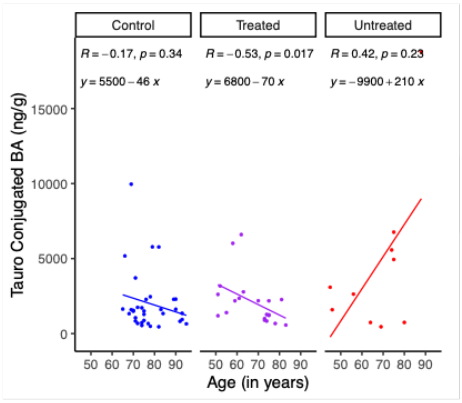
k.


Control
Treated
Untreated
R = −0.24, p = 0.17
R = −0.66, p = 0.001
R = 0.41, p = 0.24
y = 36000 − 310 x
y = 55000 − 640 x
y = −140000 + 2600 x
Conjugated BA (ng/g)
Age (in years)

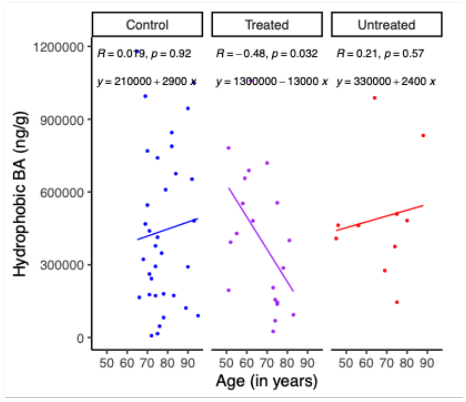
l.


Control
Treated
Untreated
R = −0.27, p = 0.12
R = −0.64, p = 0.002
R = 0.44, p = 0.21
y = 31000 − 270 x
y = 48000 − 570 x
y = −130000 + 2400 x
Glyco Conjugated BA (ng/g)
Age (in years)

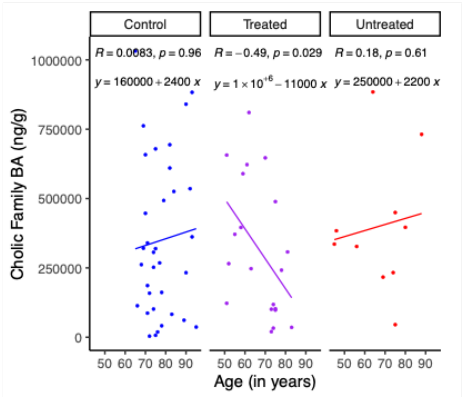
m.


Control
Treated
Untreated
R = −0.17, p = 0.34
R = −0.53, p = 0.017
R = 0.42, p = 0.23
y = 5500 − 46 x
y = 6800 − 70 x
y = −9900 + 210 x
Tauro Conjugated BA (ng/g)
Age (in years)

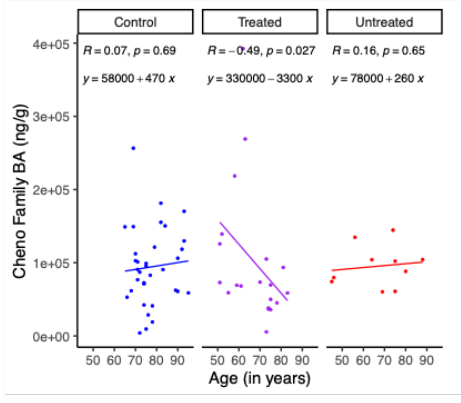
n.


Control
Treated
Untreated
R = 0.019, p = 0.92
R = −0.48, p = 0.032
R = 0.21, p = 0.57
y = 210000 + 2900 x
y = 1300000 − 13000 x
y = 330000 + 2400 x
Hydrophobic BA (ng/g)
Age (in years)

o.


Control
Treated
Untreated
R = 0.0083, p = 0.96
R = −0.49, p = 0.029
R = 0.18, p = 0.61
y = 160000 + 2400 x
y = 1 × 10^+6 − 11000 x
y = 250000 + 2200 x
Cholic Family BA (ng/g)
Age (in years)

p.


Control
Treated
Untreated
R = 0.07, p = 0.69
R = −0.49, p = 0.027
R = 0.16, p = 0.65
y = 58000 + 470 x
y = 330000 − 3300 x
y = 78000 + 260 x
Cheno Family BA (ng/g)
Age (in years)

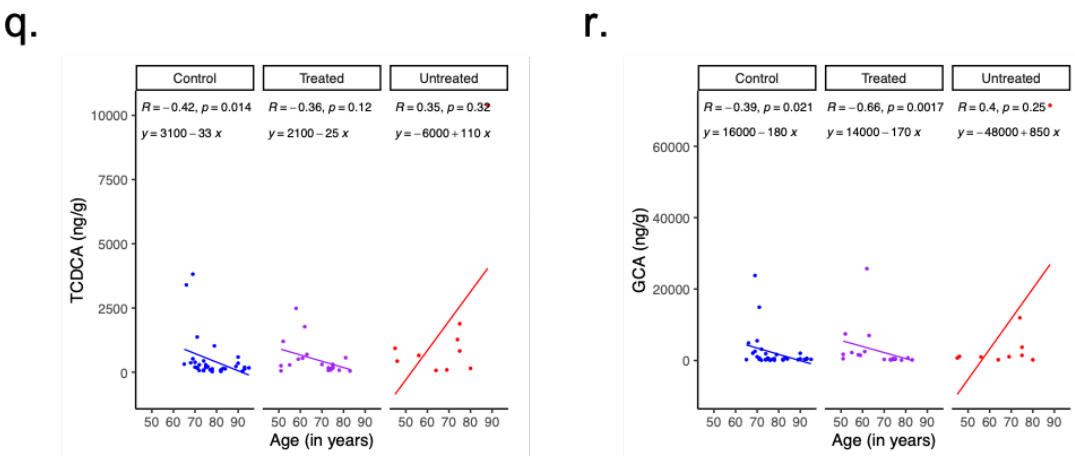


Figure 3.28: **Assessment of faecal bile acids correlation with age from Parkinson's Disease patients, relative to healthy individuals.** (a-r) Spearman correlation assessment and significantly altered classes and individual BAs; the degree of correlation of change is indicated by R value, and significance is indicated by p value Control *n*=34, Treated PD *n*=20, Untreated PD *n*=10., Data was represented as Mean ± standard deviation (SD). Spearman correlation (R value) and statistical significance is calculated using using RStudio software version 2021.09.0 and indicated (*= p<0.05; **=p<0.01; ***=p<0.001; ****=p<0.0001). Abbreviations see *Table 2.9*.

3.2.2.8 Specific faecal bile acid concentrations correlate with disease severity in Parkinson's Disease patients.

Alterations in faecal BAs were examined to correlate BA signatures with PD disease severity scores. Disease severity was assessed using the Unified Parkinson's Disease Rating Scale (UPDRS) in Treated and Untreated PD patients. PD patients in this faecal sample study had UPDRS scores, measuring best to worst, that ranged from a very low score of 2, to a score of 38, out of the highest, worst, possible score of 147. The relationship between faecal BAs and UPDRS was analysed using Spearman correlation. Individual faecal BA, CA (p=0.029) negatively correlated with increased UPDRS score in Untreated PD patients (*Figure 3.29* (a)), suggesting that perhaps higher concentrations of it are negatively associated with PD severity. Interestingly, GHCA (p=0.014) positively correlated with increased UPDRS score in Untreated PD patients (*Figure 3.29* (b)), suggesting that perhaps higher concentrations of it are

associated with PD severity, and positively contribute to disease progression. No other correlations to BA family or individual BAs were associated with mild or severe disease.

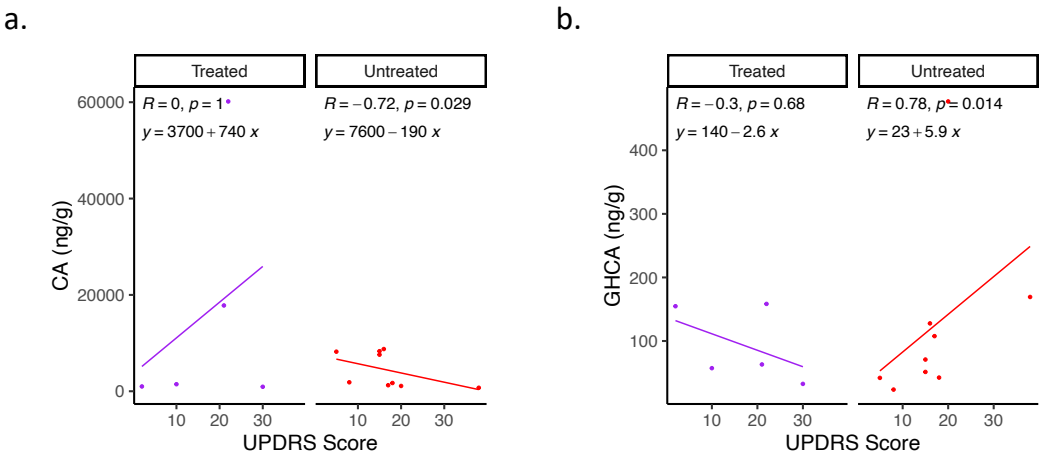


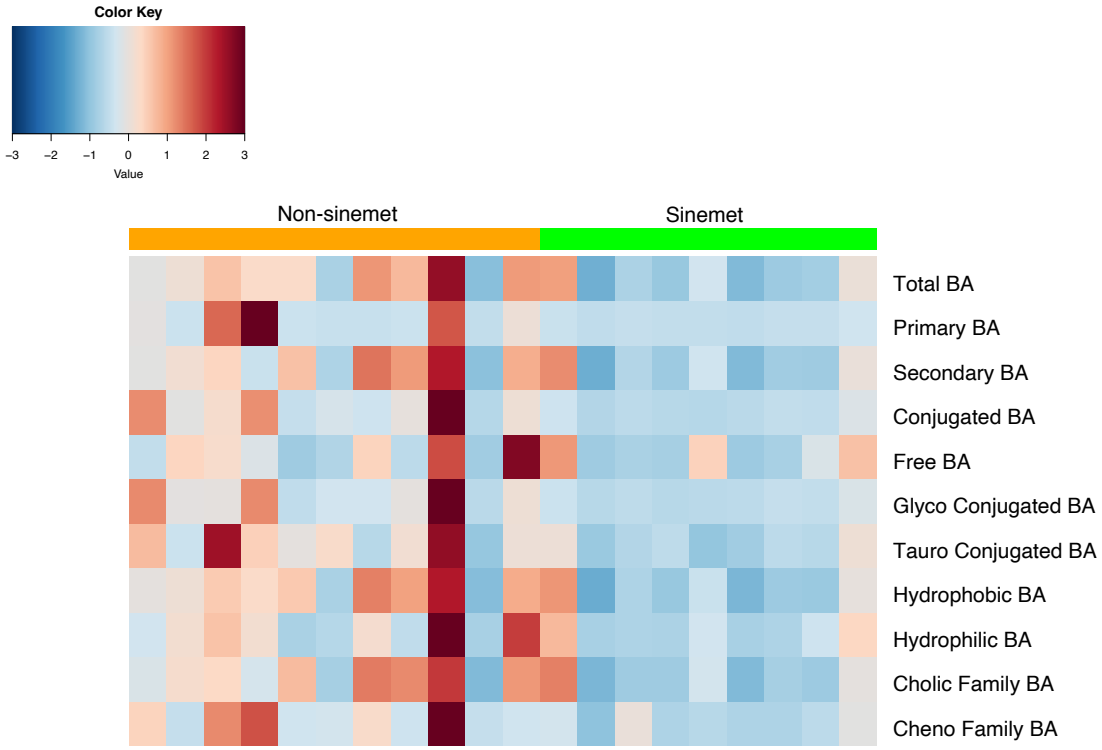
Figure 3.29: **Assessment of faecal bile acids correlation with UPDRS score from Parkinson's Disease patients.** (a-b) Spearman correlation assessment and significantly altered individual BAs; the degree of correlation of change is indicated by R value, and significance is indicated by p value using RStudio software version 2021.09.0. Treated PD *n*=5, Untreated PD *n*=9. Spearman correlation (R value) and statistical significance is indicated (*= p<0.05; **=p<0.01; ***=p<0.001; ****=p<0.0001). Abbreviations see *Table 2.9*.

3.2.2.9 Sinemet-Treated Parkinson's Disease patients have lower concentrations of faecal bile acids compared to Non-Sinemet-Treated patients.

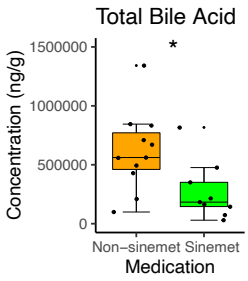
Faecal BAs may change, depending on whether PD patients are receiving PD medication. Sinemet is one of the most commonly prescribed medications to treat PD. We examined whether Sinemet itself can alter faecal BAs by dividing the groups into Treated PD patients (*n*=9) and Non-Treated PD patients (*n*=11). Initial analysis using spearman correlation heatplots, indicate that Non-Treated PD patients showed higher levels of all classes of BA (*Figure 3.30* (a)), and each BA individually (*Figure 3.30* (k)), compared to Treated PD patients. Examining faecal BAs showed that Non-Treated PD patients had significantly higher concentrations of total BAs, primary BAs, secondary BAs, conjugated BAs, glyco conjugated BAs, tauro conjugated BAs,

hydrophobic BAs, cholic acid family of BAs and chenodeoxycholic acid family of BAs, compared to Treated PD patients (*Figure 3.30* (b-j)). At the individual BA moiety level, significantly higher concentrations of individual faecal BAs: CA, GCA, TCA, DCA, GDCA, TDCA, CDCA, GCDCA, LCA, UDCA and GUDCA, were detected from Non-Treated PD patients compared to those treated (*Figure 3.30* (l-v)). This data suggests that Sinemet appears to have the potential to reduce faecal BA concentration levels in PD patients.

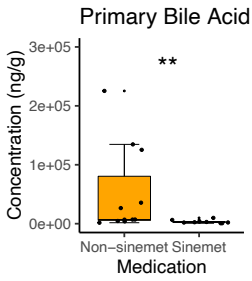
a.


Color Key
−3 −2 −1 0 1 2 3
Value
Non-sinemet
Sinemet
Total BA
Primary BA
Secondary BA
Conjugated BA
Free BA
Glyco Conjugated BA
Tauro Conjugated BA
Hydrophobic BA
Hydrophilic BA
Cholic Family BA
Cheno Family BA

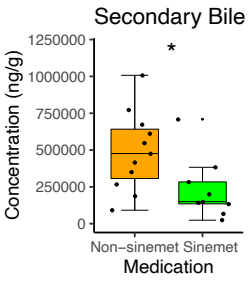
b.


Total Bile Acid
Concentration (ng/g)
1500000
1000000
500000
0
*
Non−sinemet Sinemet
Medication

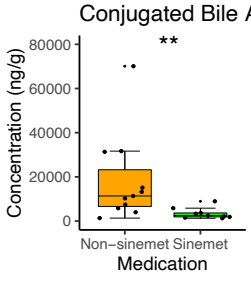
c.


Primary Bile Acid
Concentration (ng/g)
3e+05
2e+05
1e+05
0e+00
**
Non−sinemet Sinemet
Medication

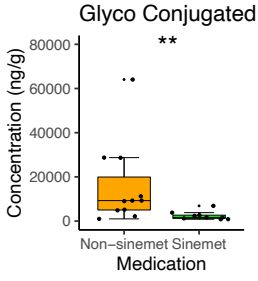
d.


Secondary Bile Acid
Concentration (ng/g)
1250000
1000000
750000
500000
250000
0
*
Non−sinemet Sinemet
Medication

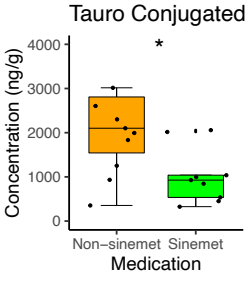
e.


Conjugated Bile Acid
Concentration (ng/g)
80000
60000
40000
20000
0
**
Non−sinemet Sinemet
Medication

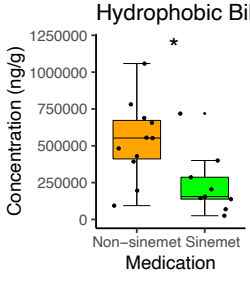
f.


Glyco Conjugated Bile Acid
Concentration (ng/g)
80000
60000
40000
20000
0
**
Non−sinemet Sinemet
Medication

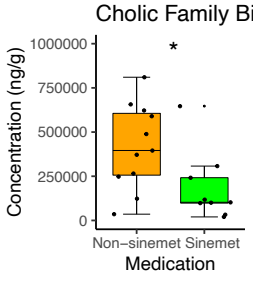
g.


Tauro Conjugated Bile Acid
Concentration (ng/g)
4000
3000
2000
1000
0
*
Non−sinemet Sinemet
Medication

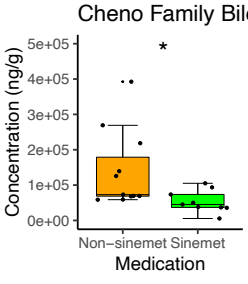
h.


Hydrophobic Bile Acid
Concentration (ng/g)
1250000
1000000
750000
500000
250000
0
*
Non−sinemet Sinemet
Medication

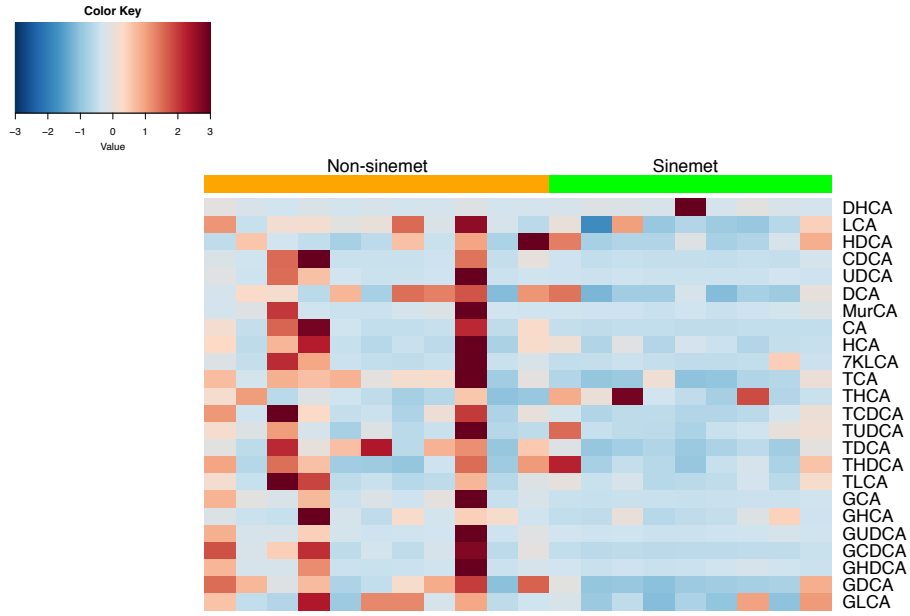
i.


Cholic Family Bile Acid
Concentration (ng/g)
1000000
750000
500000
250000
0
*
Non−sinemet Sinemet
Medication

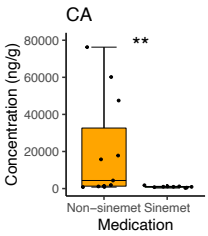
j.


Cheno Family Bile Acid
Concentration (ng/g)
5e+05
4e+05
3e+05
2e+05
1e+05
0e+00
*
Non−sinemet Sinemet
Medication

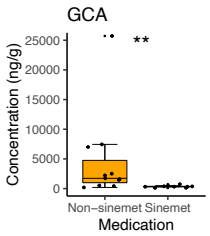
k.



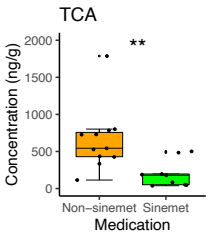
l.



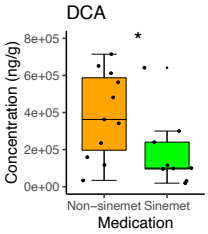
m.



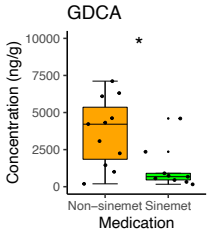
n.



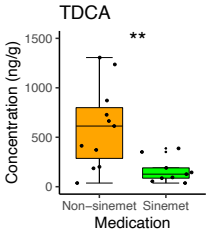
o.



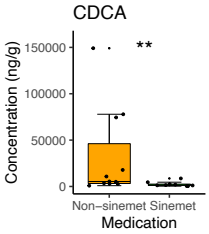
p.



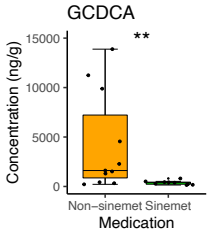
q.



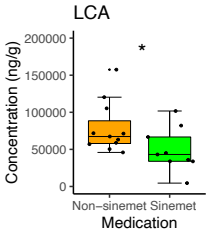
r.



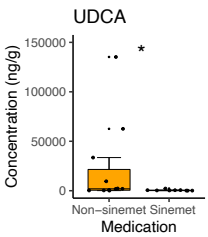
s.



t.



u.



v.

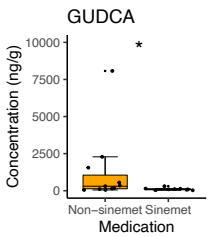


Figure 3.30: **Assessment of faecal bile acids from Parkinson's Disease patients receiving Sinemet medication.** Spearman correlation heatmap of (a) classes and (k) individual BAs; the degree of correlation of change is indicated, with red as positive and blue as negative generated using RStudio software version 2021.09.0, mean ± standard deviation (SD). Significantly altered (b-j) classes and (l-v) individual BAs were quantified against standard curves for each analyte and normalized according to internal standards and using Targetlynx^{TM} (Waters) software. Non-Sinemet-Treated PD patients *n*=11, Sinemet-Treated PD patients *n*=9. Statistical significance is indicated and calculated using Wilcoxon test (*= p<0.05; **=p<0.01; ***=p<0.001; ****=p<0.0001). Abbreviations see *Table 2.9*.

3.2.2.10 Specific circulating fatty acids are enriched in Parkinson's Disease patients.

Circulating FAs (Ellen Joyce and Susan Joyce (2017)) were analysed using Targetlynx^{TM} (Waters) software to establish alterations in circulating FAs in PD patients and whether these changes are reflected in the gut of PD patients. Principle Component Analysis (PCA) showed that FAs remained quite similar across all sample groups, with Parkinson's Disease patients perhaps slightly more spread than Control volunteers (*Figure 3.31*). There was no clear separation between Control volunteers and Parkinson's Disease patients, including those being treated with PD medication (Treated) and those without (Untreated) (*Figure 3.31*).

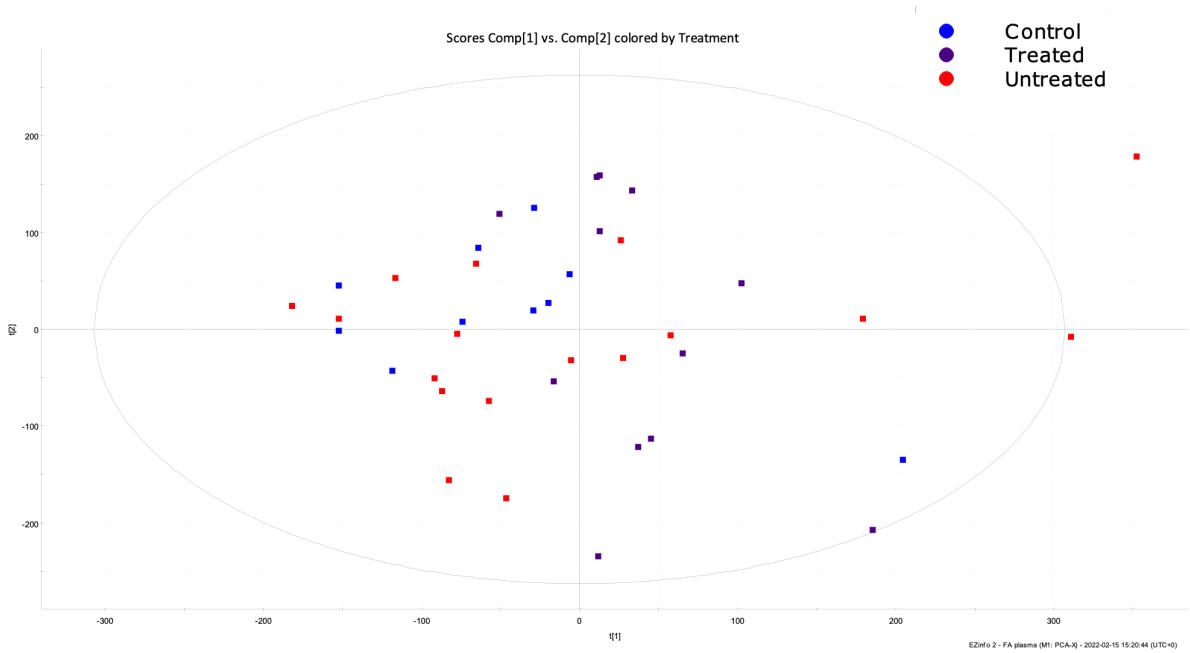
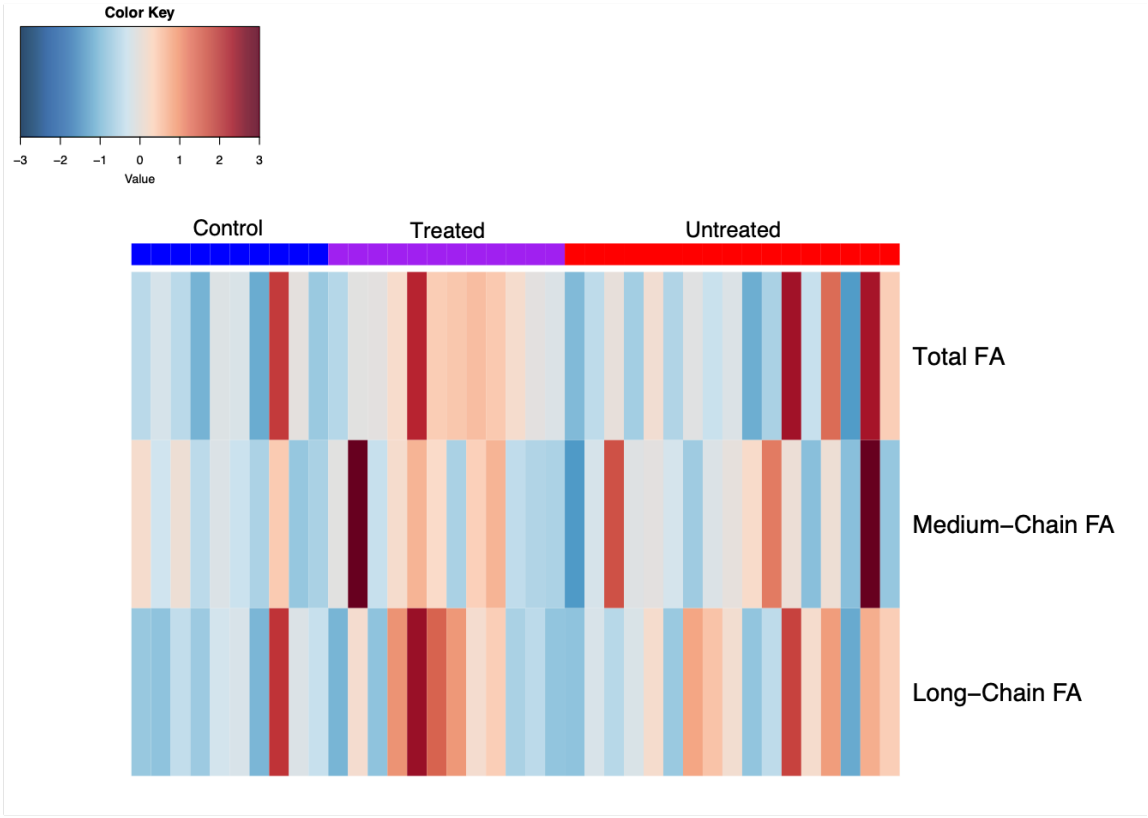


Figure 3.31: **Principal component analysis (PCA) of all detected fatty acids for plasma material.** The coloured representations are blue dots for control volunteers (*n*=10), purple dots for PD patients receiving PD medication (Treated *n*=11), and red dots for PD patients not receiving PD medication (Untreated *n*=18).

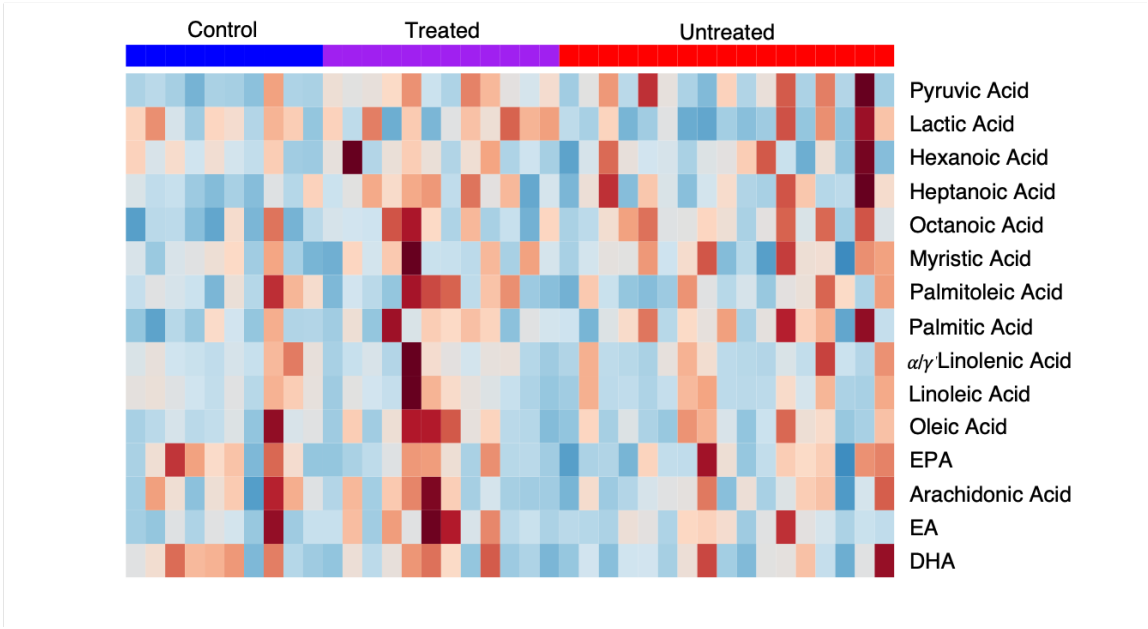
Initial spearman correlation heatplot analysis indicated that circulating FAs may be increased in PD patients (both those receiving PD medication (Treated) and those not (Untreated)) for all BA classes of (*Figure 3.32* (a)). With respect to each individual BA (*Figure 3.32* (b)), a similar effect was predicted through heatplot analysis compared to control volunteers.

Examining circulating FAs more closely showed that Treated PD patients had significantly higher concentrations of total FAs (*Figure 3.32* (i)), compared to control healthy volunteers. PD patients had significantly higher concentrations of individual circulating FA pyruvic acid (*Figure 3.32* (c)), heptanoic acid (*Figure 3.32* (e)), octanoic acid (*Figure 3.32* (f)) and palmitic acid (*Figure 3.32* (h)), compared to control volunteers. Further examination revealed Treated PD patients and Untreated PD patients both showed significantly higher concentrations of individual circulating FA pyruvic acid (*Figure 3.32* (d)) while Untreated PD patients had significantly higher concentrations of individual circulating FA octanoic acid (*Figure 3.32* (g)), compared to control volunteers. This data suggests that circulating FAs are indeed altered in PD patients compared to control volunteers, specifically in those PD patients without PD medication (Untreated). (For gender see appendix III SI.3.21).

a.


Color Key
−3
−2
−1
0
1
2
3
Value
Control
Treated
Untreated
Total FA
Medium–Chain FA
Long–Chain FA

b.


Control
Treated
Untreated
Pyruvic Acid
Lactic Acid
Hexanoic Acid
Heptanoic Acid
Octanoic Acid
Myristic Acid
Palmitoleic Acid
Palmitic Acid
α/γ Linolenic Acid
Linoleic Acid
Oleic Acid
EPA
Arachidonic Acid
EA
DHA

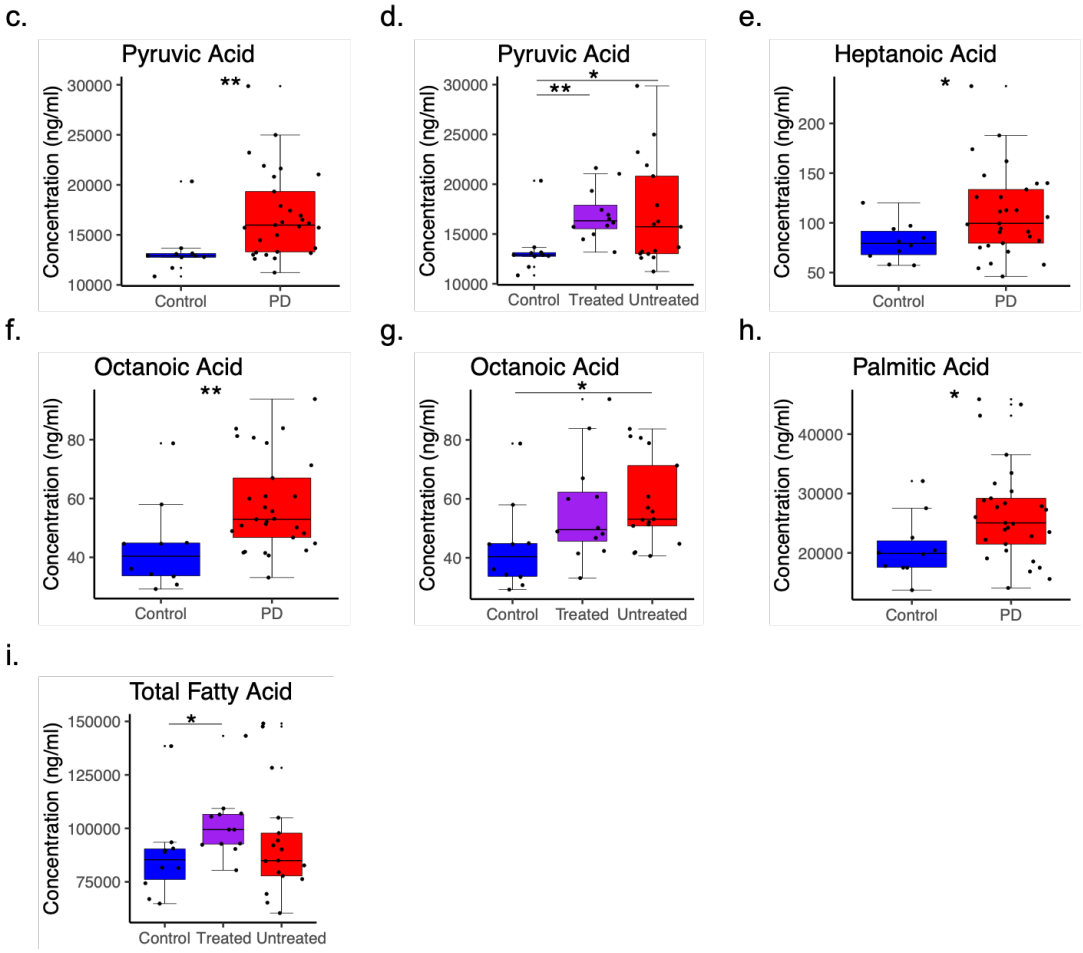


Figure 3.32: **Assessment of plasma fatty acids from Parkinson's Disease patients, compared to healthy control individuals.** Spearman correlation heatmap of (a) classes and (b) individual FAs; the degree of correlation of change is indicated, with red as positive and blue as negative generated using RStudio software version 2021.09.0. Significantly altered (c-h) individual and (i) total FAs quantified against standard curves for each analyte and normalized according to internal standards and using Targetlynx™ (Waters) software. Data was plotted using RStudio software version 2021.09.0 and is represented as mean ± standard deviation (SD). Control *n*=10, PD *n*=29: Treated PD *n*=11, Untreated PD *n*=18. Statistical significance is indicated and calculated using Wilcoxon test, and Kruskal-Wallis and Dunn's Multiple Comparison Test (*=p<0.05; **=p<0.01; ***=p<0.001; ****=p<0.0001). Abbreviations see *Table 2.10*.

3.2.2.11 Circulating fatty acids alter with age, in Parkinson's Disease patients.

We next examined whether circulating FA concentrations change with respect to PD patient's age, or perhaps as PD progresses. Initial examination of circulating FAs revealed that, in control volunteers, lactic acid (p=0.0056) and arachidonic acid (p=0.01) are negatively correlated with age (*Figure 3.33* (a) and (d)). However, in Untreated PD patients, circulating FAs palmitic acid (p=0.02), oleic acid (p=0.042), eicosahexanoic acid (p=0.00072) and docosahexanoic acid (p=0.021) are all positively correlated with age (*Figure 3.33* (b-c) and (e-f)). This data suggests that perhaps higher concentrations of specific FAs impact PD negatively, and maybe associated with disease progression.

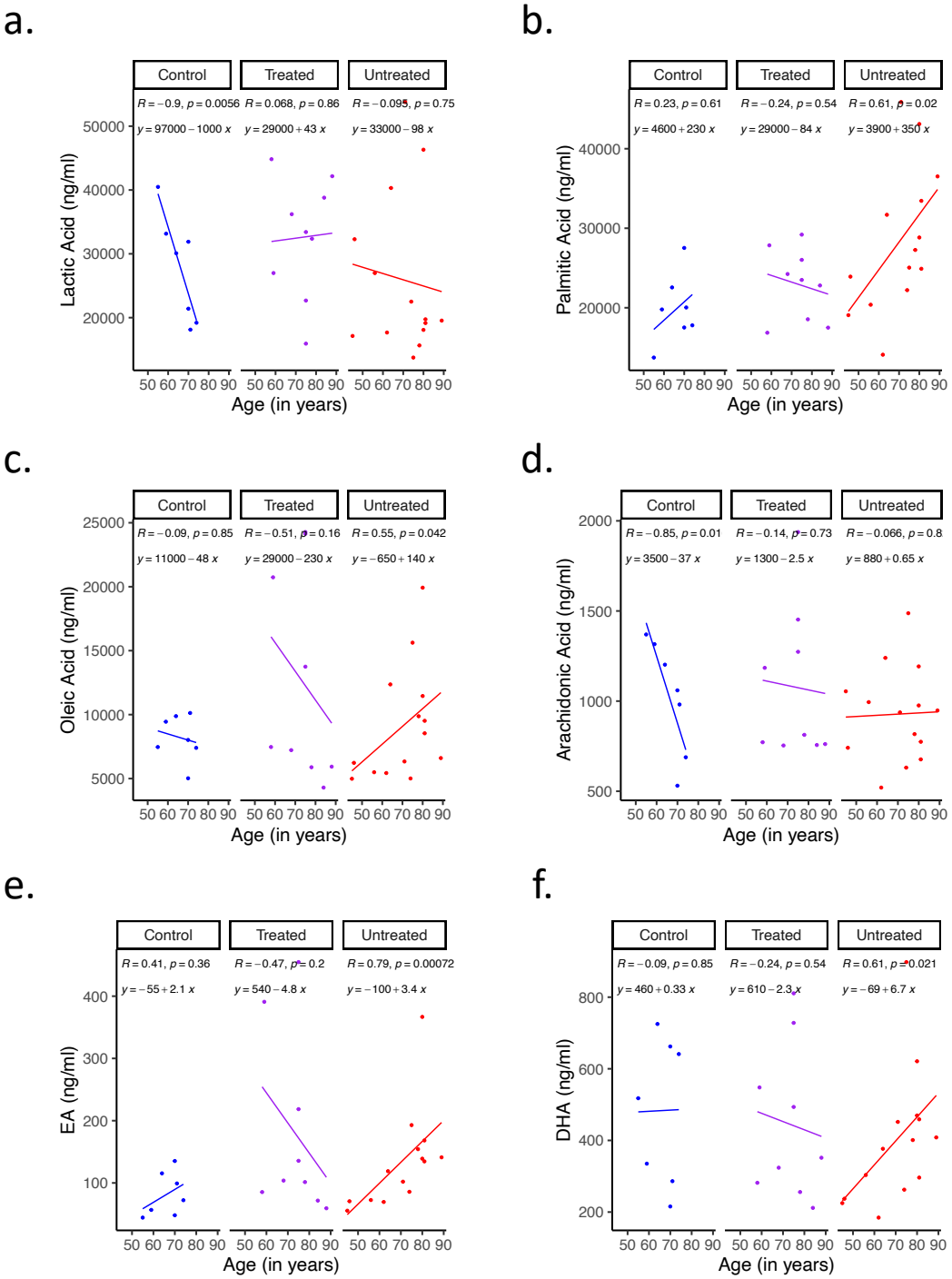


Figure 3.33: **Assessment of circulating fatty acids correlation with age from Parkinson's Disease patients, relative to healthy control volunteers.** (a-f) Spearman correlation assessment and significantly altered individual FAs; the degree of correlation of change is indicated by R value, and significance is indicated by p value using RStudio software version 2021.09.0. Control *n*=7, Treated PD *n*=9, Untreated PD *n*=14. RStudio software version 2021.09.0, mean ± standard deviation (SD).

Spearman correlation (R value) and statistical significance is indicated (*= p<0.05; **=p<0.01; ***=p<0.001; ****=p<0.0001). Abbreviations see *Table 2.10*.

3.2.2.12 Specific circulating fatty acid concentrations correlate with disease severity in Parkinson's Disease patients.

Alterations to circulating FAs are evident between medication treated and untreated PD patients. We next assessed correlation between FAs and patient disease severity using the Unified Parkinson's Disease Rating Scale (UPDRS see section 3.2.2.8 for explanation). Correlations between FAs and cognitive function were also assessed using the Montreal Cognitive Assessment (MoCA) scale from 0-30, no impairment scores >26. Our patients ranged from 14 to 29, out of a possible 30. Spearman correlation indicated that circulating FA lactic acid is positively correlated with both total UPDRS score (p=0.023) and with UPDRS motor sub-score score (p=0.0085) (*Figure 3.34* (a) and (b)). In PD patients, pyruvic acid (p=0.027) and octanoic acid (p=0.05) were both negatively correlated with MoCA score (*Figure 3.34* (c) and (d)); and upon further examination, Treated PD patients reversed the positive pyruvic acid correlation to negative correlation with MoCA score (p=0.048) (*Figure 3.34* (e)). In Treated PD patients, heptanoic acid (p=0.043) was also negatively correlated with MoCA score (*Figure 3.34* (f)). This data suggests that specific FAs, such as pyruvic acid, may be beneficial in the context of PD since it is negatively associated with PD severity, and declining cognitive function. No other correlations to FA family or individual FAs were associated with mild or severe disease (appendix III SI.3.22).

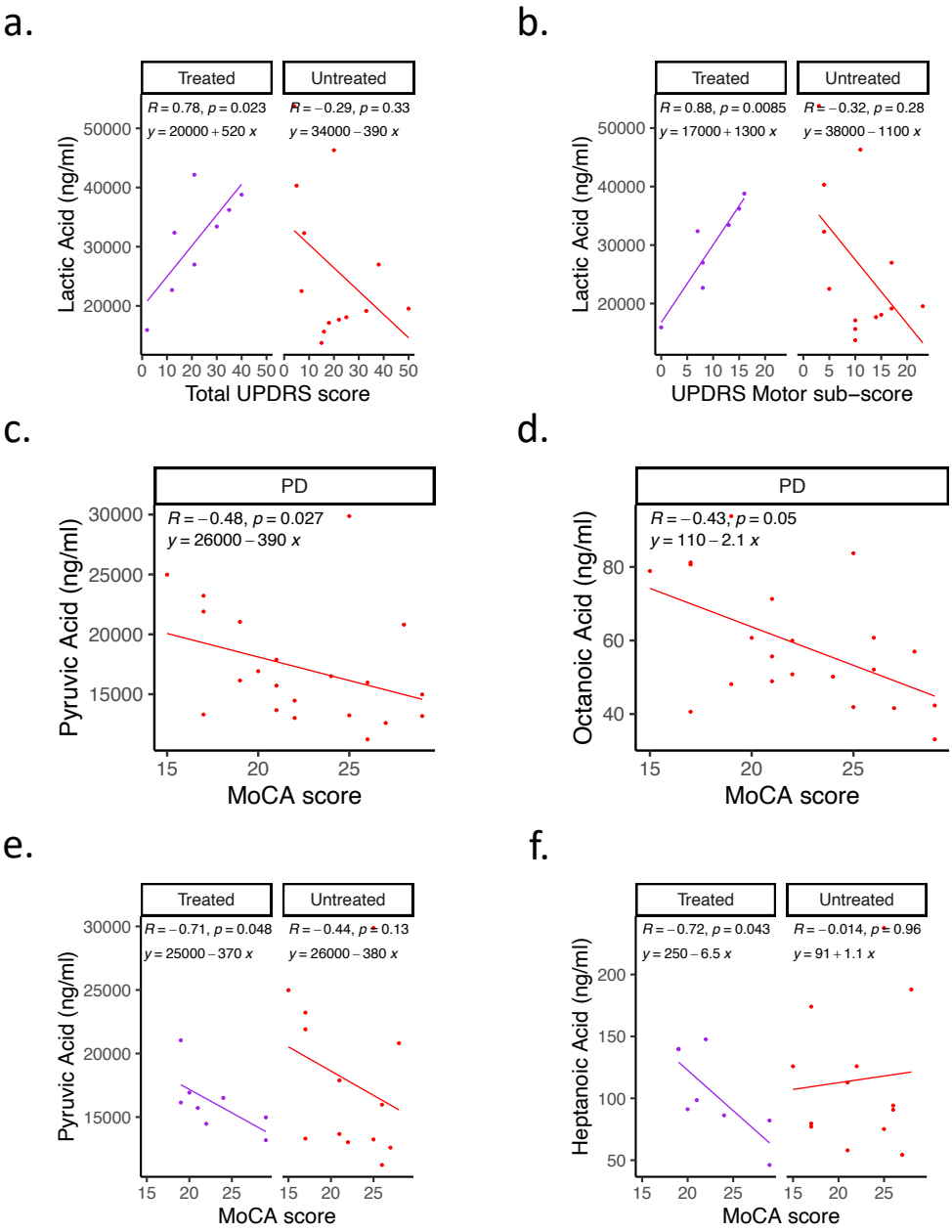


Figure 3.34: **Assessment of circulating fatty acids correlated with disease severity in Parkinson's Disease patients.** (a-f) Spearman correlation assessment and significantly altered individual FAs; the degree of correlation of change is indicated by R value, and significance is indicated by p value using RStudio software version 2021.09.0. Total UPDRS score: PD *n*=21, Treated PD *n*=8, Untreated PD *n*=13. UPDRS Motor sub-score: PD *n*=20, Treated PD *n*=7, Untreated PD *n*=13. MoCA Score PD *n*=21, Treated PD *n*=8, Untreated PD *n*=13. RStudio software version 2021.09.0. Spearman correlation (R value) and statistical significance is indicated (*= p<0.05; **=p<0.01; ***=p<0.001; ****=p<0.0001). Abbreviations see *Table 2.10*.

3.2.2.13 Specific faecal fatty acids are reduced in Parkinson's Disease patients.

To examine alterations in FA signatures, faecal FA were extracted from human PD patients and age-matched control volunteers (ELDERMET study), applied to UPLC-TMS, analysed using Targetlynx^{TM} (Waters) software (Arnav Mahajan) and graphed using RStudio software version 2021.09.0 (Materials and Methods, Section 2.3.5). Principle Component Analysis (PCA) showed that FAs remained quite similar across all sample groups (*Figure 3.35*). There was no clear separation between Control volunteers and Parkinson's Disease patients, including those being treated with PD medication (Treated) and those without (Untreated) (*Figure 3.35*). One control sample may be considered an outlier from the PCA (*Figure 3.35*), however, the sample does not demonstrate itself as an outlier in the heatplots below (*Figure 3.36*), and therefore was not categorised as a true outlier.

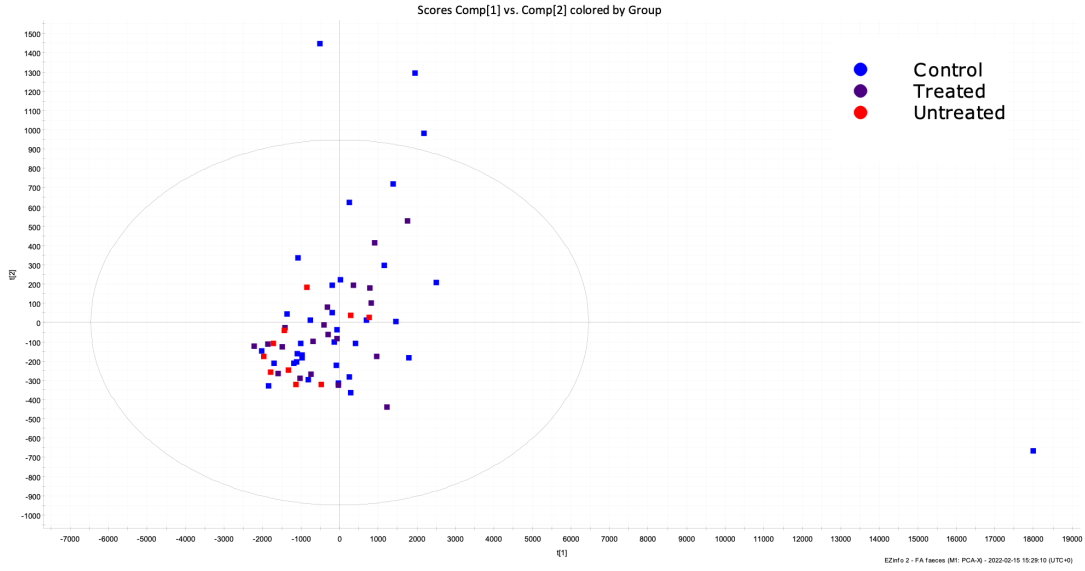
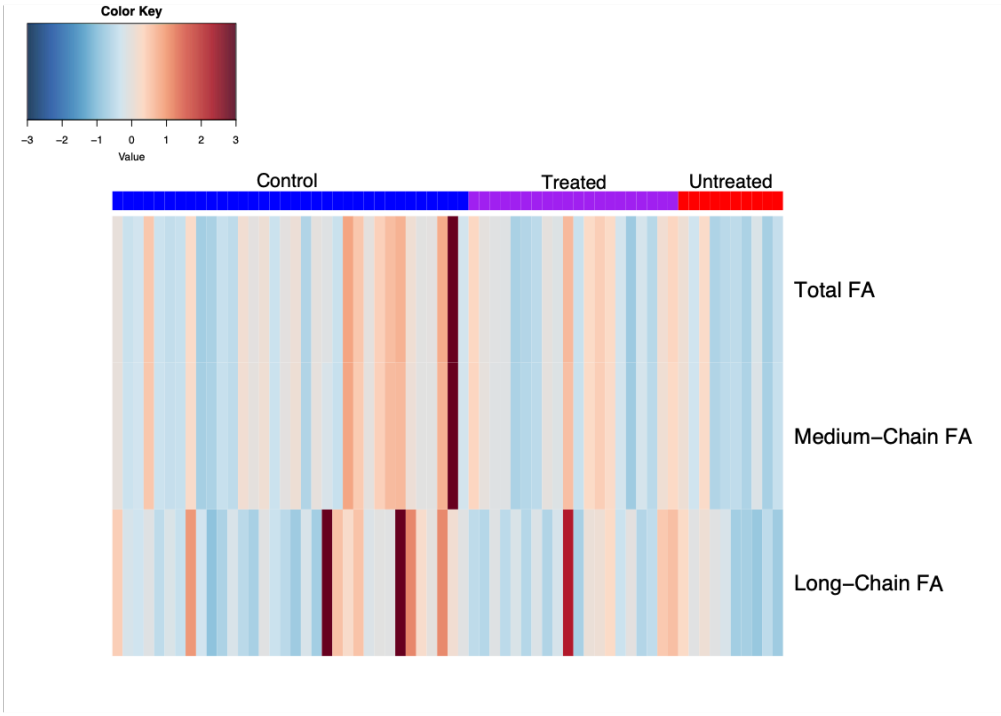


Figure 3.35: **Principal component analysis (PCA) of all detected fatty acids for faecal material.** The coloured representations are blue dots for control volunteers (*n*=34), purple dots for PD patients receiving PD medication (Treated *n*=20), and red dots for PD patients not receiving PD medication (Untreated *n*=10).

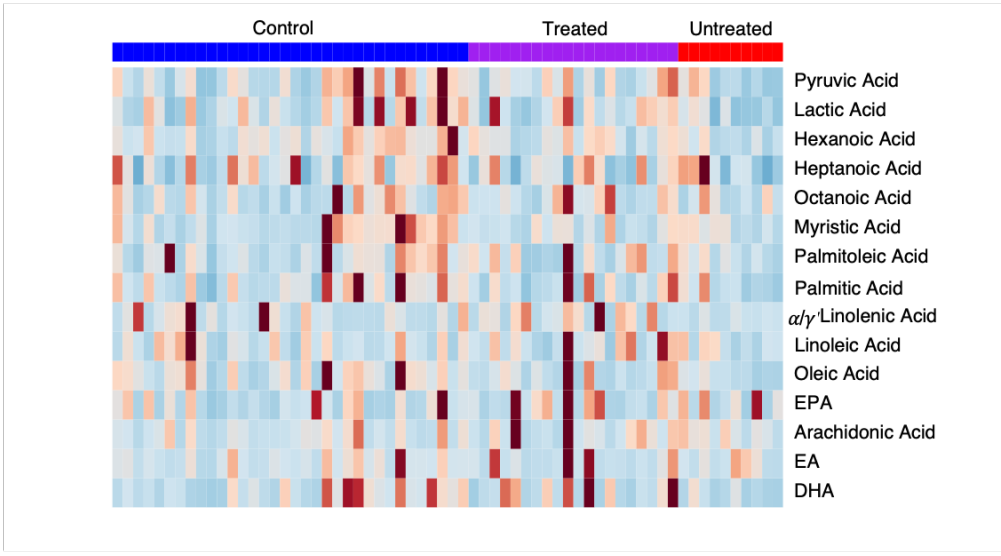
Initial analysis using spearman correlation heatplots of faecal FA signatures indicate that PD patients (both Treated and Untreated PD patients) showed correlations with lower levels of all classes of FAs (*Figure 3.36* (a)), and each individual FA (*Figure 3.36*

(b)), compared to control volunteers. Examining individual faecal FAs more closely showed that PD patients had significantly lower concentrations of oleic acid, compared to control volunteers (*Figure 3.36* (c)). This data suggests that specific faecal FAs are altered in PD patients, compared to age-matched control volunteers. (For gender see appendix III SI.3.23).

a.


Color Key
−3 −2 −1 0 1 2 3
Value
Control
Treated
Untreated
Total FA
Medium−Chain FA
Long−Chain FA

b.


Control
Treated
Untreated
Pyruvic Acid
Lactic Acid
Hexanoic Acid
Heptanoic Acid
Octanoic Acid
Myristic Acid
Palmitoleic Acid
Palmitic Acid
α/γ-Linolenic Acid
Linoleic Acid
Oleic Acid
EPA
Arachidonic Acid
EA
DHA

c.

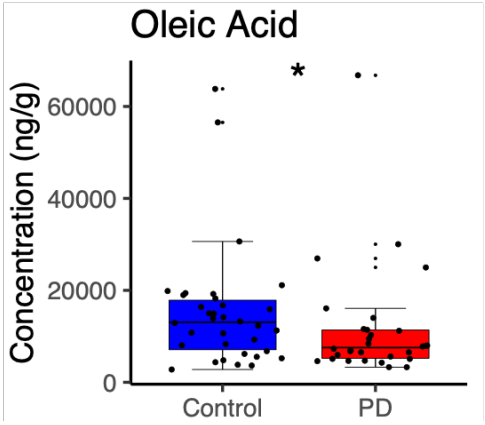

Oleic Acid
Concentration (ng/g)
60000
40000
20000
0
*
Control
PD

Figure 3.36: **Assessment of faecal fatty acids from Parkinson's Disease patients, compared to healthy control volunteers.** Spearman correlation heatmap of (a) classes and (b) individual FAs; the degree of correlation of change is indicated, with red as positive and blue as negative generated using RStudio software version 2021.09.0. (c) Significantly altered individual FA, Oleic Acid, quantified against standard curves for each analyte and normalized according to internal standards and using Targetlynx^{TM} (Waters) software. Control *n*=34, PD *n*=30: Treated PD *n*=20, Untreated PD *n*=10. RStudio software version 2021.09.0, mean ± standard deviation (SD). Statistical significance is indicated and calculated using Wilcoxon test (*=p<0.05; **=p<0.01; ***=p<0.001; ****=p<0.0001). Abbreviations see *Table 2.10*.

3.2.2.14 Faecal fatty acids alter with age, in Parkinson's Disease patients.

We next examined whether faecal FA concentrations change with respect to PD patient's age, or perhaps as PD progresses. Initial examination of faecal FAs in control volunteers revealed that the class of long-chain FAs (p=0.012), and individual FA pyruvic acid (p=0.031) positively correlate with age (*Figure 3.37* (a) and (b)). In Treated PD patients, faecal FA oleic acid (p=0.016) positively correlated with age (*Figure 3.37* (c)). Interestingly, in both control volunteers and Treated PD patients, myristic acid (p=0.00013, 0.042) and DHA (p=0.001, 0.0061) were positively correlated with age (*Figure 3.37* (d) and (e)). This data suggests that perhaps individual FAs oleic acid, myristic acid and DHA impact PD positively, and they may beneficially impact PD.

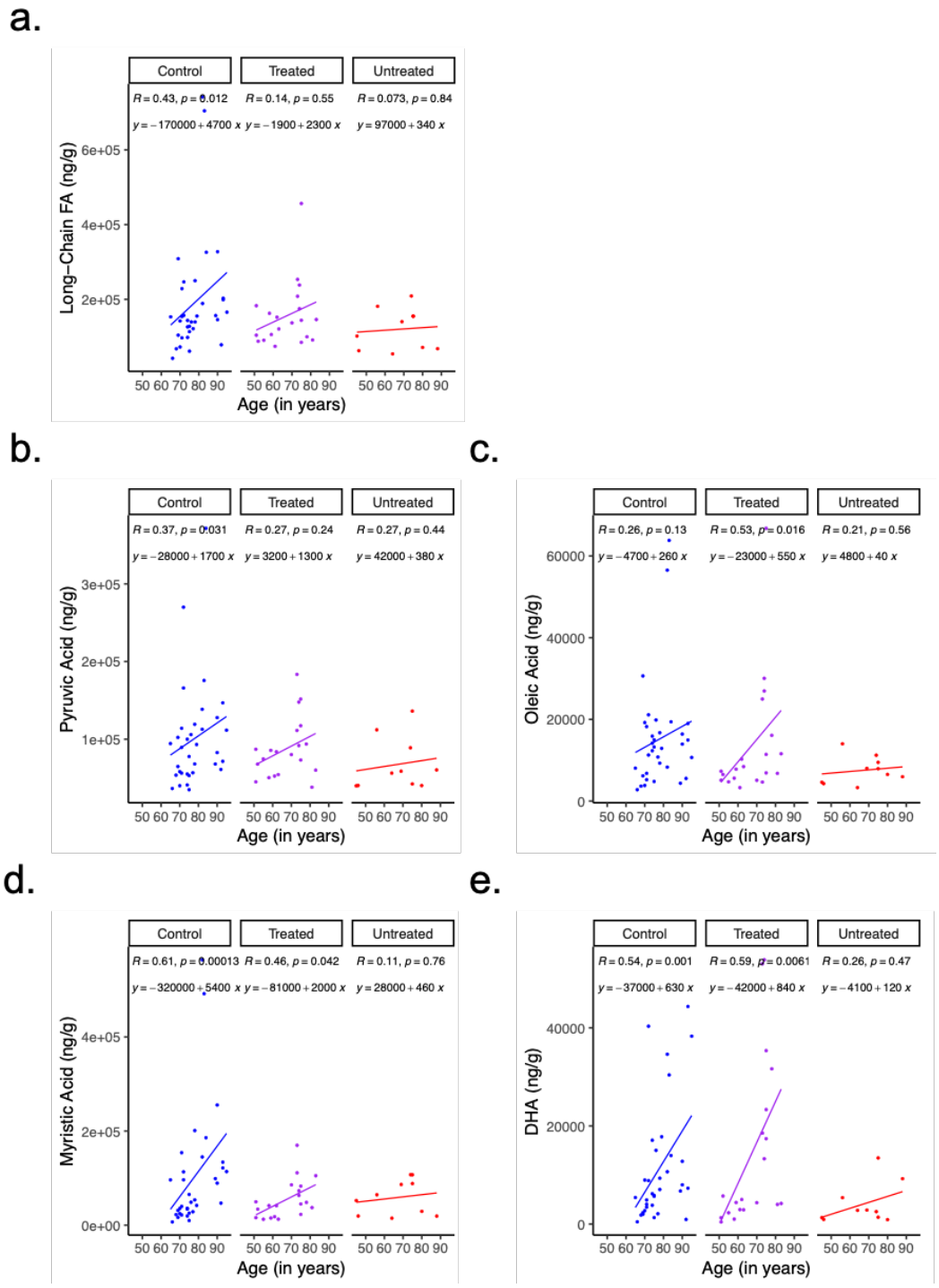


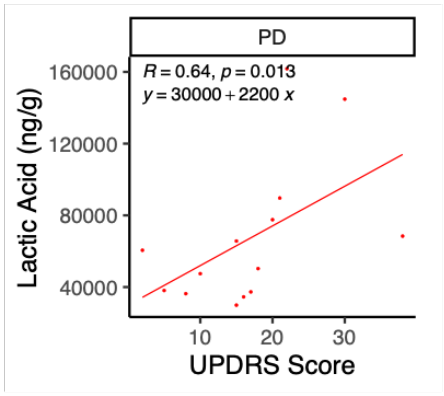
Figure 3.37: **Assessment of faecal fatty acids correlated with age in Parkinson's Disease patients, relative to healthy control volunteers.** Spearman correlation assessment and significantly altered (a) class of Long-chain FAs and (b-e) individual FAs; the degree of correlation of change is indicated by R value, and significance is indicated by p value using RStudio software version 2021.09.0. Control *n*=34, Treated

PD *n*=20, Untreated PD *n*=10. RStudio software version 2021.09.0, mean ± standard deviation (SD). Spearman correlation (R value) and statistical significance is indicated (*= p<0.05; **=p<0.01; ***=p<0.001; ****=p<0.0001). Abbreviations see *Table 2.10*.

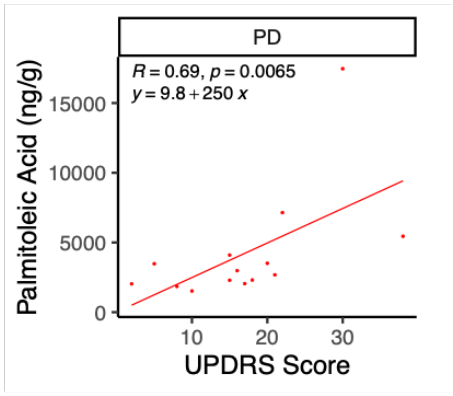
3.2.2.15 Specific faecal fatty acid concentrations correlate with disease severity in Parkinson's Disease patients.

Alterations in faecal FAs are evident between PD patients under medication or not. Similar to section 3.2.2.12, we assessed correlation between FAs and patient disease severity using the Unified Parkinson's Disease Rating Scale (UPDRS) in Treated and Untreated PD patients. UPDRS scores in our patient samples ranged from 2 to 38, out of a possible 147, measuring best to worst. Spearman correlation of FAs and UPDRS was analysed, and in PD patients, individual faecal FAs: lactic acid (p=0.013), palmitoleic acid (p=0.0065), palmitic acid (p=0.018), α/γlinolenic acid (p=0.04), linoleic acid (p=0.0031), oleic acid (p=0.024), arachidonic acid (p=0.024) and the class of FAs, long-chain FAs (p=0.0077), all positively correlated UPDRS score (*Figure 3.38* (a-h)). Upon further examination, specifically linoleic acid (p=0.017) positively correlated with UPDRS score in Treated PD patients (*Figure 3.38* (j)). In Untreated PD patients, individual faecal FAs octanoic acid (p=0.017) and oleic acid (p=0.038), and the class of FAs, long-chain FAs (p=0.021), positively correlated UPDRS score (*Figure 3.38* (i), (k) and (l)).

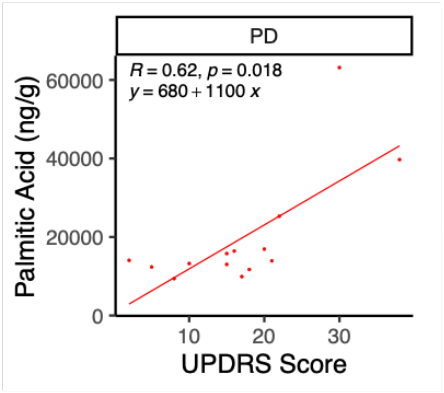
a.


PD
R = 0.64, p = 0.013
y = 30000 + 2200 x
Lactic Acid (ng/g)
160000
120000
80000
40000
10
20
30
UPDRS Score

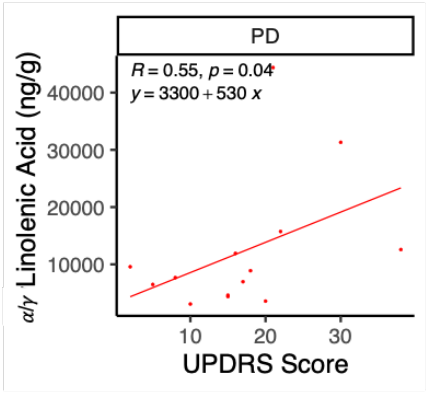
b.


PD
R = 0.69, p = 0.0065
y = 9.8 + 250 x
Palmitoleic Acid (ng/g)
15000
10000
5000
0
10
20
30
UPDRS Score

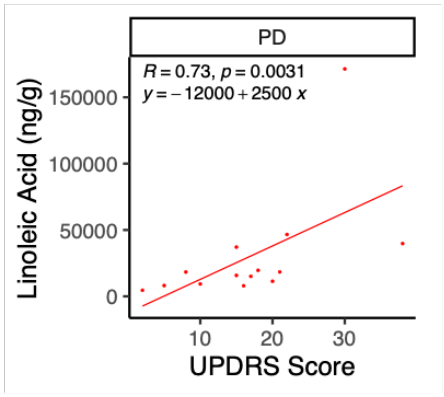
c.


PD
R = 0.62, p = 0.018
y = 680 + 1100 x
Palmitic Acid (ng/g)
60000
40000
20000
0
10
20
30
UPDRS Score

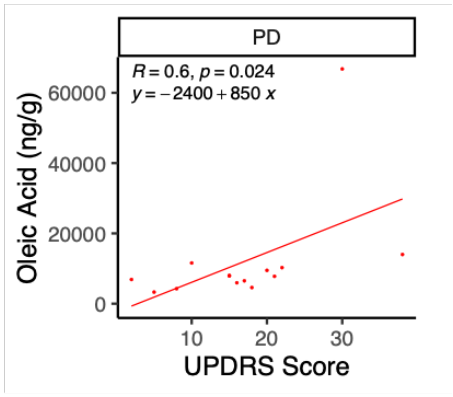
d.


PD
R = 0.55, p = 0.04
y = 3300 + 530 x
α/γ Linolenic Acid (ng/g)
40000
30000
20000
10000
10
20
30
UPDRS Score

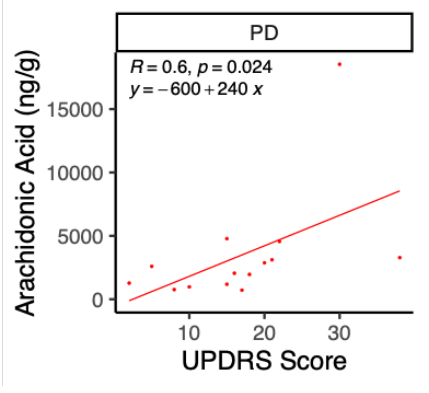
e.


PD
R = 0.73, p = 0.0031
y = −12000 + 2500 x
Linoleic Acid (ng/g)
150000
100000
50000
0
10
20
30
UPDRS Score

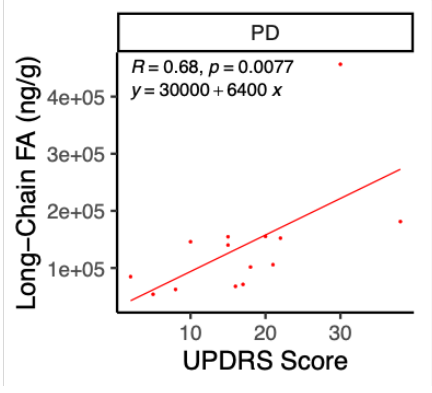
f.


PD
R = 0.6, p = 0.024
y = −2400 + 850 x
Oleic Acid (ng/g)
60000
40000
20000
0
10
20
30
UPDRS Score

g.


PD
R = 0.6, p = 0.024
y = −600 + 240 x
Arachidonic Acid (ng/g)
15000
10000
5000
0
10
20
30
UPDRS Score

h.


PD
R = 0.68, p = 0.0077
y = 30000 + 6400 x
Long−Chain FA (ng/g)
4e+05
3e+05
2e+05
1e+05
10
20
30
UPDRS Score

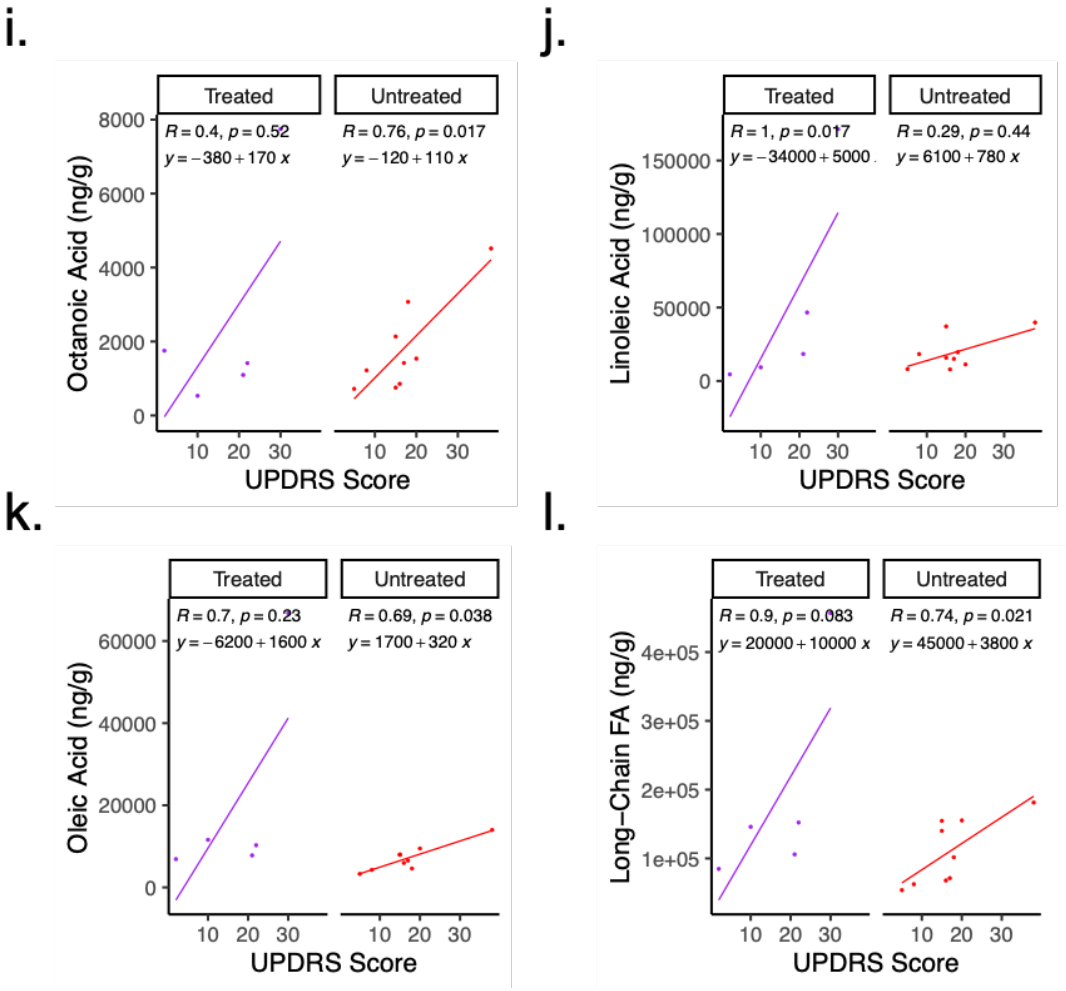


Figure 3.38: **Assessment of faecal fatty acids correlated with disease severity in Parkinson's Disease patients.** (a-l) Spearman correlation assessment and significantly altered individual FAs and Long-Chain FAs; the degree of correlation of change is indicated by R value, and significance is indicated by p value using RStudio software version 2021.09.0, mean ± standard deviation (SD). Total UPDRS score: PD *n*=14, Treated PD *n*=5, Untreated PD *n*=9. Spearman correlation (R value) and statistical significance is indicated (*= p<0.05; **=p<0.01; ***=p<0.001; ****=p<0.0001). Abbreviations *Table 2.10*.

Correlations between FAs and cognition was also assessed using the Montreal Cognitive Assessment (MoCA) scale which scores from 0-30, no impairment indicated with scores >26. MoCA scores in our patient samples ranged from 15 to 29 out of a possible 30. Interestingly, in PD patients, individual faecal FAs palmitic acid

(p=0.0065) and arachidonic acid (p=0.04) negatively correlated with MoCA score (*Figure 3.39* (a) and (b)). In Untreated PD patients, individual faecal FAs palmitic acid (p=0.0021), arachidonic acid (p=0.0021) and DHA (p=0.05), all negatively correlated with MoCA score (*Figure 3.39* (c-e)). This data suggests that specific FAs, such as palmitic acid and arachidonic, may be associated with increased motor dysfunction (UPDRS score *Figure 3.38*), but may be beneficial in the context of cognitive function (MoCA score *Figure 3.39*) in PD. This also suggests that FAs may have the potential to elicit beneficial effects and harmful effects, depending on the specific context of PD.

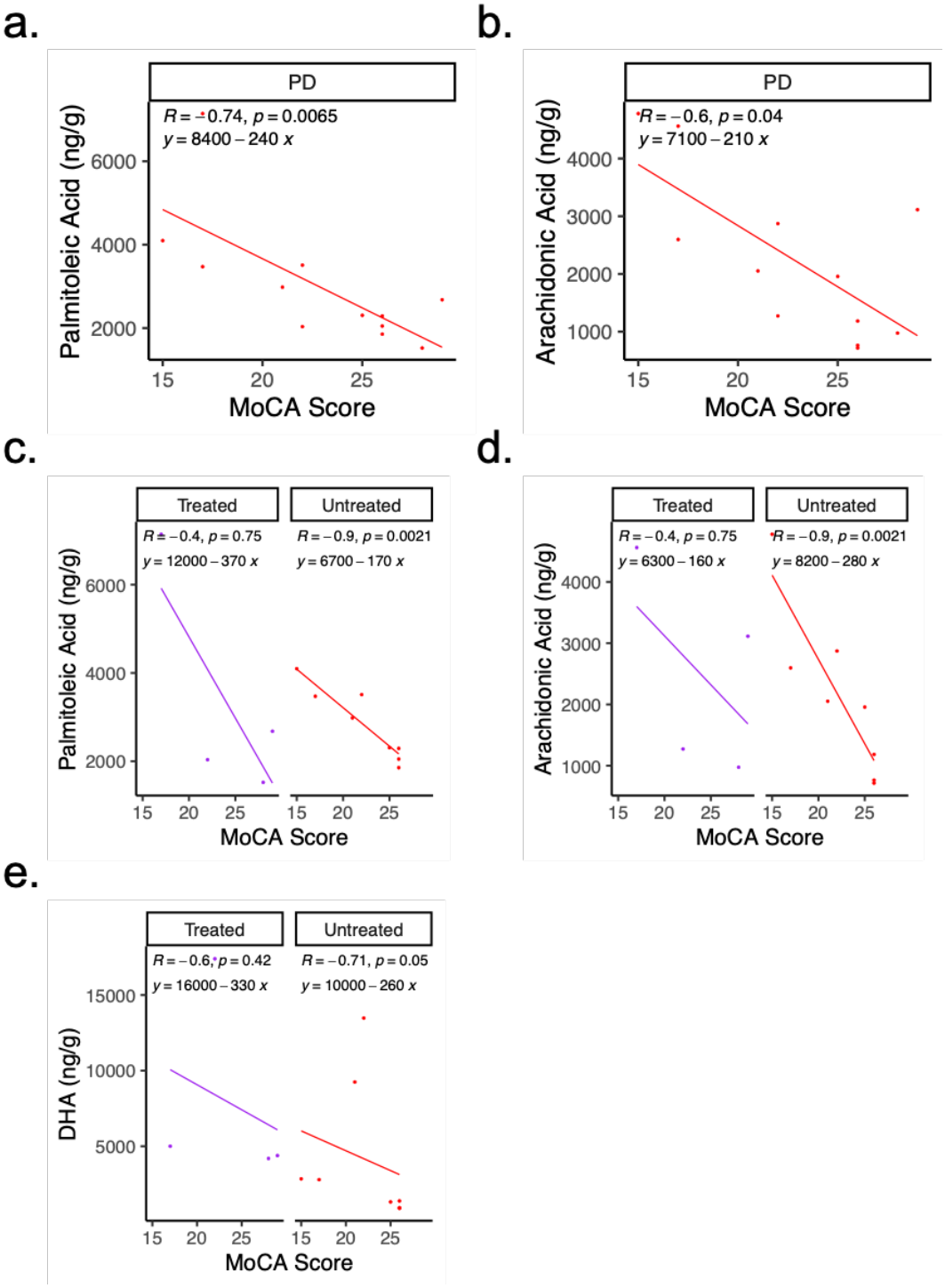


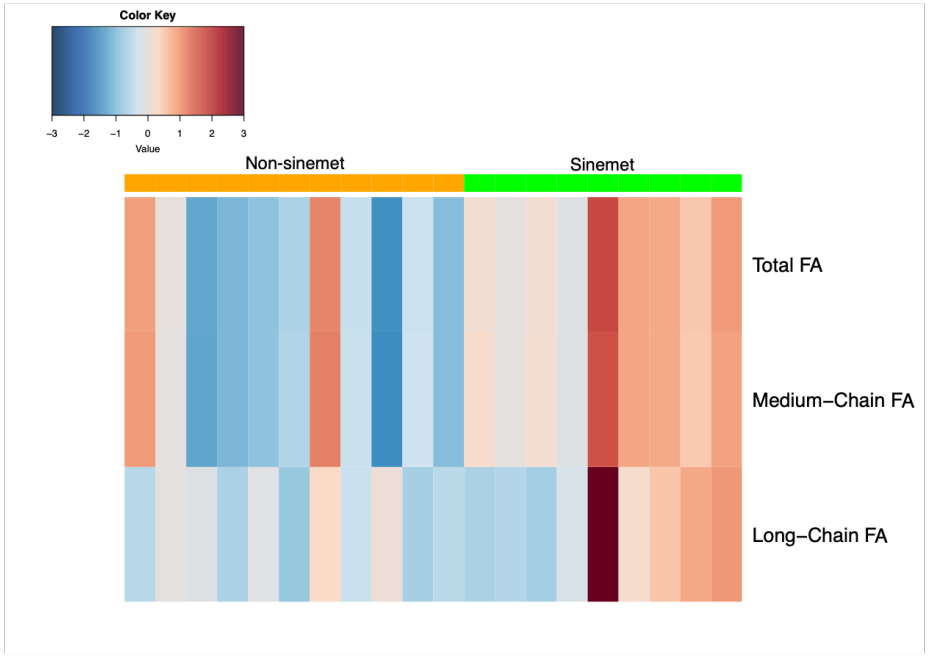
Figure 3.39: **Assessment of faecal fatty acid correlation to cognitive function in Parkinson's Disease patients.** (a-e) Spearman correlation assessment and significantly altered individual FAs; the degree of correlation of change is indicated by R value, and significance is indicated by p value using RStudio software version 2021.09.0, mean ± standard deviation (SD). MoCA Score PD *n*=12, Treated PD *n*=4,

Untreated PD *n*=8. Spearman correlation (R value) and statistical significance is indicated (*= p<0.05; **=p<0.01; ***=p<0.001; ****=p<0.0001). Abbreviations see *Table 2.10*.

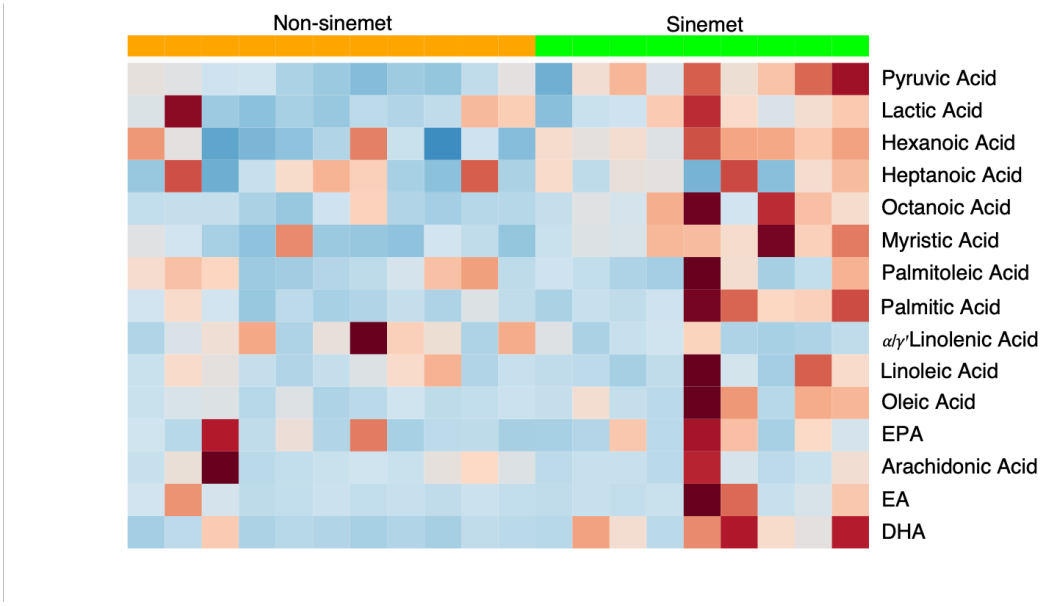
3.2.2.16 Sinemet-Treated Parkinson's Disease patients have higher concentrations of faecal fatty acids compared to Non-Sinemet-Treated patients.

Faecal FA changes, depending on whether PD patients are receiving PD medication. We next examined whether Sinemet is influential here. Initial analysis using spearman correlation heatplots of faecal FAs indicated that Sinemet was correlated with higher levels of all classes of FA (*Figure 3.40* (a)), and each individual FA (*Figure 3.40* (b)). Interestingly, Sinemet-Treated PD patients also showed significantly higher relative levels of individual FAs: pyruvic acid, hexanoic acid, octanoic acid, myristic, palmitic Acid, α/γlinolenic Acid and DHA, compared to Non-Sinemet-Treated PD patients (*Figure 3.40* (c-i)). This data suggests that faecal FAs are indeed altered in Treated PD patients compared to Untreated PD patients. Sinemet appears to have the potential to increase FA levels in PD patients.

a.


Color Key
−3
−2
−1
0
1
2
3
Value
Non-sinemet
Sinemet
Total FA
Medium−Chain FA
Long−Chain FA

b.


Non-sinemet
Sinemet
Pyruvic Acid
Lactic Acid
Hexanoic Acid
Heptanoic Acid
Octanoic Acid
Myristic Acid
Palmitoleic Acid
Palmitic Acid
α/γ'Linolenic Acid
Linoleic Acid
Oleic Acid
EPA
Arachidonic Acid
EA
DHA

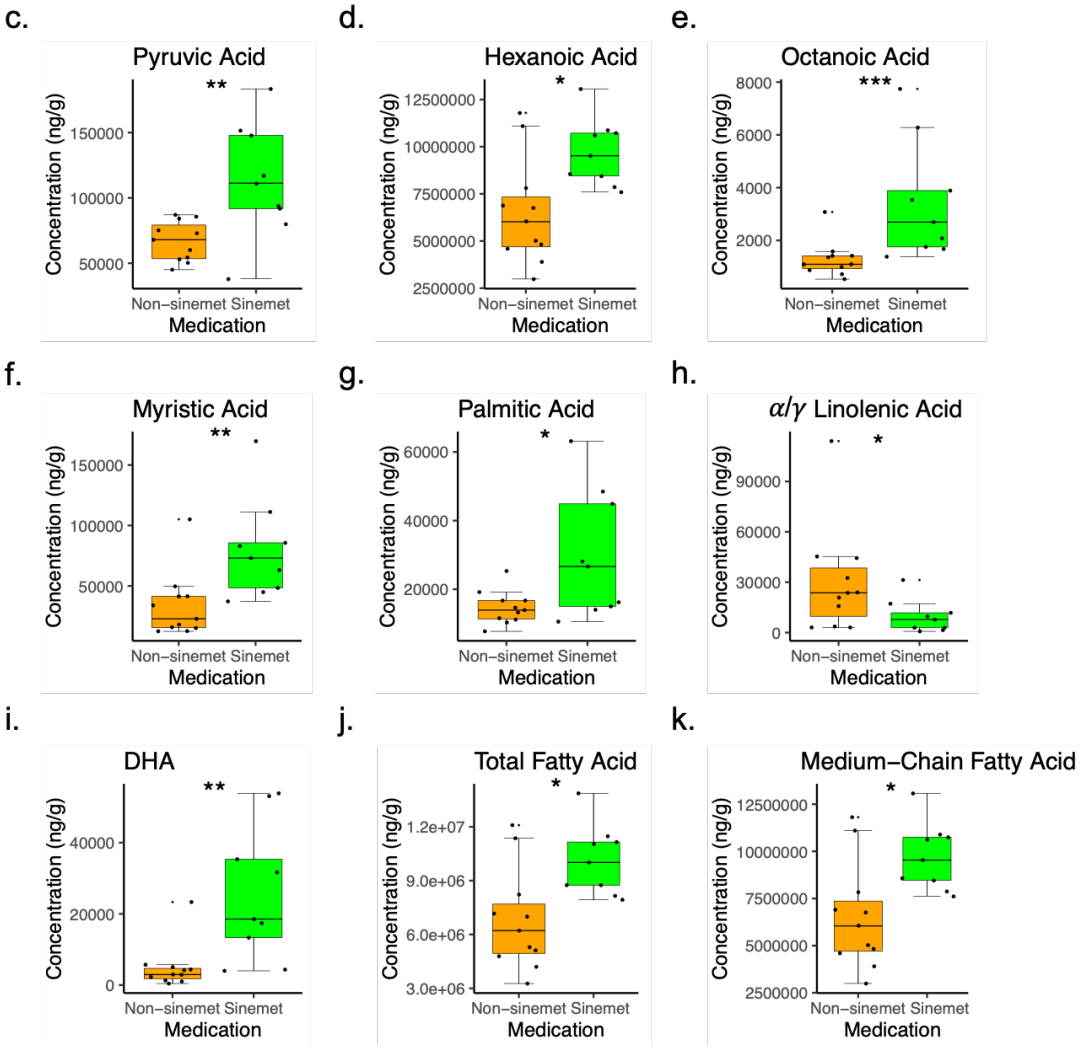


Figure 3.40: **Assessment of faecal fatty acids from Parkinson's Disease patients receiving Sinemet medication, compared to those treated with other Parkinson's Disease medications.** Spearman correlation heatmap of (a) classes and (b) individual FAs. Significantly altered (c-i) individual and (j-k) classes of FAs quantified against standard curves for each analyte and normalized according to internal standards and using Targetlynx™ (Waters) software. RStudio software version 2021.09.0. Non-Sinemet-Treated PD patients *n*=11, Sinemet-Treated PD patients *n*=9. Statistical significance is indicated and calculated using Wilcox test (*= p<0.05; **=p<0.01; ***=p<0.001; ****=p<0.0001). Abbreviations see *Table 2.10*.

3.3 Discussion

This chapter aimed to investigate a possible role for microbially produced or altered metabolites in the context of two different gut convergent diseases, one in early life (ASD - part I) and the other in later life (PD - part II) . The model applied was different for each study; ASD was studied using an animal model while PD was studied using human clinical samples. The ASD murine model is well established and respected for its congruency with the ASD social and behavioural indicators (Meyza and Blanchard, 2017). Clear metabolic differences in microbial BA metabolism were evident in the BTBR animal model. Here, microbial intervention (based on bile salt hydrolase activity) to redress the reported dysbiosis in BA metabolism in the ASD BTBR murine model, showed subtle but significant effects to influence gut health and behaviour. While the precise cause of ASD is really uncharacterized, it is believed to encompass a range of genetic mutations, epigenomic modifications as well as environmental effects, which may include microbial representation and activity (Niesler and Rappold, 2021). In examining these aspects, a note of caution is that altered metabolism and food consumption is associated with the model (Tordoff *et al.,* 2014), therefore the altered metabolites evident in our study may be a consequence rather than causative of disease.

In this study, *Lactobacillus salivarius* strain P0003 and *Bifidobacterium adolescentis* strain 2715 were selected as bacterial interventions on the basis of BA metabolism by bile salt hydrolase enzymes and their pyrogen free nature. *B. adolescentis* strain 2715 is capable of de-conjugation of BAs from taurine while *L. salivarius* strain P0003 is capable of de-conjugation of BAs from taurine and glycine. In addition, both *Lactobacillus* and *Bifidobacterium* are capable of resisting BA toxicity by the presence of efflux pumps and changes in the lipid structure of their bacterial membranes, by altering specific proteins involved in FA metabolism (Ruiz *et al.,* 2013). While missing or reduced microbial populations (*Lactobacillus* and *Bifidobacterium*) and potential functionality may in part be restored, the specific strains and functions encoded by reduced microbes may not be fully represented in the strain selection for this study. The introduction of these specific *Lactobacillus* and *Bifidobacterium* strains may indeed alter other populations of bacteria and their respective functionalities. It may well be that a population shift is responsible for the current behavioural outcome

rather than the microbes introduced per se. In the future, ASD treatment will encompass bacterial intervention in combination with dietary changes, such as treatment with a ketogenic diet, to increase microbial diversity as well as targeting specific signalling in the gut, including the release of serotonin and also the regulation of dopamine. Two weeks of oral feeding of *Lactobacillus plantarum* ST-III was reported to improve autism-like social deficits in a male mouse model of ASD and reduce self-grooming and freezing times in a female mouse model of ASD, constructed using triclosan (Guo *et al.,* 2022). In faecal samples of female mouse model of ASD, the relative abundance of *Lachnospiraceae* increased, whereas the relative abundance of *Alistipes* decreased which contributed to behavioural improvement. *L. plantarum* ST-III intervention improved social behaviour and intestinal homeostasis in a mouse model of ASD (Guo *et al.,* 2022).

The aim of this study was to apply bacterial interventions *L. salivarius* strain P0003 and *B. adolescentis* strain 2715 to BTBR ASD mouse model. The hypothesis was that these bacterial interventions would restore the deficits in BA signalling as reported in (Golubeva *et al.,* 2017). In circulation, bacterial treatments increased total tauro conjugated BA levels, namely TLCA, and LCA was the free BA with most obvious increase, in BTBR, ASD model mice. Bacterial treatments overall reduced BA signalling compared to control mice, however, both TLCA and LCA are agonists of the GPCR TGR5. Increase in TGR5 signalling in circulation, increases energy homeostasis, by converting thyroxine (T4) into thyroid hormone (T3), thermogenesis and glucose metabolism through increasing GLP-1 (Wahlström *et al.,* 2016). In the faeces, at baseline, *B. adolescentis* strain 2715 animals had significantly less βMCA, DCA and UDCA, compared to *L. salivarious* strain P0003 animals, showing variation in BA levels across BTBR groups. Individual free BA, secondary BA, LCA were at lower levels across all BTBR mice, compared to C57_Veh mice. Similarly, Golubeva *et al.*, (2017) reported that two classes of faecal BAs: tauro conjugated primary BAs and tauro secondary BAs, were reduced in BTBR mice compared to C57 control animals. At baseline week 0, such an effect was confirmed in this study. TCA, TMCA and TUDCA levels were significantly higher in BTBR mice, compared to C57_Veh. Similar to Golubeva *et al.*, (2017), BTBR_Veh concentration levels of TCDCA, TDCA and TLCA were higher in BTBR mice relative to C57_Veh control WT mice. Bacterial interventions, particularly

L. salivarious strain P0003 demonstrated the highest levels of Tauro conjugated BAs compared to all BTBR mice and C57_Veh. Despite BA concentrations at baseline, bacterial treatments increased faecal total BA levels, namely CDCA, in BTBR, ASD model mice. CA, βMCA and UDCA were similar across all groups, and total tauro conjugated BA levels were similar across all groups, with *B. adolescentis* strain 2715 specifically increasing TLCA levels. Bacterial treatments increased FXR signalling compared to BTBR, ASD model mice, which is consistent with the most potent BA ligand, CDCA, elevated in these treatment groups. FXR can induce the expression of *Fgf15* (FGF19 in humans) regulating BA homeostasis and regulate glucose metabolism by inhibiting the synthesis of GLP-1 (Wahlström *et al.,* 2016). *B. adolescentis* strain 2715 specifically increased TLCA levels, again increasing TGR5 signalling. However, in the gut, TGR5 can regulate gut motility (Alemi *et al.,* 2013) and both FXR and TGR5 have been reported to regulate immune response through caspase-1/11 activation and release of cleaved interleukin (IL)-1β (Kang *et al.,* 2021). *Bifidobacterium* species have been shown to metabolise tryptophan to compounds of the indole pathway, such as Indoleacetic acid (IAA) and indolelactic acid (ILA). Similarly, *Lactobacillus* species have the capacity to metabolise tryptophan to indolealdehyde (IAld) and ILA (Roager and Licht, 2018). The indole pathway has been reported to be involved in the regulation of GI homeostasis in the host, maintaining immune function and epithelium integrity (Bosi *et al.,* 2020). Some *Lactobacillus* species have even shown to produce serotonin from tryptophan (Bosi *et al.,* 2020), demonstrating that perhaps *L. salivarius* strain P0003 and *B. adolescentis* strain 2715 interventions are improving GI function through tryptophan metabolism, rather than altering the BA metabolism. Comparison of this data with changes in microbial composition and serotonin levels will help determine whether *L. salivarius* strain P0003 and *B. adolescentis* strain 2715 interventions could be applied to humans to improve behaviour as well as gastrointestinal traits in ASD. Overall, *L. salivarius* strain P0003 and *B. adolescentis* strain 2715 interventions have great potential to improve characteristics of the ASD behavioural phenotype, by subtle changes in gut signalling.

To determine whether bacterial interventions can be applied to improve a disease state, firstly deficits in microbial functionality, for example through BA modification

and potential BA and FA signalling, must be examined in order to target and restore these observed deficits. In the second part to this chapter, we investigated microbial functionality through BA and FA modification and potential signalling in PD. PD studies are focusing on the gut microbiota more and more for answers into disease progression and insights into new treatment therapies (Hasegawa *et al.,* 2015; Scheperjans *et al.,* 2015; Unger *et al.,* 2016; Pietrucci *et al.,* 2019; Shen, 2020). The purpose of this PD study was to investigate the composition of gut microbiota and signalling by analysing the levels of BAs and FAs in plasma and faeces in PD patients. Studies have demonstrated a connection between the gut-brain axis in PD by showing that constipation precedes the first PD motor symptom and α-synuclein is present in the PD colon up to 5 years before the extrapyramidal symptoms (Abbott *et al.,* 2007; Shannon *et al.,* 2012). Alterations in BA synthesis and metabolism have been reported in PD patients (Santos-Lobato *et al.,* 2022). Li *et al.*, (2021) reported an 18.7-fold and 5.6-fold increase in secondary BAs Lithocholic Acid (LCA) and Deoxycholic Acid (DCA), respectively, in the appendix of PD patients compared to a control group (Li *et al.,* 2021). DCA is known to be toxic to gut microbes and is a colon cancer promoter (Li and Chiang, 2014). In the ileum, Li *et al.*, (2021) found a 3.6 fold increase in LCA relative to the control group (Li *et al.,* 2021). Gut microbiota with Bile Acid Inducible (BAI) dehydroxylation activity convert primary BAs to secondary BAs. Li *et al.*, (2021) showed an increase in *Clostridiales* and *Burkholderiales* in the appendix, bacterial species capable of secondary BA synthesis (Li *et al.* 2021). Unger *et al.*, (2016) found, in faeces of PD patients, an increase in the genera *Bifidobacterium* and *Enterobacteriaceae*. There was also an increase in species *Akkermansia muciniphila*, although not significant (Unger *et al.,* 2016). Unger *et al.*, (2016) also reported a reduction in the levels of acetate, propionate and butyrate in PD faeces (Unger *et al.,* 2016). Levels of lactic acid have also been reported to be decreased in PD patients, and succinic acid is associated with disease severity (Voigt *et al.,* 2022). Sampson *et al.*, (2016) also showed an association between gut microbiota and SCFA concentrations in PD. They found that SCFA, in mice colonised with human PD microbiota, regulate microglia and augment PD extrapyramidal symptoms (Sampson *et al.,* 2016). Sampson *et al.*, (2016) found that symptoms are increased when mice, overexpressing α-synuclein, are colonised with PD patient

microbiota. They also reported that neuroinflammation and motor symptoms are enhanced in germ-free mice when administered gut microbiota from human PD patients (Sampson *et al.,* 2016). These studies suggest that changes in gut microbiome serve as a risk factor for PD onset and progression. Our study examines the concentration of BAs and FAs in PD patient plasma and faeces in order to deduce possible changes in gut microbial composition and subsequent signalling, by comparing with an age-matched control group.

Indeed, BA alterations have been reported in PD, particularly in a mouse model of prodromal PD (Graham *et al.,* 2018b) and in a follow on study examining human PD brain tissue samples (Vishweswaraiah *et al.,* 2022). Despite different sample cohorts, our study found that concentration levels of circulating and faecal BAs were generally higher in PD patients, compared to age-matched control volunteers. Conjugated BAs, for example circulating GUDCA is significantly higher in PD patients, compared to control volunteers. Interestingly, GUDCA has been reported as a plasma biomarker for PD (Zhao *et al.,* 2018). This could indicate that these bacteria with bile salt hydrolase (BSH) activity could be at lower concentrations in PD gut and so conjugated BAs are being absorbed and remaining in circulation. This level of conjugated BAs could also be damaging other microbes in the gut. If there is less deconjugation, therefore there is less liberation of amino acids glycine and taurine. Taurine has also been shown to be neuroprotective (Che *et al.,* 2018; Hou *et al.,* 2018).

Circulating and faecal concentrations of taurine were slightly lower in PD Patients compared to control volunteers, this supports our hypothesis that perhaps BSH bacteria are at low abundance and so taurine is not being freely liberated (appendix III SI.3.19). A decrease in the levels of circulating taurine in PD patients has been reported in the literature, with an association of increased disease severity as taurine itself has neuroprotective and dopaminergic protective qualities (Zhang *et al.,* 2016; Che *et al.,* 2018).

PD is more common in males than females, in fact ~1.5 times more common in males (Reekes *et al.,* 2020). Gender differences have been reported in different disease states, including PD, and particularly in relation to BA levels (Frommherz *et al.,* 2016; Sheng *et al.,* 2017; Grant and DeMorrow, 2020; Shao *et al.,* 2021). Our data also showed, particularly in circulation, female PD patients had higher levels of BAs

compared to male PD patients. Strikingly, female PD patients had significantly higher concentrations of total BAs compared to female controls. This supports that there are gender differences with respect to circulating BAs in PD patients.

It is known that BA concentrations change as we age (Bertolotti *et al.,* 2007; Frommherz *et al.,* 2016; Lee *et al.,* 2016). Concentration levels of total circulating tauro conjugated BAs and hydrophilic BAs positively correlated with age in PD patients; total BAs, total conjugated BAs, total glyco conjugated BAs, hydrophobic BAs, CA class of BAs and CDCA class of BAs, all positively correlated with age in untreated PD patients. Faecal concentration levels of total BAs, primary BAs, secondary BAs, total conjugated BAs, total glyco conjugated BAs, total tauro conjugated BAs, hydrophobic BAs CA class of BAs and CDCA class of BAs all negatively correlated with age in treated PD patients. This positive correlation of total circulating BAs with age suggests a loss of reabsorption or increase in BAs synthesis. This may be due to an over stimulation of the Farnesoid X Receptor (FXR) (Li and Chiang, 2014), and interestingly, BA FXR agonist concentration levels were significantly higher in treated PD patients compared to age-matched control volunteers. The significant negative correlation of total faecal BAs with age was in the Treated PD group, perhaps suggesting that PD medications are decreasing BA concentrations over time in the gut.

As per the Mayo Clinic, Sinemet is one of the most commonly prescribed medications to treat PD. It contains Levodopa, a chemical precursor of dopamine, and Carbidopa, a decarboxylase inhibitor. In oral Sinemet, 60% of levodopa reaches circulation and 40% is metabolised by gut microbiota (Brüssow, 2020). Enright *et al.*, (2016) summarised in their 2016 review that levodopa promotes microbial dehydroxylation in the gut, promoting the production of metabolites: *m*-tyramine and *m*-hydroxyphenylacetic acid; also, as *Helicobacter pylori* infection is very common in PD patients, this bacterial infection may reduce absorption of levodopa in the gut (Enright *et al.,* 2016). Interestingly, Enright *et al.*, (2017) reported that TCA and TDCA could impact the solubility and absorption of specific drugs. Particularly, they investigated the ratio of unconjugated and tauro conjugated forms of these primary and secondary BAs and their impact on solubility and absorption (Enright *et al.,* 2017). However, the concentrations of total BAs, primary BAs, secondary BAs and

conjugated BAs were all significantly lower in Sinemet-Treated PD Patients compared to their Non-Sinemet-Treated counterparts, indicating that Sinemet is reducing the levels of these BAs in the gut, which may be impacting its absorbance. This again supports the hypothesis that PD medications, such as Sinemet, could be influencing gut microbiota. Perhaps there is a reduction in BA synthesis and regulation of FXR may be affected by PD medications such as Sinemet.

The secondary BA UDCA is synthesized from CDCA by gut microbes in the intestine. UDCA has been shown in multiple studies to have beneficial effects in the context of PD (Ved *et al.,* 2005; Mortiboys *et al.,* 2013; Mortiboys *et al.,* 2015). TUDCA protects against the PD effects of MPTP-induced dopaminergic degeneration (Castro-Caldas *et al.,* 2012). We showed that the concentration of circulating GUDCA was at a significantly higher concentration in PD patients compared to control volunteers. Perhaps GUDCA is at higher concentrations to induce beneficial effects in the brain, trying to counteract the progression of PD in patients. GUDCA also acts as an antagonist to the nuclear receptor, FXR, which acts as a feedback regulator for BA synthesis. FXR also has important roles in lipid metabolism, glucose metabolism and metabolic rate. Indeed, concentration levels of circulating BA agonists for the VDR were significantly higher in treated PD patients, compared to control volunteers. VDR is involved in drug and BA metabolism and detoxification. Also, faecal BA agonist CA negatively correlated with UPDRS in untreated PD patients. Perhaps BA agonists of FXR and VDR decrease with age and disease progression in PD, therefore affecting overall downstream metabolism and detoxification.

In our study, we noted an increase in the concentrations of circulating total FAs in PD patients compared to control volunteers. Pyruvic acid concentrations were significantly increased in PD patients, compared to control volunteers, suggesting that ATP production in the mitochondria is reduced as pyruvic acid is not being utilized properly by the TCA cycle; instead it is circulating in the plasma. Reduced ATP levels and pyruvic acid have already been reported to have a role in PD (Mytilineou *et al.,* 1994; Ghosh *et al.,* 2016; Cai *et al.,* 2019). Circulating medium-chain FA: octanoic acid, and long-chain FA: palmitic acid are significantly increased in PD patients compared to control volunteers. Octanoic acid is associated with beneficial

effects in the context of PD and it has been shown to induce neurite processes and increase metabolic mitochondrial activity (Kamata *et al.,* 2007; Joniec-Maciejak *et al.,* 2018). It is unusual to have such high concentrations, although Jain *et al.*, (2021) reported that on bone health, octanoic acid induced significant negative effects (Jain *et al.,* 2021). Perhaps more investigation is needed on both the positive and negative effects of octanoic acid on human health. Palmitic acid can be produced endogenously or obtained from the diet and may be a potential plasma biomarker for PD (Shah *et al.,* 2019). Shah *et al.*, (2019) reported that palmitic acid has negative effects in the context of PD. They found that palmitic acid was elevated in the plasma of rats induced with PD symptoms by treatment of 6-hydroxydopamine (6-OHDA), and that high levels of palmitic acid is associated with increased motor dysfunction (Shah *et al.,* 2019). Elevated levels of palmitic acid in the plasma may have a negative effect on PD progression. Schommer *et al.*, (2018) also showed that a diet, enriched with palmitic acid, increases the levels of both the expression of tyrosine hydroxylase and the toxic protein α-synuclein (Schommer *et al.,* 2018). Fanning *et al.*, (2019) demonstrated that increased oleic acid leads to an increase in PD toxicity (Fanning *et al.,* 2019). In our study, faecal oleic acid is significantly lower in PD patients compared to control volunteers. However, it has been shown that oleic acid has a beneficial role in the diet by increasing omega-3 FAs in the blood and reducing cardiovascular disease (Nogoy *et al.,* 2020). Oleic acid has also been shown to reduce locomotor activity in rats (Contreras *et al.,* 2014). Faecal oleic acid also positively correlated with age in treated PD patients. Circulating oleic acid positively correlated with age in untreated PD patients, along with palmitic acid, EA and DHA. EA originates from oleic acid and has been reported as a biomarker for autoimmune diseases (Tsoukalas *et al.,* 2019). DHA and arachidonic acid have been shown to regulate α-synuclein (Sharon *et al.,* 2003; Iljina *et al.,* 2016). Arachidonic acid induced α-synuclein formation is said to be less toxic with arachidonic acid stimulating apoptosis by forming adducts with dopamine (Liu *et al.,* 2008). Interestingly linoleic acid, α/γlinolenic acid, and arachidonic acid metabolism have been reported to be reduced in PD (Shao *et al.,* 2021). Faecal myristic acid and DHA positively correlated with age in treated PD patients and control volunteers. PD medication may be

rescuing these FA levels to those of the control. Myristic acid has been shown to have anti-anxiety affects in rats (Contreras *et al.,* 2014). Myristic acid has also been shown to have beneficial effects in tau phosphorylation (Tsai *et al.,* 2015). DHA has been shown to have beneficial effects in the context of PD by inducing dopamine synthesis and increasing motor function (Gómez-Soler *et al.,* 2018; Chitre *et al.,* 2020).

The concentrations of total FAs and medium-chain FAs, are significantly higher in Sinemet-Treated PD patients compared to their Non-Sinemet-Treated counterparts. Studies have shown than FAs may interfere with Sinemet absorption (Babita *et al.,* 2005; Babita and Tiwary, 2005). Our findings show that Sinemet-Treated PD patients have reduced levels of faecal BAs but elevated levels of faecal FAs, therefore gut microbial composition analysis may shed more light on these findings.

Circulating lactic acid positively correlated with both total UPDRS score and UPDRS motor sub-score in treated PD patients. This suggests that lactic acid concentration levels increase as PD progresses, and lactic acid has already been reported to increase with age (Ross *et al.,* 2010). Circulating pyruvic acid and octanoic acid both negatively correlated with MoCA score in PD patients. Circulating pyruvic acid and heptanoic acid both negatively correlated with MoCA score in treated PD patients. Pyruvic acid, reflecting reduced ATP, and octanoic acid, inducing neurite processes, have already been shown to have effects in the context of PD, as mentioned earlier. Decreasing concentrations of pyruvic acid and octanoic acid would agree with negative PD progression. Faecal lactic acid, palmitoleic acid, palmitic acid, α/γlinolenic acid, linoleic acid, oleic acid, arachidonic acid and long-chain FAs all positively correlated with UPDRS score in PD patients. Faecal octanoic acid, oleic acid and long-chain FAs all positively correlated with UPDRS score in Untreated PD patients. α-Linolenic acid is needed for EPA and DHA synthesis. Positive correlation of α-linolenic acid with disease progression may indicate that it negatively effects PD. Dong *et al.*, (2014) reported a weak positive association between n-6 polyunsaturated FAs, including linoleic acid, and PD risk (Dong *et al.,* 2014). Faecal linoleic acid positively correlated with UPDRS score in treated PD patients. Faecal palmitic acid and arachidonic acid both negatively correlated with MoCA score in PD patients. Faecal palmitic acid, arachidonic acid and DHA all negatively correlated with MoCA score in Untreated PD patients. As discussed, arachidonic acid and DHA have

been shown to have beneficial effects in the context of PD despite regulating α-synuclein (Xicoy *et al.,* 2019).

Future Work

To move this work forward, this data could be compared with microbial composition. DNA extraction and 16S rRNA gene sequencing could be performed on these faecal samples to compared BA microbial modification with this BA analysis. RNA-sequencing analysis on faecal samples would allow comparison of the real-time transcriptome of PD patients against age-matched, healthy, control volunteers. This would give a snapshot into the PD profile and allow the potential to connect signalling pathways, from transcriptome analysis, directly with microbial composition. Analysis could also be carried out to determine exact activation of NRs including FXR or VDR.

To conclude, in part I - bacterial treatments increased LCA and total tauro conjugated BA levels, namely TLCA, and reduced BA signalling. As TLCA and LCA are agonists of TGR5, there is an increase energy homeostasis, thermogenesis and glucose metabolism. In the faeces, bacterial treatments increased total BA levels, namely CDCA. *B. adolescentis* strain 2715 specifically increased TLCA levels. Bacterial treatments increased FXR signalling and the most potent BA ligand, CDCA, was elevated. FXR regulates BA homeostasis and glucose metabolism. *B. adolescentis* strain 2715 specifically increased TLCA levels, again increasing TGR5 signalling. TGR5 can regulate gut motility and both FXR and TGR5 have been reported to regulate immune response. Comparison of this data with changes in microbial composition and serotonin levels will help determine whether *L. salivarius* strain P0003 and *B. adolescentis* strain 2715 interventions could be applied to humans to improve behaviour as well as gastrointestinal traits in ASD. Overall, *L. salivarius* strain P0003 and *B. adolescentis* strain 2715 interventions have great potential to improve characteristics of the ASD behavioural phenotype, by subtle changes in gut signalling.

To conclude, in part II - our data suggests that bacteria with bile salt hydrolase (BSH) activity could be at lower concentrations, therefore conjugated BAs are being

absorbed and remaining in circulation. This level of conjugated BAs could also be damaging other microbes in the gut. If there is less deconjugation, therefore there is less liberation of amino acids glycine and taurine. In addition, the positive correlation of total circulating BAs with age suggests a loss of reabsorption or increase in BA synthesis. This may be due to an over stimulation of the FXR. The significant negative correlation of total faecal BAs with age, perhaps suggests that PD medications are decreasing BA concentrations over time in the gut. We hypothesize that Sinemet is reducing the levels of BAs in the gut, which may be impacting its absorbance. This again supports the hypothesis that PD medications, such as Sinemet, could be influencing gut microbiota. Regulation of FXR may be affected by PD medications such as Sinemet. GUDCA is a biomarker of PD and was found at high levels in circulation. GUDCA also acts as an antagonist to the nuclear receptor, FXR, which acts as a feedback regulator for BA synthesis. FXR also has important roles in lipid metabolism, glucose metabolism and metabolic rate. Indeed, concentration levels of circulating BA agonists for the VDR were higher in PD patients. VDR is involved in drug and BA metabolism and detoxification. Also, faecal BA agonist CA negatively correlated with UPDRS in Untreated PD patients. Perhaps BA agonists of FXR and VDR decrease with age and disease progression in PD, therefore affecting overall downstream metabolism and detoxification. Our data also showed that there are gender differences with respect to circulating BAs in PD patients. In the circulation of PD patients, total FAs were increased, including pyruvic acid, suggesting that ATP production in the mitochondria is reduced, and palmitic acid, which is associated with increased motor dysfunction in PD. Faecal oleic acid is lower in PD patients, suggesting a reduction in omega-3 FAs. The concentrations of total FAs were significantly higher in Sinemet-Treated PD patients, suggesting they may interfere with the absorption of Sinemet in the gut.

Our studies suggest that changes in BA and FA concentration levels can reveal alterations in gut microbial composition and subsequent signalling, which can indicate risk factors for diseases such as PD. Microbial-based intervention can be applied once these alterations are known and could improve disease traits, such as behaviour and gastrointestinal dysbiosis in ASD.

Chapter 4 – Examining bile acids to determine if their activation influences lifespan in the model of aging *Caenorhabditis elegans*

4.0 Abstract

The aim of this study was to identify new mechanisms and potential therapeutic targets that could promote healthy aging, through the human gut microbiome and associated metabolism, using the nematode model of aging *Caenorhabditis elegans* (*C. elegans*). The microbiome may differentially contribute to aging and longevity. One mechanism may be through microbial alterations to signalling molecules, specifically expansion of the palate of BA moieties. Indeed, in chapter 3 we determined that BA alterations were a convergent feature of disease and that changes were also associated with aging. We note that BAs are cholesterol derivatives with the capacity, as individual moieties, to modulate receptor signalling and other functions. The same receptors are conserved in *C. elegans*, the nematode model of aging. Indeed, cholesterol derivatives (Dafachronic acids (DAs)) also differentially modulate the nematode receptors. To translate and investigate aging in humans, in this chapter, different classes of BAs, primary and secondary BAs, were applied to the simple nematode model of aging, to determine whether they may influence lifespan and development. Specifically, we wondered whether BAs could act by influencing or mimicking DAs, whether they could alter or influence DA production and hence receptor functions, to impact *C. elegans* longevity and development. This study identified specific BAs CDCA, its microbial derivative LCA and also DCA, microbially derived from liver produced CA, as impactful in either *C. elegans* lifespan or development. The potential to invoke DAs and downstream responses was evident in experiments. Furthermore, RNAseq and its analysis showed that exposure to either CDCA and LCA provided tentative evidence for their possible influence in the aging context.

4.1 Introduction

Caenorhabditis elegans (*C. elegans*) is a well characterised soil-dwelling nematode, particularly due to its short lifespan of 20-25 days, and its diet, *E. coli* species (OP50 in the lab) (Brenner, 1974). *C. elegans* is a particularly useful model of aging (Klass, 1977), as many of its pathways have homologs in humans. One such pathway is concerned with cholesterol utilization for the synthesis of dafachronic acids (DAs) in

C. elegans and a similar pathway exists in humans for the synthesis of BAs (*Figure 1.16*). DAs are synthesised from cholesterol and some activate the DAF receptors influencing *C. elegans* life cycle. The two main DAs, Δ^4-dafachronic acid (Δ^4DA) and Δ^7-dafachronic acid (Δ^7DA), both act as ligands for the DAF-12 receptor, activating its downstream pathway to stimulate and control normal *C. elegans* progression through its life cycle (Antebi *et al.,* 1998; Antebi *et al.,* 2000; Gerisch *et al.,* 2001; Gerisch *et al.,* 2007; Dumas *et al.,* 2013). BAs are also synthesised from cholesterol and some (CDCA>DCA>CA and α/βMCA) can activate the Farnesoid X Receptor (FXR), a DAF-12 human homologue, to regulate lipid and energy metabolism, circadian rhythm and to influence immune function while equally others (T/GUDCA and Tα/βMCA) can repress it (Joyce *et al.,* 2014; Li and Chiang, 2014; Perino *et al.,* 2021). BAs have been suggested to positively impact human lifespan (Cai *et al.,* 2016). They are reported to further extend it in long-lived growth hormone-releasing hormone, *Ghrhr*, mutant mice (Amador-Noguez *et al.,* 2004; Amador-Noguez *et al.,* 2007; Gems, 2007), but no mechanism, or general consensus on BAs, in the context of aging and longevity, has been reported. Indeed, the secondary BA, Lithocholic Acid (LCA), has been reported to induce lifespan extension in the fruit fly, *Drosophila melanogaster*, by altering gut microbial metabolism, as well as increasing expression of peroxisome proliferator-activated receptor-gamma coactivator-1alpha (PGC1α)-homolog *srl* (Staats *et al.,* 2018). A similar LCA effect on lifespan is reported in chronologically aging yeast *Saccharomyces cerevisiae*. Here, LCA is reported to regulate longevity through the mitochondrial membrane lipidome, affecting oxidation-reduction processes (Goldberg *et al.,* 2010; Beach *et al.,* 2015; Leonov *et al.,* 2017). Indeed, LCA, added at either of two yeast lifespan periods -both logarithmic and diauxic growth phases and during early stationary phase- could also induce lifespan extension in these chronologically aging yeast *Saccharomyces cerevisiae* under calorie restricted conditions (Burstein *et al.,* 2012). LCA was found to integrate lipid and carbohydrate metabolism, in yeast, and mitochondrial metabolism, lipo-necrotic and apoptotic modes of aging-associated cell death, to induce longevity (Arlia-Ciommo *et al.,* 2018). Furthermore, LCA extends the lifespan of yeast through a unique metabolic pattern, compared to caloric restriction. LCA can

alter the intracellular concentration of methionine, whose levels are a known aging associated modulator for global protein expression and also affect sulfur amino acid biosynthesis, and cellular ATP, ADP and AMP concentrations (Mohammad and Titorenko, 2021).

Ursodeoxycholic Acid (UDCA) is reported to protect against secondary BA Deoxycholic Acid (DCA)-induced apoptosis through EGFR/Raf-1/ERK signalling in human colorectal cancer cells, and through activation of the Akt-dependent survival signalling pathway in HCT116 cells (Im and Martinez, 2004; Im *et al.,* 2005). There is evidence that UDCA reduces hepatic lipid accumulation and decreases adipocyte and hepatocyte inflammation (Oh *et al.,* 2016). At the cellular level, UDCA elevates isocitrate dehydrogenase and complex II of the electron transport chain, while DCA inhibits Ca^{2+} absorption in the intestine. UDCA was also shown to be beneficial to airway epithelial cells by regulating Th2 cell derived cytokines and inhibiting apoptosis (Işık *et al.,* 2017) while it also averts mitochondrial dysfunction (Pérez *et al.,* 2021). These beneficial effects, have promoted its application to treat disease, including Parkinson's Disease (Sathe *et al.,* 2020). DCA (*Figure 4.1*), is a potent FXR ligand and is correlated with negative effects on overall host health. It can stimulate afferent nerve firing in the colon (Yu *et al.,* 2019). A role for DCA in intestinal carcinogenesis, through vasculogenic mimicry formation and epithelial-mesenchymal transition, is proposed via activation of the vascular endothelial growth factor receptor 2 signalling pathway (Song *et al.,* 2022). It is also associated with end-stage kidney disease and all-cause mortality in patients with chronic kidney disease (Frazier *et al.,* 2022). DCA can induce production of reactive oxidative species (ROS) and reduce signal-regulated kinase 1/2 (ERK1/2) signalling pathways. Moreover, it is shown to increase intestinal permeability (Zeng *et al.,* 2022). Both DCA, and its parent molecule Cholic Acid (CA) (*Figure 4.1*), are reported to stimulate skeletal muscle atrophy *via* TGR5 receptor by increasing atrogin-1, MuRF-1 and oxidative stress, to reduce fiber diameter and MHC protein levels, in wild-type fibers from male mice (Abrigo *et al.,* 2021). In another study, oral CA therapy was identified as an effective and safe long-term treatment for children in need of liver

transplantation and where defects in primary BA synthesis were evident (Gonzales *et al.,* 2018).

Primary BA, Chenodeoxycholic Acid (CDCA), (*Figure 4.1*), can reduce trans-epithelial electrical resistance, and increases IL-8 production and permeability in Caco-2 cells (Horikawa *et al.,* 2019). CDCA has been shown to increase insulin sensitivity in the context of Alzheimer's Disease (Bazzari *et al.,* 2019). In weaned piglets, CDCA administration altered serum metabolic profiles and the relative abundance of certain gut bacteria, whilst improving lipid digestion, intestinal morphology and barrier function to positively impact overall growth performance or bulking (Song *et al.,* 2021). CDCA has also been shown to be an effective treatment for patients with BA synthesis disorders (Kimura *et al.,* 2021).

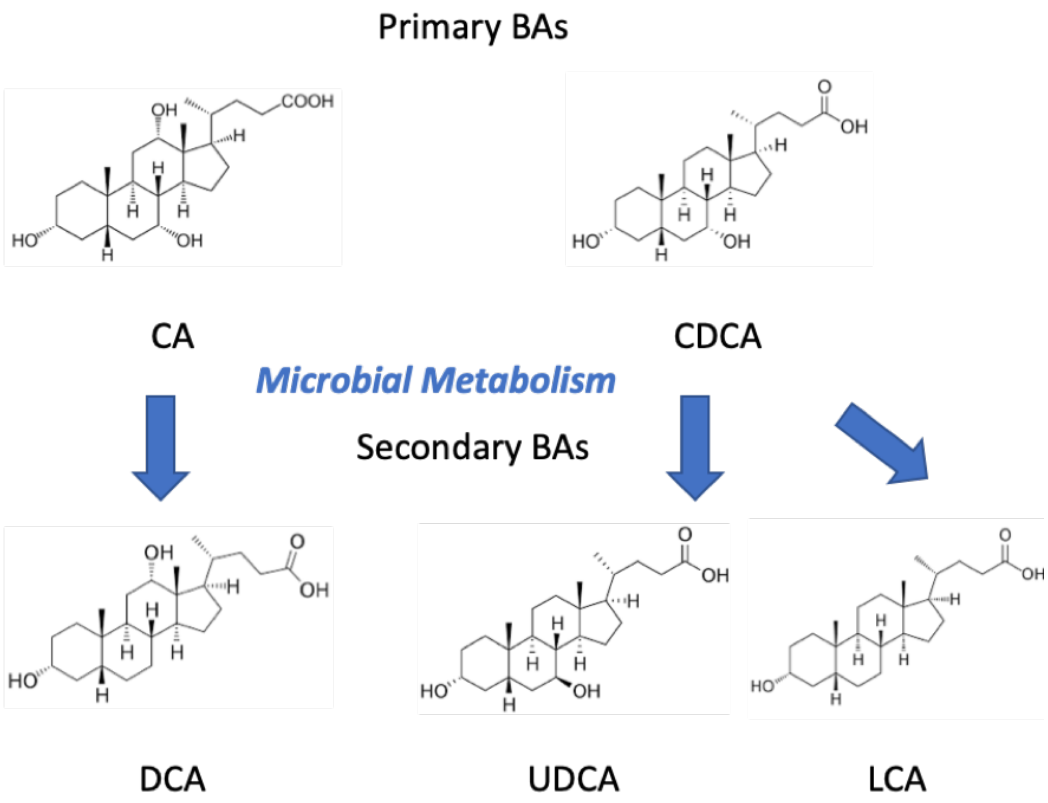


Figure 4.1: **Chemical structure of primary and secondary bile acids.** Chemical structure of liver produced primary BAs: Cholic Acid (CA) and Chenodeoxycholic Acid (CDCA); and their microbially derived secondary BAs: Deoxycholic Acid (DCA) from Cholic Acid (CA), while Ursodeoxycholic Acid (UDCA) and Lithocholic Acid (LCA) are derived from Chenodeoxycholic Acid (CDCA).

In chapter 3 we determined that BA alterations were a convergent feature of disease and indeed changes are associated to aging. We further reasoned that disease and aging might be adjusted through probiotic strain modification, where specific BA altering enzymes were expressed by such strains. We reasoned that BAs may have a central role in the aging process, given the convergent mechanism (lipid metabolism, ROS, immune functions and circadian rhythms) that BAs alter. All of these pathways influence and converge in the aging process in *C. elegans*, the model of aging. In this study we hypothesized that such effects could be tested using *C. elegans*, where BA receptor homologues are present (see Chapter 1, Introduction sections 1.7.4) and influenced by other cholesterol derivatives, namely DAs. *C. elegans* may therefore be an appropriate model in which to study the influence of BAs on the aging landscape, with origins from the gut. This work commenced in 2018, when very little was known in terms of BAs in the aging landscape, and their interactions with *C. elegans*. Primary BAs: CA and CDCA, and secondary BAs: DCA, UDCA and LCA were applied in this study at concentrations 1 mM, 5 mM and 10 mM. These BA concentrations were chosen due to their physiological relevance. Human gut BA levels can be 1 mM or lower, and can reach up to 10 mM mainly during digestion (Hofmann and Eckmann, 2006; Hamilton *et al.,* 2007; Guzior and Quinn, 2021). Here, in this chapter *C. elegans* was applied to determine whether the different classes of BAs could influence lifespan and development in a model animal.

Specifically, we wondered whether BAs could act by influencing DA receptor functions and indeed DA production to alter longevity and development. We also asked whether BAs could influence gene expression through any of the DA receptors and associated convergent pathways. This study identified DCA and CDCA as impactful in *C. elegans*, whilst LCA proved equivocal, LCA may have the potential to extend *C. elegans* lifespan. RNAseq analysis was undertaken to compare the changes in gene transcription and potential physiology in *C. elegans* nematodes that were exposed to either LCA or CDCA, to provide tentative evidence for their possible influence in the aging context.

4.2 Results

4.2.1 Assessment of *Escherichia coli* OP50 bacterial growth in the presence of individual primary and secondary bile acids.

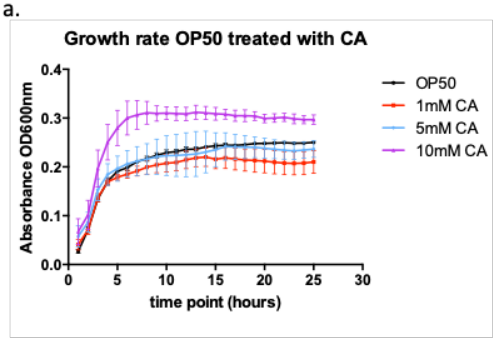
The developmental cues for *C. elegans* is a function of its food (*E. coli* bacteria) and its quality. Here, E. *coli* OP50 is supplied as a calorific source. *E. coli* are taken into the pharynx, crushed and its contents are gut delivered, including cholesterol (for DA synthesis). We reasoned that *E. coli* might deliver BAs to the nematode gut, we further reasoned that *E. coli* OP50 may be altered for fitness, in taking up BAs and that *C. elegans* reproduction and development could be influenced by BAs. The effect could be either direct or indirect through *E.coli* either as a food or as a reduced fitness resource or through signalling functions. To investigate and separate these aspects, the rate of this bacterial, *E. coli* OP50, growth in the presence of BAs was assessed, over 24 hours, in the absence and the presence of BAs CA, DCA, CDCA, UDCA and LCA at concentrations of 1 mM, 5 mM and 10 mM. To enumerate viable cells, a replicate assay was performed to facilitate bacterial serial dilutions (to 10^{-8}) at the 24-hour point. Here, dilutions were plated onto solid LB agar media, then incubated for 24 hours at 37°C (Materials and Methods, Section 2.1.3) (*Figure 4.2*).

E. coli OP50 grown under normal conditions was consistent for biomass (0.2 ODs maximum) and in its growth patterns under all experimental conditions over 24 hours. The CFUs recovered post serial dilution reflect this consistency (*n*=3). Addition of BAs to growth media elicited responses that appear to enhance biomass, by absorbance, for all BAs tested with the exception of 1 mM and 5 mM CA. (*Figure 4.2* (a), (c), (e), (g) and (i)). When viable cells were examined, biomass was not significantly enhanced by any BA treatment (*Figure 4.2* (b), (d), (f), (h) and (j)). However significant and dose dependent reductions in cell viability are evident for those cultures treated with DCA and CDCA (*Figure 4.2* (d) and (f)).

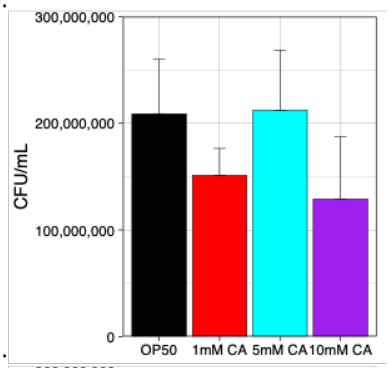
In conclusion, *E. coli* OP50 appeared to grow at a faster rate, to produce increased biomass in the presence of BAs, an effect that did not translate to viability. Instead, viability decreased in a dose dependent manner in the presence of two BAs, DCA and CDCA. The data suggest a possible background absorbance in the presence of BAs that may skew the data towards a false elevated biomass detection, an effect that is

resolved by viable pate counting and recording. In all, it appears that BAs reduces bacterial cell viability and may reduce its fitness as a food source for nematodes.

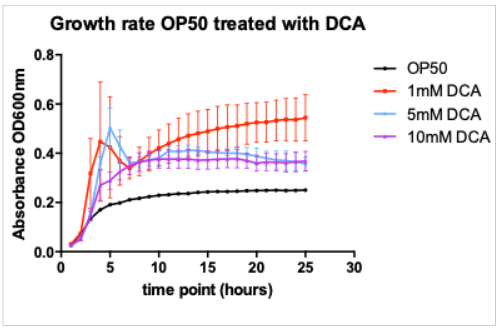
a.


Growth rate OP50 treated with CA
Absorbance OD600nm
time point (hours)
OP50
1mM CA
5mM CA
10mM CA

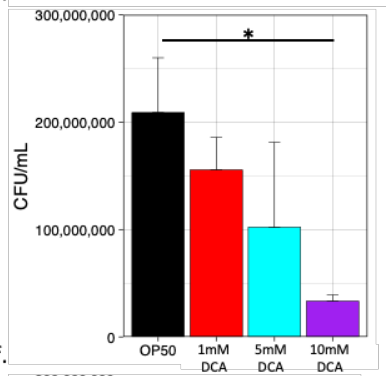
b.


CFU/mL
OP50
1mM CA
5mM CA
10mM CA

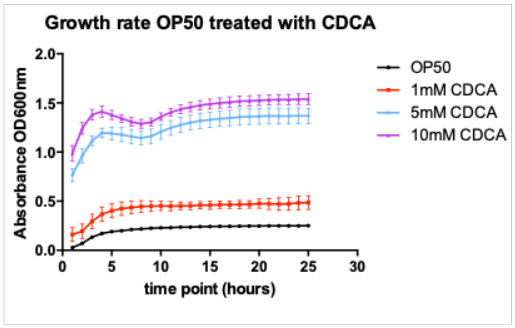
c.


Growth rate OP50 treated with DCA
Absorbance OD600nm
time point (hours)
OP50
1mM DCA
5mM DCA
10mM DCA

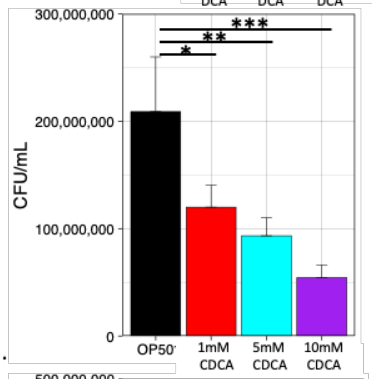
d.


CFU/mL
*
OP50
1mM DCA
5mM DCA
10mM DCA

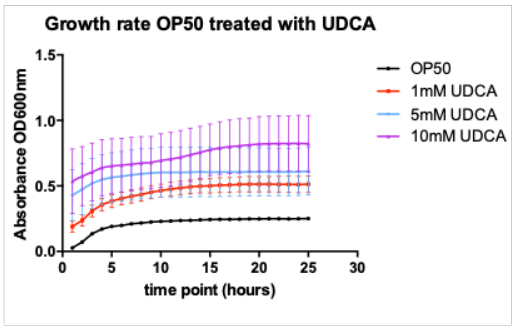
e.


Growth rate OP50 treated with CDCA
Absorbance OD600nm
time point (hours)
OP50
1mM CDCA
5mM CDCA
10mM CDCA

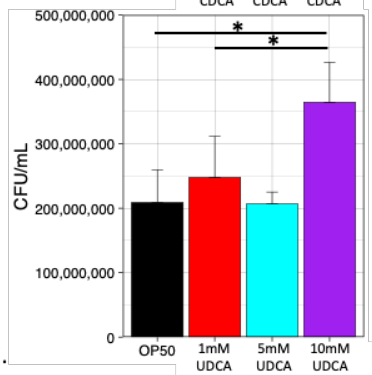
f.


CFU/mL
*
**
***
OP50
1mM CDCA
5mM CDCA
10mM CDCA

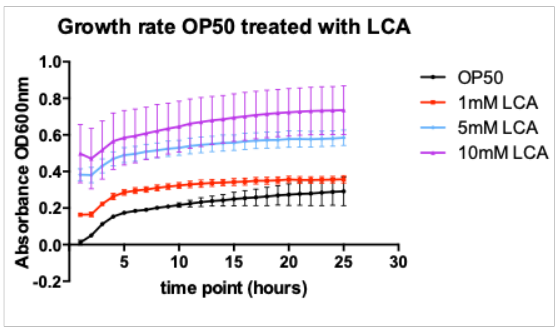
g.


Growth rate OP50 treated with UDCA
Absorbance OD600nm
time point (hours)
OP50
1mM UDCA
5mM UDCA
10mM UDCA

h.


CFU/mL
*
*
OP50
1mM UDCA
5mM UDCA
10mM UDCA

i.


Growth rate OP50 treated with LCA
Absorbance OD600nm
time point (hours)
OP50
1mM LCA
5mM LCA
10mM LCA

j.

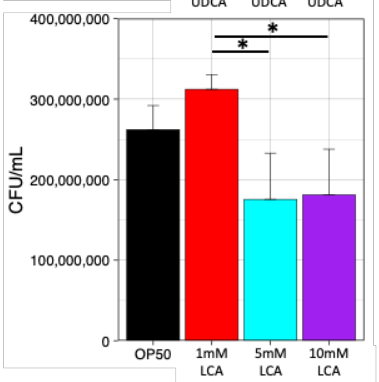

CFU/mL
*
*
OP50
1mM LCA
5mM LCA
10mM LCA

Figure 4.2: **Assessment of *Escherichia coli* OP50 bacterial growth in the absence and presence of individual primary and secondary bile acids.** Growth assessment (OD_{600nm}) recorded over 24 hours at 37°C in LB media in the presence and absence of 1, 5 and 10 mM BAs (a) Cholic Acid (CA), (c) Deoxycholic Acid (DCA), (e) Chenodeoxycholic Acid (CDCA), (g) Ursodeoxycholic Acid (UDCA) and (i) Lithocholic Acid (LCA). The corresponding viability was assessed following 24 hours exposure (or not) to these BA concentrations for (b) Cholic Acid (CA), (d) Deoxycholic Acid (DCA), (f) Chenodeoxycholic Acid (CDCA), (h) Ursodeoxycholic Acid (UDCA) and (j) Lithocholic Acid (LCA). (*n*=3) for each treatment and control (second biological replicate, appendix IV SI.4.4.1). Statistics were one-way ANOVA, Tukey multiple comparison test (* = $p<0.05$; ** = $p<0.01$; *** = $p<0.001$; **** = $p<0.0001$).

4.2.2 Primary and secondary bile acids were detected in *Escherichia coli* OP50 and gut of *Caenorhabditis elegans*, and their concentrations increased in a dose-dependent manner

BAs appear to affect the rate of growth of *E.coli* OP50 and may be toxic. We evaluated whether the bacteria could act as an effective delivery system for different BAs noting that bacteria themselves use different adaptations -including efflux systems, production of stress proteins and changing the morphology of the bacterial cell- to deal with potentially toxic chemicals and environmental stresses. We therefore evaluated whether *E.coli* OP50 could in fact retain individual BAs. This could indicate the level of delivery to the nematode gut environment. Briefly, *E. coli* OP50 was grown in the absence and presence of BAs; either 1 or 10 mM of each of CA, DCA, CDCA, UDCA, LCA were independently added to NGM agar. The co-incubations were placed at 37°C for 48 hours (Materials and Methods, Section 2.3.4). Each sample *E. coli* OP50 (*n*=3/treatment) was normalised to 1 OD_{600} per ml before it was lysed and BAs were extracted for mass spectrometry application and analysis (Material and Methods, Section 2.3.5).

Below we show that *E. coli* OP50, were capable of BA uptake in a dose dependent manner. The levels were low, reaching a maximum of 4 μg/OD_{600} and 17.4 μg/OD_{600} in the case exposure to 1 mM and 10 mM, respectively, for CA (*Figure 4.3* (a)); 39

μg/OD_{600} and 124 μg/OD_{600} in the case exposure to 1 mM and 10 mM, respectively, for DCA (*Figure 4.3* (b)); 4.5 μg/OD_{600} and 166 μg/OD_{600} in the case exposure to 1 mM and 10 mM, respectively, for CDCA (*Figure 4.3* (c)); 2.2 μg/OD_{600} and 4.6 μg/OD_{600} in the case exposure to 1 mM and 10 mM, respectively, for UDCA (*Figure 4.3* (d)); 14 μg/OD_{600} and 29 μg/OD_{600} in the case exposure to 1 mM and 10 mM, respectively, for LCA (*Figure 4.3* (e)). While this data confirmed uptake of BA by *E. coli* OP50, it was clear that uptake was BA dependent irrelevant of the dose supplied. Furthermore there was no clear distinction related to the properties of BAs, explicitly, those that were hydrophilic were not taken up and delivered to a higher level than hydrophobic BAs (*Figure 4.3*) or vice versa.

To investigate the actual delivery to nematodes, temperature sensitive mutant *C. elegans* strain SS104 were synchronised (Materials and Methods, Section 2.2.2) and 60 L1 larvae were plated onto NGM agar pre-seeded plates with *E. coli* OP50 with and without BAs at the same concentrations as above. They were then co-incubated (Materials and Methods, Section 2.3.4) at 16°C for 2 weeks. At this point *C. elegans* SS104 were represented by mixed populations, namely dauer. Nematodes were sorted and counted under light microscopy to confirm the total number of individuals associated to each treatment. A single aliquot of ~1000 mixed population, for each treatment, was washed from the agar and prepared for lysis and BA extraction in preparation for mass spectrometry application and analysis (*n*=1), (Material and Methods, Section 2.3.5). Only one replicate was prepared for UPLC-TMS, an experiment done in real time. Analysis revealed that all BAs reach the nematode gut, albeit to different levels (*Figure 4.4*). Indeed, the levels recovered did not reflect the microbial load carried/OD_{600} of bacteria, for individual BAs, with for example the highest level returned for CA (1500 ng/1000 nematodes on exposure to 10 mM) (*Figure 4.4* (a)) whereas in *E. coli* OP50 CA reached 17.4 μg/OD_{600}. For CDCA, carried by *E.coli* OP50 at 166 μg/OD_{600} much lower levels were detected in delivery, in nemaodes: 530 ng/1000 nematodes were recovered (*Figure 4.4* (c)). These data indicate a delivery difference that may be reflective of one of the mixed populations and their stage differences or of actual nematode uptake as well as the number of bacteria that may be colonising each nematode. Only one replicate is taken for each

experiment, therefore it is difficult to access the validity of the data. However, although the data indicated delivery to both bacteria and to nematodes, there was no linear relationship for individual BAs between bacterial dose and gut levels in a non-synchronised population (*Figure 4.4).* (Extraction efficiency and total nematode per treatment, appendix IV SI.4.2-6).

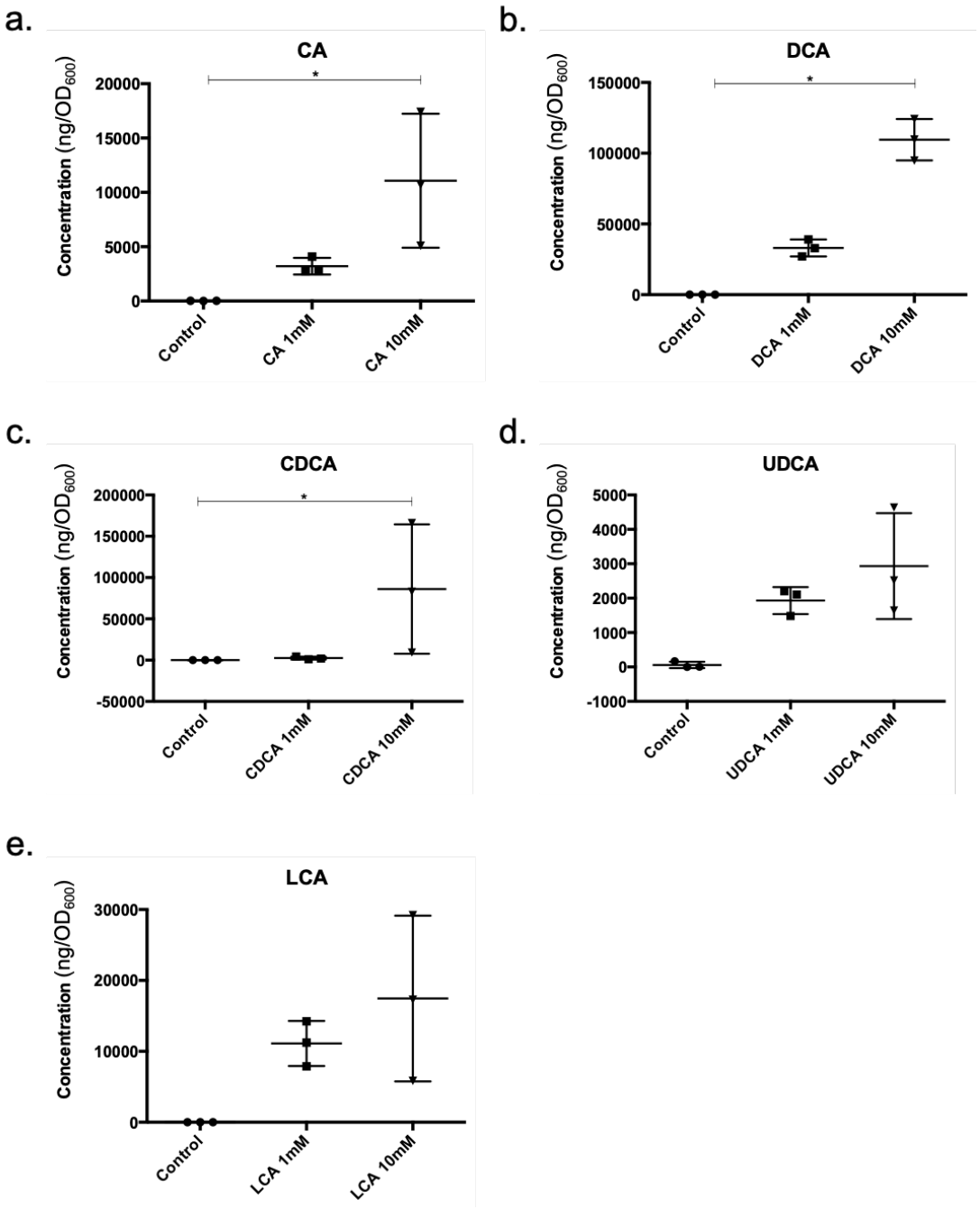


Figure 4.3: **Ultra Performance liquid Chromatography Tandem Mass spectrometry (UPLC-TMS) assessment of bile acid uptake into *Escherichia coli* OP50.** The level of

individual BA was assessed from 1 OD_{600} of *E. coli* OP50 post extraction process, where individual cultures were pre-exposed to one of 0, 1 and 10 mM of individual BAs (a) CA (b) DCA (c) CDCA (d) UDCA (e) LCA. (*n* = 3). Statistics were carried out using Kruskal-Wallis, and Dunn's Multiple comparison test (* = $p<0.05$; ** = $p<0.01$; *** = $p<0.001$; **** = $p<0.0001$).

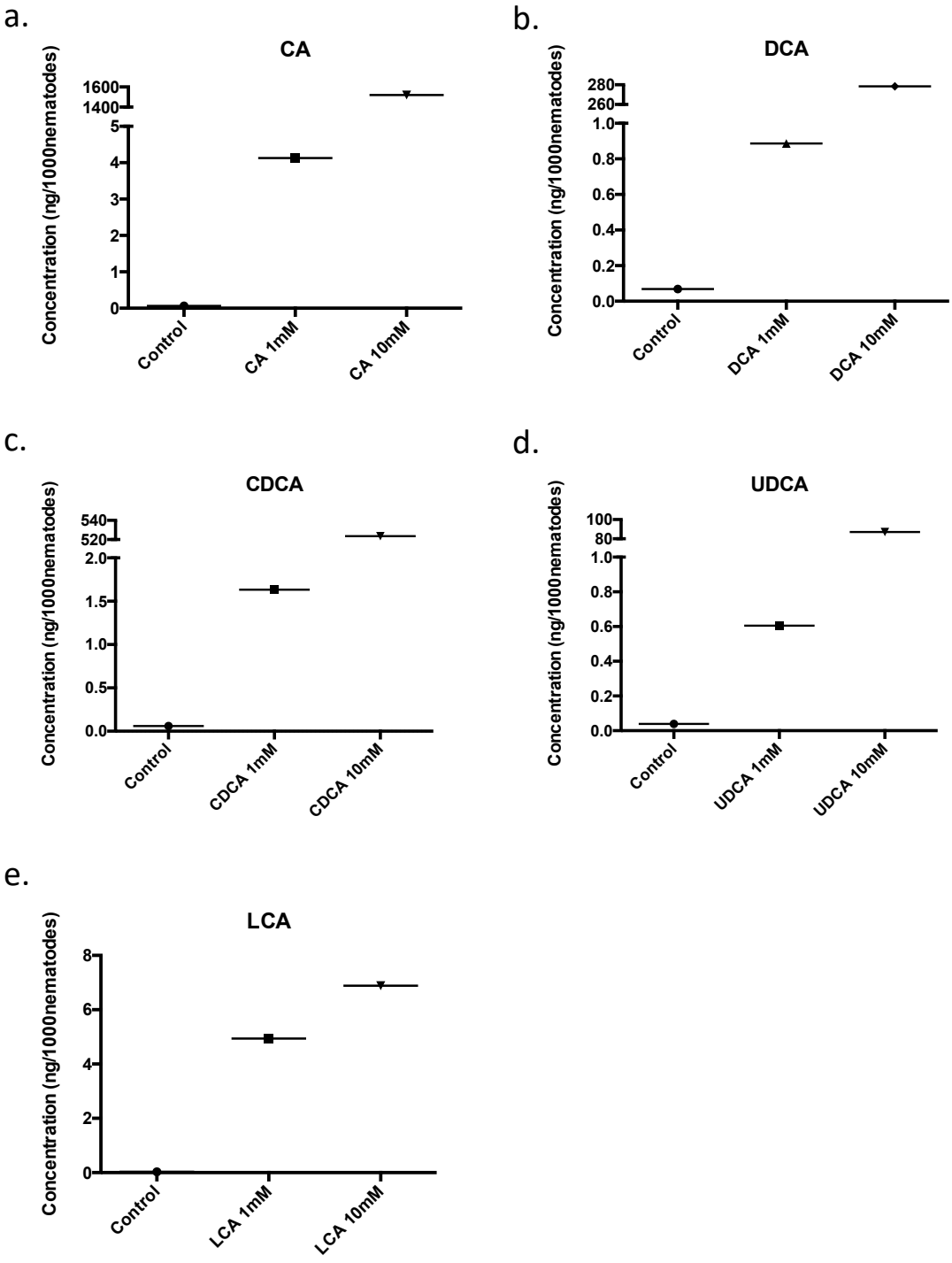


Figure 4.4: **Ultra Performance Liquid Chromatography Tandem Mass Spectrometry (UPLC-TMS) assessment of bile acid levels in *Caenorhabditis elegans* SS104 strain.** The levels of individual BAs, from those contained in agar and in bacteria, was assessed from 1000 nematodes, post extraction, where both bacteria and nematodes were pre-exposed to one of 0, 1 and 10 mM for each individual BA (a) CA (b) DCA (c) CDCA (d) UDCA (e) LCA. (*n* = 1).

4.2.3 The primary bile acid Chenodeoxycholic Acid and the secondary bile acid Deoxycholic Acid reduce *Caenorhabditis elegans* lifespan

Primary and secondary BAs were applied to *C. elegans* to determine their effects on lifespan (Materials and Methods, Section 2.2.3). Specific BAs were added directly to the NGM agar, again pre-seeded with *E. coli* OP50 at 37°C for 24 hours. *C. elegans* strain SS104 (a temperature sensitive mutant, containing the *glp-4(bn2)* mutation that is permissive for egg laying and reproduction at 16°C (Beanan and Strome 1992)), was synchronised. 10 L1 larvae (*n*=3) were added to BA containing NGM agar for lifespan assessment (Materials and Methods, Section 2.2.3). Lifespan assays were carried out at 25°C to ensure *C. elegans* strain SS104 was not confounded by egg-laying and the development of new generations of nematodes. Different concentrations of BA (1, 5 and 10 mM) were added directly to the NGM agar that were pre-seeded with *E. coli* OP50 before 10 L1 stage *C. elegans* SS104 nematodes were added, and monitored until 0% survival was reached, to determine how these BAs impacted early life and the development and progression into and through adulthood (*Figure 4.5*).

It is clear that *C. elegans* SS104 lifespan, when treated with any concentrations of CA or UDCA were not significantly different to untreated control animals (*Figure 4.5* (a) and (d)). However, a reduction on lifespan of 8 days was seen when nematodes were cultured with 1 mM and 5 mM UDCA (*Figure 4.5* (d)). In all cases, 50% of nematodes survived at 16 days. However, those nematodes exposed to 1 mM and 10 mM CA survived to day 23, while nematodes growing on 5 mM CA showed extension to day 27, 9 days less than untreated controls. Therefore, CA treatment was associated with a reduction of lifespan of 33-50% relative to the control animals. In the presence of CAs microbially produced BA DCA, 5 and 10 mM was detrimental to L1 larvae and did not survive from time 0. At lower DCA concentrations (1 mM) nematode survival was significantly reduced, by half (to 9 days only with DCA) relative to 18 days for control, non DCA treated animals (*Figure 4.5* (b), p=<0.0001). A dose dependent effect on L1 larvae survival was evident with CDCA, while lifespan (50%) was significantly reduced with the highest level (5 mM CDCA, p=0.0004) only, compared to the control *E. coli* OP50. However, although 1 mM and 10 mM concentrations appeared to reduce lifespan by 4 days, the effect was not significant (*Figure 4.5* (c)). LCA, microbially

produced from CDCA, did not significantly alter lifespan from L1 larvae, however a reduction in survival of 50% was evident in a dose dependent manner for 1 and 5 mM LCA, a toxicity point is probably reached in this interval given that the same effect was seen with 10mM LCA treatment (*Figure 4.5* (e)). Taken together these assays reveal a differential effect on both survival and lifespan that is dependent on BA moiety and on the concentration of BA, to which L1 larvae are exposed.

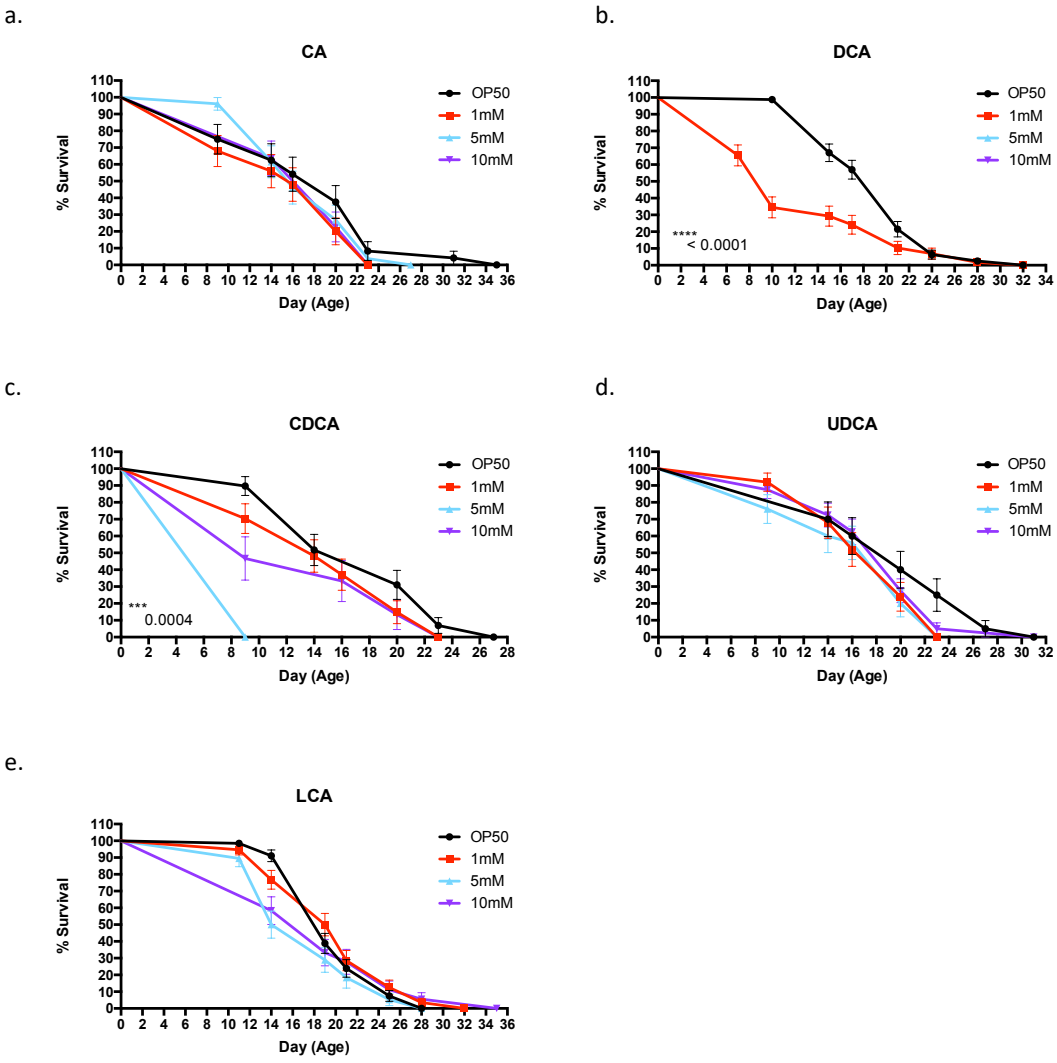


Figure 4.5: **Lifespan and longevity assessment of *Caenorhabditis elegans* strain SS104 in the presence and absence of primary and secondary bile acids.** (a) Cholic Acid (CA), (b) Deoxycholic Acid (DCA), (c) Chenodeoxycholic Acid (CDCA), (d) Ursodeoxycholic Acid (UDCA) and (e) Lithocholic Acid (LCA), were each applied at concentrations of 0, 1, 5 and 10 mM in NGM agar and their impact on *Caenorhabditis elegans* strain SS104 longevity from L1 larval stage was assessed. Survival curves

were performed and are shown for treated and untreated nematodes ((*n*=3) for all treatments and controls agar was pre-seeded with *E. coli* OP50, appendix IV SI.4.7). Statistical analysis was performed through application of the log-rank test for survival curves (*= p<0.05; **=p<0.01; ***=p<0.001; ****=p<0.0001).

These same assays were repeated (with the same BA and controls as described above) but for the WT *C. elegans* N2 Bristol strain to determine whether the observed effects may be related to the SS104 genotype specifically. *C. elegans* WT N2 strain (*n*=30) from the L1 stage were transferred onto fresh plates every second day to counter egg-laying and mixed stages, and were examined until 0% survival was reached (*n*=3) (*Figure 4.6*). Of note, *C. elegans* N2 showed a shortened lifespan of 22 days relative to up to 36 days above for *C. elegans* strain SS104.

1 mM CA, significantly reduced *C. elegans* N2 lifespan, compared to the control *E. coli* OP50 (*Figure 4.6* (a), p=0.0022). 10 mM UDCA significantly extended nematode lifespan, compared to 1 mM UDCA (*Figure 4.6* (d), p=0.0027). *C. elegans* N2 L1 survival was detectible in the presence of 5 mM and 10 mM DCA but with the effect of 50% survival and death within 2 days compared to 11 days with 1 mM DCA and 15 days with no BA treatment (*Figure 4.6* (b), p=<0.0001). Overall, DCA had a negative impact on *C. elegans* N2 lifespan (Figure *4.6* (b)).

For CDCA, the L1 survival and lifespan effect seen in strain SS104 was reproduced in *C. elegans* N2 (*Figure 4.6* (c)). Two secondary BAs, both derived from CDCA, UDCA and LCA (*Figure 4.6* (d) and (e)) showed the potential to extend longevity in the N2 Bristol strain of *C. elegans,* an effect <u>*not*</u> evident for SS104. The effect was significant with 10 mM UDCA (p=0.0027) and with 10 mM LCA (p=0.0026). These data cement some of the individual moiety effects across both strains of *C. elegans*, however some strain specific effects, possibly relating to fresh food and agar transfer, became clear with the *C. elegans* N2 Bristol strain in terms of lifespan extension effects: reduced lifespan with continual fresh food supply and with renewed BA content.

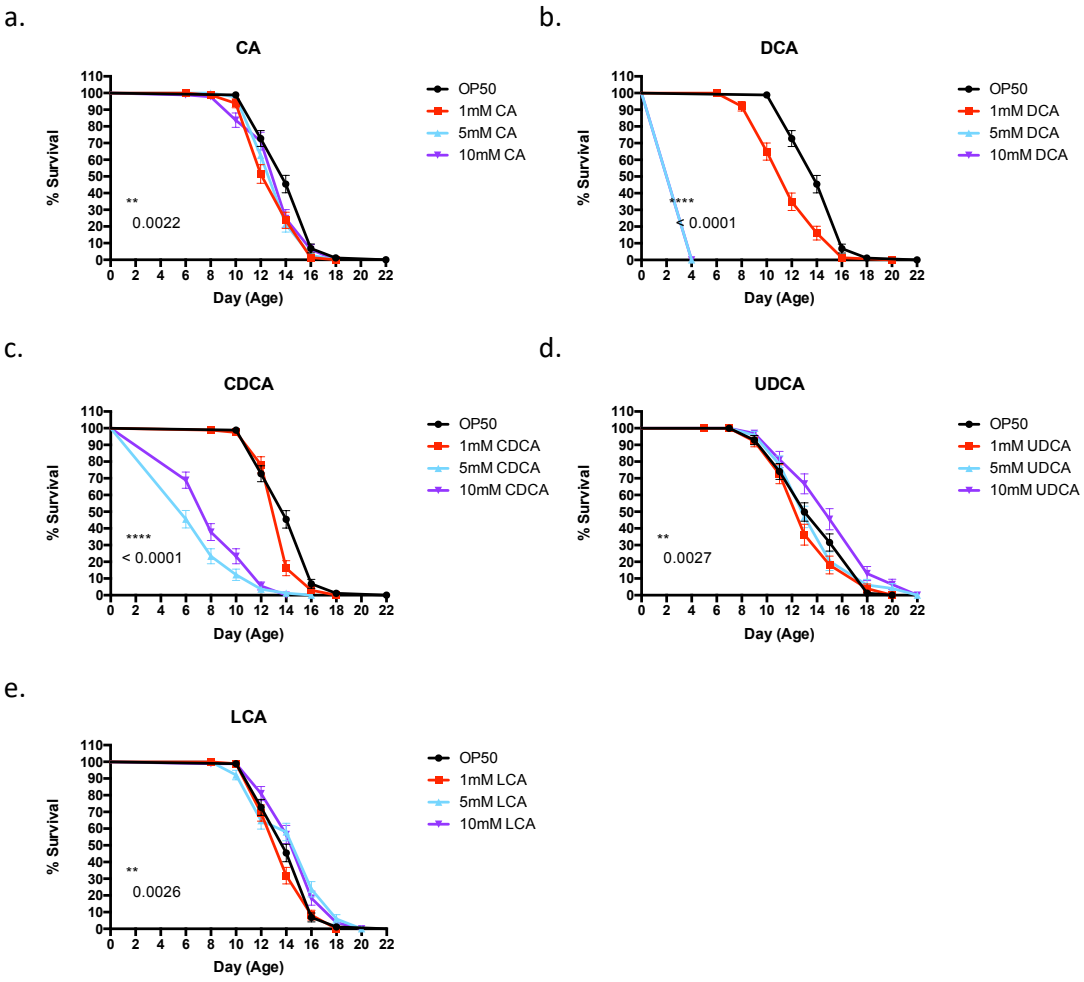


Figure 4.6: **Lifespan and longevity assessment of *Caenorhabditis elegans* wild-type (WT) Bristol strain N2 in the presence and absence of primary and secondary bile acids.** (a) Cholic Acid (CA), (b) Deoxycholic Acid (DCA), (c) Chenodeoxycholic Acid (CDCA), (d) Ursodeoxycholic Acid (UDCA) and (e) Lithocholic Acid (LCA), were each applied at concentrations of one of 0, 1, 5 and 10 mM in NGM agar and their impact on *Caenorhabditis elegans* strain SS104 longevity from L1 larval stage were assessed. Survival curves were performed and are shown for treated and untreated nematodes, all treatments and controls were pre-seeded with *E. coli* OP50. (*n*=3), second replicate see appendix IV SI.4.9. Statistical analysis was performed through application of the log-rank test for survival curves (*= p<0.05; **=p<0.01; ***=p<0.001; ****=p<0.0001).

We next wished to determine whether the effects of these BAs were developmental stage dependent or whether they were consistent across the board, for *C. elegans*.

L4 larval stage were next applied to determine whether BAs could induce changes in lifespan from reproductive adults from *C. elegans* SS104 and/or the WT N2 Bristol strain. The same BA concentrations (1, 5 and 10 mM) of BAs CA, its derivative DCA, CDCA and its derivatives UDCA and LCA were applied independently in NGM agar, pre-seeded with *E. coli* OP50, to which either 30 L4 stage *C. elegans* SS104 or 30 L4 stage wild-type N2 nematodes were applied. Here, controls lacked BAs, but they were pre-seeded with *E. coli* OP50 for 24 hours (Materials and Methods, Section 2.2.2 and 2.2.3). Nematodes were placed at 25^{o}C and assessed until 0% survival was reached. While lifespan was determined, this approach also allowed reproduction monitoring for both strains since the temperature sensitive mutation in SS104, *glp-4(bn2)*, is documented to influence *C. elegans* lifespan (Alper *et al.,* 2010; Rastogi *et al.,* 2015).

Nematode L4 larvae survival for strain SS104 reached 24 days and was equivalent to that found when L1 larvae were applied in similar assays. Noteworthy is that L4 larvae usually develop from L1 Larvae within 28 hours of their application in control situations. For all BAs tested a dose dependent effect on 50% survival was evident, relative to non BA treated controls, even with CA and UDCA (*Figure 4.7* (a), p=<0.0001 and (d)). While CA did not extend longevity as shown previously, with this stage, the UDCA lifespan extending property evident for L1 larvae was lost for L4 larvae. Furthermore, the cytotoxic effect of DCA was reduced and L4 larvae and subsequent nematodes survived at all concentrations of DCA (*Figure 4.7* (b)). However, 5 and 10 mM DCA shortened survival of 50% of nematodes to 6 and 8 days of 18 (for controls lacking BAs) respectively while 1 mM DCA, unlike previously, had no effect (*Figure 4.7* (b)). L4 stage SS104 nematodes proved equally and significantly sensitive to 5 and 10 mM CDCA in terms of 50% survival and indeed, lifespan, compared to the control *E. coli* OP50 (*Figure 4.7* (c), p=<0.0001). For UDCA, in contrast to L1 larvae, 1 mM UDCA, significantly shortened *C. elegans* SS104 L4 larvae lifespan by 4 days, compared to the control *E. coli* OP50 (*Figure 4.7* (d), p<0.0001) while 5 mM UDCA showed a smaller effect, reduction was of 2 days, compared to the control *E. coli* OP50 (*Figure 4.7* (d)). 5 mM LCA significantly extended *C. elegans* SS104 lifespan, compared to the control *E. coli* OP50 (*Figure 4.7* (e), p=0.0075). 1, 5 and 10 mM

concentrations of LCA all may have the potential to extend lifespan of *C. elegans* SS104 (*Figure 4.7* (e)).

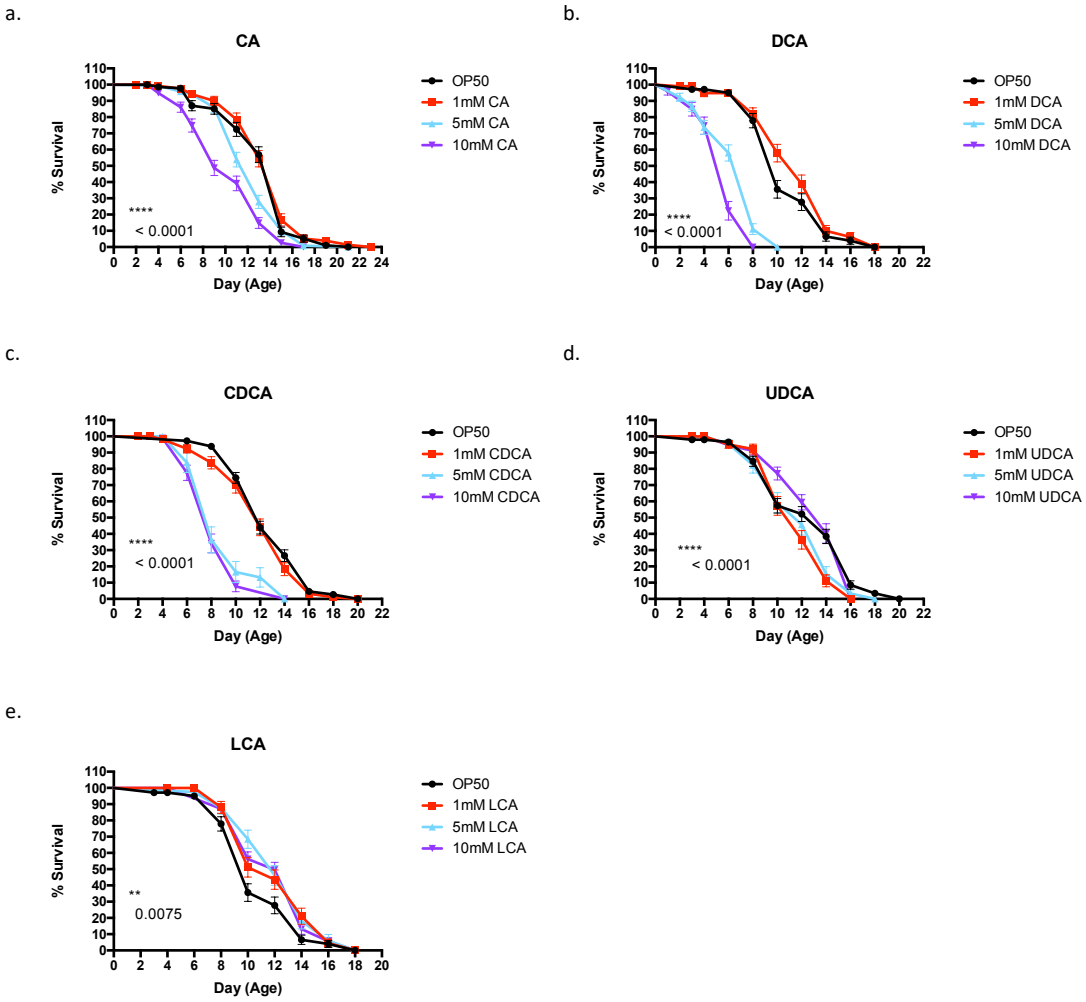


Figure 4.7: **Lifespan and longevity assessment of reproductive adulthood *Caenorhabditis elegans* temperature sensitive strain SS104 in the presence and absence of primary and secondary bile acids.** (a) Cholic Acid (CA), (b) Deoxycholic Acid (DCA), (c) Chenodeoxycholic Acid (CDCA), (d) Ursodeoxycholic Acid (UDCA) and (e) Lithocholic Acid (LCA), applied at concentrations of 0, 1, 5 and 10 mM in NGM agar. Survival curves were performed and are shown for treated and untreated nematodes, all treatments and controls were pre-seeded with *E. coli* OP50. (*n*=3) appendix IV SI.4.8. Statistical analysis was performed through application of the log-rank test for survival curves (*= p<0.05; **=p<0.01; ***=p<0.001; ****=p<0.0001).

The same assays were conducted, but with WT *C. elegans* N2 Bristol strain (*Figure 4.8* (a-e)). Here, similar to L4 larvae of *C. elegans* SS104 strain, CA elicited a dose dependent effect on 50% survival and no extension of lifespan (*Figure 4.8* (a), p=<0.0001). 10 mM UDCA significantly extended *C. elegans* N2 lifespan, compared to the control *E. coli* OP50 (*Figure 4.8* (d), p=0.0004). 1, 5 and 10 mM concentrations of UDCA may have the potential to extend lifespan of *C. elegans* N2 (*Figure 4.8* (d)). A dose dependent response was seen with DCA (*Figure 4.8* (b), p=<0.0001), an effect that was identical at the two higher concentrations and which was similar to that seen for *C. elegans* SS104. However, with the N2 Bristol strain of *C. elegans*, in contrast to SS104, where 1 mM DCA had the effect of reducing 50% survival by day 8 of the assay. A similar effect for the higher BA concentrations was seen with CDCA with L4 larvae of the *C. elegans* N2 strain, again 1 mM CDCA, resulted in reduction of 50% survival by day 11 relative to day 13 under control conditions, an effect that was not seen with L4 larvae of strain SS104 (*Figure 4.8* (c), p=<0.0001). Consistent to both strains, L4 larvae remained unaltered for survival by LCA, in contrast to SS104 L1 larvae. However, only L4 larvae of the N2 Bristol strain showed an extension of survival that was concentration dependent, up to 4 days when treated with 10 mM LCA (*Figure 4.8* (e), p=<0.0001).

Taken together, the commonality among L1 larvae for BA application was shared for larvae survival and sensitivity to CA, CDCA and to UDCA but not for DCA and LCA, although time frames differed. For L4 Larvae CA, DCA and UDCA showed common effects, mainly of lifespan reduction, between the strains but these were different to L1 larval outcomes (*Table 4.1*). Taken together, there is consistency across the assays for individual BAs at the different concentrations in terms of effect on 50% survival and on lifespan extension or reduction, namely CA, DCA, CDCA and LCA. However, these data also suggest BA moiety effects can be stage specific and strain dependent, specifically UDCA (*Table 4.1*).

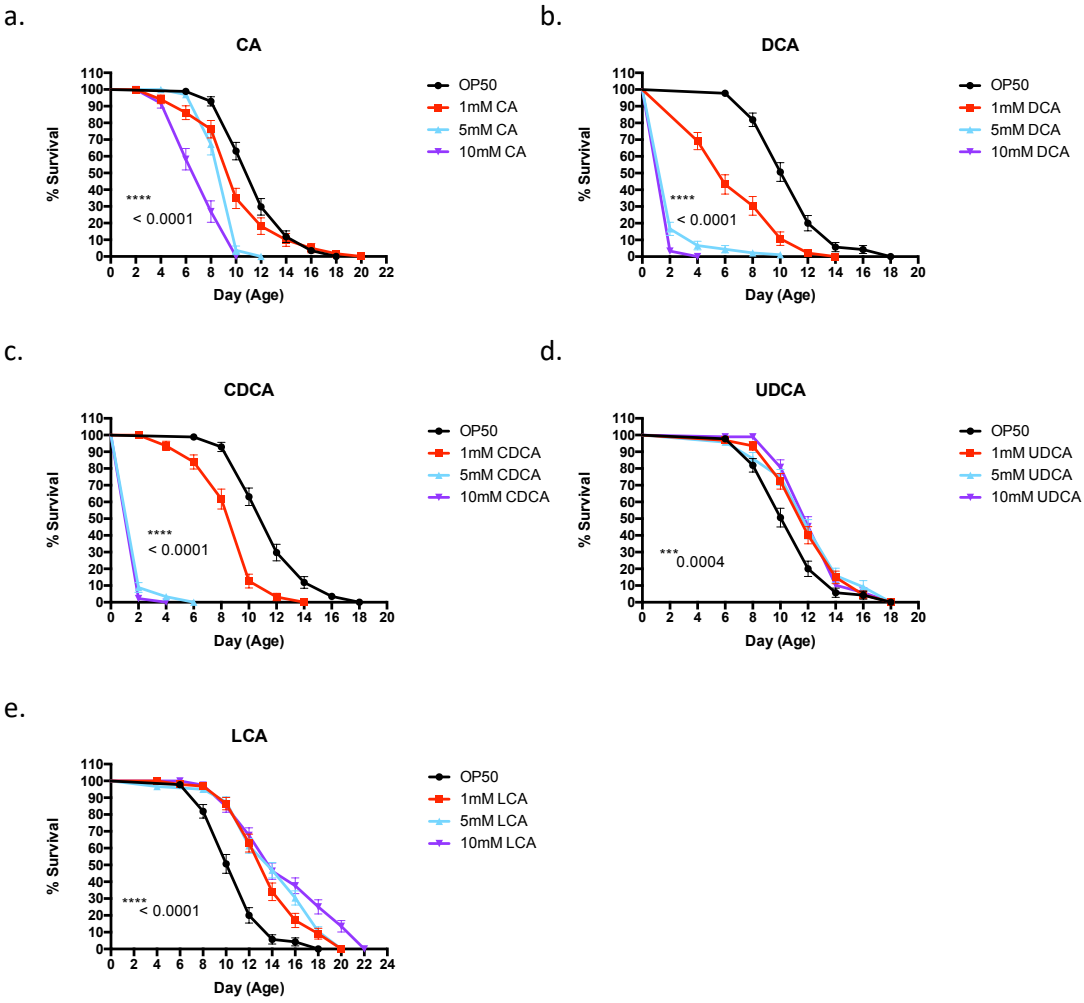


Figure 4.8: **Lifespan and longevity assessment of *Caenorhabditis elegans* wild-type (WT) Bristol strain N2 in adulthood, in the presence and absence of primary and secondary bile acids.** (a) Cholic Acid (CA), (b) Deoxycholic Acid (DCA), (c) Chenodeoxycholic Acid (CDCA), (d) Ursodeoxycholic Acid (UDCA) and (e) Lithocholic Acid (LCA), applied at concentrations of 0, 1, 5 and 10 mM in NGM agar. Survival curves were performed and are shown for treated and untreated nematodes, all treatments and controls were pre-seeded with *E. coli* OP50. (*n*=3), second replicate see appendix IV SI.4.9. Statistical analysis was performed through application of the log-rank test for survival curves (*= p<0.05; **=p<0.01; ***=p<0.001; ****=p<0.0001).

***Table 4.1*: Summary of *Caenorhabditis elegans* lifespan assays in the presence of individual bile acids**

	SS104 L1 larvae	N2 L1 larvae	SS104 L4 larvae	N2 L4 larvae
1 mM CA	-	↓	-	-
5 mM CA	-	-	↓	↓
10 mM CA	-	-	↓	↓
1 mM DCA	↓	↓	-	↓
5 mM DCA	θ	↓	↓	↓
10 mM DCA	θ	↓	↓	↓
1 mM CDCA	-	-	-	↓
5 mM CDCA	↓	↓	↓	↓
10 mM CDCA	-	↓	↓	↓
1 mM UDCA	-	-	↓	↑
5 mM UDCA	-	-	↓	↑
10 mM UDCA	-	↑	-	↑
1 mM LCA	-	-	↑	↑
5 mM LCA	-	↑	↑	↑
10 mM LCA	-	↑	↑	↑

Summary of lifespan assays in *Caenorhabditis elegans* strains SS104 and WT N2, in L1 larvae through development, and L4 larvae through adulthood, when treated with bile acids, compared to the control with no bile acids. A '-' in a cell represents unchanged lifespan. θ represents where *Caenorhabditis elegans* did not survive. A red and green arrow represents a decrease and increase in *Caenorhabditis elegans* lifespan, respectively.

4.2.4 Specific bile acids can alter *Caenorhabditis elegans* larvae developmental timing

We next sought to determine whether BA induced changes, detected over 22-36 days, altering *C. elegans* lifespan, survival and longevity could be due to alterations in development. Synchronous L1 larval stage *C. elegans* (30 nematodes/plate *n*=3 independent assays) for both the temperature-sensitive SS104 and WT N2 nematodes were independently exposed to BAs or not, as described above (and in Materials and Methods, Section 2.2.2). BAs CA, DCA, CDCA, UDCA and LCA were applied at the same concentrations -one of 1, 5 and 10 mM- and nematode development was monitored from early life into adulthood. Strain dependent temperature incubations, 25°C (for WT N2 strain) and 16°C (permissive for egg-laying in SS104), were applied and total progeny (L1 and L2 stage *C. elegans*) were counted until dauer juveniles appeared (*n*=3) (Materials and Methods, Section 2.2.4).

C. elegans SS104 L1 larvae development largely remained unchanged, with progeny appearing after 6 days, compared to untreated nematodes, irrespective of CA, UDCA or LCA concentrations applied (*Figure 4.9* (a), (d) and (e)). A similar effect was seen with the lowest level of DCA (1 mM) however, 5 mM DCA delayed progeny appearance until approx. 8 days. As expected 10 mM DCA resulted in 0 survival and no progeny generation (*Figure 4.5* (b)). Taken together the data support the lack of effect by LCA, UDCA and CA and differential effects on development and survival for the remaining BAs for SS104 L1 larvae. Dauer appeared after day 14, therefore the experiment was stopped. Nutrients were exhausted and so another variable was present from day 14.

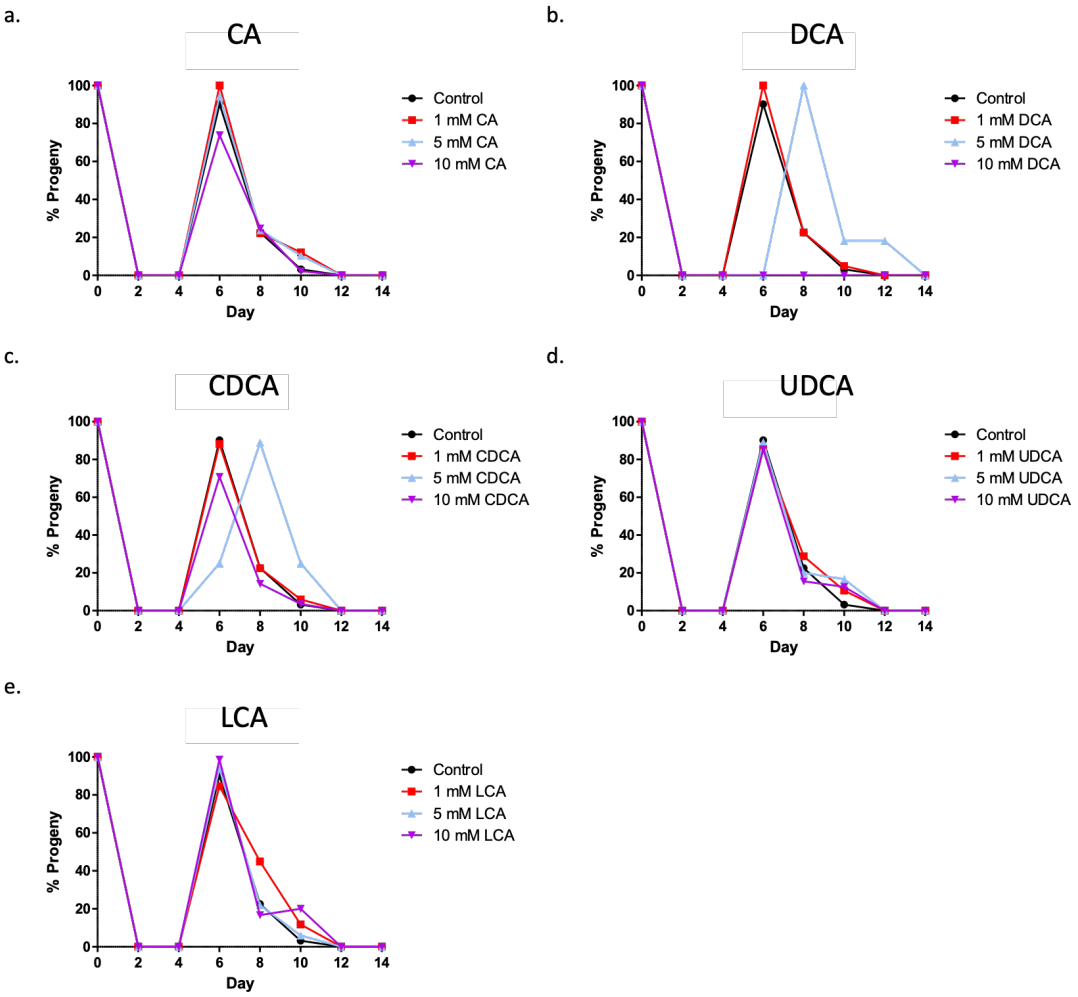


Figure 4.9: **Assessment of developmental timing of *Caenorhabditis elegans* strain SS104 in the presence and absence of primary and secondary bile acids:** one of (a) Cholic Acid (CA), (b) Deoxycholic Acid (DCA), (c) Chenodeoxycholic Acid (CDCA), (d) Ursodeoxycholic Acid (UDCA) and (e) Lithocholic Acid (LCA), were each applied to nematodes at concentrations 0, 1, 5 and 10 mM in NGM agar. Graphs represent percent of SS104 progeny (L1 and L2) over time (from day 0-14) for treated and untreated nematodes, all treatments and controls were pre-seeded with *E. coli* OP50. *n*=3 experiments were performed, Appendix IV SI.4.10, one experimental representation shown here.

The same assay was performed with WT *C. elegans* N2 Bristol strain, L1 larvae. In the absence of BAs next generation N2 L1/L2 nematodes emerged from day 6 to 8 post introduction to media (*Figure 4.10*) and summarized in *Table 4.2* below. Similar to SS104, for N2 L1 larvae, produced the next generation at 6 to 8 days post exposure

to CA, UDCA and LCA regardless of BA concentration (*Figure 4.10* (a), (d) and (e)), a rate of development (progeny production) that was equivalent to control treatments (no BAs). These time frames are in line with the documented life cycle through all stages to reproduction for the N2 strain and indicate that these BAs have no effect on nematode development.

The second generation of nematodes appeared, as expected, from 12 days post L1 larvae introduction; these L1 larvae developed into dauer (*Figure 4.10*). In the presence of BAs, the second generation began to appear at day 12 in the presence of most BAs but the process was accelerated with some concentrations specifically 5 mM CA, 1 mM DCA, 10 mM CDCA (*Figure 4.10*). The assay was not continued beyond day 14 as these L1s developed into dauer juveniles. 5 and 10 mM DCA were detrimental to *C. elegans* N2 L1 larvae, with no progeny associated to these treatments (*Figure 4.10* (b)).

In summary, 10 mM concentrations of DCA reduced the lifespan of both WT *C. elegans* N2 Bristol strain and egg-laying deficient mutant *C. elegans* SS104 strain, and inhibited the development of L1 larvae in both *C. elegans* strains. 5 mM CDCA slowed L1 larval development in both WT N2 and temperature-sensitive SS104 strains, and also reduced the lifespan of both these *C. elegans* strains. WT *C. elegans* N2 Bristol strain developed at a faster rate than the egg-laying deficient mutant *C. elegans* SS104 strain due to incubation at a higher temperature (25°C compared to 16°C). *Table 4.2* below summarises each BA's effect on each *C. elegans* strains' overall survival and lifespan.

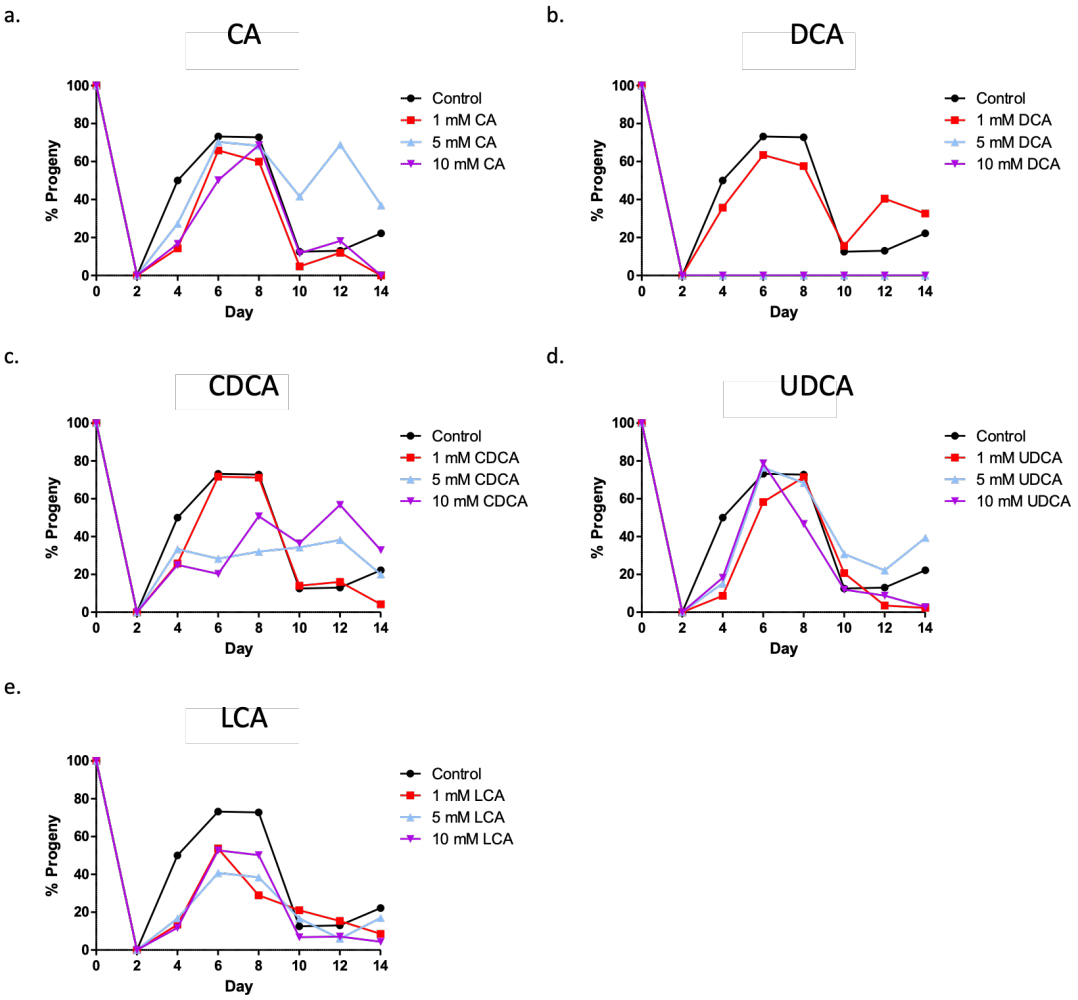


Figure 4.10: **Assessment of developmental timing of *Caenorhabditis elegans* wild-type (WT) Bristol strain N2 in the presence and absence of primary and secondary bile acids.** (a) Cholic Acid (CA), (b) Deoxycholic Acid (DCA), (c) Chenodeoxycholic Acid (CDCA), (d) Ursodeoxycholic Acid (UDCA) and (e) Lithocholic Acid (LCA), at concentrations 0, 1, 5 and 10 mM were each applied to nematodes. Graphs represent percent SS104 progeny (L1 and L2) over time (day 0-14) for treated and untreated nematodes, all treatments and controls were pre-seeded with *E. coli* OP50. *n*=3 experiments were performed, Appendix IV SI.4.11, one experimental representation shown here.

Table 4.2: **Summary of the effect of each bile acid on *Caenorhabditis elegans* lifespan and development.**

	SS104 L1 larvae	N2 L1 larvae
1 mM CA	Lifespan: - Development: -	Lifespan: ↓ Development: -
5 mM CA	Lifespan: - Development: -	Lifespan: - Development: ↑
10 mM CA	Lifespan: - Development: -	Lifespan: - Development: -
1 mM DCA	Lifespan: ↓ Development: -	Lifespan: ↓ Development: ↑
5 mM DCA	Lifespan: θ Development: ↓	Lifespan: ↓ Development: θ
10 mM DCA	Lifespan: θ Development: θ	Lifespan: ↓ Development: θ
1 mM CDCA	Lifespan: - Development: -	Lifespan: - Development: -
5 mM CDCA	Lifespan: ↓ Development: ↓	Lifespan: ↓ Development: ↓
10 mM CDCA	Lifespan: - Development: -	Lifespan: ↓ Development: ↑
1 mM UDCA	Lifespan: - Development: -	Lifespan: - Development:
5 mM UDCA	Lifespan: - Development: -	Lifespan: - Development:
10 mM UDCA	Lifespan: - Development: -	Lifespan: ↑ Development: -
1 mM LCA	Lifespan: - Development: -	Lifespan: - Development: -
5 mM LCA	Lifespan: - Development: -	Lifespan: ↑ Development: -
10 mM LCA	Lifespan: - Development: -	Lifespan: ↑ Development: -

Summary of lifespan and development assays on *Caenorhabditis elegans* strains SS104 and WT N2. Individual L1 larvae time through development, when treated with bile acids, compared to the control with no bile acids. A '-' in a cell represents unchanged lifespan. θ represents where *Caenorhabditis elegans* did not survive. A red and green arrow represents a decrease and increase in *Caenorhabditis elegans* lifespan and developmental timing, respectively.

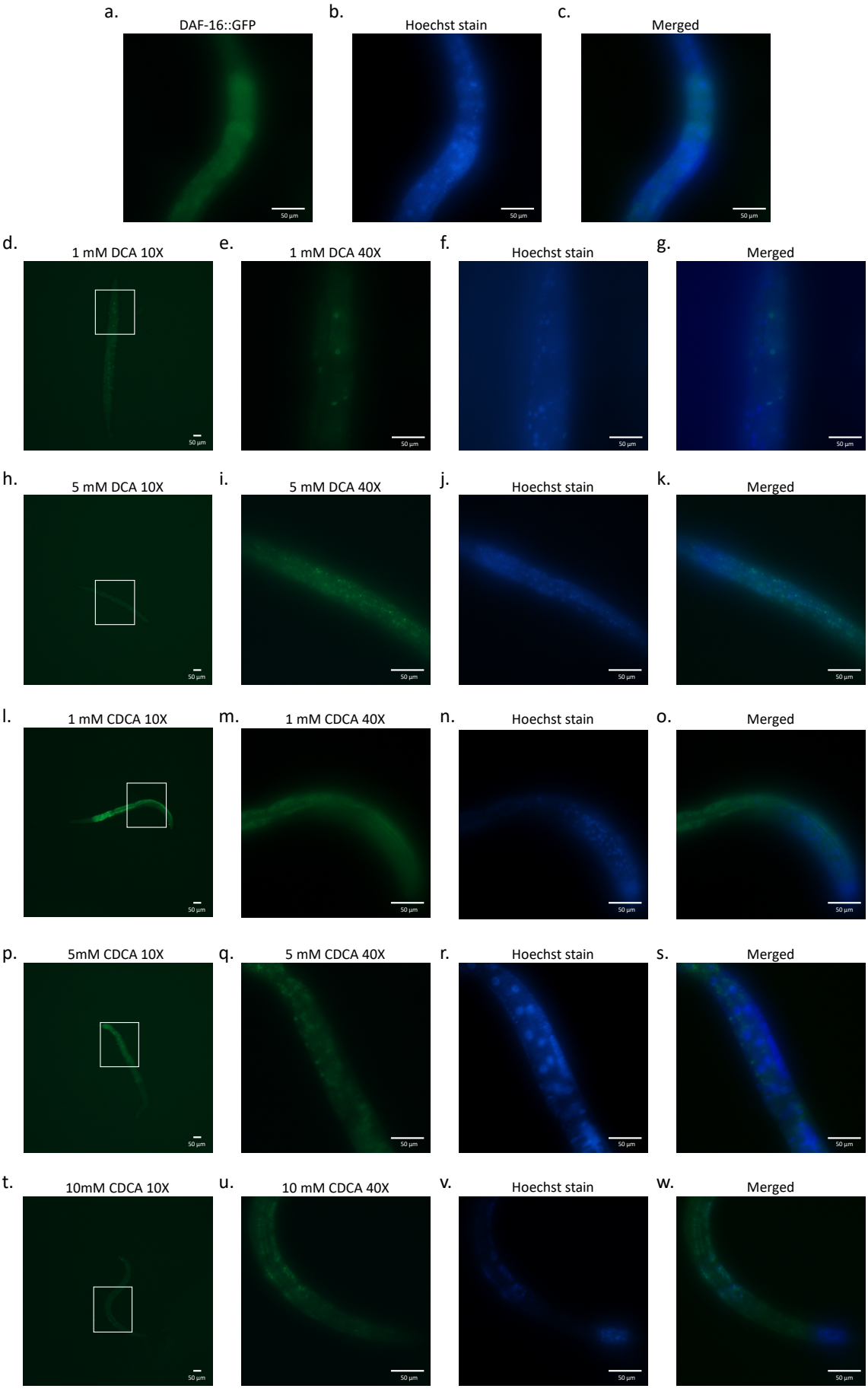
4.2.5 Specific concentrations of the primary bile acid Chenodeoxycholic Acid and the secondary bile acid Deoxycholic Acid induce nuclear translocation of *Caenorhabditis elegans* transcription factor DAF-16

The signals for development, through a range of different DAs, follow a hierarchy (*Figure 1.16* Chapter 1 and *Figure 4.13* below). They dictate longevity, lifespan and development. Dependent and independent of DAF-12, DAF-16, a homolog of human FOXO, is normally repressed by DAF-2 (InsR) through AKT-1 in both larval and adult nematodes for normal development, however, it can be activated in adults by DAF-12 under stress conditions (Aguilaniu *et al.,* 2016), (Chapter 1, sections 1.7.4.1 and 1.7.4.2). DAF-16 expression is tightly linked to longevity (Ogg *et al.,* 1997). To establish whether BAs can link to longevity we wished to examine DAF-16 expression in nematodes treated with individual BAs, noting that an NHR-8 longevity effect may not be detectible here.

C. elegans strain CF1139, *daf-16(mu86) I; muIs61 [(pKL78) daf16::GFP + rol-6(su1006)]*, (*Table 2.2*), expresses DAF-16 when the *daf-16* promoter is active, represented by green fluorescent protein expression. Briefly, primary and secondary BAs (CA, DCA, CDCA, UDCA, LCA, *Figure 4.1*) were individually applied with 10 nematodes, at L4 larval stage, to the NGM agar, pre-seeded with *E. coli* OP50 at 37°C for 24 hours (Materials and Methods, Section 2.2.6). They were incubated for 5 days at 16°C, in advance of DAF-16 expression assessment by fluorescence microscopy (Materials and Methods, Section 2.2.6) (*n*=3). A green punctate pattern is expected when DAF-16 is activated and translocates into the nucleus.

As expected, nematodes in the presence of *E. coli* OP50 (negative control) exhibited cytosolic expression of DAF-16 (*Figure 4.11* (a)), with no evidence for co-localisation with nuclei stained by Hoescht stain (*Figure 4.11* (b-c)). Nematodes treated with either 1 or 5 mM DCA generated a punctate pattern that co-localized to the nucleus (*Figure 4.11* (d-k)) suggesting DCA induced activation and translocation of DAF-16 to the nucleus. Otherwise, only 5 and 10 mM CDCA showed a punctate pattern and a nuclear localisation for DAF-16 expression (*Figure 4.11* (p-w)), CA, UDCA, LCA did not. The data suggest BA selective influences -at some level- on the regulons feeding into DAF-16 induction. Interestingly, neither CDCA nor DCA elicited a dose dependent response on survival and on lifespan across the stages. However, both were

represented at high levels in *E. coli* OP50 for delivery to nematodes when bacteria were exposed at 10 mM concentrations. The data therefore, may represent inappropriate gene activation and for that reason, transcriptomics approaches to determine the influence of BAs in the context of these nematodes were explored.


a.
DAF-16::GFP
b.
Hoechst stain
c.
Merged
d.
1 mM DCA 10X
e.
1 mM DCA 40X
f.
Hoechst stain
g.
Merged
h.
5 mM DCA 10X
i.
5 mM DCA 40X
j.
Hoechst stain
k.
Merged
l.
1 mM CDCA 10X
m.
1 mM CDCA 40X
n.
Hoechst stain
o.
Merged
p.
5mM CDCA 10X
q.
5 mM CDCA 40X
r.
Hoechst stain
s.
Merged
t.
10mM CDCA 10X
u.
10 mM CDCA 40X
v.
Hoechst stain
w.
Merged

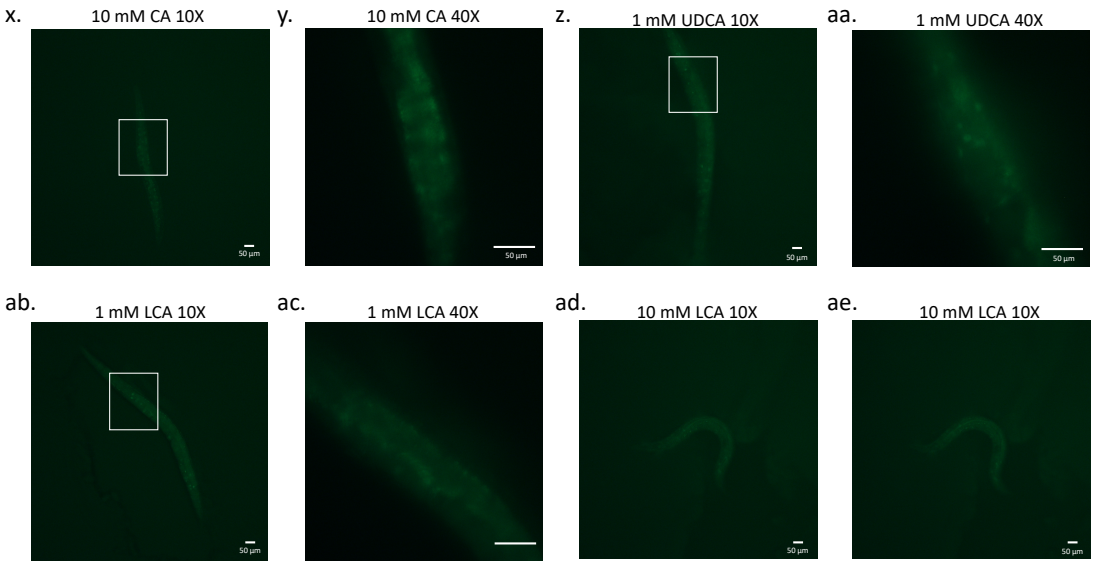


Figure 4.11: **Fluorescence microscopy assessment of bile acid-induced DAF-16:GFP expression in *Caenorhabditis elegans* CF1139 strain.** Either 10X (10X) or 40X (40X) magnification was applied to examine GFP expression (a, d, e, h, i, l, m, p, q, t, u, x-ae), Hoescht nuclear staining (b, f, j, n, r, v), and co-localized (c, g, k, o, s, w). Untreated controls (a-c), and those treated with either 1, 5 or 10 mM of individual BAs as indicated: DCA (d-k); CDCA (l-w); CA (x and y); UDCA (z and aa); and LCA (ab-ae). Hoescht stain (1 μg/ml) (*n*=3).

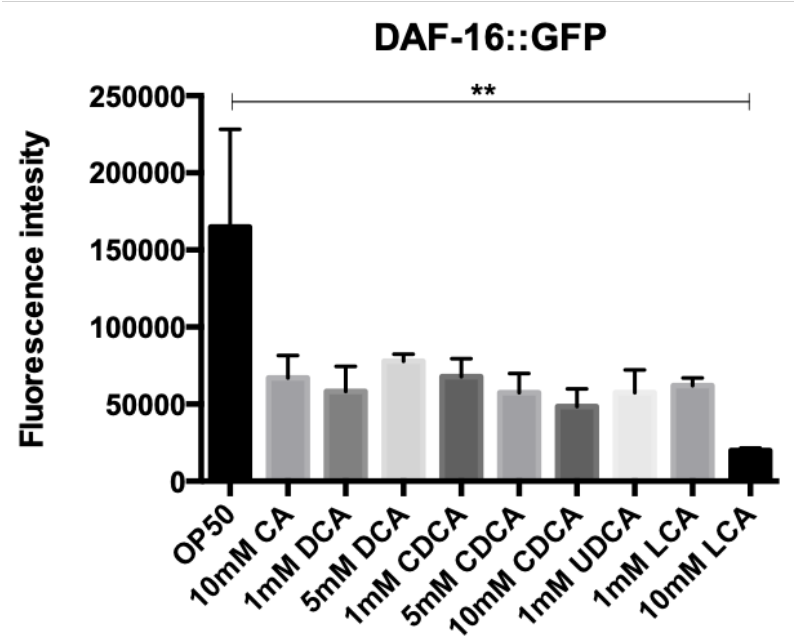


Figure 4.12: **Measurement of green fluorescence intensity representing bile acid-induced DAF-16:GFP expression in *Caenorhabditis elegans* CF1139 strain.**

Fluorescence (GFP) intensity was analysed and are shown for treated and untreated nematodes, all treatments and controls were pre-seeded with *E. coli* OP50. (*n*=3). Statistical significance was calculated using Kruskal-Wallis and Dunn's Multiple Comparison Test (*= p<0.05; **=p<0.01; ***=p<0.001; ****=p<0.0001).

4.2.6 Ultra Performance Liquid Chromatography Tandem Mass Spectrometry (UPLC-TMS) assessment of Δ^4-Dafachronic Acid and Δ^7-Dafachronic Acid levels in *Caenorhabditis elegans* strain SS104 treated with individual primary and secondary bile acids.

Given that activation through DAF-16 appears to be associated with specific BAs, we assessed whether dafachronic acids (DAs) are in fact activated in their presence. The rationale is that BAs and DAs could present a readout of inducers of either longevity pathway NHR-8 (the homologue of the human BA receptor the LXR) or DAF-12 (the homologue of the human BA receptor the FXR). They feed into DAF-16 (FOXO). Alternatively, DAs could indicate diapause control preventing dauer formation (*Figure 4.13*). Basically, DAs could be representative of BA influences at the specific time point for each individual BA application.

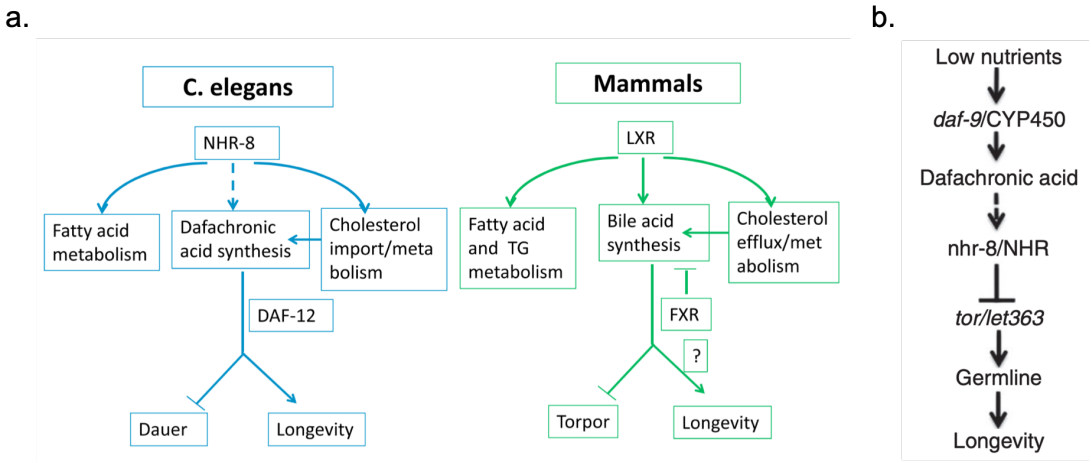


Figure 4.13: **Potential longevity pathways in *Caenorhabditis elegans* and mammals.** (a) *C. elegans* NHR-8 and Mammalian homologue LXR longevity pathways adapted from (Groen and Kuipers, 2013). (b) *C. elegans* NHR-8 activation under dietary restriction conditions, adapted from (Thondamal *et al.,* 2014).

As an initial experiment, a possible BA influence on these molecules could be established. Furthermore their production could reflect a molecular developmental readout of exposure to BAs. Dafachronic acids (DAs) are similar in nature to BAs, we applied mass spectrometry to determine if this was the case. An attempt was made to identify the different DAs based on relative mass, as predicted and similarly examined previously (Witting *et al.,* 2015; Aguilaniu *et al.,* 2016). The two main DAs: Δ^4-Dafachronic Acid (Δ^4-DA) and Δ^7-Dafachronic Acid (Δ^7-DA), are isomers that both feed into DAF-12 activation (a diapause determiner and an established longevity factor in adult nematodes). The predicted negative ion mass is 413.306 Da for both. 20 μg/ml Δ^4-DA was analysed using UPLC-TMS in negative mode. It was determined that Δ^4-DA, purified compound (Cambridge Bioscience), mass 413.306 Da, had a retention time of 22.15 minutes due to the distinct peak in the chromatogram produced by Target Lynx^{TM} software (*Figure 4.14*).



Figure 4.14: **Detection of Δ^4-Dafachronic Acid by Ultra Performance Liquid Chromatography Tandem Mass Spectrometry (UPLC-TMS).** Target Lynx^{TM} software chromatogram of purified compound Δ^4-Dafachronic Acid of mass 413.306 Da with a peak at retention time 22.15 minutes, from UPLC-TMS analysis.

We examined Δ^4-DA and Δ^7-DA levels as a result of BA exposure in *C. elegans* strain SS104 nematodes by UPLC-TMS analysis (Materials and Methods, Section 2.3.4).

Nematode extracts, showed potential Δ^4-DA at a retention time of 20.2236 (*Figure 4.15*). The data below indicates that Δ^4-DA and/or Δ^7-DA is not present in control untreated nematode extracts (*Figure 4.15*). In contrast, all BAs bar LCA elicited a Δ^4-DA and/or Δ^7-DA response, which was BA and dose dependent. DCA and CDCA may be inducing the production of Δ^4-DA, which in turn may be affecting *C. elegans* development (*Figure 4.9* and *4.10* (b)), and lifespan (*Figure 4.5, 4.6, 4.7* and *4.8* (b)) negatively.

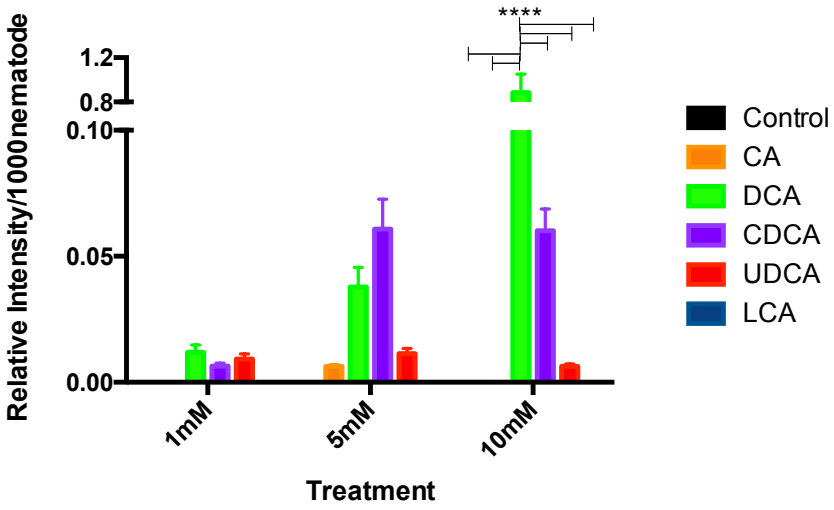


Figure 4.15: **Detection of Δ^4-Dafachronic Acid in nematode extracts with and without BA feeding.** Compound mass 413.306 Da with a retention time of 20.2236 minutes was detected in *Caenorhabditis elegans* SS104 extracts. Controls received no BA treatment, otherwise nematode populations were exposed independently to one of: 1, 5 or 10 mM of BAs: CA, DCA, CDCA, UDCA, LCA. (*n*=3). Statistical analysis applied Kruskal-Wallis, and Dunn's Multiple comparison test (* = p<0.05; ** = p<0.01; *** = p<0.001; **** = p<0.0001).

Indeed, upon further investigation of this data, there is strong evidence to suggest that *C. elegans* SS104 collected on day 14 for UPLC-TMS analysis, were in a state of dauer diapause. 60 synchronised *C. elegans* strain SS104 L1 larvae were applied to NGM agar containing specific BAs and pre-seeded with *E. coli* OP50 at 37°C for 24 hours and incubated at 16°C for 2 weeks for UPLC-TMS analysis (Materials and Methods, Section 2.3.4 and 2.3.5). Interestingly, in the development assay (Materials

and Methods, Section 2.2.4), 30 synchronised *C. elegans* strain SS104 L1 larvae were applied to NGM agar containing specific BAs and pre-seeded with *E. coli* OP50 at 37°C for 24 hours and incubated at 16°C until dauer was reached. According to *Figure 4.9*, the last timepoint was at day 14, as dauer diapause was detected thereafter, due to over-crowding and the exhaustion of nutrients over the 14 day period. In UPLC-TMS analysis, double the number of L1 larvae (*n*=60), were plated onto NGM agar compared to the development assay (*n*=30). This suggests that the *C. elegans* SS104 collected on day 14 for UPLC-TMS analysis were in a state of dauer diapause, meaning that DAs would not be present in these worms. Furthermore, the compound found did not have the exact mass as Δ^4-DA, and its retention time is approximately 2 minutes earlier than Δ^4-DA purified compound (Cambridge Bioscience). In addition, if dauer *C. elegans* DA were activated, they would be rescued from dauer and enter back into reproductive life cycle.

Interestingly, examining the exact concentration (ng/ml) of Δ^4-DA and/or Δ^7-DA (mass 413.306 Da, retention time 22.15 minutes) in each sample of *C. elegans* SS104 (*Figure 4.16* (a)) and comparing with the *E. coli* OP50 samples (*Figure 4.16* (b)), revealed that approximately the same concentration (ng/ml) of Δ^4-DA and/or Δ^7-DA was present in each treatment, regardless of whether the sample was *C. elegans* SS104 or *E. coli* OP50 (*Figure 4.16* (a-b)). For example, approximately 5 ng/ml was present in both control samples of *C. elegans* SS104 and *E. coli* OP50. Lastly, looking at the chromatograms of each of the three 10 mM DCA injections from UPLC-TMS analysis (*Figure 4.16* (c-e)), shows that none of the three injections (at mass 413.306 Da) have an exact peak at retention time 22.15, the peak varies from retention time 22.06 (*Figure 4.16* (c)), to 22.20 (*Figure 4.16* (d-e)), indicated by red arrows. In addition, a peak at retention time 22.15 is very close to the end of the 25 minute run, and so many different compounds can fall out here before the 25 minute run finishes.

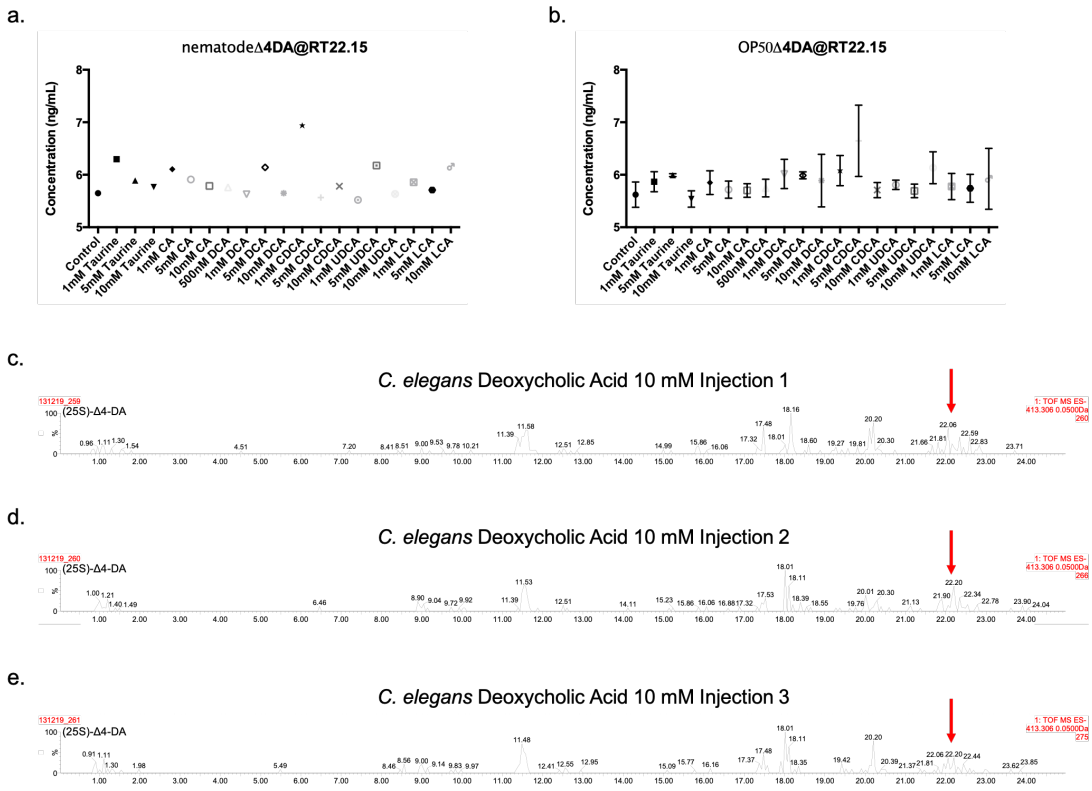


Figure 4.16: **Assessement of detection of Δ^4-Dafachronic Acid in *Caenorhabditis elegans* strain SS104 and *Escherichia coli* OP50.** Concentration (ng/ml) Δ^4-DA (mass 413.306 Da and retention time 22.15) detected in each sample of (a) *C. elegans* SS104 strain (*n*=1) and (b) *E. coli* OP50 (*n*=3), from UPLC-TMS analysis. (c-d) Chromatogram of Δ^4-DA (mass 413.306 Da and retention time 22.15) of the three UPLC-TMS injections, from *C. elegans* SS104 strain samples treated with 10 mM DCA, peaks at retention time of approximately 22.15 indicated by red arrows. Statistics were carried out using Kruskal-Wallis, and Dunn's Multiple comparison test (* = p<0.05; ** = p<0.01; *** = p<0.001; **** = p<0.0001).

In conclusion, there is a distinct possibility that BAs, particularly DCA and CDCA, affect *C. elegans* lifespan through the alteration of DA levels, and their role in DAF-12 signalling. However, to confirm this hypothesis, BAs would have to be applied to *C. elegans* eggs (before they have hatched) and collected at L2 larvae and L3 larvae for UPLC-TMS analysis, as Δ^4-DA and Δ^7-DA have a similar retention times and expression is at its highest at midlarval stages (Motola *et al.,* 2006; Schaedel *et al.,* 2012; Li *et al.,* 2013; Mahanti *et al.,* 2014; Witting *et al.,* 2015; Ma *et al.,* 2019).

4.2.7 Bile acids influence the *Caenorhabditis elegans* transcriptome towards different outcomes

To cement the influence of BA on development and longevity, RNA sequencing was performed by Genewiz Europe (Leipzig, Germany), following stage synchronized *C.elegans* exposure to primary and secondary BAs. *C. elegans* strain SS104 (*glp-4(bn2)* mutation), was maintained at 25°C to eliminate egg-laying and new generations of nematodes. in order to ensure a synchronous culture with such a large population of *C. elegans*. Synchronised L4 stage SS104 nematodes (*n*=1500) were added to NGM agar plates containing no BA (control) or 1 mM of independently added BAs: CA, DCA, CDCA, UDCA, and LCA, agar had been pre-seeded with *E. coli* OP50 at 37°C for 24 hours (*n*=4) (Materials and Methods, Section 2.2.7). 1 mM was chosen as a non-detrimental quantity for the nematodes, so that clean and reproducible mRNA could be isolated. 48 hours, was determined as a suitable point (see *Figure 4.7*) for *C. elegans* SS104 harvesting and total RNA extraction.

The mRNA was assessed for quality (according to Materials and Methods, Section 2.2.7 and 2.2.8). *Table 4.3* shows three (of the four RNA extracted samples) that had a RNA Integrity Number (RIN) value >6.0 and an A260/A280 = 1.8-2.2, so that ≥2 µg of each of these samples were delivered to Genewiz Europe (Leipzig, Germany) for cDNA library preparation and sequencing. At least three samples of good predicted quality were sent to represent each BA treatment and control non treated samples.

***Table 4.3*: *Caenorhabditis elegans* SS104 RNA samples and their quality assessed post extraction. In all samples, indicated they were appropriate for further work.**

Sample	Qubit Total conc. (ng) in 20µl	Bioanalyser RIN	Nanodrop A260/280
OP50 Control 1	7600	7.1	2.01
OP50 Control 2	5760	6.0	1.95
OP50 Control 3	8620	8.5	2.06
CA 1	3680	6.6	2.04
CA 2	4320	5.9	1.89
CA 3	9680	4.6	1.69
DCA 1	9500	8.0	2.07
DCA 2	9860	8.5	2.07
DCA 3	3200	6.4	1.90
CDCA 1	7120	8.0	2.09
CDCA 2	17600	8.1	2.02
CDCA 3	9020	9.4	2.06
UDCA 1	8000	8.3	2.05
UDCA 2	4240	8.4	2.01
UDCA 3	10200	9.2	2.07
LCA 1	7200	9.1	2.05
LCA 2	4560	8.6	2.07
LCA 3	4240	9.3	1.98

Qubit™ analysis revealed that the total RNA concentration for each sample ranged from 3.2 µg to 17.6 µg in a 20 µl sample. The BioAnalyser quality assessment gave a RNA Integrity Number (RIN) value of >4.6 and a Nanodrop 2000 spectrophotometer detected a total RNA quality A260/A280 = 1.89-2.09 for each control and bile acid treatment sample.

Genewiz Europe (Leipzig, Germany), performed their own sample quality analysis. They found that the total RNA quality and library preparation was of good quality for the following: Control (*n*=1), CA treated (*n*=1), DCA treated (*n*=1), CDCA treated (*n*=2), UDCA treated (*n*=2), and LCA treated (*n*=2) (*Table 4.4*). There are insufficient controls *n*=1, for statistical significance however, the data can be taken as a pilot indicator towards future studies (*Table 4.4*).

***Table 4.4*: Genewiz Europe quality assessment of *Caenorhabditis elegans* strain SS104 RNA samples.**

			Sample QC										
			General				Qubit			Fragment Analyzer			
Sample Name	Sampl	Genewiz ID	Date	Operator	Volume	Quantity	dilution factor	measured concentration	calculated concentration	RQN	dilution factor	concentration	
					µl	ng		ng/µl	ng/µl			measured ng/ul	calculated ng/ul
~~O1~~	1	CHK02-1-O1	10/29/2021	SF	20	2016	1	100.8	100.8	~~5.2~~	1	56.4	55.7
~~O2~~	2	CHK02-2-O2	10/29/2021	SF	20	1801	1	90.1	90.1	~~4.7~~	1	44.4	43.7
O3	3	CHK02-3-O3	10/29/2021	SF	20	3406	1	170.3	170.3	8.1	1	95.7	95.0
~~CA1~~	4	CHK02-4-CA	10/29/2021	SF	20	1346	1	67.3	67.3	~~3.9~~	1	28.8	28.1
CA2	5	CHK02-5-CA	10/29/2021	SF	20	2782	1	139.1	139.1	6.9	1	71.3	70.6
~~CA3~~	6	CHK02-6-CA	10/29/2021	SF	20	644	1	32.2	32.2	~~2.9~~	1	11.5	10.8
DC1	7	CHK02-7-DC	10/29/2021	SF	20	2856	1	142.8	142.8	7.6	1	81.7	81.0
~~DC2~~	8	CHK02-8-DC	10/29/2021	SF	20	2852	1	142.6	142.6	~~8.3~~	1	79.2	78.5
~~DC3~~	9	CHK02-9-DC	10/29/2021	SF	20	1341	1	67.0	67.0	~~3.9~~	1	28.6	27.9
CD1	10	CHK02-10-C	10/29/2021	SF	20	3182	1	159.1	159.1	7.5	1	85.1	84.4
CD2	11	CHK02-11-C	10/29/2021	SF	20	1004	1	50.2	50.2	7.8	1	20.3	19.6
~~CD3~~	12	CHK02-12-C	10/29/2021	SF	20	2558	1	127.9	127.9	~~8.7~~	1	76.3	75.6
~~U1~~	13	CHK02-13-U	10/29/2021	SF	20	2616	1	130.8	130.8	~~8.0~~	1	68.5	67.8
U2	14	CHK02-14-U	10/29/2021	SF	20	1296	1	64.8	64.8	7.6	1	33.9	33.2
U3	15	CHK02-15-U	10/29/2021	SF	20	1856	1	92.8	92.8	8.6	1	50.1	49.4
L1	16	CHK02-16-L	10/29/2021	SF	20	4994	1	249.7	249.7	9.2	1	177.8	177.1
L2	17	CHK02-17-L	10/29/2021	SF	20	1792	1	89.6	89.6	8.7	1	115.6	114.9
~~L3~~	18	CHK02-18-L	10/29/2021	SF	20	2068	1	103.4	103.4	~~8.4~~	1	65.3	64.6

The notation is as follows: O1-O3, no treatment (control), otherwise 1 mM was applied independently for each BA treatment: CA1-CA3: Cholic Acid; DC1-DC3: Deoxycholic Acid; CD1-CD3: Chenodeoxycholic Acid; U1-U3: Ursodeoxycholic Acid; L1-L3: Lithocholic Acid. RNA Quality Number (RQN) values (in red), are samples which did not reach RNA Integrity Number (RIN) value >6.0 and therefore failed Genewiz quality control. Samples with a red horizontal line are those who failed to generate a cDNA library. Samples highlighted in green are those successfully applied to RNA sequencing. Finally 6/18 samples (CDCA, UDCA and LCA samples with *n*=2), were suitable for follow analysis.

FastQC analysis revealed an RNA (cDNA) sequence length of 8-150 base pairs, consistent across all samples: CDCA treated (*n*=2), UDCA treated (*n*=2), and LCA treated (*n*=2) (*Table 4.5*). STAR (Spliced Transcripts Alignment to a Reference), was used to align reads to the *C. elegans* reference genome (WBcel235). FastQC and STAR alignment detected consistency in the number of total sequences across the forward and reverse reads of each sample (*Table 4.5*). STAR alignment analysis determined the percentage of uniquely matched reads was >74%, the mismatch rate per base was >0.17% for these 6 samples, indicating good reliable read matches to the database *C. elegans* genome (WBcel235) (*Table 4.5*).

***Table 4.5*: FastQC and STAR alignment report on RNA sequencing.**

Sample	Total Sequences		Sequences flagged as poor quality	Sequence length	% Uniquely matched reads	% Mismatch rate per base
	Forward	Reverse				
CDCA 1	37571698	37571698	0	8-150	74.63	0.16
CDCA 2	25984662	25984662	0	8-150	81.49	0.16
UDCA 2	21484290	21484290	0	8-150	77.60	0.17
UDCA 3	22169744	22169744	0	8-150	80.94	0.16
LCA 1	30741292	30741292	0	8-150	76.37	0.17
LCA 2	27561779	27561779	0	8-150	83.83	0.17

Statistics are based on FastQC report and the alignment of the sample reads relative to the *C. elegans* (WBcel235) database using STAR (Spliced Transcripts Alignment to a Reference).

Next, correlation between RNA sample replicates (*n*=2) for three BA treatments, was examined to show agreement between replicates. Correlation between all replicates was very high, R>0.93 (*Figure 4.17*), to indicate that the normalised gene counts are very similar between these replicates. Overall, this shows that there is very little variation between 2 replicates for the same treatment.

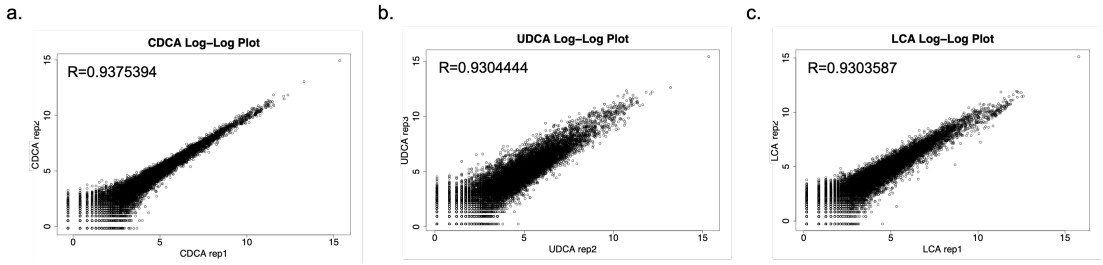


***Figure 4.17:* Correlation between paired RNA sample replicates showing Spearman's rank correlation coefficient R values.** (a) CDCA (b) UDCA (c) LCA. (*n*=2).

4.2.8 The *Caenorhabditis elegans* transcriptome was similar following treatment with bile acids Ursodeoxycholic Acid compared to Chenodeoxycholic Acid, and Lithocholic Acid compared to Ursodeoxycholic Acid

C. elegans strain SS104 gene expression treated with secondary BA UDCA, compared to the primary BA, parent CDCA, showed a similar transcriptome (*Figure 4.18*). Comparison of these transcriptomes revealed 7 genes that were differentially expressed, with an adjusted p-value <0.99 (*Table 4.6*). *C50F7.5* and *F49H6.3* were the only genes with relatively higher and lower transcription levels, $\log_2$ fold change (1 log fold = 2 fold change) of 3.08 and -3.01 respectively, both with adjusted p-values

of 0.07787, closest to a p-value of 0.05 (*Table 4.6*). *C50F7.5* is influenced by genes *daf-16*, *daf-2*, and *glp-1* (pathways involved in longevity and immune response); whereas *F49H6.3* is predicted to be an integral part of the membrane. Overall, it can be concluded that UDCA and CDCA treated SS104 strain *C. elegans* had a very similar transcriptomes.

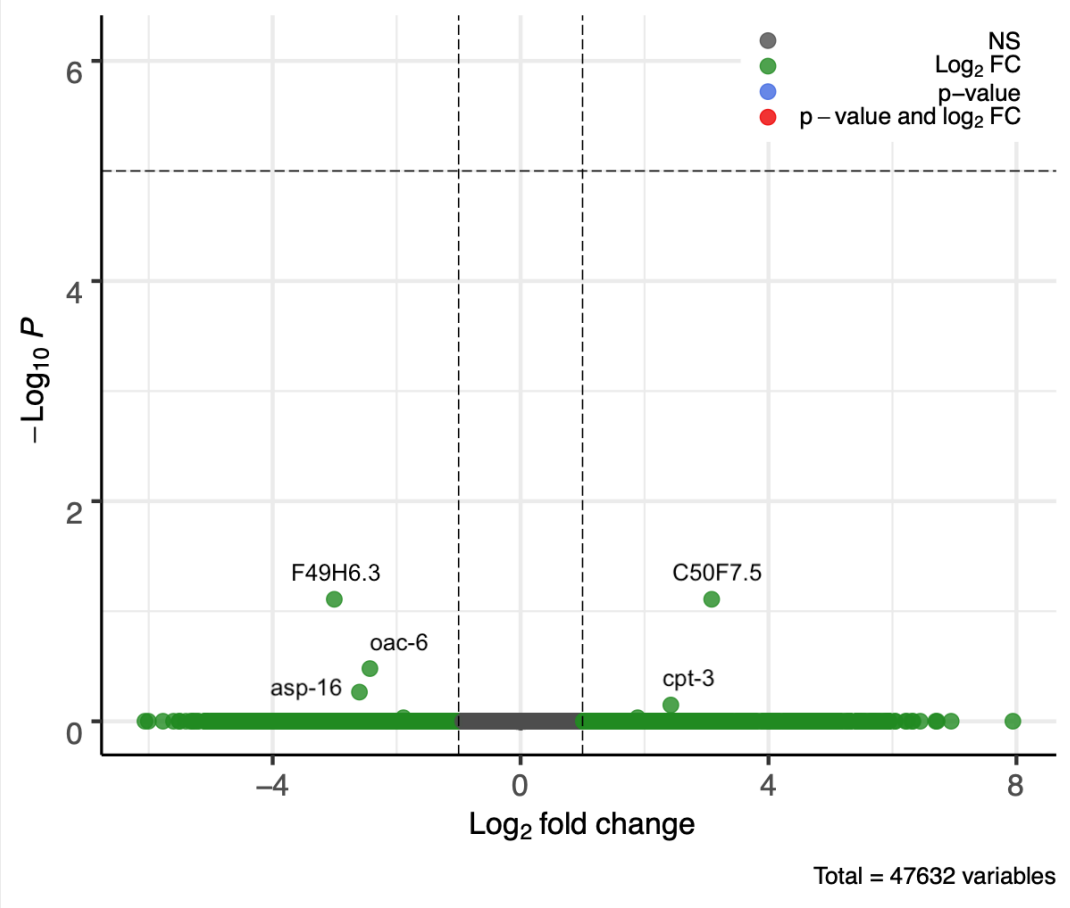


Figure 4.18: **Volcano plot of *Caenorhabditis elegans* SS104 strain top transcribed genes, when treated with bile acid UDCA compared to CDCA.**

***Table 4.6*: Differential transcriptome analysis for *C. elegans* strain SS104 strain in the presence of bile acids UDCA compared to CDCA.**

Gene Name	Proposed Function	Information of Interest	Base Mean	Log_2 Fold Change	Standard Error	p adjusted value
C50F7.5	Cell membrane protein	Possible *daf-16, fos-1* regulon	796.44	3.08	0.69	0.08
cpt-3	Carnitine Palmitoyl Transferase, located in the mitochondrion	Possible *hpl-2* regulon	105.53	2.42	0.65	0.71
nspc-17	Nematode Specific Peptide family, group C, enriched in intestine and neuronal cells	Possible *daf-16, nhr-28, nhr-77, fos-1* regulon	1046.59	1.89	0.53	0.93
K10D11.5	Integral membrane component	Possible *daf-16, nhr-28, nhr-77* regulon	258.71	-1.89	0.52	0.93
oac-6	O-ACyltransferase homolog, Integral membrane component	Possible *fos-1* regulon	118.90	-2.43	0.60	0.33
asp-16	ASpartyl Protease, Predicted to be involved in cell death, located in lysosome. An ortholog of human genes: *CTSE* (cathepsin E); *PGA4* (pepsinogen A4); and *PGC* (progastricsin)	Possible *hpl-2* regulon	83.37	-2.60	0.68	0.54
F49H6.3	Integral membrane component	Possible *nhr-2, fos-1, jun-1* regulon	86.43	-3.01	0.67	0.08

Representation and identification of 7 differentially transcribed genes following 1 mM secondary BA (UDCA compared to CDCA) treatment (n=2) with an adjusted p-value <0.99. The proposed function of each of these genes is listed including downstream genes that may be regulated according to WormBase (https://wormbase.org//#012-34-5). The base mean value, Log_2 Fold Change, Standard error and adjusted p-value are also represented.

C. elegans strain SS104 transcription, post treatment with 1 mM secondary BA LCA, was compared to the secondary BA UDCA, to reveal 13 genes that were differentially transcribed, with an adjusted p-value <0.05 (*Table 4.7*). Here, LCA was associated with higher levels of transcription of 1 gene: *clec-4*, predicted to enable carbohydrate binding activity; while 12 genes were associated with lower levels of transcription: *R05D8.9*, *E02C12.6*, *E02C12.10*, *F44E5.4*, *ugt-36*, *cyp-33C2*, *cest-35.2*, *nhr-17*, *F44E5.5*, *dhs-14*, *cyp-34A7* and *cyp-34A8* (*Figure 4.19*). *R05D8.9* and *dhs-14* are predicted to enable oxidoreductase activity; *E02C12.6* and *E02C12.10* are associated with genes *skn-1*, *rrf-3*, and *hsf-1*; and *glp-1*, *pgl-1*, and *glh-1*; respectively. *F44E5.4* is predicted to have a role in several functions including ATP binding activity, ATP hydrolysis activity and misfolded protein binding activity; similarly, *F44E5.5* is also

predicted to enable ATP binding activity and ATP hydrolysis activity; *ugt-36* is predicted to be involved in glucuronosyltransferase activity; *cyp-33C2*, *cyp-34A7* and *cyp-34A8* are predicted to have roles in organic acid metabolic processes and xenobiotic metabolic processes; *cest-35.2* is predicted to be involved in carboxylic ester hydrolase activity; and *nhr-17* is predicted to have a role in cell differentiation and regulation of transcription by RNA polymerase II. (Alliance WS285) (https://wormbase.org). All 12 genes were analysed using the gene ontology resource, powered by PANTHER (Ashburner *et al.,* 2000; Mi *et al.,* 2019; Consortium, 2021). However, this analysis revealed no significantly different biological processes. Therefore, SS104 *C. elegans* strain treated with LCA were relatively similar for gene transcription globally to those treated with UDCA.

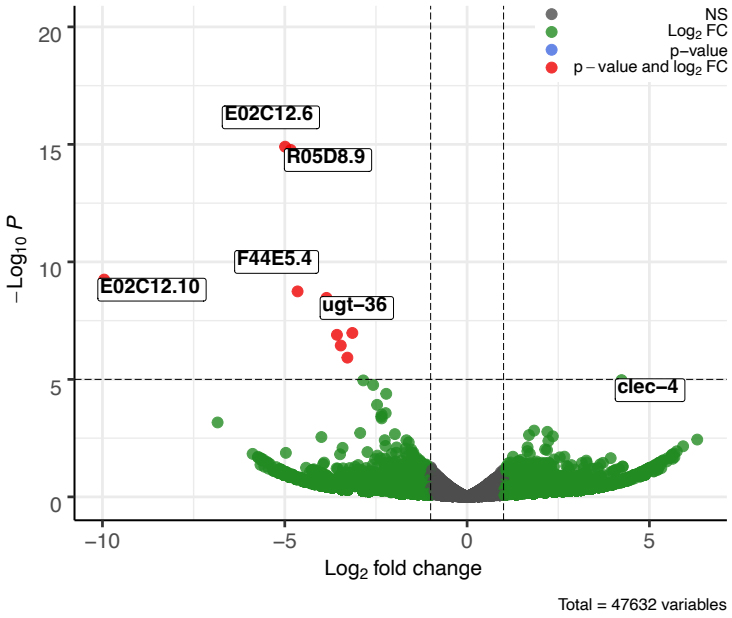


Figure 4.19: **Volcano plot of top five transcribed genes, and clec-4, in *Caenorhabditis elegans* strain SS104 treated with bile acid LCA compared to UDCA.**

***Table 4.7*: Differentially transcribed genes in *Caenorhabditis elegans* strain SS104 cultured with bile acid 1 mM LCA, compared to 1 mM UDCA.**

Gene Name	Proposed Function	Information of Interest	Base Mean	Log_2 Fold Change	Standard Error	p adjusted value
clec-4	C-type LECtin, carbohydrate binding activity, expressed in amphid neurons, human homolog TLL1 protein.	Possible *daf-16, fos-1, nhr-28, nhr-77, nhr-23, nhr-6, pqm-1* regulon	55.22	4.24	0.96	0.01
cyp-34A8	Involved in organic acid metabolic and xenobiotic metabolic processes, located in cytoplasm and intracellular membrane-bounded organelle, an ortholog of human CYP2U1 (cytochrome P450 family 2 subfamily U member 1).	Possible *daf-16, nhr-28* regulon	1111.62	-2.22	0.54	0.04
cyp-34A7	Involved in organic acid metabolic and xenobiotic metabolic processes, located in cytoplasm and intracellular membrane-bounded organelle, an ortholog of human CYP2U1 (cytochrome P450 family 2 subfamily U member 1).	Possible *daf-16, fos-1, nhr-28, nhr-6, lin-35, pha-4, pqm-1, zag-1* regulon	300.85	-2.58	0.60	0.02
dhs-14	DeHydrogenases, Short chain, ortholog of human HSD17B14 (hydroxysteroid 17-beta dehydrogenase 14).	Possible *daf-16, fos-1, nhr-28, pha-4, pqm-1* regulon	1392.64	-2.85	0.65	0.01
cyp-33C2	Involved in organic acid metabolic and xenobiotic metabolic processes, located in cytoplasm and intracellular membrane-bounded organelle, an ortholog of human CYP2J2 (cytochrome P450 family 2 subfamily J member 2).	Possible *daf-16, gei-11, nhr-28, nhr-6, lin-35, dpl-1, hpl-2, efl-1* regulon	237.40	-3.15	0.59	0.0002
F44E5.5	Enables ATP binding and hydrolysis activity, an ortholog of human HSPA1B (heat shock protein family A (Hsp70) member 1B); HSPA1L (heat shock protein family A (Hsp70) member 1 like); and HSPA6 (heat shock protein family A (Hsp70) member 6).	Possible *daf-12, daf-16, nhr-28, nhr-23, nhr-6, nhr-77, lin-35, fos-1, pha-4, zag-1, unc-62, skn-1, pqm-1* regulon	124.50	-3.28	0.68	0.001
nhr-17	Involved in cell differentiation and regulation of transcription by RNA polymerase II, located in nucleus, expressed in tail, an ortholog of human RXRA (retinoid X receptor alpha) and RXRG (retinoid X receptor gamma).	Possible *daf-12, daf-16, gei-11, nhr-28, nhr-23, nhr-6, nhr-12, nhr-129, nhr-77, fos-1, lin-35, lin-39, pha-4, unc-62, skn-1, pqm-1, hpl-2, eor-1* regulon	256.75	-3.46	0.68	0.0005
cest-35.2	Carboxyl ESTerase domain containing, enables carboxylic ester hydrolase activity, an ortholog of several human genes including CES1 (carboxylesterase 1); CES3 (carboxylesterase 3); and CES5A (carboxylesterase 5A).	Possible *daf-16, nhr-28, nhr-129, efl-1, lin-35, fos-1, pha-4, skn-1, dpl-1, gei-11* regulon	104.31	-3.57	0.68	0.0002
ugt-36	UDP-GlucuronosylTransferase, located in intracellular membrane-bounded organelle, an ortholog of several human genes including UGT1A10 (UDP glucuronosyltransferase family 1 member A10); UGT1A7 (UDP glucuronosyltransferase family 1 member A7); and UGT1A8 (UDP glucuronosyltransferase family 1 member A8).	Possible *daf-16, nhr-28* regulon	511.57	-3.86	0.65	7.69E-06
F44E5.4	Enables ATP binding, hydrolysis activity and misfolded protein binding activity, predicted to be involved in protein refolding and located in cytoplasm.	Possible *nhr-28*, nhr-12, nhr-6, *unc-39, atfs-1 pha-4, skn-1, dpl-1, gei-11* regulon	84.44	-4.65	0.77	5.08E-06
R05D8.9	Enables oxidoreductase activity, human homolog Isoform 1 of Dehydrogenase/reductase SDR family member 4, expressed in the intestine and GABAergic neuron.	Possible *ceh-26, nhr-28* regulon	468.35	-4.84	0.61	9.73E-12
E02C12.6	Expressed in the intestine and mechanosensory neurons	Possible *nhr-28, pqm-1, fos-1* regulon	629.13	-4.99	0.62	9.73E-12
E02C12.10	Expressed in the intestine and bilaterally symmetric right bipolar head neuron, ASER - major gustatory chemosensory neuron	Possible *nhr-28, pqm-1* regulon	78.84	-9.95	1.61	2.13E-06

Representation of the 13 genes that were differentially transcribed in *C. elegans* strain SS104 treated with secondary BA LCA, compared to secondary BA UDCA, with an adjusted p-value <0.05. The proposed function of each of these genes is listed including downstream genes that may be regulated according to WormBase (https://wormbase.org//#012-34-5). The base mean value, Log_2 Fold Change, Standard error and adjusted p-value are also represented.

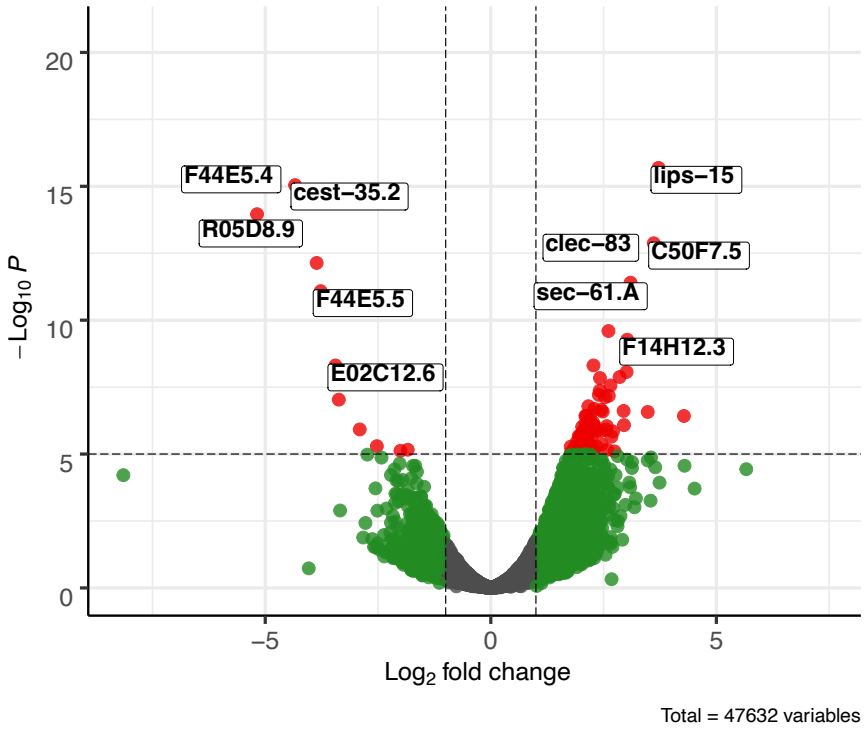
4.2.9 The microbially produced secondary bile acid, Lithocholic Acid, induced changes in the *Caenorhabditis elegans* transcriptome, compared to the parent primary bile acid, Chenodeoxycholic Acid

Comparison of transcription of *C. elegans* SS104 strain transcriptome revealed 1763 genes (Table appendix IV SI.4.12) that were differentially transcribed when nematodes were exposed to 1 mM LCA, compared to its parent molecule primary BA, CDCA, with an adjusted p-value <0.05.

Of the 1763 genes differentially transcribed in *C. elegans* strain SS104 transcriptome treated with 1 mM LCA compared to primary BA, 1 mM CDCA, 1299 genes were relatively increased while, 464 were relatively decreased for transcription. In LCA, compared to CDCA, those increased included: *lips-15*, *C50F7.5*, *clec-83*, *sec-61.A* and *F14H12.3* (*Figure 4.20* (a)). *lips-15* is predicted to be involved in lipid catabolic process; *C50F7.5* is associated with genes *daf-16*, *daf-2*, and *glp-1* (pathways established to influence longevity and immune response); *clec-83* is predicted to be involved in carbohydrate binding activity; *sec-61.A* is predicted to have a role in SRP-dependent co-translational protein targeting to membrane, translocation and posttranslational protein targeting; and *F14H12.3 5* is associated with genes *daf-16*, *daf-2* and *rrf-3* (pathways associated with longevity and immune response). Those genes reduced for transcription, in LCA compared to CDCA, included: *cest-35.2*, *F44E5.4*, *R05D8.9*, *F44E5.5* and *E02C12.6* (*Figure 4.20* (a)). *cest-35.2* is predicted to be involved in carboxylic ester hydrolase activity; *F44E5.4* is predicted to have a role in several functions including ATP binding activity, ATP hydrolysis activity and misfolded protein binding activity; similarly, *F44E5.5* is also predicted to enable ATP binding activity and ATP hydrolysis activity; *R05D8.9* is predicted to enable oxidoreductase activity; and *E02C12.6* is affected by genes *skn-1*, *rrf-3*, and *hsf-1* (Alliance WS285) (https://wormbase.org).

All LCA elevated 1299 genes were analysed using the gene ontology resource, powered by PANTHER (Ashburner *et al.,* 2000; Mi *et al.,* 2019; Consortium, 2021). This analysis revealed that LCA treatment, compared to CDCA, impacted the *C. elegans* transcriptome through each of the Notch signalling pathway, pyruvate metabolism, translation, apoptotic cell clearance, cellular response to toxic substance, detoxification, oxidative stress response, determination of adult lifespan, FA metabolism and innate immune response (*Figure 4.20* (b)). For those 464 genes with lower transcription levels, immune system process, membrane lipid biosynthetic process, cellular lipid catabolic process and response to stress were identified as central processes (*Figure 4.20* (b)).

a.



b.

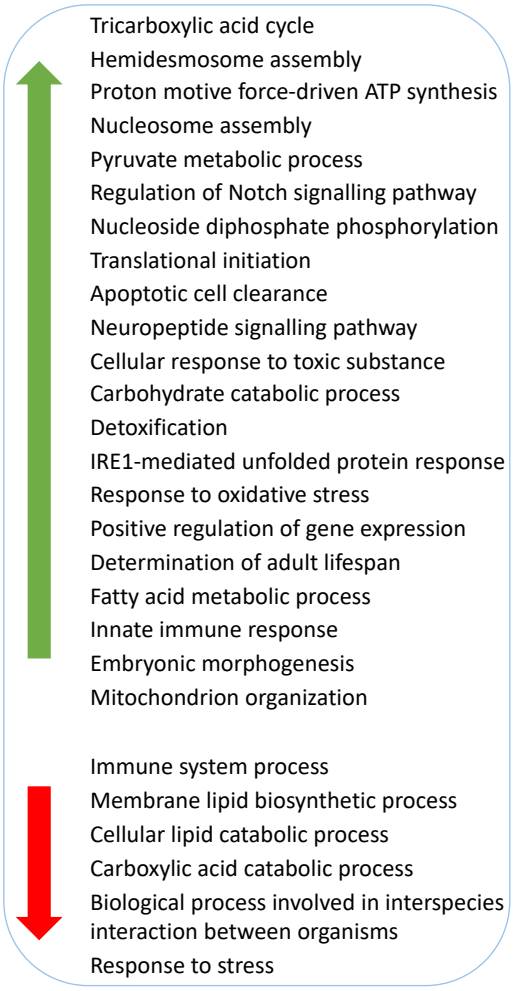


Figure 4.20: **Alterations in *Caenorhabditis elegans* SS104 strain transcriptome treated with bile acid LCA, compared to CDCA.** (a) Volcano plot of the top five differentially transcribed genes in *C. elegans* strain SS104 treated with LCA, compared to CDCA. (b) Changes in specific *C. elegans* biological pathways when treated with LCA, compared to CDCA, with a false discovery rate (FDR) $p<0.05$.

4.2.10 Alterations in *Caenorhabditis elegans* transcription of genes involved in longevity and immune response, when treated with bile acid Lithocholic Acid compared to Chenodeoxycholic Acid

Analysis of the 1763 differentially transcribed *C. elegans* genes, when treated with LCA, compared to CDCA, revealed alterations in immune response and longevity pathways. The key pathways that play a role in *C. elegans* longevity and immune

response include: DAF-2/DAF-16 pathway (*Figure 4.21* (a)), MAP kinase pathway (*Figure 4.21* (b) and (c)), TOR signalling pathway (*Figure 4.21* (d)), DBL-1 pathway (*Figure 4.21* (e)), DVE-1 pathway (*Figure 4.21* (g)), and DAF-12 signalling pathway (*Figure 4.21* (f) and (h)). *C. elegans* strain SS104 treated with LCA, compared to CDCA, revealed alterations in the transcription of genes involved in these longevity pathways (*Figure 4.21* (i)).

According to *C. elegans* strain SS104 transcriptome there were alterations in the DAF-2/DAF-16 pathway (*Figure 4.21* (a)). The *daf-28* gene is predicted to encode an insulin/insulin-like peptide ligand that is an agonist for the DAF-2 pathway. Nematode transcriptome cultured on LCA showed a relatively higher level of *daf-28* compared to those cultured on CDCA (*Figure 4.21* (a) and (i)). Genes *mtl-1* and *gst-4* showed relatively lower transcription, suggesting that the DAF-2 pathway may be activated in LCA treated nematodes, compared to CDCA. *gst-6* also demonstrated lower levels of transcription in LCA treated nematodes, compared to CDCA, implying an inhibition in innate immunity. *gst-40*, *gst-36*, *gst-33*, *gst-20* were associated with higher levels in LCA treated nematodes, compared to CDCA, suggesting a possible increase in glutathione metabolism. However, *sod-3* had relatively higher transcription, implicating alterations in the mitochondria. Similarly, DAF-16 activation induces expression of *lips-15* and *lipl-5* which are of high transcription, suggesting perhaps increased in lipolysis, however, expression of genes *lips-5* and *lipl-2* are at lower transcription levels in LCA treated nematodes, compared to CDCA. *skn-1* was associated with higher levels of transcription (*Figure 4.21* (b) and (i)) and *unc-43* involved in MAPK calcium signalling is also at higher transcription levels (*Figure 4.21* (c) and (i)).

Interestingly, the mTOR pathway, which is involved in the regulation of autophagy, appears to be associated with higher transcription levels (*Figure 4.21* (d) and (i)). *unc-51* and *igg-2*, downstream from mTOR signalling, had relatively higher levels of transcription, along with *hlh-30*. *sma-2* was associated with lower transcription, impacting the DBL-1 pathway (*Figure 4.21* (e)).

Downstream of NHR-80, *fat-4* was associated with lower transcription, but *fat-5* was associated with higher levels of transcription, suggesting alterations in FA synthesis and desaturation (*Figure 4.21* (f) and (i)). However, downstream of DAF-12 signalling,

fard-1 had lower levels of transcription but *lit-1* and *ain-1* had higher levels of transcription (*Figure 4.21* (f) and (i)). *dve-1* was at relatively lower levels of transcription, suggesting a reduction in impaired and misfolded proteins and therefore proteotoxic mitochondrial stress (*Figure 4.21* (g) and (i)).

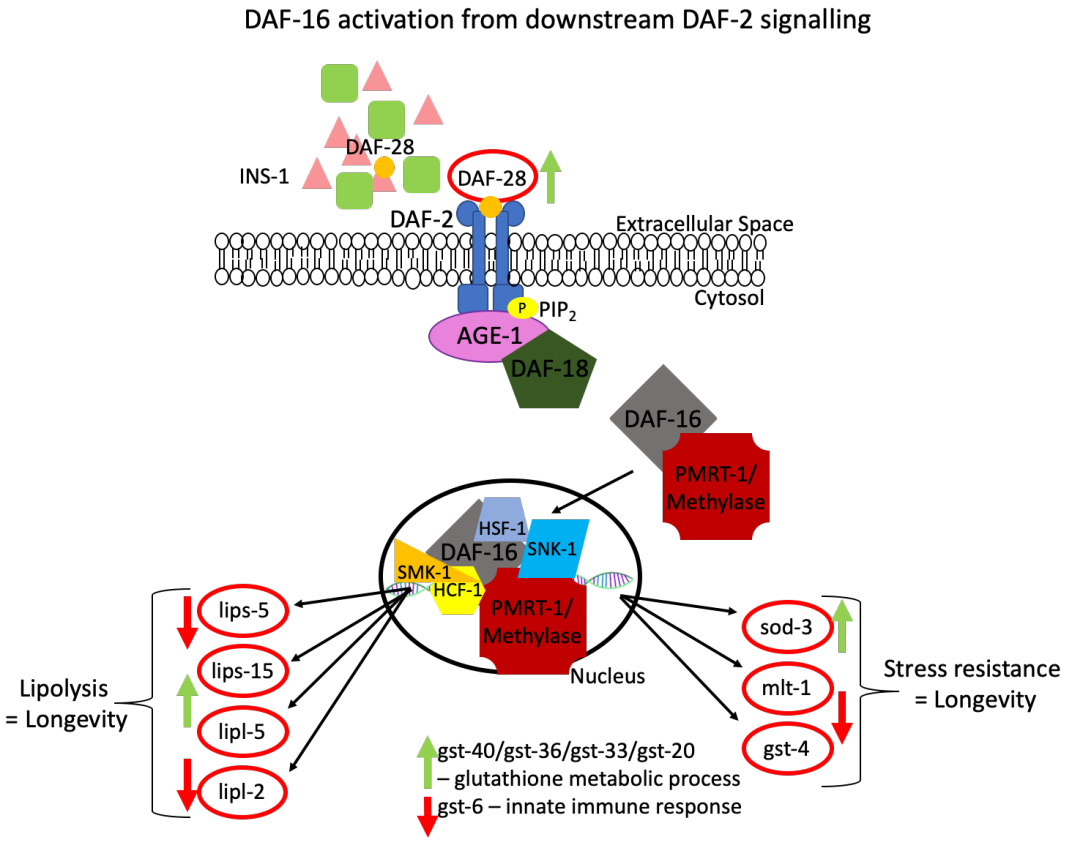
daf-22, *daf-7* and *daf-5* demonstrated relatively higher levels of transcription (*Figure 4.18* (h) and (i)). Despite an increase in pheromone *daf-22*, *daf-7* (TGF-β) is increased, and as *daf-5* is also increased, *C. elegans* strain SS104 treated with 1 mM LCA are not pushed to dauer formation. This may signify a longevity pathway through an increase in *daf* expression.

The longevity associated gene *ife-2* was also at relatively higher transcription levels, along with other genes of the same family, *ife-3* and *ife-5* suggesting an increase in *C. elegans* strain SS104 translation (*Figure 4.21* (i)). Genes of the same family of longevity associated gene *eat-2*: *eat-20* and *eat-17* were also at relatively higher transcription levels, suggesting an increase in regulation of *C. elegans* strain SS104 pharyngeal pumping (*Figure 4.21* (i)).

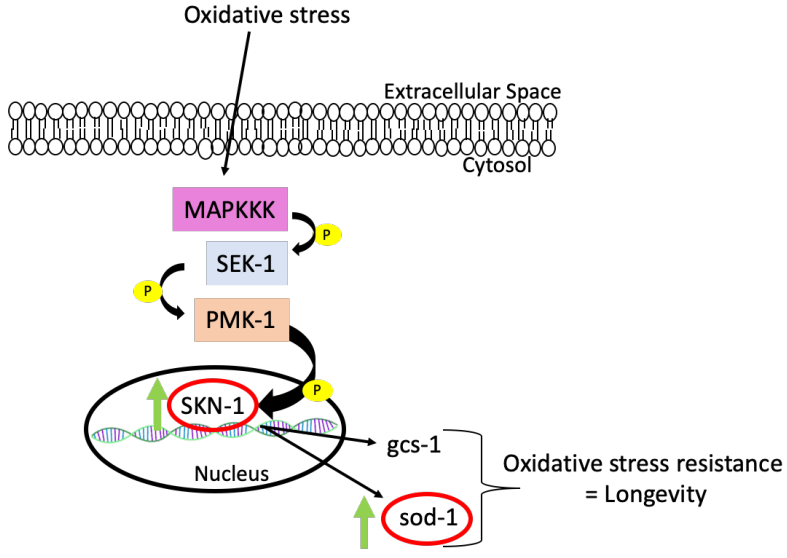
sodh-1 transcription, involved in the sorbitol pathway, was also at higher levels in *C. elegans* strain SS104 treated with LCA, compared to CDCA, the sorbitol pathway has been suggested to be involved in *C. elegans* longevity through the osmotic stress response (Chandler-Brown *et al.,* 2015).

Overall, in *C. elegans* strain SS104 treated with 1 mM LCA, compared to 1 mM CDCA, the DAF-2 signalling pathway appears to be activated, but DAF-16 activation was through mitochondria, in response to oxidative stress resistance. The transcriptome analysis also supports a reduction in mitochondrial proteotoxicity with increased autophagy resulting in longevity potential. A reduction in *C. elegans* strain SS104 immune response also suggests the potential for longevity. Finally, an alternative in *daf* gene expression shows the potential for *C. elegans* strain SS104 longevity pathway.

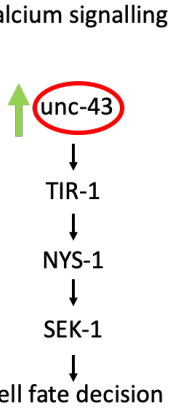
a.


DAF-16 activation from downstream DAF-2 signalling
DAF-28
INS-1
DAF-28
DAF-2
Extracellular Space
Cytosol
P
PIP2
AGE-1
DAF-18
DAF-16
PMRT-1/
Methylase
HSF-1
DAF-16
SNK-1
SMK-1
HCF-1
PMRT-1/
Methylase
Nucleus
lips-5
lips-15
lipl-5
lipl-2
Lipolysis
= Longevity
sod-3
mlt-1
gst-4
Stress resistance
= Longevity
gst-40/gst-36/gst-33/gst-20
– glutathione metabolic process
gst-6 – innate immune response

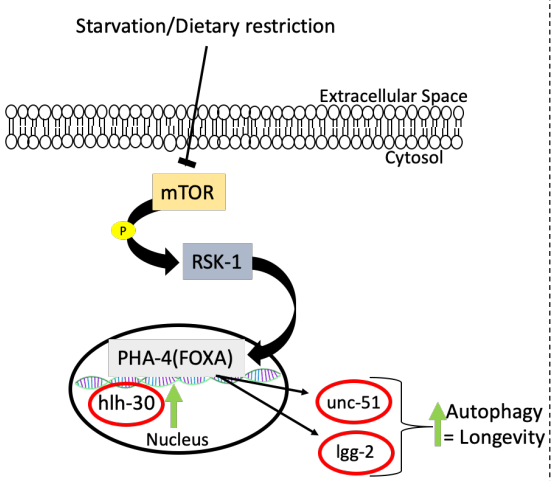
b.


Oxidative stress
Extracellular Space
Cytosol
MAPKKK
P
SEK-1
P
PMK-1
P
SKN-1
Nucleus
gcs-1
sod-1
Oxidative stress resistance
= Longevity

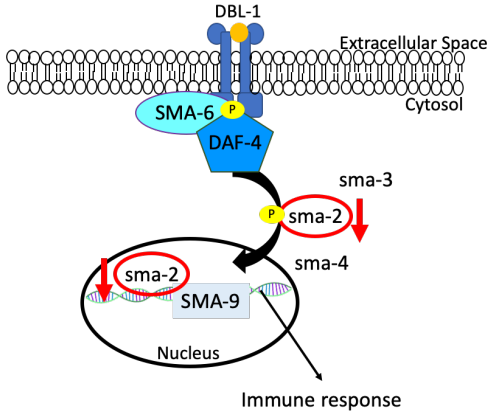
c.


Calcium signalling
unc-43
TIR-1
NYS-1
SEK-1
Cell fate decision

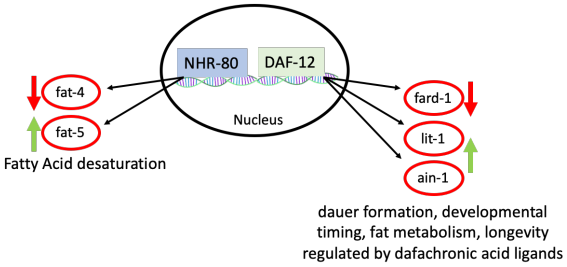
d.


mTOR signaling pathway
Starvation/Dietary restriction
Extracellular Space
Cytosol
mTOR
P
RSK-1
PHA-4(FOXA)
hlh-30
Nucleus
unc-51
lgg-2
Autophagy
= Longevity

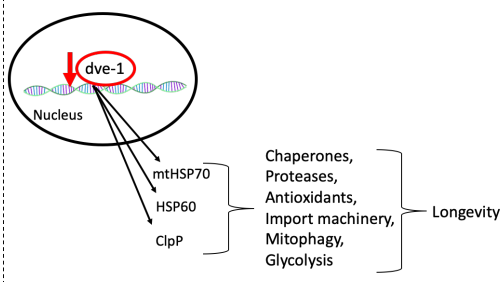
e.


DBL-1 (TGF-β) signaling pathway
DBL-1
Extracellular Space
Cytosol
SMA-6
P
DAF-4
sma-3
P
sma-2
sma-4
sma-2
SMA-9
Nucleus
Immune response

f.


NHR-80
DAF-12
Nucleus
fat-4
fat-5
Fatty Acid desaturation
fard-1
lit-1
ain-1
dauer formation, developmental
timing, fat metabolism, longevity
regulated by dafachronic acid ligands

g.


dve-1
Nucleus
mtHSP70
HSP60
ClpP
Chaperones,
Proteases,
Antioxidants,
Import machinery,
Mitophagy,
Glycolysis
Longevity

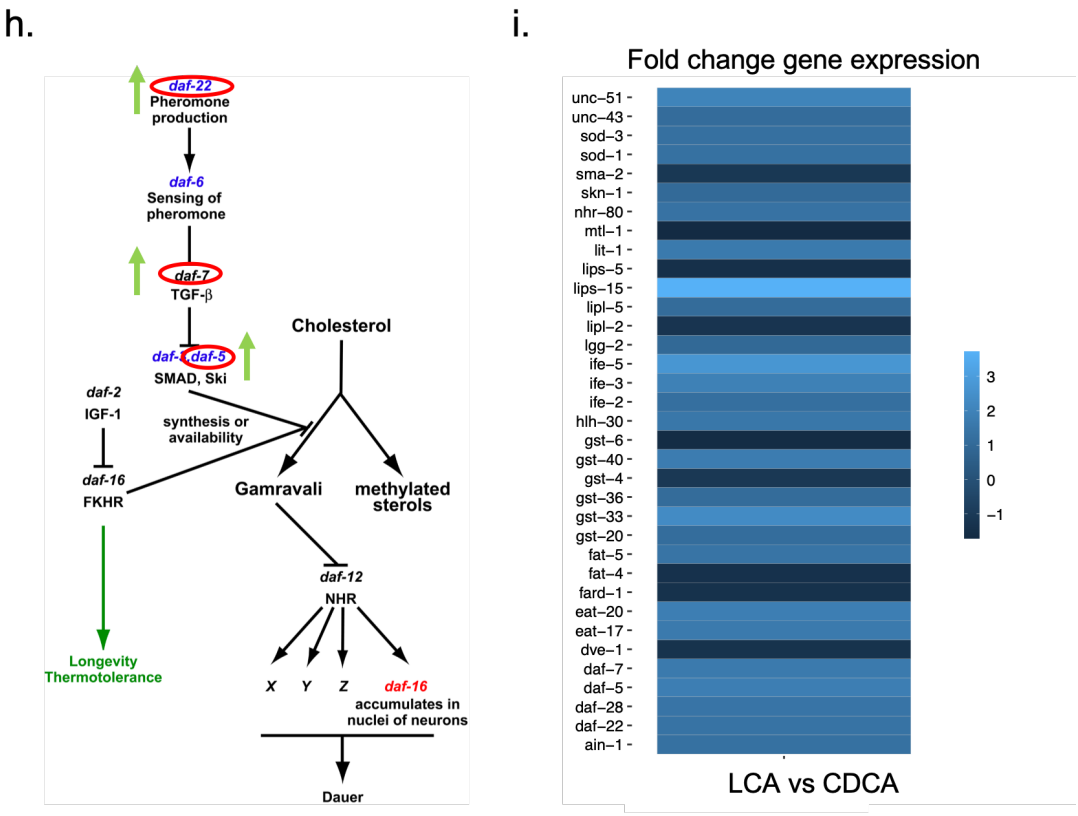


***Figure 4.21: Caenorhabditis elegans* longevity and immune response signalling pathways in bile acid LCA treated nematodes, compared to CDCA.** (a) DAF-2/DAF-16 pathway. (b) MAP kinase pathway. (c) MAP kinase calcium signalling pathway. (d) mTOR signalling pathway. (e) DBL-1 (TGF-β) signalling pathway. (f) NHR-80 and DAF-12 transcription pathway. (g) DVE-1 transcription pathway. (h) Pheromone dauer signalling pathway (adapted from (Matyash *et al.,* 2004)). (i) Heatmap showing relatively higher and lower transcription of *C. elegans* genes of interest, induced by treatment with 1 mM LCA, compared to 1 mM CDCA. Red circles in (a-h) highlight genes in (i), green arrow illustrates relatively higher transcription, red arrow illustrates relatively lower transcription.

In conclusion, the experiments shown here support the hypothesis that BAs may influence *C. elegans* longevity through DAF-12 and DA regulation (*Figure 4.22*). This work indicates that subtle effects are associated with UDCA and CDCA, however in relative comparisons with LCA and CDCA, large differences in nematode transcripts seem to point towards a range of potential system adjustments including lipolysis, signalling pathways including DAF-7 (TGF-β) and DAF-2 (insulin/IGF) pathways, which

can regulate DA production. Ultimately, through DAF-12 and DA regulation, BAs can regulate DAF-16, NHR-80 and HLH-30 pathways altering lipolysis, FA metabolism and autophagy, resulting in longevity potential (*Figure 4.22*) (Antebi, 2015).

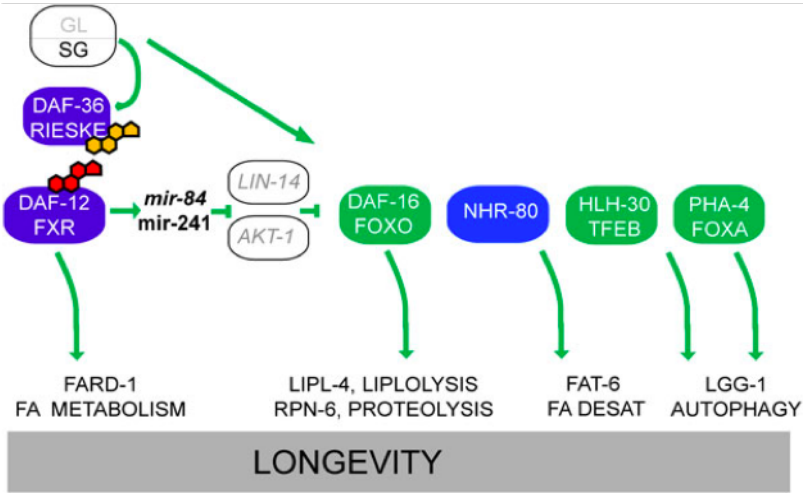


Figure 4.22: **Potential bile acid longevity pathway in *Caenorhabditis elegans*.** Signals from the germline and somatic gonad regulate DA production, extending *C. elegans* lifespan through DAF-12 activation, we propose that BAs influence longevity through regulation of this *C. elegans* pathway (Antebi, 2015).

4.3 Discussion

BA and DA signalling receptors are conserved between humans and *C. elegans*, however, a specific role for BAs in human longevity has not been established. Using the nematode model of aging, *C. elegans*, our study aimed to uncover a potential role for BAs in lifespan regulation, that may be relevant to the human situation.

This work showed that primary BA CA appeared to induce negative effects rather than positive on *C. elegans* lifespan and development. CA either reduced, or had no effect, on *C. elegans* lifespan and development. CA did not have the capacity to induce longevity, regardless of *C. elegans* strain. Interestingly, CA does not appear to induce DAF-16 expression, as cytosolic expression of DAF-16 was seen upon *C. elegans* strain CF1139 examination under fluorescence microscopy. CA has been shown to be an effective oral therapy for children in need of liver transplantation, inducing BA synthesis (Gonzales *et al.,* 2018). CA has also been found to promote lifespan in progeroid mice - progeria (Hutchinson-Gilford syndrome) is a genetic disorder that causes rapid aging (Bárcena *et al.,* 2018). Low levels of CA were found

in the serum of patients with Alzheimer's Disease, compared to healthy control volunteers, indicating CA may elicit beneficial effects in the context of Alzheimer's Disease (MahmoudianDehkordi *et al.,* 2019). However, although our study suggests that CA does not extend lifespan or induce expression of longevity genes, it may need to be considered in terms of its downstream BA, DCA.

Indeed, DCA and CDCA both significantly reduced *C. elegans* lifespan and development. DCA has previously been reported to impart, in general, negative effects on cell line and animal studies. These include: apoptosis in colonic and colorectal carcinoma cells, DNA damage and activation of transcription factors NF-κB and AP-1 (Glinghammar *et al.,* 2002; Im and Martinez, 2004; Im *et al.,* 2005), inhibiting Ca^{2+} absorption in rat duodenum (Pérez *et al.,* 2021), activation of IL-6 and IL-8 mRNA in oesophageal cells (Quilty *et al.,* 2021), intestinal carcinogenesis in a mouse model (Song *et al.,* 2022), increase of reactive oxidative species, and intestinal permeability in human colorectal adenocarcinoma cells (Zeng *et al.,* 2022). CDCA has also been reported to increase IL-8 production in human colorectal adenocarcinoma cells and increase intestinal permeability (Horikawa *et al.,* 2019) and increase tumour formation in mice (Mahmoud *et al.,* 1999). It is therefore not surprising, given the negative effects of DCA and CDCA already reported, that DCA and CDCA reduce *C. elegans* lifespan. Interestingly, DCA and CDCA both also induced translocation of DAF-16 to the nucleus for transcription of specific DAF-16 target genes, such as longevity or immune response gene expression. DCA is a hydrophobic BA, thus it has the capacity to damage mitochondria which can subsequently "leak" electrons from the electron transport chain to form superoxide (O^-) and resulting in an increase in reactive oxygen species (ROS) and overall oxidative stress (reviewed by (Payne *et al.,* 2008)). Interestingly, Payne *et al.*, (2008) describe this pathway occurring in colon cells, however, from mass spectrometry (UPLC-TMS) analysis we showed BAs are being taken up directly into the *C. elegans* strain SS104 gut. Perhaps both DCA and CDCA are acting in a similar manner as described by Payne *et al.*, (2008), reducing *C. elegans* lifespan and negatively impacting longevity.

The impact UDCA had on *C. elegans* lifespan and development appeared to be strain dependent. UDCA reduced the lifespan of *C. elegans* strain SS104 whereas, *C. elegans* strain N2 lifespan was extended. UDCA does not appear to induce DAF-16 expression, as cytosolic expression of DAF-16 was seen upon *C. elegans* strain CF1139 examination under fluorescence microscopy. Interestingly, *C. elegans* strain SS104 transcriptome analysis of UDCA treated nematodes, compared to CDCA, showed a relative decrease in transcription of *nhr-2* and *jun-1*. *nhr-2* is an ortholog of human PPARA and PPARD (peroxisome proliferator activated receptor alpha and delta, respectively) and THRA (thyroid hormone receptor alpha) (WormBase https://wormbase.org/species/c_elegans/gene/WBGene00003601#0-9f143a6-10). PPARA regulates FA β-oxidation and energy homeostasis (van Raalte *et al.,* 2004), and has been implicated in longevity through regulation of fibroblast growth factor-21 (FGF21) (McCarty, 2015). PPARD is involved in the regulation of insulin secretion and sensitivity and FA metabolism, such as uptake, transport, and β-oxidation; it has also been suggested to be cancer promoting (Gupta *et al.,* 2004). *jun-1* is an ortholog of human JUN, JUNB and JUND (Jun proto-oncogene, AP-1 transcription factor subunit) (WormBase https://wormbase.org/species/c_elegans/gene/WBGene00012005#0-9f143a6-10). JUN has been reported to have a role in colorectal cancer (Serra *et al.,* 2014) and inducing apoptosis, particularly in T cells (Baumann *et al.,* 2003). The implications of lower transcription levels of these genes, compared to CDCA, indicates that UDCA may be exhibiting beneficial effects on *C. elegans* lifespan and overall longevity. UDCA has been reported to be present at low levels in the ileum of aging mice (Wei *et al.,* 2022). In progeroid mice, an increase in secondary BA biosynthesis, including UDCA, have shown to extend lifespan (Bárcena *et al.,* 2019). UDCA has mainly been reported to protect against adverse effects, including reducing inflammation in fed mice (Oh *et al.,* 2016) and regulating Th-2 derived cytokines in a fed mouse model of chronic asthma (Işık *et al.,* 2017). UDCA has also been reported to inhibit DCA-induced apoptosis through EGFR/Raf-1/ERK and Akt/PKB-dependent survival signalling in human colon cancer cells (Im and Martinez, 2004; Im *et al.,* 2005), regulate mitochondrial function stimulating intestinal Ca^{2+} absorption in rat

duodenum (Pérez *et al.,* 2021) and UDCA has also been used as an oral therapy to treat Parkinson's disease (Sathe *et al.,* 2020).

The secondary BA LCA significantly extended *C. elegans* lifespan, regardless of strain. In the literature, LCA has been reported to have beneficial effects on the lifespan of both yeast, *Saccharomyces cerevisiae*, and fruit fly, *Drosophila melanogaster*, despite LCA being the most hydrophobic BA. LCA has been found to induce these lifespan extension effects through alteration of the mitochondria (Perino *et al.,* 2021), but these effects have been shown to be developmentally sensitive and may act through the mitochondrial membrane lipidome (Goldberg *et al.,* 2010; Burstein *et al.,* 2012; Beach *et al.,* 2013; Beach *et al.,* 2015; Leonov *et al.,* 2017; Arlia-Ciommo *et al.,* 2018; Staats *et al.,* 2018). Interestingly, various isoforms of LCA, specifically isoalloLCA, have been found to be present at high levels in centenarians, implicating that such BA derivatives of LCA are eliciting beneficial, infection reducing and gut homeostasis, effects (Sato *et al.,* 2021). On the contrary, LCA has also been reported as a plasma biomarker for Alzheimer's Disease (Marksteiner *et al.,* 2018). *C. elegans* SS104 transcriptome analysis revealed increased expression of *daf-22*, *daf-7* and *daf-5*, in nematodes treated with LCA, compared to CDCA, despite an increase in pheromone *daf-22*, which induces dauer formation. *daf-7* (TGF-β) is increased, and as *daf-5* is also increased, SS104 *C. elegans* continue their normal life cycle. In fact, this may signify a longevity pathway through increased *daf* expression. In addition, downstream of DAF-12 signalling, *fard-1* was down-regulated but *lit-1* and *ain-1* were up-regulated in *C. elegans* strain SS104 treated with LCA, compared to CDCA, suggesting a reduction in FA metabolism and an increase in development and longevity. DAF-12 has the capacity to interact with DAF-16, downstream of DAF-2 signalling pathway. DAF-2 pathway was indeed activated in LCA treated *C. elegans* strain SS104, compared to CDCA, due to up-regulated *daf-28*, and cytosolic DAF-16, leading to reduced expression of *mtl-1* and *gst-4*. This is in agreement with fluorescence microscopy analysis where DAF-16 translocation to the nucleus was seen in CDCA treated *C. elegans* CF1139 strain, but not in those treated with LCA. However, *sod-3* was up-regulated in LCA treated *C. elegans* strain SS104, compared to CDCA, suggesting that this increase in *sod-3* expression was due to alterations in

the mitochondria, induced by DAF-16 expression and subsequent transcription. Gene expression of *skn-1* was also up-regulated, indeed supporting the theory that LCA induced oxidative stress, compared to CDCA, particularly as expression of downstream *sod-1* is also relatively increased in these nematodes. Hence, the increase in DAF-16 expression and downstream *sod-3* in mitochondria is most probably in response to oxidative stress. LCA lowered the transcription of *dve-1*, compared to CDCA, suggesting a reduction in impaired and misfolded proteins and therefore proteotoxic mitochondrial stress. Similarly, *unc-43* involved in MAPK calcium signalling is at a higher level of transcription, suggesting a push towards longevity in LCA, compared to CDCA. Interestingly, the mTOR pathway which is involved in the regulation of autophagy is also relatively higher in LCA, compared to CDCA again, suggesting a push towards longevity. Expression of genes *unc-51* and *igg-2*, downstream from mTOR signalling, were at higher transcription levels in LCA, compared to CDCA, similarly *hlh-30* expression was also at higher transcription levels, inducing autophagy and potential longevity in *C. elegans* strain SS104. *sma-2* transcription levels were reduced in LCA, compared to CDCA, suggesting that the immune response in these worms is in fact reduced, perhaps supporting *C. elegans* longevity. Gene expression of *gst-6* was also at lower transcription levels in LCA, compared to CDCA, implying that there is an inhibition in innate immunity in these worms.

In LCA treated *C. elegans* strain SS104, compared to CDCA, transcriptome analysis revealed that there was an increase in oxidative stress resistance, a reduction in mitochondrial proteotoxicity, an increase in autophagy regulation and a reduction in immune response, resulting in in longevity potential. LCA inducing it's *C. elegans* longevity potential through alteration of the mitochondria is in agreement with the literature (Goldberg *et al.,* 2010; Burstein *et al.,* 2012; Beach *et al.,* 2015; Leonov *et al.,* 2017; Arlia-Ciommo *et al.,* 2018; Staats *et al.,* 2018). Comparing the secondary BA LCA, to the primary BA CDCA, was of interest, as LCA significantly extended *C. elegans* lifespan and CDCA significantly reduced *C. elegans* lifespan. Perhaps CDCA is inducing the same stress response in *C. elegans* as reviewed in Payne *et al.*, (2008), as mentioned above.

Interestingly, as 1 mM BA concentrations were assessed, this gives a glimpse into the *C. elegans'* transcriptome before significant changes in lifespan and development were induced by these BAs, specifically at 10 mM concentrations. Perhaps in some BAs, low concentrations may induce positive effects, such as longevity, rather than negative, reduction in lifespan effects. Maybe there is a threshold where these longevity genes are activated by BAs, but once concentrations are increased to a certain point, *C. elegans* can't metabolise these BAs and they become toxic and detrimental to *C. elegans* survival, particularly in the case of 5 mM and 10 mM DCA and CDCA. This *C. elegans* transcriptome analysis suggests that there is potential for BAs, particularly hydrophobic BAs, such as LCA and DCA, to effect mitochondria, autophagy, and immune response in *C. elegans*, that may switch from lifespan extension, to lifespan reduction, depending on concentration of BA administered.

In terms of longevity, there are four main long-lived mutants found in *C. elegans*, namely *daf-2*/*age-1*, *eat-2*, *clk-1*, *ife-2* (insulin/insulin-like growth factor-1, dietary restriction, mitochondrial signalling and protein translation), (Bansal *et al.,* 2015) as discussed in Chapter 1, sections 1.7.3. Transcription of *daf-2*/*age-1, eat-2* and *clk-1* were not found to be altered from the transcriptomic analysis in this study. *eat-20* and *eat-17*, genes of the same family as *eat-2* showed higher transcription levels, in LCA treated *C. elegans*, compared to CDCA, suggesting an increase in regulation of *C. elegans* strain SS104 pharyngeal pumping. Transcription levels of *ife-2* were higher in LCA treated *C. elegans*, compared to CDCA, along with other genes of the same family, *ife-3* and *ife-5*. This suggests that pharyngeal pumping and protein translation are perhaps increased in LCA treated nematodes, but reduced in those treated with CDCA. Perhaps CDCA is reducing pharyngeal pumping and protein translation, indeed inducing a concentration dependent hormesis effect. This hormesis effect being that CDCA elicits a beneficial effect on *C. elegans* at concentrations of 1 mM or lower, and induces negative effects on *C. elegans* at concentrations of 5 mM or higher. However, from the transcriptomic analysis in this study, BAs do appear to effect downstream signalling of specific nuclear hormone receptors (NHRs). Androstadienediones (ADDs), released from bacterial BA degradation, have been reported to have negative effects on the reproduction rate of *C. elegans*, induced

through NHR-69, the putative testosterone receptor (Mendelski *et al.,* 2019). We hypothesise from our data, that BAs ultimately influence *C. elegans* longevity through DAF-12 and DA regulation, effecting other downstream NHRs such as NHR-80 and NHR-6, a homolog of human NGF-1 and involved in the regulation of spermatheca organogenesis (Antebi, 2015). Transcription of NHR-6 was higher in LCA, compared to CDCA. Examination of *C. elegans* transcriptome revealed that BAs have the ability to regulate reproductive development, and in turn, the potential to coordinate nutrient sensing, metabolism, and energy homeostasis, including influencing signalling pathways DAF-7 (TGF-β) and DAF-2 (insulin/IGF) pathways. BAs, particularly LCA, can regulate mitochondrial function and induce stress response in *C. elegans*. LCA has been suggested to be toxic at high concentrations and interestingly, sulfation of LCA helps reduce its toxic effects, showing that the effects of LCA on longevity may be concentration dependent (Sheng *et al.,* 2022).

We hypothesize that BAs act through the regulation of DAF-12 and DA, to alter DAF-16, NHR-80 and HLH-30 signalling, mediating longevity potential through lipolysis, FA metabolism and autophagy. The homologs of these pathways in humans include FXR, FOXO and TFEB. FXR regulates BA homeostasis, by inducing fibroblast growth factor 19 (FGF19) expression (Holt *et al.,* 2003). It can also regulate triglyceride, cholesterol and glucose metabolism (Sinal *et al.,* 2000; Duran-Sandoval *et al.,* 2004; Zhang *et al.,* 2006) and it has an anti-inflammatory response (Li *et al.,* 2007). Lastly, FXR has recently been reported to have a role in FA β-oxidation regulation (Lu *et al.,* 2022). FOXO is involved in initiating apoptosis, cell cycle arrest or repairing DNA damage (Zhang *et al.,* 2011), as well as regulating energy metabolism through glucose homeostasis, and switching from carbohydrate to FA metabolism during starvation (Gross *et al.,* 2008). The transcription factor EB (TFEB) is involved in autophagy and lysosomal biogenesis, downstream of the mTOR pathway, as well as regulating metabolism, and inflammatory and immune responses (Zhu *et al.,* 2021). Ultimately, BAs may influence human lifespan and longevity through maturational steroids, that regulate mitochondria, as well as receptors and downstream pathways including FXR, FOXO and TFEB.

Future Work

To move this work forward, further analysis and experimentation is required to cement the effects of BAs on the *C. elegans* transcriptome and on longevity in the wild-type N2 strain treated with all primary and secondary BAs. Further experimentation and replicates would confirm these effects. Our experiments did not examine a possible BA blunting effect. A range of metabolites are established DAF-16 modulators; it may be that specific BAs could dampen such responses if they are evoked. Real-Time Quantitative Reverse Transcription PCR (qRT-PCR) could be performed to examine DAF-12 and DA regulation pathways in *C. elegans* wild-type strain N2, both at L1 larval stage and reproductive adult, treated with BAs, compared to a control with no BAs. A large-scale proteomics study could be carried out to analyse the changes in protein profiles in *C. elegans* wild-type strain N2, treated with BAs compared to a control with no BAs, identifying human protein homologs. This would have the potential to determine the specific proteins that may be involved in human longevity. This study demonstrates that BAs may act through DAF-12 and DA regulation, potentially altering DAF-16, NHR-80 and HLH-30 pathways, influencing lipolysis, FA metabolism and autophagy, and inducing longevity potential in the model of aging, *C. elegans*.

Chapter 5 – Exploring gut microbial interactions that can alter lifespan in the model of aging *Caenorhabditis elegans*

5.0 Abstract

The microbiome may differentially contribute to aging and longevity, through affecting alterations in gut microbial composition. Indeed, in chapter 4 we determined that primary and secondary BAs can influence *C. elegans* lifespan and development, and are associated with aging. Here, in this chapter 5, *C. elegans*, was also used to investigate the relationship between food and longevity, using *Escherichia coli* (*E. coli*) HM605. *E. coli* HM605 is an adherent-invasive *E. coli* (AIEC) isolated from a colonic biopsy specimen of a Crohn's Disease (CD) patient. CD is an inflammatory bowel disease (IBD) whose incidence has tripled in the last 10 years. We show that *E. coli* HM605 has the capability of reducing *C. elegans* lifespan. Its deletion mutation, Δ*dsb*A, demonstrates properties that restore *C. elegans* lifespan. Growing *C. elegans* with *E. coli* HM605 resulted in transcriptional changes that indicated that *E. coli* HM605 may be pathogenic to the nematode. Interestingly, the Δ*dsb*A mutation reversed theses changes in the *C. elegans* transcriptome, reducing *C. elegans* innate immune response, by inhibiting DAF-2/DAF-16 signalling, VHP-1 signalling, fatty acid synthesis and promoting lipid synthesis, the stress response and apoptotic pathways, promoting longevity and reducing virulent potential. The aim of this study was to demonstrate the significant consequences a single mutation in the food source (*E. coli* HM605) could have in terms of host health and longevity. It also aimed at cementing the potential use of antibacterials, rather than antibiotics, for the treatment of human infection and disease, including CD.

5.1 Introduction

Caenorhabditis elegans (*C. elegans*) is a transparent, soil-dwelling nematode that is well characterised, making it a very valuable model organism, particularly as a model of aging (Klass, 1977). Under laboratory conditions, *C. elegans* has a short lifespan of around 20-25 days with a diet of *E. coli* OP50 (Brenner, 1974). Due to its short lifespan and diet, it is a useful model of aging as a single bacterium can be applied, and its effects on the whole organism can be studied.

Crohn's disease (CD) is an inflammatory bowel disease (IBD). In Ireland in 2011, per 100,000 population, there were 5.9 new cases of CD (Irish Society for Colitis and Crohn's disease). The peak age of incidence is between the ages of 15 and 35 (Irish Society for Colitis and Crohn's disease). Currently, there is no cure for CD. Diversity of the faecal and mucosal microbiome has been reported to be reduced in CD, with an increase in adherent-invasive *Escherichia coli* (AIEC) species (Giaffer *et al.,* 1992). AIEC are believed to be one of the main causes of CD, resulting in increased inflammation. AIEC have the capacity to invade and replicate within epithelial and macrophage cells (Darfeuille-Michaud, 2002). AIEC induces TNF-α, IL-6, IL-23, CD40, and CD80 in macrophages, which can be inhibited by the glucocorticoid dexamethasone, one of the first lines of treatment for CD (Olivares-Morales *et al.,* 2018). AIEC virulence and replication within murine macrophages is tolerant of stress conditions, including superoxide stress, and depends on the induction of macrophage NF-κB signalling in order to support their invasion and survival (Tawfik *et al.,* 2019).

Studies have been carried using *E. coli* LF82 (an ileal AIEC isolated from a CD patient), to determine genes that are essential for AIEC pathogenesis. LF82 has been shown to reduce *C. elegans* lifespan and this was reported to be due to colonisation of the *C. elegans* gut and damage to the intestinal epithelial surface (Simonsen *et al.,* 2011b). Two *fim* mutants were found to allow LF82 to adhere, but prevented host cell membrane elongations. This data showed that type 1 pili are involved in the invasive process of LF82 (Boudeau *et al.,* 2001). The *fim*H gene has been shown to be involved in inducing inflammation in CD, in CEABAC10 transgenic mice, expressing human CEACAM receptors (Dreux *et al.,* 2013). The *fim*H gene encodes a fimbrial adhesin which binds oligomannose glycans on the surface of host cells (Dumych *et al.,* 2018). The *dsbA* gene encodes a periplasmic oxidoreductase and functions in the formation of a specific disulfide bond in secreted proteins in *E. coli*, such as the PapD chaperone, essential for fimbriae biogenesis (Jacob-Dubuisson *et al.,* 1994; Hu *et al.,* 1997). A study showed that insertion of a *fim* operon into an AIEC LF82-Δ*dsb*A mutant does not rescue gut adhesion and invasion (Bringer *et al.,* 2007). The *dsb*A gene also has a role in the secretion of toxins and components of Type 3 secretion systems by

catalysing the correct folding of these secretions and surface-proteins (Yu and Kroll, 1999). The *htr*A gene, encoding the stress protein HtrA, is necessary for AIEC replication within macrophages (Bringer *et al.,* 2005). However, Simonsen *et al.*, (2011) have reported that LF82 virulence is independent of the *htrA*, *omp*R, *fim*H and *dsb*A. They report that deletion of *hfq* gene, encoding an RNA chaperone mediating post-transcriptional gene regulation, results in decreased virulence through cell invasion inhibition and reduced motility (Simonsen *et al.,* 2011b).

DAF-16 can regulate *C. elegans* innate immune response and have an important role in bacterial-induced longevity (Garsin *et al.,* 2003). *Bifidobacterium longum* strain BB68 extended *C. elegans* lifespan by inducing high levels of DAF-16 nuclear accumulation, via TIR-1 and JNK-1 phosphorylation and activation, and increased expression of the DAF-16 target gene, *sod-3* (Zhao *et al.,* 2017). *Pseudomonas aeruginosa* PAO1 and *Salmonella enterica* serovar *Typhimurium* strain MST1 induce nuclear expression of DAF-16 (Palominos *et al.,* 2017). DAF-16 hyperactivation has also been reported to increase *C. elegans* susceptibility to bacterial infections (Singh and Aballay, 2009).

The *C. elegans* model of aging has been used to determine that a strain of AIEC, HM605, reduces the lifespan of the nematode (S. Walsh, unpublished data, data not shown). A total of 29 HM605 mutations were tested with *C. elegans* to determine which bacterial genes were involved in the observed reduction of lifespan. This study identified one particular HM605 deletion mutant, Δ*dsbA,* where the lifespan of *C. elegans* was rescued to that observed on *E. coli* OP50. *C. elegans* RNA sequencing and analysis was then undertaken to determine the changes in physiology in *C. elegans* that are correlated with increased lifespan.

5.2 Results

5.2.1 *Escherichia coli* HM605 and its deletion mutations affect *Caenorhabditis elegans* strain SS104 L1 larvae lifespan

It has been observed that the lifespan of *C. elegans* strain SS104 is reduced when cultured on *E. coli* HM605 compared to nematodes cultured on the *E. coli* OP50 control (S. Walsh, unpublished data, data not shown). HM605 is an AIEC and has been associated with IBD in humans (Clarke *et al.,* 2011). *E. coli* OP50 is a uracil auxotroph that is normally used as a diet source for *C. elegans*, grown under laboratory conditions (Brenner, 1974). *C. elegans* strain SS104 is a temperature sensitive mutant that contains the *glp-4(bn2)* mutation. This mutation is permissive for egg laying and reproduction at 16°C, but egg-laying is inhibited at 25°C (Beanan and Strome, 1992). Therefore, lifespan assays carried out at 25°C are not confounded by egg-laying and the development of new generations of nematodes. A total of 29 HM605 deletion mutations were screened to determine if they could rescue *C. elegans* lifespan from the L1 stage, to that of the control, *E. coli* OP50 (*Table 5.1*). Mutants were selected on their availability and also previous work indicating a role for the mutated gene in the virulence of HM605 (David Clarke, personal communication). The L1 stage was used to determine how these bacterial mutants impacted early life and the development and progression into and through adulthood. HM605 deletion mutant strains: Δ*fim*H, Δ*dsb*A, Δ*flg*G and Δ*bae*R, appeared to have the capability of restoring *C. elegans* strain SS104 L1 lifespan to that observed when nematodes are cultured on the control, *E. coli* OP50 (S. Walsh and Z. Walsh, unpublished data, data not shown).

***Table 5.1*: Identity and function of the *Escherichia coli* HM605 mutants screened in this study.**

Mutant	Function
Δ**icD**	Isocitrate dehydrogenase enables E. coli to make rapid shifts between TCA and glyoxalate bypass pathway
Δ**pfkAB**	6-phosphofructokinase I (PFK I) + 6-phosphofructokinase II
Δ***fim*H**	Encodes for a component of fimbriae that allow for cell adhesion.
Δ***dsb*A**	Periplasmic thiol:disulfide oxidoreductase. Promotes protein disulfide bond formation in E. coli.
Δ***flg*G**	FlgG is one of four proteins that comprise the rod section of the basal-body assembly of the flagellar motor.
Δ***cpx*R**	Effective binding of stationary phase cells to hydrophobic surfaces, part of the process of biofilm formation.
Δ***pho*B**	A positive regulator of the phosphate regulon.
Δ***nar*L**	Activated expression of nitrate reductase and formate dehydrogenase-N operons and represses the transcription of fumarate reductase operon.
Δ***rss*B**	Regulates the turnover of sigma S factor by promoting proteolysis in growing cells. Also regulated mRNA polyadenylation pathway during stationary phase.
Δ***yeh*T**	DNA-binding.
Δ***dcu*R**	Involved in the C4-dicarboxylate-stimulated regulation of the genes encoding the anaerobic fumarate respiratory system. Weakly regulates the aerobic C4-dicarboxylate transporter dctA.
Δ***qse*B**	Activates transcription of FIhDC, in doing so activates the flagella regulon.
Δ***rcs*B**	Response regulator. Binds to regulatory DNA regions. Regulates expression of genes such as biofilm formation, cell division, colonic acid capsule synthesis and outer membrane protein synthesis.
Δ***uvr*Y**	Regulates carbon metabolism. Activates transcription of untranslated csrB RNA and of barA in an autoregulatory loop.
Δ***arc*A**	Represses a wide variety of aerobic enzymes under anaerobic conditions. Controls the resistance of E. coli to dyes. Also involved in the osmoregulation of envelope proteins.
Δ***zra*R**	When activated acts in conjunction with sigma-54 to regulate the expression of zraP. Also involved in the positive regulation of the expression of zraSR operon.
Δ***cre*B**	Functions in catabolic regulation.
Δ***omp*R**	N-terminus of the protein required for transcriptional expression of both major outer membrane protein genes ompF and ompC. C-terminus is involved in the multimerization of the ompR protein.
Δ***ato*C**	In the presence of acetoacetate stimulates expression of atoDAEB operon, leading to short chain fatty acid catabolism and also activates the poly-®-3-hydroxybutyrate (cPHB) biosynthetic pathway. Involved in the regulation of motility and chemotaxis via transcriptional induction of the flagellar regulon.
Δ***pho*P**	Involved in the adaptation to low Mg2+ environments and the control of acid resistance genes. Mediates magnesium influx to the cytosol by activation of MgtA.
Δ***ypd*B**	Regulate expression of yhjX by binding to its promoter region.
Δ***uhp*A**	Part of the UhpABC signalling cascade that controls the expression of the hexose phosphate transporter UhpT. Activates the transcription of the uhpT gene.
Δ***che*Y**	Involved in the transmission of sensory signals from the chemoreceptors to the flagellar motors. In active form - enhanced binding switches component, FliM, at the flagellar motor to induce change from anticlockwise to clockwise flagellar rotation.
Δ***tor*R**	Involved in the anaerobic utilization of trimethylamine-N-oxide (TMAO).
Δ***rts*A**	Involved in sequence specific DNA binding.
Δ***fhi*A**	Required for induction of expression of the formate dehydrogenase H and hydrogenase-3 structural genes. Also activates expression of hyf operon (encodes the silent hydrogenase-4 gene cluster).
Δ***evg*A**	Regulates the expression of emrKY operon and yfdX. Also involved in the control of the expression of a multidrug efflux operon.
Δ***bae*R**	Responds to envelope stress. Activates expression of periplasmic chaperone spy in response to spheroplast formation. Also, baeR could have a role in the activation of CRISPR-Cas casABCDE-ygbT-ygbF operon.
Δ***nar*P**	Activates expression of nitrate reductase and formate dehydrogenase-N operons and represses transcription of fumarate reductase operon in response to nitrate/nitrite induction signal.

To confirm the earlier observations, the lifespan of *C. elegans* strain SS104 cultured on *E. coli* HM605 and the 4 deletion mutations, Δ*fim*H, Δ*dsb*A, Δ*flg*G and Δ*bae*R, was measured and compared with the control *E. coli* OP50. Briefly, *C. elegans* strain SS104 L1 stage (*n*=30), were pipetted onto NGM agar, individually inoculated with either *E. coli* OP50, HM605, Δ*fim*H, Δ*dsb*A, Δ*flg*G or Δ*bae*R (*n*=3), and incubated at 25°C. The nematodes were counted until the population reached 0% survival. It is clear that *E. coli* HM605 significantly reduced the lifespan of L1 stage *C. elegans* strain SS104 compared to that of the control, *E. coli* OP50 (*Figure 5.1* (a)). Moreover, incubation on all of the mutants showed that Δ*dsb*A had the capacity to restore nematode lifespan to that of the control, *E. coli* OP50. Δ*dsb*A significantly increased L1 stage *C. elegans* strain SS104 lifespan, compared to *E. coli* HM605 (*Figure 5.1* (b)). *C. elegans* strain SS104 L1 stage was used as an initial screen. Adulthood of both *C. elegans* strains (SS104 and WT N2) were the focus going forward.

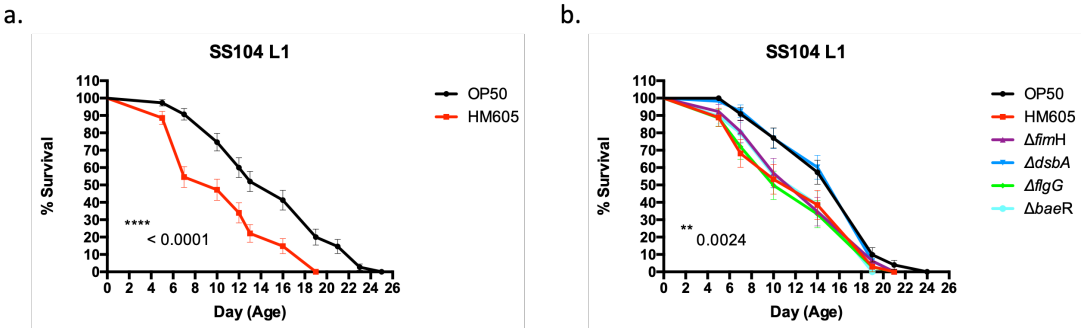


Figure 5.1: **Assessment of *Escherichia coli* HM605 and its deletion mutations on *Caenorhabditis elegans* strain SS104 L1 lifespan.** Survival curve of *C. elegans* strain SS104 L1 treated with (a) *E. coli* OP50 and *E. coli* HM605; and (b) *E. coli* OP50, *E. coli* HM605 and *E. coli* HM605 deletion mutants: Δ*fim*H, Δ*dsb*A, Δ*flg*G and Δ*bae*R. (*n*=3 technical and biological replicates, appendix V SI.5.1). Statistics were log-rank test for survival curves (*= p<0.05; **=p<0.01; ***=p<0.001; ****=p<0.0001).

5.2.2 *Escherichia coli* HM605 and its deletion mutations affect *Caenorhabditis elegans* L4 larvae lifespan

L1 stage nematodes were initially used for the lifespan assays in order to include nematode development in the measurements. To look at lifespan and adulthood,

and to see whether reproduction, i.e. the temperature sensitive mutation, *glp-4(bn2)*, influences lifespan, it was decided to examine the effect of the bacteria on the lifespan of *C. elegans* strain SS104 and *C. elegans* wild-type strain N2 nematodes at the L4 stage. Therefore, in the same way as previously described, *C. elegans* strain SS104 and *C. elegans* wild-type strain N2 at L4 stage were each synchronised (*n*=30), pipetted onto NGM agar individually inoculated with either OP50, HM605, Δ*fim*H or Δ*dsb*A (*n*=3), and incubated at 25°C. The nematodes were counted until the population reached 0% survival. *E. coli* HM605 significantly reduced the lifespan of L4 stage *C. elegans* strain SS104 (*Figure 5.2* (a)) and L4 stage *C. elegans* wild-type strain N2 (*Figure 5.2* (c)), compared to that of the *E. coli* OP50 control. Therefore, *E. coli* HM605 reduces the lifespan of both adult and L1 nematodes. Incubation on either Δ*fim*H or Δ*dsb*A mutants increased the lifespan of L4 stage *C. elegans* strain SS104, compared to *E. coli* HM605, although not significantly (*Figure 5.2* (b)), significance was found between *E. coli* OP50 and *E. coli* HM605. This confirmed the results presented using L1 stage *C. elegans* strain SS104 (*Figure 5.1* (b)) and suggests that deleting the *dsb*A gene can increase the longevity of *C. elegans* fed *E. coli* HM605. Although the phenotype isn't as dramatic in the *C. elegans* wild-type strain N2, Δ*dsb*A exhibits the largest increase in longevity, particularly at 50% survival (*Figure 5.2* (d)).

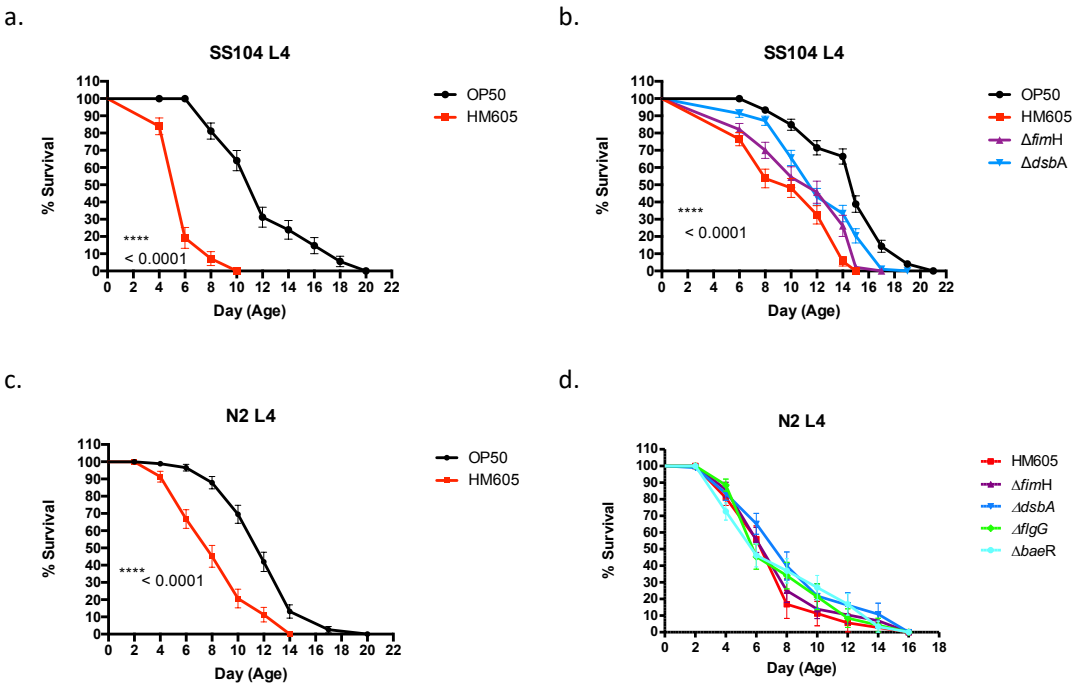


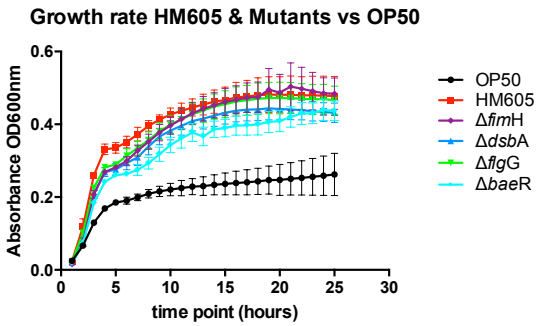
Figure 5.2: **Assessment of *Escherichia coli* HM605 and its deletion mutations on *Caenorhabditis elegans* strain SS104 and *Caenorhabditis elegans* wild-type strain N2 L4 lifespan.** Survival curve of *C. elegans* strain SS104 treated with (a*) E. coli* OP50 and *E. coli* HM605; and (b) *E. coli* OP50, *E. coli* HM605, and *E. coli* HM605 deletion mutants: Δ*fim*H and Δ*dsb*A. Survival curve of *C. elegans* wild-type strain N2 treated with (c) E. coli OP50 and E. coli HM605; and (d) E. coli OP50, E. coli HM605, and *E. coli* HM605 deletion mutants: Δ*fim*H and Δ*dsb*A, Δ*flg*G and Δ*bae*R. (*n*=3, appendix V SI.5.1). Statistics were carried out using log-rank test for survival curves (* = p<0.05; ** = p<0.01; *** = p<0.001; **** = p<0.0001).

5.2.3 Assessment of the rate of growth of *Escherichia coli* HM605 and its deletion mutants

In order to eliminate changes in the growth rates of the mutant strains as a trivial explanation for the observed increased lifespans, the growth of *E. coli* HM605 and its deletion mutations were compared to the control, *E. coli* OP50 (*Figure 5.3*). The growth of *E. coli* OP50, HM605, Δ*fim*H, Δ*dsb*A, Δ*flg*G and Δ*bae*R was recorded every hour for 24 hours in LB broth at 37°C by reading the optical density at wavelength 600nm. To enumerate viable cells serial dilutions of the bacterial cultures were also plated at the 24-hour point and colonies were counted following 18 hours at 37°C. *E.*

coli HM605 and the mutant strains Δ*fim*H, Δ*dsb*A, Δ*flg*G and Δ*bae*R all showed similar growth kinetics and they all grew better (i.e. faster and to a higher cell density) than *E. coli* OP50 (*Figure 5.3* (a)). Viable plate counts confirmed that HM605 does grow to a higher cell density to that of OP50, $1x10^9$ cfu ml^{-1} and $2.4x10^8$ cfu ml^{-1}, respectively (*Figure 5.3* (b)). All of the mutants, with the exception of Δ*bae*R, had final cell densities similar to *E. coli* HM605 indicating any observed increases in *C. elegans* lifespan was not due to reduced growth of these mutants. Therefore, the rate of growth of *E. coli* HM605 and the mutant strains Δ*fim*H, Δ*dsb*A, Δ*flg*G and Δ*bae*R, do not appear to be a determining factor for increases seen in *C. elegans* lifespan, particularly *C. elegans* strain SS104 (*Figure 5.1* and *5.2* (b)).

a.



b.

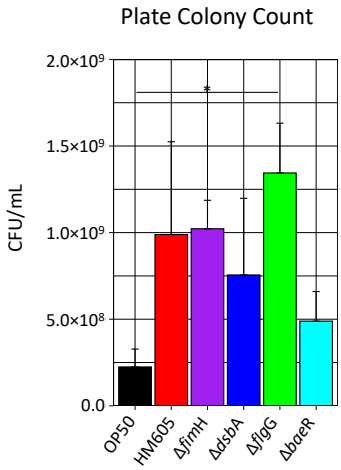


***Figure 5.3:* Assessment of the rate of growth of *Escherichia coli* HM605 and its deletion mutations, compared to control *Escherichia coli* OP50.** (a) Growth curves of *E. coli* OP50, *E. coli* HM605, and *E. coli* HM605 deletion mutants: Δ*fim*H, Δ*dsb*A, Δ*flg*G and Δ*bae*R in LB broth at 37°C. (b) Graph of CFU/ml at 24-hour timepoint and doubling time of *E. coli* OP50, *E. coli* HM605, and *E. coli* HM605 deletion mutants: Δ*fim*H, Δ*dsb*A, Δ*flg*G and Δ*bae*R. (*n*=3, second replicate see appendix V SI.5.3). Statistics were carried out using one-way ANOVA, Tukey multiple comparison test (* = p<0.05; ** = p<0.01; *** = p<0.001; **** = p<0.0001).

5.2.4 The effect of *Escherichia coli* HM605 and its deletion mutants: Δ*fim*H and Δ*dsb*A, on *Caenorhabditis elegans* developmental timing is strain dependent

E. coli HM605 significantly decreased *C. elegans* strain SS104 L1 lifespan (*Figure 5.1* (a)) and this work has shown that *C. elegans* strain SS104 L1 larvae had significantly increased longevity when cultured on Δ*dsb*A, compared to *E. coli* HM605 and the other three *E. coli* HM605 deletion mutations: Δ*fim*H, Δ*flg*G and Δ*bae*R (*Figure 5.1* (b)). The *dsb*A gene encodes a protein that functions in the formation of a specific disulfide bond in proteins that are secreted into the periplasm in Gram negative bacteria, including those proteins involved in fimbriae biogenesis and bacterial molility (Jacob-Dubuisson *et al.,* 1994; Hu *et al.,* 1997; Landeta *et al.,* 2018). Indeed, the Δ*dsb*A mutant was shown to have fimbriae but demonstrate defective colonisation, due to misfolded fimbriae as essential disulfide bonds were absent (Taylor *et al.,* 1987). Similarly, insertion of a *fim* operon into an AIEC LF82 Δ*dsb*A mutant did not rescue gut adhesion or invasion (Bringer *et al.,* 2007). Therefore, *E. coli* HM605 deletion mutant Δ*fim*H was also focused on going forward, as a control for defective fimbrial function in Δ*dsb*A. To determine whether this change in lifespan/longevity is due to changes in the development of the nematodes, synchronous L1 stage *C. elegans* strain SS104 were plated with *E. coli* HM605 and the Δ*fim*H and Δ*dsb*A mutants to monitor nematode development from early life into adulthood. Age-synchronised *C. elegans* (*n*=30) were pipetted onto NGM agar previously inoculated with the appropriate individual bacterial strain. The plates were kept at 16°C (permissive for egg-laying in *C. elegans* strain SS104) and total progeny (L1 and L2 stage nematodes) were counted until dauer juveniles appeared. Interestingly, a new generation of *C. elegans* strain SS104 L1/L2 larvae appeared on plates containing *E. coli* OP50 after approximately 6 days whilst the peak of L1/L2 nematodes growing on *E. coli* HM605 is delayed until approximately 8 days (*Figure 5.4* (a)). Therefore, *E. coli* HM605 appears to slow *C. elegans* strain SS104 nematode development. Interestingly L1 stage nematodes growing on plates containing Δ*fim*H and Δ*dsb*A mutants did exhibit a broader peak of new generation L1/L2 development suggesting a phenotype that is intermediate to that observed with *E. coli* HM605 and *E. coli* OP50 (*Figure 5.4* (a)). In the *C. elegans* wild-type N2 strain, *E. coli* HM605 and

Δ*fim*H appear to accelerate nematode development with a larger number of new generation of *C. elegans* wild-type N2 strain L1/L2 larvae after approximately 4 days, compared to *E. coli* OP50 and Δ*dsb*A (*Figure 5.4* (b)). Interestingly, Δ*dsb*A has a similar profile to the control, *E. coli* OP50. Overall, *E. coli* HM605 and Δ*fim*H appear to speed up *C. elegans* wild-type N2 strain development whilst *E. coli* OP50 and Δ*dsb*A have a similar effect on the development of *C. elegans* wild-type N2 strain L1 larvae (*Figure 5.4* (b)). WT *C. elegans* N2 Bristol strain developed at a faster rate than the egg-laying deficient mutant *C. elegans* SS104 strain due to incubation at a higher temperature (25°C compared to 16°C). L1/L2 larvae at day 10 developed into dauer, therefore the experiment was stopped. Nutrients were exhausted and so another variable was present from day 10. *C. elegans* strain SS104 L1 larvae are displaying a different phenotype compared to the *C. elegans* wild-type N2 strain, suggesting that the temperature sensitive mutation, *glp-4(bn2)*, may be influencing the effect *E. coli* HM605, Δ*fim*H and Δ*dsb*A are having on longevity and lifespan. This data suggests nematode reproduction, and perhaps immune response in the *glp-4(bn2)* mutant as mentioned above, may alter the effects of *E. coli* HM605, and deletion mutations Δ*fim*H and Δ*dsb*A.

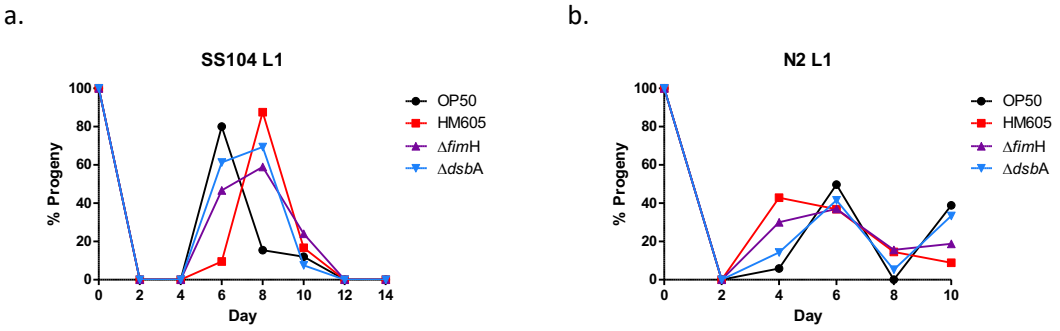


Figure 5.4: **Assessment of *Escherichia coli* HM605 and its deletion mutations on *Caenorhabditis elegans* strain SS104 and *Caenorhabditis elegans* wild-type strain N2 L1 developmental timing.** Line graph of percent (%) progeny (L1 and L2), (L1 plated day 0), from day 0-14 incubated with *E. coli* OP50, *E. coli* HM605, and *E. coli* HM605 deletion mutants: Δ*fim*H and Δ*dsb*A, of *C. elegans* strain (a) SS104, and (b) wild-type N2. *n*=3 experiments were performed, Appendix V SI.5.4-5, with one experimental representation shown here.

5.2.5 *Escherichia coli* HM605 is capable of colonising the gut of *Caenorhabditis elegans*

HM605 is an adherent invasive *E. coli* (AIEC) and its pathogenicity largely depends on its ability to invade and replicate within mammalian epithelial and macrophage cell lines (Clarke *et al.*, 2011). Therefore, it is possible that the Δ*fim*H mutant – lacking a component of fimbriae for cell adhesion, and the Δ*dsb*A mutant – disrupting periplasmic disulphide bond formation, may affect the ability of *E. coli* HM605 to colonise the *C. elegans* gut. Synchronised L4 stage nematodes were inoculated on NGM agar containing *E. coli* OP50, *E. coli* HM605, and *E. coli* HM605 deletion mutants: Δ*fim*H or Δ*dsb*A, and incubated at 25°C for 2, 4 or 6 days. L4 stage nematodes were examined to determine bacterial colonisation of a fully formed adult gut. Gut colonisation was then measured on day 2, 4 and 6, as outlined in Materials and Methods (Section 2.2.5). Percent (%) colonisation was calculated as the number of nematodes showing gut colonisation out of 10 individual nematodes examined. With *C. elegans* strain SS104, % colonisation by *E. coli* HM605 increased over time reaching a maximum level of 40% at Day 6 (*Figure 5.5* (a)). On the other hand, *E. coli* OP50, Δ*fim*H and Δ*dsb*A did not colonise as many worms as *E. coli* HM605. In addition, *E. coli* HM605 was present at significantly higher levels in the gut of colonised *C. elegans* strain SS104 on Day 6, compared to *E. coli* OP50, Δ*fim*H and Δ*dsb*A (*Figure 5.5* (b)). This data suggests that there is an inverse correlation between *E. coli* HM605 gut colonisation and lifespan in the L4 stage *C. elegans* strain SS104, indicating that *E. coli* HM605 may induce lifespan reduction in *C. elegans* strain SS104 through gut colonisation. In the *C. elegans* wild-type strain N2, an overall higher percentage of colonisation compared to the temperature sensitive *C. elegans* strain SS104 was observed (*Figure 5.5* (c)). Of the *C. elegans* wild-type strain N2 that are colonised, there appears to be a bimodal distribution of the degree of colonisation (*Figure 5.5* (d)). Some *C. elegans* wild-type strain N2 have less than 10 CFU/Nematode, while others have as many as 2000 CFU/Nematode (*Figure 5.5* (d)). *E. coli* HM605, Δ*fim*H and Δ*dsb*A do appear to colonise *C. elegans* wild-type strain N2 to a higher level compared to *E. coli* OP50, with Δ*fim*H having consistently high levels

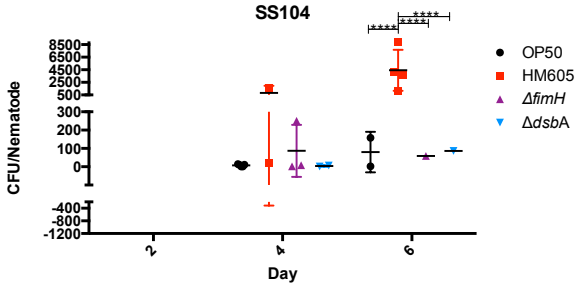
of colonisation from Day 2 to Day 6 (*Figure 5.5* (d)). Although *C. elegans* strain SS104 demonstrated a clear inverse correlation between *E. coli* HM605 gut colonisation and lifespan, this phenotype is less clear in the *C. elegans* wild-type strain N2, again suggesting a potential effect of the *glp-4(bn2)* mutation.

a.

SS104 % Colonisation

	Day 2	Day 4	Day 6
OP50	0	30	20
HM605	0	20	40
Δ*fim*H	0	30	10
Δ*dsb*A	0	20	10

b.



c.

N2 % Colonisation

	Day 2	Day 4	Day 6
OP50	40	30	90
HM605	20	70	50
Δ*fim*H	50	90	50
Δ*dsb*A	20	20	10

d.

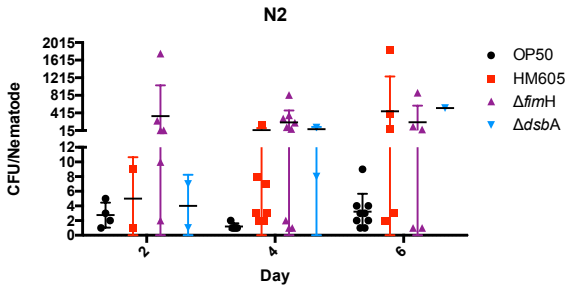


Figure 5.5: **Colonisation of the *Caenorhabditis elegans* gut by *Escherichia coli* strains.** Percent (%) colonisation, over days 2, 4 and 6, by *E. coli* OP50, *E. coli* HM605, and *E. coli* HM605 deletion mutants: Δ*fim*H and Δ*dsb*A, in *C. elegans* strain (a) SS104, and (c) wild-type N2. CFU/Nematode, over days 2, 4 and 6, of *E. coli* OP50, *E. coli* HM605, and *E. coli* HM605 deletion mutants: Δ*fim*H and Δ*dsb*A, in *C. elegans* strain (b) SS104, and (d) wild-type N2. (*n*=2, appendix V SI.5.6). Statistics were carried out using Kruskal-Wallis, Dunn's Multiple comparison test (* = p<0.05; ** = p<0.01; *** = p<0.001; **** = p<0.0001).

5.2.6 RNA extraction and sequencing to determine whether *Escherichia coli* HM605 and its deletion mutations effect *Caenorhabditis elegans* transcriptome

In this study it has been shown that *E.coli* HM605 reduces *C. elegans* lifespan and some deletion mutations, namely Δ*dsb*A, have the potential to restore lifespan to that of the control, *E.coli* OP50 (*Figure 5.1* and *5.4*). To investigate this further, RNA sequencing was performed to determine whether *E.coli* HM605, Δ*fim*H and Δ*dsb*A alter the *C. elegans* transcriptome, and, if so, what genes may be up- or down-regulated. *C. elegans* strain SS104 were used in order to ensure a synchronous culture with such a large population of *C. elegans*. Synchronised L4 stage SS104 nematodes were inoculated on NGM agar containing *E.coli* OP50, *E.coli* HM605, and *E.coli* HM605 deletion mutants: Δ*fim*H or Δ*dsb*A for two days. At this time the nematodes were harvested, washed and total RNA was then extracted, processed, sequenced and analysed (Materials and Methods, Sections 2.2.7 and 2.2.8). Two day time point was used as differences in lifespan can be seen (*Figure 5.1* (b)) but there is little to no gut colonisation (*Figure 5.5* (a and b)) to reduce bacterial RNA contamination in samples. Each sample reached the required quality for delivery to Genewiz Europe (Leipzig, Germany) for sequencing. Each RNA sample had a RIN >6.0 and an A260/A280 = 1.8-2.2 (*Table 5.2*), and ≥2 µg of each sample was delivered to Genewiz Europe (Leipzig, Germany) for sequencing.

***Table 5.2*: *Caenorhabditis elegans* strain SS104 RNA samples and their quality assessed post extraction. In all samples, indicated they were appropriate for further work.**

Sample	Qubit Total conc. (ng) in 20µl	Bioanalyser RIN	Nanodrop A260/280
OP50 Control 1	4240	6.4	1.8
OP50 Control 2	4320	6.4	2.07
OP50 Control 3	5040	6.5	2.03
HM605 1	5440	6.6	2.07
HM605 2	4640	7	2.05
HM605 3	5280	6.9	2.05
ΔdsbA 1	5840	6.3	2.04
ΔdsbA 2	6160	6.7	2.05
ΔdsbA 3	5680	6.5	2.05
ΔfimH 1	1768	7.8	1.94
ΔfimH 2	5040	6.7	2.01
ΔfimH 3	5120	6.2	2.04

Qubit™ analysis revealed that the total RNA concentration for each sample ranged from 1.77 µg to 6.16 µg in a 20 µl sample. The BioAnalyser quality assessment gave an RNA Integrity Number (RIN) value of >6.2 and a Nanodrop 2000 spectrophotometer detected a total RNA quality A260/A280 = 1.80-2.07 for each *E.coli* OP50, *E.coli* HM605, and *E.coli* HM605 deletion mutants: Δ*fim*H or Δ*dsb*A sample.

Two control samples, *E.coli* OP50 Control 2 and 3, were RNA sequenced as *E.coli* OP50 Control 1 did not meet Genwiz quality control with a RIN value of 4.4. The quality of Illumina NovaSeq 2x150 bp sequencing, 10 million read pairs, was analysed (*Table 5.3*). FastQC analysis revealed an RNA (cDNA) sequence length of 35-150 base pairs, consistent across all samples brought forward for analysis (*E.coli* OP50 (*n*=2), *E.coli* HM605 (*n*=3), Δ*fim*H (*n*=3) and Δ*dsb*A (*n*=3)), and there were no poor quality reads for these samples sequenced (*Table 5.3*). STAR (Spliced Transcripts Alignment to a Reference), was used to align our reads to the *C. elegans* reference genome, WBcel235. FastQC and STAR alignment detected consistent number of total sequences across the forward and reverse reads of each sample (*Table 5.3*). STAR alignment analysis determined that the percentage of uniquely matched reads was >81% across all samples and the mismatch rate per base was >0.20% in all samples indicating good reliable read matches to the database *C. elegans* genome (WBcel235) as expected (*Table 5.3*).

***Table 5.3*: FastQC and STAR alignment report on RNA sequencing.**

Sample	Total Sequences		Sequences flagged as poor quality	Sequence length	% Uniquely matched reads	% Mismatch rate per base
	Forward	Reverse				
OP50 Control 2	13227860	13227860	0	35-150	89.30	0.18
OP50 Control 3	17186116	17186116	0	35-150	87.42	0.19
HM605 1	19221530	19221530	0	35-150	93.05	0.17
HM605 2	19165886	19165886	0	35-150	92.52	0.17
HM605 3	15512844	15512844	0	35-150	83.72	0.17
Δ*fim*H 1	18491485	18491485	0	35-150	93.39	0.20
Δ*fim*H 2	13027398	13027398	0	35-150	83.41	0.19
Δ*fim*H 3	15900842	15900842	0	35-150	93.77	0.16
Δ*dsb*A 1	12487117	12487117	0	35-150	81.81	0.19
Δ*dsb*A 2	18871702	18871702	0	35-150	92.21	0.18
Δ*dsb*A 3	20091264	20091264	0	35-150	91.77	0.18

Statistics are based on FastQC report and the alignment of the sample reads relative to the *C. elegans* (WBcel235) database using STAR (Spliced Transcripts Alignment to a Reference).

Next, correlation between RNA sample replicates was examined to show agreement between *C. elegans* replicates. All *E.coli* OP50 controls, *E.coli* HM605, and *E.coli* HM605 deletion mutants: Δ*fim*H and Δ*dsb*A replicates had spearman R values greater than 0.9 (*Figure 5.6*), showing that there is very little variation between replicates i.e. there is very little transcriptional noise in the system.

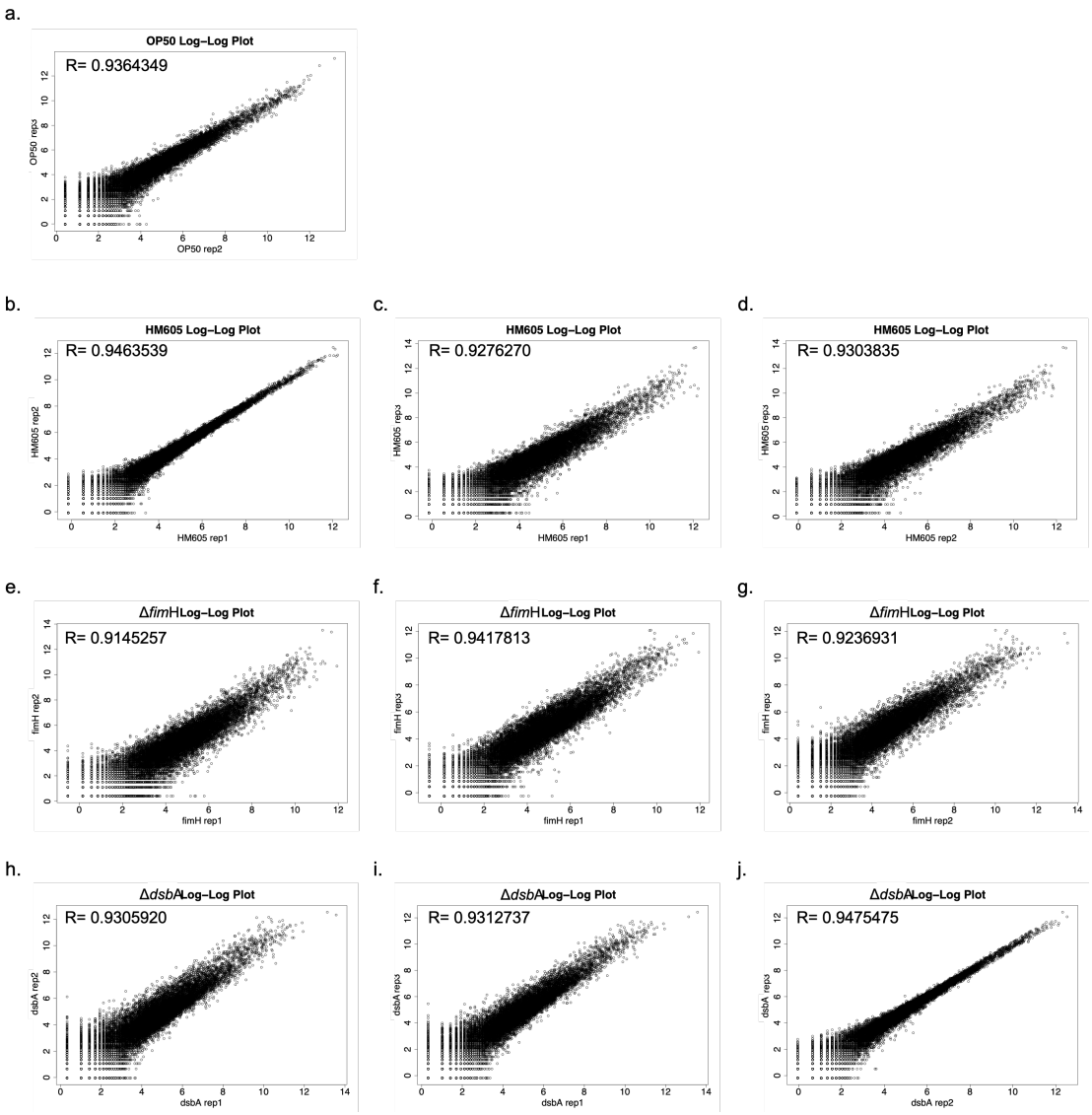


Figure 5.6: **Correlation between RNA sample replicates showing Spearman's rank correlation coefficient R values.** (a) *E. coli* OP50. (b-d) *E. coli* HM605 replicates 1-3. (e-g) Δ*fim*H replicates 1-3. (h-j) Δ*dsb*A replicates 1-3.

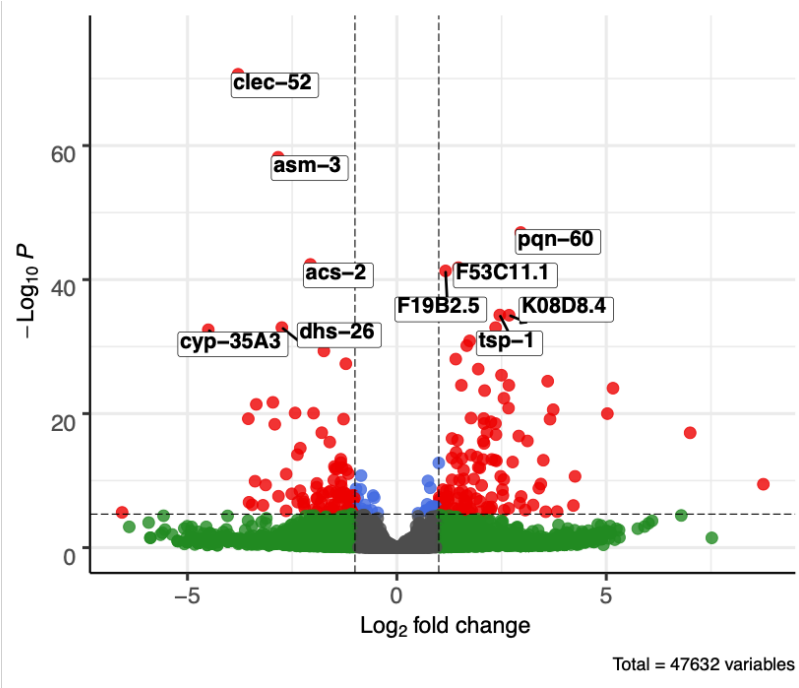
5.2.7 *Escherichia coli* HM605 induced changes in the *Caenorhabditis elegans* transcriptome, compared to the *Escherichia coli* OP50 control

Comparison of *C. elegans* strain SS104 transcriptome cultured with *E. coli* HM605 were compared with nematode cultures with *E. coli* OP50, and this analysis revealed 1647 genes that were significantly differentially expressed, with an adjusted p-value <0.05 (Table appendix V SI.5.7).

Of the 1647 genes differentially regulated, 857 genes were significantly up-regulated in nematodes cultured on *E. coli* HM605 compared to *E. coli* OP50, and 790 genes

were significantly down-regulated. The results showed that the most significantly down-regulated genes included: *clec-52*, *asm-3*, *acs-2*, *dhs-26* and *cyp-35A3* (*Figure 5.7* (a)). Interestingly, *clec-52* has been reported to be involved in defence against Gram-positive bacteria, *asm-3* in lipid droplet assembly, *acs-2* in FA metabolism, *dhs-26* in oxidoreductase activity and *cyp-35A3* is a member of the cytochrome P450 family involved in the response to xenobiotic stimulus. The most significantly up-regulated genes in the *C. elegans* strain SS104 transcriptome included: *pqn-60*, *F53C11.1*, *F19B2.5*, *tsp-1* and *K08D8.4* (*Figure 5.7* (a)). It is perhaps noteworthy that *pqn-60* is affected by *daf-16, daf-2* (pathways involved in longevity and immune response), *and skn-1; F53C11.1*, *tsp-1* and *K08D8.4* have a role in innate immune response; and *F19B2.5* has a predicted ATP binding activity (Alliance WS285) (https://wormbase.org). All 857 genes that were significantly up-regulated were analysed using the gene ontology resource, powered by PANTHER (Ashburner *et al.,* 2000; Mi *et al.,* 2019; Consortium, 2021). This analysis revealed that *E. coli* HM605 significantly increased the expression of genes in the *C. elegans* strain SS104 transcriptome that are predicted to be involved in the innate immune response, endoplasmic reticulum unfolded protein response, cellular component organisation and protein and cellular metabolic processes (*Figure 5.7* (b)). Similarly, all 790 genes that were significantly down-regulated in *C. elegans* strain SS104 transcriptome cultured with *E. coli* HM605 ,compared to *E. coli* OP50, were predicted to be involved in regulating chromatin assembly, monocarboxylic acid metabolic process, cellular nitrogen compound metabolic process and primary metabolic process (*Figure 5.7* (b)).

a.



b.

Innate immune response
Endoplasmic reticulum unfolded protein response
Cellular component organisation
Protein metabolic process
Cellular metabolic process

Chromatin assembly
Monocarboxylic acid metabolic process
Cellular nitrogen compound metabolic process

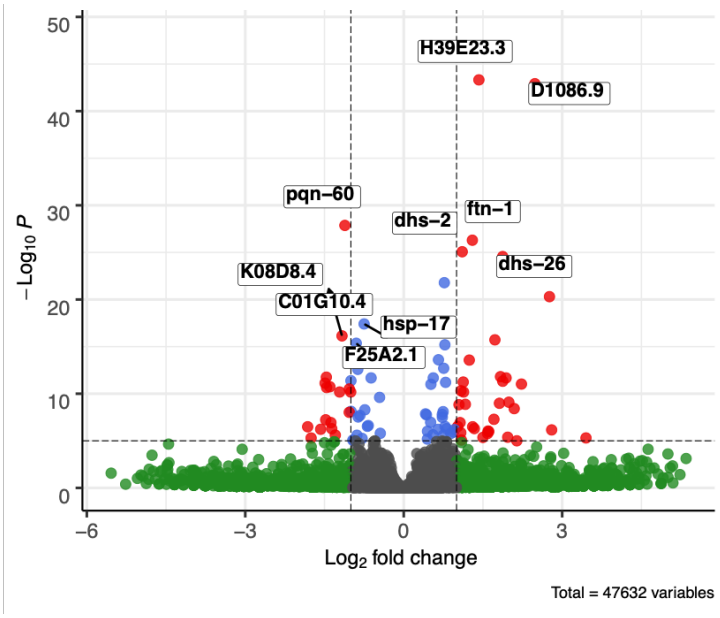
***Figure 5.7: Caenorhabditis elegans* strain SS104 transcriptome when cultured with *Escherichia coli* HM605, compared to *Escherichia coli* OP50.** (a) Volcano plot of genes in *C. elegans* strain SS104 transcriptome cultured with *E. coli* HM605, compared to *E. coli* OP50, showing the top five statistically significantly down- and up-regulated transcribed genes. (b) *C. elegans* biological pathways effected by *E. coli* HM605, compared to *E. coli* OP50, with a false discovery rate (FDR) p<0.05.

5.2.8 *Escherichia coli* HM605 deletion mutant, Δ*dsb*A, induced changes in the *Caenorhabditis elegans* transcriptome, compared to *Escherichia coli* HM605

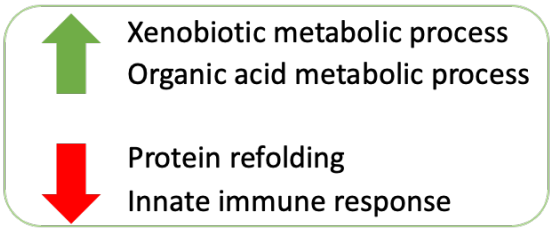
As mentioned above, Δ*fim*H was used as a control for defective fimbrial function in Δ*dsb*A. *E. coli* HM605 was used as a control to determine the specific gene changes that occur in the nematode when the *dsb*A and *fim*H genes are deleted in the AIEC HM605. Similar analysis of differentially expressed genes in *C. elegans* strain SS104 transcriptome cultured with Δ*dsb*A, compared to *E. coli* HM605, revealed 739 genes that were significantly differentially expressed in the nematode, with an adjusted p-value <0.05 (Table appendix V SI.5.9). Significantly differentially expressed genes in the *C. elegans* strain SS104 transcriptome were determined in the Δ*fim*H samples and this analysis identified 721 genes that were significantly differentially expressed compared to *E. coli* HM605, with an adjusted p-value <0.05 (Table appendix V SI.5.8). Culturing nematodes with Δ*dsb*A resulted in the significant down-regulation of 312 genes in the *C. elegans* strain SS104 transcriptome compared to nematode cultured on *E. coli* HM605. The most significantly down-regulated genes in the *C. elegans* strain SS104 transcriptome included: *pqn-60*, *C01G10.4*, *hsp-17*, *K08D8.4* and *F25A2.1* (*Figure 5.8* (a)). Interestingly, *pqn-60* and *C01G10.4* are affected by *daf-16, daf-2* (pathways involved in longevity and immune response)*, and skn-1; hsp-17* is a heat shock protein; *K08D8.4* has a role in innate immune response; and *F25A2.1* is predicted to be involved in the lipid metabolic process. On the other hand, culturing nematodes with Δ*dsb*A resulted in the significant up-regulation of 427 genes in the *C. elegans* strain SS104 transcriptome, compared to culturing with *E. coli* HM605. The most significantly up-regulated genes included: *H39E23.3*, *D1086.9*, *ftn-1*, *dhs-2* and *dhs-26* (*Figure 5.8* (a)). *H39E23.3* has a role in microtubule binding activity; *D1086.9* is affected by *daf-16, daf-2, and skn-1; ftn-1* is involved in identical protein binding activity; *dhs-2* and *dhs-26* are involved in oxidoreductase activity (Alliance WS285) (https://wormbase.org). All 427 genes that were significantly up-regulated were analysed using the gene ontology resource, powered by PANTHER (Ashburner *et al.,* 2000; Mi *et al.,* 2019; Consortium, 2021). This analysis revealed that Δ*dsb*A significantly affected genes in *C. elegans* strain SS104 transcriptome involved in xenobiotic metabolic process and organic acid metabolic process (*Figure 5.8* (b)).

Similarly, Δ*dsb*A significantly down-regulated 312 genes that were involved in *C. elegans* strain SS104 protein refolding and innate immune response (*Figure 5.8* (b)). Culturing nematodes with Δ*fim*H resulted in a transcriptome that was similar to Δ*dsb*A, but also different to *E. coli* HM605. *F19B2.5* which is predicted to be involved in ATP binding activity, was significantly down-regulated in *C. elegans* strain SS104 cultured with Δ*fim*H (*Figure 5.8* (c)) but up-regulated in *E. coli* HM605 (*Figure 5.7* (a)). *D1086.9*, affected by *daf-16, daf-2* (pathways involved in longevity and immune response)*, and skn*-1, was significantly up-regulated in *C. elegans* strain SS104 cultured with Δ*fim*H (*Figure 5.8* (c)) and Δ*dsb*A (*Figure 5.8* (a)) (Alliance WS285) (https://wormbase.org). All 465 genes that were significantly up-regulated were analysed using the gene ontology resource, powered by PANTHER (Ashburner *et al.,* 2000; Mi *et al.,* 2019; Consortium, 2021). This analysis revealed that Δ*fim*H significantly affected the *C. elegans* strain SS104 transcription of genes involved in macromolecule metabolic process, primary metabolic process, nitrogen compound metabolic process and cellular metabolic process, compared to *E. coli* HM605 (*Figure 5.8* (d)). Similarly, Δ*fim*H significantly down-regulated 256 genes that were involved in *C. elegans* strain SS104 cuticle development including: collagen and cuticulin-based cuticle molting cycle, and translation (*Figure 5.8* (d)). Δ*fim*H and *E. coli* HM605 both up-regulate cellular metabolic processes, however Δ*fim*H up-regulates primary metabolic processes, with *E. coli* HM605 down-regulating this process in the *C. elegans* strain SS104 transcriptome. *E. coli* HM605 up-regulated the innate immune response in the nematode, with Δ*dsb*A down-regulating this response in the *C. elegans* strain SS104 transcriptome. Δ*dsb*A's down-regulation of the *C. elegans* strain SS104 innate immune response may be key to its ability in extending lifespan, compared to *E. coli* HM605.

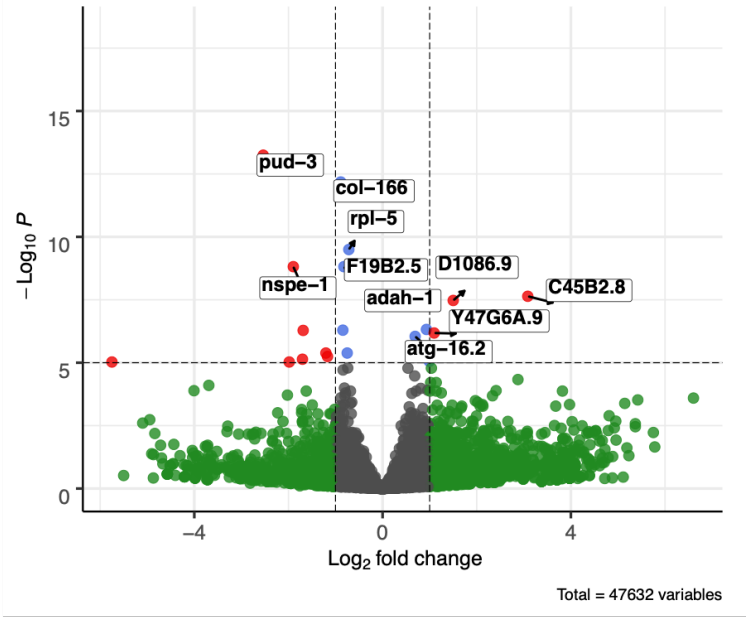
a.


H39E23.3
D1086.9
pqn–60
dhs–2
ftn–1
dhs–26
K08D8.4
C01G10.4
hsp–17
F25A2.1
50
40
30
20
10
0
−Log10 P
−6
−3
0
3
Log2 fold change
Total = 47632 variables

b.


Xenobiotic metabolic process
Organic acid metabolic process
Protein refolding
Innate immune response

c.


pud–3
col–166
rpl–5
F19B2.5
D1086.9
nspe–1
adah–1
C45B2.8
Y47G6A.9
atg–16.2
15
10
5
0
−Log10 P
−4
0
4
Log2 fold change
Total = 47632 variables

d.

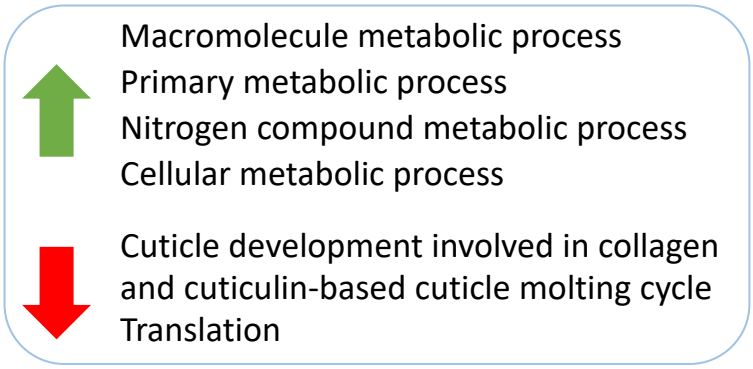


***Figure 5.8: Caenorhabditis elegans* strain SS104 transcriptome when cultured with *Escherichia coli* HM605 deletion mutants: Δ*dsb*A and Δ*fim*H, compared to *Escherichia coli* HM605.** Volcano plot of genes in *C. elegans* strain SS104 transcriptome cultured with (a) Δ*dsb*A, and (c) Δ*fim*H, compared to *E. coli* HM605, showing the top five statistically significantly down- and up-regulated transcribed genes. *C. elegans* biological pathways effected by (c) Δ*dsb*A, and (d) Δ*fim*H, compared to *E. coli* HM605, with a false discovery rate (FDR) p<0.05.

5.2.9 The transcription of *Caenorhabditis elegans* genes involved in immune response and longevity, were altered by *Escherichia coli* strains

The transcription of *C. elegans* genes involved in immune response and longevity pathways were examined. The key pathways that play a role in *C. elegans* immune response include: DAF-2/DAF-16, and KGB-1 and FOS-1 pathways (*Figure 5.9* (a)), MAP kinase calcium signalling pathway (*Figure 5.9* (b)), NHR-80 transcription pathway (*Figure 5.9* (c)) and CED-9 apoptosis pathway (*Figure 5.9* (d)).

- The *ins-8* gene is predicted to encode an insulin/insulin-like peptide ligand that is an agonist for the DAF-2 pathway (Zheng *et al.,* 2018). Nematodes cultured on *E. coli* HM605 showed a decreased level of *ins-8* expression compared to worms cultured on *E. coli* OP50, suggesting a possible increase in DAF-16 translocation into the nucleus and subsequent immune response, Δ*fim*H however, up-regulated *ins-8* expression suggesting an inhibition of DAF-16 translocation and lack of immune response (*Figure 5.9* (a)). AKT-1/AKT-2 phosphorylation prevents DAF-16 translocation into the nucleus

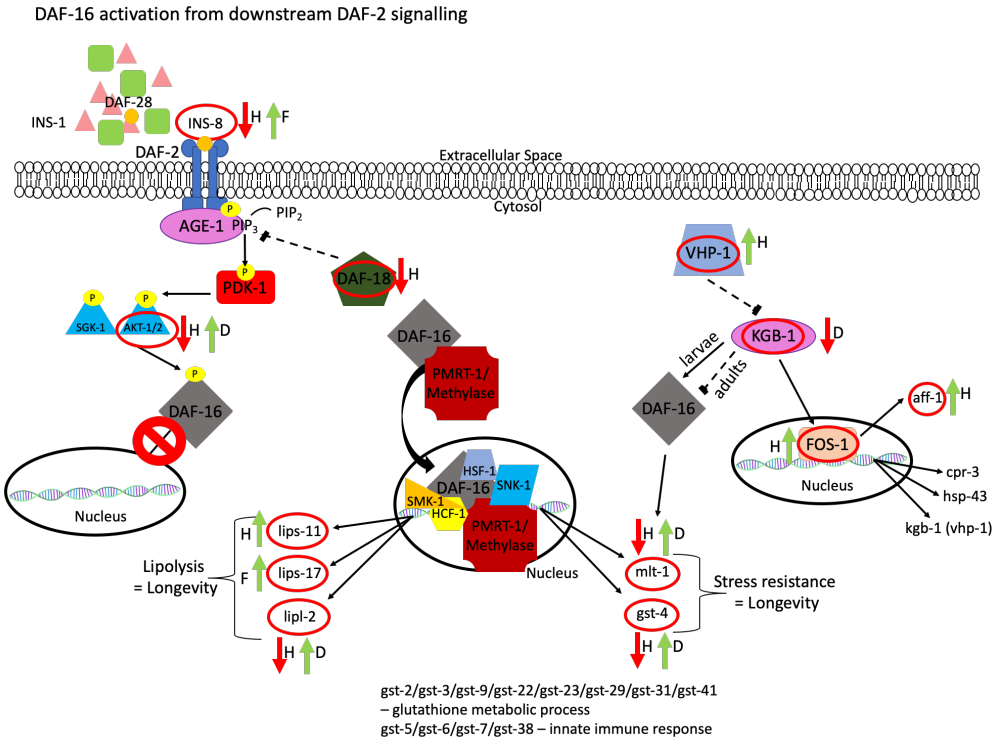
(*Figure 5.9* (a)). *akt-2* and *akt-1* are both down-regulated in *E. coli* HM605 (*Figure 5.9* (a)) suggesting DAF-16 translocation into the nucleus and activation of immune response genes. This data suggests *E. coli* HM605, through DAF-16 translocation to the nucleus, induces an innate immune response in *C. elegans* strain SS104 (*Figure 5.9* (a)). *akt-1* is up-regulated in nematodes cultured on the Δ*dsb*A mutant (*Figure 5.9* (a)) suggesting DAF-16 translocation is inhibited with a reduction in immune response (*Figure 5.9* (a)).

- Interestingly, downstream of DAF-16 signalling, *lips-11* is increased and *lipl-2* is decreased in nematodes cultured on *E. coli* HM605, compared to *E. coli* OP50. Similarly, *lips-17* and *lipl-2* are increased in nematodes cultured on Δ*fim*H and Δ*dsb*A, respectively, suggesting that lipolysis is elevated in these nematodes, compared to *E. coli* HM605 (*Figure 5.9* (a)). Indeed both *mlt-1* and *gst-4*, downstream of DAF-16 signalling, are down-regulated in *E. coli* HM605, compared to *E. coli* OP50, and up-regulated in Δ*dsb*A, compared to *E. coli* HM605, affecting the nematode's response to stress resistance (*Figure 5.9* (a)).
- *vhp-1* is up-regulated in worms cultured on *E. coli* HM605, along with downstream *fos-1* and *aff-1*, reducing stress resistance and shortening lifespan in adults (Zhang *et al.,* 2017), and oviposition and syncytium formation by plasma membrane fusion, compared to *E.coli* OP50. Interestingly, *kgb-1*, downstream of *vhp-1*, was down-regulated in Δ*dsb*A, compared to *E. coli* HM605 (*Figure 5.9* (a)).
- UNC-43 is involved in MAP kinase pathway (*Figure 5.9* (b)). *E. coli* HM605 up-regulated *unc-43*, compared to *E. coli* OP50, suggesting an increase in calcium signalling and olfactory behaviour, including a role in neuronal control of lipid metabolism.
- Downstream of NHR-80, *fat-3* and *fat-6* were down-regulated in *E. coli* HM605, compared to *E. coli* OP50, and up-regulated in Δ*dsb*A, compared to *E. coli* HM605, *fat-3* was also up-regulated in Δ*fim*H, compared to *E. coli* HM605 (*Figure 5.9* (c)), suggesting an increase in FA synthesis and

desaturation in Δ*dsb*A and Δ*fim*H, but decreased in *E. coli* HM605. *fat-7* was up-regulated in *E. coli* HM605, compared to *E. coli* OP50, and down-regulated in Δ*dsb*A, compared to *E. coli* HM605 (*Figure 5.9* (c)), suggesting an increase in lipid synthesis in nematodes cultured with *E. coli* HM605, but a decrease in Δ*dsb*A.

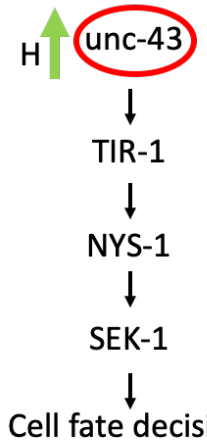
- *hus-1* was down-regulated in nematodes grown on the Δ*dsb*A mutant, compared to *E. coli* HM605 (*Figure 5.9* (d)), suggesting a decrease in DNA damage and subsequent CED-9 apoptosis pathway.
- *clk-1* is a gene involved in biological timing, in which a mutation *(qm30)* induces longevity in *C. elegans* (Wong *et al.,* 1995). Both *E. coli* HM605 and Δ*dsb*A significantly down-regulated *C. elegans* strain SS104 *clk-1* expression (*Figure 5.9* (e)).
- *sodh-1* was up-regulated in nematodes grown on the Δ*dsb*A mutant, compared to *E. coli* HM605. This gene is involved in the sorbitol pathway, which has been suggested to be involved in *C. elegans* longevity through the osmotic stress response (Chandler-Brown *et al.,* 2015).
- Other genes examined have a role heat shock response (*hsp*), neurodegeneration (*asp*), egg-laying defects (*egl*) and apoptosis.

a.

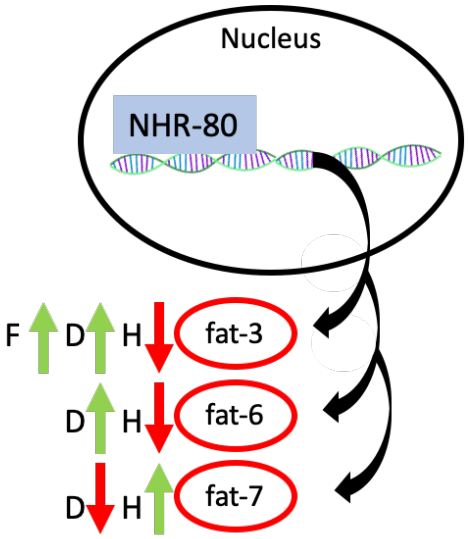


b.

Calcium signalling

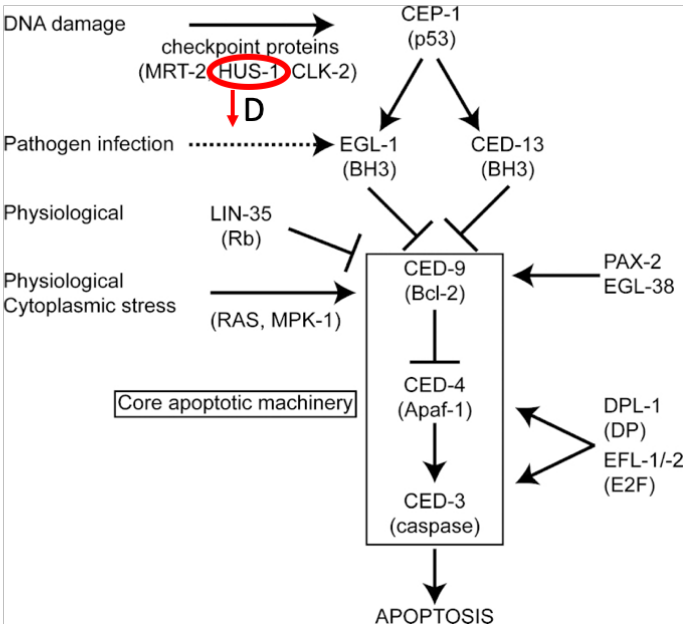


c.



Fatty Acid desaturation
Lipid synthesis

d.


DNA damage
checkpoint proteins
(MRT-2 HUS-1 CLK-2)
D
CEP-1
(p53)
Pathogen infection
EGL-1
(BH3)
CED-13
(BH3)
Physiological
LIN-35
(Rb)
Physiological
Cytoplasmic stress
(RAS, MPK-1)
CED-9
(Bcl-2)
PAX-2
EGL-38
Core apoptotic machinery
CED-4
(Apaf-1)
DPL-1
(DP)
EFL-1/-2
(E2F)
CED-3
(caspase)
APOPTOSIS

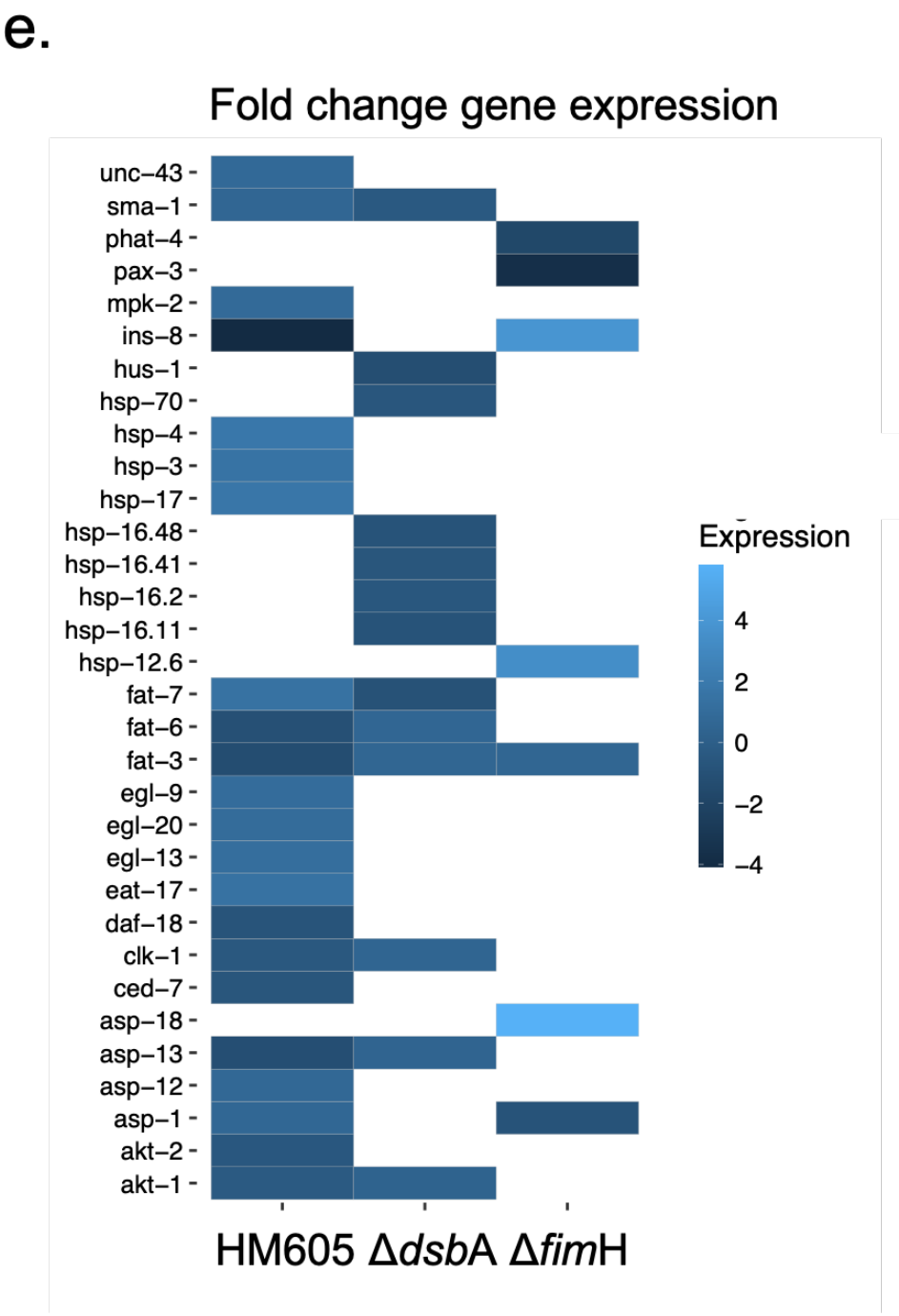


Figure 5.9: Caenorhabditis elegans **longevity and immune response signalling pathways.** (a) DAF-2/DAF-16, and KGB-1 and FOS-1 pathways. (b) MAP kinase calcium signalling pathway. (c) NHR-80 transcription pathway. (d) CED-9 apoptosis pathway (Gartner *et al.* 2008). (e) Heatmap showing significantly up- and down-regulated genes of interest of *C. elegans* strain SS104 transcriptome, induced by *E. coli* HM605, Δ*fim*H and Δ*dsb*A. Red circles in (a-d) highlight genes of interest in, green arrows illustrate significantly up-regulated genes, red arrows illustrate significantly

down-regulated genes, a 'H' next to the arrow indicates that this is present in *E. coli* HM605, an 'F' next to the arrow indicates that this is present in Δ*fim*H and a 'D' next to the arrow indicates that this is present in Δ*dsb*A.

In conclusion, from this data, it is clear that HM605, Δ*fim*H and Δ*dsb*A all have distinct effects on *C. elegans* strain SS104 transcriptome. We hypothesise that *E. coli* HM605 ultimately reduces *C. elegans* lifespan through increasing the innate immune response by promoting DAF-2/DAF-16 signalling, VHP-1 signalling, lipid synthesis and inhibiting FA synthesis. Deleting the *dsb*A gene in *E. coli* HM605 reverses some of these detrimental effects, extending *C. elegans* lifespan to that of *E. coli* OP50 and reversing the changes in the *C. elegans* transcriptome observed when the nematodes are cultured on *E. coli* HM605.

5.3 Discussion

Adherent invasive *Escherichia coli* (AIEC), HM605, is associated with Crohn's disease (CD), a debilitating disease with no cure (Clarke *et al.,* 2011). This study has shown that *E. coli* HM605 consistently reduced *C. elegans* lifespan both in temperature-sensitive SS104 strain at L1 and L4 larval stages, and wild-type N2 strain at the L4 larval stage. This is consistent with the *C. elegans* lifespan reduction previously reported for the AIEC LF82 (Simonsen *et al.,* 2011b). Similar to *E. coli* LF82, *C. elegans* lifespan reduction was abolished when cultured on heat-killed *E. coli* HM605 (appendix V SI.5.2). This suggests that live *E. coli* HM605, with an active metabolism, are required for the observed reduction in *C. elegans* lifespan. *E. coli* HM605 also consistently reduced the lifespan of CB1370, a *C. elegans* strain with a *daf-2* mutation (appendix V SI.5.2). As the *E. coli* HM605 phenotype remained unchanged, it is suggested that *daf-2* is not required for *E. coli* HM605 lifespan reduction, as was also observed with *E. coli* LF82 (Simonsen *et al.,* 2011a), although this does not rule out a role for *daf-16* in *E. coli* HM605 reduction in *C. elegans* lifespan. *E. coli* HM605 also consistently colonises the *C. elegans* gut, with the level of colonisation increasing over time, but any associated histological changes associated with this colonisation were not examined. *E. coli* LF82 has already been reported to colonise the *C. elegans*

gut and damage its epithelial surface (Simonsen *et al.,* 2011b). *E. coli* HM605 induced an increase in innate immune response in *C. elegans* strain SS104. DAF-16 can regulate innate immune response in *C. elegans* and this protein has been shown to respond to bacterial infection (Palominos *et al.,* 2017; Zhao *et al.,* 2017). The hyperactivation of DAF-16 has also been reported to increase *C. elegans* susceptibility to bacterial infections (Singh and Aballay, 2009). Nematodes cultured on *E. coli* HM605 showed a decreased level of *ins-8* expression, an insulin/insulin-like peptide ligand that is an agonist for the DAF-2 pathway (Zheng *et al.,* 2018). *akt-2* and *akt-1* were also both down-regulated in *E. coli* HM605, compared to worms cultured on *E. coli* OP50, suggesting that DAF-16 is not phosphorylated and can therefore translocate into the nucleus and activate immune response genes. Interestingly, three of the top five significantly up-regulated genes in *C. elegans* strain SS104 treated with *E. coli* HM605, compared to *E. coli* OP50, have a role in innate immune response: *F53C11.1*, *tsp-1* and *K08D8.4* (WormBase (https://wormbase.org//#012-34-5)). *mpk-2*, involved in enabling the MAP kinase pathway, was also significantly up-regulated, suggesting that *E. coli* HM605 treated *C. elegans* strain SS104, compared to *E. coli* OP50, has the potential to activate pathogen resistance pathways in *C. elegans*. *vhp-1* was also up-regulated in *E. coli* HM605, along with downstream *fos-1*, reducing stress resistance and shortening lifespan in adults (Zhang *et al.,* 2017). This transcriptome data strongly suggests that *E. coli* HM605 induces an immune response in *C. elegans*, which is key to *E. coli* HM605 virulence, resulting in reduced survival of *C. elegans*, and therefore an overall reduction in lifespan. AIEC are believed to induce increased inflammation in CD, with interferon γ (IFNγ) being spontaneously released by lymphocytes in the lamina propria of the intestine in CD patients (Fais *et al.,* 1991). Increased levels of cytokine IL-12 and T helper type 1 (Th1) cells are also found in CD (Monteleone *et al.,* 1997; Parronchi *et al.,* 1997), with *E. coli* HM605 having the capacity to invade and replicate within epithelial and macrophage cells (Thompson *et al.,* 2016). *E. coli* HM605 virulence has been shown to induce TNF-α, IL-6, IL-23, CD40, and CD80 (Olivares-Morales *et al.,* 2018), supporting our hypothesis that HM605-induced immune response is key to reducing the lifespan of *C. elegans*.

Of the 29 HM605 deletion mutations screened, Δ*dsb*A showed the most significant increase in lifespan, particularly in *C. elegans* strain SS104. This is in contrast to studies with *E. coli* LF82, where *C. elegans* strain SS104 survival remained unchanged whether cultured on *E. coli* LF82 or *E. coli* LF82 Δ*dsb*A (Simonsen *et al.,* 2011b), suggesting that perhaps *E. coli* HM605 and *E. coli* LF82 induce pathogenicity, using different mechanisms. In this study, our data also showed that the *glp-4(bn2)* mutation present in the SS104 nematode may render the worm more sensitive to the effects of Δ*dsb*A. It has been reported that the loss of the *C .elegans* germline results in extended lifespan (Hsin and Kenyon, 1999). The *glp-4(bn2)* mutation also has an increased immune response to specific pathogens (TeKippe and Aballay, 2010). Δ*dsb*A appears to reduce the innate immune response in *C. elegans*, which perhaps could be seen more clearly in the *glp-4(bn2)* mutation SS104 strain, compared to the wild-type N2 *C. elegans* strain. Interestingly, this was in contrast to the transcriptome changes induced by *E. coli* HM605. Indeed, *akt-1* was up-regulated in *C. elegans* strain SS104 cultured on Δ*dsb*A, compared to *E. coli* HM605, suggesting DAF-16 translocation is inhibited with a reduction in immune response. Indeed, only one of the top five significantly down-regulated genes in *C. elegans* strain SS104 incubated with Δ*dsb*A, compared to *E. coli* HM605, had a role in innate immune response, *K08D8.4* (WormBase (https://wormbase.org//#012-34-5)). Interestingly, HM605 significantly down-regulated gene *dhs-26*, which has a role in oxidoreductase activity, whereas Δ*dsb*A significantly up-regulated both *dhs-26* and *dhs-2*, another gene with a role in oxidoreductase activity (WormBase (https://wormbase.org//#012-34-5)). This suggests that oxidoreductase activity may also be critical for normal *C. elegans* survival and lifespan. Interestingly, Δ*dsb*A significantly down-regulated *hus-1*, a gene involved in cell death through the activation of a BH3 domain protein by p53, resulting in the expression of the proapoptotic gene *egl-1* (Hofmann *et al.,* 2002). Therefore, down-regulation of *hus-1* may promote *C. elegans* survival and lifespan. *kgb-1*, downstream of *vhp-1*, was also down-regulated in Δ*dsb*A, compared to *E. coli* HM605. *vhp-1* is upstream of *kgb-1* and is involved in reducing stress resistance and shortening lifespan in adults

(Zhang *et al.,* 2017), therefore Δ*dsb*A potentially induces lifespan extension in *C. elegans* through down-regulation of *kgb-1* and the *vhp-1* pathway.

Heat-shock proteins (HSPs) have been shown to have a role in longevity and immunity upon bacterial infection (Prithika *et al.,* 2016). Several *hsp* genes are significantly up-regulated in *C. elegans* in response to *E. coli* HM605 and comparatively significantly down-regulated in response to Δ*dsb*A. *sgk-1* is also significantly up-regulated by *E. coli* HM605 which links the DAF-2/DAF-16 pathway with the heat shock pathway (Prithika *et al.,* 2016). This again supports the hypothesis that *E. coli* HM605 is activating the *C. elegans* immune response which is reducing its lifespan, while the Δ*dsb*A mutation is preventing a *C. elegans* immune response allowing the nematode to live a longer lifespan than seen when cultured on *E. coli* HM605. Lastly, the changes seen in *fat* genes, in response to *E. coli* HM605 and Δ*dsb*A suggest they are having opposing effects on *C. elegans* fat metabolism. FA synthesis and desaturation may be increased in Δ*dsb*A and Δ*fim*H, but decreased in *E. coli* HM605, and lipid synthesis may be increased in *E. coli* HM605, but decreased in Δ*dsb*A. Indeed the *clk-1* gene, which is involved in biological timing, in which a mutation *(qm30)* induces longevity in *C. elegans* (Wong *et al.,* 1995), is significantly down-regulated in *E. coli* HM605 and Δ*dsb*A, suggesting that overall, *E. coli* HM605 and Δ*dsb*A may also be affecting *C. elegans* biological processes such as biological timing as well as fat and lipid metabolism.

Analysis of the *C. elegans* expression profile cultured with Δ*fim*H shows some similarities with that of nematodes cultured with *E. coli* HM605, but overall appears to be distinct from Δ*dsb*A. Δ*fim*H up-regulated *ins-8* expression suggesting a reduction in DAF-16 translocation into the nucleus and a decrease in immune response. Δ*fim*H also significantly up-regulated *hsp-12.6*, although *sgk-1* expression was not significantly different. Lastly, Δ*fim*H up-regulated *asp-18* expression, suggesting an increase in cell death. Δ*fim*H therefore, affects *C. elegans* transcriptome differently to *E. coli* HM605, but does not restore *C. elegans* lifespan

to that of nematodes when feeding on Δ*dsb*A, which behaves independently to Δ*fim*H.

Recently, studies have focused on anti-bacterials targeting bacterial virulence, using inhibitors such as those targeting *dsb*A, blocking the oxidative protein folding process forming virulence factors in pathogens (Bocian-Ostrzycka *et al.,* 2017; Dhouib *et al.,* 2021; Verderosa *et al.,* 2021). These inhibitors target the specific *dsb*A sites for substrate binding, to prevent correct protein folding, including: the redox (CXXC) active site, the hydrophobic patch and the cis-proline (highly-conserved, Pro151 in EcDsbA) loop (Smith *et al.,* 2016). Our analysis has shown that indeed, Δ*dsb*A reverses some of the virulent effects that *E. coli* HM605 induces on *C. elegans* lifespan and transcriptome. Δ*dsb*A reduced the innate immune response which is detrimental to *C. elegans* when cultured on *E. coli* HM605, by decreasing the DAF-2/DAF-16 signalling pathway, increasing transcription of genes involved in stress resistance, as well as down-regulating *hus-1* promoting *C. elegans* survival and lifespan. In our study, it is clear that *dsb*A may be the most valuable target of AIEC to help prevent the debilitating effects of Crohn's disease, demonstrating that a single mutation in the food source (*E. coli* HM605) can have significant consequences in terms of host gene expression and in turn, physiology.

Future Work

To move this work forward, Real-Time Quantitative Reverse Transcription PCR (qRT-PCR) could be performed to examine DAF-2/DAF-16 signalling, VHP-1 signalling and immune response signalling pathways in *C. elegans* wild-type strain N2, at reproductive adult, cultured on control *E. coli* OP50, AIEC HM605 and *E. coli* HM605 deletion mutant Δ*dsb*A. A large-scale proteomics study could be carried out to analyse the changes in protein profiles in *C. elegans* wild-type strain N2, cultured on control *E. coli* OP50, AIEC HM605 and *E. coli* HM605 deletion mutant Δ*dsb*A, identifying human protein homologs. This would have the potential to determine the specific proteins that may be involved in reducing virulence in humans and promoting longevity.

This study demonstrates that Δ*dsb*A reduces *C. elegans* innate immune response, by inhibiting DAF-2/DAF-16 signalling, VHP-1 signalling, FA synthesis and promoting lipid synthesis, the stress response and apoptosis pathways, promoting longevity and reducing virulent potential. This study cements the potential use of antibacterials, such as targeting the disulfide forming pathways of the *dsb*A gene, instead of antibiotics for the treatment of human infection and disease, such as Crohn's Disease.

Chapter 6 – General Discussion

The main findings of this study and contributions to the scientific field include:

- Bacterial intervention alters BA concentrations, restores gut health parameters and behavioural deficits in a mouse model of ASD.
- Sinemet (L-DOPA and decarboxylase inhibitor) reduces BA and increases FA levels in the gut of PD patients.
- Primary and secondary BAs influence the lifespan and development of the model of aging, *C. elegans*.
- *E. coli* HM605 reduces *C. elegans* lifespan and promotes an innate immune response, Δ*dsb*A reverses these changes.

Understanding healthy aging is becoming increasingly important to close the gap between healthy years and life expectancy, and delay the onset of age-related diseases. Scientists have focused on (1) targeting the nine biochemical hallmarks of aging: genomic instability, telomere attrition, epigenetic alterations, loss of proteostasis, deregulated nutrient sensing, mitochondrial dysfunction, cellular senescence, stem cell exhaustion, and altered intercellular communication, and (2) developing potential interventions that may help restore these aging biochemical hallmarks, namely, nutritional, pharmaceutical and genetic (López-Otín *et al.,* 2013). However, there is evidence to suggest a role for diet, gut microbes and their associated metabolites in aging. Our gut microbiome has specific immune functions and digestion roles along the gastrointestinal tract and its composition changes as we age. From birth our gut microbes are constantly changing, until they stabilise at 3 years of age, and only change based on our diet and environment, such as exposure to toxins, pathogens and intake of antibiotics (Jandhyala *et al.,* 2015). As we enter old age, our gut microbial community can alter in relation to disease states (Ghosh *et al.,* 2022). Although each gut microbiota profile is unique to each individual, the relative abundance of *Bacteroides* has been shown to be elevated in individuals over the age of 65 (Claesson *et al.,* 2011), and the relationship, between a varied diet, a diverse gut microbial community and favourable host health, has been demonstrated (Claesson *et al.,* 2012). Indeed, changes in metabolism have been reported between

adult and aged mice (Binyamin *et al.,* 2020), and faecal microbial transplants (FMTs) have shown their potential as treatment therapies for aging. FMT from aged mice to adult mice resulted in an elevation of metabolic rate (measured by respiratory quotient - ratio carbon dioxide produced to oxygen consumed), as well as an increase in insulin levels and fat body mass (Binyamin *et al.,* 2020). FMT from aged mice to young, results in impaired cognitive functions such as spatial learning and memory (D'Amato *et al.,* 2020). Interestingly, this FMT also resulted in a decrease of abundance of *Lachnospiraceae*, *Faecalibaculum*, and *Ruminococcaceae*, and *Prevotellaceae* and *Ruminococcaceae*, involved in the production of SCFAs and involved in central nervous system (CNS) disorders, respectively (D'Amato *et al.* 2020). Another study found FMT from aged mice to young mice enhanced age-associated CNS inflammation, cytokine signalling, retinal inflammation, including loss of functional proteins in the eye, and intestinal permeability, which can be reversed by FMT by young mice (Parker *et al.,* 2022). In Senescence Accelerated Mouse-Prone 8 (SAMP8) mice, FMT from young donors improved exploration and locomotor abilities, and there was a notable increase in the abundance of *Akkermansia* in young mice who had received an FMT from older mice to (Zhang *et al.,* 2022). Interestingly, FMT from young mice restored gut microbial composition and diversity in older mice (Wang *et al.,* 2022), along with an increase in ovarian function, a relative abundance of *Bifidobacterium* and *Ruminococcaceae*, anti-inflammatory cytokine IL-4 and a decrease in pro-inflammatory cytokine IFN-γ (Xu *et al.,* 2022).

In our studies, we examined metabolite changes that could be related to properties of the gut microbiota and their influences on potential cellular signalling to metabolic or systemic health, with the hypothesis that diet or bacterial intervention may help to improve the host-microbe dialogue in aging. We examined gut microbiota and metabolite changes in both disease states of the (1) young, Crohn's Disease (CD) and Autism Spectrum Disorder (ASD), as early intervention may increase overall health-span and lifespan and disease states that are (2) age-related, particularly Parkinson's Disease (PD). Diversity of the faecal and mucosal microbiome has been reported to be reduced in CD, with an increase in adherent-invasive *Escherichia coli* (AIEC) species (Giaffer *et al.,* 1992). We examined the AIEC, HM605 (Clarke *et al.,* 2011),

which is similar to LF82, an AIEC that is also capable of invading and replicating within epithelial and macrophage cells (Boudeau *et al.,* 1999). AIEC LF82 has the ability to reduce *C. elegans* lifespan, however, this effect is reversed in the absence of live culture, suggesting that live AIEC LF82, with an active metabolism, are required for the observed reduction in *C. elegans* lifespan (Simonsen *et al.,* 2011b). We have shown that AIEC HM605 works in a similar manner, needing to be metabolically active to induce its virulence. AIEC induces increased inflammation in CD, with interferon γ (IFNγ) being spontaneously released by lymphocytes in the lamina propria of the intestine in CD patients (Fais *et al.,* 1991). Increased levels of cytokine IL-12 and T helper type 1 (Th1) cells are also found in CD (Monteleone *et al.,* 1997; Parronchi *et al.,* 1997). AIEC HM605 virulence has been shown to induce TNF-α, IL-6, IL-23, CD40, and CD80 (Olivares-Morales *et al.,* 2018). We showed that AIEC HM605 increased the innate immune response in *C. elegans*. DAF-16 can regulate innate immune response in *C. elegans* and this protein been shown to respond to bacterial infection (Palominos *et al.,* 2017; Zhao *et al.,* 2017). Hyperactivation of DAF-16 has also been reported to increase *C. elegans* susceptibility to bacterial infections (Singh and Aballay, 2009). AIEC HM605 has the ability to invade and replicate within epithelial and macrophage cells (Thompson *et al.,* 2016). AIEC LF82 colonises the *C. elegans* gut, damaging its epithelial surface, and its virulence does not depend on genes *dsb*A nor *fim*H, but rather on a functioning Hfq RNA chaperone (Simonsen *et al.,* 2011b). We found AIEC HM605 also colonises the *C. elegans* gut, however, its virulence is dependent on a functioning *dsb*A gene. This study identified the AIEC HM605 deletion mutation, Δ*dsb*A, as a potential therapeutic for CD, by extending the reduced lifespan and reversing the in innate immune response of *C. elegans* when cultured on AIEC HM605. Interestingly, a recent study discusses that an AIEC strains' ability to reduce *C. elegans*' lifespan may not directly correlate with their virulence levels, indicating that pathogenicity varies between AIEC strains (de Sousa Figueiredo *et al.,* 2021). Indeed, recent studies have focused on anti-bacterials, targeting bacterial virulence, using inhibitors such as those targeting *dsb*A, blocking the oxidative protein folding process forming virulence factors in pathogens (Bocian-Ostrzycka *et al.,* 2017; Dhouib *et al.,* 2021; Verderosa *et al.,* 2021). These inhibitors target the specific *dsb*A sites for substrate binding, to prevent correct toxic secretory

protein folding, including: the redox (CXXC) active site, the hydrophobic patch and the cis-proline (highly-conserved, Pro151 in EcDsbA) loop (Smith *et al.,* 2016). This study demonstrates the significant consequences a single mutation in the food source (AIEC HM605) could have in terms of host health and longevity, also cementing the potential use of antibacterials, rather than antibiotics, for the treatment of human infection and disease, such as CD.

Manipulation of the host diet has the potential to improve aging through manipulation of gut signalling. Oral administration of specific, safe, bacterial cultures can help restore the gut microbial balance, and alterations in signalling molecules BAs and FAs can provide a read out of modification to human and dietary produced metabolites, respectively. Autism Spectrum Disorder (ASD), a neurodevelopmental disorder characterised by social and communication impairments, limited interests and repetitive behaviours, is typically diagnosed during childhood. Early intervention may improve overall health-span and lifespan. No individual gene mutation has been identified, but gastrointestinal abnormalities are associated with ASD (Madra *et al.,* 2021). Probiotic treatment has been shown to induce beneficial effects on both behavioural symptoms and GI manifestations in children with ASD (Shaaban *et al.,* 2018). *Lactobacillus* strains, including *L. plantarum*, *L. casei*, *L. acidophilus* and *L. bulgaricu*s, have been reported to ameliorate behavioural symptoms and improve immune functions in a rat model of ASD (Sunand *et al.,* 2020). In a mouse model of ASD, constructed using triclosan, oral administration of *Lactobacillus plantarum* ST-III was found to ameliorate autism-like social deficits in male mouse models and contributed to a more balanced intestinal homeostasis (Guo *et al.,* 2022). In Taiwan, orally administered *Lactobacillus plantarum* PS128 ameliorated opposition/defiance behaviours in boys with ASD (Liu *et al.,* 2019). Interestingly, another study investigating children and adolescence with ASD, found that oral administration of *Lactobacillus plantarum* PS128 improved behavioural symptoms of ASD in children and demonstrated few side effects (Mensi *et al.,* 2021). Daily intake of *Lactobacillus* strains, *L. helveticus* CCFM1076, *L. acidophilus* La28, and *L. acidophilus* JCM 1132, was reported to alleviate behavioural symptoms of ASD in valproic acid-treated rats, from weaning to sexual maturation (Kong *et al.,* 2021). *L. helveticus* CCFM1076 regulated 5-hydroxytryptamine (5HT) anabolism and catabolism and increased

oxytocin synthesis in the hypothalamus, and also reduced *Turicibacter* abundance and up-regulated butyric acid levels in the rat model of ASD (Kong *et al.,* 2021). Recently, a study by Pochakom *et al.*, (2022) applied *Lacticaseibacillus rhamnosus* or *Ligilactobacillus salivarius* to the drinking water of male juvenile BTBR mice. They reported that both strains improved behavioural symptoms of ASD, particularly in social novelty preference and *Lacticaseibacillus rhamnosus* increased the concentrations of serum and brain metabolites, 5-aminovaleric acid and choline (Pochakom *et al.,* 2022). In our study, bacterial intervention of *L. salivarius* strain P0003 showed potential in improving behavioural characteristics in BTBR mice, the murine model of ASD.

Indeed, a Microbiota Transfer Therapy (MTT) two-year follow-up study reported that children showed improvements in ASD symptoms, GI symptoms and gut microbiota, noting a significant increase in *Bifidobacteria* and bacterial diversity (Kang *et al.,* 2019). Interestingly, treatment of *Bifidobacterium* in the model of autism Sprague Dawley male rats (oral gavage of propionic acid), restored the balance of faecal *Clostridium* spp. and the levels of *brain-derived neurotrophic factor* (*BDNF*) expression, as well as increasing glutathione-S-transferase and oxytocin levels, and reducing the propionic acid-induced increase in IFN-γ levels, compared to a control group without ASD (Abuaish *et al.,* 2021; Abuaish *et al.,* 2022). In a similar study, treatment of *Bifidobacterium* in a propionic acid rat model of ASD, positively correlated with flagella biosynthesis and vitamin B12 levels, as well as negatively correlating with pyruvate metabolism, succinate biosynthesis, peptidoglycan biosynthesis, nitrogen metabolism and beta-Lactam resistance, compared to controls with no ASD (Abujamel *et al.,* 2022). Treatment of a rat model of ASD with *Bifidobacterium longum* CCFM107, alleviated behavioural symptoms of ASD, including repetitive stereotyped behaviour, learning and memory ability, and despair mood; as well as regulating glutamic acid (Glu) and Glu/γ-aminobutyric acid (GABA) levels in the brain, reducing cerebellum microglia activity (Kong *et al.* 2022). In our study, bacterial intervention *B. adolescentis* strain 2715 showed great potential in improving behavioural characteristics in BTBR mice, the murine model of ASD.

Interestingly, BAs have also been reported to be altered in ASD (Golubeva *et al.,* 2017). A rat model of ASD treated with BA Ursodeoxycholic Acid (UDCA), was

reported to improve behavioural symptoms of ASD, including sociability and anxiety (Karakas *et al.,* 2022). A FXR agonist, GW4064, was reported to ameliorate behavioural deficits in BTBR mice, a murine model of ASD (Liu *et al.,* 2022). Treatment with GW4064 inhibited BA reabsorption in BTBR mice, showing a significant increase in total BA levels in the faeces, and a significant reduction in total plasma BA levels compared to control C57 mice (Liu *et al.,* 2022). In our study, bacterial treatments increased total tauro conjugated BA levels in the plasma, namely TLCA, and interestingly LCA was the free BA with most obvious increase, in BTBR mice, murine model of ASD. Bacterial treatments overall reduced BA signalling compared to control mice, however, both TLCA and LCA are agonists of the GPCR TGR5, potentially increasing TGR5 signalling in circulation, resulting in an increase in energy homeostasis, thermogenesis and glucose metabolism (Wahlström *et al.,* 2016). In the faeces, bacterial treatments increased total BA levels, namely CDCA, in BTBR ASD model mice. CDCA is the most potent BA ligand for FXR, which can regulate BA homeostasis and glucose metabolism (Wahlström *et al.,* 2016). Total tauro conjugated BA levels were similar across all groups, with *B. adolescentis* strain 2715 specifically increasing TLCA levels. In the gut, TGR5 can regulate gut motility (Alemi *et al.,* 2013) and both FXR and TGR5 have been reported to regulate immune response (Kang *et al.,* 2021). Interestingly, *Bifidobacterium* species have been shown to metabolise tryptophan to compounds of the indole pathway such as Indoleacetic acid (IAA) and indolelactic acid (ILA), similarly, *Lactobacillus* species have the capacity to metabolise tryptophan to indolealdehyde (IAld) and ILA (Roager and Licht, 2018). The indole pathway has been reported to be involved in the regulation of GI homeostasis in the host, maintaining immune function and epithelium integrity (Bosi *et al.,* 2020). Some *Lactobacillus* species produce serotonin from tryptophan (Bosi *et al.,* 2020), demonstrating that perhaps *L. salivarius* strain P0003 and *B. adolescentis* strain 2715 interventions are improving GI function through tryptophan metabolism, rather than altering the BA metabolism profile. Interestingly, a recent study administered probiotic strains, *Bifdobacterium* spp. and *Lactobacillus* spp., to children with ASD and showed reduced anxiety and severity of ASD (Meguid *et al.,* 2022). Indeed, therapeutics for aging may soon encompass bacterial intervention in

combination with dietary changes, to increase microbial diversity and cognitive function.

The gut can be difficult to study with one's microbial composition being so diverse and unique. Examining the levels of specific BAs present in circulation, or in faeces, can give a good indication of gut health, and overall host health, particularly as these levels can alter and fluctuate as we age. In this study, we investigated microbial functionality through BA and FA modification and potential signalling in age-related Parkinson's Disease (PD). PD studies are increasingly focusing on the gut microbiota for answers into disease progression and insights into new treatment therapies (Hasegawa *et al.,* 2015; Scheperjans *et al.,* 2015; Unger *et al.,* 2016; Pietrucci *et al.,* 2019; Shen, 2020). Studies have demonstrated a connection between the gut-brain axis in PD by showing that constipation precedes the first PD motor symptom and α-synuclein is present in the PD colon up to 5 years before the extrapyramidal symptoms (Abbott *et al.,* 2007; Shannon *et al.,* 2012). Alterations in BA synthesis and metabolism have been reported in PD patients (Santos-Lobato *et al.,* 2022). Li *et al.*, (2021) reported an 18.7-fold and 5.6-fold increase in secondary BAs LCA and DCA, respectively, in the appendix of PD patients compared to a control group (Li *et al.,* 2021). DCA is known to be toxic to gut microbes and is a colon cancer promoter (Li and Chiang, 2014). In the ileum, Li *et al.*, (2021) found a 3.6 fold increase in LCA relative to the control group (Li *et al.,* 2021). Gut microbiota with Bile Acid Inducible (BAI) dehydroxylation activity convert primary to secondary BAs. Li *et al.*, (2021) showed an increase in *Clostridiales* and *Burkholderiales* in the appendix, bacterial species capable secondary BA synthesis (Li *et al.,* 2021). Our data suggests that bacteria with bile salt hydrolase (BSH) activity could be at lower concentrations, therefore conjugated BAs are being absorbed and remaining in circulation. This level of conjugated BAs could also be damaging other microbes in the gut. Interestingly, tauro-conjugated BA have been reported to be associated with disease severity and incidence of PD (Hertel *et al.,* 2019). If there is less deconjugation, therefore there is less liberation of amino acids glycine and taurine. Taurine has been shown to be protective in the context of PD (Che *et al.,* 2018; Hou *et al.,* 2018). In addition, the positive correlation of total circulating BAs with age suggests a loss of reabsorption or increase in BA synthesis, which may be due to an over stimulation of FXR. Total

primary, secondary, tertiary and free BAs have been reported to be elevated in adeno-associated virus (AAV)-α-synuclein rat model of PD, compared to controls (O'Donovan *et al.,* 2020). Interestingly, GUDCA has been reported as a biomarker of PD (Zhao *et al.,* 2018), and was found at high levels in circulation in our study. Indeed, we showed concentration levels of circulating BA agonists for the VDR were higher in PD patients, compared to controls. VDR is involved in drug and BA metabolism and detoxification (Li and Chiang, 2014). Interestingly, TGR5 is positively associated with PD pathogenesis, activation with agonist INT-777 enhances neurodegenerative pathology in a mouse model of PD (Zhang *et al.,* 2022). Also, we showed that faecal primary BA CA negatively correlated with UPDRS in Untreated PD patients. CA has been found to be elevated in adeno-associated virus (AAV)-α-synuclein rat model of PD, compared to controls (O'Donovan *et al.,* 2020). Interestingly, TUDCA and UDCA were reported to be down-regulated in prodromal PD mice (Graham *et al.,* 2018a). TUDCA and UDCA have been found to be beneficial in improving motor symptoms and mitochondrial regulation in mouse models of PD (Abdelkader *et al.,* 2016; Moreira *et al.,* 2017; Rosa *et al.,* 2018). Our data found that Sinemet reduced the levels of BAs and increased FA levels in the gut, which may be impacting its absorbance. A recent study found that bile salts do not affect the release of Levodopa while mimicking a fasted GI passage (Wollmer and Klein, 2022). Also, a lower relative abundance of *Clostridium* group IV was reported in PD patients experiencing improvements in motor impairment in response to Levodopa, suggesting that production of metabolites such as SCFA and secondary BA metabolism may be reduced (Palacios *et al.,* 2021). Unger *et al.*, (2016) reported a reduction in the levels of acetate, propionate and butyrate in PD faeces (Unger *et al.,* 2016). Levels of lactic acid have also been reported to be decreased in PD patients, and succinic acid is associated with disease severity (Voigt *et al.,* 2022). Both lactic acid and pyruvic acid are capable of reducing intracellular pH in non-toxic concentrations, activating cell protective mitophagy and autophagy after PD induction, treatment with MPP+ (Fedotova *et al.,* 2022). In our study, PD patients showed increased circulating total FAs, including pyruvic acid, suggesting that ATP production in the mitochondria is reduced (Mytilineou *et al.,* 1994; Ghosh *et al.,* 2016; Cai *et al.,* 2019); and palmitic acid, which has been reported to be elevated in the plasma of rats induced with PD

symptoms by treatment of 6-hydroxydopamine (6-OHDA), and high levels are associated with increased motor dysfunction (Shah *et al.,* 2019). A diet, enriched with palmitic acid, increased the levels of both the expression of tyrosine hydroxylase and the toxic protein α-synuclein (Schommer *et al.,* 2018). Palmitic acid has been suggested as a potential plasma biomarker for PD (Konjevod *et al.,* 2022). Sampson *et al.*, (2016) showed an association between gut microbiota and SCFA concentrations in PD, they found SCFA, in mice colonised with human PD microbiota, regulate microglia and augment PD extrapyramidal symptoms (Sampson *et al.,* 2016). They also found that symptoms are increased when mice, overexpressing α-synuclein, are colonised with PD patient microbiota; and neuroinflammation and motor symptoms are enhanced in germ-free mice when administered gut microbiota from human PD patients (Sampson *et al.,* 2016). These studies suggest that changes in gut microbiome may serve as risk factors for PD onset and progression. Our studies suggest that changes in BA and FA concentration levels can reveal alterations in gut microbial composition and subsequent signalling, which can indicate risk factors for diseases such as PD. Microbial-based intervention can be applied once these alterations are known and could improve disease traits, such as behaviour and gastrointestinal dysbiosis in ASD. As mentioned above, microbial-based intervention and dietary changes, accompanied with analysis of BA and FA changes, may also be harnessed for aging therapeutics.

Microbial metabolites, such as BAs, can indicate the microbial diversity present in the gut, due to level of BA microbial modifications. We connected BA moieties, particular those prominent in the aging spectrum, to the nematode model of aging. CA has been reported to increase lifespan and health-span of progeria mice (Bárcena *et al.,* 2018). A follow-on study found an enrichment for secondary BA biosynthesis, in addition CA, CDCA and DCA concentrations were significantly increased, in ileal content from a progeroid mouse model with FMT from wild-type mice (Bárcena *et al.,* 2019). In this study, DCA and CDCA reduced *C. elegans* lifespan. DCA has been reported to induce negative effects on cell line and animal studies, including inducing apoptosis (Glinghammar *et al.,* 2002; Im and Martinez, 2004; Im *et al.,* 2005), inhibiting Ca^{2+} absorption (Pérez *et al.,* 2021), activating IL-6 and IL-8 (Quilty *et al.,* 2021), promoting intestinal carcinogenesis (Song *et al.,* 2022), increasing reactive

oxidative species and intestinal permeability (Zeng *et al.,* 2022). Hydrophobic BAs, including DCA, may also be inducing negative effects through mitochondrial damage (Payne *et al.,* 2008). CDCA may be acting in a similar manner whereby mitochondrial damage causes electrons to "leak" from the electron transport chain, forming superoxide (O^{-}) and therefore resulting an escalation in reactive oxygen species (ROS) inducing oxidative stress (Payne *et al.,* 2008). CDCA has been reported to increase IL-8 production and permeability (Horikawa *et al.,* 2019), and promoting tumour formation in mice (Mahmoud *et al.,* 1999). Interestingly, in naked mole rats, compared to control mice, primary BAs CA and MCA, and tauro-conjugated BAs TCA and TMCA, were reduced in the plasma, however, CDCA, DCA, HDCA, UDCA and glyco-conjugated BAs GDCA, GCDCA and GHDCA were increased in the plasma, suggesting that these BAs, and their concentrations, may contribute to the longevity seen in naked mole rats (Viltard *et al.,* 2019). Interestingly, BAs CA, DCA and GCA were significantly increased in urine and faecal samples of healthy centenarians, compared to elderly people aged 60–70 years (Cai *et al.,* 2022). DCA and CDCA may induce a hormesis effect, at low concentrations, such as 1 mM and lower, these BAs may induce beneficial effects, and at high concentrations, including 5 mM and higher, they were detrimental to cell viability. The secondary BA LCA significantly extended *C. elegans* lifespan, regardless of strain. LCA has been reported to have beneficial effects on the lifespan of both yeast, *Saccharomyces cerevisiae*, and fruit fly, *Drosophila melanogaster*, despite LCA being the most hydrophobic BA. LCA has been found to induce these lifespan extension effects through alteration of the mitochondria (Perino *et al.,* 2021). LCA modulates housekeeping longevity pathways by suppressing lipid-induced necrosis, altering oxidation-reduction, suppressing mitochondria-controlled apoptosis and mitochondrial fragmentation in yeast (Goldberg *et al.,* 2010). It was found that LCA can extend longevity of yeast under caloric restriction conditions at two lifespan periods and it therefore developmentally sensitive, checkpoints that exist in logarithmic/diauxic, post-diauxic and early stationary phases (Burstein *et al.,* 2012). It was then determined that LCA extends longevity of yeast under caloric restriction conditions through the mitochondrial membrane lipidome and proteome (Beach *et al.,* 2013; Beach *et al.,* 2015; Leonov *et al.,* 2017). It was found that LCA prolongs longevity of chronologically

aging yeast through reducing age-associated cell death and promoting the survival of elderly cells (Arlia-Ciommo *et al.,* 2018). In the fruit fly, *Drosophila melanogaster*, it was reported that LCA extends lifespan through spargel (*srl*), the fly homolog of mammalian PPAR-γ co-activator 1α (PGC1α) and through unidentified changes in the metabolism of gut microbiota (Staats *et al.,* 2018). Transcriptome analysis of LCA treated *C. elegans*, compared to CDCA, revealed that LCA may too be acting through the mitochondria to induce lifespan extension. Interestingly, various isoforms of LCA, specifically isoalloLCA, have been found to present at high levels in centenarians, implicating that such BA derivatives of LCA are eliciting beneficial, infection-reducing and gut homeostasis, effects (Sato *et al.,* 2021). BAs may act through the regulation of DAF-12 and DA, to alter DAF-16, NHR-80 and HLH-30 signalling, mediating longevity potential through lipolysis, FA metabolism and autophagy in *C. elegans*. The homologs of these pathways in humans include FXR, FOXO and TFEB. Our data implicates that FXR, FOXO and TFEB may have a role in human longevity, through BA signalling. Recent reviews highlight the cross-talk between FOXO, TFEB and FGF19, which is downstream from FXR, in the regulation of autophagy, particularly under fasting conditions (Ma *et al.,* 2022; Tao *et al.,* 2022). BAs may influence human lifespan and longevity under fasting conditions through the regulation of autophagy.

This thesis focuses on elucidating associations and possible effects of microbial processes and metabolites on aging and in age-related diseases. We, with the model of aging *C. elegans*, demonstrated that DCA and CDCA may have an hormesis effect, inducing negative effects at concentrations of 5 mM and higher, and beneficial effects at concentrations of 1mM and lower. UDCA and LCA largely inducing beneficial effects on *C. elegans* health. We found conjugated BAs were significantly higher in PD patient plasma, compared to healthy control individuals. This could indicate that these bacteria with BSH activity could be at lower concentrations in PD gut and so conjugated BAs are being absorbed and remaining in circulation. This level of conjugated BAs could also be damaging other microbes in the gut. If there is less deconjugation, therefore there is less liberation of amino acids glycine and taurine. Also, the potential of FAs, in the plasma, there is an increase in the concentrations of total FAs in PD patients compared to the control. Pyruvic acid concentrations are

significantly increased in PD patients, suggesting that ATP production in the mitochondria is reduced. In the context of bacteria, this study highlights the severity of AIEC, uncovering the *dsb*A gene as a potential target of AIEC to help prevent the debilitating effects of CD; and the benefits of bacterial interventions, potentially increasing TGR5 signalling in circulation, resulting in an increase in energy homeostasis, thermogenesis and glucose metabolism; and potentially increased FXR signalling in the faeces, regulate BA homeostasis and glucose as well as TGR5, can regulating gut motility and immune response. These bacterial interventions can also regulate GI homeostasis in the host, maintaining immune function and epithelium integrity through the indole pathway, some *Lactobacillus* species have even shown to produce serotonin from tryptophan, demonstrating that perhaps *L. salivarius* strain P0003 and *B. adolescentis* strain 2715 interventions are improving GI function through tryptophan metabolism, rather than directly altering the BA metabolism profile. This work is of importance in investigating the potential of utilising BAs, FAs and Δ*dsb*A in treatment therapies for different diseases, particularly age-related diseases such as PD, and young-onset diseases, such as CD, to prolong health-span and lifespan. In the context of bacteria, it highlights the severity of AIEC and the benefits of bacterial interventions in some diseases, such as ASD, and the potential for bacterial interventions to be harnessed to benefit other diseases with GI dysbiosis, such as CD and PD.

Future Work

Indeed, studies have shown that metabolism and signalling are altered in aging. We examined gut microbiota and metabolite changes in both disease states of the young, Crohn's Disease (CD) and Autism Spectrum Disorder (ASD), as early intervention may effect age and increase overall health-span and lifespan. We demonstrated that a single mutation in a bacteria (food source *E. coli* HM605) has the potential to induce significant consequences on host health and longevity. We showed that *E. coli* HM605 has the capability of reducing *C. elegans* lifespan and altering *C. elegans* transcriptome promoting an innate immune response. We demonstrated that *E. coli* HM605 deletion mutation Δ*dsb*A restored *C. elegans* lifespan and reversed theses changes in the *C. elegans* transcriptome, reduced innate immune response by

inhibiting DAF-2/DAF-16 signalling, VHP-1 signalling, FA synthesis and promoting lipid synthesis, the stress response and apoptotic pathways, promoting longevity and reducing virulent potential. To move this work forward, targeting *dsb*A could be applied as a clinical trial to patients suffering from CD. This study cements the potential use of antibacterials, such as targeting the disulfide forming pathways of the *dsb*A gene, instead of antibiotics for the treatment of human infection and disease, such as CD. In disease states of early and advanced life stages, where symptoms of gut dysbiosis are apparent, we examined the microbial metabolites BAs and FAs, who represent a read out of modification to human and dietary produced metabolites, respectively. We advanced the work of Golubeva *et al.*, (2017) and identified BA alterations that were strain specific, and further identified restoration of gut health parameters and behavioural deficits in a model of Autism Spectrum disorder (ASD). To move this work forward, *L. salivarius* strain P0003 and *B. adolescentis* strain 2715 could potentially be applied to humans in a clinical trial. This would determine if these bacteria could help improve both gut and behavioural symptoms in ASD. We examined and identified key moieties that were affected by PD prescribed treatments, in particular for Sinemet, which may be related to transport functions as BAs and FAs appear elevated in the gut. Our analysis suggests a role for BA receptor activation for these and for detoxification functions. Indeed BAs may have an important role in promoting healthy aging. To move this work forward, this data could be compared with microbial composition. DNA extraction and 16S rRNA gene sequencing could be performed on these PD faecal samples to compared BA microbial modification with this BA analysis. RNA-sequencing analysis on faecal samples would allow comparison of the real-time transcriptome of PD patients against age-matched, healthy, control volunteers. This would give a snapshot into the PD profile and allow the potential to connect signalling pathways, from transcriptome analysis, directly with microbial composition. Our studies show that primary and secondary BAs have the potential to influence the lifespan and development of the model of aging, *C. elegans*. We identified primary BA CDCA, its microbial derivative LCA and also DCA, microbially derived from liver produced CA, as impactful in either *C. elegans* lifespan or development with the potential to act through DAF-12 (homologue of human FXR). To move this work forward, further

analysis and experimentation is required to cement the effects of BAs on the *C. elegans* transcriptome and on longevity in the wild-type N2 strain. Real-Time Quantitative Reverse Transcription PCR (qRT-PCR) could be performed to examine DAF-12 and DA regulation pathways in *C. elegans* wild-type strain N2, both at L1 larval stage and reproductive adult, treated with BAs, compared to a control with no BAs. A large-scale proteomics study could be carried out to analyse the changes in protein profiles in *C. elegans* wild-type strain N2, treated with BAs compared to a control with no BAs, identifying human protein homologs. This would have the potential to determine the specific proteins that may be involved in human longevity.

The aim of this study was to demonstrate that host- and dietary-produced factors e.g. BAs and FAs, are central to human aging and age-related disease processes because these outputs will be altered as the gut microbiota change. This work is of importance in highlighting the crucial roles of BAs and FAs in the progression of age-related diseases, particularly PD, and the bacterial *dsb*A gene as a potential therapeutic target to improve quality of life in young-onset diseases, such as CD, to prolong health-span and lifespan. This study shows the potential for bacterial interventions, that alter BAs and FAs, to be harnessed to benefit diseases with GI dysbiosis, including CD, ASD and PD.

Chapter 7 – References

Abbas, S. and Wink, M. (2010) 'Epigallocatechin gallate inhibits beta amyloid oligomerization in Caenorhabditis elegans and affects the daf-2/insulin-like signaling pathway', *Phytomedicine*, 17(11), 902-9, available: http://dx.doi.org/10.1016/j.phymed.2010.03.008.

Abbott, R.D., Ross, G.W., Petrovitch, H., Tanner, C.M., Davis, D.G., Masaki, K.H., Launer, L.J., Curb, J.D. and White, L.R. (2007) 'Bowel movement frequency in late-life and incidental Lewy bodies', *Mov Disord*, 22(11), 1581-6, available: http://dx.doi.org/10.1002/mds.21560.

Abdelkader, N.F., Safar, M.M. and Salem, H.A. (2016) 'Ursodeoxycholic Acid Ameliorates Apoptotic Cascade in the Rotenone Model of Parkinson's Disease: Modulation of Mitochondrial Perturbations', *Mol Neurobiol*, 53(2), 810-817, available: http://dx.doi.org/10.1007/s12035-014-9043-8.

Abrigo, J., Gonzalez, F., Aguirre, F., Tacchi, F., Gonzalez, A., Meza, M.P., Simon, F., Cabrera, D., Arrese, M., Karpen, S. and Cabello-Verrugio, C. (2021) 'Cholic acid and deoxycholic acid induce skeletal muscle atrophy through a mechanism dependent on TGR5 receptor', *J Cell Physiol*, 236(1), 260-272, available: http://dx.doi.org/10.1002/jcp.29839.

Abuaish, S., Al-Otaibi, N.M., Aabed, K., Abujamel, T.S., Alzahrani, S.A., Alotaibi, S.M., Bhat, R.S., Arzoo, S., Algahtani, N., Moubayed, N.M. and El-Ansary, A. (2022) 'The Efficacy of Fecal Transplantation and Bifidobacterium Supplementation in Ameliorating Propionic Acid-Induced Behavioral and Biochemical Autistic Features in Juvenile Male Rats', *J Mol Neurosci*, 72(2), 372-381, available: http://dx.doi.org/10.1007/s12031-021-01959-8.

Abuaish, S., Al-Otaibi, N.M., Abujamel, T.S., Alzahrani, S.A., Alotaibi, S.M., AlShawakir, Y.A., Aabed, K. and El-Ansary, A. (2021) 'Fecal Transplant and', *Brain Sci*, 11(8), available: http://dx.doi.org/10.3390/brainsci11081038.

Abujamel, T.S., Al-Otaibi, N.M., Abuaish, S., AlHarbi, R.H., Assas, M.B., Alzahrani, S.A., Alotaibi, S.M., El-Ansary, A. and Aabed, K. (2022) 'Different Alterations in Gut Microbiota between', *Nutrients*, 14(3), available: http://dx.doi.org/10.3390/nu14030608.

Aghayeva, U., Bhattacharya, A., Sural, S., Jaeger, E., Churgin, M., Fang-Yen, C. and Hobert, O. (2021) 'DAF-16/FoxO and DAF-12/VDR control cellular plasticity both cell-autonomously and via interorgan signaling', *PLoS Biol*, 19(4), e3001204, available: http://dx.doi.org/10.1371/journal.pbio.3001204.

Aguilaniu, H., Fabrizio, P. and Witting, M. (2016) 'The Role of Dafachronic Acid Signaling in Development and Longevity in Caenorhabditis elegans: Digging Deeper Using Cutting-Edge Analytical Chemistry', *Front Endocrinol (Lausanne)*, 7, 12, available: http://dx.doi.org/10.3389/fendo.2016.00012.

Alemi, F., Poole, D.P., Chiu, J., Schoonjans, K., Cattaruzza, F., Grider, J.R., Bunnett, N.W. and Corvera, C.U. (2013) 'The receptor TGR5 mediates the prokinetic actions of intestinal bile acids and is required for normal defecation in mice', *Gastroenterology*, 144(1), 145-54, available: http://dx.doi.org/10.1053/j.gastro.2012.09.055.

Alharthi, A., Alhazmi, S., Alburae, N. and Bahieldin, A. (2022) 'The Human Gut Microbiome as a Potential Factor in Autism Spectrum Disorder', *Int J Mol Sci*, 23(3), available: http://dx.doi.org/10.3390/ijms23031363.

Alliance, g.r. (WS285) 'WormBase'.

Alper, S., McElwee, M.K., Apfeld, J., Lackford, B., Freedman, J.H. and Schwartz, D.A. (2010) 'The Caenorhabditis elegans germ line regulates distinct signaling pathways to control lifespan and innate immunity', *J Biol Chem*, 285(3), 1822-8, available: http://dx.doi.org/10.1074/jbc.M109.057323.

Alshammari, M.K., AlKhulaifi, M.M., Al Farraj, D.A., Somily, A.M. and Albarrag, A.M. (2020) 'Incidence of Clostridium perfringens and its toxin genes in the gut of children with autism spectrum disorder', *Anaerobe*, 61, 102114, available: http://dx.doi.org/10.1016/j.anaerobe.2019.102114.

Altun, Z.F. and Hall, D.H. (2009) 'Introduction'.

Amador-Noguez, D., Dean, A., Huang, W., Setchell, K., Moore, D. and Darlington, G. (2007) 'Alterations in xenobiotic metabolism in the long-lived Little mice', *Aging Cell*, 6(4), 453-70, available: http://dx.doi.org/10.1111/j.1474-9726.2007.00300.x.

Amador-Noguez, D., Yagi, K., Venable, S. and Darlington, G. (2004) 'Gene expression profile of long-lived Ames dwarf mice and Little mice', *Aging Cell*, 3(6), 423-41, available: http://dx.doi.org/10.1111/j.1474-9728.2004.00125.x.

Annar, D., Feher, P., Madarasi, A., Mascie-Taylor, N., Kekesi, A., Kalabiska, I., Muzsnai, A. and Zsakai, A. (2022) 'Body structural and cellular aging of women with low socioeconomic status in Hungary: A pilot study', *Am J Hum Biol*, 34(3), e23662, available: http://dx.doi.org/10.1002/ajhb.23662.

Antebi (2015) 'Nuclear receptor signal transduction in C. elegans'.

Antebi, A., Culotti, J.G. and Hedgecock, E.M. (1998) 'daf-12 regulates developmental age and the dauer alternative in Caenorhabditis elegans',

Development, 125(7), 1191-205, available: http://dx.doi.org/10.1242/dev.125.7.1191.

Antebi, A., Yeh, W.H., Tait, D., Hedgecock, E.M. and Riddle, D.L. (2000) 'daf-12 encodes a nuclear receptor that regulates the dauer diapause and developmental age in C. elegans', *Genes Dev*, 14(12), 1512-27.

Arlia-Ciommo, A., Leonov, A., Mohammad, K., Beach, A., Richard, V.R., Bourque, S.D., Burstein, M.T., Goldberg, A.A., Kyryakov, P., Gomez-Perez, A., Koupaki, O. and Titorenko, V.I. (2018) 'Mechanisms through which lithocholic acid delays yeast chronological aging under caloric restriction conditions', *Oncotarget*, 9(79), 34945-34971, available: http://dx.doi.org/10.18632/oncotarget.26188.

Arnsten, A.F.T., Datta, D., Leslie, S., Yang, S.T., Wang, M. and Nairn, A.C. (2019) 'Alzheimer's-like pathology in aging rhesus macaques: Unique opportunity to study the etiology and treatment of Alzheimer's disease', *Proc Natl Acad Sci U S A*, available: http://dx.doi.org/10.1073/pnas.1903671116.

Ashburner, M., Ball, C.A., Blake, J.A., Botstein, D., Butler, H., Cherry, J.M., Davis, A.P., Dolinski, K., Dwight, S.S., Eppig, J.T., Harris, M.A., Hill, D.P., Issel-Tarver, L., Kasarskis, A., Lewis, S., Matese, J.C., Richardson, J.E., Ringwald, M., Rubin, G.M. and Sherlock, G. (2000) 'Gene ontology: tool for the unification of biology. The Gene Ontology Consortium', *Nat Genet*, 25(1), 25-9, available: http://dx.doi.org/10.1038/75556.

Avery, L. (1993) 'The genetics of feeding in Caenorhabditis elegans', *Genetics*, 133(4), 897-917, available: http://dx.doi.org/10.1093/genetics/133.4.897.

Baba, T., Ara, T., Hasegawa, M., Takai, Y., Okumura, Y., Baba, M., Datsenko, K.A., Tomita, M., Wanner, B.L. and Mori, H. (2006) 'Construction of Escherichia coli K-12 in-frame, single-gene knockout mutants: the Keio collection', *Mol Syst Biol*, 2, 2006.0008, available: http://dx.doi.org/10.1038/msb4100050.

Babita, K., Rana, V. and Tiwary, A.K. (2005) 'Lipid synthesis inhibitors: effect on epidermal lipid conformational changes and percutaneous permeation of levodopa', *AAPS PharmSciTech*, 6(3), E473-81, available: http://dx.doi.org/10.1208/pt060359.

Babita, K. and Tiwary, A.K. (2005) 'Transcutaneous delivery of levodopa: enhancement by fatty acid synthesis inhibition', *Mol Pharm*, 2(1), 57-63, available: http://dx.doi.org/10.1021/mp049926u.

Badal, V.D., Vaccariello, E.D., Murray, E.R., Yu, K.E., Knight, R., Jeste, D.V. and Nguyen, T.T. (2020) 'The Gut Microbiome, Aging, and Longevity: A Systematic Review', *Nutrients*, 12(12), available: http://dx.doi.org/10.3390/nu12123759.

Bansal, A., Zhu, L.J., Yen, K. and Tissenbaum, H.A. (2015) 'Uncoupling lifespan and healthspan in Caenorhabditis elegans longevity mutants', *Proc Natl Acad Sci U S A*, 112(3), E277-86, available: http://dx.doi.org/10.1073/pnas.1412192112.

Bao, K., Liu, W., Song, Z., Feng, J., Mao, Z., Bao, L., Sun, T., Hu, Z. and Li, J. (2022) 'Crotamiton derivative JM03 extends lifespan and improves oxidative and hypertonic stress resistance in', *Elife*, 11, available: http://dx.doi.org/10.7554/eLife.72410.

Barbieri, M., Bonafè, M., Franceschi, C. and Paolisso, G. (2003) 'Insulin/IGF-I-signaling pathway: an evolutionarily conserved mechanism of longevity from yeast to humans', *Am J Physiol Endocrinol Metab*, 285(5), E1064-71, available: http://dx.doi.org/10.1152/ajpendo.00296.2003.

Barlic, J., Zhang, Y., Foley, J.F. and Murphy, P.M. (2006) 'Oxidized lipid-driven chemokine receptor switch, CCR2 to CX3CR1, mediates adhesion of human macrophages to coronary artery smooth muscle cells through a peroxisome proliferator-activated receptor gamma-dependent pathway', *Circulation*, 114(8), 807-19, available: http://dx.doi.org/10.1161/CIRCULATIONAHA.105.602359.

Basisty, N., Kale, A., Jeon, O.H., Kuehnemann, C., Payne, T., Rao, C., Holtz, A., Shah, S., Sharma, V., Ferrucci, L., Campisi, J. and Schilling, B. (2020) 'A proteomic atlas of senescence-associated secretomes for aging biomarker development', *PLoS Biol*, 18(1), e3000599, available: http://dx.doi.org/10.1371/journal.pbio.3000599.

Baumann, S., Hess, J., Eichhorst, S.T., Krueger, A., Angel, P., Krammer, P.H. and Kirchhoff, S. (2003) 'An unexpected role for FosB in activation-induced cell death of T cells', *Oncogene*, 22(9), 1333-9, available: http://dx.doi.org/10.1038/sj.onc.1206126.

Bazzari, F.H., Abdallah, D.M. and El-Abhar, H.S. (2019) 'Chenodeoxycholic Acid Ameliorates AlCl', *Molecules*, 24(10), available: http://dx.doi.org/10.3390/molecules24101992.

Beach, A., Richard, V.R., Bourque, S., Boukh-Viner, T., Kyryakov, P., Gomez-Perez, A., Arlia-Ciommo, A., Feldman, R., Leonov, A., Piano, A., Svistkova, V. and Titorenko, V.I. (2015) 'Lithocholic bile acid accumulated in yeast mitochondria orchestrates a development of an anti-aging cellular pattern by causing age-related changes in cellular proteome', *Cell Cycle*, 14(11), 1643-56, available: http://dx.doi.org/10.1080/15384101.2015.1026493.

Beach, A., Richard, V.R., Leonov, A., Burstein, M.T., Bourque, S.D., Koupaki, O., Juneau, M., Feldman, R., Iouk, T. and Titorenko, V.I. (2013) 'Mitochondrial

membrane lipidome defines yeast longevity', *Aging (Albany NY)*, 5(7), 551-74, available: http://dx.doi.org/10.18632/aging.100578.

Beanan, M.J. and Strome, S. (1992) 'Characterization of a germ-line proliferation mutation in C. elegans', *Development*, 116(3), 755-66, available: http://dx.doi.org/10.1242/dev.116.3.755.

Berendzen, K.M., Sharma, R., Mandujano, M.A., Wei, Y., Rogers, F.D., Simmons, T.C., Seelke, A.M.H., Bond, J.M., Larios, R., Goodwin, N.L., Sherman, M., Parthasarthy, S., Espineda, I., Knoedler, J.R., Beery, A., Bales, K.L., Shah, N.M. and Manoli, D.S. (2022) 'Oxytocin receptor is not required for social attachment in prairie voles', *Neuron*, available: http://dx.doi.org/10.1016/j.neuron.2022.12.011.

Bertolotti, M., Gabbi, C., Anzivino, C., Crestani, M., Mitro, N., Del Puppo, M., Godio, C., De Fabiani, E., Macchioni, D., Carulli, L., Rossi, A., Ricchi, M., Loria, P. and Carulli, N. (2007) 'Age-related changes in bile acid synthesis and hepatic nuclear receptor expression', *Eur J Clin Invest*, 37(6), 501-8, available: http://dx.doi.org/10.1111/j.1365-2362.2007.01808.x.

Biagi, E., Franceschi, C., Rampelli, S., Severgnini, M., Ostan, R., Turroni, S., Consolandi, C., Quercia, S., Scurti, M., Monti, D., Capri, M., Brigidi, P. and Candela, M. (2016) 'Gut Microbiota and Extreme Longevity', *Curr Biol*, 26(11), 1480-5, available: http://dx.doi.org/10.1016/j.cub.2016.04.016.

Bian, G., Gloor, G.B., Gong, A., Jia, C., Zhang, W., Hu, J., Zhang, H., Zhang, Y., Zhou, Z., Zhang, J., Burton, J.P., Reid, G., Xiao, Y., Zeng, Q., Yang, K. and Li, J. (2017) 'The Gut Microbiota of Healthy Aged Chinese Is Similar to That of the Healthy Young', *mSphere*, 2(5), available: http://dx.doi.org/10.1128/mSphere.00327-17.

Binyamin, D., Werbner, N., Nuriel-Ohayon, M., Uzan, A., Mor, H., Abbas, A., Ziv, O., Teperino, R., Gutman, R. and Koren, O. (2020) 'The aging mouse microbiome has obesogenic characteristics', *Genome Med*, 12(1), 87, available: http://dx.doi.org/10.1186/s13073-020-00784-9.

Bitto, A., Ito, T.K., Pineda, V.V., LeTexier, N.J., Huang, H.Z., Sutlief, E., Tung, H., Vizzini, N., Chen, B., Smith, K., Meza, D., Yajima, M., Beyer, R.P., Kerr, K.F., Davis, D.J., Gillespie, C.H., Snyder, J.M., Treuting, P.M. and Kaeberlein, M. (2016) 'Transient rapamycin treatment can increase lifespan and healthspan in middle-aged mice', *Elife*, 5, available: http://dx.doi.org/10.7554/eLife.16351.

Bocian-Ostrzycka, K.M., Grzeszczuk, M.J., Banaś, A.M. and Jagusztyn-Krynicka, E.K. (2017) 'Bacterial thiol oxidoreductases - from basic research to new antibacterial strategies', *Appl Microbiol Biotechnol*, 101(10), 3977-3989, available: http://dx.doi.org/10.1007/s00253-017-8291-8.

Bodkin, N.L., Alexander, T.M., Ortmeyer, H.K., Johnson, E. and Hansen, B.C. (2003) 'Mortality and morbidity in laboratory-maintained Rhesus monkeys and effects of long-term dietary restriction', *J Gerontol A Biol Sci Med Sci*, 58(3), 212-9, available: http://dx.doi.org/10.1093/gerona/58.3.b212.

Bosi, A., Banfi, D., Bistoletti, M., Giaroni, C. and Baj, A. (2020) 'Tryptophan Metabolites Along the Microbiota-Gut-Brain Axis: An Interkingdom Communication System Influencing the Gut in Health and Disease', *Int J Tryptophan Res*, 13, 1178646920928984, available: http://dx.doi.org/10.1177/1178646920928984.

Bouchard, C., Blair, S.N. and Katzmarzyk, P.T. (2015) 'Less Sitting, More Physical Activity, or Higher Fitness?', *Mayo Clin Proc*, 90(11), 1533-40, available: http://dx.doi.org/10.1016/j.mayocp.2015.08.005.

Boudeau, J., Barnich, N. and Darfeuille-Michaud, A. (2001) 'Type 1 pili-mediated adherence of Escherichia coli strain LF82 isolated from Crohn's disease is involved in bacterial invasion of intestinal epithelial cells', *Mol Microbiol*, 39(5), 1272-84, available: http://dx.doi.org/10.1111/j.1365-2958.2001.02315.x.

Boudeau, J., Glasser, A.L., Masseret, E., Joly, B. and Darfeuille-Michaud, A. (1999) 'Invasive ability of an Escherichia coli strain isolated from the ileal mucosa of a patient with Crohn's disease', *Infect Immun*, 67(9), 4499-509, available: http://dx.doi.org/10.1128/IAI.67.9.4499-4509.1999.

Braak, H., Rüb, U., Gai, W.P. and Del Tredici, K. (2003) 'Idiopathic Parkinson's disease: possible routes by which vulnerable neuronal types may be subject to neuroinvasion by an unknown pathogen', *J Neural Transm (Vienna)*, 110(5), 517-36, available: http://dx.doi.org/10.1007/s00702-002-0808-2.

Brady, M., Beltramini, A., Vaughan, G. and Bechard, A.R. (2022) 'Benefits of a ketogenic diet on repetitive motor behavior in mice', *Behav Brain Res*, 422, 113748, available: http://dx.doi.org/10.1016/j.bbr.2022.113748.

Braniste, V., Al-Asmakh, M., Kowal, C., Anuar, F., Abbaspour, A., Tóth, M., Korecka, A., Bakocevic, N., Ng, L.G., Guan, N.L., Kundu, P., Gulyás, B., Halldin, C., Hultenby, K., Nilsson, H., Hebert, H., Volpe, B.T., Diamond, B. and Pettersson, S. (2014) 'The gut microbiota influences blood-brain barrier permeability in mice', *Sci Transl Med*, 6(263), 263ra158, available: http://dx.doi.org/10.1126/scitranslmed.3009759.

Bravo, J.A., Forsythe, P., Chew, M.V., Escaravage, E., Savignac, H.M., Dinan, T.G., Bienenstock, J. and Cryan, J.F. (2011) 'Ingestion of Lactobacillus strain regulates emotional behavior and central GABA receptor expression in a

mouse via the vagus nerve', *Proc Natl Acad Sci U S A*, 108(38), 16050-5, available: http://dx.doi.org/10.1073/pnas.1102999108.

Brenner, S. (1974) 'The genetics of Caenorhabditis elegans', *Genetics*, 77(1), 71-94.

Bringer, M.A., Barnich, N., Glasser, A.L., Bardot, O. and Darfeuille-Michaud, A. (2005) 'HtrA stress protein is involved in intramacrophagic replication of adherent and invasive Escherichia coli strain LF82 isolated from a patient with Crohn's disease', *Infect Immun*, 73(2), 712-21, available: http://dx.doi.org/10.1128/IAI.73.2.712-721.2005.

Bringer, M.A., Rolhion, N., Glasser, A.L. and Darfeuille-Michaud, A. (2007) 'The oxidoreductase DsbA plays a key role in the ability of the Crohn's disease-associated adherent-invasive Escherichia coli strain LF82 to resist macrophage killing', *J Bacteriol*, 189(13), 4860-71, available: http://dx.doi.org/10.1128/JB.00233-07.

Brunet, A. (2020) 'Old and new models for the study of human ageing', *Nat Rev Mol Cell Biol*, 21(9), 491-493, available: http://dx.doi.org/10.1038/s41580-020-0266-4.

Brüssow, H. (2020) 'Parkinson disease, levodopa and the gut microbiota-when microbiology meets pharmacology', *Environ Microbiol*, 22(3), 808-812, available: http://dx.doi.org/10.1111/1462-2920.14919.

Burstein, M.T., Kyryakov, P., Beach, A., Richard, V.R., Koupaki, O., Gomez-Perez, A., Leonov, A., Levy, S., Noohi, F. and Titorenko, V.I. (2012) 'Lithocholic acid extends longevity of chronologically aging yeast only if added at certain critical periods of their lifespan', *Cell Cycle*, 11(18), 3443-62, available: http://dx.doi.org/10.4161/cc.21754.

Bárcena, C., Quirós, P.M., Durand, S., Mayoral, P., Rodríguez, F., Caravia, X.M., Mariño, G., Garabaya, C., Fernández-García, M.T., Kroemer, G., Freije, J.M.P. and López-Otín, C. (2018) 'Methionine Restriction Extends Lifespan in Progeroid Mice and Alters Lipid and Bile Acid Metabolism', *Cell Rep*, 24(9), 2392-2403, available: http://dx.doi.org/10.1016/j.celrep.2018.07.089.

Bárcena, C., Valdés-Mas, R., Mayoral, P., Garabaya, C., Durand, S., Rodríguez, F., Fernández-García, M.T., Salazar, N., Nogacka, A.M., Garatachea, N., Bossut, N., Aprahamian, F., Lucia, A., Kroemer, G., Freije, J.M.P., Quirós, P.M. and López-Otín, C. (2019) 'Healthspan and lifespan extension by fecal microbiota transplantation into progeroid mice', *Nat Med*, 25(8), 1234-1242, available: http://dx.doi.org/10.1038/s41591-019-0504-5.

Cabreiro, F., Au, C., Leung, K.Y., Vergara-Irigaray, N., Cochemé, H.M., Noori, T., Weinkove, D., Schuster, E., Greene, N.D. and Gems, D. (2013) 'Metformin retards aging in C. elegans by altering microbial folate and methionine

metabolism', *Cell*, 153(1), 228-39, available: http://dx.doi.org/10.1016/j.cell.2013.02.035.

Cahill, G.F. (1970) 'Starvation in man', *N Engl J Med*, 282(12), 668-75, available: http://dx.doi.org/10.1056/NEJM197003192821209.

Cai, D., Zhao, S., Li, D., Chang, F., Tian, X., Huang, G., Zhu, Z., Liu, D., Dou, X., Li, S., Zhao, M. and Li, Q. (2016) 'Nutrient Intake Is Associated with Longevity Characterization by Metabolites and Element Profiles of Healthy Centenarians', *Nutrients*, 8(9), available: http://dx.doi.org/10.3390/nu8090564.

Cai, D., Zhao, Z., Zhao, L., Dong, Y., Wang, L., Zhao, S. and Li, Q. (2022) 'The Age-Accompanied and Diet-Associated Remodeling of the Phospholipid, Amino Acid, and SCFA Metabolism of Healthy Centenarians from a Chinese Longevous Region: A Window into Exceptional Longevity', *Nutrients*, 14(20), available: http://dx.doi.org/10.3390/nu14204420.

Cai, R., Zhang, Y., Simmering, J.E., Schultz, J.L., Li, Y., Fernandez-Carasa, I., Consiglio, A., Raya, A., Polgreen, P.M., Narayanan, N.S., Yuan, Y., Chen, Z., Su, W., Han, Y., Zhao, C., Gao, L., Ji, X., Welsh, M.J. and Liu, L. (2019) 'Enhancing glycolysis attenuates Parkinson's disease progression in models and clinical databases', *J Clin Invest*, 129(10), 4539-4549, available: http://dx.doi.org/10.1172/JCI129987.

Calder, P.C. (2011) 'Fatty acids and inflammation: the cutting edge between food and pharma', *Eur J Pharmacol*, 668 Suppl 1, S50-8, available: http://dx.doi.org/10.1016/j.ejphar.2011.05.085.

Carabotti, M., Scirocco, A., Maselli, M.A. and Severi, C. (2015) 'The gut-brain axis: interactions between enteric microbiota, central and enteric nervous systems', *Ann Gastroenterol*, 28(2), 203-209.

Castro-Caldas, M., Carvalho, A.N., Rodrigues, E., Henderson, C.J., Wolf, C.R., Rodrigues, C.M. and Gama, M.J. (2012) 'Tauroursodeoxycholic acid prevents MPTP-induced dopaminergic cell death in a mouse model of Parkinson's disease', *Mol Neurobiol*, 46(2), 475-86, available: http://dx.doi.org/10.1007/s12035-012-8295-4.

Chandler-Brown, D., Choi, H., Park, S., Ocampo, B.R., Chen, S., Le, A., Sutphin, G.L., Shamieh, L.S., Smith, E.D. and Kaeberlein, M. (2015) 'Sorbitol treatment extends lifespan and induces the osmotic stress response in Caenorhabditis elegans', *Front Genet*, 6, 316, available: http://dx.doi.org/10.3389/fgene.2015.00316.

Chapuis, S., Ouchchane, L., Metz, O., Gerbaud, L. and Durif, F. (2005) 'Impact of the motor complications of Parkinson's disease on the quality of life', *Mov Disord*, 20(2), 224-30, available: http://dx.doi.org/10.1002/mds.20279.

Che, Y., Hou, L., Sun, F., Zhang, C., Liu, X., Piao, F., Zhang, D., Li, H. and Wang, Q. (2018) 'Taurine protects dopaminergic neurons in a mouse Parkinson's disease model through inhibition of microglial M1 polarization', *Cell Death Dis*, 9(4), 435, available: http://dx.doi.org/10.1038/s41419-018-0468-2.

Check Hayden, E. (2014) 'Pet dogs set to test anti-ageing drug', *Nature*, 514(7524), 546, available: http://dx.doi.org/10.1038/514546a.

Chen, W., Rezaizadehnajafi, L. and Wink, M. (2013) 'Influence of resveratrol on oxidative stress resistance and life span in Caenorhabditis elegans', *J Pharm Pharmacol*, 65(5), 682-8, available: http://dx.doi.org/10.1111/jphp.12023.

Chiang, J.Y. (2013) 'Bile acid metabolism and signaling', *Compr Physiol*, 3(3), 1191-212, available: http://dx.doi.org/10.1002/cphy.c120023.

Chitre, N.M., Wood, B.J., Ray, A., Moniri, N.H. and Murnane, K.S. (2020) 'Docosahexaenoic acid protects motor function and increases dopamine synthesis in a rat model of Parkinson's disease via mechanisms associated with increased protein kinase activity in the striatum', *Neuropharmacology*, 167, 107976, available: http://dx.doi.org/10.1016/j.neuropharm.2020.107976.

Christensen, H.R., Frøkiaer, H. and Pestka, J.J. (2002) 'Lactobacilli differentially modulate expression of cytokines and maturation surface markers in murine dendritic cells', *J Immunol*, 168(1), 171-8, available: http://dx.doi.org/10.4049/jimmunol.168.1.171.

Chávez-Carbajal, A., Pizano-Zárate, M.L., Hernández-Quiroz, F., Ortiz-Luna, G.F., Morales-Hernández, R.M., De Sales-Millán, A., Hernández-Trejo, M., García-Vite, A., Beltrán-Lagunes, L., Hoyo-Vadillo, C. and García-Mena, J. (2020) 'Characterization of the Gut Microbiota of Individuals at Different T2D Stages Reveals a Complex Relationship with the Host', *Microorganisms*, 8(1), available: http://dx.doi.org/10.3390/microorganisms8010094.

Claesson, M.J., Cusack, S., O'Sullivan, O., Greene-Diniz, R., de Weerd, H., Flannery, E., Marchesi, J.R., Falush, D., Dinan, T., Fitzgerald, G., Stanton, C., van Sinderen, D., O'Connor, M., Harnedy, N., O'Connor, K., Henry, C., O'Mahony, D., Fitzgerald, A.P., Shanahan, F., Twomey, C., Hill, C., Ross, R.P. and O'Toole, P.W. (2011) 'Composition, variability, and temporal stability of the intestinal microbiota of the elderly', *Proc Natl Acad Sci U S A*, 108 Suppl 1, 4586-91, available: http://dx.doi.org/10.1073/pnas.1000097107.

Claesson, M.J., Jeffery, I.B., Conde, S., Power, S.E., O'Connor, E.M., Cusack, S., Harris, H.M., Coakley, M., Lakshminarayanan, B., O'Sullivan, O., Fitzgerald, G.F., Deane, J., O'Connor, M., Harnedy, N., O'Connor, K., O'Mahony, D., van Sinderen, D., Wallace, M., Brennan, L., Stanton, C., Marchesi, J.R., Fitzgerald, A.P., Shanahan, F., Hill, C., Ross, R.P. and O'Toole, P.W. (2012) 'Gut microbiota composition correlates with diet and health in the elderly', *Nature*, 488(7410), 178-84, available: http://dx.doi.org/10.1038/nature11319.

Clarke, D.J., Chaudhuri, R.R., Martin, H.M., Campbell, B.J., Rhodes, J.M., Constantinidou, C., Pallen, M.J., Loman, N.J., Cunningham, A.F., Browning, D.F. and Henderson, I.R. (2011) 'Complete genome sequence of the Crohn's disease-associated adherent-invasive Escherichia coli strain HM605', *J Bacteriol*, 193(17), 4540, available: http://dx.doi.org/10.1128/JB.05374-11.

Collino, S., Montoliu, I., Martin, F.P., Scherer, M., Mari, D., Salvioli, S., Bucci, L., Ostan, R., Monti, D., Biagi, E., Brigidi, P., Franceschi, C. and Rezzi, S. (2013) 'Metabolic signatures of extreme longevity in northern Italian centenarians reveal a complex remodeling of lipids, amino acids, and gut microbiota metabolism', *PLoS One*, 8(3), e56564, available: http://dx.doi.org/10.1371/journal.pone.0056564.

COLLINS, D.C. (1960) 'Pseudomembranous enterocolitis. Further observations on the value of donor fecal enemata as an adjunct in the treatment of pseudomembranous enterocolitis', *Am J Proctol*, 2, 389-91.

Colman, R.J., Beasley, T.M., Kemnitz, J.W., Johnson, S.C., Weindruch, R. and Anderson, R.M. (2014) 'Caloric restriction reduces age-related and all-cause mortality in rhesus monkeys', *Nat Commun*, 5, 3557, available: http://dx.doi.org/10.1038/ncomms4557.

Connell, E., Le Gall, G., Pontifex, M.G., Sami, S., Cryan, J.F., Clarke, G., Müller, M. and Vauzour, D. (2022) 'Microbial-derived metabolites as a risk factor of age-related cognitive decline and dementia', *Mol Neurodegener*, 17(1), 43, available: http://dx.doi.org/10.1186/s13024-022-00548-6.

Consortium, G.O. (2021) 'The Gene Ontology resource: enriching a GOld mine', *Nucleic Acids Res*, 49(D1), D325-D334, available: http://dx.doi.org/10.1093/nar/gkaa1113.

Contreras, C.M., Rodríguez-Landa, J.F., García-Ríos, R.I., Cueto-Escobedo, J., Guillen-Ruiz, G. and Bernal-Morales, B. (2014) 'Myristic acid produces anxiolytic-like effects in Wistar rats in the elevated plus maze', *Biomed Res Int*, 2014, 492141, available: http://dx.doi.org/10.1155/2014/492141.

Coretti, L., Paparo, L., Riccio, M.P., Amato, F., Cuomo, M., Natale, A., Borrelli, L., Corrado, G., Comegna, M., Buommino, E., Castaldo, G., Bravaccio, C.,

Chiariotti, L., Berni Canani, R. and Lembo, F. (2018) 'Gut Microbiota Features in Young Children With Autism Spectrum Disorders', *Front Microbiol*, 9, 3146, available: http://dx.doi.org/10.3389/fmicb.2018.03146.

Coretti, L., Paparo, L., Riccio, M.P., Amato, F., Cuomo, M., Natale, A., Borrelli, L., Corrado, G., De Caro, C., Comegna, M., Buommino, E., Castaldo, G., Bravaccio, C., Chiariotti, L., Berni Canani, R. and Lembo, F. (2019) 'Corrigendum: Gut Microbiota Features in Young Children With Autism Spectrum Disorders', *Front Microbiol*, 10, 920, available: http://dx.doi.org/10.3389/fmicb.2019.00920.

Corsi, A.K., Wightman, B. and Chalfie, M. (2015) 'A Transparent Window into Biology: A Primer on Caenorhabditis elegans', *Genetics*, 200(2), 387-407, available: http://dx.doi.org/10.1534/genetics.115.176099.

Cruz, M.M., Lopes, A.B., Crisma, A.R., de Sá, R.C.C., Kuwabara, W.M.T., Curi, R., de Andrade, P.B.M. and Alonso-Vale, M.I.C. (2018) 'Palmitoleic acid (16:1n7) increases oxygen consumption, fatty acid oxidation and ATP content in white adipocytes', *Lipids Health Dis*, 17(1), 55, available: http://dx.doi.org/10.1186/s12944-018-0710-z.

Cryan, J.F., O'Riordan, K.J., Cowan, C.S.M., Sandhu, K.V., Bastiaanssen, T.F.S., Boehme, M., Codagnone, M.G., Cussotto, S., Fulling, C., Golubeva, A.V., Guzzetta, K.E., Jaggar, M., Long-Smith, C.M., Lyte, J.M., Martin, J.A., Molinero-Perez, A., Moloney, G., Morelli, E., Morillas, E., O'Connor, R., Cruz-Pereira, J.S., Peterson, V.L., Rea, K., Ritz, N.L., Sherwin, E., Spichak, S., Teichman, E.M., van de Wouw, M., Ventura-Silva, A.P., Wallace-Fitzsimons, S.E., Hyland, N., Clarke, G. and Dinan, T.G. (2019) 'The Microbiota-Gut-Brain Axis', *Physiol Rev*, 99(4), 1877-2013, available: http://dx.doi.org/10.1152/physrev.00018.2018.

Cummings, J.L. (1992) 'Depression and Parkinson's disease: a review', *Am J Psychiatry*, 149(4), 443-54, available: http://dx.doi.org/10.1176/ajp.149.4.443.

D'Amato, A., Di Cesare Mannelli, L., Lucarini, E., Man, A.L., Le Gall, G., Branca, J.J.V., Ghelardini, C., Amedei, A., Bertelli, E., Regoli, M., Pacini, A., Luciani, G., Gallina, P., Altera, A., Narbad, A., Gulisano, M., Hoyles, L., Vauzour, D. and Nicoletti, C. (2020) 'Faecal microbiota transplant from aged donor mice affects spatial learning and memory via modulating hippocampal synaptic plasticity- and neurotransmission-related proteins in young recipients', *Microbiome*, 8(1), 140, available: http://dx.doi.org/10.1186/s40168-020-00914-w.

Darfeuille-Michaud, A. (2002) 'Adherent-invasive Escherichia coli: a putative new E. coli pathotype associated with Crohn's disease', *Int J Med Microbiol*, 292(3-4), 185-93, available: http://dx.doi.org/10.1078/1438-4221-00201.

Das, U.N. (2006) 'Essential Fatty acids - a review', *Curr Pharm Biotechnol*, 7(6), 467-82, available: http://dx.doi.org/10.2174/138920106779116856.

Datsenko, K.A. and Wanner, B.L. (2000) 'One-step inactivation of chromosomal genes in Escherichia coli K-12 using PCR products', *Proc Natl Acad Sci U S A*, 97(12), 6640-5, available: http://dx.doi.org/10.1073/pnas.120163297.

de Aguiar Vallim, T.Q., Tarling, E.J., Ahn, H., Hagey, L.R., Romanoski, C.E., Lee, R.G., Graham, M.J., Motohashi, H., Yamamoto, M. and Edwards, P.A. (2015) 'MAFG is a transcriptional repressor of bile acid synthesis and metabolism', *Cell Metab*, 21(2), 298-311, available: http://dx.doi.org/10.1016/j.cmet.2015.01.007.

de la Cuesta-Zuluaga, J., Kelley, S.T., Chen, Y., Escobar, J.S., Mueller, N.T., Ley, R.E., McDonald, D., Huang, S., Swafford, A.D., Knight, R. and Thackray, V.G. (2019) 'Age- and Sex-Dependent Patterns of Gut Microbial Diversity in Human Adults', *mSystems*, 4(4), available: http://dx.doi.org/10.1128/mSystems.00261-19.

de Sousa Figueiredo, M.B., Pradel, E., George, F., Mahieux, S., Houcke, I., Pottier, M., Fradin, C., Neut, C., Daniel, C., Bongiovanni, A., Foligné, B. and Titécat, M. (2021) 'Adherent-Invasive and Non-Invasive', *Microorganisms*, 9(9), available: http://dx.doi.org/10.3390/microorganisms9091823.

Deelen, J., Evans, D.S., Arking, D.E., Tesi, N., Nygaard, M., Liu, X., Wojczynski, M.K., Biggs, M.L., van der Spek, A., Atzmon, G., Ware, E.B., Sarnowski, C., Smith, A.V., Seppälä, I., Cordell, H.J., Dose, J., Amin, N., Arnold, A.M., Ayers, K.L., Barzilai, N., Becker, E.J., Beekman, M., Blanché, H., Christensen, K., Christiansen, L., Collerton, J.C., Cubaynes, S., Cummings, S.R., Davies, K., Debrabant, B., Deleuze, J.F., Duncan, R., Faul, J.D., Franceschi, C., Galan, P., Gudnason, V., Harris, T.B., Huisman, M., Hurme, M.A., Jagger, C., Jansen, I., Jylhä, M., Kähönen, M., Karasik, D., Kardia, S.L.R., Kingston, A., Kirkwood, T.B.L., Launer, L.J., Lehtimäki, T., Lieb, W., Lyytikäinen, L.P., Martin-Ruiz, C., Min, J., Nebel, A., Newman, A.B., Nie, C., Nohr, E.A., Orwoll, E.S., Perls, T.T., Province, M.A., Psaty, B.M., Raitakari, O.T., Reinders, M.J.T., Robine, J.M., Rotter, J.I., Sebastiani, P., Smith, J., Sørensen, T.I.A., Taylor, K.D., Uitterlinden, A.G., van der Flier, W., van der Lee, S.J., van Duijn, C.M., van Heemst, D., Vaupel, J.W., Weir, D., Ye, K., Zeng, Y., Zheng, W., Holstege, H., Kiel, D.P., Lunetta, K.L., Slagboom, P.E. and Murabito, J.M. (2019) 'A meta-analysis of genome-wide association studies identifies multiple longevity genes', *Nat Commun*, 10(1), 3669, available: http://dx.doi.org/10.1038/s41467-019-11558-2.

Degirolamo, C., Rainaldi, S., Bovenga, F., Murzilli, S. and Moschetta, A. (2014) 'Microbiota modification with probiotics induces hepatic bile acid synthesis

via downregulation of the Fxr-Fgf15 axis in mice', *Cell Rep*, 7(1), 12-8, available: http://dx.doi.org/10.1016/j.celrep.2014.02.032.

Desbonnet, L., Clarke, G., Shanahan, F., Dinan, T.G. and Cryan, J.F. (2014) 'Microbiota is essential for social development in the mouse', *Mol Psychiatry*, 19(2), 146-8, available: http://dx.doi.org/10.1038/mp.2013.65.

Dhouib, R., Vagenas, D., Hong, Y., Verderosa, A.D., Martin, J.L., Heras, B. and Totsika, M. (2021) 'Antivirulence DsbA inhibitors attenuate', *FASEB Bioadv*, 3(4), 231-242, available: http://dx.doi.org/10.1096/fba.2020-00100.

Dirksen, P., Marsh, S.A., Braker, I., Heitland, N., Wagner, S., Nakad, R., Mader, S., Petersen, C., Kowallik, V., Rosenstiel, P., Félix, M.A. and Schulenburg, H. (2016) 'The native microbiome of the nematode Caenorhabditis elegans: gateway to a new host-microbiome model', *BMC Biol*, 14, 38, available: http://dx.doi.org/10.1186/s12915-016-0258-1.

Dong, J., Beard, J.D., Umbach, D.M., Park, Y., Huang, X., Blair, A., Kamel, F. and Chen, H. (2014) 'Dietary fat intake and risk for Parkinson's disease', *Mov Disord*, 29(13), 1623-30, available: http://dx.doi.org/10.1002/mds.26032.

Dreux, N., Denizot, J., Martinez-Medina, M., Mellmann, A., Billig, M., Kisiela, D., Chattopadhyay, S., Sokurenko, E., Neut, C., Gower-Rousseau, C., Colombel, J.F., Bonnet, R., Darfeuille-Michaud, A. and Barnich, N. (2013) 'Point mutations in FimH adhesin of Crohn's disease-associated adherent-invasive Escherichia coli enhance intestinal inflammatory response', *PLoS Pathog*, 9(1), e1003141, available: http://dx.doi.org/10.1371/journal.ppat.1003141.

Dumas, K.J., Guo, C., Shih, H.J. and Hu, P.J. (2013) 'Influence of steroid hormone signaling on life span control by Caenorhabditis elegans insulin-like signaling', *G3 (Bethesda)*, 3(5), 841-50, available: http://dx.doi.org/10.1534/g3.112.005116.

Dumas, K.J., Guo, C., Wang, X., Burkhart, K.B., Adams, E.J., Alam, H. and Hu, P.J. (2010) 'Functional divergence of dafachronic acid pathways in the control of C. elegans development and lifespan', *Dev Biol*, 340(2), 605-12, available: http://dx.doi.org/10.1016/j.ydbio.2010.02.022.

Dumych, T., Yamakawa, N., Sivignon, A., Garenaux, E., Robakiewicz, S., Coddeville, B., Bongiovanni, A., Bray, F., Barnich, N., Szunerits, S., Slomianny, C., Herrmann, M., Gouin, S.G., Lutsyk, A.D., Munoz, L.E., Lafont, F., Rolando, C., Bilyy, R. and Bouckaert, J.M.J. (2018) 'Oligomannose-Rich Membranes of Dying Intestinal Epithelial Cells Promote Host Colonization by Adherent-Invasive', *Front Microbiol*, 9, 742, available: http://dx.doi.org/10.3389/fmicb.2018.00742.

Duparc, T., Plovier, H., Marrachelli, V.G., Van Hul, M., Essaghir, A., Ståhlman, M., Matamoros, S., Geurts, L., Pardo-Tendero, M.M., Druart, C., Delzenne, N.M., Demoulin, J.B., van der Merwe, S.W., van Pelt, J., Bäckhed, F., Monleon, D., Everard, A. and Cani, P.D. (2017) 'Hepatocyte MyD88 affects bile acids, gut microbiota and metabolome contributing to regulate glucose and lipid metabolism', *Gut*, 66(4), 620-632, available: http://dx.doi.org/10.1136/gutjnl-2015-310904.

Duran-Sandoval, D., Mautino, G., Martin, G., Percevault, F., Barbier, O., Fruchart, J.C., Kuipers, F. and Staels, B. (2004) 'Glucose regulates the expression of the farnesoid X receptor in liver', *Diabetes*, 53(4), 890-8, available: http://dx.doi.org/10.2337/diabetes.53.4.890.

Dyke, B., Gage, T.B., Mamelka, P.M., Goy, R.W. and Stone, W.H. (1986) 'A demographic analysis of the Wisconsin Regional Primate Center rhesus colony, 1962-1982', *Am J Primatol*, 10(3), 257-269, available: http://dx.doi.org/10.1002/ajp.1350100306.

Edwards, C., Canfield, J., Copes, N., Rehan, M., Lipps, D. and Bradshaw, P.C. (2014) 'D-beta-hydroxybutyrate extends lifespan in C. elegans', *Aging (Albany NY)*, 6(8), 621-44, available: http://dx.doi.org/10.18632/aging.100683.

EISEMAN, B., SILEN, W., BASCOM, G.S. and KAUVAR, A.J. (1958) 'Fecal enema as an adjunct in the treatment of pseudomembranous enterocolitis', *Surgery*, 44(5), 854-9.

Endo, N., Makinodan, M., Somayama, N., Komori, T., Kishimoto, T. and Nishi, M. (2019) 'Characterization of behavioral phenotypes in the BTBR T', *Exp Anim*, 68(3), 319-330, available: http://dx.doi.org/10.1538/expanim.18-0177.

Enright, E.F., Gahan, C.G., Joyce, S.A. and Griffin, B.T. (2016) 'The Impact of the Gut Microbiota on Drug Metabolism and Clinical Outcome', *Yale J Biol Med*, 89(3), 375-382.

Enright, E.F., Joyce, S.A., Gahan, C.G. and Griffin, B.T. (2017) 'Impact of Gut Microbiota-Mediated Bile Acid Metabolism on the Solubilization Capacity of Bile Salt Micelles and Drug Solubility', *Mol Pharm*, 14(4), 1251-1263, available: http://dx.doi.org/10.1021/acs.molpharmaceut.6b01155.

Erny, D., Hrabě de Angelis, A.L., Jaitin, D., Wieghofer, P., Staszewski, O., David, E., Keren-Shaul, H., Mahlakoiv, T., Jakobshagen, K., Buch, T., Schwierzeck, V., Utermöhlen, O., Chun, E., Garrett, W.S., McCoy, K.D., Diefenbach, A., Staeheli, P., Stecher, B., Amit, I. and Prinz, M. (2015) 'Host microbiota constantly control maturation and function of microglia in the CNS', *Nat Neurosci*, 18(7), 965-77, available: http://dx.doi.org/10.1038/nn.4030.

Ewbank, J.J., Barnes, T.M., Lakowski, B., Lussier, M., Bussey, H. and Hekimi, S. (1997) 'Structural and functional conservation of the Caenorhabditis elegans timing gene clk-1', *Science*, 275(5302), 980-3, available: http://dx.doi.org/10.1126/science.275.5302.980.

Fais, S., Capobianchi, M.R., Pallone, F., Di Marco, P., Boirivant, M., Dianzani, F. and Torsoli, A. (1991) 'Spontaneous release of interferon gamma by intestinal lamina propria lymphocytes in Crohn's disease. Kinetics of in vitro response to interferon gamma inducers', *Gut*, 32(4), 403-7, available: http://dx.doi.org/10.1136/gut.32.4.403.

Fallani, M., Amarri, S., Uusijarvi, A., Adam, R., Khanna, S., Aguilera, M., Gil, A., Vieites, J.M., Norin, E., Young, D., Scott, J.A., Doré, J., Edwards, C.A. and The Infabio Team (2011) 'Determinants of the human infant intestinal microbiota after the introduction of first complementary foods in infant samples from five European centres', *Microbiology (Reading)*, 157(Pt 5), 1385-1392, available: http://dx.doi.org/10.1099/mic.0.042143-0.

Fanning, S., Haque, A., Imberdis, T., Baru, V., Barrasa, M.I., Nuber, S., Termine, D., Ramalingam, N., Ho, G.P.H., Noble, T., Sandoe, J., Lou, Y., Landgraf, D., Freyzon, Y., Newby, G., Soldner, F., Terry-Kantor, E., Kim, T.E., Hofbauer, H.F., Becuwe, M., Jaenisch, R., Pincus, D., Clish, C.B., Walther, T.C., Farese, R.V., Srinivasan, S., Welte, M.A., Kohlwein, S.D., Dettmer, U., Lindquist, S. and Selkoe, D. (2019) 'Lipidomic Analysis of α-Synuclein Neurotoxicity Identifies Stearoyl CoA Desaturase as a Target for Parkinson Treatment', *Mol Cell*, 73(5), 1001-1014.e8, available: http://dx.doi.org/10.1016/j.molcel.2018.11.028.

Fedotova, E.I., Dolgacheva, L.P., Abramov, A.Y. and Berezhnov, A.V. (2022) 'Lactate and Pyruvate Activate Autophagy and Mitophagy that Protect Cells in Toxic Model of Parkinson's Disease', *Mol Neurobiol*, 59(1), 177-190, available: http://dx.doi.org/10.1007/s12035-021-02583-8.

Fehily, S.R., Basnayake, C., Wright, E.K. and Kamm, M.A. (2021) 'Fecal microbiota transplantation therapy in Crohn's disease: Systematic review', *J Gastroenterol Hepatol*, 36(10), 2672-2686, available: http://dx.doi.org/10.1111/jgh.15598.

Felkai, S., Ewbank, J.J., Lemieux, J., Labbé, J.C., Brown, G.G. and Hekimi, S. (1999) 'CLK-1 controls respiration, behavior and aging in the nematode Caenorhabditis elegans', *EMBO J*, 18(7), 1783-92, available: http://dx.doi.org/10.1093/emboj/18.7.1783.

Finegold, S.M., Summanen, P.H., Downes, J., Corbett, K. and Komoriya, T. (2017) 'Detection of Clostridium perfringens toxin genes in the gut microbiota of autistic children', *Anaerobe*, 45, 133-137, available: http://dx.doi.org/10.1016/j.anaerobe.2017.02.008.

Forbes, J.D., Van Domselaar, G. and Bernstein, C.N. (2016) 'Microbiome Survey of the Inflamed and Noninflamed Gut at Different Compartments Within the Gastrointestinal Tract of Inflammatory Bowel Disease Patients', *Inflamm Bowel Dis*, 22(4), 817-25, available: http://dx.doi.org/10.1097/MIB.0000000000000684.

Forsyth, C.B., Shannon, K.M., Kordower, J.H., Voigt, R.M., Shaikh, M., Jaglin, J.A., Estes, J.D., Dodiya, H.B. and Keshavarzian, A. (2011) 'Increased intestinal permeability correlates with sigmoid mucosa alpha-synuclein staining and endotoxin exposure markers in early Parkinson's disease', *PLoS One*, 6(12), e28032, available: http://dx.doi.org/10.1371/journal.pone.0028032.

Fortin, C.F., Larbi, A., Lesur, O., Douziech, N. and Fulop, T. (2006) 'Impairment of SHP-1 down-regulation in the lipid rafts of human neutrophils under GM-CSF stimulation contributes to their age-related, altered functions', *J Leukoc Biol*, 79(5), 1061-72, available: http://dx.doi.org/10.1189/jlb.0805481.

Franceschi, C., Bonafè, M., Valensin, S., Olivieri, F., De Luca, M., Ottaviani, E. and De Benedictis, G. (2000) 'Inflamm-aging. An evolutionary perspective on immunosenescence', *Ann N Y Acad Sci*, 908, 244-54, available: http://dx.doi.org/10.1111/j.1749-6632.2000.tb06651.x.

Frank, D.N., St Amand, A.L., Feldman, R.A., Boedeker, E.C., Harpaz, N. and Pace, N.R. (2007) 'Molecular-phylogenetic characterization of microbial community imbalances in human inflammatory bowel diseases', *Proc Natl Acad Sci U S A*, 104(34), 13780-5, available: http://dx.doi.org/10.1073/pnas.0706625104.

Frazier, R., Cai, X., Lee, J., Bundy, J.D., Jovanovich, A., Chen, J., Deo, R., Lash, J.P., Anderson, A.H., Go, A.S., Feldman, H.I., Shafi, T., Rhee, E.P., Miyazaki, M., Chonchol, M., Isakova, T. and Investigators, C.R.I.C.C.S. (2022) 'Deoxycholic Acid and Risks of Cardiovascular Events, ESKD, and Mortality in CKD: The CRIC Study', *Kidney Med*, 4(1), 100387, available: http://dx.doi.org/10.1016/j.xkme.2021.09.004.

Frehner, S.S., Dooley, K.T., Palumbo, M.C., Smith, A.L., Goodman, M.M., Bales, K.L. and Freeman, S.M. (2022) 'Effect of sex and autism spectrum disorder on oxytocin receptor binding and mRNA expression in the dopaminergic pars compacta of the human substantia nigra', *Philos Trans R Soc Lond B Biol Sci*, 377(1858), 20210118, available: http://dx.doi.org/10.1098/rstb.2021.0118.

Friedman, D.B. and Johnson, T.E. (1988a) 'A mutation in the age-1 gene in Caenorhabditis elegans lengthens life and reduces hermaphrodite fertility', *Genetics*, 118(1), 75-86.

Friedman, D.B. and Johnson, T.E. (1988b) 'Three mutants that extend both mean and maximum life span of the nematode, Caenorhabditis elegans, define the

age-1 gene', *J Gerontol*, 43(4), B102-9, available: http://dx.doi.org/10.1093/geronj/43.4.b102.

Frommherz, L., Bub, A., Hummel, E., Rist, M.J., Roth, A., Watzl, B. and Kulling, S.E. (2016) 'Age-Related Changes of Plasma Bile Acid Concentrations in Healthy Adults--Results from the Cross-Sectional KarMeN Study', *PLoS One*, 11(4), e0153959, available: http://dx.doi.org/10.1371/journal.pone.0153959.

Galkin, F., Mamoshina, P., Aliper, A., Putin, E., Moskalev, V., Gladyshev, V.N. and Zhavoronkov, A. (2020) 'Human Gut Microbiome Aging Clock Based on Taxonomic Profiling and Deep Learning', *iScience*, 23(6), 101199, available: http://dx.doi.org/10.1016/j.isci.2020.101199.

Gao, J., He, J., Zhai, Y., Wada, T. and Xie, W. (2009) 'The constitutive androstane receptor is an anti-obesity nuclear receptor that improves insulin sensitivity', *J Biol Chem*, 284(38), 25984-92, available: http://dx.doi.org/10.1074/jbc.M109.016808.

Garrigues, C., Goupil-Feuillerat, N., Cocaign-Bousquet, M., Renault, P., Lindley, N.D. and Loubiere, P. (2001) 'Glucose metabolism and regulation of glycolysis in Lactococcus lactis strains with decreased lactate dehydrogenase activity', *Metab Eng*, 3(3), 211-7, available: http://dx.doi.org/10.1006/mben.2001.0182.

Garsin, D.A., Villanueva, J.M., Begun, J., Kim, D.H., Sifri, C.D., Calderwood, S.B., Ruvkun, G. and Ausubel, F.M. (2003) 'Long-lived C. elegans daf-2 mutants are resistant to bacterial pathogens', *Science*, 300(5627), 1921, available: http://dx.doi.org/10.1126/science.1080147.

Gartner, A., Boag, P.R. and Blackwell, T.K. (2008) 'Germline Survival and Apoptosis'.

Gems, D. (2007) 'Long-lived dwarf mice: are bile acids a longevity signal?', *Aging Cell*, 6(4), 421-3, available: http://dx.doi.org/10.1111/j.1474-9726.2007.00309.x.

Gerisch, B., Rottiers, V., Li, D., Motola, D.L., Cummins, C.L., Lehrach, H., Mangelsdorf, D.J. and Antebi, A. (2007) 'A bile acid-like steroid modulates Caenorhabditis elegans lifespan through nuclear receptor signaling', *Proc Natl Acad Sci U S A*, 104(12), 5014-9, available: http://dx.doi.org/10.1073/pnas.0700847104.

Gerisch, B., Weitzel, C., Kober-Eisermann, C., Rottiers, V. and Antebi, A. (2001) 'A hormonal signaling pathway influencing C. elegans metabolism, reproductive development, and life span', *Dev Cell*, 1(6), 841-51, available: http://dx.doi.org/10.1016/s1534-5807(01)00085-5.

Ghosh, A., Tyson, T., George, S., Hildebrandt, E.N., Steiner, J.A., Madaj, Z., Schulz, E., Machiela, E., McDonald, W.G., Escobar Galvis, M.L., Kordower, J.H., Van Raamsdonk, J.M., Colca, J.R. and Brundin, P. (2016) 'Mitochondrial pyruvate carrier regulates autophagy, inflammation, and neurodegeneration in experimental models of Parkinson's disease', *Sci Transl Med*, 8(368), 368ra174, available: http://dx.doi.org/10.1126/scitranslmed.aag2210.

Ghosh, T.S., Rampelli, S., Jeffery, I.B., Santoro, A., Neto, M., Capri, M., Giampieri, E., Jennings, A., Candela, M., Turroni, S., Zoetendal, E.G., Hermes, G.D.A., Elodie, C., Meunier, N., Brugere, C.M., Pujos-Guillot, E., Berendsen, A.M., De Groot, L.C.P.G., Feskins, E.J.M., Kaluza, J., Pietruszka, B., Bielak, M.J., Comte, B., Maijo-Ferre, M., Nicoletti, C., De Vos, W.M., Fairweather-Tait, S., Cassidy, A., Brigidi, P., Franceschi, C. and O'Toole, P.W. (2020) 'Mediterranean diet intervention alters the gut microbiome in older people reducing frailty and improving health status: the NU-AGE 1-year dietary intervention across five European countries', *Gut*, 69(7), 1218-1228, available: http://dx.doi.org/10.1136/gutjnl-2019-319654.

Ghosh, T.S., Shanahan, F. and O'Toole, P.W. (2022) 'The gut microbiome as a modulator of healthy ageing', *Nat Rev Gastroenterol Hepatol*, 19(9), 565-584, available: http://dx.doi.org/10.1038/s41575-022-00605-x.

Giaffer, M.H., Holdsworth, C.D. and Duerden, B.I. (1992) 'Virulence properties of Escherichia coli strains isolated from patients with inflammatory bowel disease', *Gut*, 33(5), 646-50, available: http://dx.doi.org/10.1136/gut.33.5.646.

Gibson, J., Russ, T.C., Clarke, T.K., Howard, D.M., Hillary, R.F., Evans, K.L., Walker, R.M., Bermingham, M.L., Morris, S.W., Campbell, A., Hayward, C., Murray, A.D., Porteous, D.J., Horvath, S., Lu, A.T., McIntosh, A.M., Whalley, H.C. and Marioni, R.E. (2019) 'A meta-analysis of genome-wide association studies of epigenetic age acceleration', *PLoS Genet*, 15(11), e1008104, available: http://dx.doi.org/10.1371/journal.pgen.1008104.

Gill, S.R., Pop, M., Deboy, R.T., Eckburg, P.B., Turnbaugh, P.J., Samuel, B.S., Gordon, J.I., Relman, D.A., Fraser-Liggett, C.M. and Nelson, K.E. (2006) 'Metagenomic analysis of the human distal gut microbiome', *Science*, 312(5778), 1355-9, available: http://dx.doi.org/10.1126/science.1124234.

Gingras, A.C., Raught, B. and Sonenberg, N. (1999) 'eIF4 initiation factors: effectors of mRNA recruitment to ribosomes and regulators of translation', *Annu Rev Biochem*, 68, 913-63, available: http://dx.doi.org/10.1146/annurev.biochem.68.1.913.

Glinghammar, B., Inoue, H. and Rafter, J.J. (2002) 'Deoxycholic acid causes DNA damage in colonic cells with subsequent induction of caspases, COX-2 promoter activity and the transcription factors NF-kB and AP-1',

Carcinogenesis, 23(5), 839-45, available: http://dx.doi.org/10.1093/carcin/23.5.839.

Goldberg, A.A., Richard, V.R., Kyryakov, P., Bourque, S.D., Beach, A., Burstein, M.T., Glebov, A., Koupaki, O., Boukh-Viner, T., Gregg, C., Juneau, M., English, A.M., Thomas, D.Y. and Titorenko, V.I. (2010) 'Chemical genetic screen identifies lithocholic acid as an anti-aging compound that extends yeast chronological life span in a TOR-independent manner, by modulating housekeeping longevity assurance processes', *Aging (Albany NY)*, 2(7), 393-414, available: http://dx.doi.org/10.18632/aging.100168.

Golden, J.W. and Riddle, D.L. (1984) 'The Caenorhabditis elegans dauer larva: developmental effects of pheromone, food, and temperature', *Dev Biol*, 102(2), 368-78, available: http://dx.doi.org/10.1016/0012-1606(84)90201-x.

Golubeva, A.V., Joyce, S.A., Moloney, G., Burokas, A., Sherwin, E., Arboleya, S., Flynn, I., Khochanskiy, D., Moya-Pérez, A., Peterson, V., Rea, K., Murphy, K., Makarova, O., Buravkov, S., Hyland, N.P., Stanton, C., Clarke, G., Gahan, C.G.M., Dinan, T.G. and Cryan, J.F. (2017) 'Microbiota-related Changes in Bile Acid & Tryptophan Metabolism are Associated with Gastrointestinal Dysfunction in a Mouse Model of Autism', *EBioMedicine*, 24, 166-178, available: http://dx.doi.org/10.1016/j.ebiom.2017.09.020.

Gonzales, E., Matarazzo, L., Franchi-Abella, S., Dabadie, A., Cohen, J., Habes, D., Hillaire, S., Guettier, C., Taburet, A.M., Myara, A. and Jacquemin, E. (2018) 'Cholic acid for primary bile acid synthesis defects: a life-saving therapy allowing a favorable outcome in adulthood', *Orphanet J Rare Dis*, 13(1), 190, available: http://dx.doi.org/10.1186/s13023-018-0920-5.

Goodwin, M.S., Cowen, M.A. and Goodwin, T.C. (1971) 'Malabsorption and cerebral dysfunction: a multivariate and comparative study of autistic children', *J Autism Child Schizophr*, 1(1), 48-62, available: http://dx.doi.org/10.1007/BF01537742.

Gopal-Srivastava, R. and Hylemon, P.B. (1988) 'Purification and characterization of bile salt hydrolase from Clostridium perfringens', *J Lipid Res*, 29(8), 1079-85.

Govindarajan, K., MacSharry, J., Casey, P.G., Shanahan, F., Joyce, S.A. and Gahan, C.G. (2016) 'Unconjugated Bile Acids Influence Expression of Circadian Genes: A Potential Mechanism for Microbe-Host Crosstalk', *PLoS One*, 11(12), e0167319, available: http://dx.doi.org/10.1371/journal.pone.0167319.

Graham, S.F., Rey, N.L., Ugur, Z., Yilmaz, A., Sherman, E., Maddens, M., Bahado-Singh, R.O., Becker, K., Schulz, E., Meyerdirk, L.K., Steiner, J.A., Ma, J. and Brundin, P. (2018a) 'Metabolomic Profiling of Bile Acids in an Experimental

Model of Prodromal Parkinson's Disease', *Metabolites*, 8(4), available: http://dx.doi.org/10.3390/metabo8040071.

Graham, S.F., Rey, N.L., Yilmaz, A., Kumar, P., Madaj, Z., Maddens, M., Bahado-Singh, R.O., Becker, K., Schulz, E., Meyerdirk, L.K., Steiner, J.A., Ma, J. and Brundin, P. (2018b) 'Biochemical Profiling of the Brain and Blood Metabolome in a Mouse Model of Prodromal Parkinson's Disease Reveals Distinct Metabolic Profiles', *J Proteome Res*, 17(7), 2460-2469, available: http://dx.doi.org/10.1021/acs.jproteome.8b00224.

Grant, S.M. and DeMorrow, S. (2020) 'Bile Acid Signaling in Neurodegenerative and Neurological Disorders', *Int J Mol Sci*, 21(17), available: http://dx.doi.org/10.3390/ijms21175982.

Groen, A.K. and Kuipers, F. (2013) 'Bile acid look-alike controls life span in C. elegans', *Cell Metab*, 18(2), 151-2, available: http://dx.doi.org/10.1016/j.cmet.2013.07.009.

Gross, D.N., van den Heuvel, A.P. and Birnbaum, M.J. (2008) 'The role of FoxO in the regulation of metabolism', *Oncogene*, 27(16), 2320-36, available: http://dx.doi.org/10.1038/onc.2008.25.

Guo, G.L., Lambert, G., Negishi, M., Ward, J.M., Brewer, H.B., Kliewer, S.A., Gonzalez, F.J. and Sinal, C.J. (2003) 'Complementary roles of farnesoid X receptor, pregnane X receptor, and constitutive androstane receptor in protection against bile acid toxicity', *J Biol Chem*, 278(46), 45062-71, available: http://dx.doi.org/10.1074/jbc.M307145200.

Guo, M., Li, R., Wang, Y., Ma, S., Zhang, Y., Li, S., Zhang, H., Liu, Z., You, C. and Zheng, H. (2022) 'Lactobacillus plantarum ST-III modulates abnormal behavior and gut microbiota in a mouse model of autism spectrum disorder', *Physiol Behav*, 257, 113965, available: http://dx.doi.org/10.1016/j.physbeh.2022.113965.

Gupta, R.A., Wang, D., Katkuri, S., Wang, H., Dey, S.K. and DuBois, R.N. (2004) 'Activation of nuclear hormone receptor peroxisome proliferator-activated receptor-delta accelerates intestinal adenoma growth', *Nat Med*, 10(3), 245-7, available: http://dx.doi.org/10.1038/nm993.

Guzior, D.V. and Quinn, R.A. (2021) 'Review: microbial transformations of human bile acids', *Microbiome*, 9(1), 140, available: http://dx.doi.org/10.1186/s40168-021-01101-1.

Gåfvels, M., Olin, M., Chowdhary, B.P., Raudsepp, T., Andersson, U., Persson, B., Jansson, M., Björkhem, I. and Eggertsen, G. (1999) 'Structure and chromosomal assignment of the sterol 12alpha-hydroxylase gene (CYP8B1) in human and mouse: eukaryotic cytochrome P-450 gene devoid of introns',

Genomics, 56(2), 184-96, available: http://dx.doi.org/10.1006/geno.1998.5606.

Gómez-Soler, M., Cordobilla, B., Morató, X., Fernández-Dueñas, V., Domingo, J.C. and Ciruela, F. (2018) 'Triglyceride Form of Docosahexaenoic Acid Mediates Neuroprotection in Experimental Parkinsonism', *Front Neurosci*, 12, 604, available: http://dx.doi.org/10.3389/fnins.2018.00604.

Hamilton, J.P., Xie, G., Raufman, J.P., Hogan, S., Griffin, T.L., Packard, C.A., Chatfield, D.A., Hagey, L.R., Steinbach, J.H. and Hofmann, A.F. (2007) 'Human cecal bile acids: concentration and spectrum', *Am J Physiol Gastrointest Liver Physiol*, 293(1), G256-63, available: http://dx.doi.org/10.1152/ajpgi.00027.2007.

Hammell, C.M., Karp, X. and Ambros, V. (2009) 'A feedback circuit involving let-7-family miRNAs and DAF-12 integrates environmental signals and developmental timing in Caenorhabditis elegans', *Proc Natl Acad Sci U S A*, 106(44), 18668-73, available: http://dx.doi.org/10.1073/pnas.0908131106.

Han, B., Sivaramakrishnan, P., Lin, C.J., Neve, I.A.A., He, J., Tay, L.W.R., Sowa, J.N., Sizovs, A., Du, G., Wang, J., Herman, C. and Wang, M.C. (2017) 'Microbial Genetic Composition Tunes Host Longevity', *Cell*, 169(7), 1249-1262.e13, available: http://dx.doi.org/10.1016/j.cell.2017.05.036.

Han, S., Li, T., Ellis, E., Strom, S. and Chiang, J.Y. (2010) 'A novel bile acid-activated vitamin D receptor signaling in human hepatocytes', *Mol Endocrinol*, 24(6), 1151-64, available: http://dx.doi.org/10.1210/me.2009-0482.

Hansen, M., Taubert, S., Crawford, D., Libina, N., Lee, S.J. and Kenyon, C. (2007) 'Lifespan extension by conditions that inhibit translation in Caenorhabditis elegans', *Aging Cell*, 6(1), 95-110, available: http://dx.doi.org/10.1111/j.1474-9726.2006.00267.x.

Harrison, D.E., Strong, R., Sharp, Z.D., Nelson, J.F., Astle, C.M., Flurkey, K., Nadon, N.L., Wilkinson, J.E., Frenkel, K., Carter, C.S., Pahor, M., Javors, M.A., Fernandez, E. and Miller, R.A. (2009) 'Rapamycin fed late in life extends lifespan in genetically heterogeneous mice', *Nature*, 460(7253), 392-5, available: http://dx.doi.org/10.1038/nature08221.

Hasegawa, S., Goto, S., Tsuji, H., Okuno, T., Asahara, T., Nomoto, K., Shibata, A., Fujisawa, Y., Minato, T., Okamoto, A., Ohno, K. and Hirayama, M. (2015) 'Intestinal Dysbiosis and Lowered Serum Lipopolysaccharide-Binding Protein in Parkinson's Disease', *PLoS One*, 10(11), e0142164, available: http://dx.doi.org/10.1371/journal.pone.0142164.

He, J., Zhang, P., Shen, L., Niu, L., Tan, Y., Chen, L., Zhao, Y., Bai, L., Hao, X., Li, X., Zhang, S. and Zhu, L. (2020) 'Short-Chain Fatty Acids and Their Association

with Signalling Pathways in Inflammation, Glucose and Lipid Metabolism', *Int J Mol Sci*, 21(17), available: http://dx.doi.org/10.3390/ijms21176356.

Health, T.I.o.P. (2020) *Ageing and Public Health - an overview of key statistics in Ireland and Northern Ireland*, available: https://publichealth.ie/wp-content/uploads/2020/04/20200416-AGEING-PUBLIC-HEALTH-SUMMARY.pdf [accessed.

Heinken, A., Ravcheev, D.A., Baldini, F., Heirendt, L., Fleming, R.M.T. and Thiele, I. (2019) 'Systematic assessment of secondary bile acid metabolism in gut microbes reveals distinct metabolic capabilities in inflammatory bowel disease', *Microbiome*, 7(1), 75, available: http://dx.doi.org/10.1186/s40168-019-0689-3.

Heitman, J., Movva, N.R. and Hall, M.N. (1991) 'Targets for cell cycle arrest by the immunosuppressant rapamycin in yeast', *Science*, 253(5022), 905-9, available: http://dx.doi.org/10.1126/science.1715094.

Hertel, J., Harms, A.C., Heinken, A., Baldini, F., Thinnes, C.C., Glaab, E., Vasco, D.A., Pietzner, M., Stewart, I.D., Wareham, N.J., Langenberg, C., Trenkwalder, C., Krüger, R., Hankemeier, T., Fleming, R.M.T., Mollenhauer, B. and Thiele, I. (2019) 'Integrated Analyses of Microbiome and Longitudinal Metabolome Data Reveal Microbial-Host Interactions on Sulfur Metabolism in Parkinson's Disease', *Cell Rep*, 29(7), 1767-1777.e8, available: http://dx.doi.org/10.1016/j.celrep.2019.10.035.

Heuer, E., Rosen, R.F., Cintron, A. and Walker, L.C. (2012) 'Nonhuman primate models of Alzheimer-like cerebral proteopathy', *Curr Pharm Des*, 18(8), 1159-69, available: http://dx.doi.org/10.2174/138161212799315885.

Higashi, T., Watanabe, S., Tomaru, K., Yamazaki, W., Yoshizawa, K., Ogawa, S., Nagao, H., Minato, K., Maekawa, M. and Mano, N. (2017) 'Unconjugated bile acids in rat brain: Analytical method based on LC/ESI-MS/MS with chemical derivatization and estimation of their origin by comparison to serum levels', *Steroids*, 125, 107-113, available: http://dx.doi.org/10.1016/j.steroids.2017.07.001.

Hoban, A.E., Moloney, R.D., Golubeva, A.V., McVey Neufeld, K.A., O'Sullivan, O., Patterson, E., Stanton, C., Dinan, T.G., Clarke, G. and Cryan, J.F. (2016) 'Behavioural and neurochemical consequences of chronic gut microbiota depletion during adulthood in the rat', *Neuroscience*, 339, 463-477, available: http://dx.doi.org/10.1016/j.neuroscience.2016.10.003.

Hoban, A.E., Moloney, R.D., Golubeva, A.V., McVey Neufeld, K.A., O'Sullivan, O., Patterson, E., Stanton, C., Dinan, T.G., Clarke, G. and Cryan, J.F. (2017) 'Corrigendum to "Behavioural and neurochemical consequences of chronic gut microbiota depletion during adulthood in the rat" [Neuroscience 339

(2016) 463-477]', *Neuroscience*, 344, 418, available: http://dx.doi.org/10.1016/j.neuroscience.2017.01.008.

Hoehn, M.M. and Yahr, M.D. (1967) 'Parkinsonism: onset, progression and mortality', *Neurology*, 17(5), 427-42, available: http://dx.doi.org/10.1212/wnl.17.5.427.

Hofmann, A.F., Cravetto, C., Molino, G., Belforte, G. and Bona, B. (1987) 'Simulation of the metabolism and enterohepatic circulation of endogenous deoxycholic acid in humans using a physiologic pharmacokinetic model for bile acid metabolism', *Gastroenterology*, 93(4), 693-709, available: http://dx.doi.org/10.1016/0016-5085(87)90430-6.

Hofmann, A.F. and Eckmann, L. (2006) 'How bile acids confer gut mucosal protection against bacteria', *Proc Natl Acad Sci U S A*, 103(12), 4333-4, available: http://dx.doi.org/10.1073/pnas.0600780103.

Hofmann, E.R., Milstein, S., Boulton, S.J., Ye, M., Hofmann, J.J., Stergiou, L., Gartner, A., Vidal, M. and Hengartner, M.O. (2002) 'Caenorhabditis elegans HUS-1 is a DNA damage checkpoint protein required for genome stability and EGL-1-mediated apoptosis', *Curr Biol*, 12(22), 1908-18, available: http://dx.doi.org/10.1016/s0960-9822(02)01262-9.

Holman, R.R., Paul, S.K., Bethel, M.A., Matthews, D.R. and Neil, H.A. (2008) '10-year follow-up of intensive glucose control in type 2 diabetes', *N Engl J Med*, 359(15), 1577-89, available: http://dx.doi.org/10.1056/NEJMoa0806470.

Holt, J.A., Luo, G., Billin, A.N., Bisi, J., McNeill, Y.Y., Kozarsky, K.F., Donahee, M., Wang, D.Y., Mansfield, T.A., Kliewer, S.A., Goodwin, B. and Jones, S.A. (2003) 'Definition of a novel growth factor-dependent signal cascade for the suppression of bile acid biosynthesis', *Genes Dev*, 17(13), 1581-91, available: http://dx.doi.org/10.1101/gad.1083503.

Honda, A., Miyazaki, T., Iwamoto, J., Hirayama, T., Morishita, Y., Monma, T., Ueda, H., Mizuno, S., Sugiyama, F., Takahashi, S. and Ikegami, T. (2020) 'Regulation of bile acid metabolism in mouse models with hydrophobic bile acid composition', *J Lipid Res*, 61(1), 54-69, available: http://dx.doi.org/10.1194/jlr.RA119000395.

Horikawa, T., Oshima, T., Li, M., Kitayama, Y., Eda, H., Nakamura, K., Tamura, A., Ogawa, T., Yamasaki, T., Okugawa, T., Kondo, T., Kono, T., Tozawa, K., Tomita, T., Fukui, H., Watari, J. and Miwa, H. (2019) 'Chenodeoxycholic Acid Releases Proinflammatory Cytokines from Small Intestinal Epithelial Cells Through the Farnesoid X Receptor', *Digestion*, 100(4), 286-294, available: http://dx.doi.org/10.1159/000496687.

Horton, J.D., Goldstein, J.L. and Brown, M.S. (2002) 'SREBPs: activators of the complete program of cholesterol and fatty acid synthesis in the liver', *J Clin Invest*, 109(9), 1125-31, available: http://dx.doi.org/10.1172/JCI15593.

Hou, L., Che, Y., Sun, F. and Wang, Q. (2018) 'Taurine protects noradrenergic locus coeruleus neurons in a mouse Parkinson's disease model by inhibiting microglial M1 polarization', *Amino Acids*, 50(5), 547-556, available: http://dx.doi.org/10.1007/s00726-018-2547-1.

Hoyles, L., Snelling, T., Umlai, U.K., Nicholson, J.K., Carding, S.R., Glen, R.C. and McArthur, S. (2018) 'Microbiome-host systems interactions: protective effects of propionate upon the blood-brain barrier', *Microbiome*, 6(1), 55, available: http://dx.doi.org/10.1186/s40168-018-0439-y.

Hsiao, E.Y., McBride, S.W., Hsien, S., Sharon, G., Hyde, E.R., McCue, T., Codelli, J.A., Chow, J., Reisman, S.E., Petrosino, J.F., Patterson, P.H. and Mazmanian, S.K. (2013) 'Microbiota modulate behavioral and physiological abnormalities associated with neurodevelopmental disorders', *Cell*, 155(7), 1451-63, available: http://dx.doi.org/10.1016/j.cell.2013.11.024.

Hsin, H. and Kenyon, C. (1999) 'Signals from the reproductive system regulate the lifespan of C. elegans', *Nature*, 399(6734), 362-6, available: http://dx.doi.org/10.1038/20694.

Hu, Q., Peng, J., Jiang, L., Li, W., Su, Q., Zhang, J., Li, H., Song, M., Cheng, B., Xia, J. and Wu, T. (2020) 'Metformin as a senostatic drug enhances the anticancer efficacy of CDK4/6 inhibitor in head and neck squamous cell carcinoma', *Cell Death Dis*, 11(10), 925, available: http://dx.doi.org/10.1038/s41419-020-03126-0.

Hu, S.H., Peek, J.A., Rattigan, E., Taylor, R.K. and Martin, J.L. (1997) 'Structure of TcpG, the DsbA protein folding catalyst from Vibrio cholerae', *J Mol Biol*, 268(1), 137-46, available: http://dx.doi.org/10.1006/jmbi.1997.0940.

Huang, S., Haiminen, N., Carrieri, A.P., Hu, R., Jiang, L., Parida, L., Russell, B., Allaband, C., Zarrinpar, A., Vázquez-Baeza, Y., Belda-Ferre, P., Zhou, H., Kim, H.C., Swafford, A.D., Knight, R. and Xu, Z.Z. (2020) 'Human Skin, Oral, and Gut Microbiomes Predict Chronological Age', *mSystems*, 5(1), available: http://dx.doi.org/10.1128/mSystems.00630-19.

Huang, Y., Liao, J., Liu, X., Zhong, Y., Cai, X. and Long, L. (2021) 'Review: The Role of Intestinal Dysbiosis in Parkinson's Disease', *Front Cell Infect Microbiol*, 11, 615075, available: http://dx.doi.org/10.3389/fcimb.2021.615075.

Håversen, L., Danielsson, K.N., Fogelstrand, L. and Wiklund, O. (2009) 'Induction of proinflammatory cytokines by long-chain saturated fatty acids in human

macrophages', *Atherosclerosis*, 202(2), 382-93, available: http://dx.doi.org/10.1016/j.atherosclerosis.2008.05.033.

Ichikawa, R., Takayama, T., Yoneno, K., Kamada, N., Kitazume, M.T., Higuchi, H., Matsuoka, K., Watanabe, M., Itoh, H., Kanai, T., Hisamatsu, T. and Hibi, T. (2012) 'Bile acids induce monocyte differentiation toward interleukin-12 hypo-producing dendritic cells via a TGR5-dependent pathway', *Immunology*, 136(2), 153-62, available: http://dx.doi.org/10.1111/j.1365-2567.2012.03554.x.

Iljina, M., Tosatto, L., Choi, M.L., Sang, J.C., Ye, Y., Hughes, C.D., Bryant, C.E., Gandhi, S. and Klenerman, D. (2016) 'Arachidonic acid mediates the formation of abundant alpha-helical multimers of alpha-synuclein', *Sci Rep*, 6, 33928, available: http://dx.doi.org/10.1038/srep33928.

Im, E., Akare, S., Powell, A. and Martinez, J.D. (2005) 'Ursodeoxycholic acid can suppress deoxycholic acid-induced apoptosis by stimulating Akt/PKB-dependent survival signaling', *Nutr Cancer*, 51(1), 110-6, available: http://dx.doi.org/10.1207/s15327914nc5101_15.

Im, E. and Martinez, J.D. (2004) 'Ursodeoxycholic acid (UDCA) can inhibit deoxycholic acid (DCA)-induced apoptosis via modulation of EGFR/Raf-1/ERK signaling in human colon cancer cells', *J Nutr*, 134(2), 483-6, available: http://dx.doi.org/10.1093/jn/134.2.483.

Inagaki, T., Choi, M., Moschetta, A., Peng, L., Cummins, C.L., McDonald, J.G., Luo, G., Jones, S.A., Goodwin, B., Richardson, J.A., Gerard, R.D., Repa, J.J., Mangelsdorf, D.J. and Kliewer, S.A. (2005) 'Fibroblast growth factor 15 functions as an enterohepatic signal to regulate bile acid homeostasis', *Cell Metab*, 2(4), 217-25, available: http://dx.doi.org/10.1016/j.cmet.2005.09.001.

Irish Society for Colitis and Crohn's disease, I.

Iske, J., Seyda, M., Heinbokel, T., Maenosono, R., Minami, K., Nian, Y., Quante, M., Falk, C.S., Azuma, H., Martin, F., Passos, J.F., Niemann, C.U., Tchkonia, T., Kirkland, J.L., Elkhal, A. and Tullius, S.G. (2020) 'Senolytics prevent mt-DNA-induced inflammation and promote the survival of aged organs following transplantation', *Nat Commun*, 11(1), 4289, available: http://dx.doi.org/10.1038/s41467-020-18039-x.

Ivanov, I.I., Frutos, R.e.L., Manel, N., Yoshinaga, K., Rifkin, D.B., Sartor, R.B., Finlay, B.B. and Littman, D.R. (2008) 'Specific microbiota direct the differentiation of IL-17-producing T-helper cells in the mucosa of the small intestine', *Cell Host Microbe*, 4(4), 337-49, available: http://dx.doi.org/10.1016/j.chom.2008.09.009.

Iwauchi, M., Horigome, A., Ishikawa, K., Mikuni, A., Nakano, M., Xiao, J.Z., Odamaki, T. and Hironaka, S. (2019) 'Relationship between oral and gut microbiota in elderly people', *Immun Inflamm Dis*, 7(3), 229-236, available: http://dx.doi.org/10.1002/iid3.266.

Işık, S., Karaman, M., Çilaker Micili, S., Çağlayan-Sözmen, Ş., Bağrıyanık, H.A., Arıkan-Ayyıldız, Z., Uzuner, N. and Karaman, Ö. (2017) 'Beneficial effects of ursodeoxycholic acid via inhibition of airway remodelling, apoptosis of airway epithelial cells, and Th2 immune response in murine model of chronic asthma', *Allergol Immunopathol (Madr)*, 45(4), 339-349, available: http://dx.doi.org/10.1016/j.aller.2016.12.003.

Jacob-Dubuisson, F., Pinkner, J., Xu, Z., Striker, R., Padmanhaban, A. and Hultgren, S.J. (1994) 'PapD chaperone function in pilus biogenesis depends on oxidant and chaperone-like activities of DsbA', *Proc Natl Acad Sci U S A*, 91(24), 11552-6, available: http://dx.doi.org/10.1073/pnas.91.24.11552.

Jain, S., Rai, R., Singh, D. and Vohora, D. (2021) 'Octanoic acid a major component of widely consumed medium-chain triglyceride ketogenic diet is detrimental to bone', *Sci Rep*, 11(1), 7003, available: http://dx.doi.org/10.1038/s41598-021-86468-9.

Jandhyala, S.M., Talukdar, R., Subramanyam, C., Vuyyuru, H., Sasikala, M. and Nageshwar Reddy, D. (2015) 'Role of the normal gut microbiota', *World J Gastroenterol*, 21(29), 8787-803, available: http://dx.doi.org/10.3748/wjg.v21.i29.8787.

Jang, M., Cai, L., Udeani, G.O., Slowing, K.V., Thomas, C.F., Beecher, C.W., Fong, H.H., Farnsworth, N.R., Kinghorn, A.D., Mehta, R.G., Moon, R.C. and Pezzuto, J.M. (1997) 'Cancer chemopreventive activity of resveratrol, a natural product derived from grapes', *Science*, 275(5297), 218-20, available: http://dx.doi.org/10.1126/science.275.5297.218.

Johnke, J., Dirksen, P. and Schulenburg, H. (2020) 'Community assembly of the native C. elegans microbiome is influenced by time, substrate and individual bacterial taxa', *Environ Microbiol*, 22(4), 1265-1279, available: http://dx.doi.org/10.1111/1462-2920.14932.

Jonassen, T., Larsen, P.L. and Clarke, C.F. (2001) 'A dietary source of coenzyme Q is essential for growth of long-lived Caenorhabditis elegans clk-1 mutants', *Proc Natl Acad Sci U S A*, 98(2), 421-6, available: http://dx.doi.org/10.1073/pnas.98.2.421.

Joniec-Maciejak, I., Wawer, A., Turzyńska, D., Sobolewska, A., Maciejak, P., Szyndler, J., Mirowska-Guzel, D. and Płaźnik, A. (2018) 'Octanoic acid prevents reduction of striatal dopamine in the MPTP mouse model of

Parkinson's disease', *Pharmacol Rep*, 70(5), 988-992, available: http://dx.doi.org/10.1016/j.pharep.2018.04.008.

Jost, W.H. and Schimrigk, K. (1991) 'Constipation in Parkinson's disease', *Klin Wochenschr*, 69(20), 906-9, available: http://dx.doi.org/10.1007/BF01798536.

Joyce, S.A. and Gahan, C.G. (2016) 'Bile Acid Modifications at the Microbe-Host Interface: Potential for Nutraceutical and Pharmaceutical Interventions in Host Health', *Annu Rev Food Sci Technol*, 7, 313-33, available: http://dx.doi.org/10.1146/annurev-food-041715-033159.

Joyce, S.A., Kamil, A., Fleige, L. and Gahan, C.G.M. (2019) 'The Cholesterol-Lowering Effect of Oats and Oat Beta Glucan: Modes of Action and Potential Role of Bile Acids and the Microbiome', *Front Nutr*, 6, 171, available: http://dx.doi.org/10.3389/fnut.2019.00171.

Joyce, S.A., MacSharry, J., Casey, P.G., Kinsella, M., Murphy, E.F., Shanahan, F., Hill, C. and Gahan, C.G. (2014) 'Regulation of host weight gain and lipid metabolism by bacterial bile acid modification in the gut', *Proc Natl Acad Sci U S A*, 111(20), 7421-6, available: http://dx.doi.org/10.1073/pnas.1323599111.

Kaeberlein, M., Creevy, K.E. and Promislow, D.E. (2016) 'The dog aging project: translational geroscience in companion animals', *Mamm Genome*, 27(7-8), 279-88, available: http://dx.doi.org/10.1007/s00335-016-9638-7.

Kamata, Y., Shiraga, H., Tai, A., Kawamoto, Y. and Gohda, E. (2007) 'Induction of neurite outgrowth in PC12 cells by the medium-chain fatty acid octanoic acid', *Neuroscience*, 146(3), 1073-81, available: http://dx.doi.org/10.1016/j.neuroscience.2007.03.001.

Kang, D.W., Adams, J.B., Coleman, D.M., Pollard, E.L., Maldonado, J., McDonough-Means, S., Caporaso, J.G. and Krajmalnik-Brown, R. (2019) 'Long-term benefit of Microbiota Transfer Therapy on autism symptoms and gut microbiota', *Sci Rep*, 9(1), 5821, available: http://dx.doi.org/10.1038/s41598-019-42183-0.

Kang, D.W., Adams, J.B., Gregory, A.C., Borody, T., Chittick, L., Fasano, A., Khoruts, A., Geis, E., Maldonado, J., McDonough-Means, S., Pollard, E.L., Roux, S., Sadowsky, M.J., Lipson, K.S., Sullivan, M.B., Caporaso, J.G. and Krajmalnik-Brown, R. (2017) 'Microbiota Transfer Therapy alters gut ecosystem and improves gastrointestinal and autism symptoms: an open-label study', *Microbiome*, 5(1), 10, available: http://dx.doi.org/10.1186/s40168-016-0225-7.

Kang, D.W., Park, J.G., Ilhan, Z.E., Wallstrom, G., Labaer, J., Adams, J.B. and Krajmalnik-Brown, R. (2013) 'Reduced incidence of Prevotella and other fermenters in intestinal microflora of autistic children', *PLoS One*, 8(7), e68322, available: http://dx.doi.org/10.1371/journal.pone.0068322.

Kang, J.H., Kim, M. and Yim, M. (2021) 'FXR/TGR5 mediates inflammasome activation and host resistance to bacterial infection', *Biochem Biophys Rep*, 27, 101051, available: http://dx.doi.org/10.1016/j.bbrep.2021.101051.

Kaplan, R.E., Chen, Y., Moore, B.T., Jordan, J.M., Maxwell, C.S., Schindler, A.J. and Baugh, L.R. (2015) 'dbl-1/TGF-β and daf-12/NHR Signaling Mediate Cell-Nonautonomous Effects of daf-16/FOXO on Starvation-Induced Developmental Arrest', *PLoS Genet*, 11(12), e1005731, available: http://dx.doi.org/10.1371/journal.pgen.1005731.

Karakas, L., Solmaz, V., Bagcioglu, E., ozkul, b., sogut, i., uyanikgil, y. and erbas, o. (2022) 'Lowering Propionic Acid Levels by Regulating Gut Microbiota with Ursodeoxycholic Acid Appears to Regress Autism Symptoms: An Animal Study', *Research Square*, available: http://dx.doi.org/10.21203/rs.3.rs-1963818/v1.

Kashiwaya, Y., Takeshima, T., Mori, N., Nakashima, K., Clarke, K. and Veech, R.L. (2000) 'D-beta-hydroxybutyrate protects neurons in models of Alzheimer's and Parkinson's disease', *Proc Natl Acad Sci U S A*, 97(10), 5440-4, available: http://dx.doi.org/10.1073/pnas.97.10.5440.

Kashtanova, D.A., Klimenko, N.S., Strazhesko, I.D., Starikova, E.V., Glushchenko, O.E., Gudkov, D.A. and Tkacheva, O.N. (2020) 'A Cross-Sectional Study of the Gut Microbiota Composition in Moscow Long-Livers', *Microorganisms*, 8(8), available: http://dx.doi.org/10.3390/microorganisms8081162.

Katsuma, S., Hirasawa, A. and Tsujimoto, G. (2005) 'Bile acids promote glucagon-like peptide-1 secretion through TGR5 in a murine enteroendocrine cell line STC-1', *Biochem Biophys Res Commun*, 329(1), 386-90, available: http://dx.doi.org/10.1016/j.bbrc.2005.01.139.

Kawamata, Y., Fujii, R., Hosoya, M., Harada, M., Yoshida, H., Miwa, M., Fukusumi, S., Habata, Y., Itoh, T., Shintani, Y., Hinuma, S., Fujisawa, Y. and Fujino, M. (2003) 'A G protein-coupled receptor responsive to bile acids', *J Biol Chem*, 278(11), 9435-40, available: http://dx.doi.org/10.1074/jbc.M209706200.

Ke, Y., Li, D., Zhao, M., Liu, C., Liu, J., Zeng, A., Shi, X., Cheng, S., Pan, B., Zheng, L. and Hong, H. (2018) 'Gut flora-dependent metabolite Trimethylamine-N-oxide accelerates endothelial cell senescence and vascular aging through oxidative stress', *Free Radic Biol Med*, 116, 88-100, available: http://dx.doi.org/10.1016/j.freeradbiomed.2018.01.007.

Kealy, R.D., Lawler, D.F., Ballam, J.M., Mantz, S.L., Biery, D.N., Greeley, E.H., Lust, G., Segre, M., Smith, G.K. and Stowe, H.D. (2002) 'Effects of diet restriction on life span and age-related changes in dogs', *J Am Vet Med Assoc*, 220(9), 1315-20, available: http://dx.doi.org/10.2460/javma.2002.220.1315.

Keitel, V., Donner, M., Winandy, S., Kubitz, R. and Häussinger, D. (2008) 'Expression and function of the bile acid receptor TGR5 in Kupffer cells', *Biochem Biophys Res Commun*, 372(1), 78-84, available: http://dx.doi.org/10.1016/j.bbrc.2008.04.171.

Kenyon, C., Chang, J., Gensch, E., Rudner, A. and Tabtiang, R. (1993) 'A C. elegans mutant that lives twice as long as wild type', *Nature*, 366(6454), 461-4, available: http://dx.doi.org/10.1038/366461a0.

Keşli, R., Gökçen, C., Buluğ, U. and Terzi, Y. (2014) 'Investigation of the relation between anaerobic bacteria genus clostridium and late-onset autism etiology in children', *J Immunoassay Immunochem*, 35(1), 101-9, available: http://dx.doi.org/10.1080/15321819.2013.792834.

Killinger, B.A., Madaj, Z., Sikora, J.W., Rey, N., Haas, A.J., Vepa, Y., Lindqvist, D., Chen, H., Thomas, P.M., Brundin, P., Brundin, L. and Labrie, V. (2018) 'The vermiform appendix impacts the risk of developing Parkinson's disease', *Sci Transl Med*, 10(465), available: http://dx.doi.org/10.1126/scitranslmed.aar5280.

Kim, B.S., Choi, C.W., Shin, H., Jin, S.P., Bae, J.S., Han, M., Seo, E.Y., Chun, J. and Chung, J.H. (2019) 'Comparison of the Gut Microbiota of Centenarians in Longevity Villages of South Korea with Those of Other Age Groups', *J Microbiol Biotechnol*, 29(3), 429-440, available: http://dx.doi.org/10.4014/jmb.1811.11023.

Kimura, A., Mizuochi, T., Takei, H., Ohtake, A., Mori, J., Shinoda, K., Hashimoto, T., Kasahara, M., Togawa, T., Murai, T., Iida, T. and Nittono, H. (2021) 'Bile Acid Synthesis Disorders in Japan: Long-Term Outcome and Chenodeoxycholic Acid Treatment', *Dig Dis Sci*, 66(11), 3885-3892, available: http://dx.doi.org/10.1007/s10620-020-06722-4.

Kimura, K.D., Tissenbaum, H.A., Liu, Y. and Ruvkun, G. (1997) 'daf-2, an insulin receptor-like gene that regulates longevity and diapause in Caenorhabditis elegans', *Science*, 277(5328), 942-6, available: http://dx.doi.org/10.1126/science.277.5328.942.

Kirkwood, T.B. (2005) 'Understanding the odd science of aging', *Cell*, 120(4), 437-47, available: http://dx.doi.org/10.1016/j.cell.2005.01.027.

Klass, M.R. (1977) 'Aging in the nematode Caenorhabditis elegans: major biological and environmental factors influencing life span', *Mech Ageing Dev*, 6(6), 413-29, available: http://dx.doi.org/10.1016/0047-6374(77)90043-4.

Klass, M.R. (1983) 'A method for the isolation of longevity mutants in the nematode Caenorhabditis elegans and initial results', *Mech Ageing Dev*, 22(3-4), 279-86, available: http://dx.doi.org/10.1016/0047-6374(83)90082-9.

Kollanus, V., Tiittanen, P. and Lanki, T. (2021) 'Mortality risk related to heatwaves in Finland - Factors affecting vulnerability', *Environ Res*, 201, 111503, available: http://dx.doi.org/10.1016/j.envres.2021.111503.

Kong, F., Hua, Y., Zeng, B., Ning, R., Li, Y. and Zhao, J. (2016) 'Gut microbiota signatures of longevity', *Curr Biol*, 26(18), R832-R833, available: http://dx.doi.org/10.1016/j.cub.2016.08.015.

Kong, Q., Chen, Q., Mao, X., Wang, G., Zhao, J., Zhang, H. and Chen, W. (2022) 'CCFM1077 Ameliorated Neurotransmitter Disorder and Neuroinflammation Closely Linked to Regulation in the Kynurenine Pathway of Autistic-like Rats', *Nutrients*, 14(8), available: http://dx.doi.org/10.3390/nu14081615.

Kong, Q., Wang, B., Tian, P., Li, X., Zhao, J., Zhang, H., Chen, W. and Wang, G. (2021) 'Daily intake of Lactobacillus alleviates autistic-like behaviors by ameliorating the 5-hydroxytryptamine metabolic disorder in VPA-treated rats during weaning and sexual maturation', *Food Funct*, 12(6), 2591-2604, available: http://dx.doi.org/10.1039/d0fo02375b.

Konjevod, M., Sáiz, J., Barbas, C., Bergareche, A., Ardanaz, E., Huerta, J.M., Vinagre-Aragón, A., Erro, M.E., Chirlaque, M.D., Abilleira, E., Ibarluzea, J.M. and Amiano, P. (2022) 'A Set of Reliable Samples for the Study of Biomarkers for the Early Diagnosis of Parkinson's Disease', *Front Neurol*, 13, 844841, available: http://dx.doi.org/10.3389/fneur.2022.844841.

Kuai, X.Y., Yao, X.H., Xu, L.J., Zhou, Y.Q., Zhang, L.P., Liu, Y., Pei, S.F. and Zhou, C.L. (2021) 'Evaluation of fecal microbiota transplantation in Parkinson's disease patients with constipation', *Microb Cell Fact*, 20(1), 98, available: http://dx.doi.org/10.1186/s12934-021-01589-0.

Kumar, S., Egan, B.M., Kocsisova, Z., Schneider, D.L., Murphy, J.T., Diwan, A. and Kornfeld, K. (2019) 'Lifespan Extension in C. elegans Caused by Bacterial Colonization of the Intestine and Subsequent Activation of an Innate Immune Response', *Dev Cell*, 49(1), 100-117.e6, available: http://dx.doi.org/10.1016/j.devcel.2019.03.010.

Kumaresan, M. and Khan, S. (2021) 'Spectrum of Non-Motor Symptoms in Parkinson's Disease', *Cureus*, 13(2), e13275, available: http://dx.doi.org/10.7759/cureus.13275.

La-Ongkham, O., Nakphaichit, M., Nakayama, J., Keawsompong, S. and Nitisinprasert, S. (2020) 'Age-related changes in the gut microbiota and the core gut microbiome of healthy Thai humans', *3 Biotech*, 10(6), 276, available: http://dx.doi.org/10.1007/s13205-020-02265-7.

Laffitte, B.A., Chao, L.C., Li, J., Walczak, R., Hummasti, S., Joseph, S.B., Castrillo, A., Wilpitz, D.C., Mangelsdorf, D.J., Collins, J.L., Saez, E. and Tontonoz, P. (2003) 'Activation of liver X receptor improves glucose tolerance through coordinate regulation of glucose metabolism in liver and adipose tissue', *Proc Natl Acad Sci U S A*, 100(9), 5419-24, available: http://dx.doi.org/10.1073/pnas.0830671100.

Lakowski, B. and Hekimi, S. (1996) 'Determination of life-span in Caenorhabditis elegans by four clock genes', *Science*, 272(5264), 1010-3, available: http://dx.doi.org/10.1126/science.272.5264.1010.

Lakowski, B. and Hekimi, S. (1998) 'The genetics of caloric restriction in Caenorhabditis elegans', *Proc Natl Acad Sci U S A*, 95(22), 13091-6, available: http://dx.doi.org/10.1073/pnas.95.22.13091.

Landeta, C., Boyd, D. and Beckwith, J. (2018) 'Disulfide bond formation in prokaryotes', *Nat Microbiol*, 3(3), 270-280, available: http://dx.doi.org/10.1038/s41564-017-0106-2.

Larsen, P.L., Albert, P.S. and Riddle, D.L. (1995) 'Genes that regulate both development and longevity in Caenorhabditis elegans', *Genetics*, 139(4), 1567-83, available: http://dx.doi.org/10.1093/genetics/139.4.1567.

Lawler, D.F., Ballam, J.M., Meadows, R., Larson, B.T., Li, Q., Stowe, H.D. and Kealy, R.D. (2007) 'Influence of lifetime food restriction on physiological variables in Labrador retriever dogs', *Exp Gerontol*, 42(3), 204-14, available: http://dx.doi.org/10.1016/j.exger.2006.09.010.

Lee, G., Lee, H., Hong, J., Lee, S.H. and Jung, B.H. (2016) 'Quantitative profiling of bile acids in rat bile using ultrahigh-performance liquid chromatography-orbitrap mass spectrometry: Alteration of the bile acid composition with aging', *J Chromatogr B Analyt Technol Biomed Life Sci*, 1031, 37-49, available: http://dx.doi.org/10.1016/j.jchromb.2016.07.017.

Lee, I.M. and Paffenbarger, R.S. (1998) 'Physical activity and stroke incidence: the Harvard Alumni Health Study', *Stroke*, 29(10), 2049-54, available: http://dx.doi.org/10.1161/01.str.29.10.2049.

Lees, A.J., Hardy, J. and Revesz, T. (2009) 'Parkinson's disease', *Lancet*, 373(9680), 2055-66, available: http://dx.doi.org/10.1016/S0140-6736(09)60492-X.

Lehmann, J.M., Kliewer, S.A., Moore, L.B., Smith-Oliver, T.A., Oliver, B.B., Su, J.L., Sundseth, S.S., Winegar, D.A., Blanchard, D.E., Spencer, T.A. and Willson, T.M. (1997) 'Activation of the nuclear receptor LXR by oxysterols defines a new hormone response pathway', *J Biol Chem*, 272(6), 3137-40, available: http://dx.doi.org/10.1074/jbc.272.6.3137.

Lenaerts, I., Walker, G.A., Van Hoorebeke, L., Gems, D. and Vanfleteren, J.R. (2008) 'Dietary restriction of Caenorhabditis elegans by axenic culture reflects nutritional requirement for constituents provided by metabolically active microbes', *J Gerontol A Biol Sci Med Sci*, 63(3), 242-52, available: http://dx.doi.org/10.1093/gerona/63.3.242.

Lennard-Jones, J.E. (1989) 'Classification of inflammatory bowel disease', *Scand J Gastroenterol Suppl*, 170, 2-6; discussion 16-9, available: http://dx.doi.org/10.3109/00365528909091339.

Leonov, A., Arlia-Ciommo, A., Bourque, S.D., Koupaki, O., Kyryakov, P., Dakik, P., McAuley, M., Medkour, Y., Mohammad, K., Di Maulo, T. and Titorenko, V.I. (2017) 'Specific changes in mitochondrial lipidome alter mitochondrial proteome and increase the geroprotective efficiency of lithocholic acid in chronologically aging yeast', *Oncotarget*, 8(19), 30672-30691, available: http://dx.doi.org/10.18632/oncotarget.16766.

Levi Mortera, S., Vernocchi, P., Basadonne, I., Zandonà, A., Chierici, M., Durighello, M., Marzano, V., Gardini, S., Gasbarrini, A., Urbani, A., Vicari, S., Roncada, P., Furlanello, C., Venuti, P. and Putignani, L. (2022) 'A metaproteomic-based gut microbiota profiling in children affected by autism spectrum disorders', *J Proteomics*, 251, 104407, available: http://dx.doi.org/10.1016/j.jprot.2021.104407.

Li, N., Chen, H., Cheng, Y., Xu, F., Ruan, G., Ying, S., Tang, W., Chen, L., Chen, M., Lv, L., Ping, Y., Chen, D. and Wei, Y. (2021) 'Fecal Microbiota Transplantation Relieves Gastrointestinal and Autism Symptoms by Improving the Gut Microbiota in an Open-Label Study', *Front Cell Infect Microbiol*, 11, 759435, available: http://dx.doi.org/10.3389/fcimb.2021.759435.

Li, P., Killinger, B.A., Ensink, E., Beddows, I., Yilmaz, A., Lubben, N., Lamp, J., Schilthuis, M., Vega, I.E., Woltjer, R., Pospisilik, J.A., Brundin, P., Brundin, L., Graham, S.F. and Labrie, V. (2021) 'Gut Microbiota Dysbiosis Is Associated with Elevated Bile Acids in Parkinson's Disease', *Metabolites*, 11(1), available: http://dx.doi.org/10.3390/metabo11010029.

Li, T. and Chiang, J.Y. (2014) 'Bile acid signaling in metabolic disease and drug therapy', *Pharmacol Rev*, 66(4), 948-83, available: http://dx.doi.org/10.1124/pr.113.008201.

Li, T.M., Chen, J., Li, X., Ding, X.J., Wu, Y., Zhao, L.F., Chen, S., Lei, X. and Dong, M.Q. (2013) 'Absolute quantification of a steroid hormone that regulates development in Caenorhabditis elegans', *Anal Chem*, 85(19), 9281-7, available: http://dx.doi.org/10.1021/ac402025c.

Li, Y.T., Swales, K.E., Thomas, G.J., Warner, T.D. and Bishop-Bailey, D. (2007) 'Farnesoid x receptor ligands inhibit vascular smooth muscle cell inflammation and migration', *Arterioscler Thromb Vasc Biol*, 27(12), 2606-11, available: http://dx.doi.org/10.1161/ATVBAHA.107.152694.

Li-Hawkins, J., Lund, E.G., Bronson, A.D. and Russell, D.W. (2000) 'Expression cloning of an oxysterol 7alpha-hydroxylase selective for 24-hydroxycholesterol', *J Biol Chem*, 275(22), 16543-9, available: http://dx.doi.org/10.1074/jbc.M001810200.

Lima, A.A., Mridha, M.F., Das, S.C., Kabir, M.M., Islam, M.R. and Watanobe, Y. (2022) 'A Comprehensive Survey on the Detection, Classification, and Challenges of Neurological Disorders', *Biology (Basel)*, 11(3), available: http://dx.doi.org/10.3390/biology11030469.

Liu, J., Liu, C., Gao, Z., Zhou, L., Gao, J., Luo, Y., Liu, T. and Fan, X. (2022) 'GW4064 Alters Gut Microbiota Composition and Counteracts Autism-Associated Behaviors in BTBR T+tf/J Mice', *Front Cell Infect Microbiol*, 12, 911259, available: http://dx.doi.org/10.3389/fcimb.2022.911259.

Liu, L., Guo, P., Wang, P., Zheng, S., Qu, Z. and Liu, N. (2021) 'The Review of Anti-aging Mechanism of Polyphenols on', *Front Bioeng Biotechnol*, 9, 635768, available: http://dx.doi.org/10.3389/fbioe.2021.635768.

Liu, X., Jiang, N., Hughes, B., Bigras, E., Shoubridge, E. and Hekimi, S. (2005) 'Evolutionary conservation of the clk-1-dependent mechanism of longevity: loss of mclk1 increases cellular fitness and lifespan in mice', *Genes Dev*, 19(20), 2424-34, available: http://dx.doi.org/10.1101/gad.1352905.

Liu, X., Yamada, N., Maruyama, W. and Osawa, T. (2008) 'Formation of dopamine adducts derived from brain polyunsaturated fatty acids: mechanism for Parkinson disease', *J Biol Chem*, 283(50), 34887-95, available: http://dx.doi.org/10.1074/jbc.M805682200.

Liu, Y.W., Liong, M.T., Chung, Y.E., Huang, H.Y., Peng, W.S., Cheng, Y.F., Lin, Y.S., Wu, Y.Y. and Tsai, Y.C. (2019) 'Effects of', *Nutrients*, 11(4), available: http://dx.doi.org/10.3390/nu11040820.

Long, S.L., Gahan, C.G.M. and Joyce, S.A. (2017) 'Interactions between gut bacteria and bile in health and disease', *Mol Aspects Med*, 56, 54-65, available: http://dx.doi.org/10.1016/j.mam.2017.06.002.

Lu, D., Liu, Y., Luo, Y., Zhao, J., Feng, C., Xue, L., Xu, J., Wang, Q., Yan, T., Xiao, P., Krausz, K.W., Gonzalez, F.J. and Xie, C. (2022) 'Intestinal farnesoid X receptor signaling controls hepatic fatty acid oxidation', *Biochim Biophys Acta Mol Cell Biol Lipids*, 1867(2), 159089, available: http://dx.doi.org/10.1016/j.bbalip.2021.159089.

Luckey, T.D. (1972) 'Introduction to intestinal microecology', *Am J Clin Nutr*, 25(12), 1292-4, available: http://dx.doi.org/10.1093/ajcn/25.12.1292.

Luczynski, P., McVey Neufeld, K.A., Oriach, C.S., Clarke, G., Dinan, T.G. and Cryan, J.F. (2016) 'Growing up in a Bubble: Using Germ-Free Animals to Assess the Influence of the Gut Microbiota on Brain and Behavior', *Int J Neuropsychopharmacol*, 19(8), available: http://dx.doi.org/10.1093/ijnp/pyw020.

Luo, G.Z., Blanco, M.A., Greer, E.L., He, C. and Shi, Y. (2015) 'DNA N(6)-methyladenine: a new epigenetic mark in eukaryotes?', *Nat Rev Mol Cell Biol*, 16(12), 705-10, available: http://dx.doi.org/10.1038/nrm4076.

López-Otín, C., Blasco, M.A., Partridge, L., Serrano, M. and Kroemer, G. (2013) 'The hallmarks of aging', *Cell*, 153(6), 1194-217, available: http://dx.doi.org/10.1016/j.cell.2013.05.039.

Ma, G., Wang, T., Korhonen, P.K., Young, N.D., Nie, S., Ang, C.S., Williamson, N.A., Reid, G.E. and Gasser, R.B. (2019) 'Dafachronic acid promotes larval development in Haemonchus contortus by modulating dauer signalling and lipid metabolism', *PLoS Pathog*, 15(7), e1007960, available: http://dx.doi.org/10.1371/journal.ppat.1007960.

Ma, Q., Long, S., Gan, Z., Tettamanti, G., Li, K. and Tian, L. (2022) 'Transcriptional and Post-Transcriptional Regulation of Autophagy', *Cells*, 11(3), available: http://dx.doi.org/10.3390/cells11030441.

MacNeil, L.G., Tarnopolsky, M.A. and Crane, J.D. (2021) 'Acute, Exercise-Induced Alterations in Cytokines and Chemokines in the Blood Distinguish Physically Active and Sedentary Aging', *J Gerontol A Biol Sci Med Sci*, 76(5), 811-818, available: http://dx.doi.org/10.1093/gerona/glaa310.

Madra, M., Ringel, R. and Margolis, K.G. (2021) 'Gastrointestinal Issues and Autism Spectrum Disorder', *Psychiatr Clin North Am*, 44(1), 69-81, available: http://dx.doi.org/10.1016/j.psc.2020.11.006.

Magner, D.B., Wollam, J., Shen, Y., Hoppe, C., Li, D., Latza, C., Rottiers, V., Hutter, H. and Antebi, A. (2013) 'The NHR-8 nuclear receptor regulates cholesterol and bile acid homeostasis in C. elegans', *Cell Metab*, 18(2), 212-24, available: http://dx.doi.org/10.1016/j.cmet.2013.07.007.

Mahanti, P., Bose, N., Bethke, A., Judkins, J.C., Wollam, J., Dumas, K.J., Zimmerman, A.M., Campbell, S.L., Hu, P.J., Antebi, A. and Schroeder, F.C. (2014) 'Comparative metabolomics reveals endogenous ligands of DAF-12, a nuclear hormone receptor, regulating C. elegans development and lifespan', *Cell Metab*, 19(1), 73-83, available: http://dx.doi.org/10.1016/j.cmet.2013.11.024.

Mahley, R.W. and Rall, S.C. (2000) 'Apolipoprotein E: far more than a lipid transport protein', *Annu Rev Genomics Hum Genet*, 1, 507-37, available: http://dx.doi.org/10.1146/annurev.genom.1.1.507.

Mahmoud, N.N., Dannenberg, A.J., Bilinski, R.T., Mestre, J.R., Chadburn, A., Churchill, M., Martucci, C. and Bertagnolli, M.M. (1999) 'Administration of an unconjugated bile acid increases duodenal tumors in a murine model of familial adenomatous polyposis', *Carcinogenesis*, 20(2), 299-303, available: http://dx.doi.org/10.1093/carcin/20.2.299.

MahmoudianDehkordi, S., Arnold, M., Nho, K., Ahmad, S., Jia, W., Xie, G., Louie, G., Kueider-Paisley, A., Moseley, M.A., Thompson, J.W., St John Williams, L., Tenenbaum, J.D., Blach, C., Baillie, R., Han, X., Bhattacharyya, S., Toledo, J.B., Schafferer, S., Klein, S., Koal, T., Risacher, S.L., Kling, M.A., Motsinger-Reif, A., Rotroff, D.M., Jack, J., Hankemeier, T., Bennett, D.A., De Jager, P.L., Trojanowski, J.Q., Shaw, L.M., Weiner, M.W., Doraiswamy, P.M., van Duijn, C.M., Saykin, A.J., Kastenmüller, G., Kaddurah-Daouk, R. and Consortium, A.s.D.N.I.a.t.A.D.M. (2019) 'Altered bile acid profile associates with cognitive impairment in Alzheimer's disease-An emerging role for gut microbiome', *Alzheimers Dement*, 15(1), 76-92, available: http://dx.doi.org/10.1016/j.jalz.2018.07.217.

Makishima, M., Lu, T.T., Xie, W., Whitfield, G.K., Domoto, H., Evans, R.M., Haussler, M.R. and Mangelsdorf, D.J. (2002) 'Vitamin D receptor as an intestinal bile acid sensor', *Science*, 296(5571), 1313-6, available: http://dx.doi.org/10.1126/science.1070477.

Malecki, K.M.C., Andersen, J.K., Geller, A.M., Harry, G.J., Jackson, C.L., James, K.A., Miller, G.W. and Ottinger, M.A. (2022) 'Integrating Environment and Aging Research: Opportunities for Synergy and Acceleration', *Front Aging Neurosci*, 14, 824921, available: http://dx.doi.org/10.3389/fnagi.2022.824921.

Marksteiner, J., Blasko, I., Kemmler, G., Koal, T. and Humpel, C. (2018) 'Bile acid quantification of 20 plasma metabolites identifies lithocholic acid as a putative biomarker in Alzheimer's disease', *Metabolomics*, 14(1), 1, available: http://dx.doi.org/10.1007/s11306-017-1297-5.

Maruyama, T., Miyamoto, Y., Nakamura, T., Tamai, Y., Okada, H., Sugiyama, E., Itadani, H. and Tanaka, K. (2002) 'Identification of membrane-type receptor

for bile acids (M-BAR)', *Biochem Biophys Res Commun*, 298(5), 714-9, available: http://dx.doi.org/10.1016/s0006-291x(02)02550-0.

Maruyama, T., Tanaka, K., Suzuki, J., Miyoshi, H., Harada, N., Nakamura, T., Miyamoto, Y., Kanatani, A. and Tamai, Y. (2006) 'Targeted disruption of G protein-coupled bile acid receptor 1 (Gpbar1/M-Bar) in mice', *J Endocrinol*, 191(1), 197-205, available: http://dx.doi.org/10.1677/joe.1.06546.

Mathew, R., Pal Bhadra, M. and Bhadra, U. (2017) 'Insulin/insulin-like growth factor-1 signalling (IIS) based regulation of lifespan across species', *Biogerontology*, 18(1), 35-53, available: http://dx.doi.org/10.1007/s10522-016-9670-8.

Mattison, J.A., Colman, R.J., Beasley, T.M., Allison, D.B., Kemnitz, J.W., Roth, G.S., Ingram, D.K., Weindruch, R., de Cabo, R. and Anderson, R.M. (2017) 'Caloric restriction improves health and survival of rhesus monkeys', *Nat Commun*, 8, 14063, available: http://dx.doi.org/10.1038/ncomms14063.

Mattison, J.A., Roth, G.S., Beasley, T.M., Tilmont, E.M., Handy, A.M., Herbert, R.L., Longo, D.L., Allison, D.B., Young, J.E., Bryant, M., Barnard, D., Ward, W.F., Qi, W., Ingram, D.K. and de Cabo, R. (2012) 'Impact of caloric restriction on health and survival in rhesus monkeys from the NIA study', *Nature*, 489(7415), 318-21, available: http://dx.doi.org/10.1038/nature11432.

Matyash, V., Entchev, E.V., Mende, F., Wilsch-Bräuninger, M., Thiele, C., Schmidt, A.W., Knölker, H.J., Ward, S. and Kurzchalia, T.V. (2004) 'Sterol-derived hormone(s) controls entry into diapause in Caenorhabditis elegans by consecutive activation of DAF-12 and DAF-16', *PLoS Biol*, 2(10), e280, available: http://dx.doi.org/10.1371/journal.pbio.0020280.

Mazmanian, S.K., Liu, C.H., Tzianabos, A.O. and Kasper, D.L. (2005) 'An immunomodulatory molecule of symbiotic bacteria directs maturation of the host immune system', *Cell*, 122(1), 107-18, available: http://dx.doi.org/10.1016/j.cell.2005.05.007.

McCartney, D.L., Min, J.L., Richmond, R.C., Lu, A.T., Sobczyk, M.K., Davies, G., Broer, L., Guo, X., Jeong, A., Jung, J., Kasela, S., Katrinli, S., Kuo, P.L., Matias-Garcia, P.R., Mishra, P.P., Nygaard, M., Palviainen, T., Patki, A., Raffield, L.M., Ratliff, S.M., Richardson, T.G., Robinson, O., Soerensen, M., Sun, D., Tsai, P.C., van der Zee, M.D., Walker, R.M., Wang, X., Wang, Y., Xia, R., Xu, Z., Yao, J., Zhao, W., Correa, A., Boerwinkle, E., Dugué, P.A., Durda, P., Elliott, H.R., Gieger, C., de Geus, E.J.C., Harris, S.E., Hemani, G., Imboden, M., Kähönen, M., Kardia, S.L.R., Kresovich, J.K., Li, S., Lunetta, K.L., Mangino, M., Mason, D., McIntosh, A.M., Mengel-From, J., Moore, A.Z., Murabito, J.M., Ollikainen, M., Pankow, J.S., Pedersen, N.L., Peters, A., Polidoro, S., Porteous, D.J., Raitakari, O., Rich, S.S., Sandler, D.P., Sillanpää, E., Smith, A.K., Southey, M.C., Strauch, K., Tiwari, H., Tanaka, T., Tillin, T., Uitterlinden, A.G., Van Den Berg, D.J., van

Dongen, J., Wilson, J.G., Wright, J., Yet, I., Arnett, D., Bandinelli, S., Bell, J.T., Binder, A.M., Boomsma, D.I., Chen, W., Christensen, K., Conneely, K.N., Elliott, P., Ferrucci, L., Fornage, M., Hägg, S., Hayward, C., Irvin, M., Kaprio, J., Lawlor, D.A., Lehtimäki, T., Lohoff, F.W., Milani, L., Milne, R.L., Probst-Hensch, N., Reiner, A.P., Ritz, B., Rotter, J.I.*, et al.* (2021) 'Genome-wide association studies identify 137 genetic loci for DNA methylation biomarkers of aging', *Genome Biol*, 22(1), 194, available: http://dx.doi.org/10.1186/s13059-021-02398-9.

McCarty, M.F. (2015) 'Practical prospects for boosting hepatic production of the "pro-longevity" hormone FGF21', *Horm Mol Biol Clin Investig*, 30(2), available: http://dx.doi.org/10.1515/hmbci-2015-0057.

McKay, J.P., Raizen, D.M., Gottschalk, A., Schafer, W.R. and Avery, L. (2004) 'eat-2 and eat-18 are required for nicotinic neurotransmission in the Caenorhabditis elegans pharynx', *Genetics*, 166(1), 161-9, available: http://dx.doi.org/10.1534/genetics.166.1.161.

Meguid, N.A., Mawgoud, Y.I.A., Bjørklund, G., Mehanne, N.S., Anwar, M., Effat, B.A.E., Chirumbolo, S. and Elrahman, M.M.A. (2022) 'Molecular Characterization of Probiotics and Their Influence on Children with Autism Spectrum Disorder', *Mol Neurobiol*, 59(11), 6896-6902, available: http://dx.doi.org/10.1007/s12035-022-02963-8.

Mellies, J.L., Barron, A.M., Haack, K.R., Korson, A.S. and Oldridge, D.A. (2006) 'The global regulator Ler is necessary for enteropathogenic Escherichia coli colonization of Caenorhabditis elegans', *Infect Immun*, 74(1), 64-72, available: http://dx.doi.org/10.1128/IAI.74.1.64-72.2006.

Mendelski, M.N., Dölling, R., Feller, F.M., Hoffmann, D., Ramos Fangmeier, L., Ludwig, K.C., Yücel, O., Mährlein, A., Paul, R.J. and Philipp, B. (2019) 'Steroids originating from bacterial bile acid degradation affect Caenorhabditis elegans and indicate potential risks for the fauna of manured soils', *Sci Rep*, 9(1), 11120, available: http://dx.doi.org/10.1038/s41598-019-47476-y.

Mensi, M.M., Rogantini, C., Marchesi, M., Borgatti, R. and Chiappedi, M. (2021) 'PS128 and Other Probiotics in Children and Adolescents with Autism Spectrum Disorder: A Real-World Experience', *Nutrients*, 13(6), available: http://dx.doi.org/10.3390/nu13062036.

Meyza, K.Z. and Blanchard, D.C. (2017) 'The BTBR mouse model of idiopathic autism - Current view on mechanisms', *Neurosci Biobehav Rev*, 76(Pt A), 99-110, available: http://dx.doi.org/10.1016/j.neubiorev.2016.12.037.

Mi, H., Muruganujan, A., Ebert, D., Huang, X. and Thomas, P.D. (2019) 'PANTHER version 14: more genomes, a new PANTHER GO-slim and improvements in

enrichment analysis tools', *Nucleic Acids Res*, 47(D1), D419-D426, available: http://dx.doi.org/10.1093/nar/gky1038.

Miao, J., Fang, S., Bae, Y. and Kemper, J.K. (2006) 'Functional inhibitory cross-talk between constitutive androstane receptor and hepatic nuclear factor-4 in hepatic lipid/glucose metabolism is mediated by competition for binding to the DR1 motif and to the common coactivators, GRIP-1 and PGC-1alpha', *J Biol Chem*, 281(21), 14537-46, available: http://dx.doi.org/10.1074/jbc.M510713200.

Miller, R.A., Harrison, D.E., Astle, C.M., Baur, J.A., Boyd, A.R., de Cabo, R., Fernandez, E., Flurkey, K., Javors, M.A., Nelson, J.F., Orihuela, C.J., Pletcher, S., Sharp, Z.D., Sinclair, D., Starnes, J.W., Wilkinson, J.E., Nadon, N.L. and Strong, R. (2011) 'Rapamycin, but not resveratrol or simvastatin, extends life span of genetically heterogeneous mice', *J Gerontol A Biol Sci Med Sci*, 66(2), 191-201, available: http://dx.doi.org/10.1093/gerona/glq178.

Miller, R.A., Harrison, D.E., Astle, C.M., Fernandez, E., Flurkey, K., Han, M., Javors, M.A., Li, X., Nadon, N.L., Nelson, J.F., Pletcher, S., Salmon, A.B., Sharp, Z.D., Van Roekel, S., Winkleman, L. and Strong, R. (2014) 'Rapamycin-mediated lifespan increase in mice is dose and sex dependent and metabolically distinct from dietary restriction', *Aging Cell*, 13(3), 468-77, available: http://dx.doi.org/10.1111/acel.12194.

Miller, W.L. (1988) 'Molecular biology of steroid hormone synthesis', *Endocr Rev*, 9(3), 295-318, available: http://dx.doi.org/10.1210/edrv-9-3-295.

Mitani, S. (2017) 'Comprehensive functional genomics using Caenorhabditis elegans as a model organism', *Proc Jpn Acad Ser B Phys Biol Sci*, 93(8), 561-577, available: http://dx.doi.org/10.2183/pjab.93.036.

Miyadera, H., Amino, H., Hiraishi, A., Taka, H., Murayama, K., Miyoshi, H., Sakamoto, K., Ishii, N., Hekimi, S. and Kita, K. (2001) 'Altered quinone biosynthesis in the long-lived clk-1 mutants of Caenorhabditis elegans', *J Biol Chem*, 276(11), 7713-6, available: http://dx.doi.org/10.1074/jbc.C000889200.

Mohammad, K. and Titorenko, V.I. (2021) 'Caloric restriction creates a metabolic pattern of chronological aging delay that in budding yeast differs from the metabolic design established by two other geroprotectors', *Oncotarget*, 12(7), 608-625, available: http://dx.doi.org/10.18632/oncotarget.27926.

Molenaars, M., Janssens, G.E., Santermans, T., Lezzerini, M., Jelier, R., MacInnes, A.W. and Houtkooper, R.H. (2018) 'Mitochondrial ubiquinone-mediated longevity is marked by reduced cytoplasmic mRNA translation', *Life Sci Alliance*, 1(5), available: http://dx.doi.org/10.26508/lsa.201800082.

Monaghan, R.M., Barnes, R.G., Fisher, K., Andreou, T., Rooney, N., Poulin, G.B. and Whitmarsh, A.J. (2015) 'A nuclear role for the respiratory enzyme CLK-1 in regulating mitochondrial stress responses and longevity', *Nat Cell Biol*, 17(6), 782-92, available: http://dx.doi.org/10.1038/ncb3170.

Monteleone, G., Biancone, L., Marasco, R., Morrone, G., Marasco, O., Luzza, F. and Pallone, F. (1997) 'Interleukin 12 is expressed and actively released by Crohn's disease intestinal lamina propria mononuclear cells', *Gastroenterology*, 112(4), 1169-78, available: http://dx.doi.org/10.1016/s0016-5085(97)70128-8.

Moore, L.B., Maglich, J.M., McKee, D.D., Wisely, B., Willson, T.M., Kliewer, S.A., Lambert, M.H. and Moore, J.T. (2002) 'Pregnane X receptor (PXR), constitutive androstane receptor (CAR), and benzoate X receptor (BXR) define three pharmacologically distinct classes of nuclear receptors', *Mol Endocrinol*, 16(5), 977-86, available: http://dx.doi.org/10.1210/mend.16.5.0828.

Moreira, S., Fonseca, I., Nunes, M.J., Rosa, A., Lemos, L., Rodrigues, E., Carvalho, A.N., Outeiro, T.F., Rodrigues, C.M.P., Gama, M.J. and Castro-Caldas, M. (2017) 'Nrf2 activation by tauroursodeoxycholic acid in experimental models of Parkinson's disease', *Exp Neurol*, 295, 77-87, available: http://dx.doi.org/10.1016/j.expneurol.2017.05.009.

Morgan, B.R., Ibrahim, G.M., Vogan, V.M., Leung, R.C., Lee, W. and Taylor, M.J. (2019) 'Characterization of Autism Spectrum Disorder across the Age Span by Intrinsic Network Patterns', *Brain Topogr*, 32(3), 461-471, available: http://dx.doi.org/10.1007/s10548-019-00697-w.

Morris, J.Z., Tissenbaum, H.A. and Ruvkun, G. (1996) 'A phosphatidylinositol-3-OH kinase family member regulating longevity and diapause in Caenorhabditis elegans', *Nature*, 382(6591), 536-9, available: http://dx.doi.org/10.1038/382536a0.

Mortiboys, H., Aasly, J. and Bandmann, O. (2013) 'Ursocholanic acid rescues mitochondrial function in common forms of familial Parkinson's disease', *Brain*, 136(Pt 10), 3038-50, available: http://dx.doi.org/10.1093/brain/awt224.

Mortiboys, H., Furmston, R., Bronstad, G., Aasly, J., Elliott, C. and Bandmann, O. (2015) 'UDCA exerts beneficial effect on mitochondrial dysfunction in LRRK2(G2019S) carriers and in vivo', *Neurology*, 85(10), 846-52, available: http://dx.doi.org/10.1212/WNL.0000000000001905.

Motola, D.L., Cummins, C.L., Rottiers, V., Sharma, K.K., Li, T., Li, Y., Suino-Powell, K., Xu, H.E., Auchus, R.J., Antebi, A. and Mangelsdorf, D.J. (2006) 'Identification of ligands for DAF-12 that govern dauer formation and reproduction in C.

elegans', *Cell*, 124(6), 1209-23, available: http://dx.doi.org/10.1016/j.cell.2006.01.037.

Mukherjee, M., Chaudhari, S.N., Balachandran, R.S., Vagasi, A.S. and Kipreos, E.T. (2017) 'Dafachronic acid inhibits C. elegans germ cell proliferation in a DAF-12-dependent manner', *Dev Biol*, 432(2), 215-221, available: http://dx.doi.org/10.1016/j.ydbio.2017.10.014.

Murasko, D.M., Nelson, B.J., Silver, R., Matour, D. and Kaye, D. (1986) 'Immunologic response in an elderly population with a mean age of 85', *Am J Med*, 81(4), 612-8, available: http://dx.doi.org/10.1016/0002-9343(86)90546-2.

Mytilineou, C., Werner, P., Molinari, S., Di Rocco, A., Cohen, G. and Yahr, M.D. (1994) 'Impaired oxidative decarboxylation of pyruvate in fibroblasts from patients with Parkinson's disease', *J Neural Transm Park Dis Dement Sect*, 8(3), 223-8, available: http://dx.doi.org/10.1007/BF02260943.

Narhi, L., Wood, S.J., Steavenson, S., Jiang, Y., Wu, G.M., Anafi, D., Kaufman, S.A., Martin, F., Sitney, K., Denis, P., Louis, J.C., Wypych, J., Biere, A.L. and Citron, M. (1999) 'Both familial Parkinson's disease mutations accelerate alpha-synuclein aggregation', *J Biol Chem*, 274(14), 9843-6, available: http://dx.doi.org/10.1074/jbc.274.14.9843.

Nasreddine, Z.S., Phillips, N.A., Bédirian, V., Charbonneau, S., Whitehead, V., Collin, I., Cummings, J.L. and Chertkow, H. (2005) 'The Montreal Cognitive Assessment, MoCA: a brief screening tool for mild cognitive impairment', *J Am Geriatr Soc*, 53(4), 695-9, available: http://dx.doi.org/10.1111/j.1532-5415.2005.53221.x.

Needham, B.D., Adame, M.D., Serena, G., Rose, D.R., Preston, G.M., Conrad, M.C., Campbell, A.S., Donabedian, D.H., Fasano, A., Ashwood, P. and Mazmanian, S.K. (2021) 'Plasma and Fecal Metabolite Profiles in Autism Spectrum Disorder', *Biol Psychiatry*, 89(5), 451-462, available: http://dx.doi.org/10.1016/j.biopsych.2020.09.025.

Neumann, B., Baror, R., Zhao, C., Segel, M., Dietmann, S., Rawji, K.S., Foerster, S., McClain, C.R., Chalut, K., van Wijngaarden, P. and Franklin, R.J.M. (2019) 'Metformin Restores CNS Remyelination Capacity by Rejuvenating Aged Stem Cells', *Cell Stem Cell*, 25(4), 473-485.e8, available: http://dx.doi.org/10.1016/j.stem.2019.08.015.

Nicholas, J.S., Charles, J.M., Carpenter, L.A., King, L.B., Jenner, W. and Spratt, E.G. (2008) 'Prevalence and characteristics of children with autism-spectrum disorders', *Ann Epidemiol*, 18(2), 130-6, available: http://dx.doi.org/10.1016/j.annepidem.2007.10.013.

Niesler, B. and Rappold, G.A. (2021) 'Emerging evidence for gene mutations driving both brain and gut dysfunction in autism spectrum disorder', *Mol Psychiatry*, 26(5), 1442-1444, available: http://dx.doi.org/10.1038/s41380-020-0778-5.

Nishiwaki, H., Ito, M., Ishida, T., Hamaguchi, T., Maeda, T., Kashihara, K., Tsuboi, Y., Ueyama, J., Shimamura, T., Mori, H., Kurokawa, K., Katsuno, M., Hirayama, M. and Ohno, K. (2020) 'Meta-Analysis of Gut Dysbiosis in Parkinson's Disease', *Mov Disord*, 35(9), 1626-1635, available: http://dx.doi.org/10.1002/mds.28119.

Nogoy, K.M.C., Kim, H.J., Lee, Y., Zhang, Y., Yu, J., Lee, D.H., Li, X.Z., Smith, S.B., Seong, H.A. and Choi, S.H. (2020) 'High dietary oleic acid in olive oil-supplemented diet enhanced omega-3 fatty acid in blood plasma of rats', *Food Sci Nutr*, 8(7), 3617-3625, available: http://dx.doi.org/10.1002/fsn3.1644.

Norlin, M., Toll, A., Björkhem, I. and Wikvall, K. (2000) '24-hydroxycholesterol is a substrate for hepatic cholesterol 7alpha-hydroxylase (CYP7A)', *J Lipid Res*, 41(10), 1629-39.

O'Byrne, J., Hunt, M.C., Rai, D.K., Saeki, M. and Alexson, S.E. (2003) 'The human bile acid-CoA:amino acid N-acyltransferase functions in the conjugation of fatty acids to glycine', *J Biol Chem*, 278(36), 34237-44, available: http://dx.doi.org/10.1074/jbc.M300987200.

O'Donovan, S.M., Crowley, E.K., Brown, J.R., O'Sullivan, O., O'Leary, O.F., Timmons, S., Nolan, Y.M., Clarke, D.J., Hyland, N.P., Joyce, S.A., Sullivan, A.M. and O'Neill, C. (2020) 'Nigral overexpression of α-synuclein in a rat Parkinson's disease model indicates alterations in the enteric nervous system and the gut microbiome', *Neurogastroenterol Motil*, 32(1), e13726, available: http://dx.doi.org/10.1111/nmo.13726.

Odamaki, T., Kato, K., Sugahara, H., Hashikura, N., Takahashi, S., Xiao, J.Z., Abe, F. and Osawa, R. (2016) 'Age-related changes in gut microbiota composition from newborn to centenarian: a cross-sectional study', *BMC Microbiol*, 16, 90, available: http://dx.doi.org/10.1186/s12866-016-0708-5.

Ogg, S., Paradis, S., Gottlieb, S., Patterson, G.I., Lee, L., Tissenbaum, H.A. and Ruvkun, G. (1997) 'The Fork head transcription factor DAF-16 transduces insulin-like metabolic and longevity signals in C. elegans', *Nature*, 389(6654), 994-9, available: http://dx.doi.org/10.1038/40194.

Oh, A.R., Bae, J.S., Lee, J., Shin, E., Oh, B.C., Park, S.C. and Cha, J.Y. (2016) 'Ursodeoxycholic acid decreases age-related adiposity and inflammation in mice', *BMB Rep*, 49(2), 105-10, available: http://dx.doi.org/10.5483/bmbrep.2016.49.2.173.

Olivares-Morales, M.J., De La Fuente, M.K., Dubois-Camacho, K., Parada, D., Diaz-Jiménez, D., Torres-Riquelme, A., Xu, X., Chamorro-Veloso, N., Naves, R., Gonzalez, M.J., Quera, R., Figueroa, C., Cidlowski, J.A., Vidal, R.M. and Hermoso, M.A. (2018) 'Glucocorticoids Impair Phagocytosis and Inflammatory Response Against Crohn's Disease-Associated Adherent-Invasive', *Front Immunol*, 9, 1026, available: http://dx.doi.org/10.3389/fimmu.2018.01026.

Olsen, A. and Gill, M.S. (2016) *Ageing: Lessons from C. elegans*, Cham, Switzerland: Springer.

Ong, S.M., Hadadi, E., Dang, T.M., Yeap, W.H., Tan, C.T., Ng, T.P., Larbi, A. and Wong, S.C. (2018) 'The pro-inflammatory phenotype of the human non-classical monocyte subset is attributed to senescence', *Cell Death Dis*, 9(3), 266, available: http://dx.doi.org/10.1038/s41419-018-0327-1.

Onken, B. and Driscoll, M. (2010) 'Metformin induces a dietary restriction-like state and the oxidative stress response to extend C. elegans Healthspan via AMPK, LKB1, and SKN-1', *PLoS One*, 5(1), e8758, available: http://dx.doi.org/10.1371/journal.pone.0008758.

Palacios, N., Hannoun, A., Flahive, J., Ward, D., Goostrey, K., Deb, A. and Smith, K.M. (2021) 'Effect of Levodopa Initiation on the Gut Microbiota in Parkinson's Disease', *Front Neurol*, 12, 574529, available: http://dx.doi.org/10.3389/fneur.2021.574529.

Palominos, M.F., Verdugo, L., Gabaldon, C., Pollak, B., Ortíz-Severín, J., Varas, M.A., Chávez, F.P. and Calixto, A. (2017) 'Transgenerational Diapause as an Avoidance Strategy against Bacterial Pathogens in', *mBio*, 8(5), available: http://dx.doi.org/10.1128/mBio.01234-17.

Park, S.H., Kim, K.A., Ahn, Y.T., Jeong, J.J., Huh, C.S. and Kim, D.H. (2015) 'Comparative analysis of gut microbiota in elderly people of urbanized towns and longevity villages', *BMC Microbiol*, 15, 49, available: http://dx.doi.org/10.1186/s12866-015-0386-8.

Parker, A., Romano, S., Ansorge, R., Aboelnour, A., Le Gall, G., Savva, G.M., Pontifex, M.G., Telatin, A., Baker, D., Jones, E., Vauzour, D., Rudder, S., Blackshaw, L.A., Jeffery, G. and Carding, S.R. (2022) 'Fecal microbiota transfer between young and aged mice reverses hallmarks of the aging gut, eye, and brain', *Microbiome*, 10(1), 68, available: http://dx.doi.org/10.1186/s40168-022-01243-w.

Parronchi, P., Romagnani, P., Annunziato, F., Sampognaro, S., Becchio, A., Giannarini, L., Maggi, E., Pupilli, C., Tonelli, F. and Romagnani, S. (1997) 'Type 1 T-helper cell predominance and interleukin-12 expression in the gut of patients with Crohn's disease', *Am J Pathol*, 150(3), 823-32.

Payne, C.M., Bernstein, C., Dvorak, K. and Bernstein, H. (2008) 'Hydrophobic bile acids, genomic instability, Darwinian selection, and colon carcinogenesis', *Clin Exp Gastroenterol*, 1, 19-47, available: http://dx.doi.org/10.2147/ceg.s4343.

Pearson, K.J., Baur, J.A., Lewis, K.N., Peshkin, L., Price, N.L., Labinskyy, N., Swindell, W.R., Kamara, D., Minor, R.K., Perez, E., Jamieson, H.A., Zhang, Y., Dunn, S.R., Sharma, K., Pleshko, N., Woollett, L.A., Csiszar, A., Ikeno, Y., Le Couteur, D., Elliott, P.J., Becker, K.G., Navas, P., Ingram, D.K., Wolf, N.S., Ungvari, Z., Sinclair, D.A. and de Cabo, R. (2008) 'Resveratrol delays age-related deterioration and mimics transcriptional aspects of dietary restriction without extending life span', *Cell Metab*, 8(2), 157-68, available: http://dx.doi.org/10.1016/j.cmet.2008.06.011.

Perino, A., Demagny, H., Velazquez-Villegas, L. and Schoonjans, K. (2021) 'Molecular Physiology of Bile Acid Signaling in Health, Disease, and Aging', *Physiol Rev*, 101(2), 683-731, available: http://dx.doi.org/10.1152/physrev.00049.2019.

Petersen, J.D., Wehberg, S., Packness, A., Svensson, N.H., Hyldig, N., Raunsgaard, S., Andersen, M.K., Ryg, J., Mercer, S.W., Søndergaard, J. and Waldorff, F.B. (2021) 'Association of Socioeconomic Status With Dementia Diagnosis Among Older Adults in Denmark', *JAMA Netw Open*, 4(5), e2110432, available: http://dx.doi.org/10.1001/jamanetworkopen.2021.10432.

Pietrucci, D., Cerroni, R., Unida, V., Farcomeni, A., Pierantozzi, M., Mercuri, N.B., Biocca, S., Stefani, A. and Desideri, A. (2019) 'Dysbiosis of gut microbiota in a selected population of Parkinson's patients', *Parkinsonism Relat Disord*, 65, 124-130, available: http://dx.doi.org/10.1016/j.parkreldis.2019.06.003.

Pikuleva, I.A., Babiker, A., Waterman, M.R. and Björkhem, I. (1998) 'Activities of recombinant human cytochrome P450c27 (CYP27) which produce intermediates of alternative bile acid biosynthetic pathways', *J Biol Chem*, 273(29), 18153-60, available: http://dx.doi.org/10.1074/jbc.273.29.18153.

Pinti, M., Cevenini, E., Nasi, M., De Biasi, S., Salvioli, S., Monti, D., Benatti, S., Gibellini, L., Cotichini, R., Stazi, M.A., Trenti, T., Franceschi, C. and Cossarizza, A. (2014) 'Circulating mitochondrial DNA increases with age and is a familiar trait: Implications for "inflamm-aging"', *Eur J Immunol*, 44(5), 1552-62, available: http://dx.doi.org/10.1002/eji.201343921.

Plagg, B.Z., Stefan. (2021) 'How does the environment affect human ageing? An interdisciplinary review', available: http://dx.doi.org/10.36150/2499-6564-420.

Pochakom, A., Mu, C., Rho, J.M., Tompkins, T.A., Mayengbam, S. and Shearer, J. (2022) 'Selective Probiotic Treatment Positively Modulates the Microbiota-

Gut-Brain Axis in the BTBR Mouse Model of Autism', *Brain Sci*, 12(6), available: http://dx.doi.org/10.3390/brainsci12060781.

Postuma, R.B., Gagnon, J.F., Pelletier, A. and Montplaisir, J. (2013) 'Prodromal autonomic symptoms and signs in Parkinson's disease and dementia with Lewy bodies', *Mov Disord*, 28(5), 597-604, available: http://dx.doi.org/10.1002/mds.25445.

Prete, R., Long, S.L., Gallardo, A.L., Gahan, C.G., Corsetti, A. and Joyce, S.A. (2020) 'Beneficial bile acid metabolism from Lactobacillus plantarum of food origin', *Sci Rep*, 10(1), 1165, available: http://dx.doi.org/10.1038/s41598-020-58069-5.

Prithika, U., Deepa, V. and Balamurugan, K. (2016) 'External induction of heat shock stimulates the immune response and longevity of Caenorhabditis elegans towards pathogen exposure', *Innate Immun*, 22(6), 466-78, available: http://dx.doi.org/10.1177/1753425916654557.

Pryor, R. and Cabreiro, F. (2015) 'Repurposing metformin: an old drug with new tricks in its binding pockets', *Biochem J*, 471(3), 307-22, available: http://dx.doi.org/10.1042/BJ20150497.

Pryor, R., Norvaisas, P., Marinos, G., Best, L., Thingholm, L.B., Quintaneiro, L.M., De Haes, W., Esser, D., Waschina, S., Lujan, C., Smith, R.L., Scott, T.A., Martinez-Martinez, D., Woodward, O., Bryson, K., Laudes, M., Lieb, W., Houtkooper, R.H., Franke, A., Temmerman, L., Bjedov, I., Cochemé, H.M., Kaleta, C. and Cabreiro, F. (2019) 'Host-Microbe-Drug-Nutrient Screen Identifies Bacterial Effectors of Metformin Therapy', *Cell*, 178(6), 1299-1312.e29, available: http://dx.doi.org/10.1016/j.cell.2019.08.003.

Pérez, A., Rivoira, M.A., Rodríguez, V., Marchionatti, A. and Tolosa de Talamoni, N. (2021) 'Role of mitochondria in the differential action of sodium deoxycholate and ursodeoxycholic acid on rat duodenum', *Can J Physiol Pharmacol*, 99(3), 270-277, available: http://dx.doi.org/10.1139/cjpp-2019-0561.

Qi, B. and Han, M. (2018) 'Microbial Siderophore Enterobactin Promotes Mitochondrial Iron Uptake and Development of the Host via Interaction with ATP Synthase', *Cell*, 175(2), 571-582.e11, available: http://dx.doi.org/10.1016/j.cell.2018.07.032.

Qi, Q., Liu, Y., Cheng, Y., Glanville, J., Zhang, D., Lee, J.Y., Olshen, R.A., Weyand, C.M., Boyd, S.D. and Goronzy, J.J. (2014) 'Diversity and clonal selection in the human T-cell repertoire', *Proc Natl Acad Sci U S A*, 111(36), 13139-44, available: http://dx.doi.org/10.1073/pnas.1409155111.

Quilty, F., Freeley, M., Gargan, S., Gilmer, J. and Long, A. (2021) 'Deoxycholic acid induces proinflammatory cytokine production by model oesophageal cells via lipid rafts', *J Steroid Biochem Mol Biol*, 214, 105987, available: http://dx.doi.org/10.1016/j.jsbmb.2021.105987.

Rahayu, E.S., Utami, T., Mariyatun, M., Hasan, P.N., Kamil, R.Z., Setyawan, R.H., Pamungkaningtyas, F.H., Harahap, I.A., Wiryohanjoyo, D.V., Pramesi, P.C., Cahyanto, M.N., Sujaya, I.N. and Juffrie, M. (2019) 'Gut microbiota profile in healthy Indonesians', *World J Gastroenterol*, 25(12), 1478-1491, available: http://dx.doi.org/10.3748/wjg.v25.i12.1478.

Raizen, D.M., Lee, R.Y. and Avery, L. (1995) 'Interacting genes required for pharyngeal excitation by motor neuron MC in Caenorhabditis elegans', *Genetics*, 141(4), 1365-82, available: http://dx.doi.org/10.1093/genetics/141.4.1365.

Rampelli, S., Soverini, M., D'Amico, F., Barone, M., Tavella, T., Monti, D., Capri, M., Astolfi, A., Brigidi, P., Biagi, E., Franceschi, C., Turroni, S. and Candela, M. (2020) 'Shotgun Metagenomics of Gut Microbiota in Humans with up to Extreme Longevity and the Increasing Role of Xenobiotic Degradation', *mSystems*, 5(2), available: http://dx.doi.org/10.1128/mSystems.00124-20.

Rapamune, s. (1999) 'Initial U.S. Approval'.

Rastogi, S., Borgo, B., Pazdernik, N., Fox, P., Mardis, E.R., Kohara, Y., Havranek, J. and Schedl, T. (2015) 'Caenorhabditis elegans glp-4 Encodes a Valyl Aminoacyl tRNA Synthetase', *G3 (Bethesda)*, 5(12), 2719-28, available: http://dx.doi.org/10.1534/g3.115.021899.

Raulin, A.C., Doss, S.V., Trottier, Z.A., Ikezu, T.C., Bu, G. and Liu, C.C. (2022) 'ApoE in Alzheimer's disease: pathophysiology and therapeutic strategies', *Mol Neurodegener*, 17(1), 72, available: http://dx.doi.org/10.1186/s13024-022-00574-4.

Reekes, T.H., Higginson, C.I., Ledbetter, C.R., Sathivadivel, N., Zweig, R.M. and Disbrow, E.A. (2020) 'Sex specific cognitive differences in Parkinson disease', *NPJ Parkinsons Dis*, 6, 7, available: http://dx.doi.org/10.1038/s41531-020-0109-1.

Renaud, S. and de Lorgeril, M. (1992) 'Wine, alcohol, platelets, and the French paradox for coronary heart disease', *Lancet*, 339(8808), 1523-6, available: http://dx.doi.org/10.1016/0140-6736(92)91277-f.

Repa, J.J., Liang, G., Ou, J., Bashmakov, Y., Lobaccaro, J.M., Shimomura, I., Shan, B., Brown, M.S., Goldstein, J.L. and Mangelsdorf, D.J. (2000) 'Regulation of mouse sterol regulatory element-binding protein-1c gene (SREBP-1c) by

oxysterol receptors, LXRalpha and LXRbeta', *Genes Dev*, 14(22), 2819-30, available: http://dx.doi.org/10.1101/gad.844900.

Richards, S.E., Wang, Y., Claus, S.P., Lawler, D., Kochhar, S., Holmes, E. and Nicholson, J.K. (2013) 'Metabolic phenotype modulation by caloric restriction in a lifelong dog study', *J Proteome Res*, 12(7), 3117-27, available: http://dx.doi.org/10.1021/pr301097k.

Riddle, D.L., Swanson, M.M. and Albert, P.S. (1981) 'Interacting genes in nematode dauer larva formation', *Nature*, 290(5808), 668-71, available: http://dx.doi.org/10.1038/290668a0.

Ridlon, J.M. and Hylemon, P.B. (2012) 'Identification and characterization of two bile acid coenzyme A transferases from Clostridium scindens, a bile acid 7α-dehydroxylating intestinal bacterium', *J Lipid Res*, 53(1), 66-76, available: http://dx.doi.org/10.1194/jlr.M020313.

Roager, H.M. and Licht, T.R. (2018) 'Microbial tryptophan catabolites in health and disease', *Nat Commun*, 9(1), 3294, available: http://dx.doi.org/10.1038/s41467-018-05470-4.

Rosa, A.I., Duarte-Silva, S., Silva-Fernandes, A., Nunes, M.J., Carvalho, A.N., Rodrigues, E., Gama, M.J., Rodrigues, C.M.P., Maciel, P. and Castro-Caldas, M. (2018) 'Tauroursodeoxycholic Acid Improves Motor Symptoms in a Mouse Model of Parkinson's Disease', *Mol Neurobiol*, 55(12), 9139-9155, available: http://dx.doi.org/10.1007/s12035-018-1062-4.

Ross, C., Salmon, A., Strong, R., Fernandez, E., Javors, M., Richardson, A. and Tardif, S. (2015) 'Metabolic consequences of long-term rapamycin exposure on common marmoset monkeys (Callithrix jacchus)', *Aging (Albany NY)*, 7(11), 964-73, available: http://dx.doi.org/10.18632/aging.100843.

Ross, J.M., Öberg, J., Brené, S., Coppotelli, G., Terzioglu, M., Pernold, K., Goiny, M., Sitnikov, R., Kehr, J., Trifunovic, A., Larsson, N.G., Hoffer, B.J. and Olson, L. (2010) 'High brain lactate is a hallmark of aging and caused by a shift in the lactate dehydrogenase A/B ratio', *Proc Natl Acad Sci U S A*, 107(46), 20087-92, available: http://dx.doi.org/10.1073/pnas.1008189107.

Ruiz, L., Margolles, A. and Sánchez, B. (2013) 'Bile resistance mechanisms in Lactobacillus and Bifidobacterium', *Front Microbiol*, 4, 396, available: http://dx.doi.org/10.3389/fmicb.2013.00396.

Ruiz-Ruiz, S., Sanchez-Carrillo, S., Ciordia, S., Mena, M.C., Méndez-García, C., Rojo, D., Bargiela, R., Zubeldia-Varela, E., Martínez-Martínez, M., Barbas, C., Ferrer, M. and Moya, A. (2020) 'Functional microbiome deficits associated with ageing: Chronological age threshold', *Aging Cell*, 19(1), e13063, available: http://dx.doi.org/10.1111/acel.13063.

Sampson, T.R., Debelius, J.W., Thron, T., Janssen, S., Shastri, G.G., Ilhan, Z.E., Challis, C., Schretter, C.E., Rocha, S., Gradinaru, V., Chesselet, M.F., Keshavarzian, A., Shannon, K.M., Krajmalnik-Brown, R., Wittung-Stafshede, P., Knight, R. and Mazmanian, S.K. (2016) 'Gut Microbiota Regulate Motor Deficits and Neuroinflammation in a Model of Parkinson's Disease', *Cell*, 167(6), 1469-1480.e12, available: http://dx.doi.org/10.1016/j.cell.2016.11.018.

Samuel, B.S., Rowedder, H., Braendle, C., Félix, M.A. and Ruvkun, G. (2016) 'Caenorhabditis elegans responses to bacteria from its natural habitats', *Proc Natl Acad Sci U S A*, 113(27), E3941-9, available: http://dx.doi.org/10.1073/pnas.1607183113.

Santos-Lobato, B.L., Gardinassi, L.G., Bortolanza, M., Peti, A.P.F., Pimentel, Â., Faccioli, L.H., Del-Bel, E.A. and Tumas, V. (2022) 'Metabolic Profile in Plasma AND CSF of LEVODOPA-induced Dyskinesia in Parkinson's Disease: Focus on Neuroinflammation', *Mol Neurobiol*, 59(2), 1140-1150, available: http://dx.doi.org/10.1007/s12035-021-02625-1.

Sathe, A.G., Tuite, P., Chen, C., Ma, Y., Chen, W., Cloyd, J., Low, W.C., Steer, C.J., Lee, B.Y., Zhu, X.H. and Coles, L.D. (2020) 'Pharmacokinetics, Safety, and Tolerability of Orally Administered Ursodeoxycholic Acid in Patients With Parkinson's Disease-A Pilot Study', *J Clin Pharmacol*, 60(6), 744-750, available: http://dx.doi.org/10.1002/jcph.1575.

Sato, Y., Atarashi, K., Plichta, D.R., Arai, Y., Sasajima, S., Kearney, S.M., Suda, W., Takeshita, K., Sasaki, T., Okamoto, S., Skelly, A.N., Okamura, Y., Vlamakis, H., Li, Y., Tanoue, T., Takei, H., Nittono, H., Narushima, S., Irie, J., Itoh, H., Moriya, K., Sugiura, Y., Suematsu, M., Moritoki, N., Shibata, S., Littman, D.R., Fischbach, M.A., Uwamino, Y., Inoue, T., Honda, A., Hattori, M., Murai, T., Xavier, R.J., Hirose, N. and Honda, K. (2021) 'Novel bile acid biosynthetic pathways are enriched in the microbiome of centenarians', *Nature*, 599(7885), 458-464, available: http://dx.doi.org/10.1038/s41586-021-03832-5.

Schaedel, O.N., Gerisch, B., Antebi, A. and Sternberg, P.W. (2012) 'Hormonal signal amplification mediates environmental conditions during development and controls an irreversible commitment to adulthood', *PLoS Biol*, 10(4), e1001306, available: http://dx.doi.org/10.1371/journal.pbio.1001306.

Scheperjans, F., Aho, V., Pereira, P.A., Koskinen, K., Paulin, L., Pekkonen, E., Haapaniemi, E., Kaakkola, S., Eerola-Rautio, J., Pohja, M., Kinnunen, E., Murros, K. and Auvinen, P. (2015) 'Gut microbiota are related to Parkinson's disease and clinical phenotype', *Mov Disord*, 30(3), 350-8, available: http://dx.doi.org/10.1002/mds.26069.

Schloss, P.D., Schubert, A.M., Zackular, J.P., Iverson, K.D., Young, V.B. and Petrosino, J.F. (2012) 'Stabilization of the murine gut microbiome following weaning', *Gut Microbes*, 3(4), 383-93, available: http://dx.doi.org/10.4161/gmic.21008.

Schommer, J., Marwarha, G., Nagamoto-Combs, K. and Ghribi, O. (2018) 'Palmitic Acid-Enriched Diet Increases α-Synuclein and Tyrosine Hydroxylase Expression Levels in the Mouse Brain', *Front Neurosci*, 12, 552, available: http://dx.doi.org/10.3389/fnins.2018.00552.

Schwan, A., Sjölin, S., Trottestam, U. and Aronsson, B. (1983) 'Relapsing clostridium difficile enterocolitis cured by rectal infusion of homologous faeces', *Lancet*, 2(8354), 845, available: http://dx.doi.org/10.1016/s0140-6736(83)90753-5.

Schönfeld, P. and Wojtczak, L. (2016) 'Short- and medium-chain fatty acids in energy metabolism: the cellular perspective', *J Lipid Res*, 57(6), 943-54, available: http://dx.doi.org/10.1194/jlr.R067629.

Sen, P., Sherwin, E., Sandhu, K., Bastiaanssen, T.F.S., Moloney, G.M., Golubeva, A., Fitzgerald, P., Paula Ventura Da Silva, A., Chruścicka-Smaga, B., Olavarría-Ramírez, L., Druelle, C., Campos, D., Jayaprakash, P., Rea, K., Jeffery, I.B., Savignac, H., Chetal, S., Mulder, I., Schellekens, H., Dinan, T.G. and Cryan, J.F. (2022) 'The live biotherapeutic Blautia stercoris MRx0006 attenuates social deficits, repetitive behaviour, and anxiety-like behaviour in a mouse model relevant to autism', *Brain Behav Immun*, 106, 115-126, available: http://dx.doi.org/10.1016/j.bbi.2022.08.007.

Serra, R.W., Fang, M., Park, S.M., Hutchinson, L. and Green, M.R. (2014) 'A KRAS-directed transcriptional silencing pathway that mediates the CpG island methylator phenotype', *Elife*, 3, e02313, available: http://dx.doi.org/10.7554/eLife.02313.

Shaaban, S.Y., El Gendy, Y.G., Mehanna, N.S., El-Senousy, W.M., El-Feki, H.S.A., Saad, K. and El-Asheer, O.M. (2018) 'The role of probiotics in children with autism spectrum disorder: A prospective, open-label study', *Nutr Neurosci*, 21(9), 676-681, available: http://dx.doi.org/10.1080/1028415X.2017.1347746.

Shah, A., Han, P., Wong, M.Y., Chang, R.C. and Legido-Quigley, C. (2019) 'Palmitate and Stearate are Increased in the Plasma in a 6-OHDA Model of Parkinson's Disease', *Metabolites*, 9(2), available: http://dx.doi.org/10.3390/metabo9020031.

Shaham, S. (2006) 'WormBook: 'Methods in Cell Biology' WormBook, ed. The *C. elegans* Research Community, WormBook http://www.wormbook.org'.

Shannon, K.M., Keshavarzian, A., Dodiya, H.B., Jakate, S. and Kordower, J.H. (2012) 'Is alpha-synuclein in the colon a biomarker for premotor Parkinson's disease? Evidence from 3 cases', *Mov Disord*, 27(6), 716-9, available: http://dx.doi.org/10.1002/mds.25020.

Shao, Y., Li, T., Liu, Z., Wang, X., Xu, X., Li, S., Xu, G. and Le, W. (2021) 'Comprehensive metabolic profiling of Parkinson's disease by liquid chromatography-mass spectrometry', *Mol Neurodegener*, 16(1), 4, available: http://dx.doi.org/10.1186/s13024-021-00425-8.

Sharma, K.K., Wang, Z., Motola, D.L., Cummins, C.L., Mangelsdorf, D.J. and Auchus, R.J. (2009) 'Synthesis and activity of dafachronic acid ligands for the C. elegans DAF-12 nuclear hormone receptor', *Mol Endocrinol*, 23(5), 640-8, available: http://dx.doi.org/10.1210/me.2008-0415.

Sharon, G., Cruz, N.J., Kang, D.W., Gandal, M.J., Wang, B., Kim, Y.M., Zink, E.M., Casey, C.P., Taylor, B.C., Lane, C.J., Bramer, L.M., Isern, N.G., Hoyt, D.W., Noecker, C., Sweredoski, M.J., Moradian, A., Borenstein, E., Jansson, J.K., Knight, R., Metz, T.O., Lois, C., Geschwind, D.H., Krajmalnik-Brown, R. and Mazmanian, S.K. (2019) 'Human Gut Microbiota from Autism Spectrum Disorder Promote Behavioral Symptoms in Mice', *Cell*, 177(6), 1600-1618.e17, available: http://dx.doi.org/10.1016/j.cell.2019.05.004.

Sharon, R., Bar-Joseph, I., Mirick, G.E., Serhan, C.N. and Selkoe, D.J. (2003) 'Altered fatty acid composition of dopaminergic neurons expressing alpha-synuclein and human brains with alpha-synucleinopathies', *J Biol Chem*, 278(50), 49874-81, available: http://dx.doi.org/10.1074/jbc.M309127200.

Shaw, W. (2010) 'Increased urinary excretion of a 3-(3-hydroxyphenyl)-3-hydroxypropionic acid (HPHPA), an abnormal phenylalanine metabolite of Clostridia spp. in the gastrointestinal tract, in urine samples from patients with autism and schizophrenia', *Nutr Neurosci*, 13(3), 135-43, available: http://dx.doi.org/10.1179/147683010X12611460763968.

Shen, L. (2020) 'Gut, oral and nasal microbiota and Parkinson's disease', *Microb Cell Fact*, 19(1), 50, available: http://dx.doi.org/10.1186/s12934-020-01313-4.

Sheng, L., Jena, P.K., Liu, H.X., Kalanetra, K.M., Gonzalez, F.J., French, S.W., Krishnan, V.V., Mills, D.A. and Wan, Y.Y. (2017) 'Gender Differences in Bile Acids and Microbiota in Relationship with Gender Dissimilarity in Steatosis Induced by Diet and FXR Inactivation', *Sci Rep*, 7(1), 1748, available: http://dx.doi.org/10.1038/s41598-017-01576-9.

Sheng, W., Ji, G. and Zhang, L. (2022) 'The Effect of Lithocholic Acid on the Gut-Liver Axis', *Front Pharmacol*, 13, 910493, available: http://dx.doi.org/10.3389/fphar.2022.910493.

Shi, Y., Su, W., Zhang, L., Shi, C., Zhou, J., Wang, P., Wang, H., Shi, X., Wei, S., Wang, Q., Auwerx, J., Schoonjans, K., Yu, Y., Pan, R., Zhou, H. and Lu, L. (2020) 'TGR5 Regulates Macrophage Inflammation in Nonalcoholic Steatohepatitis by Modulating NLRP3 Inflammasome Activation', *Front Immunol*, 11, 609060, available: http://dx.doi.org/10.3389/fimmu.2020.609060.

Shimazu, T., Hirschey, M.D., Newman, J., He, W., Shirakawa, K., Le Moan, N., Grueter, C.A., Lim, H., Saunders, L.R., Stevens, R.D., Newgard, C.B., Farese, R.V., de Cabo, R., Ulrich, S., Akassoglou, K. and Verdin, E. (2013) 'Suppression of oxidative stress by β-hydroxybutyrate, an endogenous histone deacetylase inhibitor', *Science*, 339(6116), 211-4, available: http://dx.doi.org/10.1126/science.1227166.

Shostak, Y., Van Gilst, M.R., Antebi, A. and Yamamoto, K.R. (2004) 'Identification of C. elegans DAF-12-binding sites, response elements, and target genes', *Genes Dev*, 18(20), 2529-44, available: http://dx.doi.org/10.1101/gad.1218504.

Siemann, E.H.a.C., L.L. (1992) 'Concentration of the phytoalexin resveratrol in wine'.

Silhavy, T.J., Hartig-Beecken, I. and Boos, W. (1976) 'Periplasmic protein related to the sn-glycerol-3-phosphate transport system of Escherichia coli', *J Bacteriol*, 126(2), 951-8, available: http://dx.doi.org/10.1128/jb.126.2.951-958.1976.

Simonsen, K.T., Møller-Jensen, J., Kristensen, A.R., Andersen, J.S., Riddle, D.L. and Kallipolitis, B.H. (2011a) 'Quantitative proteomics identifies ferritin in the innate immune response of C. elegans', *Virulence*, 2(2), 120-30, available: http://dx.doi.org/10.4161/viru.2.2.15270.

Simonsen, K.T., Nielsen, G., Bjerrum, J.V., Kruse, T., Kallipolitis, B.H. and Møller-Jensen, J. (2011b) 'A role for the RNA chaperone Hfq in controlling adherent-invasive Escherichia coli colonization and virulence', *PLoS One*, 6(1), e16387, available: http://dx.doi.org/10.1371/journal.pone.0016387.

Sinal, C.J., Tohkin, M., Miyata, M., Ward, J.M., Lambert, G. and Gonzalez, F.J. (2000) 'Targeted disruption of the nuclear receptor FXR/BAR impairs bile acid and lipid homeostasis', *Cell*, 102(6), 731-44, available: http://dx.doi.org/10.1016/s0092-8674(00)00062-3.

Singh, V. and Aballay, A. (2009) 'Regulation of DAF-16-mediated Innate Immunity in Caenorhabditis elegans', *J Biol Chem*, 284(51), 35580-7, available: http://dx.doi.org/10.1074/jbc.M109.060905.

Smith, R.P., Paxman, J.J., Scanlon, M.J. and Heras, B. (2016) 'Targeting Bacterial Dsb Proteins for the Development of Anti-Virulence Agents', *Molecules*, 21(7), available: http://dx.doi.org/10.3390/molecules21070811.

Society, M.D. (2008) 'The MDS-sponsored Revision of the Unified Parkinson's Disease Rating Scale'.

Song, M., Zhang, F., Chen, L., Yang, Q., Su, H., Yang, X., He, H., Ling, M., Zheng, J., Duan, C., Lai, X., Pan, M., Zhu, X., Wang, L., Gao, P., Shu, G., Jiang, Q. and Wang, S. (2021) 'Dietary chenodeoxycholic acid improves growth performance and intestinal health by altering serum metabolic profiles and gut bacteria in weaned piglets', *Anim Nutr*, 7(2), 365-375, available: http://dx.doi.org/10.1016/j.aninu.2020.07.011.

Song, X., An, Y., Chen, D., Zhang, W., Wu, X., Li, C., Wang, S., Dong, W., Wang, B., Liu, T., Zhong, W., Sun, T. and Cao, H. (2022) 'Microbial metabolite deoxycholic acid promotes vasculogenic mimicry formation in intestinal carcinogenesis', *Cancer Sci*, 113(2), 459-477, available: http://dx.doi.org/10.1111/cas.15208.

Soto-Beasley, A.I., Walton, R.L., Valentino, R.R., Hook, P.W., Labbé, C., Heckman, M.G., Johnson, P.W., Goff, L.A., Uitti, R.J., McLean, P.J., Springer, W., McCallion, A.S., Wszolek, Z.K. and Ross, O.A. (2020) 'Screening non-MAPT genes of the Chr17q21 H1 haplotype in Parkinson's disease', *Parkinsonism Relat Disord*, 78, 138-144, available: http://dx.doi.org/10.1016/j.parkreldis.2020.07.022.

Staats, S., Rimbach, G., Kuenstner, A., Graspeuntner, S., Rupp, J., Busch, H., Sina, C., Ipharraguerre, I.R. and Wagner, A.E. (2018) 'Lithocholic Acid Improves the Survival of Drosophila Melanogaster', *Mol Nutr Food Res*, 62(20), e1800424, available: http://dx.doi.org/10.1002/mnfr.201800424.

Staiger, H., Staiger, K., Stefan, N., Wahl, H.G., Machicao, F., Kellerer, M. and Häring, H.U. (2004) 'Palmitate-induced interleukin-6 expression in human coronary artery endothelial cells', *Diabetes*, 53(12), 3209-16, available: http://dx.doi.org/10.2337/diabetes.53.12.3209.

Sterne, J. (1957) 'Du nouveau dans les antidiabetiques. La NN dimethylamine guanyl guanide (NNDG)'.

Stiernagle, T. (2006) ''Maintenance of C*. elegans'* WormBook, ed. The C*. elegans* Research Community, WormBook http://www.wormbook.org'.

Strati, F., Cavalieri, D., Albanese, D., De Felice, C., Donati, C., Hayek, J., Jousson, O., Leoncini, S., Renzi, D., Calabrò, A. and De Filippo, C. (2017) 'New evidences on the altered gut microbiota in autism spectrum disorders', *Microbiome*, 5(1), 24, available: http://dx.doi.org/10.1186/s40168-017-0242-1.

Ståhlberg, D. (1995) 'Effects of pregnenolone-16 alpha-carbonitrile on the metabolism of cholesterol in rat liver microsomes', *Lipids*, 30(4), 361-4, available: http://dx.doi.org/10.1007/BF02536046.

Sulston, J.E. and Brenner, S. (1974) 'The DNA of Caenorhabditis elegans', *Genetics*, 77(1), 95-104, available: http://dx.doi.org/10.1093/genetics/77.1.95.

Sun, L., Xie, C., Wang, G., Wu, Y., Wu, Q., Wang, X., Liu, J., Deng, Y., Xia, J., Chen, B., Zhang, S., Yun, C., Lian, G., Zhang, X., Zhang, H., Bisson, W.H., Shi, J., Gao, X., Ge, P., Liu, C., Krausz, K.W., Nichols, R.G., Cai, J., Rimal, B., Patterson, A.D., Gonzalez, F.J. and Jiang, C. (2018) 'Gut microbiota and intestinal FXR mediate the clinical benefits of metformin', *Nat Med*, 24(12), 1919-1929, available: http://dx.doi.org/10.1038/s41591-018-0222-4.

Sunand, K., Krishna Mohan, G. and Bakshi, V. (2020) 'Supplementation of Lactobacillus Probiotic Strains Supports Gut- Brain-Axis and Defends Autistic Deficits Occurred by Valproic Acid-Induced Prenatal Model of Autism', *Pharmacognosy Journal*, 12(6), available: http://dx.doi.org/10.5530/pj.2020.12.226.

Suriyalaksh, M., Raimondi, C., Mains, A., Segonds-Pichon, A., Mukhtar, S., Murdoch, S., Aldunate, R., Krueger, F., Guimerà, R., Andrews, S., Sales-Pardo, M. and Casanueva, O. (2022) 'Gene regulatory network inference in long-lived', *iScience*, 25(1), 103663, available: http://dx.doi.org/10.1016/j.isci.2021.103663.

Syntichaki, P., Troulinaki, K. and Tavernarakis, N. (2007) 'eIF4E function in somatic cells modulates ageing in Caenorhabditis elegans', *Nature*, 445(7130), 922-6, available: http://dx.doi.org/10.1038/nature05603.

Tan, A., Sullenbarger, B., Prakash, R. and McDaniel, J.C. (2018) 'Supplementation with eicosapentaenoic acid and docosahexaenoic acid reduces high levels of circulating proinflammatory cytokines in aging adults: A randomized, controlled study', *Prostaglandins Leukot Essent Fatty Acids*, 132, 23-29, available: http://dx.doi.org/10.1016/j.plefa.2018.03.010.

Tao, Z., Aslam, H., Parke, J., Sanchez, M. and Cheng, Z. (2022) 'Mechanisms of autophagic responses to altered nutritional status', *J Nutr Biochem*, 103, 108955, available: http://dx.doi.org/10.1016/j.jnutbio.2022.108955.

Tawfik, A., Knight, P., Duckworth, C.A., Pritchard, D.M., Rhodes, J.M. and Campbell, B.J. (2019) 'Replication of Crohn's Disease Mucosal', *Pathogens*, 8(2), available: http://dx.doi.org/10.3390/pathogens8020074.

Taylor, R.K., Miller, V.L., Furlong, D.B. and Mekalanos, J.J. (1987) 'Use of phoA gene fusions to identify a pilus colonization factor coordinately regulated with

cholera toxin', *Proc Natl Acad Sci U S A*, 84(9), 2833-7, available: http://dx.doi.org/10.1073/pnas.84.9.2833.

TeKippe, M. and Aballay, A. (2010) 'C. elegans germline-deficient mutants respond to pathogen infection using shared and distinct mechanisms', *PLoS One*, 5(7), e11777, available: http://dx.doi.org/10.1371/journal.pone.0011777.

Thomas, R.H., Meeking, M.M., Mepham, J.R., Tichenoff, L., Possmayer, F., Liu, S. and MacFabe, D.F. (2012) 'The enteric bacterial metabolite propionic acid alters brain and plasma phospholipid molecular species: further development of a rodent model of autism spectrum disorders', *J Neuroinflammation*, 9, 153, available: http://dx.doi.org/10.1186/1742-2094-9-153.

Thompson, A.P., O'Neill, I., Smith, E.J., Catchpole, J., Fagan, A., Burgess, K.E.V., Carmody, R.J. and Clarke, D.J. (2016) 'Glycolysis and pyrimidine biosynthesis are required for replication of adherent-invasive Escherichia coli in macrophages', *Microbiology (Reading)*, 162(6), 954-965, available: http://dx.doi.org/10.1099/mic.0.000289.

Thondamal, M., Witting, M., Schmitt-Kopplin, P. and Aguilaniu, H. (2014) 'Steroid hormone signalling links reproduction to lifespan in dietary-restricted Caenorhabditis elegans', *Nat Commun*, 5, 4879, available: http://dx.doi.org/10.1038/ncomms5879.

Tieu, K., Perier, C., Caspersen, C., Teismann, P., Wu, D.C., Yan, S.D., Naini, A., Vila, M., Jackson-Lewis, V., Ramasamy, R. and Przedborski, S. (2003) 'D-beta-hydroxybutyrate rescues mitochondrial respiration and mitigates features of Parkinson disease', *J Clin Invest*, 112(6), 892-901, available: http://dx.doi.org/10.1172/JCI18797.

Tigges, J., Gordon, T.P., McClure, H.M., Hall, E.C. and Peters, A. (1988) 'Survival rate and life span of rhesus monkeys at the Yerkes regional primate research center', *Am J Primatol*, 15(3), 263-273, available: http://dx.doi.org/10.1002/ajp.1350150308.

Tomova, A., Husarova, V., Lakatosova, S., Bakos, J., Vlkova, B., Babinska, K. and Ostatnikova, D. (2015) 'Gastrointestinal microbiota in children with autism in Slovakia', *Physiol Behav*, 138, 179-87, available: http://dx.doi.org/10.1016/j.physbeh.2014.10.033.

Tomova, A., Soltys, K., Repiska, G., Palkova, L., Filcikova, D., Minarik, G., Turna, J., Prochotska, K., Babinska, K. and Ostatnikova, D. (2020) 'Specificity of gut microbiota in children with autism spectrum disorder in Slovakia and its correlation with astrocytes activity marker and specific behavioural patterns', *Physiol Behav*, 214, 112745, available: http://dx.doi.org/10.1016/j.physbeh.2019.112745.

Tordoff, M.G., Downing, A. and Voznesenskaya, A. (2014) 'Macronutrient selection by seven inbred mouse strains and three taste-related knockout strains', *Physiol Behav*, 135, 49-54, available: http://dx.doi.org/10.1016/j.physbeh.2014.05.039.

Tsai, S.Y., Pokrass, M.J., Klauer, N.R., Nohara, H. and Su, T.P. (2015) 'Sigma-1 receptor regulates Tau phosphorylation and axon extension by shaping p35 turnover via myristic acid', *Proc Natl Acad Sci U S A*, 112(21), 6742-7, available: http://dx.doi.org/10.1073/pnas.1422001112.

Tsoukalas, D., Fragoulakis, V., Sarandi, E., Docea, A.O., Papakonstaninou, E., Tsilimidos, G., Anamaterou, C., Fragkiadaki, P., Aschner, M., Tsatsakis, A., Drakoulis, N. and Calina, D. (2019) 'Targeted Metabolomic Analysis of Serum Fatty Acids for the Prediction of Autoimmune Diseases', *Front Mol Biosci*, 6, 120, available: http://dx.doi.org/10.3389/fmolb.2019.00120.

Tuikhar, N., Keisam, S., Labala, R.K., Imrat, Ramakrishnan, P., Arunkumar, M.C., Ahmed, G., Biagi, E. and Jeyaram, K. (2019) 'Comparative analysis of the gut microbiota in centenarians and young adults shows a common signature across genotypically non-related populations', *Mech Ageing Dev*, 179, 23-35, available: http://dx.doi.org/10.1016/j.mad.2019.02.001.

Tye, C., Runicles, A.K., Whitehouse, A.J.O. and Alvares, G.A. (2018) 'Characterizing the Interplay Between Autism Spectrum Disorder and Comorbid Medical Conditions: An Integrative Review', *Front Psychiatry*, 9, 751, available: http://dx.doi.org/10.3389/fpsyt.2018.00751.

Unger, M.M., Spiegel, J., Dillmann, K.U., Grundmann, D., Philippeit, H., Bürmann, J., Faßbender, K., Schwiertz, A. and Schäfer, K.H. (2016) 'Short chain fatty acids and gut microbiota differ between patients with Parkinson's disease and age-matched controls', *Parkinsonism Relat Disord*, 32, 66-72, available: http://dx.doi.org/10.1016/j.parkreldis.2016.08.019.

van der Hee, B. and Wells, J.M. (2021) 'Microbial Regulation of Host Physiology by Short-chain Fatty Acids', *Trends Microbiol*, 29(8), 700-712, available: http://dx.doi.org/10.1016/j.tim.2021.02.001.

van Raalte, D.H., Li, M., Pritchard, P.H. and Wasan, K.M. (2004) 'Peroxisome proliferator-activated receptor (PPAR)-alpha: a pharmacological target with a promising future', *Pharm Res*, 21(9), 1531-8, available: http://dx.doi.org/10.1023/b:pham.0000041444.06122.8d.

van Soest, A.P.M., Hermes, G.D.A., Berendsen, A.A.M., van de Rest, O., Zoetendal, E.G., Fuentes, S., Santoro, A., Franceschi, C., de Groot, L.C.P.G. and de Vos, W.M. (2020) 'Associations between Pro- and Anti-Inflammatory Gastro-Intestinal Microbiota, Diet, and Cognitive Functioning in Dutch Healthy

Older Adults: The NU-AGE Study', *Nutrients*, 12(11), available: http://dx.doi.org/10.3390/nu12113471.

Ved, R., Saha, S., Westlund, B., Perier, C., Burnam, L., Sluder, A., Hoener, M., Rodrigues, C.M., Alfonso, A., Steer, C., Liu, L., Przedborski, S. and Wolozin, B. (2005) 'Similar patterns of mitochondrial vulnerability and rescue induced by genetic modification of alpha-synuclein, parkin, and DJ-1 in Caenorhabditis elegans', *J Biol Chem*, 280(52), 42655-42668, available: http://dx.doi.org/10.1074/jbc.M505910200.

Vellai, T., Takacs-Vellai, K., Zhang, Y., Kovacs, A.L., Orosz, L. and Müller, F. (2003) 'Genetics: influence of TOR kinase on lifespan in C. elegans', *Nature*, 426(6967), 620, available: http://dx.doi.org/10.1038/426620a.

Verderosa, A.D., Dhouib, R., Hong, Y., Anderson, T.K., Heras, B. and Totsika, M. (2021) 'A high-throughput cell-based assay pipeline for the preclinical development of bacterial DsbA inhibitors as antivirulence therapeutics', *Sci Rep*, 11(1), 1569, available: http://dx.doi.org/10.1038/s41598-021-81007-y.

Viltard, M., Durand, S., Pérez-Lanzón, M., Aprahamian, F., Lefevre, D., Leroy, C., Madeo, F., Kroemer, G. and Friedlander, G. (2019) 'The metabolomic signature of extreme longevity: naked mole rats', *Aging (Albany NY)*, 11(14), 4783-4800, available: http://dx.doi.org/10.18632/aging.102116.

Vishweswaraiah, S., Akyol, S., Yilmaz, A., Ugur, Z., Gordevičius, J., Oh, K.J., Brundin, P., Radhakrishna, U., Labrie, V. and Graham, S.F. (2022) 'Methylated Cytochrome P450 and the Solute Carrier Family of Genes Correlate With Perturbations in Bile Acid Metabolism in Parkinson's Disease', *Front Neurosci*, 16, 804261, available: http://dx.doi.org/10.3389/fnins.2022.804261.

Voigt, R.M., Wang, Z., Brown, J.M., Engen, P.A., Naqib, A., Goetz, C.G., Hall, D.A., Metman, L.V., Shaikh, M., Forsyth, C.B. and Keshavarzian, A. (2022) 'Gut microbial metabolites in Parkinson's disease: Association with lifestyle, disease characteristics, and treatment status', *Neurobiol Dis*, 170, 105780, available: http://dx.doi.org/10.1016/j.nbd.2022.105780.

Wahlström, A., Sayin, S.I., Marschall, H.U. and Bäckhed, F. (2016) 'Intestinal Crosstalk between Bile Acids and Microbiota and Its Impact on Host Metabolism', *Cell Metab*, 24(1), 41-50, available: http://dx.doi.org/10.1016/j.cmet.2016.05.005.

Wang, B., Wu, L., Chen, J., Dong, L., Chen, C., Wen, Z., Hu, J., Fleming, I. and Wang, D.W. (2021) 'Metabolism pathways of arachidonic acids: mechanisms and potential therapeutic targets', *Signal Transduct Target Ther*, 6(1), 94, available: http://dx.doi.org/10.1038/s41392-020-00443-w.

Wang, C., Lau, C.Y., Ma, F. and Zheng, C. (2021) 'Genome-wide screen identifies curli amyloid fibril as a bacterial component promoting host neurodegeneration', *Proc Natl Acad Sci U S A*, 118(34), available: http://dx.doi.org/10.1073/pnas.2106504118.

Wang, N., Li, R., Lin, H., Fu, C., Wang, X., Zhang, Y., Su, M., Huang, P., Qian, J., Jiang, F., Wang, H., Jiang, L., Yu, X., Liu, J., Chen, Y. and Jiang, Q. (2019) 'Enriched taxa were found among the gut microbiota of centenarians in East China', *PLoS One*, 14(10), e0222763, available: http://dx.doi.org/10.1371/journal.pone.0222763.

Wang, W., Wang, J., Li, J., Yan, P., Jin, Y., Zhang, R., Yue, W., Guo, Q. and Geng, J. (2018) 'Cholecystectomy Damages Aging-Associated Intestinal Microbiota Construction', *Front Microbiol*, 9, 1402, available: http://dx.doi.org/10.3389/fmicb.2018.01402.

Wang, X.X., Luo, Y., Wang, D., Adorini, L., Pruzanski, M., Dobrinskikh, E. and Levi, M. (2017) 'A dual agonist of farnesoid X receptor (FXR) and the G protein-coupled receptor TGR5, INT-767, reverses age-related kidney disease in mice', *J Biol Chem*, 292(29), 12018-12024, available: http://dx.doi.org/10.1074/jbc.C117.794982.

Wang, Y., Tang, J., Lv, Q., Tan, Y., Dong, X., Liu, H., Zhao, N., He, Z., Kou, Y., Liu, X.A., Wang, L., Liu, Y.Y. and Dai, L. (2022) 'Establishment and resilience of transplanted gut microbiota in aged mice', *iScience*, 25(1), 103654, available: http://dx.doi.org/10.1016/j.isci.2021.103654.

Wang, Y.D., Chen, W.D., Wang, M., Yu, D., Forman, B.M. and Huang, W. (2008) 'Farnesoid X receptor antagonizes nuclear factor kappaB in hepatic inflammatory response', *Hepatology*, 48(5), 1632-43, available: http://dx.doi.org/10.1002/hep.22519.

Watanabe, M., Houten, S.M., Mataki, C., Christoffolete, M.A., Kim, B.W., Sato, H., Messaddeq, N., Harney, J.W., Ezaki, O., Kodama, T., Schoonjans, K., Bianco, A.C. and Auwerx, J. (2006) 'Bile acids induce energy expenditure by promoting intracellular thyroid hormone activation', *Nature*, 439(7075), 484-9, available: http://dx.doi.org/10.1038/nature04330.

Wei, D., Li, Y., Che, M., Li, C., Wu, Q. and Sun, C. (2022) 'Melatonin relieves hepatic lipid dysmetabolism caused by aging via modifying the secondary bile acid pattern of gut microbes', *Cell Mol Life Sci*, 79(10), 527, available: http://dx.doi.org/10.1007/s00018-022-04412-0.

Weimann, E., Silva, M.B.B., Murata, G.M., Bortolon, J.R., Dermargos, A., Curi, R. and Hatanaka, E. (2018) 'Topical anti-inflammatory activity of palmitoleic acid improves wound healing', *PLoS One*, 13(10), e0205338, available: http://dx.doi.org/10.1371/journal.pone.0205338.

Weindruch, R., Walford, R.L., Fligiel, S. and Guthrie, D. (1986) 'The retardation of aging in mice by dietary restriction: longevity, cancer, immunity and lifetime energy intake', *J Nutr*, 116(4), 641-54, available: http://dx.doi.org/10.1093/jn/116.4.641.

Weis, S., Schwiertz, A., Unger, M.M., Becker, A., Faßbender, K., Ratering, S., Kohl, M., Schnell, S., Schäfer, K.H. and Egert, M. (2019) 'Effect of Parkinson's disease and related medications on the composition of the fecal bacterial microbiota', *NPJ Parkinsons Dis*, 5, 28, available: http://dx.doi.org/10.1038/s41531-019-0100-x.

White, J.G., Southgate, E., Thomson, J.N. and Brenner, S. (1986) 'The structure of the nervous system of the nematode Caenorhabditis elegans', *Philos Trans R Soc Lond B Biol Sci*, 314(1165), 1-340, available: http://dx.doi.org/10.1098/rstb.1986.0056.

Wilmanski, T., Diener, C., Rappaport, N., Patwardhan, S., Wiedrick, J., Lapidus, J., Earls, J.C., Zimmer, A., Glusman, G., Robinson, M., Yurkovich, J.T., Kado, D.M., Cauley, J.A., Zmuda, J., Lane, N.E., Magis, A.T., Lovejoy, J.C., Hood, L., Gibbons, S.M., Orwoll, E.S. and Price, N.D. (2021) 'Gut microbiome pattern reflects healthy ageing and predicts survival in humans', *Nat Metab*, 3(2), 274-286, available: http://dx.doi.org/10.1038/s42255-021-00348-0.

Witting, M., Rudloff, H.C., Thondamal, M., Aguilaniu, H. and Schmitt-Kopplin, P. (2015) 'Fast separation and quantification of steroid hormones Δ4- and Δ7-dafachronic acid in Caenorhabditis elegans', *J Chromatogr B Analyt Technol Biomed Life Sci*, 978-979, 118-21, available: http://dx.doi.org/10.1016/j.jchromb.2014.12.005.

Wollam, J., Magner, D.B., Magomedova, L., Rass, E., Shen, Y., Rottiers, V., Habermann, B., Cummins, C.L. and Antebi, A. (2012) 'A novel 3-hydroxysteroid dehydrogenase that regulates reproductive development and longevity', *PLoS Biol*, 10(4), e1001305, available: http://dx.doi.org/10.1371/journal.pbio.1001305.

Wollmer, E. and Klein, S. (2022) 'Patient-specific in vitro drug release testing coupled with in silico PBPK modeling to forecast the in vivo performance of oral extended-release levodopa formulations in Parkinson's disease patients', *Eur J Pharm Biopharm*, 180, 101-118, available: http://dx.doi.org/10.1016/j.ejpb.2022.09.015.

Wong, A., Boutis, P. and Hekimi, S. (1995) 'Mutations in the clk-1 gene of Caenorhabditis elegans affect developmental and behavioral timing', *Genetics*, 139(3), 1247-59, available: http://dx.doi.org/10.1093/genetics/139.3.1247.

Wood, J.G., Rogina, B., Lavu, S., Howitz, K., Helfand, S.L., Tatar, M. and Sinclair, D. (2004) 'Sirtuin activators mimic caloric restriction and delay ageing in metazoans', *Nature*, 430(7000), 686-9, available: http://dx.doi.org/10.1038/nature02789.

Wu, G., Jiang, Z., Pu, Y., Chen, S., Wang, T., Wang, Y., Xu, X., Wang, S., Jin, M., Yao, Y., Liu, Y., Ke, S. and Liu, S. (2022) 'Serum short-chain fatty acids and its correlation with motor and non-motor symptoms in Parkinson's disease patients', *BMC Neurol*, 22(1), 13, available: http://dx.doi.org/10.1186/s12883-021-02544-7.

Wu, H., Esteve, E., Tremaroli, V., Khan, M.T., Caesar, R., Mannerås-Holm, L., Ståhlman, M., Olsson, L.M., Serino, M., Planas-Fèlix, M., Xifra, G., Mercader, J.M., Torrents, D., Burcelin, R., Ricart, W., Perkins, R., Fernàndez-Real, J.M. and Bäckhed, F. (2017) 'Metformin alters the gut microbiome of individuals with treatment-naive type 2 diabetes, contributing to the therapeutic effects of the drug', *Nat Med*, 23(7), 850-858, available: http://dx.doi.org/10.1038/nm.4345.

Wu, J., Li, Q. and Fu, X. (2019) 'Fusobacterium nucleatum Contributes to the Carcinogenesis of Colorectal Cancer by Inducing Inflammation and Suppressing Host Immunity', *Transl Oncol*, 12(6), 846-851, available: http://dx.doi.org/10.1016/j.tranon.2019.03.003.

Wu, L., Zeng, T., Zinellu, A., Rubino, S., Kelvin, D.J. and Carru, C. (2019) 'A Cross-Sectional Study of Compositional and Functional Profiles of Gut Microbiota in Sardinian Centenarians', *mSystems*, 4(4), available: http://dx.doi.org/10.1128/mSystems.00325-19.

Xicoy, H., Wieringa, B. and Martens, G.J.M. (2019) 'The Role of Lipids in Parkinson's Disease', *Cells*, 8(1), available: http://dx.doi.org/10.3390/cells8010027.

Xie, H., Shao, R., Yang, Y., Cruz, R. and Zhou, X. (2022) 'Impacts of Built Environment on Risk of Women's Lung Cancer: A Case Study of China', *Int J Environ Res Public Health*, 19(12), available: http://dx.doi.org/10.3390/ijerph19127157.

Xie, W., Radominska-Pandya, A., Shi, Y., Simon, C.M., Nelson, M.C., Ong, E.S., Waxman, D.J. and Evans, R.M. (2001) 'An essential role for nuclear receptors SXR/PXR in detoxification of cholestatic bile acids', *Proc Natl Acad Sci U S A*, 98(6), 3375-80, available: http://dx.doi.org/10.1073/pnas.051014398.

Xu, C., Zhu, H. and Qiu, P. (2019) 'Aging progression of human gut microbiota', *BMC Microbiol*, 19(1), 236, available: http://dx.doi.org/10.1186/s12866-019-1616-2.

Xu, L., Zhang, Q., Dou, X., Wang, Y., Wang, J., Zhou, Y., Liu, X. and Li, J. (2022) 'Fecal microbiota transplantation from young donor mice improves ovarian

function in aged mice', *J Genet Genomics*, available: http://dx.doi.org/10.1016/j.jgg.2022.05.006.

Yamaguchi, A., Nishida, Y., Maeshige, N., Moriguchi, M., Uemura, M., Ma, X., Miyoshi, M., Kondo, H. and Fujino, H. (2021) 'Preventive effect of docosahexaenoic acid (DHA) and eicosapentaenoic acid (EPA) against endotoxin-induced muscle atrophy', *Clin Nutr ESPEN*, 45, 503-506, available: http://dx.doi.org/10.1016/j.clnesp.2021.07.017.

Yamawaki, T.M., Berman, J.R., Suchanek-Kavipurapu, M., McCormick, M., Gaglia, M.M., Lee, S.J. and Kenyon, C. (2010) 'The somatic reproductive tissues of C. elegans promote longevity through steroid hormone signaling', *PLoS Biol*, 8(8), available: http://dx.doi.org/10.1371/journal.pbio.1000468.

Yang, Y., Qian, J., Mei, J., Zhong, K. and Niu, C. (2020) 'In vivo detection of metabolic changes in the striatum of proteasomal inhibition-induced Parkinson's disease in rats using proton MR spectroscopy at 9.4 T', *Int J Neurosci*, 130(2), 153-160, available: http://dx.doi.org/10.1080/00207454.2019.1667783.

Yap, C.X., Henders, A.K., Alvares, G.A., Wood, D.L.A., Krause, L., Tyson, G.W., Restuadi, R., Wallace, L., McLaren, T., Hansell, N.K., Cleary, D., Grove, R., Hafekost, C., Harun, A., Holdsworth, H., Jellett, R., Khan, F., Lawson, L.P., Leslie, J., Frenk, M.L., Masi, A., Mathew, N.E., Muniandy, M., Nothard, M., Miller, J.L., Nunn, L., Holtmann, G., Strike, L.T., de Zubicaray, G.I., Thompson, P.M., McMahon, K.L., Wright, M.J., Visscher, P.M., Dawson, P.A., Dissanayake, C., Eapen, V., Heussler, H.S., McRae, A.F., Whitehouse, A.J.O., Wray, N.R. and Gratten, J. (2021) 'Autism-related dietary preferences mediate autism-gut microbiome associations', *Cell*, 184(24), 5916-5931.e17, available: http://dx.doi.org/10.1016/j.cell.2021.10.015.

Yatsunenko, T., Rey, F.E., Manary, M.J., Trehan, I., Dominguez-Bello, M.G., Contreras, M., Magris, M., Hidalgo, G., Baldassano, R.N., Anokhin, A.P., Heath, A.C., Warner, B., Reeder, J., Kuczynski, J., Caporaso, J.G., Lozupone, C.A., Lauber, C., Clemente, J.C., Knights, D., Knight, R. and Gordon, J.I. (2012) 'Human gut microbiome viewed across age and geography', *Nature*, 486(7402), 222-7, available: http://dx.doi.org/10.1038/nature11053.

Yi, H., Brooks, E.D., Thurberg, B.L., Fyfe, J.C., Kishnani, P.S. and Sun, B. (2014) 'Correction of glycogen storage disease type III with rapamycin in a canine model', *J Mol Med (Berl)*, 92(6), 641-50, available: http://dx.doi.org/10.1007/s00109-014-1127-4.

Yu, J. and Kroll, J.S. (1999) 'DsbA: a protein-folding catalyst contributing to bacterial virulence', *Microbes Infect*, 1(14), 1221-8, available: http://dx.doi.org/10.1016/s1286-4579(99)00239-7.

Yu, T., Wang, C., Yang, J., Guo, Y., Wu, Y. and Li, X. (2017) 'Metformin inhibits SUV39H1-mediated migration of prostate cancer cells', *Oncogenesis*, 6(5), e324, available: http://dx.doi.org/10.1038/oncsis.2017.28.

Yu, Y., Villalobos-Hernandez, E.C., Pradhananga, S., Baker, C.C., Keating, C., Grundy, D., Lomax, A.E. and Reed, D.E. (2019) 'Deoxycholic acid activates colonic afferent nerves via 5-HT', *Am J Physiol Gastrointest Liver Physiol*, 317(3), G275-G284, available: http://dx.doi.org/10.1152/ajpgi.00016.2019.

Zeng, H., Safratowich, B.D., Cheng, W.H., Larson, K.J. and Briske-Anderson, M. (2022) 'Deoxycholic Acid Modulates Cell-Junction Gene Expression and Increases Intestinal Barrier Dysfunction', *Molecules*, 27(3), available: http://dx.doi.org/10.3390/molecules27030723.

Zhang, F., Weckhorst, J.L., Assié, A., Hosea, C., Ayoub, C.A., Khodakova, A.S., Cabrera, M.L., Vidal Vilchis, D., Félix, M.A. and Samuel, B.S. (2021) 'Natural genetic variation drives microbiome selection in the Caenorhabditis elegans gut', *Curr Biol*, 31(12), 2603-2618.e9, available: http://dx.doi.org/10.1016/j.cub.2021.04.046.

Zhang, J., Cao, Q., Li, S., Lu, X., Zhao, Y., Guan, J.S., Chen, J.C., Wu, Q. and Chen, G.Q. (2013) '3-Hydroxybutyrate methyl ester as a potential drug against Alzheimer's disease via mitochondria protection mechanism', *Biomaterials*, 34(30), 7552-62, available: http://dx.doi.org/10.1016/j.biomaterials.2013.06.043.

Zhang, L., Yuan, Y., Tong, Q., Jiang, S., Xu, Q., Ding, J., Zhang, R. and Zhang, K. (2016) 'Reduced plasma taurine level in Parkinson's disease: association with motor severity and levodopa treatment', *Int J Neurosci*, 126(7), 630-6, available: http://dx.doi.org/10.3109/00207454.2015.1051046.

Zhang, N., Zhang, Y., Wang, Z., Pan, F., Ren, R., Li, Z., Zhao, H., Luo, X., Wang, L., Mo, R., Sun, G., Peng, L., Ni, M. and Yang, Y. (2022) 'Regular fecal microbiota transplantation to Senescence Accelerated Mouse-Prone 8 (SAMP8) mice delayed the aging of locomotor and exploration ability by rejuvenating the gut microbiota', *Front Aging Neurosci*, 14, 991157, available: http://dx.doi.org/10.3389/fnagi.2022.991157.

Zhang, S., Zeng, B., Chen, Y., Yang, M., Kong, F., Wei, L., Li, F., Zhao, J. and Li, Y. (2021) 'Gut microbiota in healthy and unhealthy long-living people', *Gene*, 779, 145510, available: http://dx.doi.org/10.1016/j.gene.2021.145510.

Zhang, X., Rielland, M., Yalcin, S. and Ghaffari, S. (2011) 'Regulation and function of FoxO transcription factors in normal and cancer stem cells: what have we learned?', *Curr Drug Targets*, 12(9), 1267-83, available: http://dx.doi.org/10.2174/138945011796150325.

Zhang, Y., Lee, F.Y., Barrera, G., Lee, H., Vales, C., Gonzalez, F.J., Willson, T.M. and Edwards, P.A. (2006) 'Activation of the nuclear receptor FXR improves hyperglycemia and hyperlipidemia in diabetic mice', *Proc Natl Acad Sci U S A*, 103(4), 1006-11, available: http://dx.doi.org/10.1073/pnas.0506982103.

Zhang, Y., Sun, X., Kang, Z., Cai, L., Ding, J., Lu, M. and Hu, G. (2022) 'GPBAR1 preserves neurite and synapse of dopaminergic neurons via RAD21-OPCML signaling: Role in preventing Parkinson's disease in mouse model and human patients', *Pharmacol Res*, 184, 106459, available: http://dx.doi.org/10.1016/j.phrs.2022.106459.

Zhang, Z., Liu, L., Twumasi-Boateng, K., Block, D.H. and Shapira, M. (2017) 'FOS-1 functions as a transcriptional activator downstream of the C. elegans JNK homolog KGB-1', *Cell Signal*, 30, 1-8, available: http://dx.doi.org/10.1016/j.cellsig.2016.11.010.

Zhao, H., Wang, C., Zhao, N., Li, W., Yang, Z., Liu, X., Le, W. and Zhang, X. (2018) 'Potential biomarkers of Parkinson's disease revealed by plasma metabolic profiling', *J Chromatogr B Analyt Technol Biomed Life Sci*, 1081-1082, 101-108, available: http://dx.doi.org/10.1016/j.jchromb.2018.01.025.

Zhao, L., Zhao, Y., Liu, R., Zheng, X., Zhang, M., Guo, H., Zhang, H. and Ren, F. (2017) 'The Transcription Factor DAF-16 is Essential for Increased Longevity in C. elegans Exposed to Bifidobacterium longum BB68', *Sci Rep*, 7(1), 7408, available: http://dx.doi.org/10.1038/s41598-017-07974-3.

Zheng, S., Chiu, H., Boudreau, J., Papanicolaou, T., Bendena, W. and Chin-Sang, I. (2018) 'A functional study of all 40', *J Biol Chem*, 293(43), 16912-16922, available: http://dx.doi.org/10.1074/jbc.RA118.004542.

Zhou, C., King, N., Chen, K.Y. and Breslow, J.L. (2009) 'Activation of PXR induces hypercholesterolemia in wild-type and accelerates atherosclerosis in apoE deficient mice', *J Lipid Res*, 50(10), 2004-13, available: http://dx.doi.org/10.1194/jlr.M800608-JLR200.

Zhou, L., Liu, J., Bu, L.L., Liao, D.F., Cheng, S.W. and Zheng, X.L. (2021) 'Curcumin Acetylsalicylate Extends the Lifespan of', *Molecules*, 26(21), available: http://dx.doi.org/10.3390/molecules26216609.

Zhou, Z.X., Mou, S.F., Chen, X.Q., Gong, L.L. and Ge, W.S. (2018) 'Anti-inflammatory activity of resveratrol prevents inflammation by inhibiting NF-κB in animal models of acute pharyngitis', *Mol Med Rep*, 17(1), 1269-1274, available: http://dx.doi.org/10.3892/mmr.2017.7933.

Zhu, S.Y., Yao, R.Q., Li, Y.X., Zhao, P.Y., Ren, C., Du, X.H. and Yao, Y.M. (2021) 'The Role and Regulatory Mechanism of Transcription Factor EB in Health and

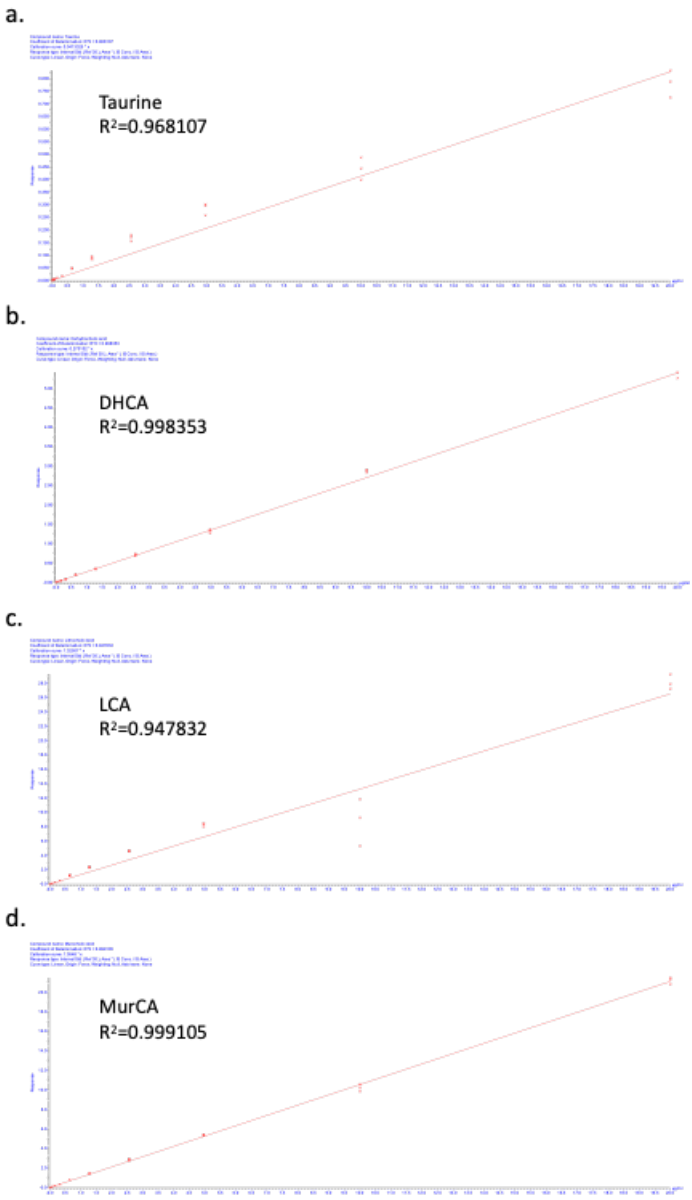
Diseases', *Front Cell Dev Biol*, 9, 667750, available: http://dx.doi.org/10.3389/fcell.2021.667750.

Zoetendal, E.G., Raes, J., van den Bogert, B., Arumugam, M., Booijink, C.C., Troost, F.J., Bork, P., Wels, M., de Vos, W.M. and Kleerebezem, M. (2012) 'The human small intestinal microbiota is driven by rapid uptake and conversion of simple carbohydrates', *ISME J*, 6(7), 1415-26, available: http://dx.doi.org/10.1038/ismej.2011.212.

Appendix I – Chapter 1 – Introduction

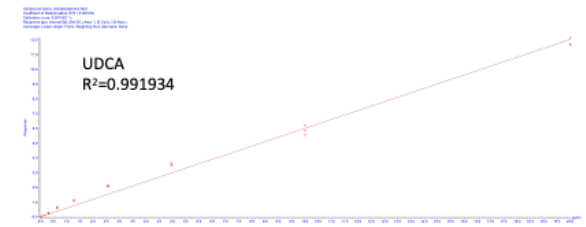
Appendix II – Chapter 2 – Materials and Methods

Appendix III – Chapter 3 – Supplementary Information

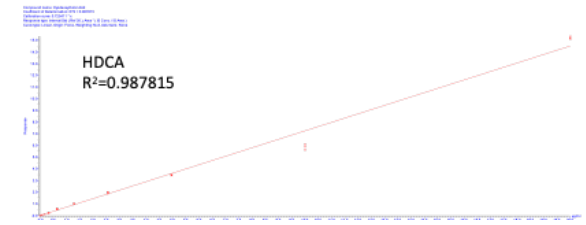


SI.3.1: Standard curves of individual plasma bile acids obtained from UPLC-TMS analysis. X axis represents the concentration of each bile acid (µg/ml) and the Y axis represents the response.

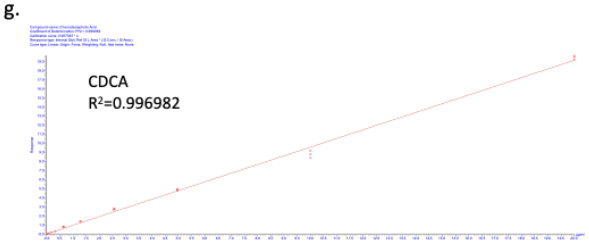
e.



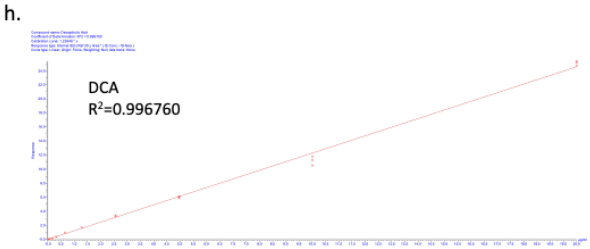
f.



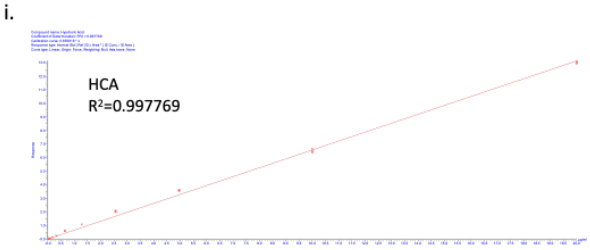
g.



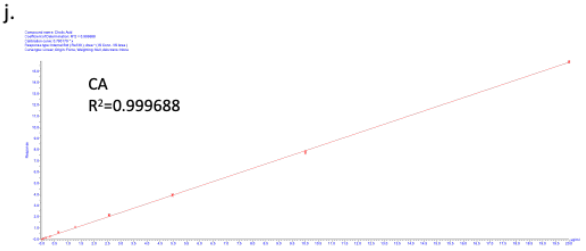
h.



i.

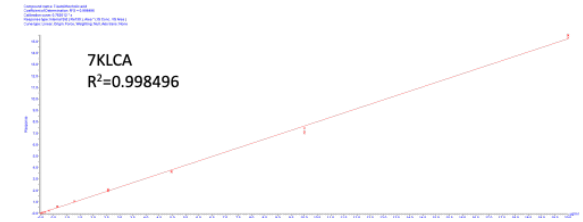


j.

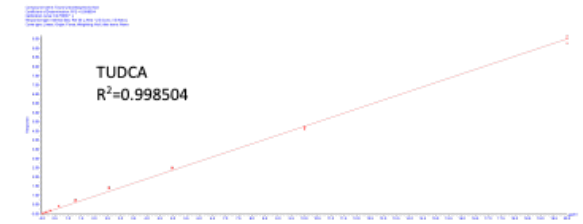


SI.3.1 continued: Standard curves of individual plasma bile acids obtained from UPLC-TMS analysis. X axis represents the concentration of each bile acid (µg/ml) and the Y axis represents the response.

k.



l.



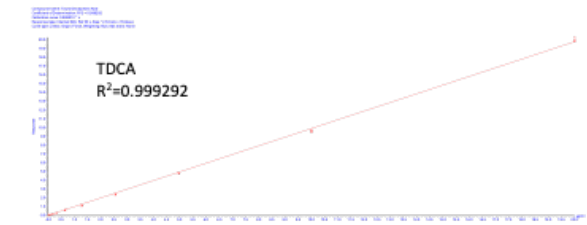
m.



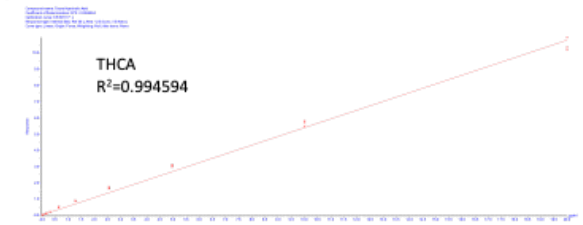
n.



o.

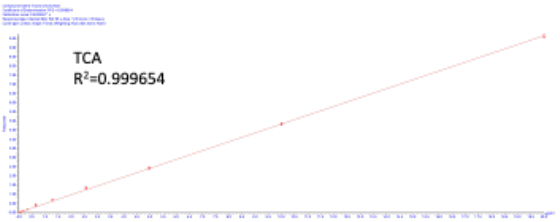


p.

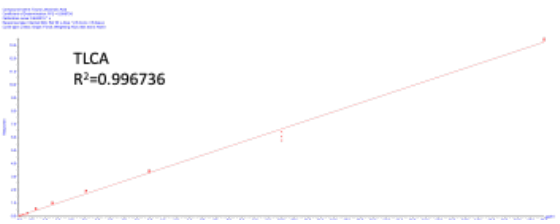


SI.3.1 continued: Standard curves of individual plasma bile acids obtained from UPLC-TMS analysis. X axis represents the concentration of each bile acid (µg/ml) and the Y axis represents the response.

q.



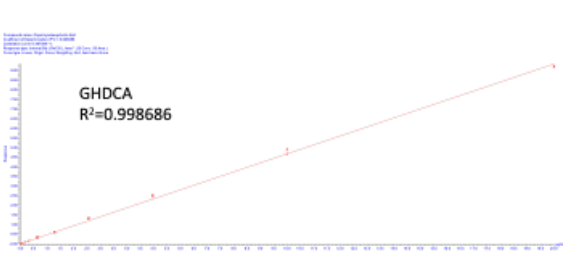
r.



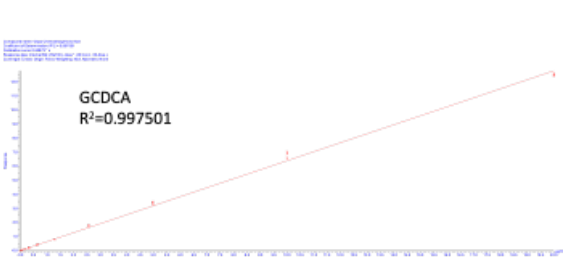
s.



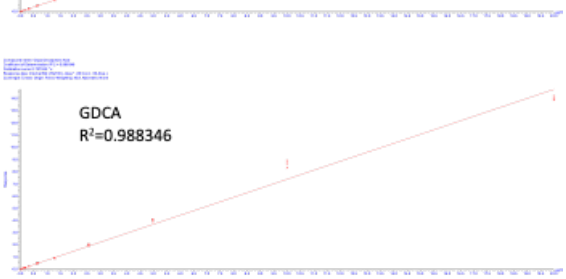
t.



u.

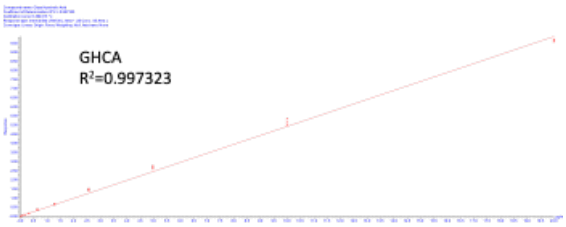


v.



SI.3.1 continued: Standard curves of individual plasma bile acids obtained from UPLC-TMS analysis. X axis represents the concentration of each bile acid (µg/ml) and the Y axis represents the response.

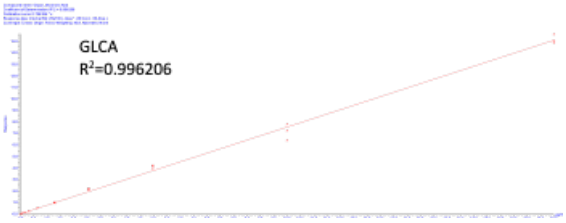
w.



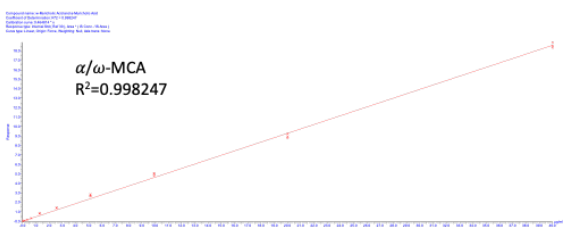
x.



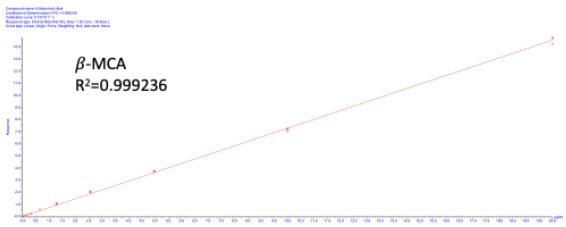
y.



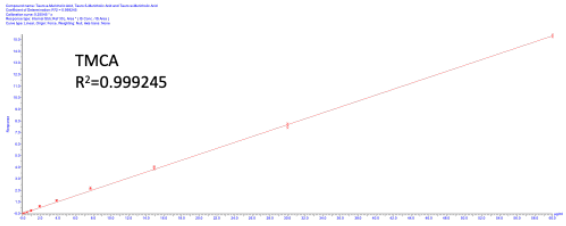
z.



aa.

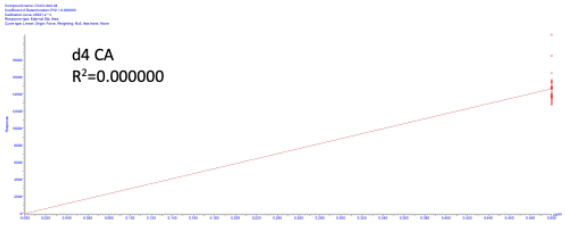


ab.



SI.3.1 continued: Standard curves of individual plasma bile acids obtained from UPLC-TMS analysis. X axis represents the concentration of each bile acid (µg/ml) and the Y axis represents the response.

ac.



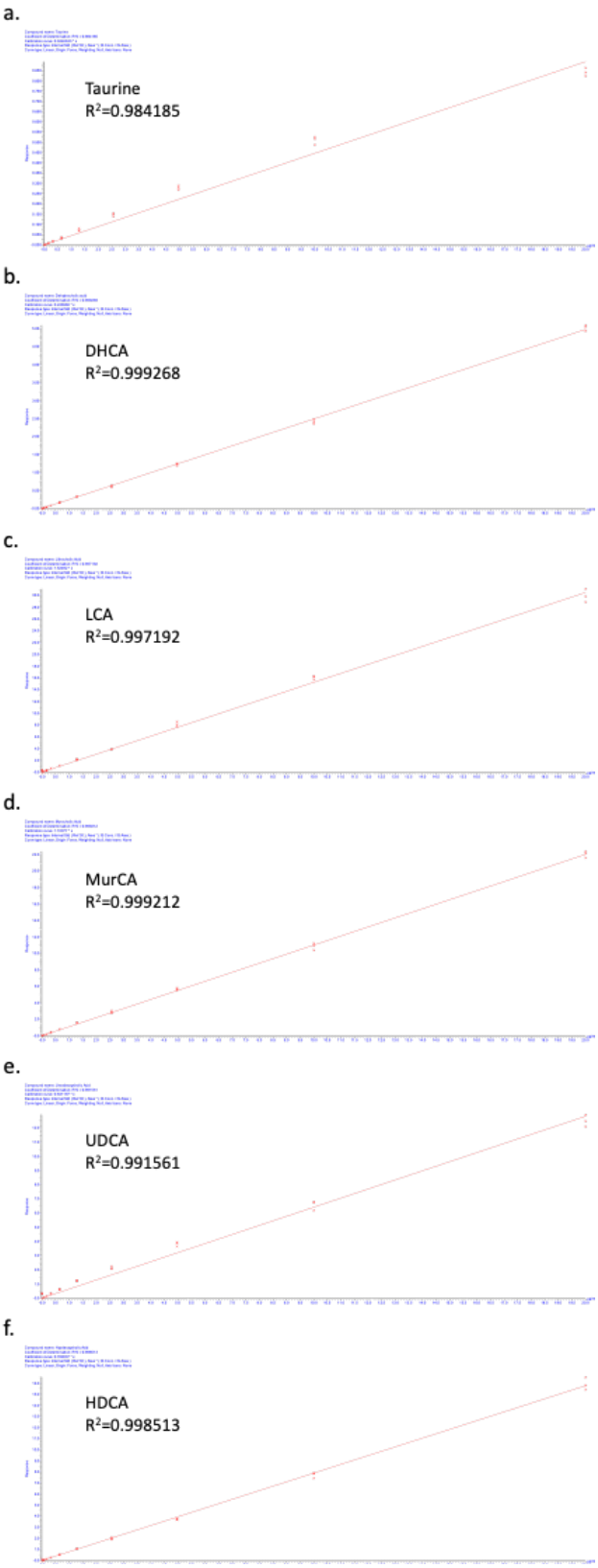
ad.



SI.3.1 continued: Standard curves of individual plasma bile acids obtained from UPLC-TMS analysis. X axis represents the concentration of each bile acid (µg/ml) and the Y axis represents the response.

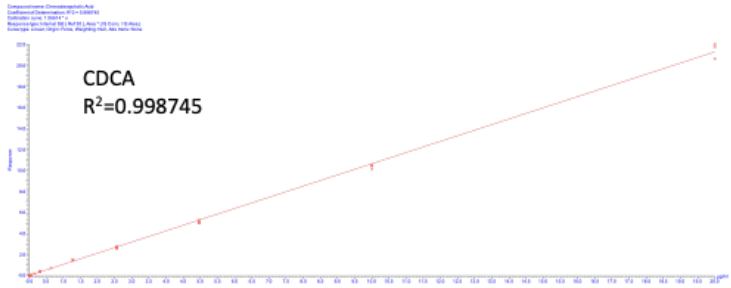
SI.3.2: Table summary of targeted UPLC-TMS application for BA circulating metabolite quantitation (*n*=30) applied to murine BTBR model. The study is described in Chapter 3. BAs are listed with their negative ion mode Molecular weight (MW-), their retention time (RT), R^2 value (which indicates reliability of standard curve) and concentration range (µg/ml) of individual standards for detection.

Number	Analyte	$[MW]^{-H}$	Neutral Formula	RT	Actual RT Top	Actual RT Middle	Actual RT End	R2 value	Range (µg/ml)
1	Taurine	124.0068	$C_2H_7NO_3S$	0.75	0.86	0.86	0.86	0.968107	0.0064-20.00
2	Dehydrocholic Acid	401.2328	$C_{24}H_{34}O_5$	2.00	1.93	1.93	1.93	0.998353	0.0064-20.00
3	Lithocholic Acid	375.2899	$C_{24}H_{40}O_3$	21.72	21.71	21.71	21.71	0.947832	0.0064-20.00
4	Ursodeoxycholic Acid	391.2848	$C_{24}H_{40}O_4$	9.87	8.65	8.65	8.65	0.991937	0.0064-20.00
5	Chenodeoxycholic Acid	391.2848	$C_{24}H_{40}O_4$	19.17	17.53	17.53	17.53	0.996982	0.0064-20.00
6	Hyodeoxycholic Acid	391.2848	$C_{24}H_{40}O_4$	12.54	10.60	10.60	10.60	0.987815	0.0064-20.00
7	Deoxycholic Acid	391.2848	$C_{24}H_{40}O_4$	20.20	18.20	18.20	18.20	0.996760	0.0064-20.00
8	Murocholic Acid	391.2848	$C_{24}H_{40}O_4$	8.25	7.00	7.00	7.05	0.999105	0.0064-20.00
9	Cholic Acid	407.2797	$C_{24}H_{40}O_5$	11.76	11.67	11.67	11.72	0.999688	0.0064-20.00
10	Hyocholic Acid	407.2797	$C_{24}H_{40}O_5$	10.39	8.95	8.95	9.00	0.997769	0.0064-20.00
11	7-Ketolithocholic Acid	389.2692	$C_{24}H_{38}O_4$	11.83	9.92	9.92	9.97	0.998496	0.0064-20.00
12	Taurocholic Acid	514.2838	$C_{26}H_{45}NO_7S$	4.82	4.37	4.37	4.42	0.999654	0.0064-20.00
13	Taurohyocholic Acid	514.2838	$C_{26}H_{45}NO_7S$	3.06	2.67	2.72	2.72	0.994594	0.0064-20.00
14	Taurochenodeoxycholic Acid	498.2889	$C_{26}H_{45}NO_6S$	9.03	7.74	7.78	7.78	0.999002	0.0064-20.00
15	Tauroursodeoxycholic Acid	498.2889	$C_{26}H_{45}NO_6S$	3.16	2.76	2.76	2.81	0.998504	0.0064-20.00
16	Taurodeoxycholic Acid	498.2889	$C_{26}H_{45}NO_6S$	10.39	8.65	8.65	8.70	0.999292	0.0064-20.00
17	Taurohyodeoxycholic Acid	498.2889	$C_{26}H_{45}NO_6S$	3.76	3.16	3.20	3.20	0.996002	0.0064-20.00
18	Taurolithocholic Acid	482.2940	$C_{26}H_{45}NO_5S$	15.19	13.72	13.72	13.77	0.996736	0.0064-20.00
19	Glycocholic Acid	464.3012	$C_{26}H_{43}NO_6$	7.44	5.69	5.69	5.74	0.990186	0.0064-20.00
20	Glycohyocholic Acid	464.3012	$C_{26}H_{43}NO_6$	4.67	3.44	3.44	3.44	0.997323	0.0064-20.00
21	Glycoursodeoxycholic Acid	448.3063	$C_{26}H_{43}NO_5$	4.57	3.49	3.49	3.49	0.991084	0.0064-20.00
22	Glycochenodeoxycholic Acid	448.3063	$C_{26}H_{43}NO_5$	12.64	9.44	9.48	9.48	0.997501	0.0064-20.00
23	Glycohyodeoxycholic Acid	448.3063	$C_{26}H_{43}NO_5$	5.67	4.13	4.13	4.13	0.998686	0.0064-20.00
24	Glycodeoxycholic Acid	448.3063	$C_{26}H_{43}NO_5$	14.05	10.75	10.81	10.81	0.988346	0.0064-20.00
25	Glycolithocholic Acid	432.3114	$C_{26}H_{43}NO_4$	18.19	15.48	15.48	15.53	0.996206	0.0064-20.00
26	α-Muricholic Acid	407.2797	$C_{24}H_{40}O_5$	7.18	5.93	5.93	5.93	0.998247	0.0064-20.00
27	β-Muricholic Acid	407.2797	$C_{24}H_{40}O_5$	7.59	6.37	6.37	6.37	0.999236	0.0064-20.00
28	ω-Muricholic Acid	407.2797	$C_{24}H_{40}O_5$	7.08	5.93	5.93	5.93	0.998247	0.0064-20.00
29	Tauro α-Muricholic Acid	514.2838	$C_{26}H_{45}NO_7S$	2.00	1.79	1.79	1.74	0.999245	0.0064-20.00
30	Tauro β-Muricholic Acid	514.2838	$C_{26}H_{45}NO_7S$	2.16	1.79	1.79	1.74	0.999245	0.0064-20.00
31	Tauro ω-Muricholic Acid	514.2838	$C_{26}H_{45}NO_7S$	2.37	1.79	1.79	1.74	0.999245	0.0064-20.00
D1	Cholic Acid d4	411.3049	$C_{24}H_{36}D_4O_5$	11.74	11.67	11.67	11.67	0.000000	
D2	Chenodeoxycholic Acid d4	395.3099	$C_{24}H_{36}D_4O_4$	19.00	17.48	17.48	17.48	0.000000	

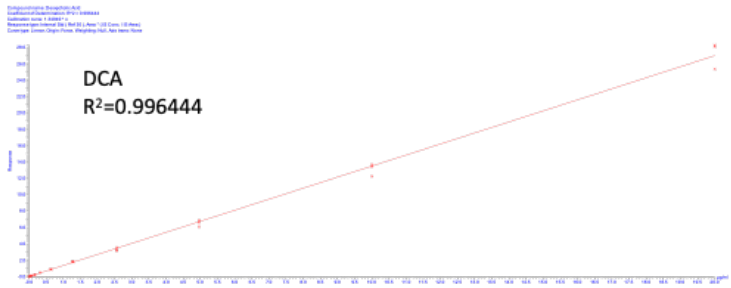


SI.3.3: Standard curves of individual faecal bile acids obtained from UPLC-TMS analysis. X axis represents the concentration of each bile acid (µg/ml) and the Y axis represents the response.

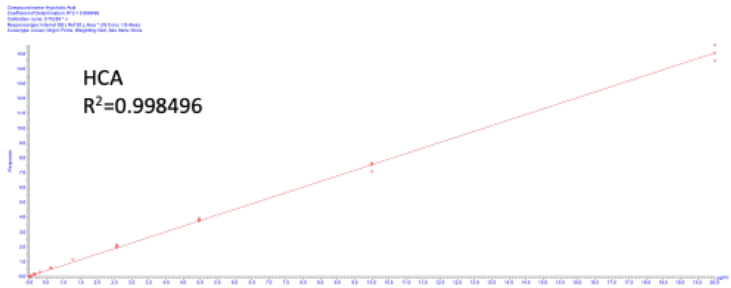
g.



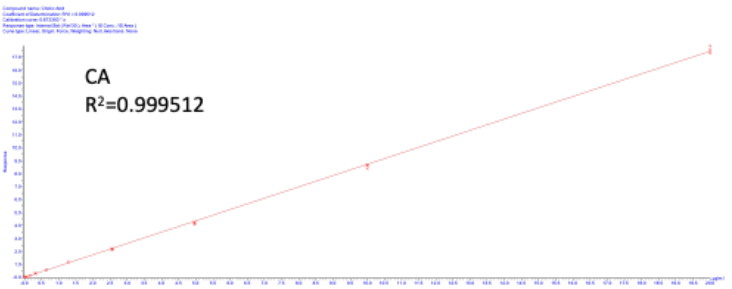
h.



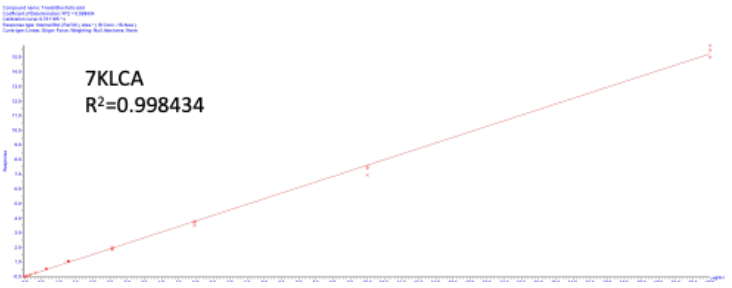
i.



j.

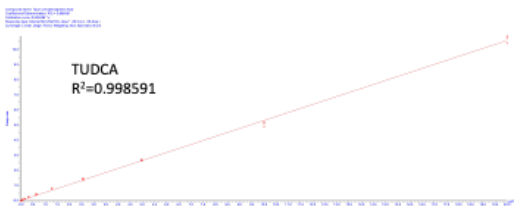


k.

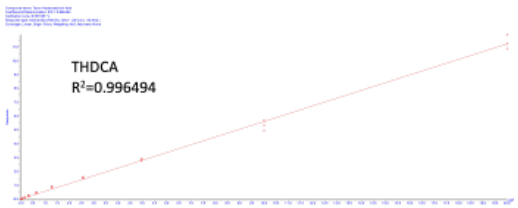


SI.3.3 continued: Standard curves of individual faecal bile acids obtained from UPLC-TMS analysis. X axis represents the concentration of each bile acid (µg/ml) and the Y axis represents the response.

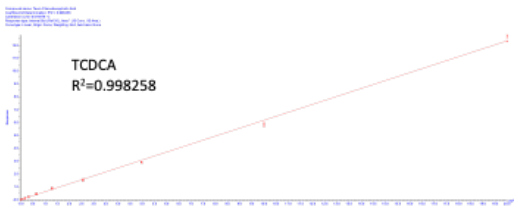
l.



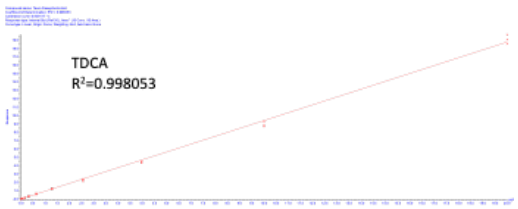
m.



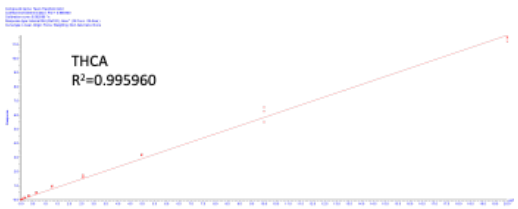
n.



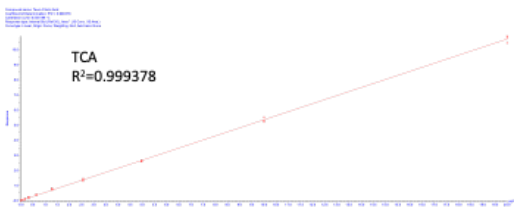
o.



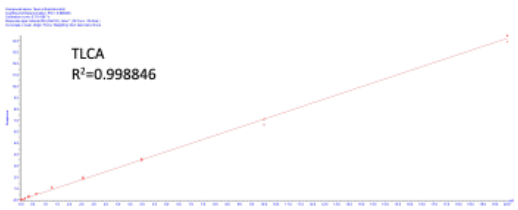
p.



q.



r.

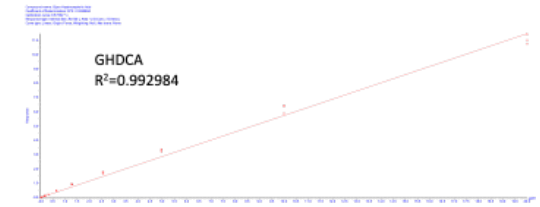


SI.3.3 continued: Standard curves of individual faecal bile acids obtained from UPLC-TMS analysis. X axis represents the concentration of each bile acid (µg/ml) and the Y axis represents the response.

s.



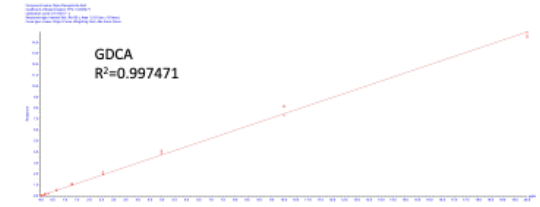
t.



u.



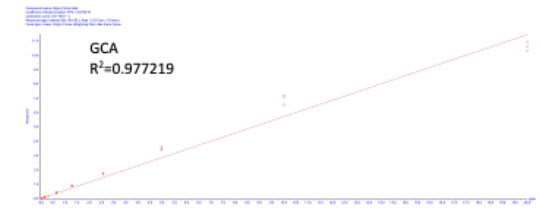
v.



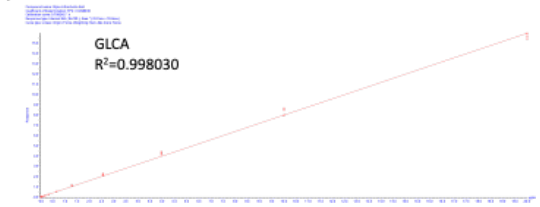
w.



x.

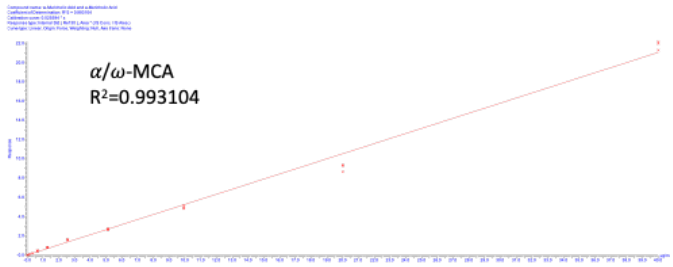


y.

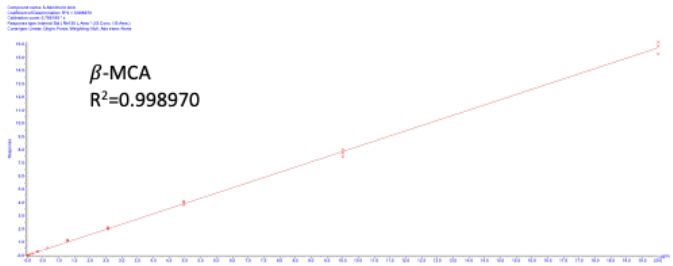


SI.3.3 continued: Standard curves of individual faecal bile acids obtained from UPLC-TMS analysis. X axis represents the concentration of each bile acid (µg/ml) and the Y axis represents the response.

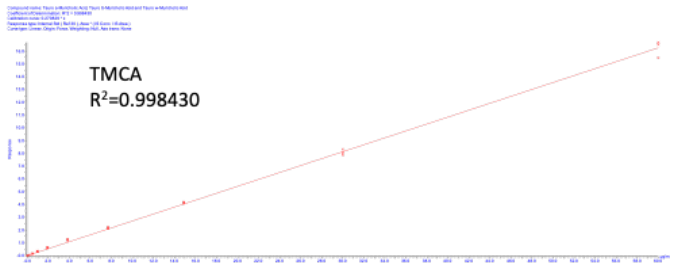
z.



aa.



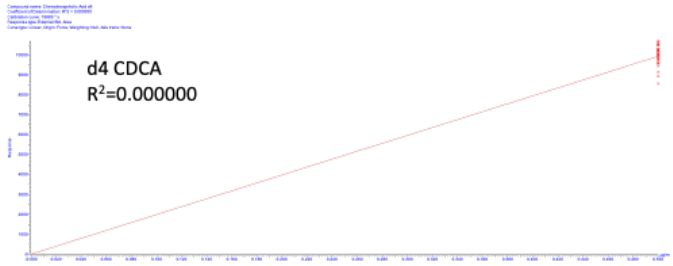
ab.



ac.



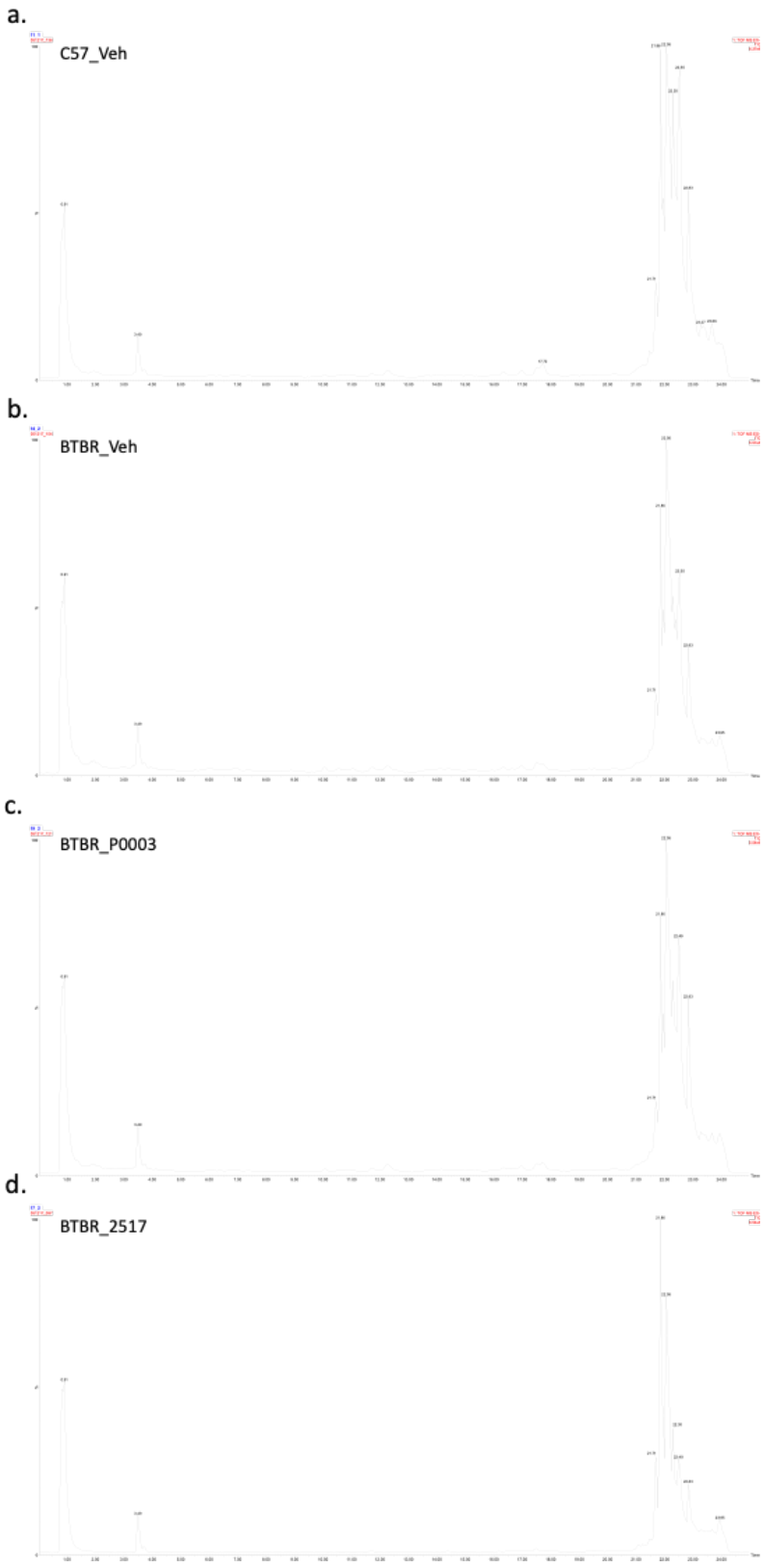
ad.



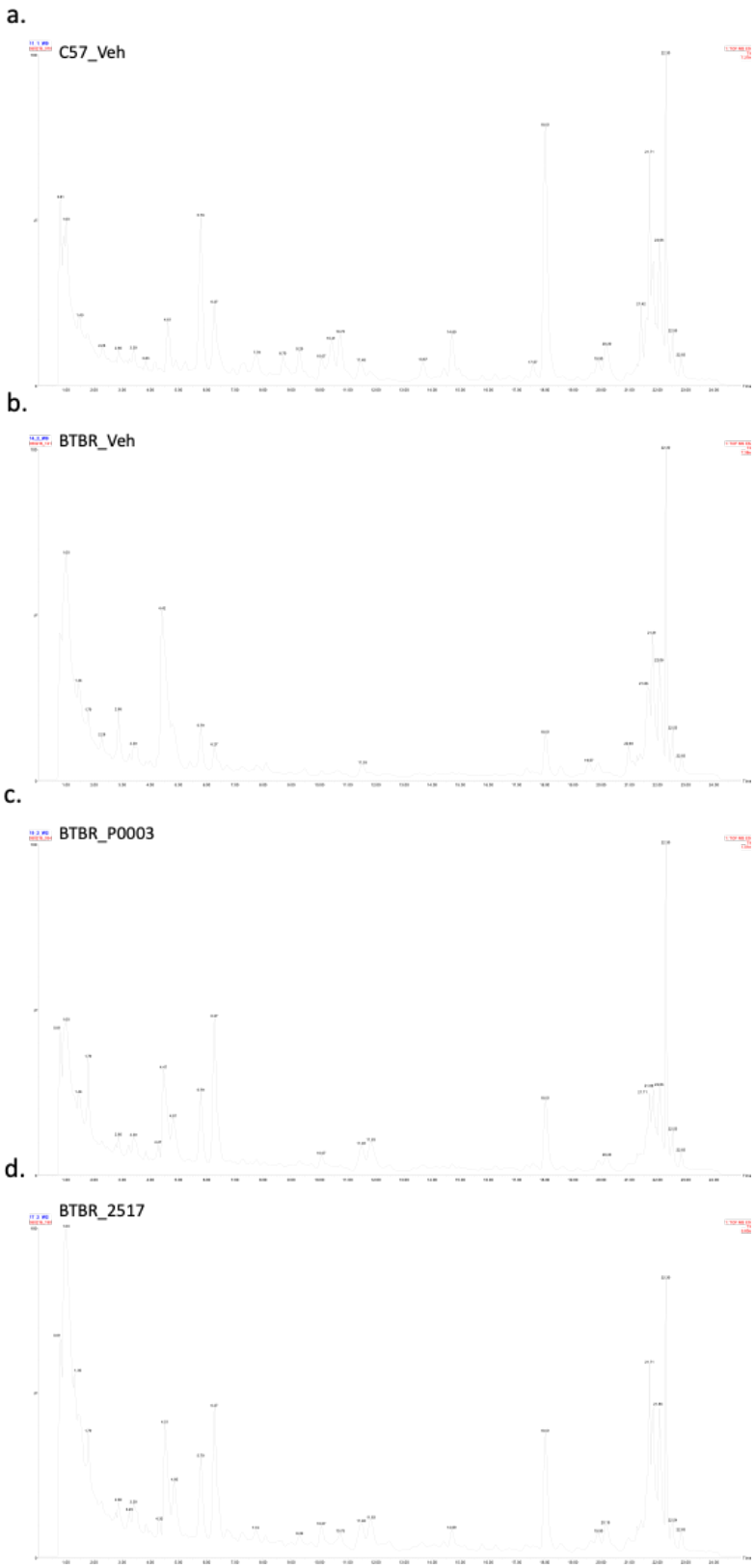
SI.3.3 continued: Standard curves of individual faecal bile acids obtained from UPLC-TMS analysis. X axis represents the concentration of each bile acid (µg/ml) and the Y axis represents the response.

SI.3.4: Table summary of targeted UPLC-TMS application for faecal BA metabolite quantitation (*n*=30) applied to murine BTBR model. The study is described in Chapter 3. BAs are listed with their negative ion mode Molecular weight (MW-), their retention time (RT), R^2 value (which indicates reliability of standard curve) and concentration range (µg/ml) of individual standards for detection.

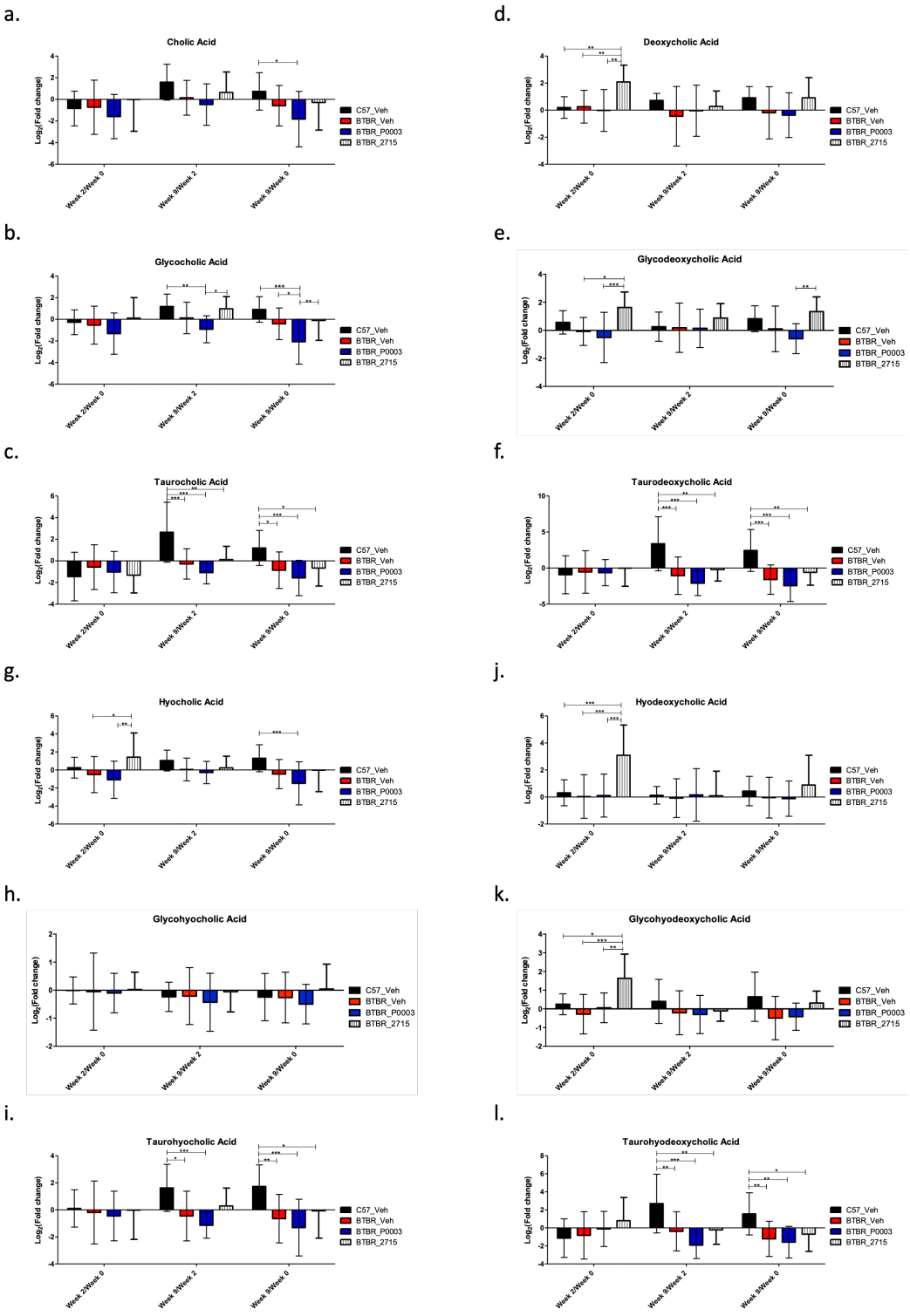
Number	Analyte	$[MW]^{-H}$	Neutral Formula	RT	Actual RT Top	Actual RT Middle	Actual RT End	R2 value	Range (µg/ml)
1	Taurine	124.0068	$C_2H_7NO_3S$	0.75	0.81	0.81	0.81	0.984185	0.0064-20.00
2	Dehydrocholic Acid	401.2328	$C_{24}H_{34}O_5$	2.00	0.96	0.96	1.06	0.999269	0.0064-20.00
3	Lithocholic Acid	375.2899	$C_{24}H_{40}O_3$	21.72	21.71	21.71	21.71	0.997192	0.0064-20.00
4	Ursodeoxycholic Acid	391.2848	$C_{24}H_{40}O_4$	9.87	8.51	8.51	8.51	0.991561	0.0064-20.00
5	Chenodeoxycholic Acid	391.2848	$C_{24}H_{40}O_4$	19.17	17.57	17.57	17.57	0.998745	0.0064-20.00
6	Hyodeoxycholic Acid	391.2848	$C_{24}H_{40}O_4$	12.54	10.27	10.27	10.27	0.998513	0.0064-20.00
7	Deoxycholic Acid	391.2848	$C_{24}H_{40}O_4$	20.20	18.01	18.01	18.01	0.996444	0.0064-20.00
8	Murocholic Acid	391.2848	$C_{24}H_{40}O_4$	8.25	6.90	6.90	6.90	0.999212	0.0064-20.00
9	Cholic Acid	407.2797	$C_{24}H_{40}O_5$	11.76	11.48	11.48	11.48	0.999512	0.0064-20.00
10	Hyocholic Acid	407.2797	$C_{24}H_{40}O_5$	10.39	8.27	8.22	8.22	0.998496	0.0064-20.00
11	7-Ketolithocholic Acid	389.2692	$C_{24}H_{38}O_4$	11.83	10.75	10.75	10.75	0.998434	0.0064-20.00
12	Taurocholic Acid	514.2838	$C_{26}H_{45}NO_7S$	4.82	4.32	4.32	4.32	0.999378	0.0064-20.00
13	Taurohyocholic Acid	514.2838	$C_{26}H_{45}NO_7S$	3.06	2.28	2.28	2.28	0.995960	0.0064-20.00
14	Taurochenodeoxycholic Acid	498.2889	$C_{26}H_{45}NO_6S$	9.03	7.68	7.68	7.68	0.998258	0.0064-20.00
15	Tauroursodeoxycholic Acid	498.2889	$C_{26}H_{45}NO_6S$	3.16	2.76	2.76	2.76	0.998591	0.0064-20.00
16	Taurodeoxycholic Acid	498.2889	$C_{26}H_{45}NO_6S$	10.39	8.60	8.60	8.60	0.998053	0.0064-20.00
17	Taurohyodeoxycholic Acid	498.2889	$C_{26}H_{45}NO_6S$	3.76	3.49	3.49	3.49	0.996494	0.0064-20.00
18	Taurolithocholic Acid	482.2940	$C_{26}H_{45}NO_5S$	15.19	13.62	13.67	13.62	0.998846	0.0064-20.00
19	Glycocholic Acid	464.3012	$C_{26}H_{43}NO_6$	7.44	5.79	5.79	5.74	0.977219	0.0064-20.00
20	Glycohyocholic Acid	464.3012	$C_{26}H_{43}NO_6$	4.67	3.64	3.44	3.16	0.997612	0.0064-20.00
21	Glycoursodeoxycholic Acid	448.3063	$C_{26}H_{43}NO_5$	4.57	3.74	3.74	3.69	0.997853	0.0064-20.00
22	Glycochenodeoxycholic Acid	448.3063	$C_{26}H_{43}NO_5$	12.64	9.09	8.90	8.65	0.996093	0.0064-20.00
23	Glycohyodeoxycholic Acid	448.3063	$C_{26}H_{43}NO_5$	5.67	3.93	3.93	4.18	0.992984	0.0064-20.00
24	Glycodeoxycholic Acid	448.3063	$C_{26}H_{43}NO_5$	14.05	10.90	10.95	10.85	0.997471	0.0064-20.00
25	Glycolithocholic Acid	432.3114	$C_{26}H_{43}NO_4$	18.19	14.90	14.84	14.84	0.998030	0.0064-20.00
26	α-Muricholic Acid	407.2797	$C_{24}H_{40}O_5$	7.18	5.79	5.79	5.79	0.993104	0.0064-20.00
27	β-Muricholic Acid	407.2797	$C_{24}H_{40}O_5$	7.59	6.27	6.27	6.27	0.998970	0.0064-20.00
28	ω-Muricholic Acid	407.2797	$C_{24}H_{40}O_5$	7.08	5.79	5.79	5.79	0.993104	0.0064-20.00
29	Tauro α-Muricholic Acid	514.2838	$C_{26}H_{45}NO_7S$	2.00	1.79	1.79	1.79	0.998430	0.0064-20.00
30	Tauro β-Muricholic Acid	514.2838	$C_{26}H_{45}NO_7S$	2.16	1.79	1.79	1.79	0.998430	0.0064-20.00
31	Tauro ω-Muricholic Acid	514.2838	$C_{26}H_{45}NO_7S$	2.37	1.79	1.79	1.79	0.998430	0.0064-20.00
D1	Cholic Acid d4	411.3049	$C_{24}H_{36}D_4O_5$	11.74	11.48	11.44	11.44	0.000000	
D2	Chenodeoxycholic Acid d4	395.3099	$C_{24}H_{36}D_4O_4$	19.00	17.32	17.32	17.32	0.000000	



SI.3.5: Representative Chromatograms displaying the full mass spectra of plasma bile acids for controls: a) C57_Veh, b) BTBR_Veh and each treatment group: c) BTBR_P0003, d) BTBR_2715.

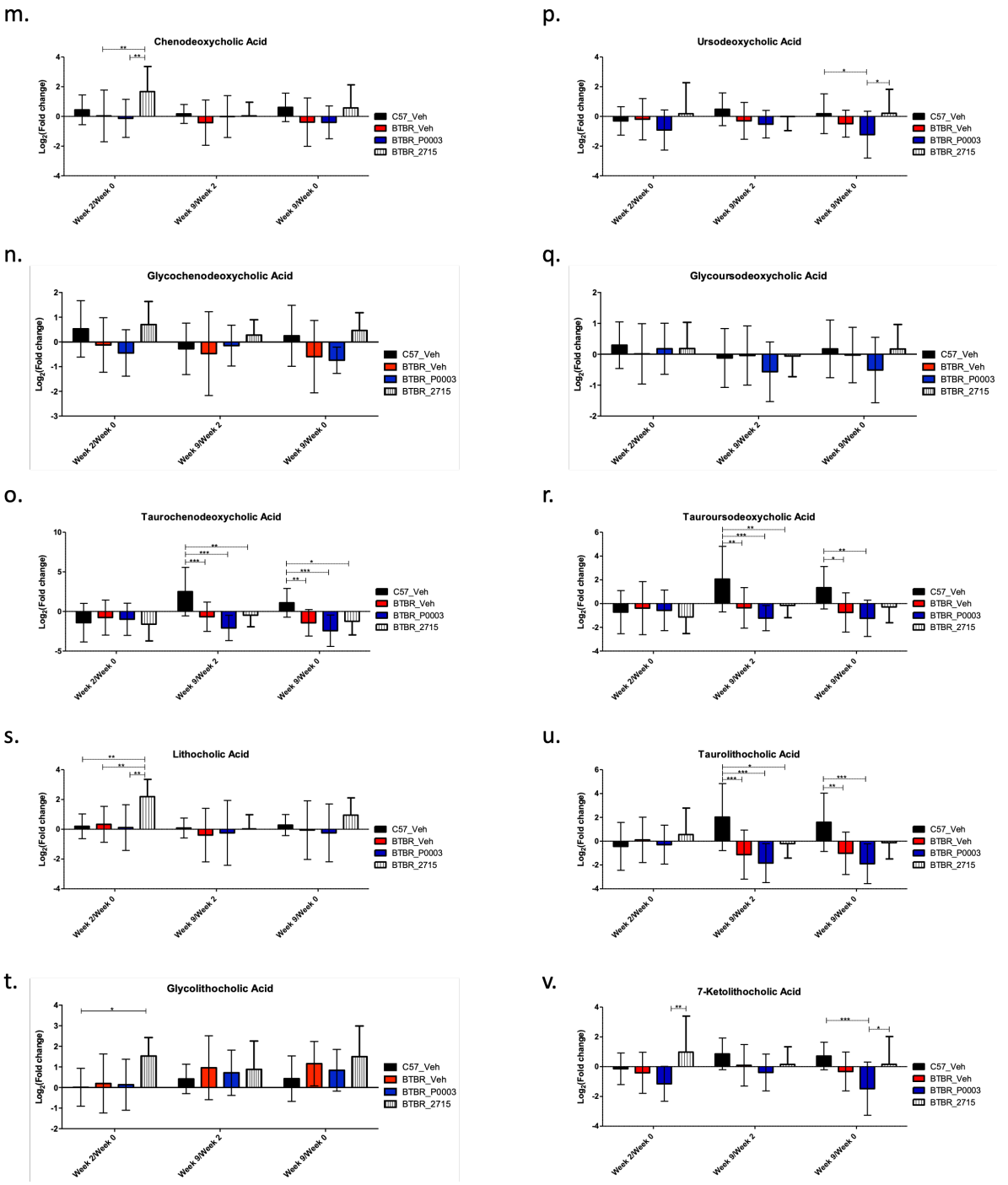


SI.3.6: Representative Chromatograms displaying the full mass spectra of faecal bile acids, for controls: a) C57_Veh, b) BTBR_Veh and each treatment group: c) BTBR_P0003, d) BTBR_2715.



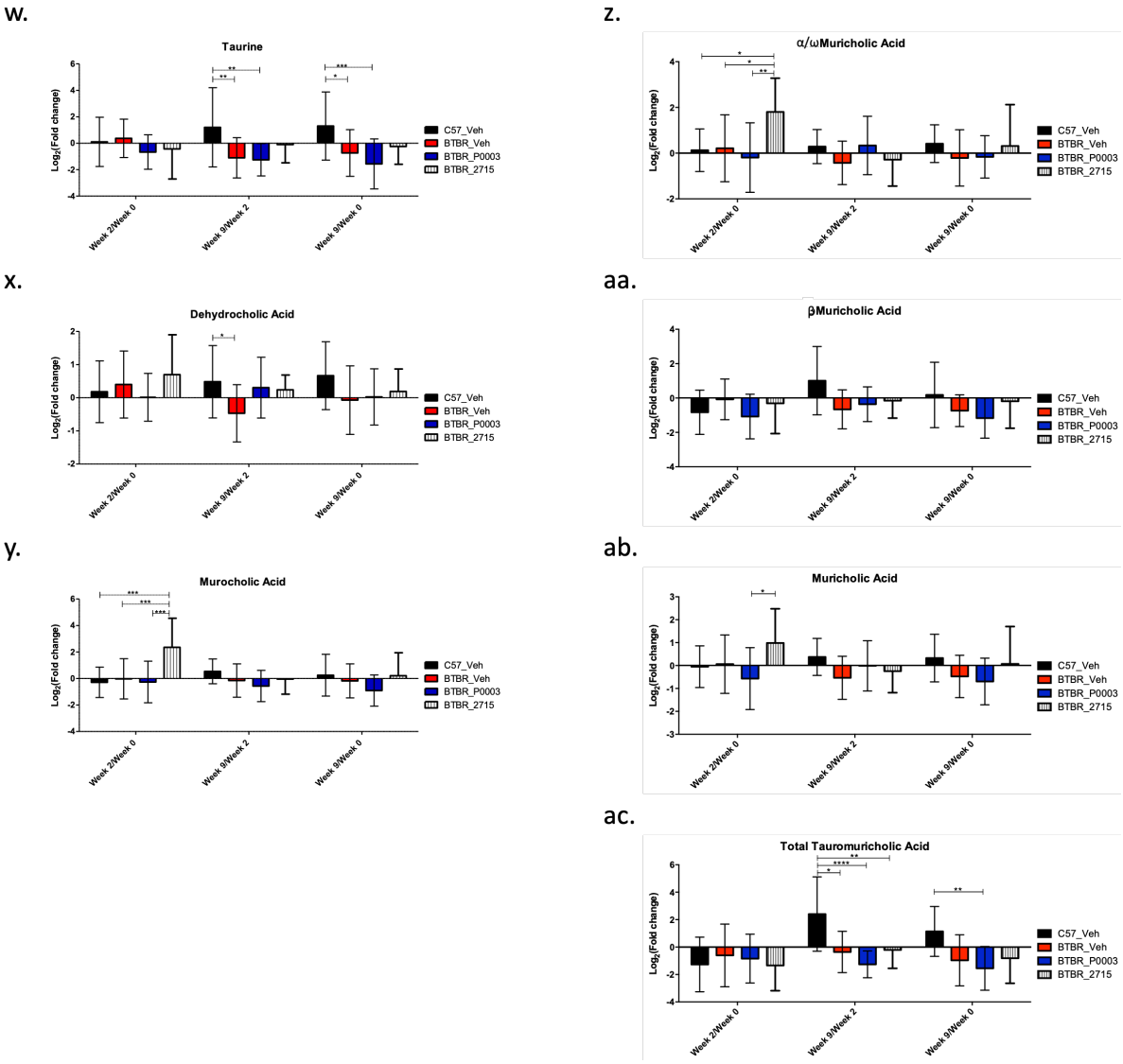
SI.3.7: Log_2 fold change of individual faecal bile acids: (a) primary bile acid CA, (b) secondary bile acid DCA, (g) hyocholic acid and (j) hyodeoxycholic acid, and their corresponding glyco (b, e, h and k) and tauro conjugated moieties (c, f, i and l), across weeks 0, 2 and 9, for controls: C57_Veh, BTBR_Veh and each treatment group: BTBR_P0003, BTBR_2715.

Statistical significance is indicated and calculated using Bonferroni's Multiple Comparison Test (*= p<0.05; **=p<0.01; ***=p<0.001; ****=p<0.0001).

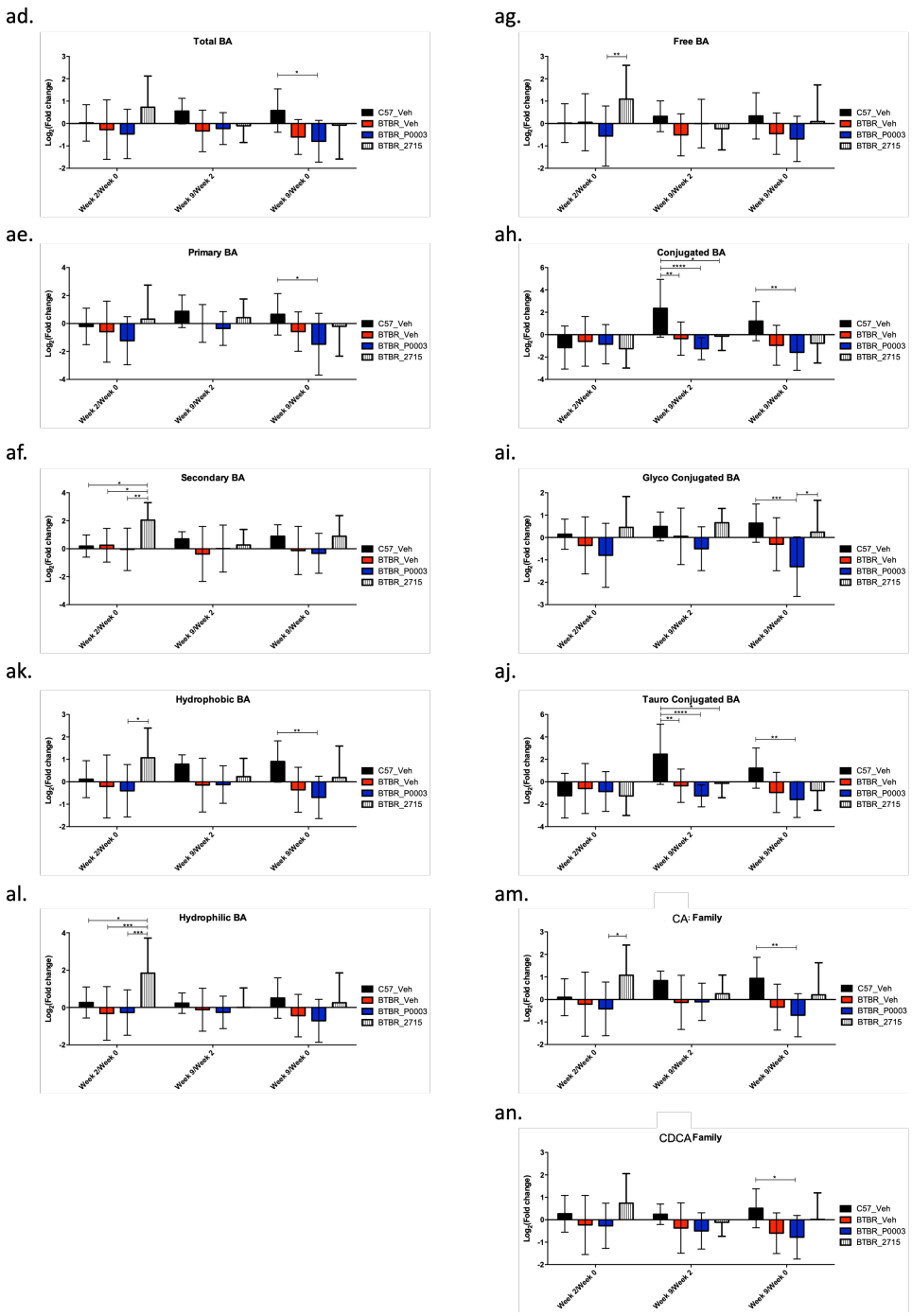


SI.3.7 continued: Log_2 fold change of individual faecal bile acids: (m) primary bile acid CDCA, (p and s) secondary bile acids UDCA and LCA, and their corresponding glyco (n, q and t) and tauro conjugated moieties (o, r and u), and (v) 7-ketolithocholic acid, across weeks 0, 2 and 9 for controls: C57_Veh, BTBR_Veh and each treatment group: BTBR_P0003, BTBR_2715.

Statistical significance is indicated and calculated using Bonferroni's Multiple Comparison Test (*= p<0.05; **=p<0.01; ***=p<0.001; ****=p<0.0001).



SI.3.7 continued: Log_2 fold change of individual faecal bile acids: (w) taurine, (x) dehydrocholic acid, (y) murocholic acid and (z-ac) muricholic bile acids, across weeks 0, 2 and 9 for controls: C57_Veh, BTBR_Veh and each treatment group: BTBR_P0003, BTBR_2715. Statistical significance is indicated and calculated using Bonferroni's Multiple Comparison Test (*= p<0.05; **=p<0.01; ***=p<0.001; ****=p<0.0001).



SI.3.7 continued: Log_2 fold change of individual faecal bile acids: (ad) Total bile acids, (ae) Primary bile acids, (af) Secondary bile acids, (ag) Free bile acids, (ah) Total conjugated bile acids, (ai) Glyco-conjugated bile acids, (aj) Tauro-conjugated bile acids (ak) Hydrophobic bile acids, (al) Hydrophilic bile acids, (am) Cholic Acid class of bile acids and (an) Chenodeoxycholic Acid class of bile acids, across weeks 0, 2 and 9 for controls: C57_Veh, BTBR_Veh and each treatment group: BTBR_P0003, BTBR_2715. Statistical significance is indicated and calculated using Bonferroni's Multiple Comparison Test (*= p<0.05; **=p<0.01; ***=p<0.001; ****=p<0.0001).

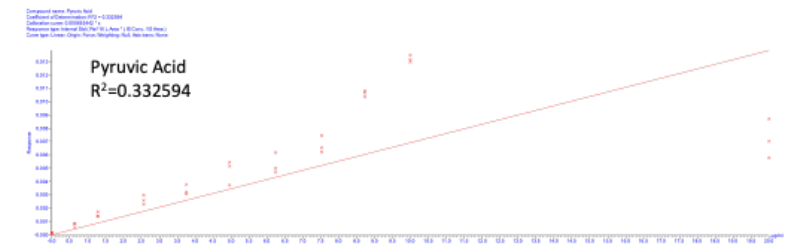
SI.3.8: Table summary of targeted UPLC-TMS application for BA circulating metabolite quantitation (*n*=30) applied to Parkinson's Disease patients and healthy individuals. The study is described in Chapter 3. BAs are listed with their negative ion mode Molecular weight (MW-), their retention time (RT), R^2 value (which indicates reliability of standard curve) and concentration range (µg/ml) of individual standards for detection.

Number	Analyte	$[MW]^{-H}$	Neutral Formula	RT	Actual RT Top	Actual RT Middle	Actual RT End	R2 value	Range (µg/ml)
1	Taurine	124.0068	$C_2H_7NO_3S$	0.75	0.81	0.81	0.81	0.923432	0.0064-20.00
2	Dehydrocholic Acid	401.2328	$C_{24}H_{34}O_5$	2.00	2.13	2.13	2.13	0.988876	0.0064-20.00
3	Lithocholic Acid	375.2899	$C_{24}H_{40}O_3$	21.72	22.00	22.00	22.00	0.974655	0.0064-20.00
4	Ursodeoxycholic Acid	391.2848	$C_{24}H_{40}O_4$	9.87	10.16	10.12	10.12	0.978293	0.0064-20.00
5	Chenodeoxycholic Acid	391.2848	$C_{24}H_{40}O_4$	19.17	19.62	19.57	19.57	0.980594	0.0064-20.00
6	Hyodeoxycholic Acid	391.2848	$C_{24}H_{40}O_4$	12.54	12.85	12.85	12.85	0.991064	0.0064-20.00
7	Deoxycholic Acid	391.2848	$C_{24}H_{40}O_4$	20.20	20.55	20.44	20.44	0.988372	0.0064-20.00
8	Murocholic Acid	391.2848	$C_{24}H_{40}O_4$	8.25	8.12	8.07	8.07	0.989616	0.0064-20.00
9	Cholic Acid	407.2797	$C_{24}H_{40}O_5$	11.76	13.97	13.97	13.97	0.982910	0.0064-20.00
10	Hyocholic Acid	407.2797	$C_{24}H_{40}O_5$	10.39	10.65	10.60	10.60	0.978977	0.0064-20.00
11	7-Ketolithocholic Acid	389.2692	$C_{24}H_{38}O_4$	11.83	11.88	11.88	11.88	0.990330	0.0064-20.00
12	Taurocholic Acid	514.2838	$C_{26}H_{45}NO_7S$	4.82	5.39	5.35	5.35	0.977604	0.0064-20.00
13	Taurohyocholic Acid	514.2838	$C_{26}H_{45}NO_7S$	3.06	3.16	3.16	3.16	0.990026	0.0064-20.00
14	Taurochenodeoxycholic Acid	498.2889	$C_{26}H_{45}NO_6S$	9.03	9.14	9.09	9.09	0.990822	0.0064-20.00
15	Tauroursodeoxycholic Acid	498.2889	$C_{26}H_{45}NO_6S$	3.16	3.25	3.20	3.20	0.963736	0.0064-20.00
16	Taurodeoxycholic Acid	498.2889	$C_{26}H_{45}NO_6S$	10.39	10.32	10.32	10.32	0.990657	0.0064-20.00
17	Taurohyodeoxycholic Acid	498.2889	$C_{26}H_{45}NO_6S$	3.76	3.79	3.79	3.79	0.989911	0.0064-20.00
18	Taurolithocholic Acid	482.2940	$C_{26}H_{45}NO_5S$	15.19	15.18	15.13	15.13	0.988410	0.0064-20.00
19	Glycocholic Acid	464.3012	$C_{26}H_{43}NO_6$	7.44	6.71	6.65	6.65	0.999456	0.0064-20.00
20	Glycohyocholic Acid	464.3012	$C_{26}H_{43}NO_6$	4.67	3.98	3.98	3.98	0.998975	0.0064-20.00
21	Glycoursodeoxycholic Acid	448.3063	$C_{26}H_{43}NO_5$	4.57	4.03	3.98	3.98	0.993045	0.0064-20.00
22	Glycochenodeoxycholic Acid	448.3063	$C_{26}H_{43}NO_5$	12.64	11.14	11.09	11.09	0.999521	0.0064-20.00
23	Glycohyodeoxycholic Acid	448.3063	$C_{26}H_{43}NO_5$	5.67	4.86	4.81	4.86	0.999416	0.0064-20.00
24	Glycodeoxycholic Acid	448.3063	$C_{26}H_{43}NO_5$	14.05	12.79	12.74	12.74	0.999678	0.0064-20.00
25	Glycolithocholic Acid	432.3114	$C_{26}H_{43}NO_4$	18.19	17.13	17.09	17.09	0.999751	0.0064-20.00
26	α-Muricholic Acid	407.2797	$C_{24}H_{40}O_5$	7.18	7.05	7.00	7.00	0.984351	0.0064-20.00
27	β-Muricholic Acid	407.2797	$C_{24}H_{40}O_5$	7.59	7.44	7.44	7.44	0.985821	0.0064-20.00
28	ω-Muricholic Acid	407.2797	$C_{24}H_{40}O_5$	7.08	7.05	7.00	7.00	0.984351	0.0064-20.00
29	Tauro α-Muricholic Acid	514.2838	$C_{26}H_{45}NO_7S$	2.00	2.03	2.03	2.03	0.987022	0.0064-20.00
30	Tauro β-Muricholic Acid	514.2838	$C_{26}H_{45}NO_7S$	2.16	2.03	2.03	2.03	0.987022	0.0064-20.00
31	Tauro ω-Muricholic Acid	514.2838	$C_{26}H_{45}NO_7S$	2.37	2.03	2.03	2.03	0.987022	0.0064-20.00
D1	Cholic Acid d4	411.3049	$C_{24}H_{36}D_4O_5$	11.74	13.97	13.97	13.97	0.000000	
D2	Chenodeoxycholic Acid d4	395.3099	$C_{24}H_{36}D_4O_4$	19.00	19.62	19.57	19.52	0.000000	

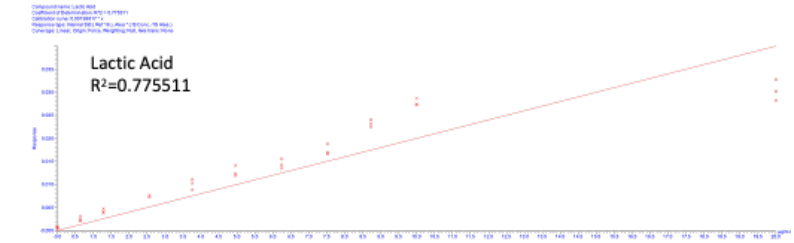
SI.3.9: Table summary of targeted UPLC-TMS application for faecal BA metabolite quantitation (*n*=30) applied to Parkinson's Disease patients and healthy individuals. The study is described in Chapter 3. BAs are listed with their negative ion mode Molecular weight (MW-), their retention time (RT), R^2 value (which indicates reliability of standard curve) and concentration range (µg/ml) of individual standards for detection.

Number	Analyte	$[MW]^{-H}$	Neutral Formula	RT	Actual RT Top	Actual RT Middle	Actual RT End	R2 value	Range (µg/ml)
1	Taurine	124.0068	$C_2H_7NO_3S$	0.75	0.81	0.81	0.81	0.972775	0.0064-20.00
2	Dehydrocholic Acid	401.2328	$C_{24}H_{34}O_5$	2.00	1.88	1.88	1.88	0.996518	0.0064-20.00
3	Lithocholic Acid	375.2899	$C_{24}H_{40}O_3$	21.72	21.71	21.71	21.71	0.994159	0.0064-20.00
4	Ursodeoxycholic Acid	391.2848	$C_{24}H_{40}O_4$	9.87	8.51	8.51	8.51	0.978781	0.0064-20.00
5	Chenodeoxycholic Acid	391.2848	$C_{24}H_{40}O_4$	19.17	17.32	17.32	17.32	0.998445	0.0064-20.00
6	Hyodeoxycholic Acid	391.2848	$C_{24}H_{40}O_4$	12.54	10.41	10.41	10.41	0.999259	0.0064-20.00
7	Deoxycholic Acid	391.2848	$C_{24}H_{40}O_4$	20.20	18.01	18.01	18.01	0.998806	0.0064-20.00
8	Murocholic Acid	391.2848	$C_{24}H_{40}O_4$	8.25	6.90	6.90	6.90	0.996933	0.0064-20.00
9	Cholic Acid	407.2797	$C_{24}H_{40}O_5$	11.76	11.48	11.48	11.48	0.998840	0.0064-20.00
10	Hyocholic Acid	407.2797	$C_{24}H_{40}O_5$	10.39	8.81	8.81	8.81	0.994796	0.0064-20.00
11	7-Ketolithocholic Acid	389.2692	$C_{24}H_{38}O_4$	11.83	9.78	9.78	9.78	0.998595	0.0064-20.00
12	Taurocholic Acid	514.2838	$C_{26}H_{45}NO_7S$	4.82	4.37	4.37	4.37	0.998579	0.0064-20.00
13	Taurohyocholic Acid	514.2838	$C_{26}H_{45}NO_7S$	3.06	2.67	2.67	2.67	0.988100	0.0064-20.00
14	Taurochenodeoxycholic Acid	498.2889	$C_{26}H_{45}NO_6S$	9.03	7.74	7.74	7.74	0.998869	0.0064-20.00
15	Tauroursodeoxycholic Acid	498.2889	$C_{26}H_{45}NO_6S$	3.16	2.76	2.76	2.76	0.997182	0.0064-20.00
16	Taurodeoxycholic Acid	498.2889	$C_{26}H_{45}NO_6S$	10.39	8.60	8.65	8.65	0.996258	0.0064-20.00
17	Taurohyodeoxycholic Acid	498.2889	$C_{26}H_{45}NO_6S$	3.76	3.16	3.16	3.16	0.996838	0.0064-20.00
18	Taurolithocholic Acid	482.2940	$C_{26}H_{45}NO_5S$	15.19	13.67	13.67	13.67	0.998531	0.0064-20.00
19	Glycocholic Acid	464.3012	$C_{26}H_{43}NO_6$	7.44	5.63	5.63	5.63	0.971917	0.0064-20.00
20	Glycohyocholic Acid	464.3012	$C_{26}H_{43}NO_6$	4.67	3.39	3.39	3.39	0.990290	0.0064-20.00
21	Glycoursodeoxycholic Acid	448.3063	$C_{26}H_{43}NO_5$	4.57	3.44	3.44	3.44	0.979925	0.0064-20.00
22	Glycochenodeoxycholic Acid	448.3063	$C_{26}H_{43}NO_5$	12.64	9.34	9.34	9.39	0.988811	0.0064-20.00
23	Glycohyodeoxycholic Acid	448.3063	$C_{26}H_{43}NO_5$	5.67	4.07	4.07	4.07	0.989284	0.0064-20.00
24	Glycodeoxycholic Acid	448.3063	$C_{26}H_{43}NO_5$	14.05	10.65	10.65	10.65	0.987063	0.0064-20.00
25	Glycolithocholic Acid	432.3114	$C_{26}H_{43}NO_4$	18.19	15.38	15.38	15.38	0.991825	0.0064-20.00
26	α-Muricholic Acid	407.2797	$C_{24}H_{40}O_5$	7.18	5.79	5.79	5.79	0.999296	0.0064-20.00
27	β-Muricholic Acid	407.2797	$C_{24}H_{40}O_5$	7.59	6.27	6.27	6.27	0.998682	0.0064-20.00
28	ω-Muricholic Acid	407.2797	$C_{24}H_{40}O_5$	7.08	5.79	5.79	5.79	0.999296	0.0064-20.00
29	Tauro α-Muricholic Acid	514.2838	$C_{26}H_{45}NO_7S$	2.00	1.79	1.79	1.79	0.997946	0.0064-20.00
30	Tauro β-Muricholic Acid	514.2838	$C_{26}H_{45}NO_7S$	2.16	1.79	1.79	1.79	0.997946	0.0064-20.00
31	Tauro ω-Muricholic Acid	514.2838	$C_{26}H_{45}NO_7S$	2.37	1.79	1.79	1.79	0.997946	0.0064-20.00
D1	Cholic Acid d4	411.3049	$C_{24}H_{36}D_4O_5$	11.74	11.44	11.48	11.48	0.000000	
D2	Chenodeoxycholic Acid d4	395.3099	$C_{24}H_{36}D_4O_4$	19.00	17.32	17.32	17.32	0.000000	

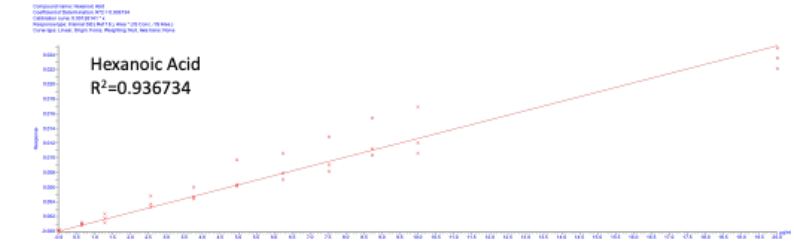
a.



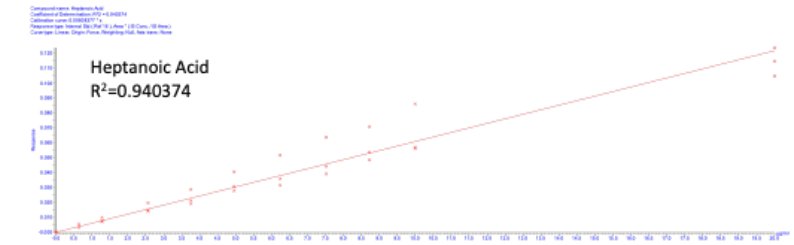
b.



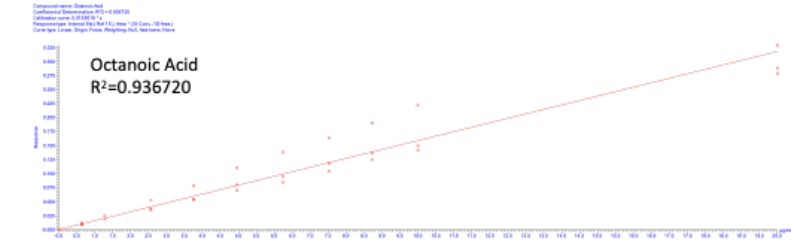
c.



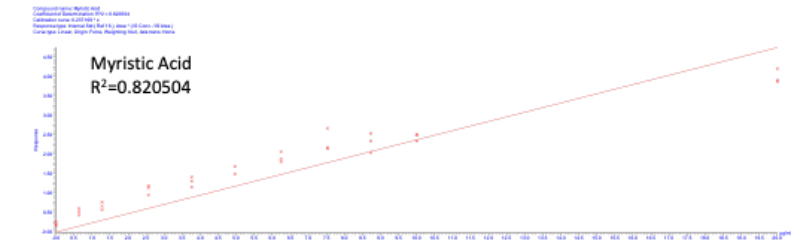
d.



e.

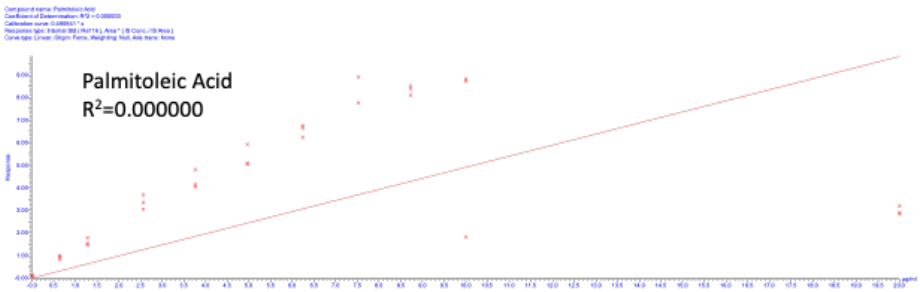


f.

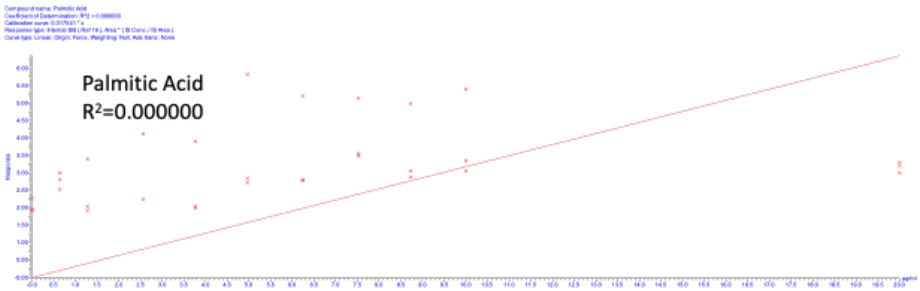


SI.3.10: Standard curves of individual plasma fatty acids obtained from UPLC-TMS analysis for PD study. X axis represents the concentration of each fatty acid (µg/ml) and the Y axis represents the response.

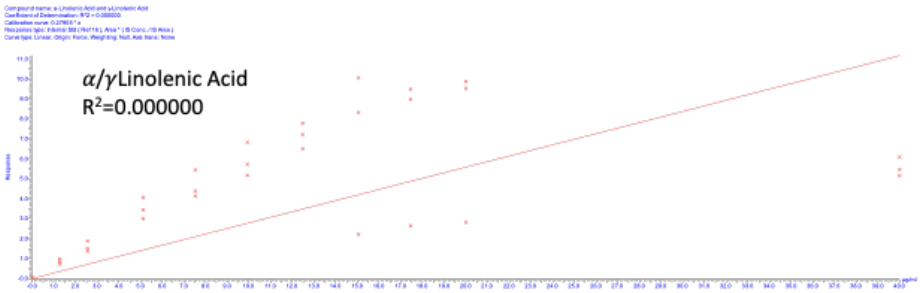
g.



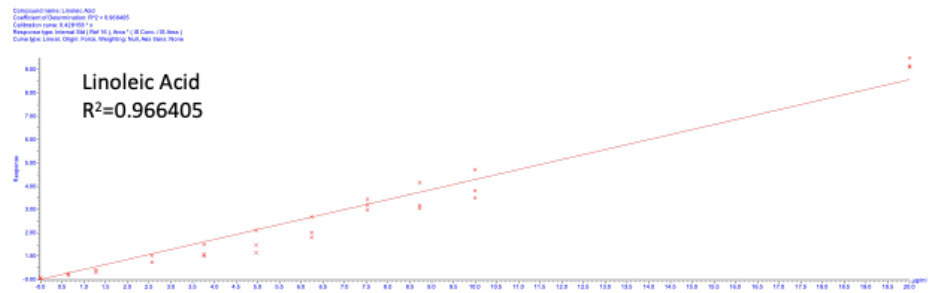
h.



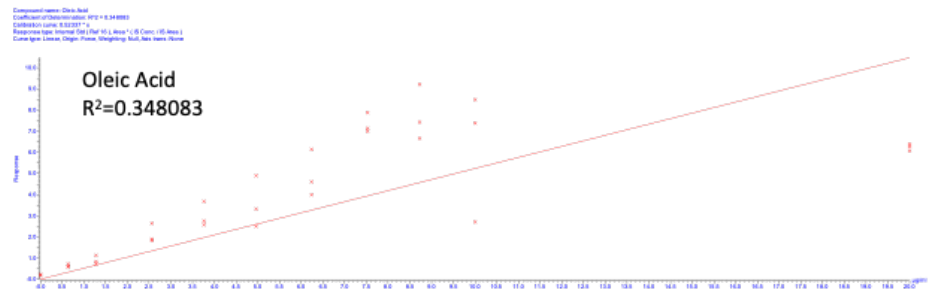
i.



j.

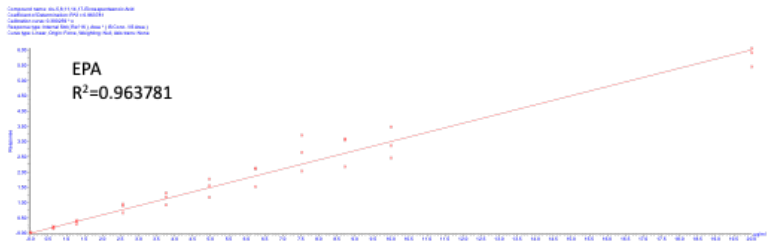


k.

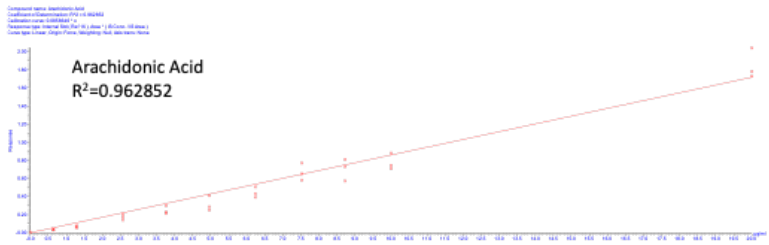


SI.3.10 continued: Standard curves of individual plasma fatty acids obtained from UPLC-TMS analysis for PD study. X axis represents the concentration of each fatty acid (µg/ml) and the Y axis represents the response.

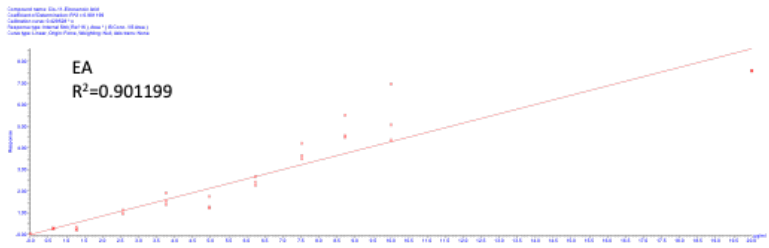
m.



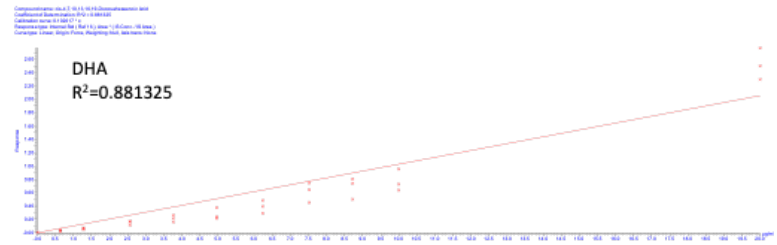
n.



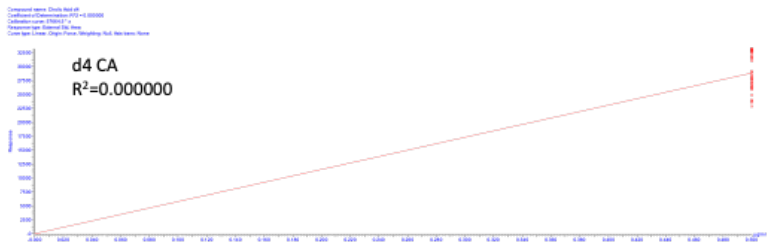
o.



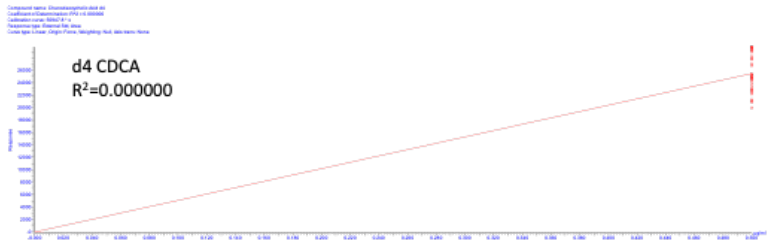
p.



q.



r.



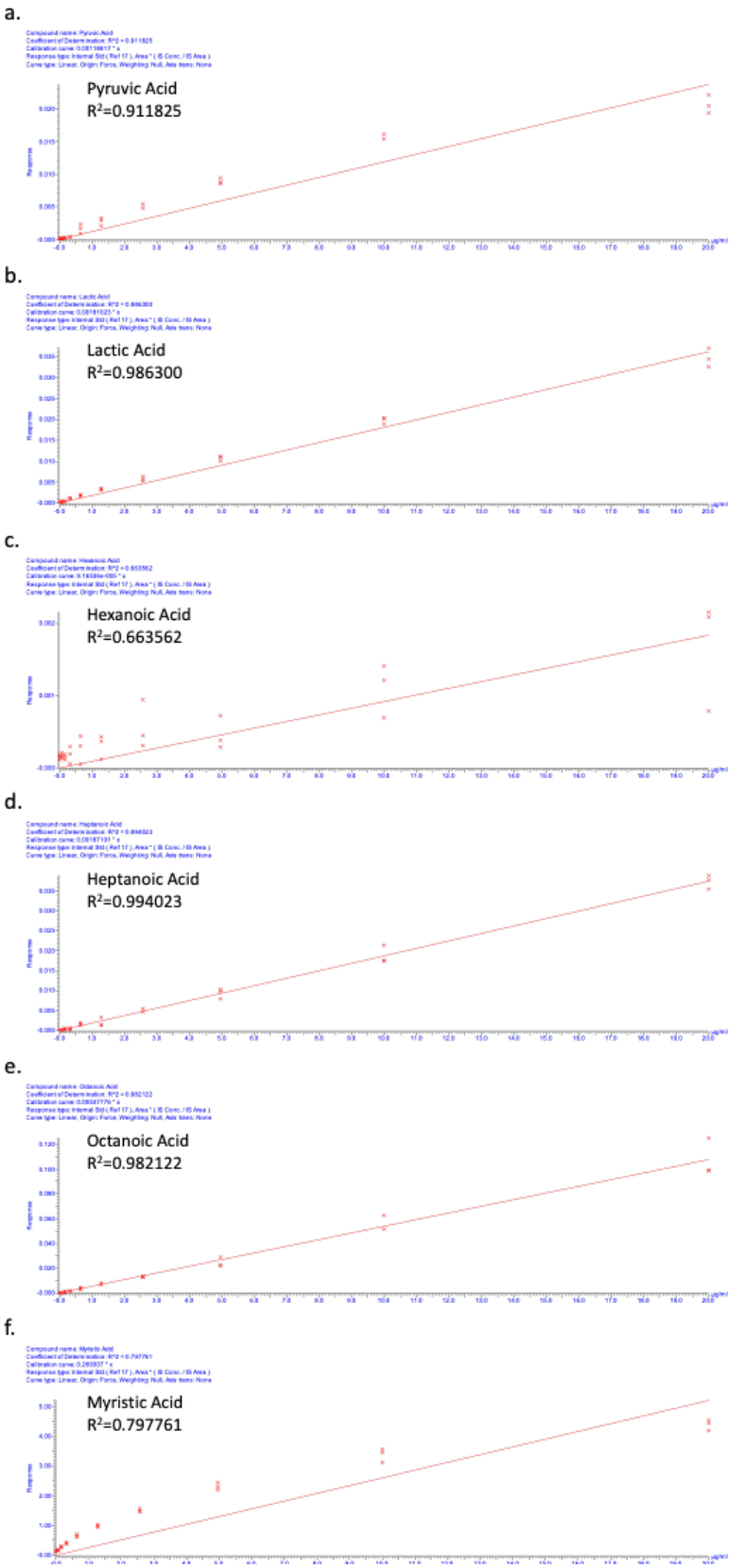
SI.3.10 continued: Standard curves of individual plasma fatty acids obtained from UPLC-TMS analysis for PD study. X axis represents the concentration of each fatty acid (µg/ml) and the Y axis represents the response.

SI.3.11: Table summary of targeted UPLC-TMS application for FA circulating metabolite quantitation (*n*=16) applied to Parkinson's Disease patients and healthy individuals. The study is described in Chapter 3. FAs are listed with their negative ion mode Molecular weight (MW-), their retention time (RT), R^2 value (which indicates reliability of standard curve) and concentration range (µg/ml) of individual standards for detection.

	Analyte	$[MW]^{-H}$	Neutral Formula	RT	Actual RT Top	Actual RT Middle	Actual RT End	R2 value	Range (µg/ml)
	Pyruvic acid	87.0082	$C_3H_4O_3$	0.81	0.81	0.81	0.81	0.332594	0.0064-20.00
	Lactic acid	89.0239	$C_3H_6O_3$	0.80	0.86	0.86	0.86	0.775511	0.0064-20.00
Medium-Chain Fatty Acid	Hexanoic Acid	115.0759	$C_6H_{12}O_2$	1.93	1.98	1.98	1.98	0.936734	0.0064-20.00
	Heptanoic Acid	129.0916	$C_7H_{14}O_2$	2.95	3.05	3.00	3.05	0.940374	0.0064-20.00
	Octanoic Acid	143.1072	$C_8H_{16}O_2$	5.05	5.05	5.05	5.05	0.936720	0.0064-20.00
Long-Chain Fatty Acid	Myristic Acid	227.2011	$C_{14}H_{28}O_2$	22.20	22.25	22.25	22.25	0.820504	0.0064-20.00
	Palmitoleic Acid	253.2168	$C_{16}H_{30}O_2$	22.25	22.34	22.34	22.34	0.000000	0.0064-20.00
	Palmitic Acid	255.2324	$C_{16}H_{32}O_2$	22.55	22.69	22.69	22.69	0.000000	0.0064-20.00
	y-Linolelic Acid	277.2168	$C_{18}H_{30}O_2$	22.20	22.30	22.25	22.25	0.000000	0.0064-20.00
	α-Linolenic acid	277.2168	$C_{18}H_{30}O_2$	22.15	21.42	21.42	21.42	0.000000	0.0064-20.00
	Linoleic Acid	279.2324	$C_{18}H_{32}O_2$	22.34	22.49	22.49	22.44	0.966405	0.0064-20.00
	Oleic Acid	281.2481	$C_{18}H_{34}O_2$	22.59	22.74	22.74	22.74	0.348083	0.0064-20.00
	cis-5,8,11,14,17-Eicosapentaenoic acid	301.2168	$C_{20}H_{30}O_2$	22.15	22.20	22.20	22.20	0.963781	0.0064-20.00
	Arachidonic Acid	303.2324	$C_{20}H_{32}O_2$	22.30	22.39	22.39	22.39	0.962852	0.0064-20.00
	Cis-11-Eicosenoic acid	309.2794	$C_{20}H_{38}O_2$	22.97	23.18	23.18	23.18	0.901199	0.0064-20.00
	Cis-4,7,10,13,16,19-Docosahexaenoic acid	327.2324	$C_{22}H_{32}O_2$	22.25	22.34	22.34	22.34	0.881235	0.0064-20.00
IS	Cholic Acid d4	411.3049	$C_{24}H_{36}D_4O_5$	14.02	13.97	13.97	13.97	0.000000	
	Chenodeoxycholic Acid d4	395.3099	$C_{24}H_{36}D_4O_4$	19.57	19.62	19.57	19.52	0.000000	

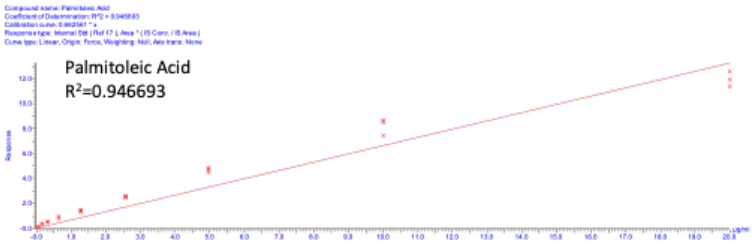
SI.3.12: Table summary of targeted UPLC-TMS application for faecal FA metabolite quantitation (*n*=16) applied to Parkinson's Disease patients and healthy individuals. The study is described in Chapter 3. FAs are listed with their negative ion mode Molecular weight (MW-), their retention time (RT), R^2 value (which indicates reliability of standard curve) and concentration range (µg/ml) of individual standards for detection.

	Analyte	$[MW]^{-H}$	Neutral Formula	RT	Actual RT Top	Actual RT Middle	Actual RT End	R2 value	Range (µg/ml)
	Pyruvic acid	87.0082	$C_3H_4O_3$	0.81	0.81	0.81	0.81	0.911825	0.0064-20.00
	Lactic acid	89.0239	$C_3H_6O_3$	0.80	0.86	0.86	0.86	0.986300	0.0064-20.00
Medium-Chain Fatty Acid	Hexanoic Acid	115.0759	$C_6H_{12}O_2$	1.93	0.81	0.91	0.91	0.663562	0.0064-20.00
	Heptanoic Acid	129.0916	$C_7H_{14}O_2$	2.95	2.76	2.76	2.76	0.994023	0.0064-20.00
	Octanoic Acid	143.1072	$C_8H_{16}O_2$	5.05	4.42	4.42	4.42	0.982122	0.0064-20.00
Long-Chain Fatty Acid	Myristic Acid	227.2011	$C_{14}H_{28}O_2$	22.20	22.06	22.06	22.06	0.797761	0.0064-20.00
	Palmitoleic Acid	253.2168	$C_{16}H_{30}O_2$	22.25	22.20	22.15	22.15	0.946693	0.0064-20.00
	Palmitic Acid	255.2324	$C_{16}H_{32}O_2$	22.55	22.49	22.49	22.49	0.971132	0.0064-20.00
	y-Linolelic Acid	277.2168	$C_{18}H_{30}O_2$	22.20	22.10	22.10	22.11	0.963201	0.0064-20.00
	α-Linolenic acid	277.2168	$C_{18}H_{30}O_2$	22.15	22.10	22.10	22.11	0.963201	0.0064-20.00
	Linoleic Acid	279.2324	$C_{18}H_{32}O_2$	22.34	22.30	22.30	22.30	0.989844	0.0064-20.00
	Oleic Acid	281.2481	$C_{18}H_{34}O_2$	22.59	22.55	22.55	22.55	0.990036	0.0064-20.00
	Stearic Acid	283.2637	$C_{18}H_{36}O_2$	22.97	22.83	22.83	22.83	0.737882	0.0064-20.00
	cis-5,8,11,14,17-Eicosapentaenoic acid	301.2168	$C_{20}H_{30}O_2$	22.15	22.06	22.06	22.06	0.988885	0.0064-20.00
	Arachidonic Acid	303.2324	$C_{20}H_{32}O_2$	22.30	22.25	22.25	22.25	0.991674	0.0064-20.00
	Cis-11-Eicosenoic acid	309.2794	$C_{20}H_{38}O_2$	22.97	22.88	22.88	22.88	0.976318	0.0064-20.00
	Cis-4,7,10,13,16,19-Docosahexaenoic acid	327.2324	$C_{22}H_{32}O_2$	22.25	22.25	22.20	22.20	0.988207	0.0064-20.00
IS	Cholic Acid d4	411.3049	$C_{24}H_{36}D_4O_5$	14.02	11.48	11.48	11.48	0.000000	-
	Chenodeoxycholic Acid d4	395.3099	$C_{24}H_{36}D_4O_4$	19.57	17.32	17.32	17.32	0.000000	-

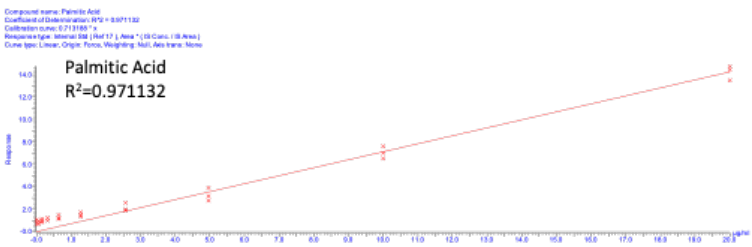


SI.3.13: Standard curves of individual faecal fatty acids obtained from UPLC-TMS analysis for PD study. X axis represents the concentration of each fatty acid (µg/ml) and the Y axis represents the response.

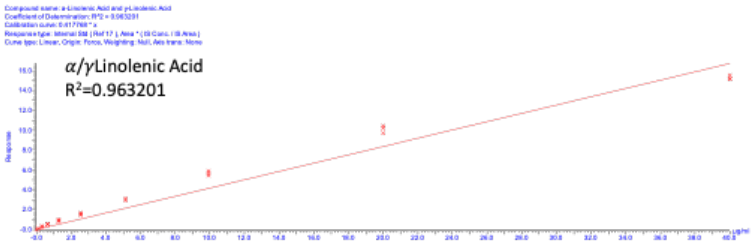
g.



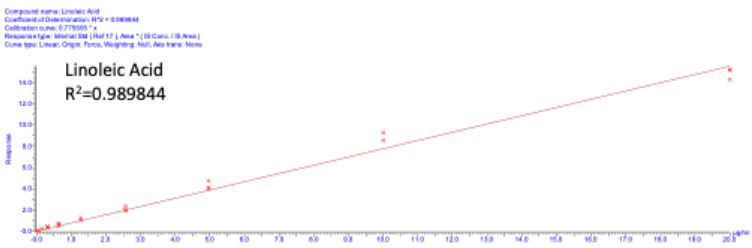
h.



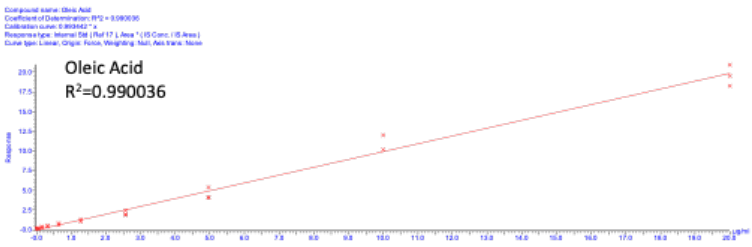
i.



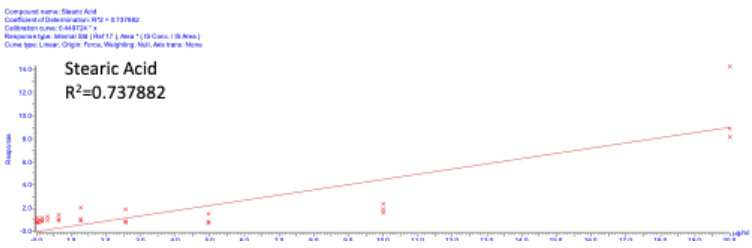
j.



k.

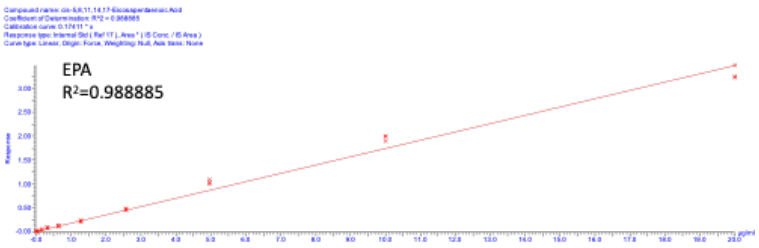


l.

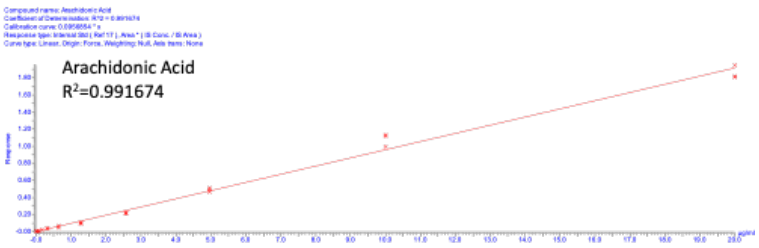


SI.3.13 continued: Standard curves of individual faecal fatty acids obtained from UPLC-TMS analysis for PD study. X axis represents the concentration of each fatty acid (µg/ml) and the Y axis represents the response.

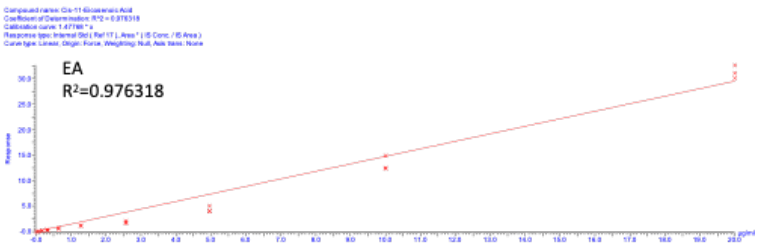
m.



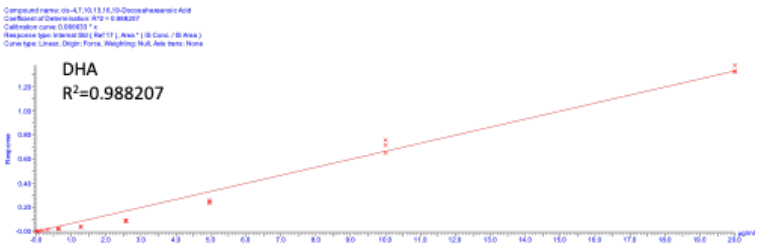
n.



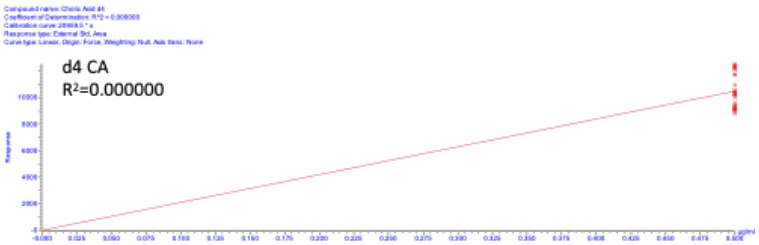
o.



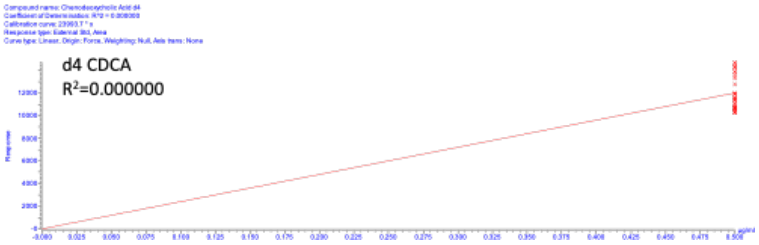
p.



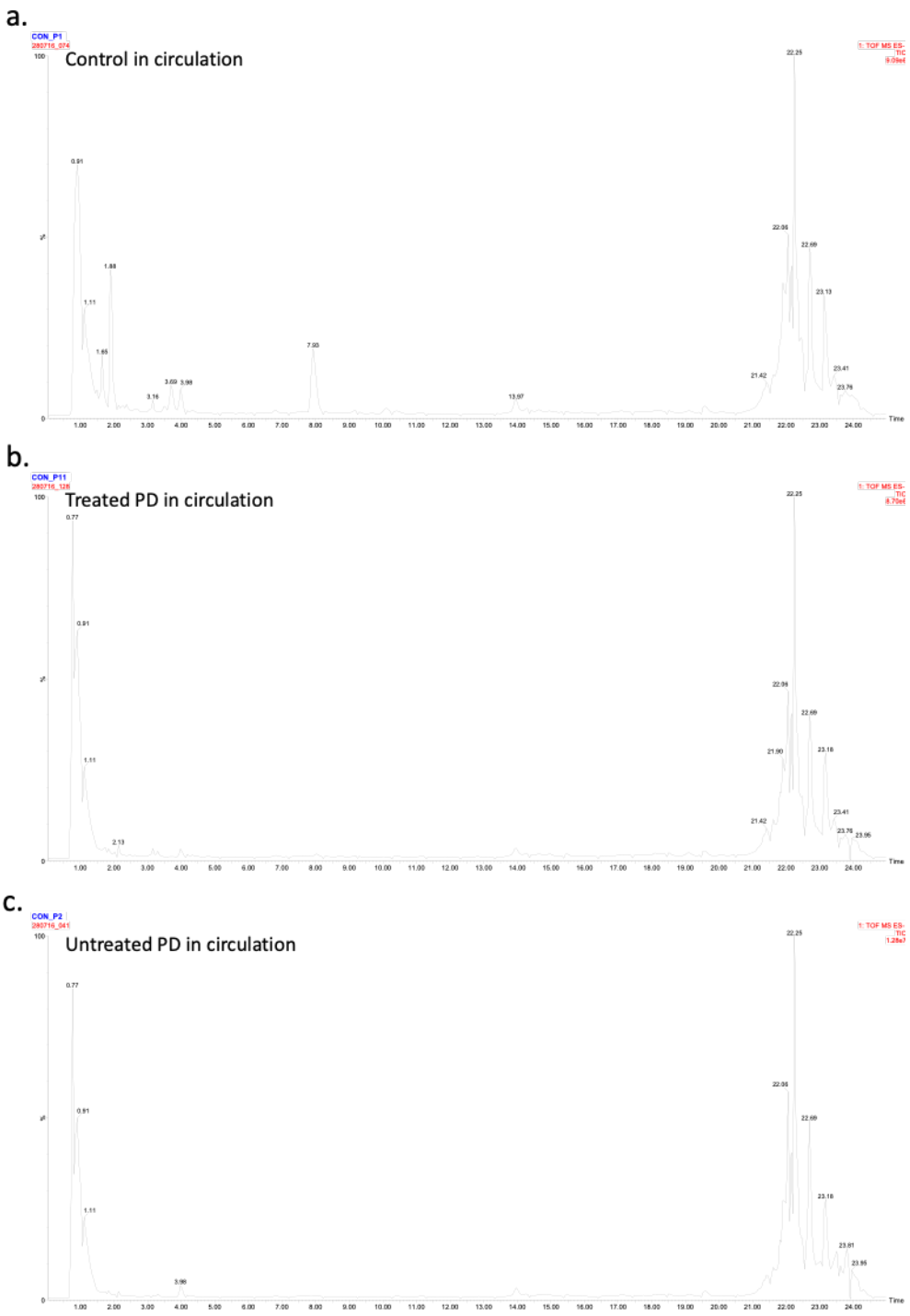
q.



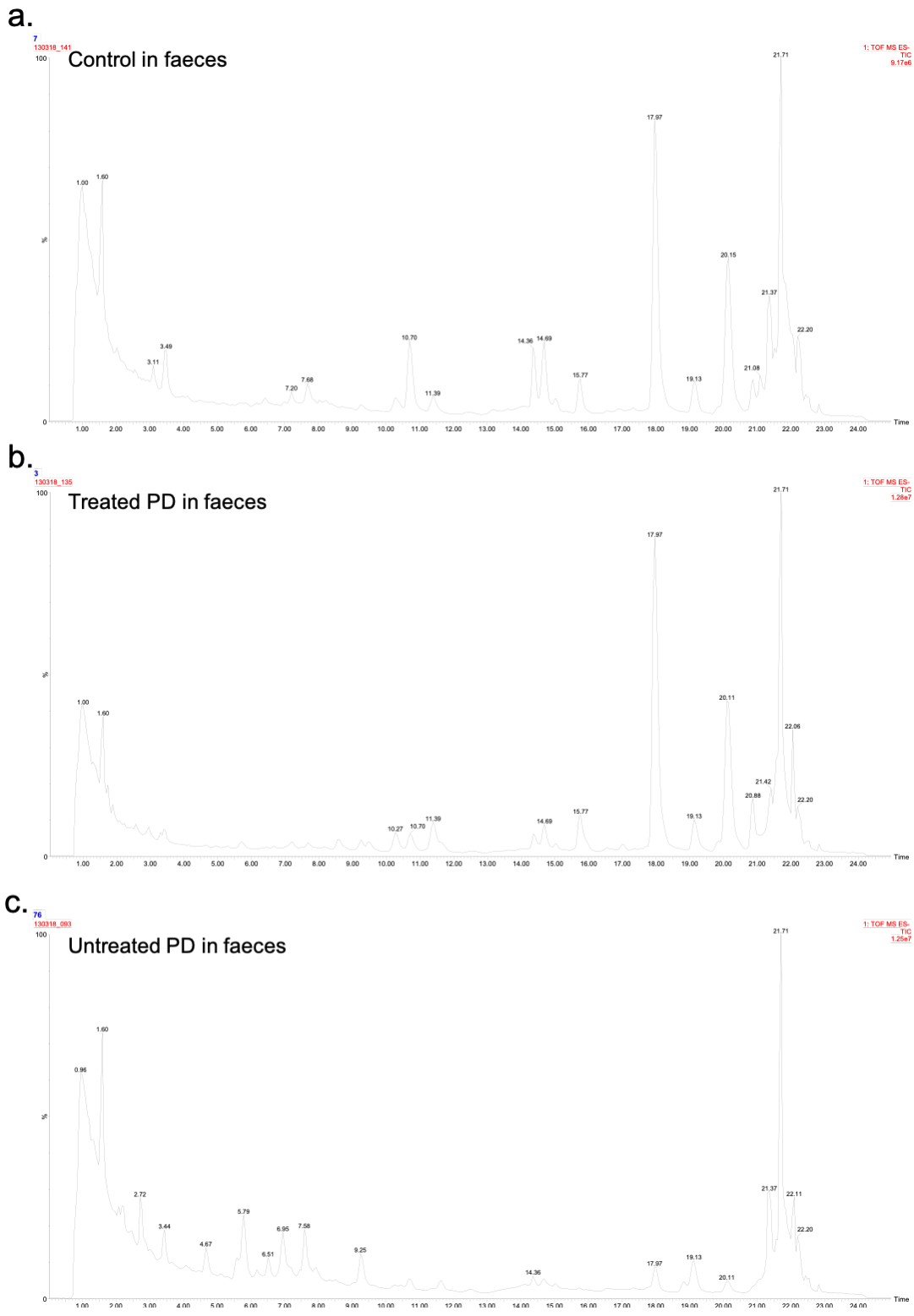
r.



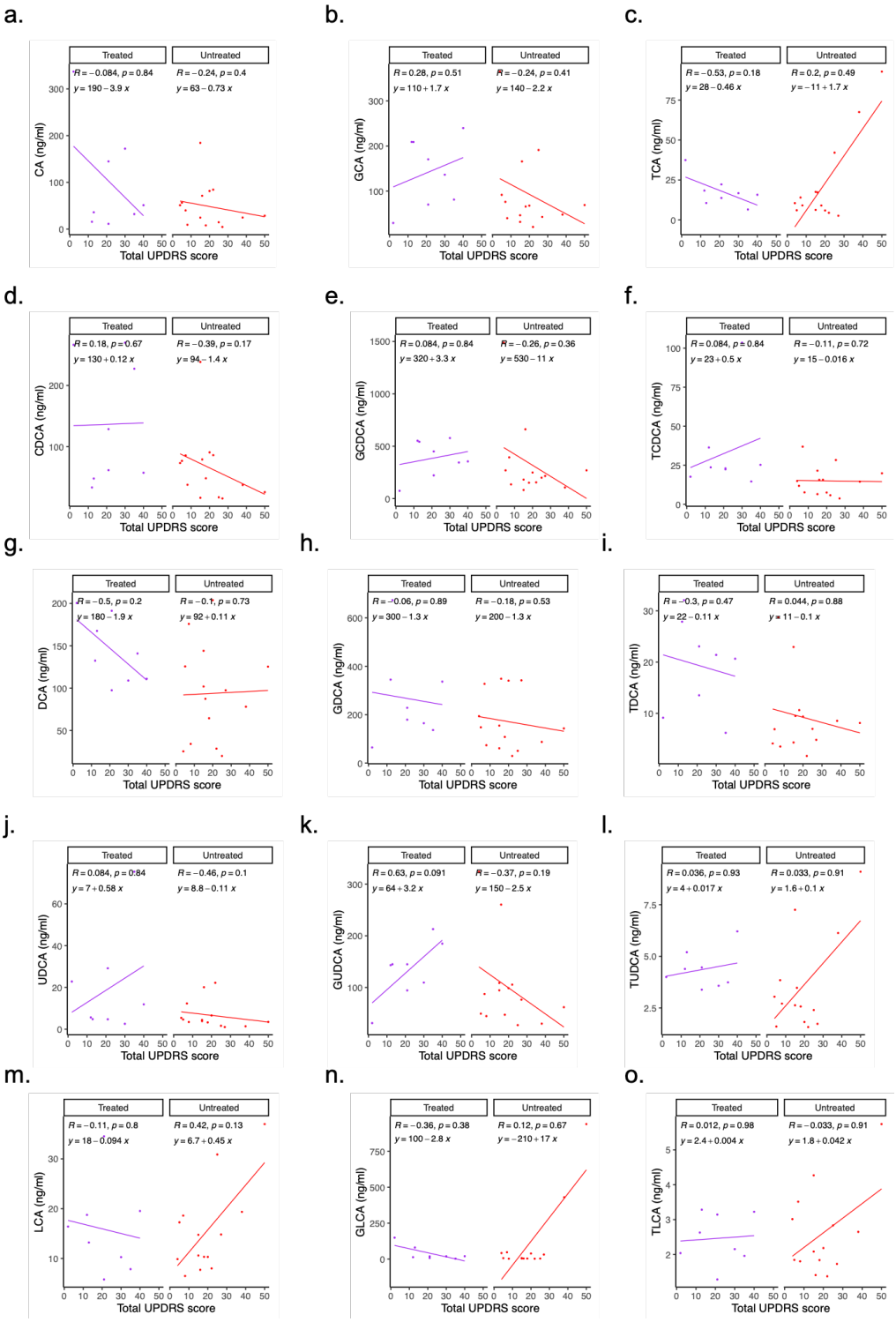
SI.3.33 continued: Standard curves of individual faecal fatty acids obtained from UPLC-TMS analysis for PD study. X axis represents the concentration of each fatty acid (µg/ml) and the Y axis represents the response.



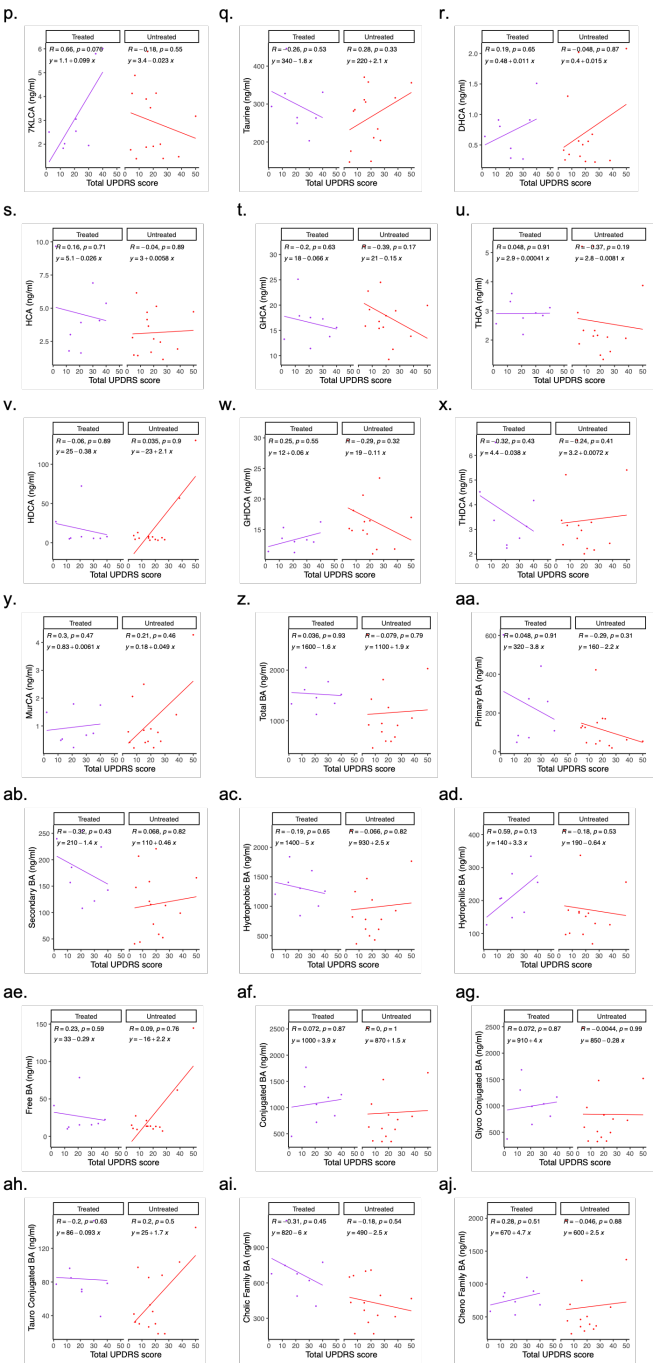
SI.3.14: Representative Chromatograms displaying the full mass spectra of plasma bile and fatty acids for controls: a) healthy volunteers and PD patients: b) Treated PD patients, d) Untreated PD patients.



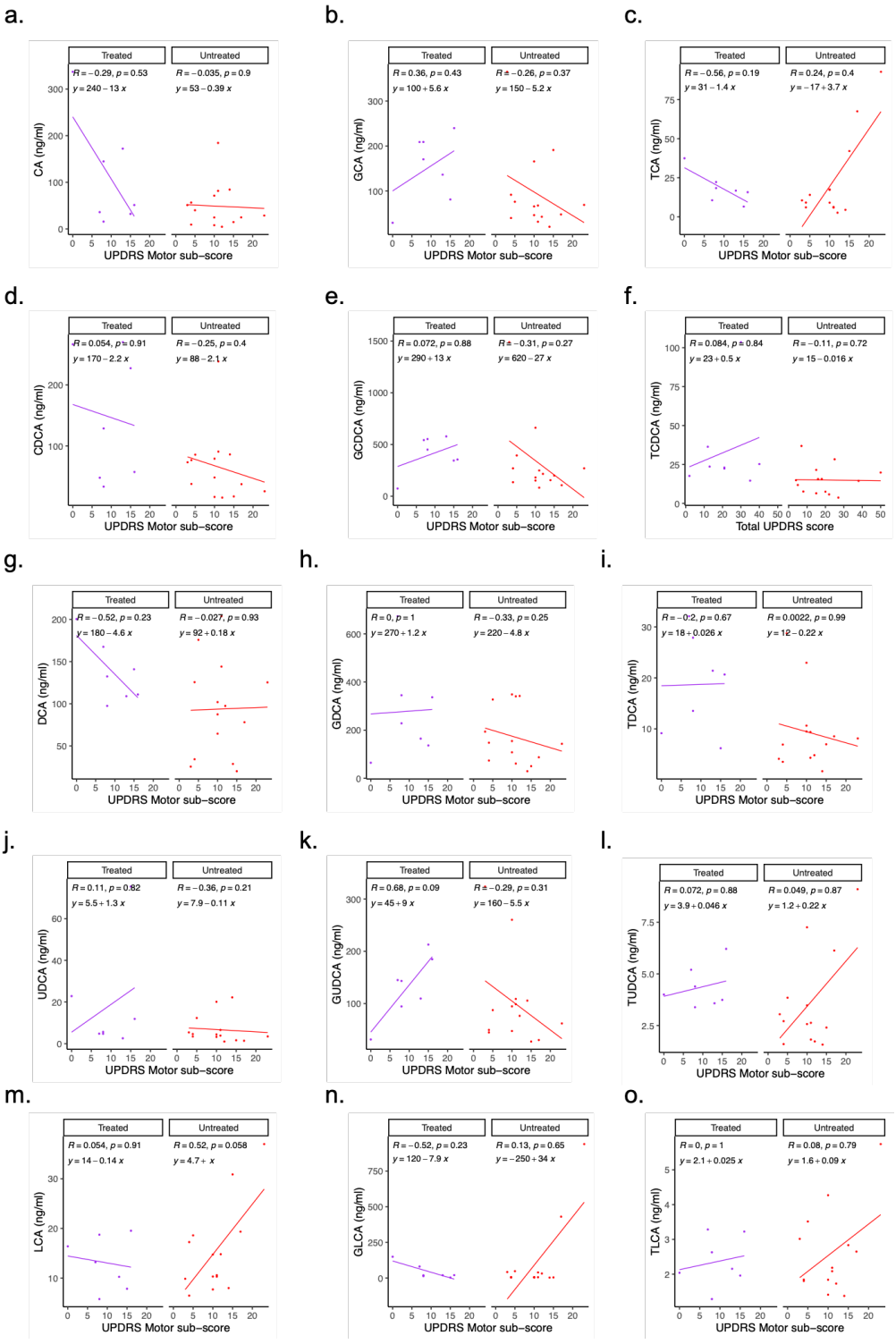
SI.3.15: Representative Chromatograms displaying the full mass spectra of faecal bile and fatty acids for controls: a) healthy volunteers and PD patients: b) Treated PD patients, d) Untreated PD patients.



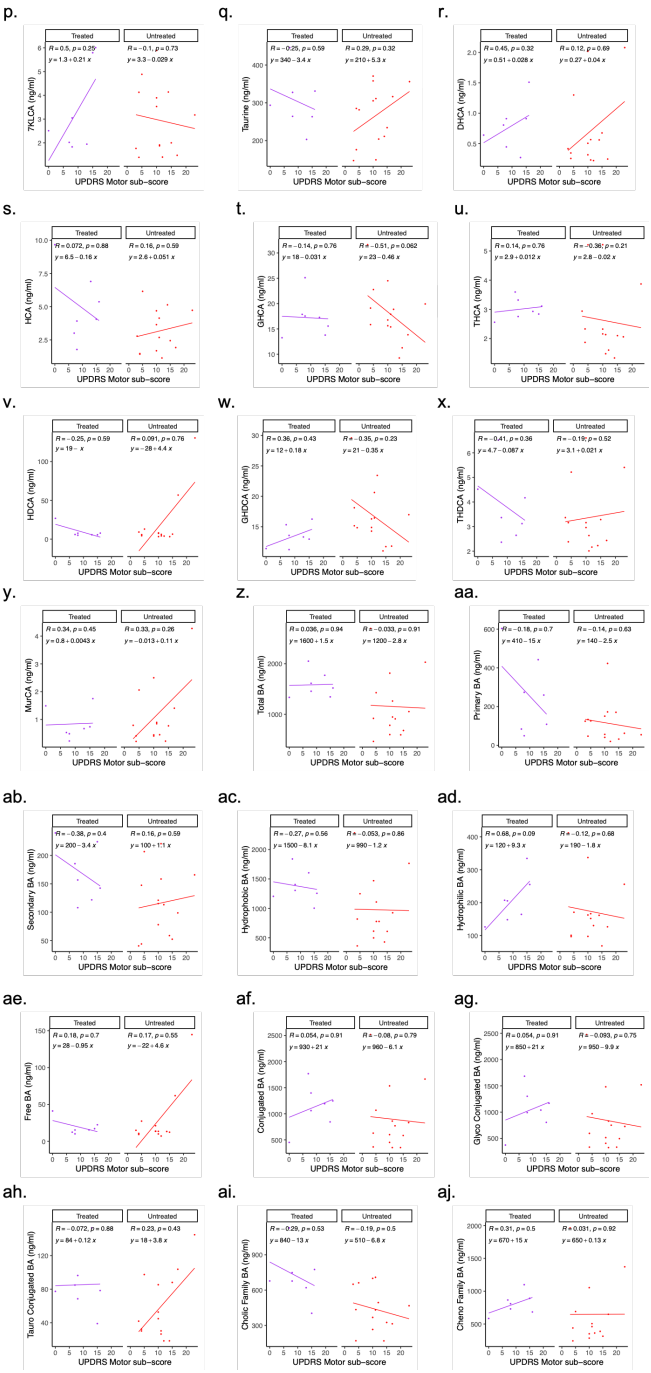
SI.3.16: Absolute quantity of PD study plasma UPDRS correlation with treated and untreated PD patients (a, d) primary bile acids, (g, j, m) secondary bile acids, and their corresponding glyco (b, e, h, k, n) and tauro conjugated moieties (c, f, i, l, o). Data was plotted using RStudio software version 2021.09.0. Spearman correlation (R value) and statistical significance is indicated (*= p<0.05; **=p<0.01; ***=p<0.001; ****=p<0.0001).



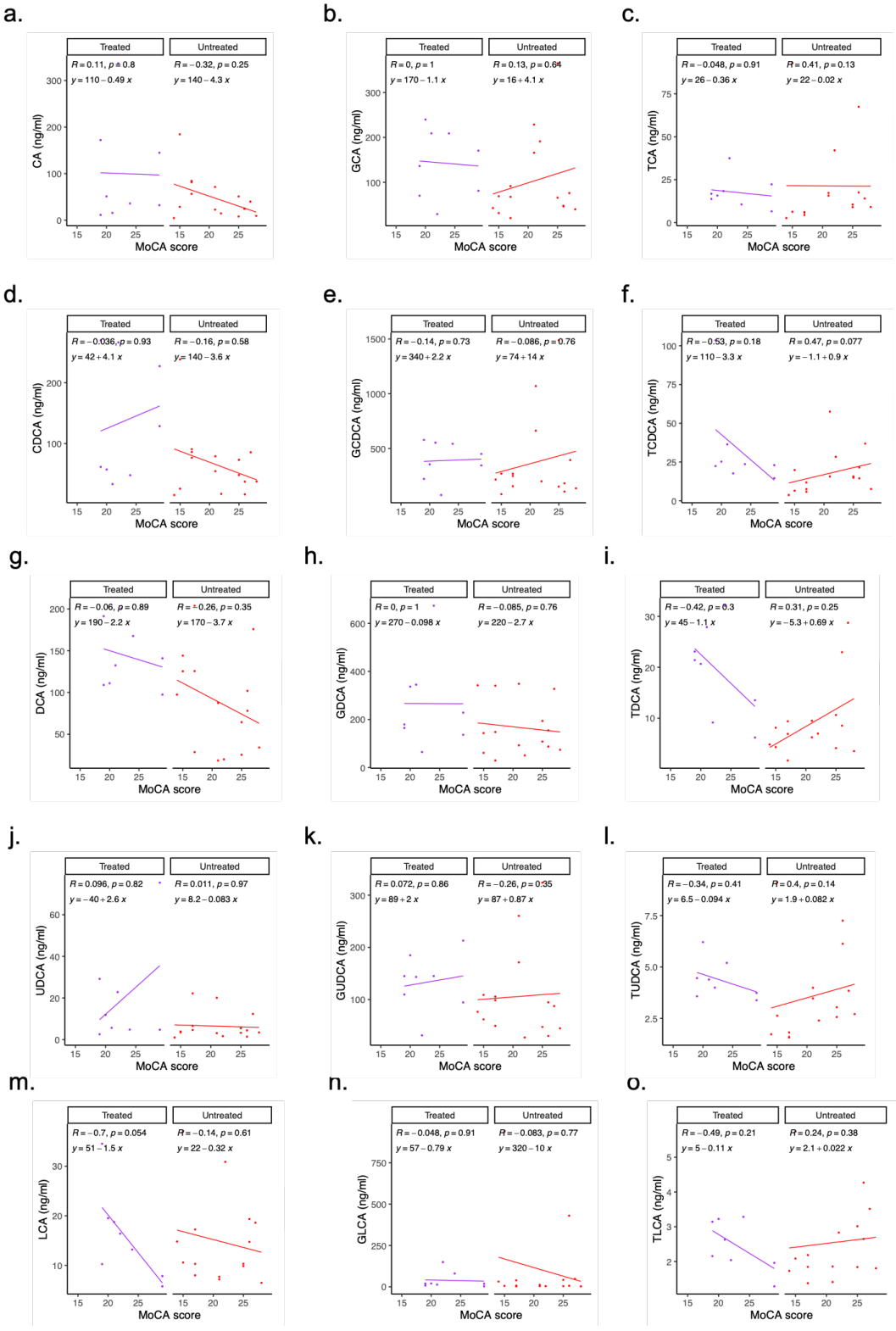
SI.3.16 continued: Absolute quantity of PD study plasma UPDRS correlation with treated and untreated PD patients (p) 7-ketolithocholic acid, (q) taurine, (r) dehydrocholic acid, (s) hyocholic acid, (v) hyodeoxycholic acid and their corresponding glyco (t, w) and tauro conjugated moiety (u, x), (y) murocholic acid, (z) Total bile acids, (aa) Primary bile acids, (ab) Secondary bile acids, (ac) Hydrophobic bile acids, (ad) Hydrophilic bile acids, (ae) Free bile acids, (af) Total conjugated bile acids, (ag) Glyco-conjugated bile acids, (ah) Tauro-conjugated bile acids, (ai) Cholic Acid class of bile acids and (aj) Chenodeoxycholic Acid class of bile acids. RStudio software version 2021.09.0. Spearman correlation (R value) and statistical significance is indicated (*= p<0.05; **=p<0.01; ***=p<0.001; ****=p<0.0001).



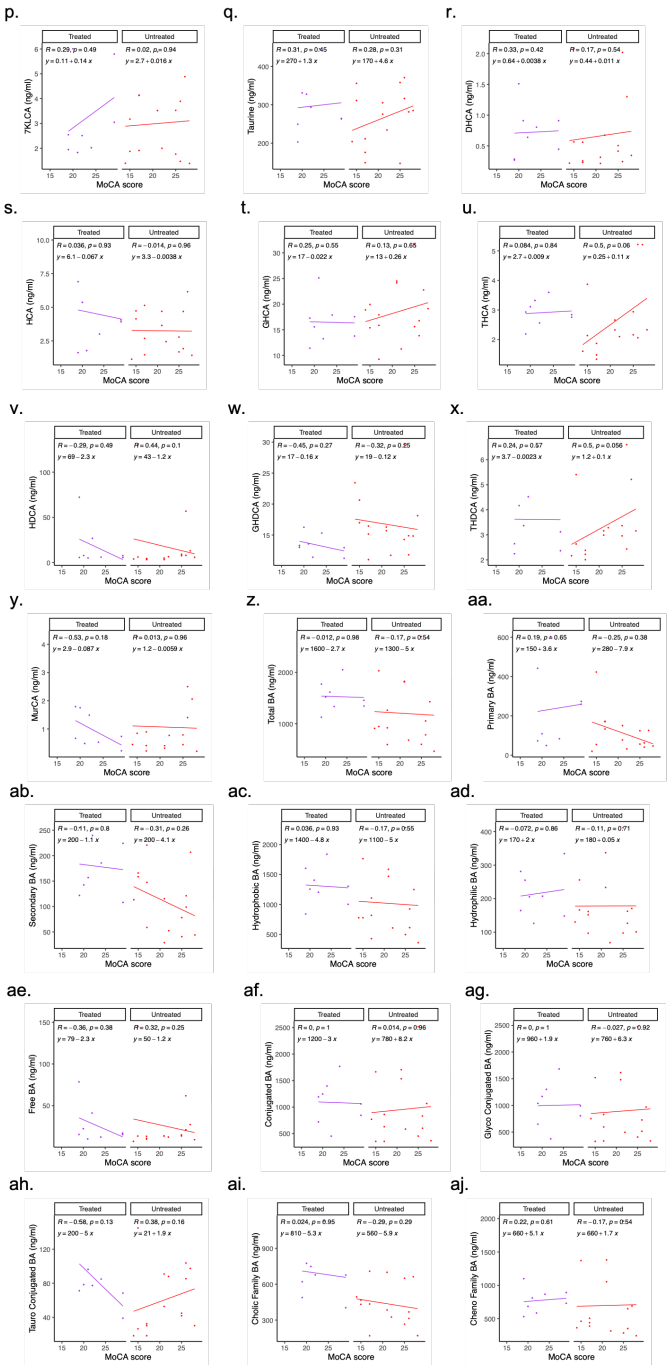
SI.3.17: Absolute quantity of PD study plasma UPDRS Motor sub-score correlation, with treated and untreated PD patients (a, d) primary bile acids, (g, j, m) secondary bile acids, and their corresponding glyco (b, e, h, k, n) and tauro conjugated moieties (c, f, i, l, o). Data was plotted using RStudio software version 2021.09.0. Spearman correlation (R value) and statistical significance is indicated (*= p<0.05; **=p<0.01; ***=p<0.001; ****=p<0.0001).



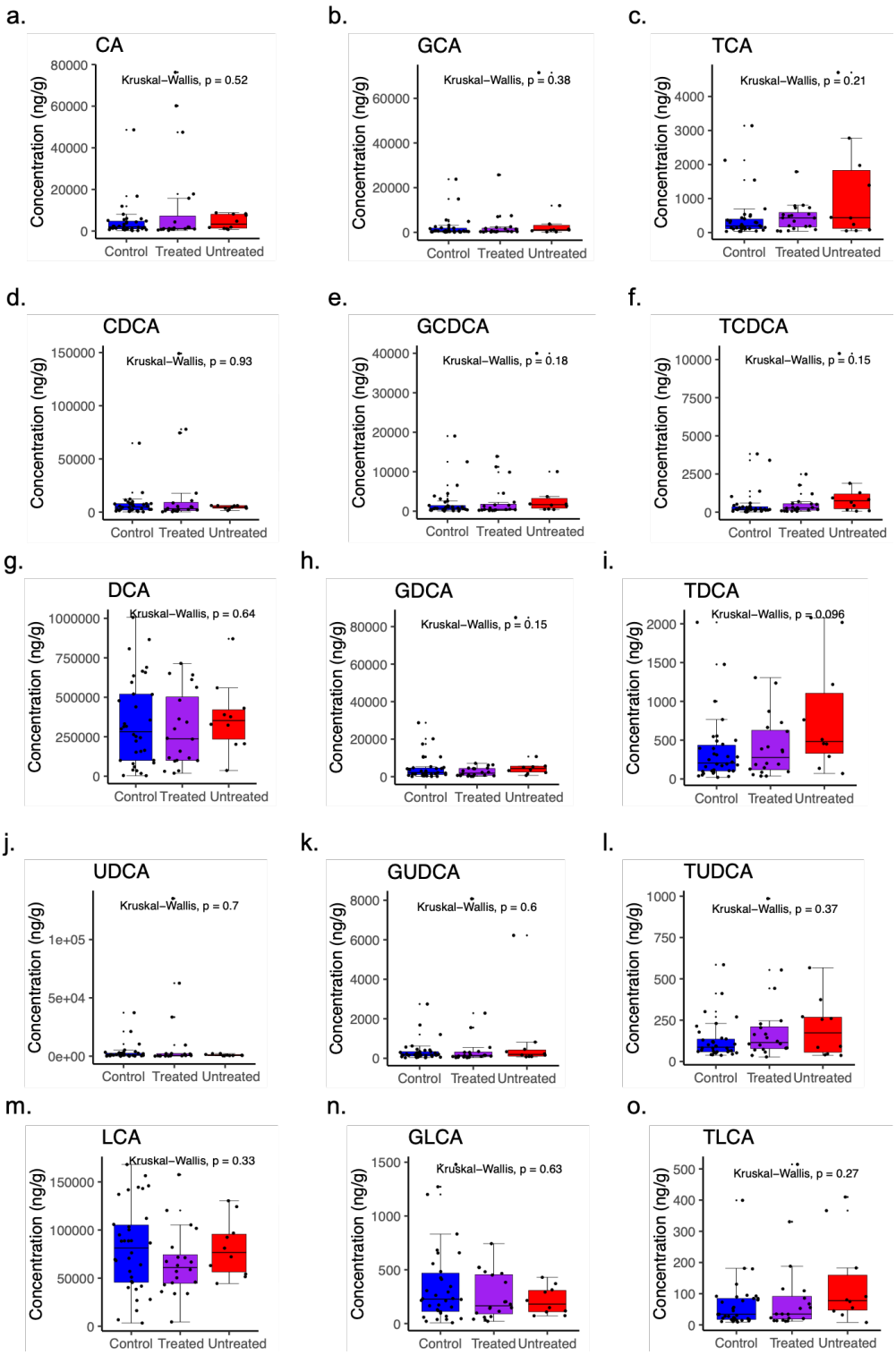
SI.3.17 continued: Absolute quantity of PD study plasma UPDRS Motor sub-score correlation, with treated and untreated PD patients (p) 7-ketolithocholic acid, (q) taurine, (r) dehydrocholic acid, (s) hyocholic acid, (v) hyodeoxycholic acid and their corresponding glyco (t, w) and tauro conjugated moiety (u, x), (y) murocholic acid, (z) Total bile acids, (aa) Primary bile acids, (ab) Secondary bile acids, (ac) Hydrophobic bile acids, (ad) Hydrophilic bile acids, (ae) Free bile acids, (af) Total conjugated bile acids, (ag) Glyco-conjugated bile acids, (ah) Tauro-conjugated bile acids, (ai) Cholic Acid class of bile acids and (aj) Chenodeoxycholic Acid class of bile acids.RStudio software version 2021.09.0. Spearman correlation (R value) and statistical significance is indicated (*= p<0.05; **=p<0.01; ***=p<0.001; ****=p<0.0001).



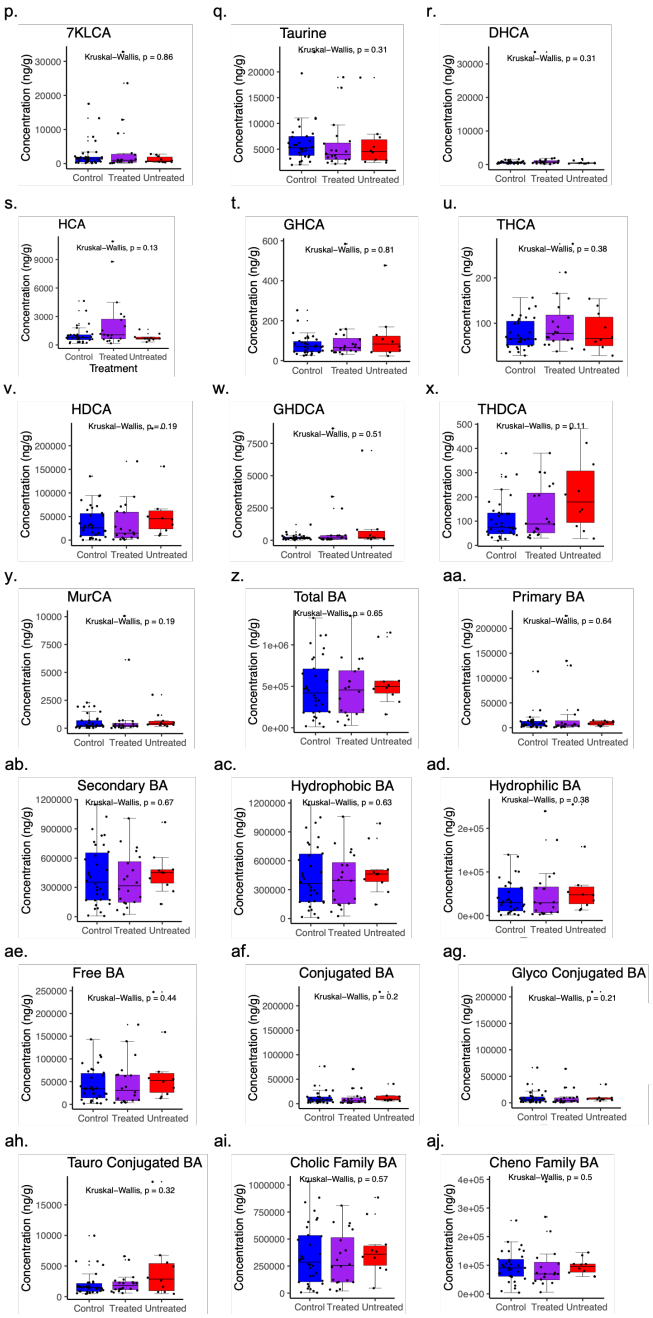
SI.3.18: Absolute quantity of PD study plasma MoCA correlation, with treated and untreated PD patients (a, d) primary bile acids, (g, j, m) secondary bile acids, and their corresponding glyco (b, e, h, k, n) and tauro conjugated moieties (c, f, i, l, o). Data was plotted using RStudio software version 2021.09.0. Spearman correlation (R value) and statistical significance is indicated (*= p<0.05; **=p<0.01; ***=p<0.001; ****=p<0.0001).



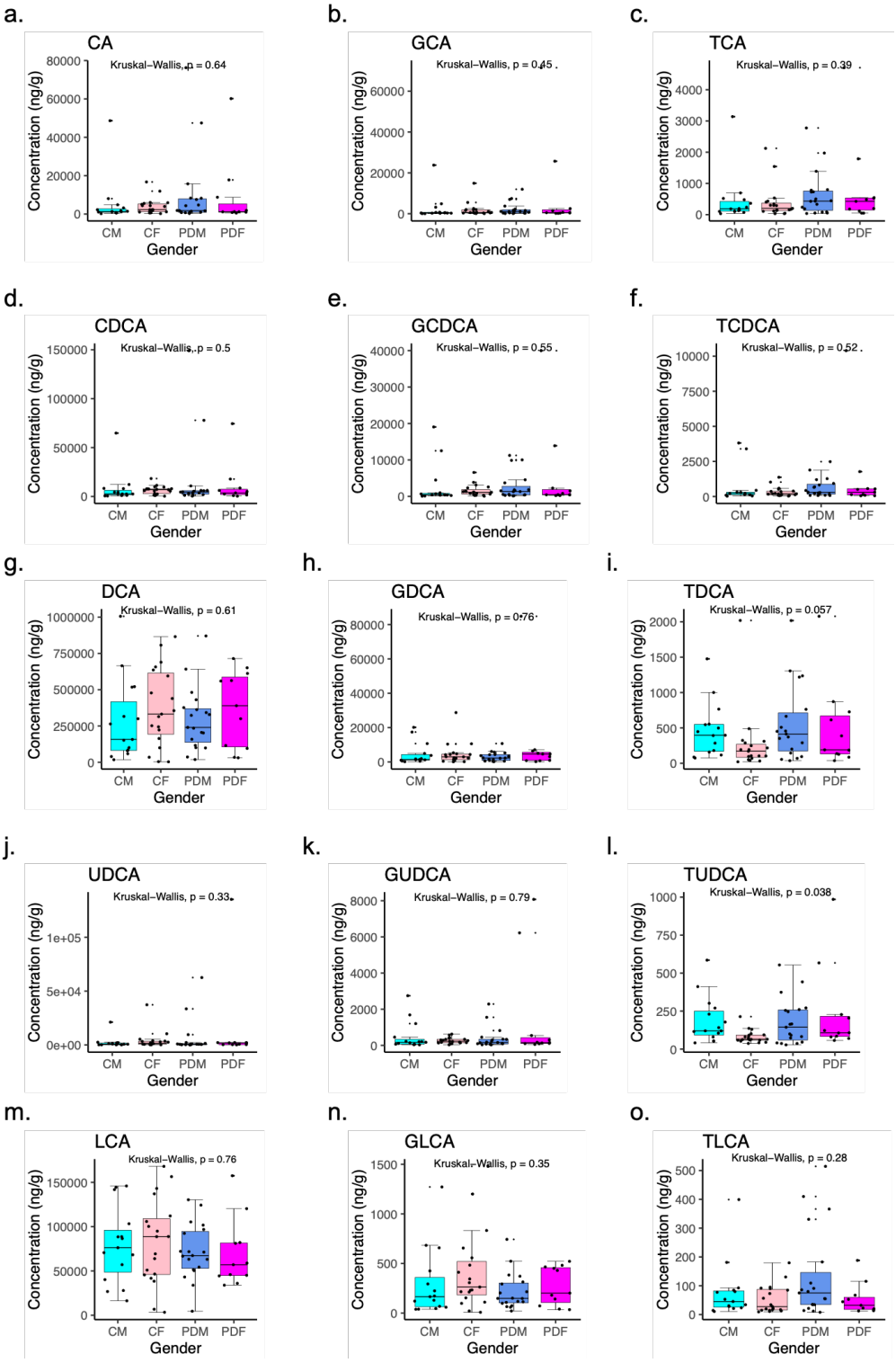
SI.3.18 continued: Absolute quantity of PD study plasma MoCA correlation, with treated and untreated PD patients (p) 7-ketolithocholic acid, (q) taurine, (r) dehydrocholic acid, (s) hyocholic acid, (v) hyodeoxycholic acid and their corresponding glyco (t, w) and tauro conjugated moiety (u, x), (y) murocholic acid, (z) Total bile acids, (aa) Primary bile acids, (ab) Secondary bile acids, (ac) Hydrophobic bile acids, (ad) Hydrophilic bile acids, (ae) Free bile acids, (af) Total conjugated bile acids, (ag) Glyco-conjugated bile acids, (ah) Tauro-conjugated bile acids, (ai) Cholic Acid class of bile acids and (aj) Chenodeoxycholic Acid class of bile acids. RStudio software version 2021.09.0. Spearman correlation (R value) and statistical significance is indicated (*= p<0.05; **=p<0.01; ***=p<0.001; ****=p<0.0001).



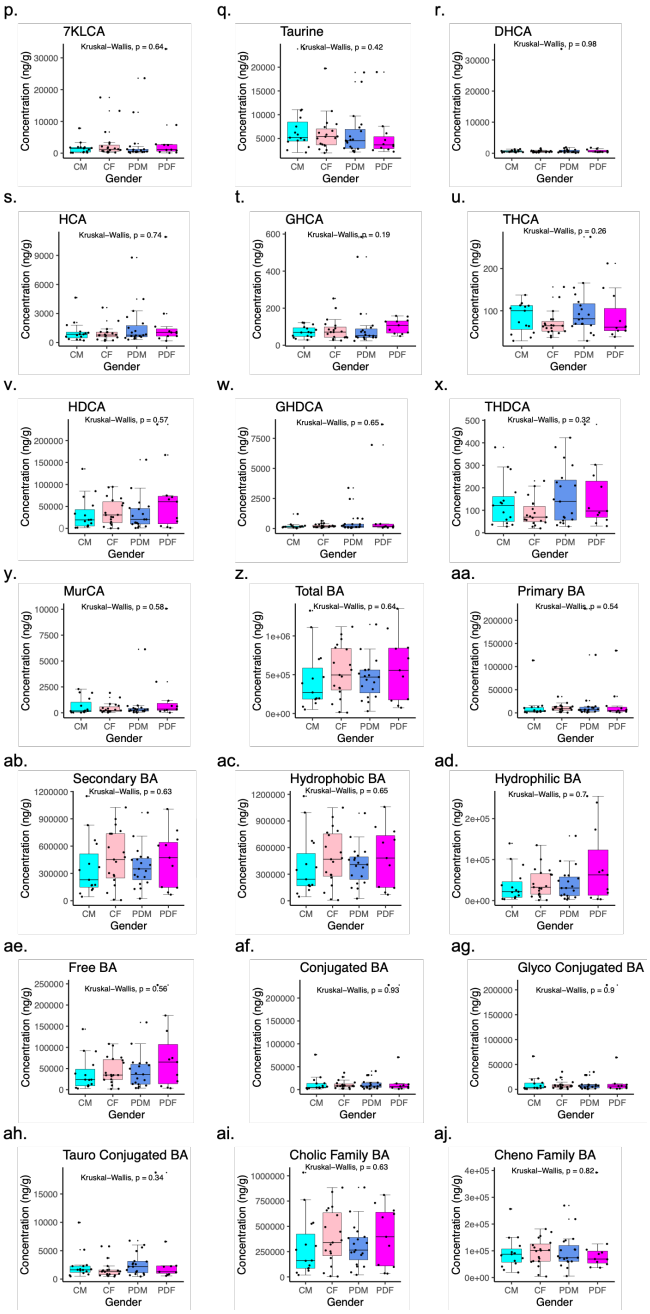
SI.3.19: Absolute quantity of PD study faeces of control vs PD treated vs PD untreated (a, d) primary bile acids, (g, j, m) secondary bile acids, and their corresponding glyco (b, e, h, k, n) and tauro conjugated moieties (c, f, i, l, o). Data was plotted using RStudio software version 2021.09.0 and is represented as mean ± SD. Statistical significance is indicated and calculated using using Kruskal-Wallis and Dunn's Multiple Comparison Test (*= p<0.05; **=p<0.01; ***=p<0.001; ****=p<0.0001).



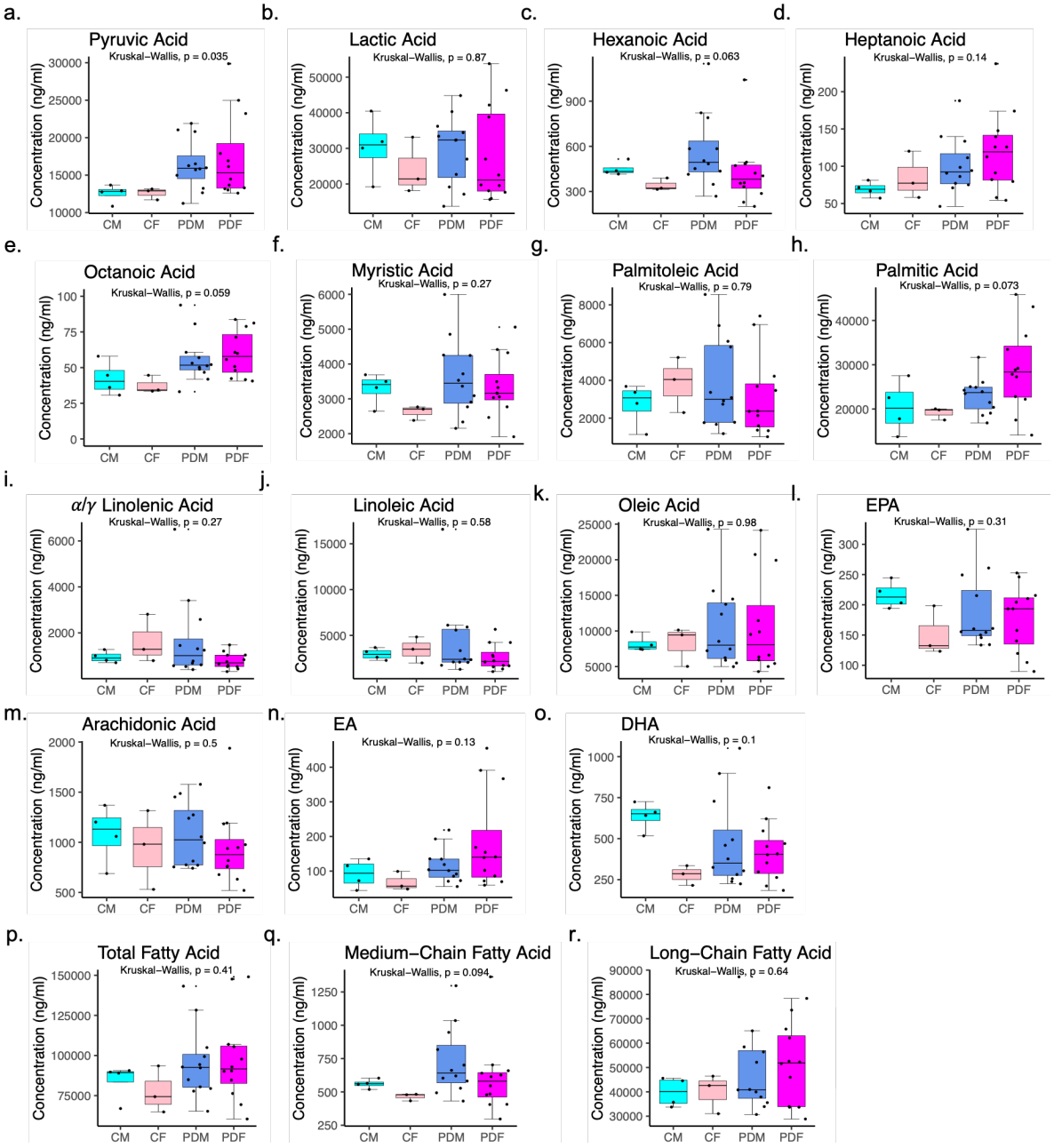
SI.3.19 continued: Absolute quantity of PD study faeces of control vs PD treated vs PD untreated (p) 7-ketolithocholic acid, (q) taurine, (r) dehydrocholic acid, (s) hyocholic acid, (v) hyodeoxycholic acid and their corresponding glyco (t, w) and tauro conjugated moieties (u, x), (y) murocholic acid, (z) Total bile acids, (aa) Primary bile acids, (ab) Secondary bile acids, (ac) Hydrophobic bile acids (ad) Hydrophilic bile acids (ae) Free bile acids, (af) Total conjugated bile acids, (ag) Glyco-conjugated bile acids, (ah) Tauro-conjugated bile acids, (ai) Cholic Acid class of bile acids and (aj) Chenodeoxycholic Acid class of bile acids. RStudio software version 2021.09.0. Statistical significance is indicated and calculated using using Kruskal-Wallis and Dunn's Multiple Comparison Test (*= p<0.05; **=p<0.01; ***=p<0.001; ****=p<0.0001).



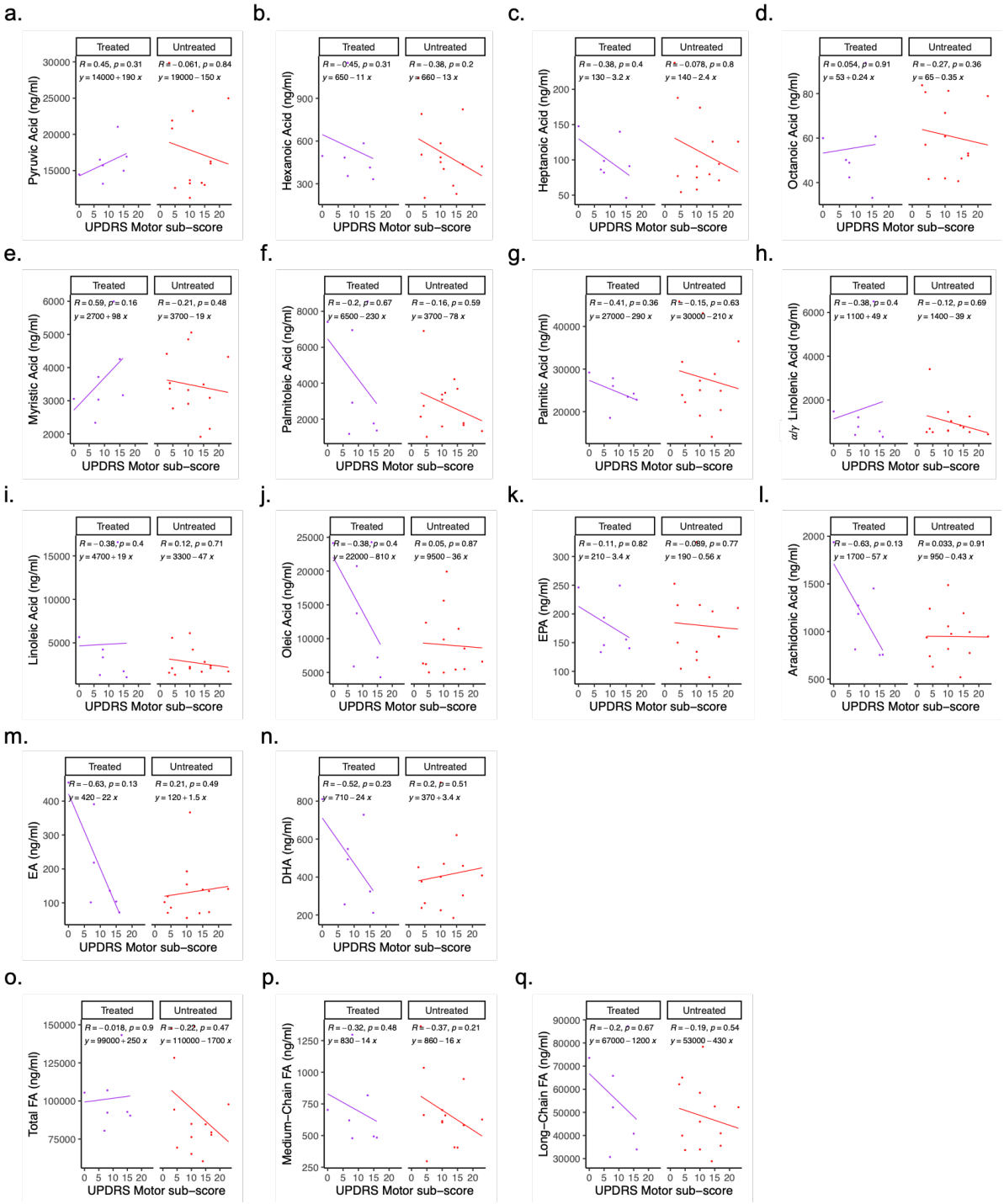
SI.3.20: Absolute quantity of PD study faeces gender (a, d) primary bile acids, (g, j, m) secondary bile acids, and their corresponding glyco (b, e, h, k, n) and tauro conjugated moieties (c, f, i, l, o). Data was plotted using RStudio software version 2021.09.0 and is represented as mean ± SD. Statistical significance is indicated and calculated using using Kruskal-Wallis and Dunn's Multiple Comparison Test (*= p<0.05; **=p<0.01; ***=p<0.001; ****=p<0.0001).



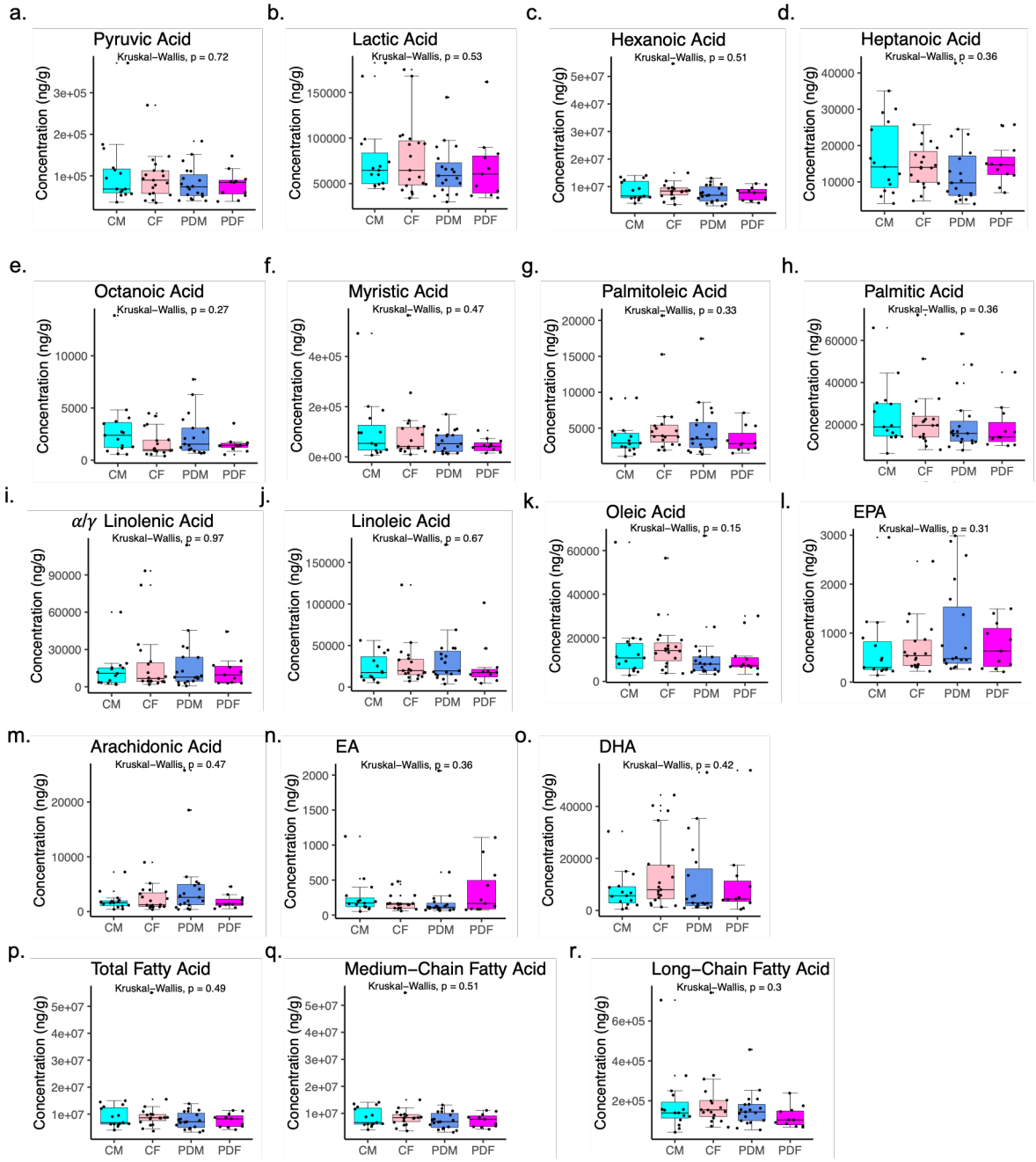
SI.3.20 continued: Absolute quantity of PD study faeces gender (p) 7-ketolithocholic acid, (q) taurine, (r) dehydrocholic acid, (s) hyocholic acid, (v) hyodeoxycholic acid and their corresponding glyco (t, w) and tauro conjugated moieties (u, x), (y) murocholic acid, (z) Total bile acids, (aa) Primary bile acids, (ab) Secondary bile acids, (ac) Hydrophobic bile acids (ad) Hydrophilic bile acids (ae) Free bile acids, (af) Total conjugated bile acids, (ag) Glyco-conjugated bile acids, (ah) Tauro-conjugated bile acids, (ai) Cholic Acid class of bile acids and (aj) Chenodeoxycholic Acid class of bile acids. RStudio software version 2021.09.0. Statistical significance is indicated and calculated using using Kruskal-Wallis and Dunn's Multiple Comparison Test (*= p<0.05; **=p<0.01; ***=p<0.001; ****=p<0.0001)



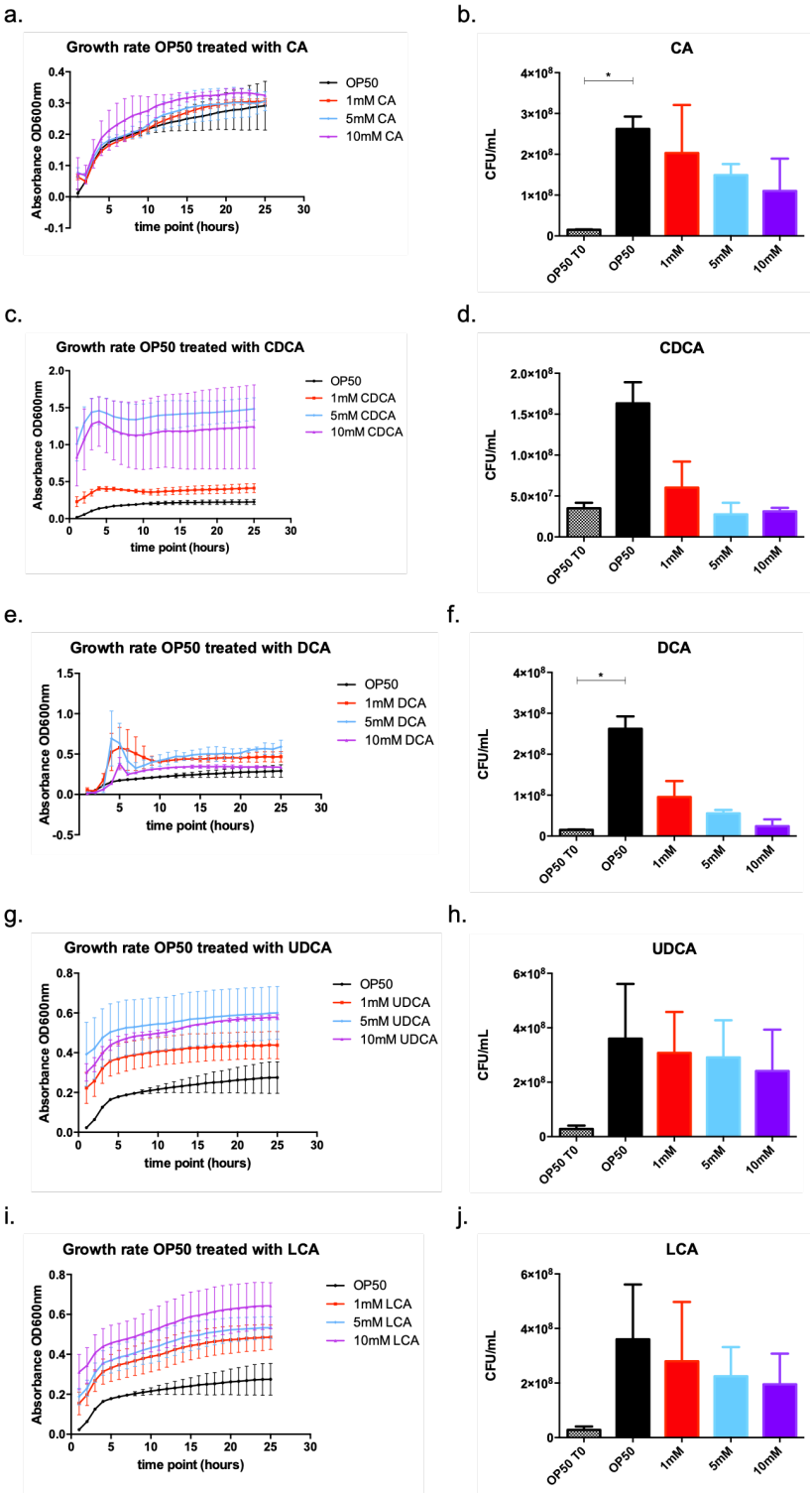
SI.3.21: Absolute quantity of PD study fatty acid plasma gender (a) pyruvic acid, (b) lactic acid, (c) hexanoic acid, (d) heptanoic acid, (e) octanoic acid, (f) myristic acid, (g) palmitoleic acid, (h) palmitic acid, (i) α/γlinolenic acid, (j) linoleic acid, (k) oleic acid, (l) eicosapentaenoic acid, (m) arachidonic acid, (n) eicosenoic acid, (o) docosahexaenoic acid, (p) Total fatty acids, (q) medium-chain fatty acids and (r) long-chain fatty acids. All concentrations were quantified against standard curves for each analyte and normalised according to internal standards using Targetlynx^{TM} (Waters Ltd.) software. RStudio software version 2021.09.0. Statistical significance is indicated and calculated using Kruskal-Wallis and Dunn's Multiple Comparison Test (*= p<0.05; **=p<0.01; ***=p<0.001; ****=p<0.0001).



SI.3.22: Absolute quantity of PD study fatty acid plasma UPDRS Motor sub-score correlation, with treated and untreated PD (a) pyruvic acid, (b) hexanoic acid, (c) heptanoic acid, (d) octanoic acid, (e) myristic acid, (f) palmitoleic acid, (g) palmitic acid, (h) α/γlinolenic acid, (i) linoleic acid, (j) oleic acid, (k) eicosapentaenoic acid, (l) arachidonic acid, (m) eicosenoic acid, (n) docosahexaenoic acid, (o) Total fatty acids, (p) medium-chain fatty acids and (q) long-chain fatty acids. RStudio software version 2021.09.0. Spearman correlation (R value) and statistical significance is indicated (*= p<0.05; **=p<0.01; ***=p<0.001; ****=p<0.0001).



SI.3.23: Absolute quantity of PD study fatty acid faeces gender (a) pyruvic acid, (b) lactic acid, (c) hexanoic acid, (d) heptanoic acid, (e) octanoic acid, (f) myristic acid, (g) palmitoleic acid, (h) palmitic acid, (i) α/γlinolenic acid, (j) linoleic acid, (k) oleic acid, (l) eicosapentaenoic acid, (m) arachidonic acid, (n) eicosenoic acid, (o) docosahexaenoic acid, (p) Total fatty acids, (q) medium-chain fatty acids and (r) long-chain fatty acids. RStudio software version 2021.09.0. Statistical significance is indicated and calculated using Kruskal-Wallis and Dunn's Multiple Comparison Test (*= p<0.05; **=p<0.01; ***=p<0.001; ****=p<0.0001).

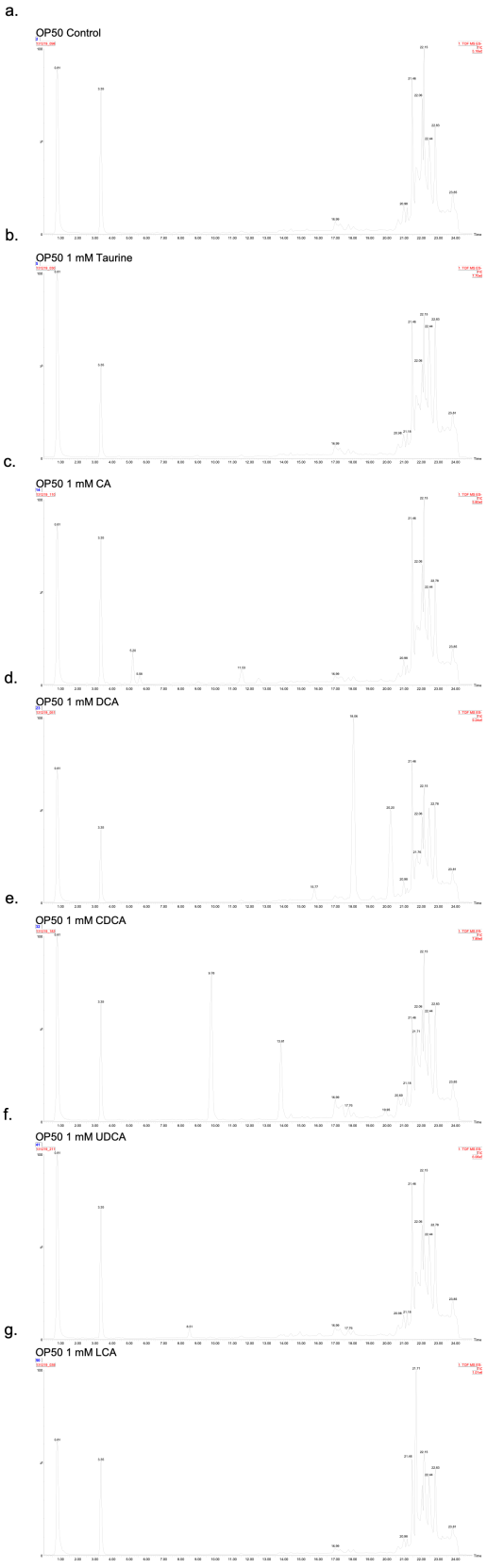


SI.4.1: Replicate experiment depicting: Growth rate of *Escherichia coli* OP50 in presence (a-d) primary bile acids, (g-j) secondary bile acids. GraphPrism v6. Statistics were carried out

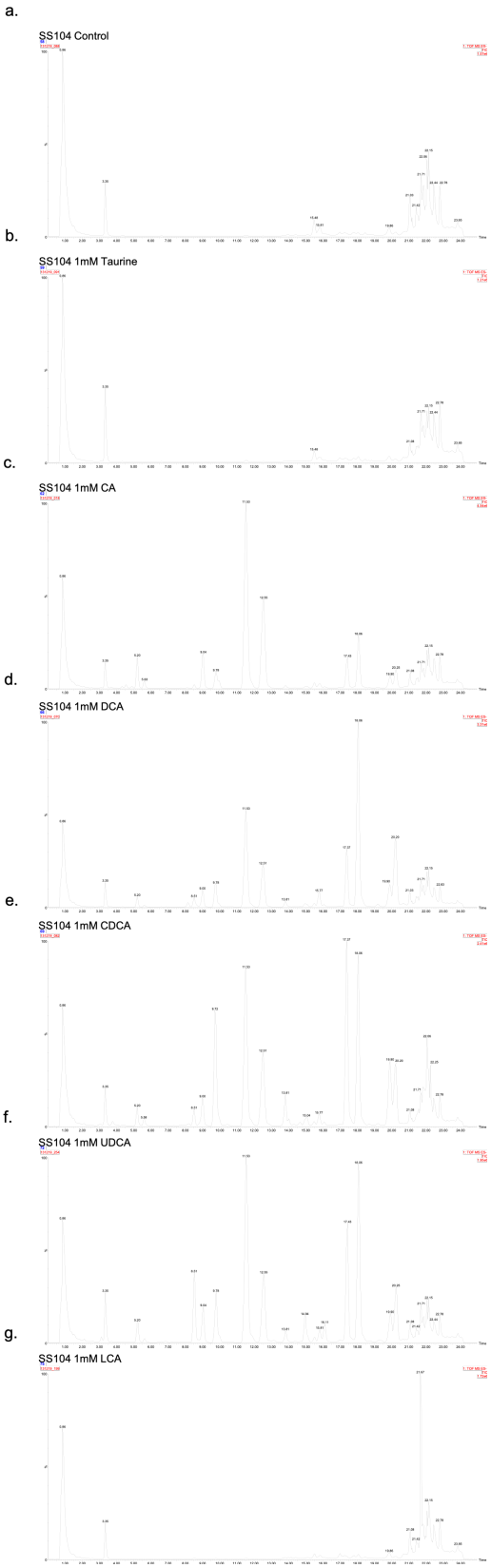
using one-way ANOVA, Tukey multiple comparison test (* = p<0.05; ** = p<0.01; *** = p<0.001; **** = p<0.0001).

SI.4.2: Table detailing the 58 bile acid metabolites potentially examined using UPLC-TMS, for *E. coli* and *C. elegans* study, their retention time (RT), R^2 value and concentration range (µg/ml). Only primary and secondary BAs were examined. Abbreviations: MW- Molecular weight, RT- retention time in minutes, R^2 value- coefficient of determination, IS- internal standard

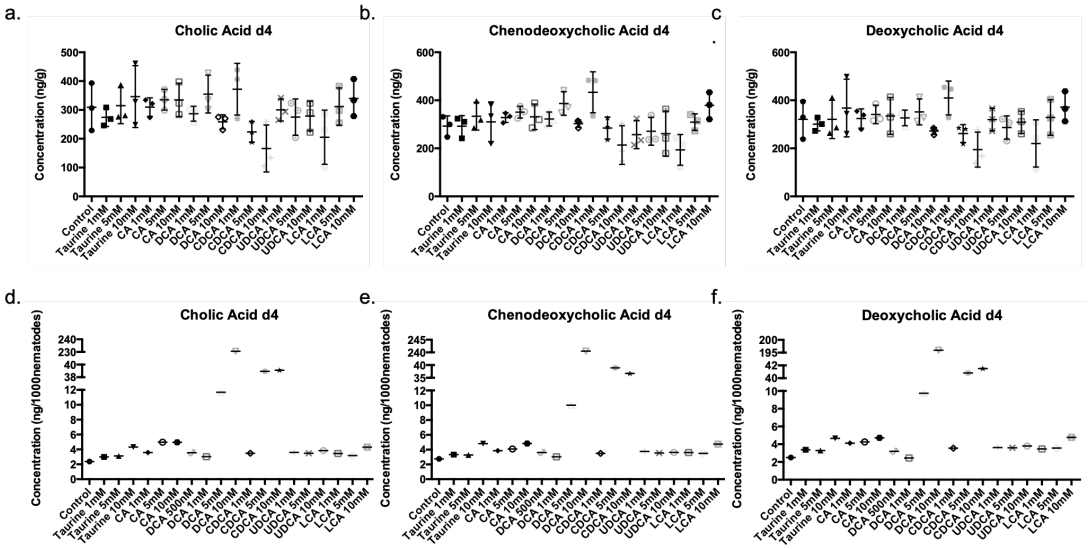
Number	Analyte	Abbreviation	$[MW]^{-H}$	Neutral Formula	RT Original	RT 2020	Actual RT Top	Actual RT Middle	Actual RT End	R2 value	Range (µg/ml)
1	Taurine	Taurine	124.0068	$C_2H_7NO_3S$	0.75	0.77	0.77	0.77	0.77	0.993875	0.0064-20.00
2	Dehydrocholic Acid	DHCA	401.2328	$C_{24}H_{34}O_5$	2.00	1.79	1.84	1.84	1.84	0.922988	0.0064-20.00
3	Dehydrolithocholic	DHLCA	373.2743	$C_{24}H_{38}O_3$	21.27	21.27	21.08	21.08	21.08	0.969911	0.0064-20.00
4	3,7-Diketocholanic acid	3,7DKCnA	387.2535	$C_{24}H_{36}O_4$	7.39	7.39	7.49	7.44	7.44	0.660553	0.0064-20.00
5	3,6-Diketocholanic acid	3,6DKCnA	387.2535	$C_{24}H_{36}O_4$	7.68	7.68	7.68	7.74	7.74	0.692528	0.0064-20.00
6	Allolithocholic Acid	AlloLCA	375.2899	$C_{24}H_{40}O_3$	19.08	18.78	19.04	19.04	19.08	0.992597	0.0064-20.00
7	Isolithocholic Acid	IsoLCA	375.2899	$C_{24}H_{40}O_3$	18.99	18.99	blank	blank	blank	0.992596	0.0064-20.00
8	Lithocholic Acid	LCA	375.2899	$C_{24}H_{40}O_3$	21.72	21.66	21.71	21.66	21.67	0.990496	0.0064-20.00
9	Murocholic Acid	MurCA	391.2848	$C_{24}H_{40}O_4$	8.25	6.76	6.90	6.90	6.90	0.993302	0.0064-20.00
10	Ursodeoxycholic aAid	UDCA	391.2848	$C_{24}H_{40}O_4$	9.87	8.37	8.51	8.51	8.51	0.993484	0.0064-20.00
11	β-Hyodeoxycholic Acid	β-HDCA	391.2848	$C_{24}H_{40}O_4$	9.68	9.29	9.53	9.53	9.53	0.995158	0.0064-20.00
12	Hyodeoxycholic Acid	HDCA	391.2848	$C_{24}H_{40}O_4$	12.54	10.21	10.51	10.46	10.46	0.995106	0.0064-20.00
13	β-Deoxycholic Acid	β-DCA	391.2848	$C_{24}H_{40}O_4$	11.19	11.19	blank	blank	blank	-	0.0064-20.00
14	Chenodeoxycholic Acid	CDCA	391.2848	$C_{24}H_{40}O_4$	19.17	17.23	17.43	17.43	17.43	0.992176	0.0064-20.00
15	Deoxycholic Acid	DCA	391.2848	$C_{24}H_{40}O_4$	20.20	17.86	18.11	18.06	18.06	0.997737	0.0064-20.00
16	Isodeoxycholic Acid	IsoDCA	391.2848	$C_{24}H_{40}O_4$	20.50	20.06	20.34	20.34	20.34	0.995951	0.0064-20.00
17	Ursocholic Acid	UCA	407.2797	$C_{24}H_{40}O_5$	3.44	3.20	3.35	3.35	3.35	0.981690	0.0064-20.00
18	α-Muricholic Acid	α-MCA	407.2797	$C_{24}H_{40}O_5$	7.18	5.63	5.79	5.79	5.79	0.997771	0.0064-20.00
19	ω-Muricholic Acid	ω-MCA	407.2797	$C_{24}H_{40}O_5$	7.08	5.63	5.20	5.20	5.20	0.997771	0.0064-20.00
20	β-Muricholic Acid	β-MCA	407.2797	$C_{24}H_{40}O_5$	7.59	6.07	6.23	6.23	6.23	0.996574	0.0064-20.00
21	Hyocholic Acid	HCA	407.2797	$C_{24}H_{40}O_5$	10.39	8.65	8.85	8.85	8.85	0.989188	0.0064-20.00
22	Cholic Acid	CA	407.2797	$C_{24}H_{40}O_5$	11.76	11.29	11.58	11.53	11.58	0.997557	0.0064-20.00
23	Allocholic Acid	AlloCA	407.2797	$C_{24}H_{40}O_5$	12.21	11.77	12.07	12.07	12.07	0.997565	0.0064-20.00
24	Ursocholanic Acid	UCnA	359.2950	$C_{24}H_{40}O_2$	23.62	23.57	23.57	23.62	23.57	0.823528	0.0064-20.00
25	7-Ketolithocholic Acid	7KLCA	389.2692	$C_{24}H_{38}O_4$	11.83	9.58	9.78	9.78	9.78	0.994359	0.0064-20.00
26	12-Ketolithocholic Acid	12KLCA	389.2692	$C_{24}H_{38}O_4$	10.95	10.46	10.75	10.70	10.70	0.995295	0.0064-20.00
27	3-Oxochenodeoxycholic Acid	3OCDCA	389.2692	$C_{24}H_{38}O_4$	14.30	14.16	14.36	14.30	14.36	0.989009	0.0064-20.00
28	3-Oxodeoxycholic Acid	3ODCA	389.2692	$C_{24}H_{38}O_4$	14.55	14.55	blank	blank	blank	0.990249	0.0064-20.00
29	Norursodeoxycholic Acid	NorUDCA	377.2692	$C_{23}H_{38}O_4$	4.86	4.86	4.71	4.71	4.71	0.997704	0.0064-20.00
30	Nordeoxycholic Acid	NorDCA	377.2692	$C_{23}H_{38}O_4$	13.97	13.97	blank	blank	blank	0.000000	0.0064-20.00
31	Norcholic Acid	NorCA	393.2641	$C_{23}H_{38}O_5$	6.71	6.71	6.90	6.90	6.90	0.000000	0.0064-20.00
32	7,12-Diketolithocholic acid	7,12DKLCA	403.2484	$C_{24}H_{36}O_5$	2.37	2.18	2.23	2.23	2.23	0.995756	0.0064-20.00
33	6,7-Diketolithocholic acid	6,7DKLCA	403.2484	$C_{24}H_{36}O_5$	9.48	9.48	blank	blank	blank	0.939122	0.0064-20.00
34	12-Dehydrocholic Acid	12DHCA	405.2641	$C_{24}H_{38}O_5$	4.51	4.32	4.37	4.37	4.37	0.776529	0.0064-20.00
35	7-Dehydrocholic Acid	7DHCA	405.2641	$C_{24}H_{38}O_5$	5.39	5.16	5.20	5.20	5.20	0.995108	0.0064-20.00
36	7-Oxohyocholic acid (Takeda ketol)	7OHCA	405.2641	$C_{24}H_{38}O_5$	5.44	5.44	5.79	5.79	5.79	0.994842	0.0064-20.00
37	3-Dehydrocholic Acid	3DHCA	405.2641	$C_{24}H_{38}O_5$	7.93	7.74	7.74	7.78	7.74	0.988056	0.0064-20.00
38	Tauroursodeoxycholic Acid	TUDCA	498.2889	$C_{26}H_{45}NO_6S$	3.16	2.76	2.86	2.86	2.86	0.994893	0.0064-20.00
39	Taurohyodeoxycholic Acid	THDCA	498.2889	$C_{26}H_{45}NO_6S$	3.76	3.16	3.30	3.30	3.30	0.991427	0.0064-20.00
40	Taurochenodeoxycholic Acid	TCDCA	498.2889	$C_{26}H_{45}NO_6S$	9.03	7.88	8.07	8.07	8.07	0.991847	0.0064-20.00
41	Taurodeoxycholic Acid	TDCA	498.2889	$C_{26}H_{45}NO_6S$	10.39	8.85	9.09	9.09	9.09	0.993995	0.0064-20.00
42	Tauro α-Muricholic Acid	α-TMCA	514.2838	$C_{26}H_{45}NO_7S$	2.00	1.74	1.79	1.84	1.79	0.992274	0.0064-20.00
43	Tauro β-Muricholic Acid	β-TMCA	514.2838	$C_{26}H_{45}NO_7S$	2.16	1.74	1.79	1.84	1.79	0.992274	0.0064-20.00
44	Tauro ω-Muricholic Acid	ω-TMCA	514.2838	$C_{26}H_{45}NO_7S$	2.37	1.74	1.79	1.84	1.79	0.992274	0.0064-20.00
45	Taurohyocholic Acid	THCA	514.2838	$C_{26}H_{45}NO_7S$	3.06	2.67	2.76	2.76	2.76	0.992501	0.0064-20.00
46	Taurocholic Acid	TCA	514.2838	$C_{26}H_{45}NO_7S$	4.82	4.42	4.61	4.61	4.61	0.995597	0.0064-20.00
47	Taurolithocholic Acid	TLCA	482.2940	$C_{26}H_{45}NO_5S$	15.19	13.92	14.16	14.11	14.11	0.992438	0.0064-20.00
48	Taurodehydrocholic acid	TDHCA	508.2369	$C_{26}H_{39}NO_7S$	1.00	1.00	1.79	0.96	1.11	0.854634	0.0064-20.00
49	Tauroursocholanic Acid	TUCnA	466.2991	$C_{26}H_{45}NO_4S$	22.30	22.30	22.34	22.34	22.34	0.980344	0.0064-20.00
50	Glycoursodeoxycholic Acid	GUDCA	448.3063	$C_{26}H_{43}NO_5$	4.57	3.25	3.39	3.39	3.39	0.991414	0.0064-20.00
51	Glycohyodeoxycholic Acid	GHDCA	448.3063	$C_{26}H_{43}NO_5$	5.67	3.83	4.03	4.03	4.03	0.980736	0.0064-20.00
52	Glycochenodeoxycholic Acid	GCDCA	448.3063	$C_{26}H_{43}NO_5$	12.64	9.14	9.39	9.39	9.39	0.982927	0.0064-20.00
53	Glycodeoxycholic Acid	GDCA	448.3063	$C_{26}H_{43}NO_5$	14.05	10.41	10.70	10.70	10.70	0.986917	0.0064-20.00
54	β-Glycomuricholic Acid	β-GMCA	464.3012	$C_{26}H_{43}NO_6$	2.09	2.09	blank	blank	blank	0.593900	0.0064-20.00
55	Glycohyocholic Acid	GHCA	464.3012	$C_{26}H_{43}NO_6$	4.67	3.20	3.35	3.35	3.35	0.994290	0.0064-20.00
56	Glycocholic Acid	GCA	464.3012	$C_{26}H_{43}NO_6$	7.44	5.39	5.58	5.58	5.58	0.985872	0.0064-20.00
57	Glycolithocholic Acid	GLCA	432.3114	$C_{26}H_{43}NO_4$	18.19	15.23	15.43	15.43	15.43	0.839345	0.0064-20.00
58	Glycodehydrocholic acid	GDHCA	458.2543	$C_{26}H_{37}NO_6$	1.06	1.06	blank	blank	blank	0.000000	0.0064-20.00
D1	Cholic Acid d4	CA d4	411.3049	$C_{24}H_{36}D_4O_5$	11.74	11.23	11.53	11.53	11.53	0.000000	0.0064-20.00
D2	Chenodeoxycholic Acid d4	CDCA d4	395.3099	$C_{24}H_{36}D_4O_4$	19.00	17.18	17.37	17.37	17.37	0.000000	0.0064-20.00
D3	Deoxycholic Acid d4	DCA d4	395.3099	$C_{24}H_{36}D_4O_4$	20.20	17.86	18.06	18.06	18.06	0.000000	0.0064-20.00



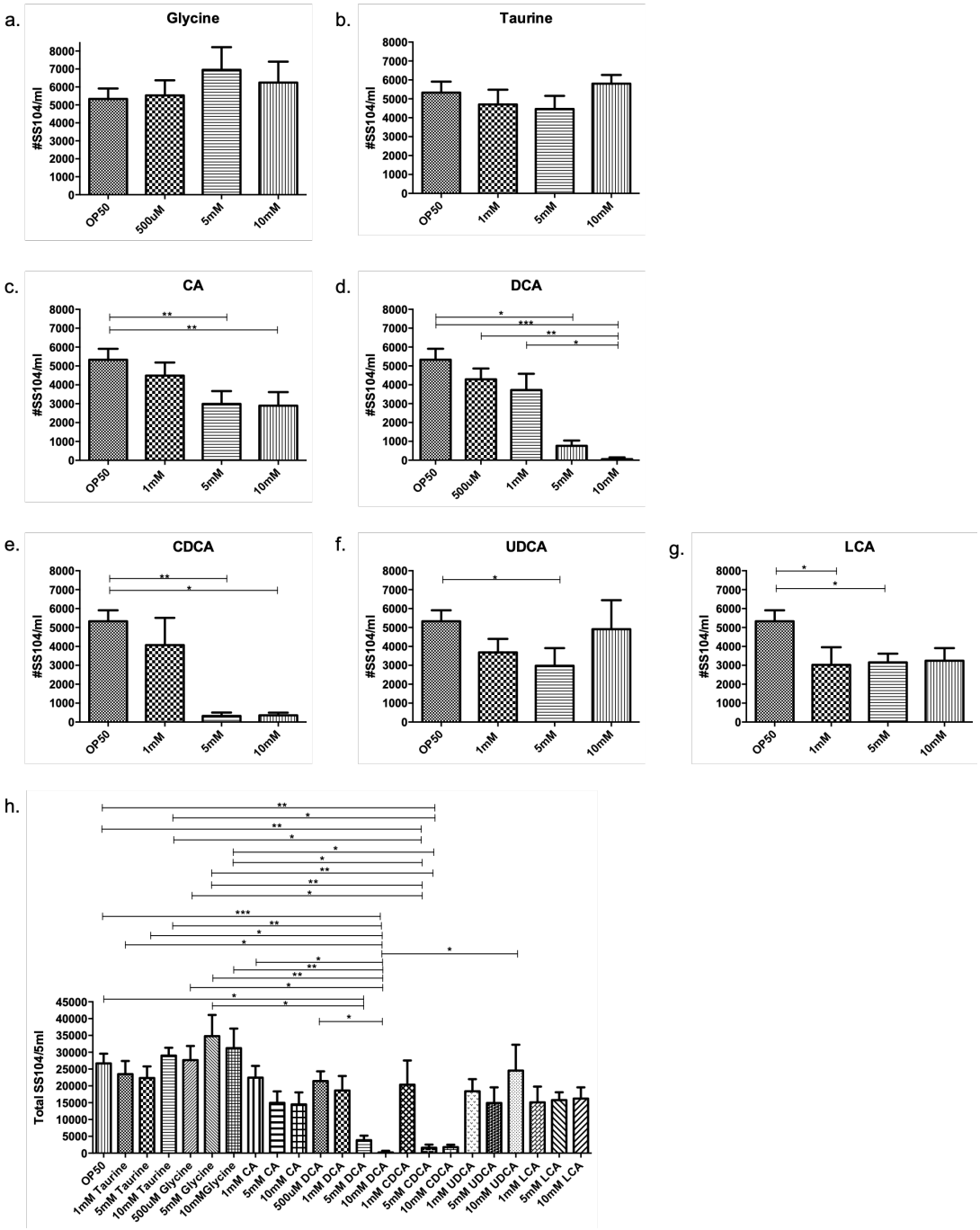
SI.4.3: Representative Chromatograms displaying the full mass spectra of *E. coli* OP50 bile acids for control: (a) no bile acid and treatments: (b) taurine, (c-d) primary bile acids and (e-g) secondary bile acids.



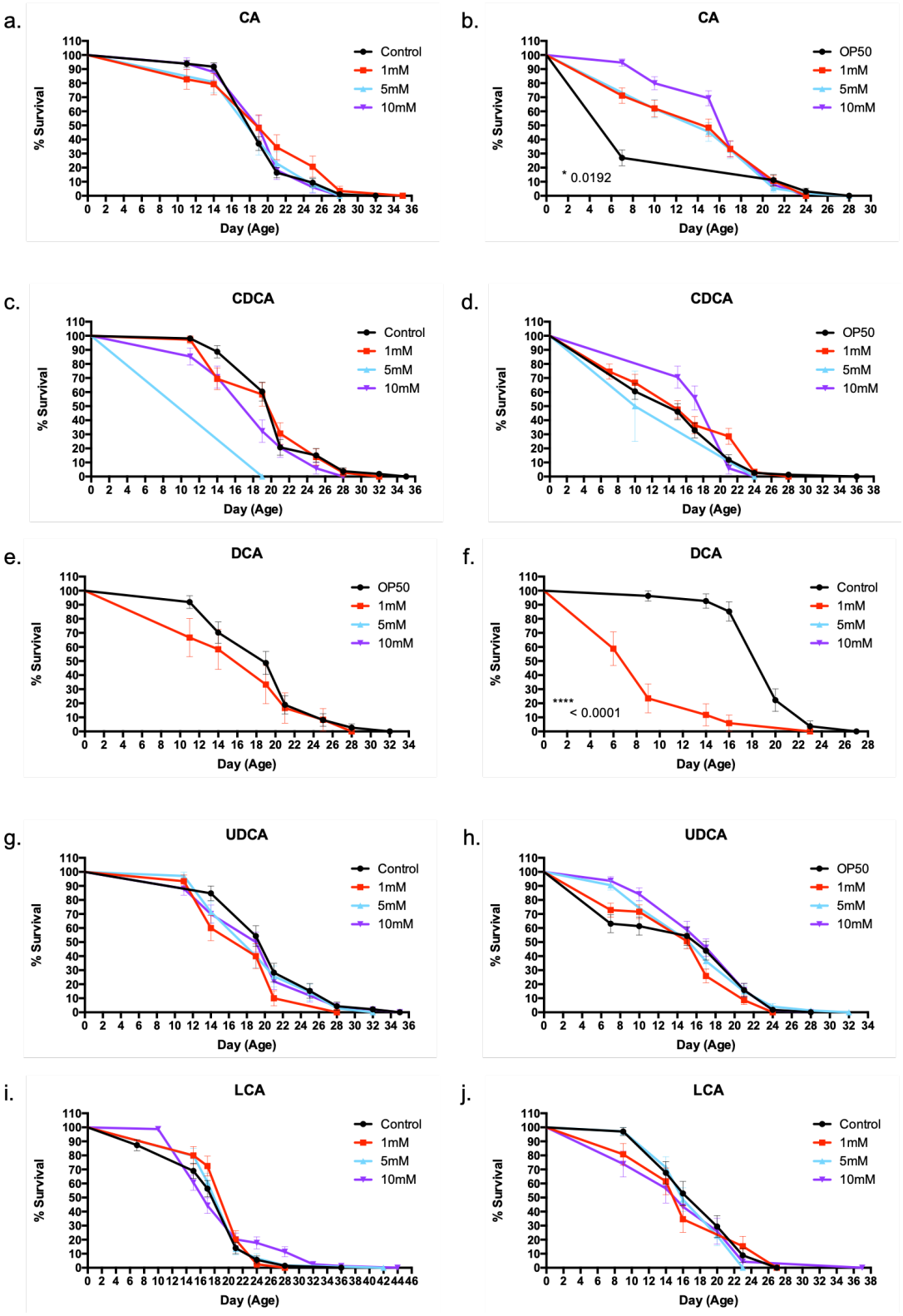
SI.4.4: Representative Chromatograms displaying the full mass spectra of *C. elegans* SS104 bile acids for control: (a) no bile acid and treatments: (b) taurine, (c-d) primary bile acids and (e-g) secondary bile acids.



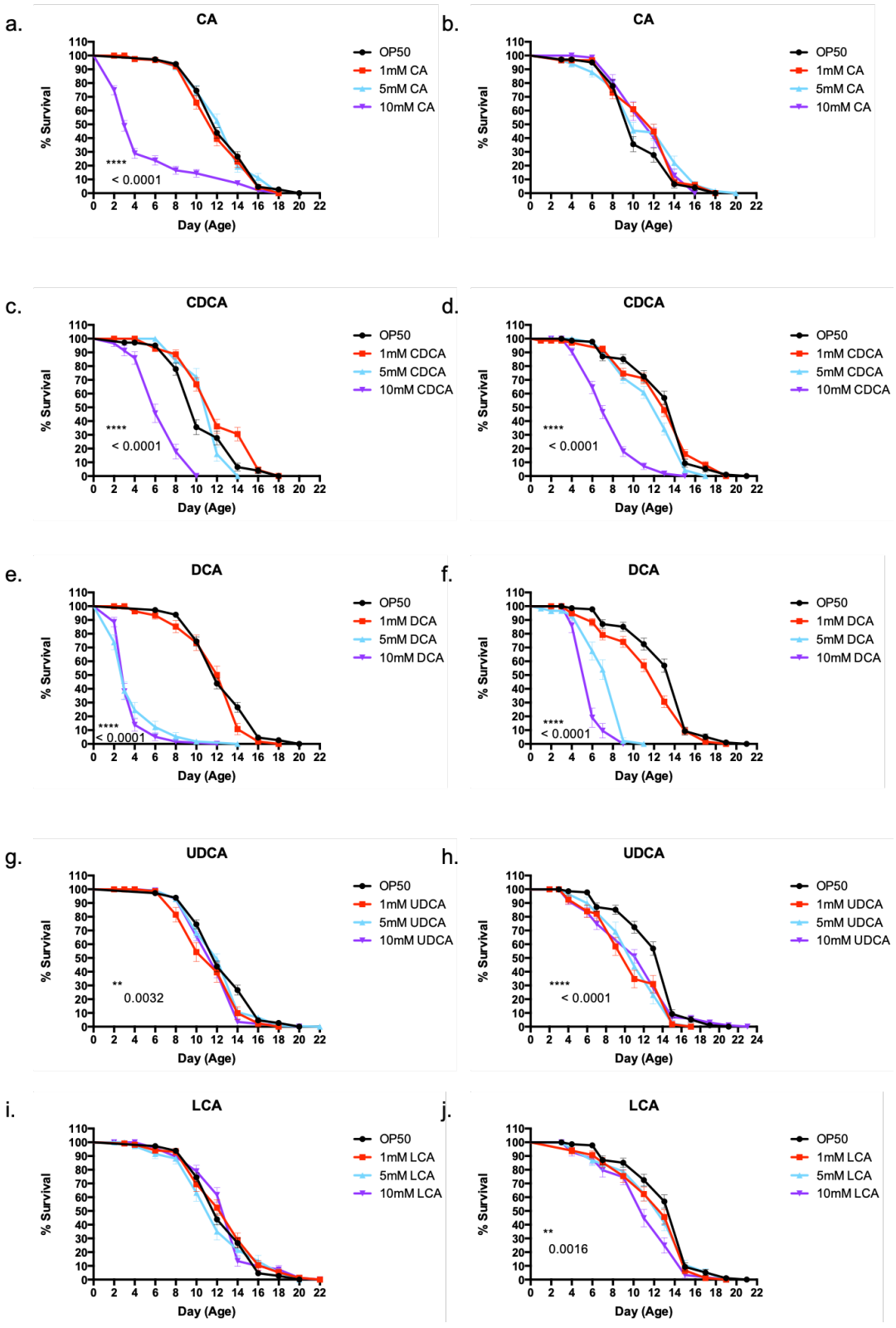
SI.4.5: Internal standard Cholic Acid d4 extraction efficiency for *E. coli* and *C. elegans* study. All concentrations were quantified against standard curves for each analyte and normalised according to internal standards using Targetlynx^{TM} (Waters Ltd.) software. Data was plotted using GraphPrism v6 and is represented as mean ± SD. Statistical significance is indicated and calculated using Kruskal-Wallis and Dunn's Multiple Comparison Test (*= p<0.05; **=p<0.01; ***=p<0.001; ****=p<0.0001).



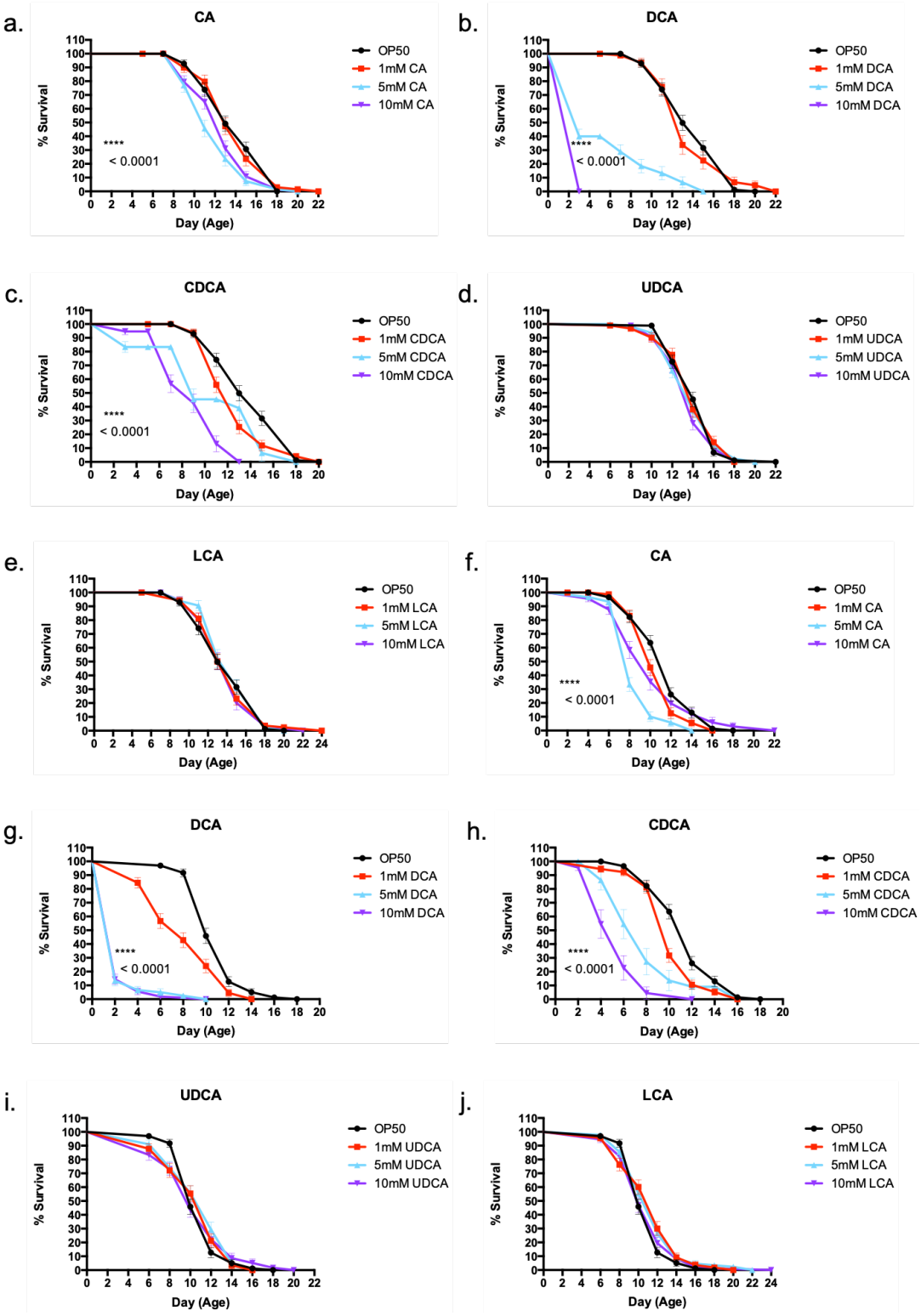
SI.4.6: Quantity of *C. elegans* collected for UPLC-MS. (a) glycine, (b) taurine, (c and e) primary bile acids and (d, f and g) secondary bile acids, (h) summary of all treatments. All concentrations were quantified against standard curves for each analyte and normalised according to internal standards using Targetlynx™ (Waters Ltd.) software. Data was plotted using GraphPrism v6 and is represented as mean ± SD. Statistical significance is indicated and calculated using Kruskal-Wallis and Dunn's Multiple Comparison Test (*= p<0.05; **=p<0.01; ***=p<0.001; ****=p<0.0001).



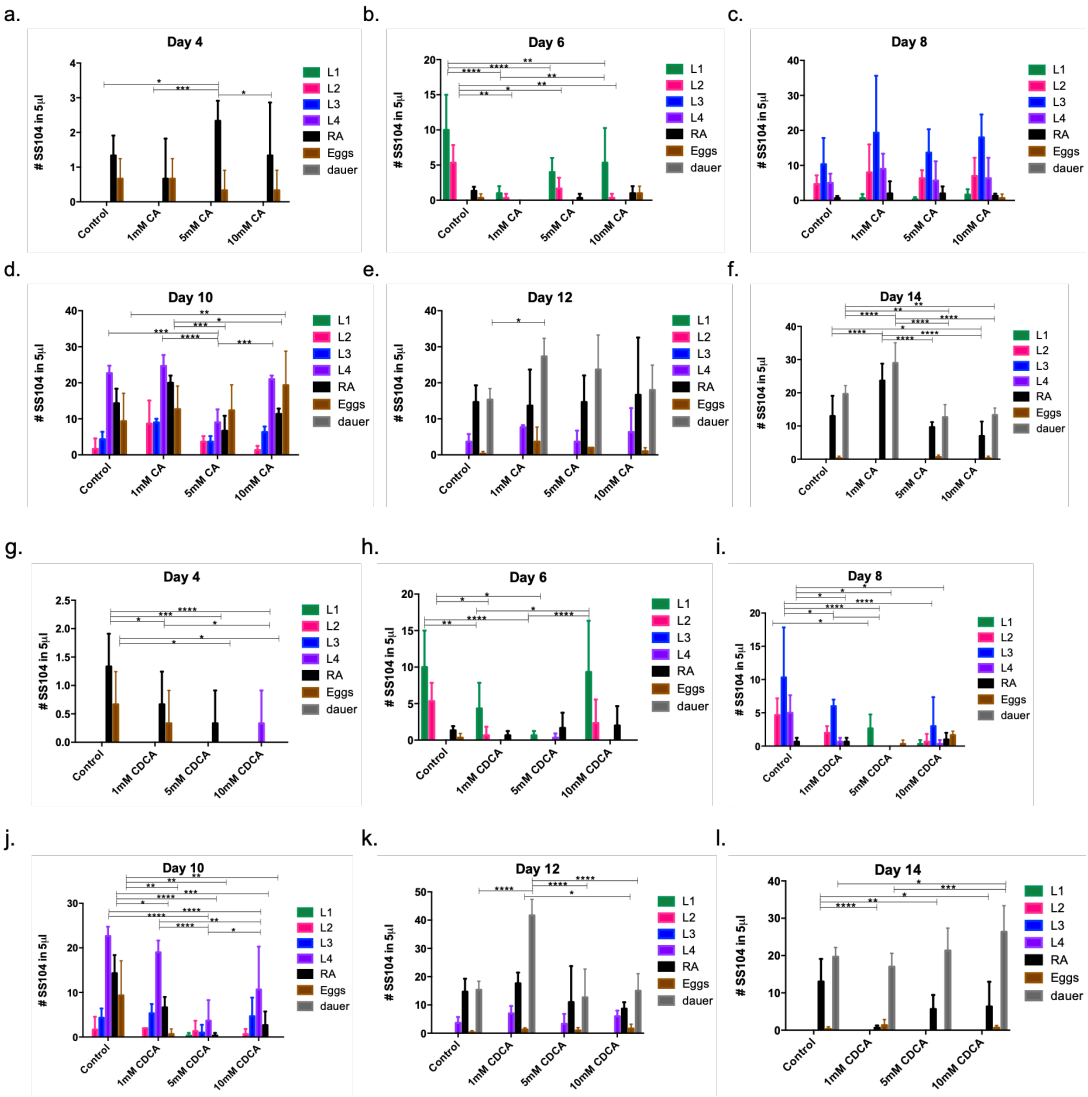
SI.4.7: Replicate lifespan *C. elegans* strain SS104 L1 larvae (a-d) primary bile acids and (e-j) secondary bile acids. Data was plotted using GraphPrism v6. Statistical analysis was performed through application of the log-rank test for survival curves (*= p<0.05; **=p<0.01; ***=p<0.001; ****=p<0.0001).



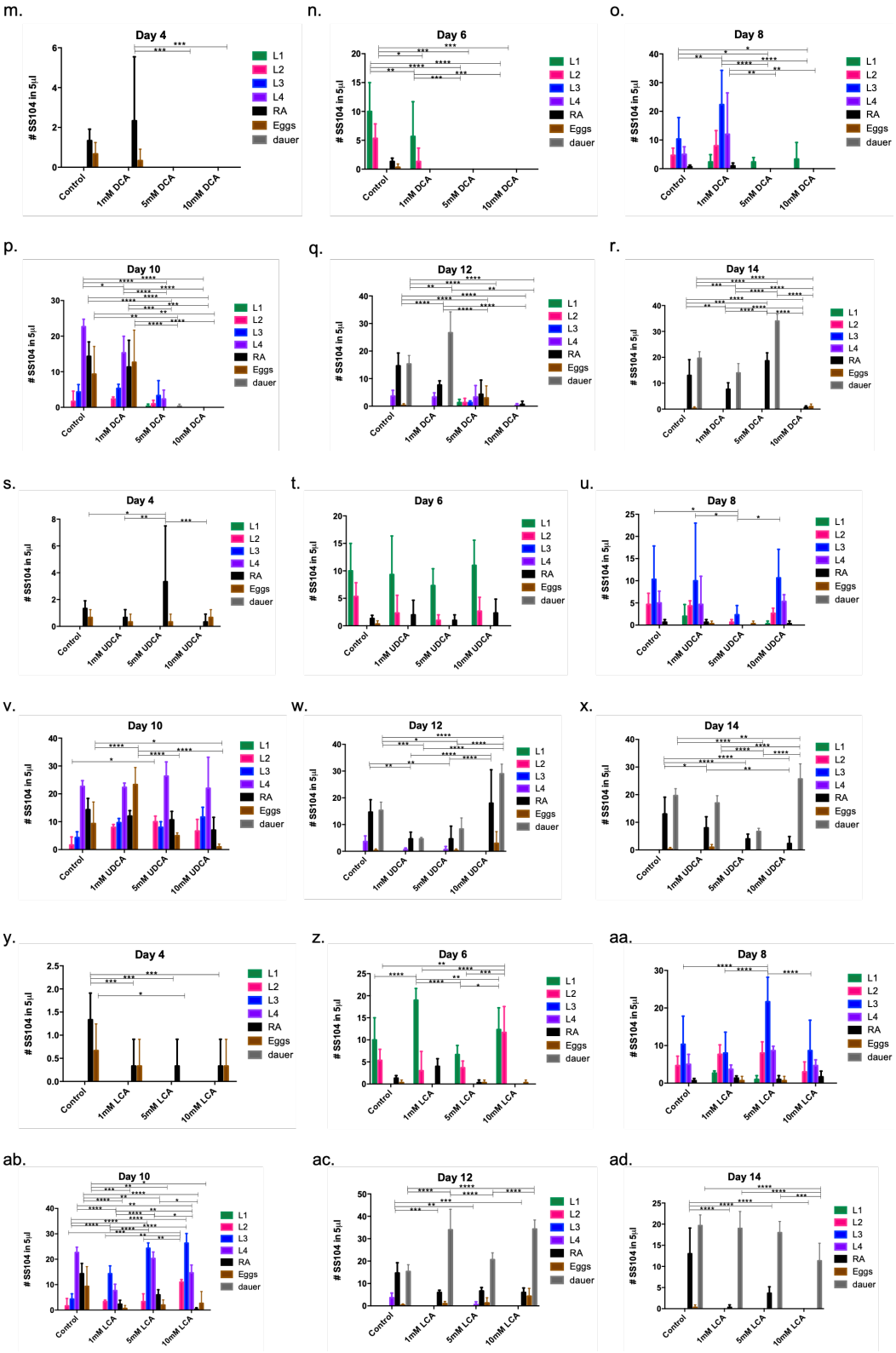
SI.4.8: Replicate lifespan *C. elegans* strain SS104 L4 larvae (a-d) primary bile acids and (e-j) secondary bile acids. Data was plotted using GraphPrism v6. Statistical analysis was performed through application of the log-rank test for survival curves (*= p<0.05; **=p<0.01; ***=p<0.001; ****=p<0.0001).



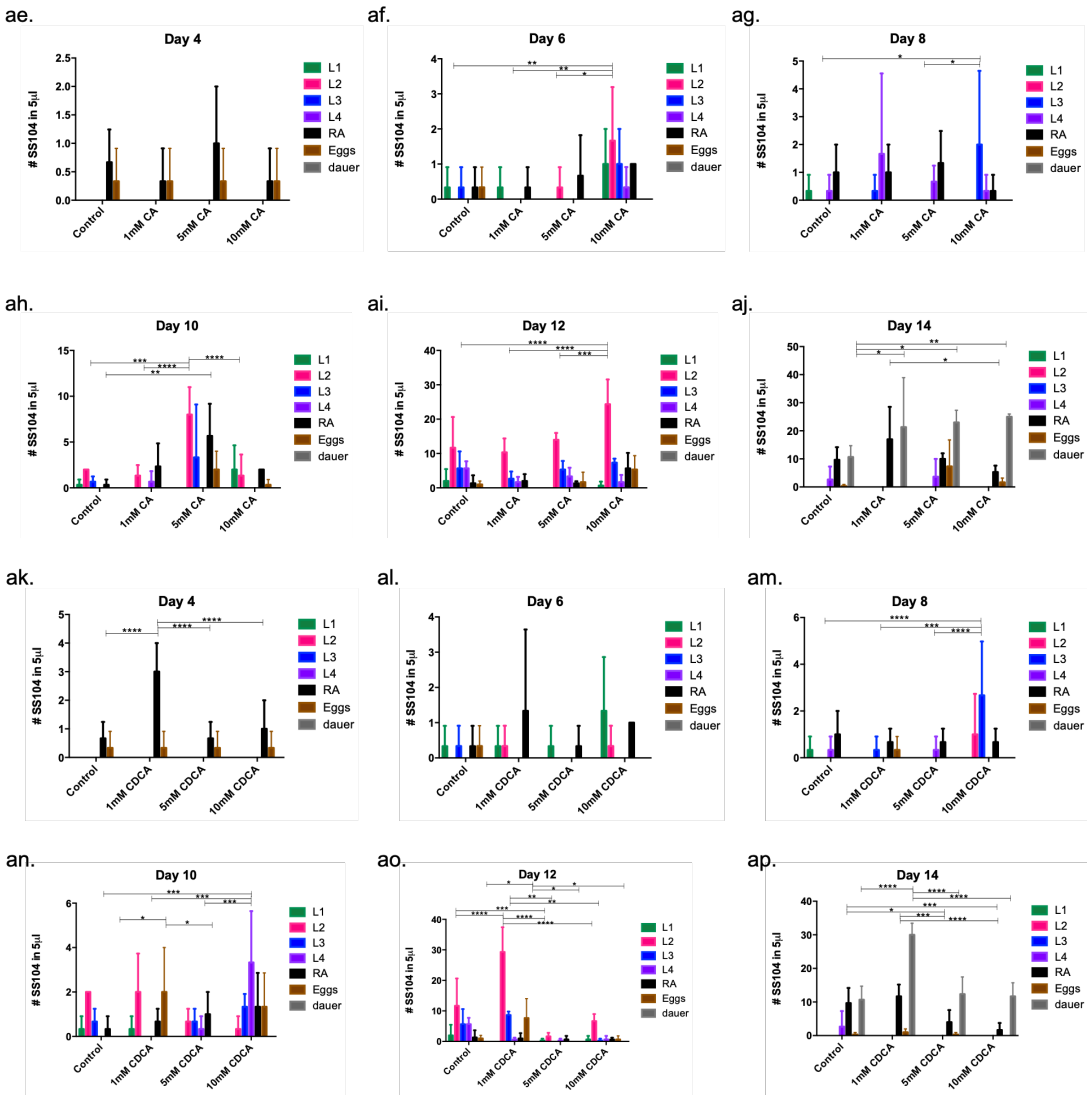
SI.4.9: Lifespan *C. elegans* strain N2 L1 larvae (a and c) primary bile acids and (b, d and e) secondary bile acids; and L4 larvae (f and h) primary bile acids and (g, i and j) secondary bile acids. Data was plotted using GraphPrism v6. Statistical analysis was performed through application of the log-rank test for survival curves (*= p<0.05; **=p<0.01; ***=p<0.001; ****=p<0.0001).



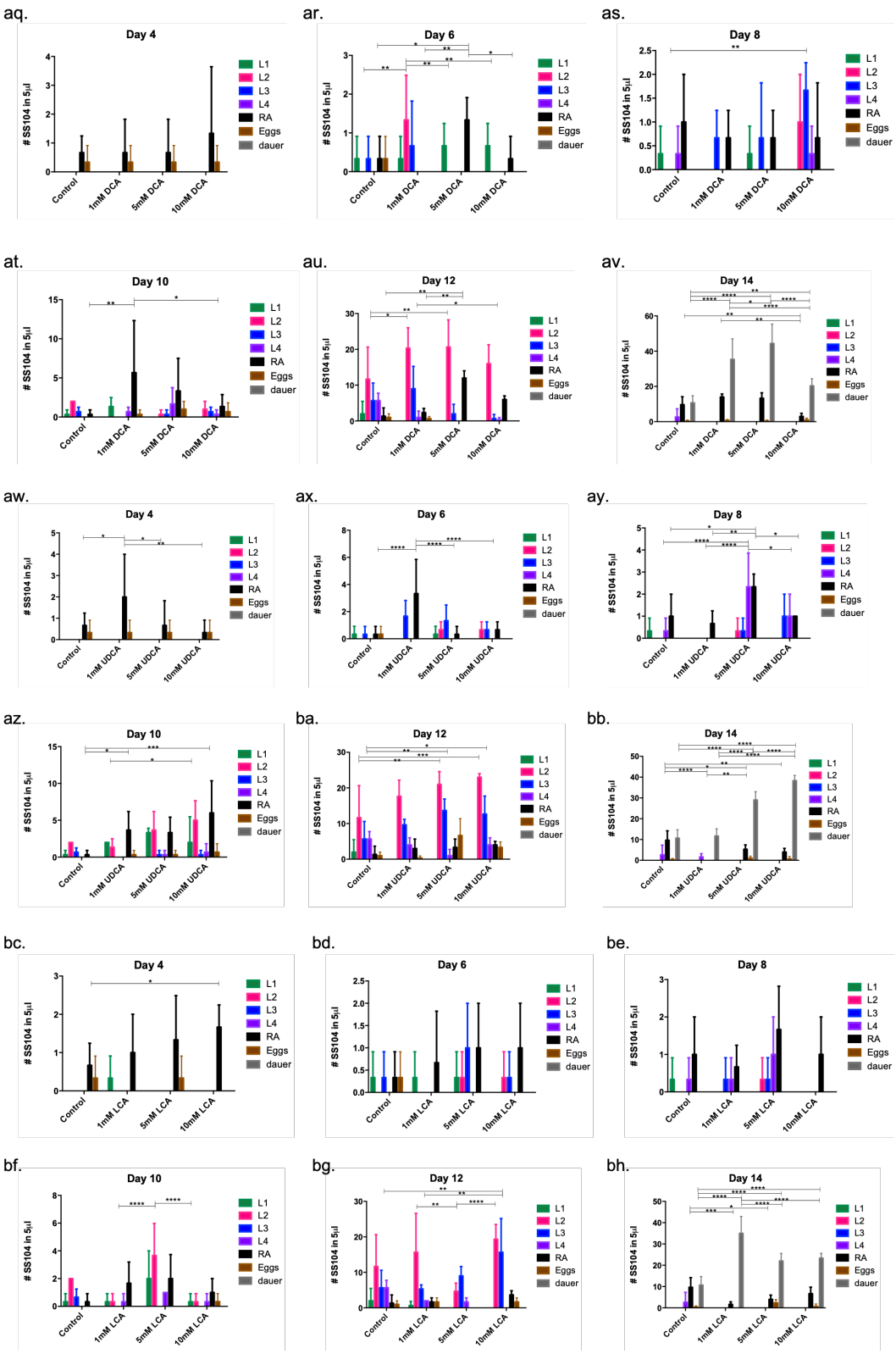
SI.4.10: Development *C. elegans* strain SS104 L1 larvae (a-l) primary bile acids from day 4 to day 14. Data was plotted using GraphPrism v6. Statistical significance is indicated and calculated using Kruskal-Wallis, Dunn's Multiple Comparison Test and Tukey's Multiple Comparison Test (*= p<0.05; **=p<0.01; ***=p<0.001; ****=p<0.0001).



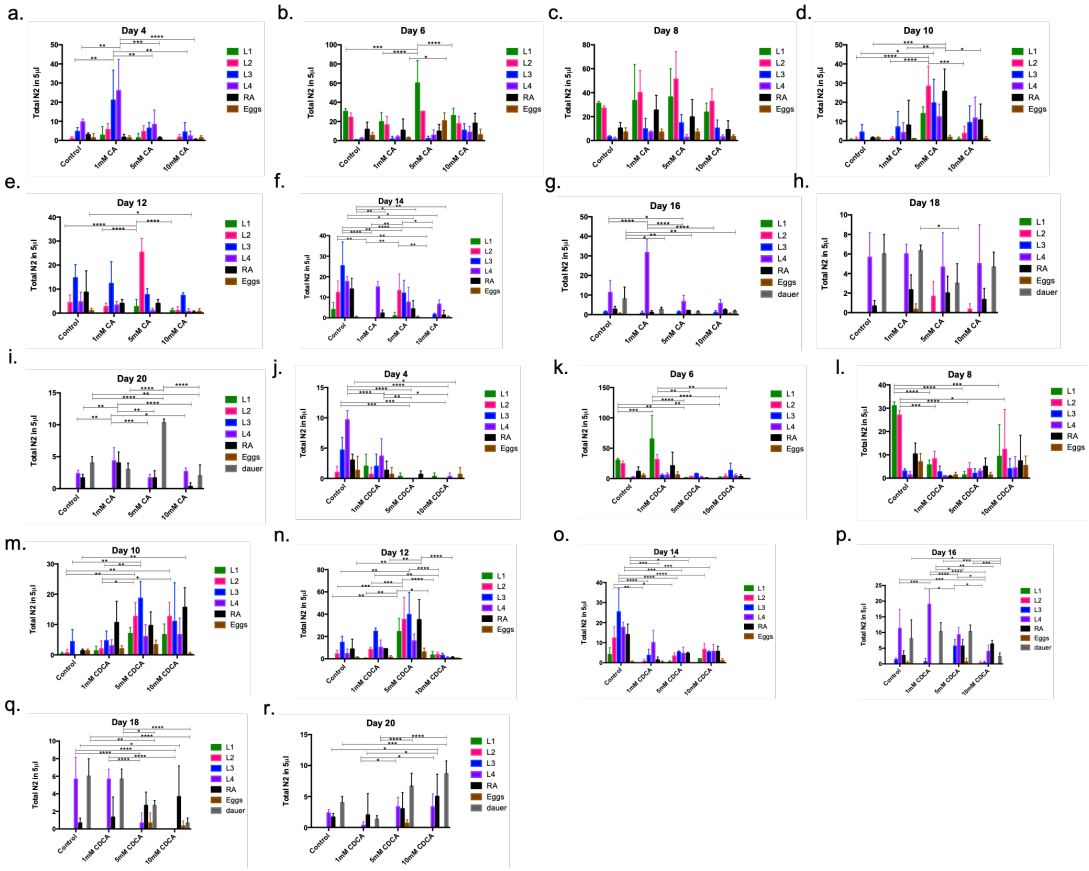
SI.4.10 continued: Development *C. elegans* strain SS104 L1 larvae (m-ad) secondary bile acids from day 4 to day 14. Data was plotted using GraphPrism v6. Statistical significance is indicated and calculated using Kruskal-Wallis, Dunn's Multiple Comparison Test and Tukey's Multiple Comparison Test (*= p<0.05; **=p<0.01; ***=p<0.001; ****=p<0.0001).



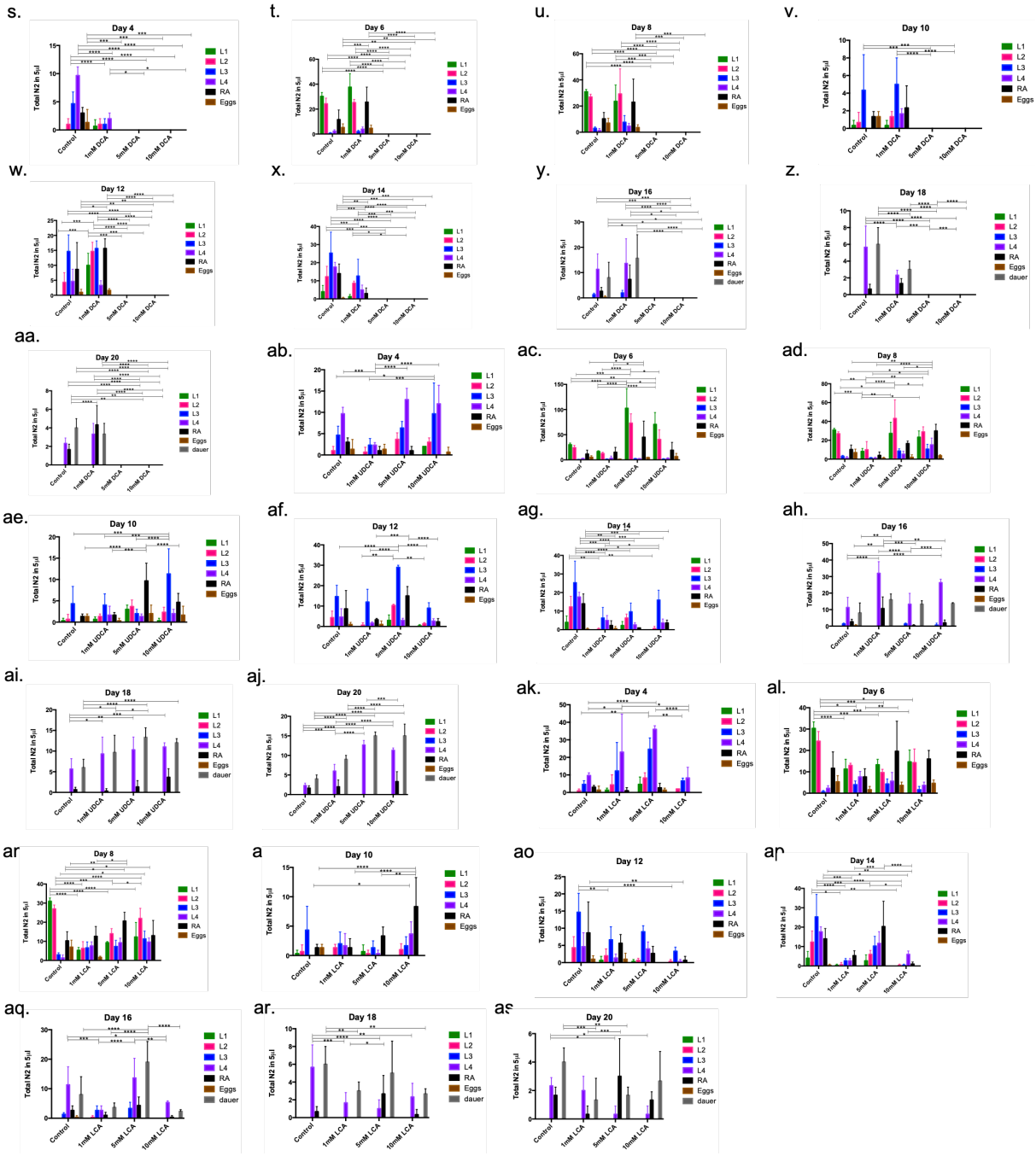
SI.4.10 continued: Development *C. elegans* strain SS104 L1 larvae (ae-ap) primary bile acids from day 4 to day 14. Data was plotted using GraphPrism v6. Statistical significance is indicated and calculated using Kruskal-Wallis, Dunn's Multiple Comparison Test and Tukey's Multiple Comparison Test (*= p<0.05; **=p<0.01; ***=p<0.001; ****=p<0.0001).



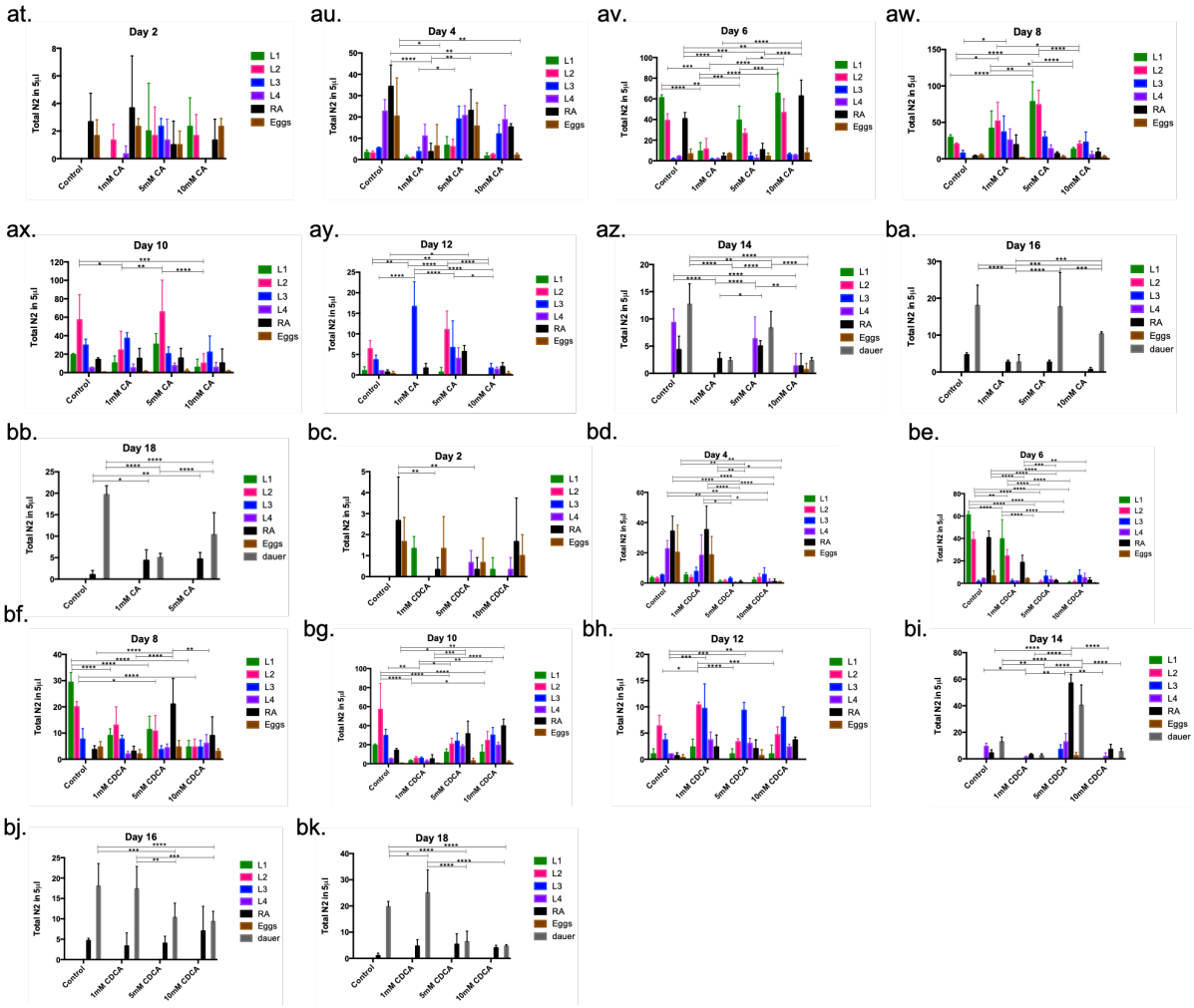
SI.4.10 continued: Development *C. elegans* strain SS104 L1 larvae (aq-bh) secondary bile acids from day 4 to day 14. Data was plotted using GraphPrism v6. Statistical significance is indicated and calculated using Kruskal-Wallis, Dunn's Multiple Comparison Test and Tukey's Multiple Comparison Test (*= p<0.05; **=p<0.01; ***=p<0.001; ****=p<0.0001).



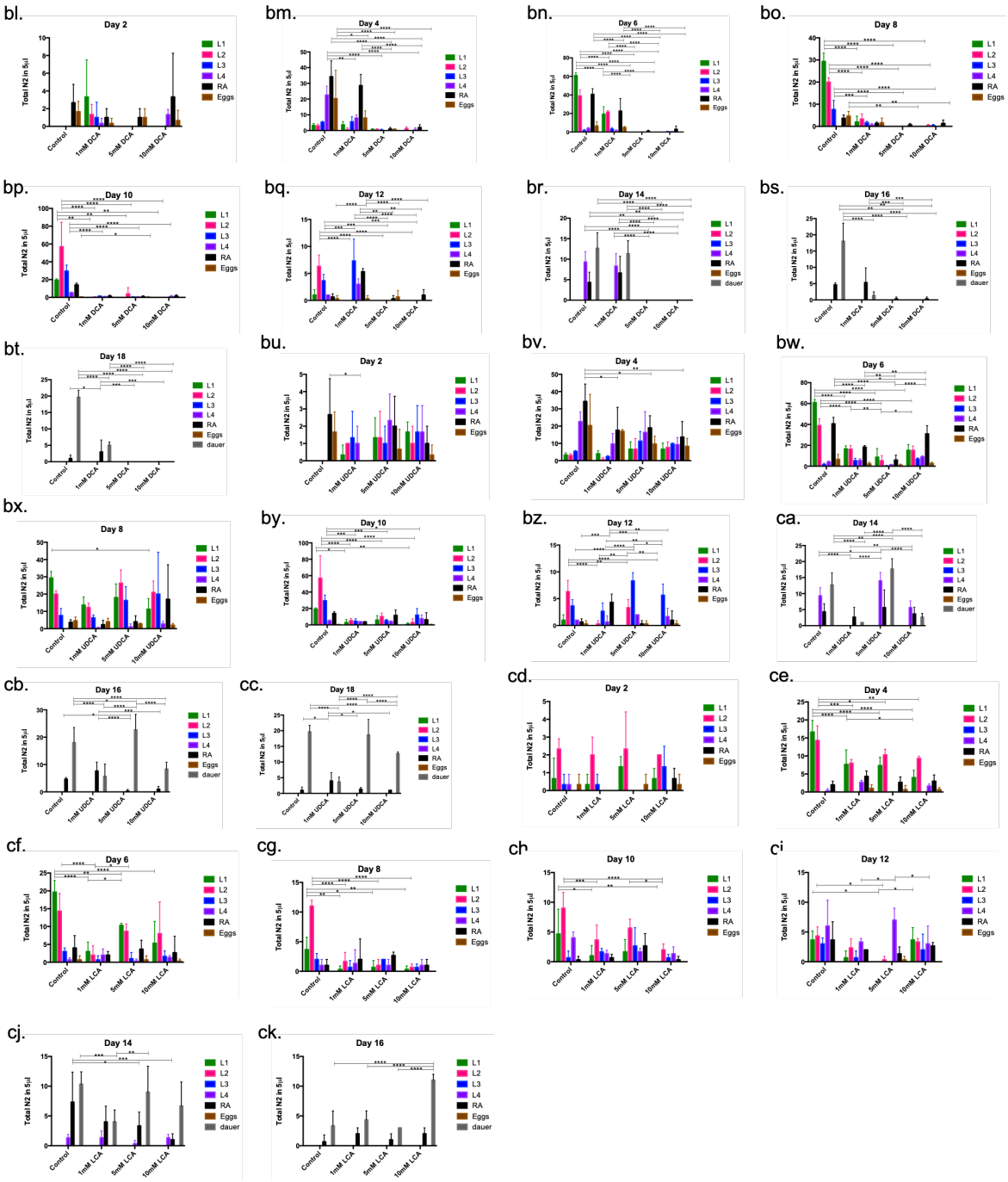
SI.4.11: Development *C. elegans* strain N2 L1 larvae (a-r) primary bile acids, from day 4 to day 20. Data was plotted using GraphPrism v6. Statistical significance is indicated and calculated using Kruskal-Wallis, Dunn's Multiple Comparison Test and Tukey's Multiple Comparison Test (*= $p<0.05$; **=$p<0.01$; ***=$p<0.001$; ****=$p<0.0001$).



SI.4.11 continued: Development *C. elegans* strain N2 L1 larvae (s-as) secondary bile acids, from day 4 to day 20. Data was plotted using GraphPrism v6. Statistical significance is indicated and calculated using Kruskal-Wallis, Dunn's Multiple Comparison Test and Tukey's Multiple Comparison Test (*= p<0.05; **=p<0.01; ***=p<0.001; ****=p<0.0001).



SI.4.11 continued: Development *C. elegans* strain N2 L1 larvae (at-bk) primary bile acids, from day 2 to day 18. Data was plotted using GraphPrism v6. Statistical significance is indicated and calculated using Kruskal-Wallis, Dunn's Multiple Comparison Test and Tukey's Multiple Comparison Test (*= p<0.05; **=p<0.01; ***=p<0.001; ****=p<0.0001).



SI.4.11 continued: Development *C. elegans* strain N2 L1 larvae (bl-ck) secondary bile acids, from day 4 to day 18. Data was plotted using GraphPrism v6. Statistical significance is indicated and calculated using Kruskal-Wallis, Dunn's Multiple Comparison Test and Tukey's Multiple Comparison Test (*= p<0.05; **=p<0.01; ***=p<0.001; ****=p<0.0001).

SI.4.12: Table of total differentially transcribed genes with adjusted p-value >0.05, in *C. elegans* strain SS104 cultured with bile acid 1 mM LCA, compared to 1 mM CDCA. The base mean value, Log_2 Fold Change, Standard error and adjusted p-value are represented.

Gene name	Mean	Fold Change (log2)	Standard Error	adjusted p-value
lips-15	726.095978	3.71697904	0.40121903	2.05E-16
cest-35.2	211.743037	-4.3386145	0.48052948	9.05E-16
F44E5.4	150.727883	-5.1818182	0.59524189	1.10E-14
C50F7.5	1239.1348	3.61191372	0.43084733	1.34E-13
R05D8.9	302.451764	-3.8605737	0.47340365	7.29E-13
clec-83	1738.02665	3.09817541	0.39093528	3.96E-12
F44E5.5	211.198658	-3.7706834	0.48254506	8.24E-12
sec-61.A	1803.27747	2.6082539	0.35475005	2.54E-10
F14H12.3	735.089696	3.02388024	0.41789254	5.35E-10
F32A5.4	3172.21714	3.05583839	0.43585679	2.47E-09
cpn-4	4076.60551	2.27591012	0.33039068	4.90E-09
E02C12.6	282.092097	-3.4440828	0.49970354	4.90E-09
E01G4.5	525.524833	3.00973987	0.44284252	8.60E-09
gpx-3	401.439565	2.85428883	0.42455974	1.33E-08
rnst-2	983.882031	2.41869586	0.36099045	1.45E-08
nspc-1	795.701578	2.65223252	0.40206445	2.74E-08
kat-1	1114.49724	2.41379207	0.37015226	4.28E-08
nspc-14	3241.17451	2.39414274	0.37072763	6.15E-08
thn-1	615.574168	2.61465139	0.4061418	6.65E-08
vap-1	341.652288	2.5295184	0.39458529	7.56E-08
nhr-17	299.693222	-3.3695787	0.52883061	9.28E-08
lec-2	8437.49407	2.16256296	0.34452206	1.64E-07
mthf-1	582.688012	2.29475144	0.36804624	2.05E-07
nspc-7	701.029804	2.44785008	0.39390012	2.24E-07
F35B12.9	567.98548	2.94369812	0.47526032	2.45E-07
srap-1	644.953529	2.48090228	0.40150891	2.59E-07
inf-1	184.781231	3.47821271	0.56395479	2.68E-07
gtbp-1	728.144626	2.20388816	0.36169171	3.78E-07
col-158	1505.89693	2.11219959	0.3467891	3.78E-07
aqp-7	6032.71469	2.09809567	0.34421783	3.78E-07
cht-1	67.7241112	4.28058217	0.70152863	3.78E-07

drr-2	434.819573	2.26559914	0.37776029	6.53E-07
odc-1	1041.69362	2.10074083	0.35134579	7.09E-07
F21F3.6	2584.95246	2.23320319	0.37405016	7.26E-07
marg-1	714.456116	2.95216893	0.49668372	8.30E-07
Y54G2A.10	751.321938	2.27795401	0.38491827	8.94E-07
acly-1	684.811168	2.17960596	0.36792239	8.94E-07
nlp-14	1740.65694	2.30678858	0.38965664	8.94E-07
acs-13	528.133588	2.5718003	0.43506527	9.07E-07
F55H12.4	6622.22617	2.02563272	0.34343361	9.58E-07
wwp-1	677.339456	2.1345904	0.36273273	9.90E-07
K09C6.9	713.94382	2.12727419	0.36131974	9.90E-07
glt-1	1014.4151	2.09224984	0.3567078	1.09E-06
chat-1	636.883993	2.2831144	0.39008684	1.15E-06
ugt-36	347.481764	-2.9057552	0.49749604	1.20E-06
hip-1	1879.20641	2.18389124	0.37430471	1.22E-06
maph-1.1	1012.97122	2.24650678	0.38555732	1.23E-06
aqp-2	643.609609	2.55310319	0.43793599	1.23E-06
flp-9	3371.95099	2.11567075	0.36414681	1.33E-06
ifa-1	968.947981	2.44951371	0.4221155	1.36E-06
paa-1	1552.23308	2.10759518	0.36358779	1.38E-06
hsp-12.2	3379.97415	2.14929546	0.37165394	1.43E-06
dlst-1	2144.38235	2.03518131	0.35203269	1.43E-06
xbx-6	809.455502	2.33818346	0.40415731	1.43E-06
uaf-1	156.96915	2.70805925	0.4689385	1.43E-06
snx-1	543.193524	2.13862861	0.3703188	1.43E-06
mdh-2	7321.97807	1.94982661	0.34156147	2.08E-06
ncs-2	1176.51099	1.98045465	0.3471252	2.09E-06
sup-26	514.891752	2.24221265	0.39328437	2.10E-06
hrg-1	429.822927	2.67311647	0.47000981	2.24E-06
tre-2	495.193932	2.10811963	0.37202451	2.49E-06
mbf-1	689.521724	2.02749443	0.35814916	2.49E-06
F53A9.1	886.20063	1.96332378	0.34676334	2.49E-06
lap-2	1496.69519	2.01207523	0.35618665	2.63E-06
T21D12.12	715.938519	2.01591538	0.35896605	3.14E-06
ida-1	1338.56682	2.09743071	0.37506993	3.54E-06
clik-3	1003.36459	2.15917276	0.38646987	3.54E-06
adss-1	6268.56552	1.90389758	0.34072588	3.54E-06
nlp-6	1647.51137	2.07113925	0.37213245	3.95E-06

sqt-3	639.213432	2.09206331	0.37649122	4.08E-06
nspc-19	1571.13172	1.94014357	0.34926076	4.08E-06
gpx-5	1961.20112	1.98989614	0.358453	4.10E-06
T28D6.5	443.024678	2.4535625	0.44291394	4.33E-06
dpy-18	580.483788	2.2166134	0.4009107	4.54E-06
Y53H1B.2	5234.51725	1.97529681	0.35784572	4.71E-06
R107.5	315.557911	-2.5263643	0.45894263	5.07E-06
egl-21	10807.0521	2.11249613	0.38407255	5.14E-06
ubxn-1	313.427049	2.21351931	0.40309008	5.21E-06
nlp-11	1592.4844	2.00343639	0.36479021	5.21E-06
srp-1	1331.77175	1.93837281	0.35300591	5.21E-06
clec-1	8654.8254	1.77178546	0.32292013	5.27E-06
T22F3.11	5915.38263	2.34267471	0.42720605	5.30E-06
prmt-1	2202.47762	2.08032358	0.37962349	5.34E-06
cpl-1	19751.7484	1.87144537	0.34192696	5.48E-06
gpb-1	1917.5896	2.17633861	0.39831855	5.71E-06
unc-51	617.451193	2.0100569	0.36800782	5.71E-06
fln-1	2158.35308	1.85222297	0.33963478	5.92E-06
C29H12.2	810.313887	1.92979933	0.35418149	6.01E-06
Y9C2UA.1	334.613975	2.5835501	0.47640758	6.87E-06
dod-24	2749.80467	-1.8413131	0.33969536	6.89E-06
gba-4	608.177003	-2.0025209	0.37068823	7.54E-06
inx-12	1133.34539	2.05320648	0.38105589	7.98E-06
F13E9.15	892.210623	2.74333311	0.50907208	7.98E-06
sti-1	327.649218	2.28436597	0.42413198	7.99E-06
unc-54	14664.5975	1.7760246	0.33092082	8.79E-06
sdha-1	2758.17943	1.90725613	0.35564024	8.90E-06
F09G2.2	702.750702	1.90938616	0.3571038	9.62E-06
F20G2.2	645.873767	2.00487518	0.37527211	9.76E-06
twf-2	624.194354	2.24161623	0.41997959	9.93E-06
W05B5.1	841.998581	2.09961045	0.39365847	1.00E-05
Y110A2AL.9	4166.31176	1.91605626	0.35969899	1.03E-05
Y71F9B.13	1351.97484	1.78294518	0.33510729	1.05E-05
egl-3	4881.29028	2.21514764	0.41649924	1.05E-05
T16G1.4	130.784434	-2.736857	0.51452334	1.05E-05
sbt-1	6001.30423	2.10053859	0.3956204	1.09E-05
W04G3.5	454.317482	2.0265864	0.38207111	1.11E-05
ntl-2	678.682071	1.90786551	0.36045323	1.16E-05

lec-10	1352.88193	1.77516431	0.3354608	1.16E-05
pyc-1	1469.52817	1.84353784	0.3482321	1.16E-05
fum-1	3665.45702	1.87665584	0.35485945	1.17E-05
rmd-2	2058.02232	1.75420878	0.33183322	1.17E-05
H10E21.5	274.886958	2.81464198	0.53294092	1.19E-05
dab-1	761.700382	1.88202472	0.35692342	1.24E-05
ret-1	2506.50811	1.76959169	0.33593537	1.26E-05
pdhb-1	647.671529	1.87275561	0.356222	1.32E-05
cTel55X.1	511.019138	1.93713406	0.3685145	1.32E-05
lido-9	61.9374812	3.55151629	0.67616886	1.34E-05
T02B11.3	3256.17469	1.83967508	0.350363	1.34E-05
B0454.6	424.258685	2.2100754	0.42112309	1.35E-05
K02A11.4	1484.16527	-2.4224747	0.46202177	1.36E-05
Y54E2A.4	220.326911	2.26083248	0.43114521	1.36E-05
hmg-1.1	5124.99347	1.90823126	0.36488093	1.45E-05
clec-82	438.989678	2.19622506	0.42040133	1.48E-05
ZK1058.9	1434.86197	1.74685706	0.33503973	1.55E-05
Y8A9A.2	3520.22229	2.01880197	0.38751838	1.58E-05
nspc-10	4139.65888	1.80350821	0.34660065	1.62E-05
Y48G1BR.1	252.436855	2.46122224	0.47341273	1.63E-05
cts-1	9463.2956	1.72846885	0.3325544	1.63E-05
C07A12.2	110.868486	3.02313313	0.58144224	1.63E-05
flp-3	1988.86479	2.11284382	0.40668243	1.64E-05
K08E3.5	2608.08143	1.86385693	0.35948623	1.72E-05
hpo-19	77.0864017	3.47831196	0.67124109	1.73E-05
F37H8.5	9413.51199	1.6614118	0.32117883	1.81E-05
myo-1	804.234636	2.4484492	0.47410428	1.88E-05
F09C6.13	87.9989153	3.12973407	0.6073878	1.98E-05
nex-1	7348.00854	1.759944	0.34294541	2.20E-05
rncs-1	41740.6821	-2.0206646	0.39433106	2.27E-05
rab-1	2976.66576	1.73403734	0.33866549	2.31E-05
clik-2	2139.42811	2.22415842	0.43517078	2.40E-05
C15C7.4	365.668562	2.51390286	0.49311463	2.56E-05
Y37E3.17	1564.99571	1.72021525	0.33810391	2.68E-05
unc-42	41.1891907	4.29424492	0.84487974	2.73E-05
ZC395.5	4297.32974	-1.6751097	0.32974092	2.75E-05
C08F11.13	1787.59874	-1.7262679	0.33997827	2.77E-05
nspc-17	1154.0154	1.8686229	0.3683897	2.82E-05

clec-4	69.7983424	3.6457082	0.72161865	3.12E-05
glc-2	219.514015	2.3967601	0.4745835	3.13E-05
eef-1A.2	16647.8088	1.60521384	0.31803387	3.16E-05
dpf-5	987.494334	1.78293138	0.35384509	3.28E-05
Y52B11A.4	95.095046	3.12920365	0.6214998	3.32E-05
unc-15	10752.2182	1.6073167	0.31992409	3.49E-05
pygl-1	3511.99793	1.78130845	0.35470117	3.51E-05
srd-28	35.5157204	5.66326239	1.12994013	3.67E-05
C04H5.7	931.18082	-2.1356	0.4264799	3.73E-05
tkt-1	4171.69001	1.76659077	0.35322308	3.78E-05
C14C6.2	1611.8979	1.6684874	0.33354077	3.78E-05
ncx-2	805.916136	2.65359427	0.53033047	3.78E-05
dcar-1	1059.11895	1.86334082	0.37321538	3.93E-05
W04B5.3	316.718651	2.00163177	0.40299636	4.43E-05
dli-1	358.446486	2.05901044	0.41446442	4.43E-05
hsp-25	4610.78155	1.6678807	0.33610585	4.51E-05
F48C1.9	8425.18264	-1.6365611	0.33004584	4.57E-05
myo-3	1068.28434	1.6882468	0.34086149	4.68E-05
clc-3	132.006527	2.53914753	0.51344755	4.83E-05
dnpp-1	324.038902	2.04280229	0.41361218	4.96E-05
lfi-1	1157.95816	1.69002028	0.34247554	5.04E-05
F37C4.6	557.272277	1.78401603	0.3616135	5.04E-05
sdhb-1	2766.19596	1.60629672	0.32615265	5.24E-05
F13D12.9	593.794578	2.26494745	0.46059045	5.36E-05
ldh-1	1451.86418	1.80499586	0.36693999	5.36E-05
cmd-1	3598.36693	1.80839198	0.36779999	5.36E-05
T08B1.4	1271.67144	1.93906014	0.39516639	5.61E-05
W10C8.5	2236.40987	1.64683346	0.33599877	5.67E-05
pqn-41	201.571019	2.15648573	0.439937	5.67E-05
F20D1.3	1864.63965	1.89156961	0.38592015	5.67E-05
sqst-1	636.144686	1.82951802	0.37368542	5.80E-05
cey-1	4238.40354	1.58354108	0.32417239	6.06E-05
Y54G2A.11	606.985113	2.16209115	0.44278105	6.06E-05
C07G1.15	182.657503	-2.2136699	0.45336266	6.06E-05
C33E10.10	108.769939	2.7656375	0.56610887	6.06E-05
pde-6	526.628473	1.92701934	0.39539576	6.14E-05
pqn-42	227.690276	2.07449454	0.4252181	6.14E-05
F59A7.5	217.234029	2.53859691	0.52086662	6.14E-05

E02C12.10	27.7577749	-8.1451755	1.67027518	6.14E-05
unc-27	10348.5695	1.60982871	0.33023577	6.14E-05
cah-4	1039.67431	2.39086839	0.49056452	6.14E-05
pho-14	5527.50082	1.56505723	0.32158192	6.33E-05
pghm-1	5074.89698	2.01783416	0.41552779	6.64E-05
fgt-1	1290.53196	1.72323797	0.35518713	6.75E-05
arrd-13	115.839496	2.59973462	0.53655092	6.94E-05
F35F10.13	221.801061	2.2746084	0.47028533	7.21E-05
rpt-5	333.284935	1.90582021	0.39467113	7.45E-05
ttr-2	8093.45481	1.69414092	0.35089337	7.45E-05
cdka-1	237.749704	2.39868196	0.49788679	7.80E-05
best-20	265.104928	1.9719409	0.40951553	7.86E-05
lec-3	334.988385	2.03018157	0.42194001	7.93E-05
H01G02.1	1257.53321	1.89800525	0.39442801	7.93E-05
ugt-44	608.752595	-1.7630626	0.36663528	8.00E-05
snf-3	414.282997	1.94846301	0.40574329	8.18E-05
zyx-1	1541.95324	1.61374557	0.33598685	8.18E-05
F53F8.4	539.046164	1.82742911	0.3806471	8.20E-05
far-6	2991.48842	1.77227515	0.36927404	8.22E-05
tct-1	12876.5396	1.7666538	0.36832562	8.29E-05
Y77E11A.14	564.680428	1.85337511	0.38657538	8.34E-05
hxk-2	477.987653	1.77421932	0.37035061	8.45E-05
F41D9.2	246.27043	2.0412895	0.42617585	8.45E-05
K02F2.5	382.948344	2.2514702	0.47065412	8.63E-05
chch-3	591.088336	1.75037499	0.36584596	8.63E-05
fipr-26	338.019161	-1.9538898	0.40983152	9.26E-05
nlp-38	414.089954	2.18482668	0.45820915	9.26E-05
vig-1	4347.59432	1.55468384	0.32620205	9.27E-05
W07E11.1	1229.73216	1.67353877	0.35118528	9.27E-05
T04F8.8	6950.50503	1.61572202	0.33918119	9.31E-05
unc-17	273.737926	2.27377431	0.47805857	9.52E-05
clx-1	151.205881	2.21464845	0.4656089	9.52E-05
anmt-3	1923.60596	1.95334934	0.41067186	9.52E-05
B0272.3	750.81133	1.67866814	0.35317961	9.63E-05
cyp-34A7	280.908243	-2.0911099	0.4401916	9.71E-05
enol-1	19706.2783	1.57384786	0.33138868	9.72E-05
gfat-1	1501.14623	1.81026082	0.38179931	0.000100589
hsp-70	230.298901	-2.0477816	0.43216913	0.000101176

somi-1	153.872651	2.26961063	0.4789246	0.000101176
nlp-73	479.604505	1.74057636	0.36783851	0.000103991
R148.5	327.909977	2.10466642	0.44537595	0.000106793
ZC21.3	315.036491	2.18919162	0.46377423	0.000108759
gln-3	17641.9978	1.64075292	0.34761121	0.000108759
nspc-13	2121.18906	1.74912416	0.37133097	0.000113542
mec-12	535.643788	1.93479696	0.41118701	0.000115617
Y49G5B.1	173.142045	2.34657706	0.49874787	0.000115617
tag-10	849.280303	1.63208019	0.34695816	0.000115662
tag-353	875.52057	1.62365993	0.34524269	0.000115736
srd-27	60.9278756	3.07076568	0.65326215	0.000116536
tag-191	51.174123	3.7404218	0.79598251	0.000116913
cey-4	6721.12987	1.68932614	0.35985936	0.000119133
ncx-1	553.344716	2.0641539	0.43988592	0.000119752
glna-1	96.6475234	2.57283924	0.54892264	0.000122436
Y54F10BM.22	889.234556	-1.6429925	0.35101636	0.000125259
W09D6.5	1633.23553	1.65910507	0.3544492	0.000125259
tni-4	750.887548	2.1257143	0.45493601	0.000129768
dmd-6	753.750854	1.92355325	0.41194596	0.000131209
F56A8.3	603.52698	1.76468418	0.37811763	0.000131944
F29B9.8	1488.22916	1.73904432	0.37265949	0.000131944
perm-4	34257.7795	1.5122563	0.32424529	0.000133106
Y119D3B.12	244.976207	1.93758114	0.41585669	0.000135456
slrp-1	558.568888	1.73407444	0.37222775	0.000135456
unc-108	1422.79126	1.77028612	0.38015192	0.000135573
F53A9.6	952.365537	1.72606574	0.37060885	0.000135573
Y69H2.3	11178.7042	1.61087524	0.34669116	0.000141984
scrm-1	646.408805	1.84745315	0.39788401	0.000143619
eif-3.B	2052.8226	1.6378201	0.35279564	0.000143619
his-35	2506.24876	1.57431903	0.33930079	0.000144136
gsp-1	995.486212	1.64702019	0.35502257	0.000144136
tnt-2	5543.77124	1.5233161	0.32825641	0.000144136
lin-24	134.316738	2.27549774	0.49084863	0.000145916
atln-1	396.339897	1.87388077	0.40444374	0.000147193
F01F1.15	112.404499	2.41903943	0.52267778	0.000149885
Y54G2A.32	235.971049	2.35892961	0.50981241	0.000149885
F59B1.2	1641.80401	1.56485842	0.33815019	0.000149885
cab-1	5297.19951	1.62727488	0.3520915	0.000153185

nuo-5	2130.55955	1.58884641	0.34422945	0.00015713
brp-1	23143.9071	1.53501038	0.3326762	0.000157688
dod-19	1100.87654	1.61956162	0.35163147	0.000163256
Y43F8B.1	1833.42277	1.56843359	0.34056953	0.000163256
pas-1	402.852233	1.8437006	0.40057541	0.000164758
C17H12.8	6498.42973	-1.4777989	0.32129369	0.0001666
Y74C10AL.2	703.830927	1.77084271	0.38510739	0.000166947
Y48E1B.3	189.739512	2.000387	0.43590479	0.000173875
ncs-5	74.5210963	3.08802909	0.67314972	0.000174569
pqn-74	273.912791	2.80765031	0.61297899	0.000179927
R31.2	2687.68553	1.51881417	0.33196986	0.000183754
nep-11	191.134127	2.60790408	0.57032445	0.000185265
Y25C1A.7	242.21893	1.88245015	0.4122405	0.000190198
F49H6.3	100.482239	-2.5567472	0.56016647	0.00019143
vha-12	1904.3324	1.53973713	0.33747757	0.000192353
W09G12.9	141.266618	2.1491418	0.47116725	0.000192727
trap-1	2324.63588	1.61373694	0.35417546	0.000195106
vha-1	2740.12633	1.48746096	0.32643247	0.000195106
kcnl-1	133.884049	2.61259585	0.57341737	0.000195106
F53B3.6	32.0230771	4.51744026	0.99160102	0.000195106
tba-4	1329.62187	1.53334998	0.33677735	0.000196918
Y54E5A.8	430.86271	1.77389589	0.3899587	0.000200056
cah-3	631.073456	1.63223859	0.35926847	0.00020482
Y39E4B.6	665.869644	1.68717422	0.37180312	0.000209403
C54E4.5	708.736754	1.72315189	0.38005225	0.000212487
xbp-1	1265.27474	1.63354273	0.36049887	0.000213663
ftt-2	10065.6624	1.63702144	0.36122632	0.000213663
ubxn-3	489.929085	1.77831427	0.39320018	0.000221833
rgs-4	421.051967	1.71408425	0.37933701	0.000225319
F37C4.5	14774.5299	1.61188416	0.35683229	0.000225554
ech-9	889.020767	-1.8437078	0.40817575	0.000225554
hrpr-1	529.819729	1.67255931	0.37061278	0.000228266
hsp-3	1766.1732	1.68250665	0.37281301	0.000228266
C09G9.1	868.24564	1.64930811	0.36621045	0.00023761
C18D11.1	723.596986	1.73700693	0.38600191	0.000240346
mdl-1	1114.94613	1.68851328	0.37523862	0.000240346
rpt-6	657.217154	1.64514361	0.36587768	0.000243404
F53B2.8	389.939308	1.73810616	0.38681808	0.00024613

Y45G5AM.6	153.071222	2.10060198	0.46769044	0.00024751
vdac-1	8811.76775	1.44498442	0.32188287	0.000249331
C51E3.9	151.984039	2.25857129	0.50328457	0.000250255
pod-1	2225.0322	1.51421376	0.33767626	0.000253487
clec-66	828.340916	1.65083479	0.36902503	0.00026565
ebp-2	495.60226	1.79367089	0.40102052	0.000265689
let-2	3745.37718	1.5774219	0.35284455	0.000267528
mop-25.1	543.160755	1.61736582	0.36206929	0.00027115
nlp-13	1882.17076	1.68902234	0.37818974	0.000271448
dmd-9	140.132504	2.12947114	0.47736556	0.0002772
pgk-1	4688.48321	1.49110728	0.33454398	0.000279937
car-1	978.817123	1.73629102	0.38959205	0.000279937
ZK622.4	256.951492	2.10670195	0.47265638	0.000279937
pccb-1	11249.6452	1.45707944	0.32703672	0.00028072
M01H9.3	7456.01652	1.43802149	0.32358848	0.000295099
rsp-2	746.028045	1.57371299	0.35450163	0.000300731
Y54G2A.26	284.319709	1.85536337	0.41809594	0.000301117
eef-1G	23365.9587	1.79863961	0.40531998	0.000301117
rab-7	1675.72794	1.47621135	0.3327483	0.000301343
nhr-142	146.157149	-2.1132659	0.47638412	0.000301343
did-2	706.872354	1.55831546	0.3514415	0.000303179
C05D12.7	131.107815	2.74901461	0.6203258	0.000305757
hecd-1	840.855235	1.55359118	0.35080139	0.000308891
math-39	188.680666	-1.9517242	0.4409752	0.000311899
vps-54	145.483796	-2.0778976	0.46967434	0.000313539
nhr-86	137.743902	2.14688914	0.48547337	0.000315279
cct-2	449.813726	1.69239838	0.38280929	0.000316149
nol-56	318.000973	1.80896346	0.40972308	0.000323908
tlk-1	262.811922	1.80148739	0.40812573	0.000324468
nlp-8	885.564357	1.70544635	0.3866885	0.000327992
flp-4	1032.37065	1.54005704	0.34915369	0.000327992
his-72	1629.0855	1.49407068	0.33908522	0.000333408
zag-1	122.662619	2.73240302	0.62047309	0.000336159
dld-1	3323.54497	1.51257095	0.3436487	0.000338619
cri-2	866.319686	1.62188737	0.36856084	0.000339014
let-92	989.267635	1.60504639	0.36487925	0.000340738
xbx-9	163.937426	2.21097855	0.50318804	0.000347473
arp-1	410.437629	1.77833855	0.40489539	0.000349393

K10D11.5	290.140441	-1.8450174	0.42016835	0.000349888
flp-27	1072.33494	1.6099421	0.36690915	0.000353117
C12D12.1	617.066924	1.78119665	0.40590816	0.000353117
ltah-1.2	320.645387	1.76491177	0.40230699	0.000353489
F15A4.6	10106.988	1.73835461	0.39669232	0.000360397
paqr-1	216.993705	1.84805454	0.42183316	0.000361184
men-1	981.887993	1.52571751	0.34839823	0.000363072
emc-1	218.5835	1.84846178	0.42269229	0.000369221
Y46G5A.18	478.746701	1.6457083	0.37633037	0.000369221
K02E2.11	1958.39355	-1.5496266	0.35425488	0.000369221
H18N23.2	1473.20748	1.47963365	0.33835387	0.000369221
lin-17	151.202894	2.0672106	0.47285653	0.000370332
atx-2	570.266037	1.5695941	0.35927533	0.000374329
pyp-1	5847.95982	1.50757219	0.34538171	0.000378893
adk-1	2037.61615	1.52527525	0.34946779	0.000378893
cgp-1	173.805742	2.1145001	0.48450438	0.000378893
cif-1	335.937731	1.77315343	0.40688574	0.000389011
Y87G2A.19	926.67844	1.63184727	0.37459017	0.000390597
flp-5	2012.10716	1.60539914	0.36859619	0.000391119
idha-1	3761.52598	1.40976908	0.3238001	0.000392905
ZC123.4	132.020004	2.09774673	0.48192364	0.000393529
M01G5.3	341.596727	1.67835453	0.38579974	0.000396993
F40F8.4	2896.98595	1.51200458	0.34769235	0.000398856
gpx-2	120.02321	2.39195165	0.55098686	0.000411516
clec-51	278.611223	-1.821913	0.41982482	0.000413213
ZK686.3	709.572001	1.5500317	0.35724964	0.000413772
Y69A2AR.1	226.64585	1.82733071	0.42128577	0.000415043
K05B2.2	89.7293162	2.41101642	0.55605963	0.000416948
F21F3.7	105.625165	2.38298178	0.54992848	0.000418518
rps-6	23777.738	1.69714588	0.39155762	0.000418518
aqp-1	2439.48354	1.77747805	0.4101766	0.000418518
C08F11.12	748.088071	-1.5433448	0.35627401	0.000419953
Y45G5AL.1	555.240437	1.63634165	0.37797676	0.000423963
ubc-13	250.650685	1.87011204	0.43234143	0.000429912
F49C12.14	991.058459	-1.6593599	0.3837347	0.000431299
spl-3	2111.99362	1.49602183	0.34602822	0.000431754
Y75B8A.28	317.299071	-1.7079181	0.39512768	0.000432479
msrp-7	1882.23217	1.90197917	0.44037102	0.000435698

F01D5.5	235.745073	1.81399261	0.41996224	0.000435698
nlp-9	1367.34936	1.55246695	0.35938845	0.000435698
pbs-6	605.900991	1.56391318	0.36230986	0.000438472
myo-2	3675.61181	2.10172585	0.48690937	0.000438472
sucl-1	3027.35344	1.47049817	0.34077933	0.00044001
F40H7.12	49.0412186	3.2165676	0.74650577	0.00045148
cnp-2	110.881587	2.20482685	0.51211567	0.000457474
toh-1	281.82467	1.94892447	0.45291279	0.000460912
F58B4.5	250.435498	-1.8813319	0.43737562	0.000462299
Y43F8C.3	273.032878	1.97732232	0.45970716	0.000462299
siah-1	440.318408	1.97183102	0.45879019	0.000468164
capa-1	417.863578	1.693465	0.39442767	0.000476343
rhr-1	886.247425	1.53302198	0.35731997	0.000481877
scm-1	1154.6435	1.4739728	0.34391288	0.000490343
ucr-2.1	6261.7234	1.40846794	0.32900474	0.000499961
his-24	1745.39988	1.69850508	0.3968617	0.00050127
M04G7.1	2209.60313	1.67229245	0.39121444	0.00051185
nlp-15	1753.76968	1.56993183	0.36770513	0.000522304
map-2	1024.23789	1.51248757	0.35478848	0.000536297
F13B6.3	95.8837477	2.54929861	0.59830901	0.000540296
cul-2	268.986525	1.71436104	0.4025641	0.000544342
T20B12.7	3002.47982	1.41589374	0.33263787	0.000547944
acer-1	4890.40144	1.42606753	0.335194	0.000551067
F46C5.1	1864.77448	1.491069	0.35049664	0.000551067
laat-1	38.8039199	3.5414822	0.83264054	0.000551764
tsn-1	440.553669	1.59437466	0.37516207	0.000559016
kin-1	1120.18666	1.62423591	0.38229327	0.000560524
ZK218.5	137.293097	2.15888485	0.50847658	0.000566343
camt-1	879.343923	1.54247261	0.3636058	0.000572738
asp-8	308.514904	1.83203133	0.43185671	0.000572738
C23H3.5	147.859624	-2.0405942	0.48138392	0.00057937
flp-28	4761.18174	1.47429275	0.34802184	0.000585212
dhhc-7	69.9743301	2.62788526	0.62073098	0.000585538
dcn-1	112.089112	2.23218011	0.52706431	0.000585538
dod-6	25975.1041	1.3541947	0.31988914	0.000585538
clec-198	100.671788	2.35788543	0.55696832	0.000585538
vha-13	1968.43627	1.40386067	0.33159252	0.000585538
eif-3.I	646.920694	1.61470851	0.38154212	0.000587413

swt-1	965.688784	1.49023904	0.35218855	0.000587792
ppk-2	397.965473	1.63313381	0.38640583	0.000599262
clec-146	1502.13262	1.44701487	0.34307028	0.000621168
vps-32.1	694.534781	1.50302713	0.35694578	0.000637762
snx-14	321.059087	1.99253393	0.47313819	0.000637762
sgt-1	691.166881	1.49477358	0.35504101	0.000638083
nlp-49	7008.02552	1.4970104	0.35591488	0.000648072
C12D5.3	112.080833	2.31085618	0.54990574	0.000657519
nmt-1	294.901955	1.7203553	0.40958426	0.000661406
cebp-1	487.429983	1.74366921	0.41517271	0.000661406
F32B5.6	1299.6832	1.47177812	0.35053385	0.000663311
mtl-1	35090.1174	-1.6932459	0.40380523	0.000677856
faah-2	1658.30637	-1.6060678	0.38313306	0.000680122
pab-1	23803.2592	1.44236557	0.34414621	0.000680889
cyp-33C2	159.365751	-2.1253752	0.50739119	0.000686249
gsy-1	1397.12165	1.59933747	0.38190448	0.000687186
Y32F6A.4	490.944435	-1.6375308	0.3910562	0.000687186
F19C7.8	127.905659	2.33783411	0.55839922	0.000687958
Y41D4A.4	1069.50083	1.49424177	0.35701571	0.000690312
C50D2.6	158.027924	1.93760324	0.46320586	0.000695836
bam-2	138.040007	2.08158733	0.49882594	0.000722661
ucr-1	5260.97955	1.34639284	0.32258704	0.000722661
atg-18	529.047937	1.57906922	0.37845943	0.000722661
F53F1.6	539.152294	-1.6461464	0.39453979	0.000722661
cmk-1	115.813722	2.52195426	0.60480658	0.000728856
zipt-11	265.974437	1.68687777	0.40470565	0.000732608
fat-5	8132.65398	1.39450124	0.334603	0.000732638
hlh-30	1299.72755	1.5222172	0.36531957	0.000733601
unc-50	306.413934	1.6375252	0.39329306	0.000741271
ima-3	899.004269	1.51639878	0.36422126	0.000741271
clic-1	887.286756	1.47482543	0.3548515	0.000760824
F13C5.5	789.104413	1.7376532	0.41811673	0.000760824
fkh-9	472.145308	1.57405071	0.37869044	0.000760824
F47G3.4	423.656625	2.09571251	0.50436406	0.000761596
pas-6	766.828712	1.67199399	0.40251862	0.000764314
nspc-4	1021.97539	1.48241695	0.35711872	0.000771935
cct-6	549.259172	1.51406041	0.36488564	0.000775741
gdi-1	3351.52957	1.3617681	0.32843194	0.000784696

adh-5	1604.78132	1.52401551	0.36767262	0.000787194
R05A10.3	55.5437052	2.98478613	0.72026017	0.000788867
K09E4.4	444.157631	1.71101518	0.41331934	0.000802181
nlp-21	2546.37013	1.48158455	0.35795798	0.000802866
tni-3	1671.64622	1.51631805	0.36644782	0.000804974
tram-1	502.810661	1.52282756	0.36877862	0.000833486
prdx-2	10471.9782	1.3722304	0.33239734	0.000835183
F32A11.1	127.235852	2.38961072	0.57889192	0.000835183
cpr-2	1010.43512	1.83733207	0.44539198	0.000843206
dct-6	866.083125	-1.4332261	0.34757382	0.000845714
R08F11.1	374.233836	1.76323484	0.42755584	0.000845714
pisy-1	380.170373	1.56095738	0.37860188	0.000845948
Y17G7B.20	629.128247	1.47900954	0.35894327	0.000851476
nspc-9	3284.12146	1.45816099	0.35385397	0.000851476
lis-1	498.115092	1.61469195	0.39192494	0.000851686
ttr-18	1321.80733	1.39630105	0.33917546	0.000861547
slcr-46.3	343.859824	-1.6611823	0.40366576	0.000865258
F35E12.9	692.266804	-1.466231	0.35633362	0.000865258
F31E9.11	1763.78858	-1.4724141	0.35827386	0.000882416
ccf-1	775.467559	1.50589109	0.36655293	0.000886251
cbs-1	458.288187	-1.8395873	0.44796645	0.000890976
gcn-1	245.811063	1.732178	0.42202858	0.000897277
Y43B11AR.1	715.470661	1.52338814	0.37157177	0.000911271
B0294.1	237.602653	1.88805721	0.46048905	0.000911271
Y95B8A.6	1409.40397	1.41487482	0.34546084	0.000926128
T07D3.9	286.016856	1.80901122	0.44199518	0.00093339
phat-3	651.913758	1.61754732	0.39520826	0.00093339
imp-2	275.454783	1.63894361	0.40071336	0.000942608
C46F11.6	516.35743	1.65821127	0.4055358	0.000945211
hgap-1	362.78603	1.61195257	0.39428988	0.000946076
F15D4.4	286.312287	1.83665968	0.44938089	0.000948809
flp-15	1760.00785	1.43211849	0.35059906	0.000956318
ZC116.1	60.8460201	2.62520234	0.64282401	0.00095811
gpx-4	44.716137	3.18511928	0.78065293	0.000971841
icl-1	24494.6469	1.36017584	0.33360513	0.000979844
ZK813.2	1909.74046	1.50811921	0.36985906	0.000979844
sams-4	458.143716	1.56678714	0.38464306	0.000992125
ife-3	354.89764	1.89444471	0.46508306	0.000992125

cpt-1	1108.20566	1.46946107	0.360886	0.000993577
rpl-3	24299.1643	1.5137062	0.37175267	0.000993577
C18B2.4	949.562797	1.46323532	0.35937808	0.000993577
cars-1	355.112533	1.58409277	0.38945189	0.001009086
R53.5	1448.85119	1.35661673	0.33384802	0.001022095
klf-1	169.577956	1.85430107	0.45632457	0.001022095
ptr-21	593.642274	1.71567543	0.42258968	0.001036099
mab-20	123.922579	2.15050304	0.53000756	0.001042639
mec-8	124.472818	2.71350367	0.66868709	0.001042639
hex-1	1346.81772	1.51161046	0.3730082	0.00106308
nlp-61	498.218668	1.73306545	0.42793344	0.001072975
E04F6.15	81.3086005	-2.3123558	0.57127587	0.001080678
F07C6.4	313.300915	1.61209831	0.398641	0.001093832
nas-9	541.068627	1.63308153	0.40383491	0.001093832
Y38C1AA.9	209.915909	1.89601688	0.46891953	0.001094264
vha-4	3102.80817	1.35733947	0.33577096	0.001096371
F41G3.18	502.762619	-1.5253065	0.37764355	0.001105343
fem-2	242.644986	1.85461261	0.4592003	0.001105343
flp-10	671.137992	1.49778589	0.37073368	0.001105343
F20A1.1	7109.18117	1.39196462	0.34467141	0.001105343
C39D10.2	1043.57802	1.37788005	0.34120931	0.001105343
H17B01.5	286.191794	1.88054661	0.4665758	0.001138006
T28B11.1	332.365824	1.66847194	0.41396524	0.001138006
F53E2.2	3376.86583	1.33129731	0.33050512	0.001147409
nlp-1	896.913764	1.67177133	0.41528574	0.001157285
hil-2	294.483088	2.2243648	0.55369004	0.001193861
gdh-1	13875.1832	1.28857232	0.32072963	0.001193861
unc-44	4013.34879	1.3006276	0.32395942	0.001202832
Y44A6D.2	456.37075	1.58872354	0.39572998	0.001202832
R02F11.2	115.772127	2.48257708	0.61934081	0.001232703
ins-26	330.589078	1.72373048	0.43014552	0.001235666
tag-18	1056.03768	1.47419547	0.36791063	0.001235666
ttr-16	17016.302	1.29956499	0.32440532	0.001238245
nhr-88	654.071675	1.50192581	0.37516605	0.001244909
acr-18	110.788435	2.21798222	0.55396177	0.001244909
clec-48	2258.30281	1.35897814	0.33944002	0.001244909
zipt-2.2	222.623966	2.22943106	0.55696915	0.001245541
F37A8.5	365.605007	1.61863113	0.40450702	0.00125002

unc-52	569.786183	1.5896373	0.39783838	0.001278615
C42D4.13	36.7385436	-3.3412892	0.8365474	0.001284533
T20B3.1	151.729174	1.8410661	0.46109392	0.001289259
cyp-35A3	107.588137	-2.514601	0.63018645	0.001300864
C02B8.3	471.104298	1.71963364	0.43106843	0.001303968
ubc-20	742.841936	1.41772835	0.35570093	0.001320874
calf-1	124.298896	2.03918291	0.51172374	0.001322852
daf-5	439.153932	1.81440921	0.45569079	0.001338625
trap-3	1923.26849	1.370925	0.34514665	0.001391491
dlhd-1	481.37877	1.75416515	0.44180198	0.001392628
inx-6	103.898958	2.43286151	0.61271132	0.001392628
scl-5	6967.96043	1.63940979	0.41287375	0.001392628
Y40H7A.10	3800.42008	-1.5781896	0.39760444	0.00139725
hum-7	190.844872	1.84798224	0.46566756	0.001399272
arx-3	355.853791	1.55988519	0.39325427	0.001406207
rab-6.2	820.738144	1.40748644	0.35485267	0.001406207
nlp-34	1047.56172	1.42744212	0.36009087	0.001417095
F02E11.2	288.753055	1.67712573	0.42334147	0.001429251
zig-11	1540.73353	1.42247036	0.35924047	0.001438488
Y52B11A.8	1106.95419	1.39419704	0.35263383	0.001472309
F40A3.1	417.019134	1.60179637	0.40523803	0.001475388
flp-13	1418.91455	1.54197069	0.39045837	0.001495014
pdi-1	2073.67156	1.35042468	0.34245526	0.001528657
cchl-1	265.819361	1.60336281	0.40690387	0.001542235
far-2	139036.468	1.30310312	0.33070604	0.001542235
C08G5.7	226.646917	1.75679155	0.44592715	0.00154412
tbb-2	13810.29	1.33478581	0.33897122	0.001553461
msi-1	288.667247	1.70554765	0.43334328	0.001563407
lron-10	208.968958	1.99134821	0.50609472	0.001567454
Y45G12B.3	417.20048	1.5416152	0.39221257	0.001592042
mag-1	295.168293	1.60597433	0.40884884	0.001603043
tmbi-4	982.530697	1.42982244	0.36398425	0.001603043
ipla-7	2612.62083	-1.421554	0.36243108	0.00163896
Y17G7B.17	699.259118	1.42267134	0.36295557	0.001653704
mca-1	1422.87973	1.33638276	0.3410285	0.001657621
lem-3	512.294294	-1.4758352	0.37678903	0.001664163
gst-6	794.643107	-1.6186643	0.41324591	0.001664163
gei-15	541.914431	1.44020194	0.36799063	0.001683264

cysl-2	2407.70983	1.43935064	0.36809943	0.001704599
B0432.14	445.290438	1.56576618	0.40057236	0.001711472
C16B8.3	760.734163	1.39723826	0.35779281	0.001734528
K10C2.12	521.212461	-1.7915902	0.45884098	0.001734837
nlp-76	154.32228	1.87724756	0.48081982	0.001734837
fip-6	733.047703	-1.3920165	0.35673889	0.00174764
elo-6	14245.6592	-1.3127115	0.33665765	0.00176496
B0001.4	346.107876	1.52948811	0.39245169	0.001776351
haf-2	521.695313	-1.4204738	0.36458254	0.001781311
cah-5	242.933801	1.63724094	0.42036117	0.001785547
C29F7.3	1188.44467	1.40373477	0.36041777	0.001785547
atp-3	14458.0769	1.3335647	0.34262145	0.001800945
rab-35	197.214946	1.73394024	0.44590793	0.001825279
Y71H2B.4	7395.29205	1.29673075	0.33361926	0.00183494
rpl-19	39854.454	1.65736097	0.42655122	0.001842105
maph-1.3	53.5241685	2.62335378	0.67558331	0.001850758
dhs-14	917.026295	-1.7549195	0.45187869	0.001850758
C10B5.3	645.530727	1.42223489	0.3662626	0.001850758
lido-12	244.402168	1.59343982	0.41044777	0.001854399
tbc-17	274.77306	1.94568103	0.5013607	0.001861892
Y65B4A.6	400.705617	1.66533464	0.42937031	0.001871224
Y71G12B.42	1564.91604	-1.4963887	0.38580096	0.001871224
tag-120	1374.37992	-1.4424216	0.37191765	0.001871224
T26C5.4	246.046718	2.12225955	0.54736241	0.001876411
Y42G9A.2	897.837375	1.56570806	0.40393612	0.001881856
F41G3.10	3956.46432	1.50283627	0.38778919	0.001884325
act-2	4309.80903	1.45126396	0.37456895	0.001888128
casy-1	1731.56182	1.57223336	0.40622428	0.001917179
hsp-16.41	1346.26771	-1.6970157	0.43875117	0.001930957
cct-7	1292.11714	1.39599578	0.36092873	0.001930957
K02F3.2	802.911356	1.37351544	0.35550828	0.001961668
cgt-3	1093.25691	-1.4440984	0.37381735	0.001961692
csn-1	572.715689	-1.4913325	0.38684462	0.002023497
H20E11.3	84.4520296	-2.1679788	0.56293383	0.002052606
K11D12.8	206.814644	1.84871515	0.48009282	0.002053101
R07E5.7	185.824786	1.71305797	0.44511956	0.00206481
T13F3.7	51.1633416	2.87432794	0.74679448	0.00206481
ubc-12	481.33533	1.41719308	0.36844697	0.002076846

cpd-2	69.3016753	2.40034452	0.62406677	0.002076846
umps-1	296.595699	1.70369096	0.44314327	0.00208812
daf-22	909.050716	1.37173265	0.35691728	0.002095581
smo-1	337.420491	1.49917633	0.39072295	0.002146935
tomm-20	469.317951	1.47667957	0.38497377	0.002153329
T21C9.6	413.085903	-1.5952034	0.41602461	0.002162026
ant-1.1	139388.723	1.40241383	0.36609209	0.002190557
pfd-3	241.137312	1.71923332	0.44891532	0.002196028
erm-1	431.100556	1.51128148	0.39490525	0.002213902
W09D10.1	225.984868	1.62358274	0.42423647	0.002213902
K07D4.9	1541.19951	1.32350523	0.34613048	0.002239451
tbb-1	3226.96098	1.62425678	0.42525375	0.002274371
lit-1	337.423762	1.62339277	0.42537411	0.002294617
pin-2	318.570899	-1.5836729	0.41494722	0.002294617
best-1	616.950073	1.46190885	0.38308893	0.002294617
alh-5	276.971665	1.67815128	0.4398368	0.002297523
M163.1	86.345087	2.23080939	0.5851568	0.002322472
K11D2.4	438.250244	1.47566793	0.38724353	0.002334064
cnc-2	2302.79159	-1.3260878	0.34852348	0.002385815
isp-1	11997.874	1.27370058	0.33484286	0.002391595
yop-1	1119.68215	1.43435671	0.37754566	0.00243363
nlp-81	215.907681	1.82266926	0.48008744	0.002455583
Y59C2A.1	1257.99557	1.33895604	0.3527501	0.002459293
kin-10	1628.78993	1.30589685	0.3442827	0.002481913
vab-10	1377.27381	1.27418844	0.33611625	0.002499788
gsa-1	145.899896	1.85061799	0.48853271	0.002524102
Y69A2AR.18	16872.984	1.25787163	0.33220521	0.002533193
T27C4.1	6663.59849	1.54107993	0.4069935	0.002533193
nlp-2	406.732956	1.60129188	0.42295565	0.002533985
mrpl-40	265.341126	1.54592219	0.40868146	0.002563243
bath-40	310.893849	1.51522065	0.40069851	0.002572165
dod-23	1987.12033	1.57341359	0.41705308	0.002659938
T23F11.6	224.265071	-1.6903291	0.44838525	0.002686572
Y110A2AL.3	2107.15266	1.27728365	0.33912641	0.002715071
got-2.2	11278.2105	1.2134278	0.32217238	0.002715071
ubxn-2	187.163759	1.78981694	0.47545628	0.002732306
C15C7.5	309.827137	1.48337708	0.39413956	0.002737166
cct-1	892.526455	1.38300833	0.36771665	0.002760485

dpm-3	1840.5929	-1.5946932	0.42463909	0.00281924
pfn-1	1441.50698	1.28143102	0.34132933	0.002828042
Y39G10AR.9	144.905213	1.76467224	0.47036925	0.002852656
W06H8.6	80.5146633	2.21498035	0.59049963	0.002855579
eif-3.J	382.612874	1.44803093	0.38612142	0.002856183
F23D12.3	298.402612	1.75678601	0.46843109	0.002856183
H14A12.3	76.3781823	2.7247188	0.72716513	0.002887834
pqn-87	832.167285	1.29782608	0.34651828	0.002903088
cdc-48.1	564.732137	1.35967095	0.36329752	0.002930522
ttr-6	3468.77885	1.21571754	0.3249502	0.002941652
pfd-6	1485.93376	-1.2593186	0.33693896	0.002978784
pqn-27	285.569669	1.58344451	0.42372877	0.002978784
mogs-1	458.457434	-1.4406285	0.38550806	0.002978784
sup-1	421.636161	1.47149389	0.39391596	0.002990542
prdh-1	518.222481	-1.36726	0.36614539	0.002997483
C39D10.7	2230.21752	1.44766893	0.38767443	0.002997483
cdc-37	618.342369	1.52407697	0.40865397	0.003049229
F14E5.2	240.970756	-1.7222999	0.4620414	0.003063627
R05H10.1	93.984169	2.45153183	0.65774663	0.003063627
cpt-3	97.0285726	2.08595829	0.55963104	0.003063627
sdz-24	443.208401	1.43656971	0.38564729	0.003079658
F22F4.5	383.492263	-1.7239155	0.46277118	0.003079658
R02F2.1	18328.3136	1.26794673	0.34060397	0.003104944
K07A1.6	337.935832	-1.5662328	0.42092099	0.003120911
lmp-1	4359.43109	1.21330938	0.32617357	0.003130296
R01H10.4	141.615774	1.73798869	0.46728223	0.003131435
src-2	202.111732	1.67172269	0.44954071	0.003134424
glb-11	130.1693	1.80956662	0.48682584	0.003150389
Y94H6A.10	879.56752	-1.3217658	0.35573427	0.003160808
F58B4.3	550.702843	1.45815859	0.39245493	0.003160808
K03H6.5	41.2842014	2.81851476	0.75895559	0.003178696
his-41	639.463754	1.60641357	0.43287653	0.003207442
pqn-48	829.227293	1.39846331	0.37725837	0.003255059
C17C3.3	83.9116556	-2.115753	0.57187792	0.003329684
pudl-1	1079.41075	1.50071693	0.40552754	0.003329684
tald-1	2358.83857	1.31246146	0.35473977	0.003329684
W03G11.4	154.865305	1.75467977	0.47426502	0.003329684
hsp-16.2	1116.27165	-1.6031574	0.43345272	0.003338988

K01A11.1	195.484225	1.58899033	0.42995831	0.003372227
F35A5.2	1014.98601	1.48327575	0.40166567	0.003405542
clp-1	998.435194	1.26220211	0.34191429	0.003417121
F12E12.11	575.232199	1.38569086	0.37570261	0.003451714
F42A10.6	606.090979	1.35110399	0.36632071	0.003451714
atgp-1	241.18132	1.5308019	0.41518294	0.003463101
K04G2.9	103.362484	1.95357747	0.53022431	0.003493772
Y65B4BR.1	925.307452	1.26228874	0.34296301	0.003542427
toe-4	884.496866	1.32334342	0.35961921	0.003546885
gsk-3	514.595712	1.36285862	0.37042863	0.003551551
C44H9.5	372.031642	-1.6064734	0.43732913	0.003626736
dlat-1	1832.39619	1.22803054	0.33433533	0.003626736
C17C3.15	178.787141	-2.2126412	0.6027236	0.003649646
ins-27	483.269395	1.34513926	0.36650149	0.003656593
fat-4	16325.6937	-1.3989767	0.38123528	0.003660265
F19G12.9	587.888607	-1.3849412	0.37757264	0.003677582
ins-17	1226.96609	1.4613426	0.39854516	0.003691283
ets-9	231.202231	-1.6345311	0.44595692	0.003707217
acox-1.5	544.422602	-1.8441641	0.50334926	0.003722712
pod-2	7300.74353	1.2316382	0.33630982	0.003740284
F23F12.12	21010.5182	-1.1889036	0.32471452	0.003747075
F32F2.4	43.8242804	-2.7790823	0.75913946	0.003749738
vha-9	2002.06873	1.23915731	0.33886431	0.003800867
F37C12.10	1006.09445	-1.413291	0.3865011	0.003800867
feh-1	73.4221052	2.42881814	0.66435094	0.003805434
col-89	168.299542	1.77156995	0.48466288	0.003805434
C54D10.3	4779.72426	1.4240778	0.38960055	0.003805434
sma-10	733.458423	-1.3973344	0.38236819	0.003806566
W05H9.3	2784.48297	-1.2940166	0.35408896	0.003806566
C30G7.2	154.536822	2.03713055	0.55792833	0.003847369
F43C9.2	1052.5351	1.33531079	0.36574257	0.003847369
ZK1290.10	247.124915	-1.5683516	0.42986678	0.003874029
B0491.5	4092.50547	1.21661362	0.33344814	0.003874029
aman-2	3314.32744	-1.2565367	0.34451479	0.003886604
aakg-1	348.064227	1.47128422	0.40356423	0.003904463
ZK632.10	1300.8062	1.22841997	0.33714441	0.003931308
F10C5.3	139.577322	1.73877834	0.47770791	0.003983666
oac-46	490.76975	1.59147563	0.43754386	0.004012383

imph-1	240.464552	1.69452255	0.46587821	0.004012383
T23D8.3	1899.90191	-1.2929488	0.35583508	0.004064763
ZK470.2	1938.97391	1.20230998	0.331184	0.004110137
osta-3	243.336899	1.55683976	0.42916787	0.004137834
bed-2	261.160942	1.4643312	0.40367194	0.004137834
dnj-19	280.646274	1.49485986	0.41208427	0.004137834
F56B3.2	80.0168527	2.10643094	0.581039	0.004168161
sod-1	5117.26873	1.28701242	0.35510737	0.004178408
Y54G2A.18	4481.47389	1.27947072	0.35316105	0.004183428
sams-1	549.481724	1.50779014	0.41614459	0.004183428
col-181	89343.4016	1.27803955	0.3527033	0.004183428
pqn-75	4305.92412	1.88338425	0.52008067	0.004203259
T04B8.5	540.308073	1.33856135	0.36973016	0.004213046
atp-1	17195.7712	1.22239601	0.3379987	0.004263698
wbp-2	111.612878	1.89829381	0.5248714	0.004263698
K03B4.4	271.29592	1.65487904	0.45763254	0.004264377
sea-2	407.9013	1.38336916	0.38264355	0.004273041
C33G8.4	2565.35907	1.27627396	0.35306201	0.004274178
E02H4.7	1059.06637	-1.3001651	0.35975455	0.004282185
nas-11	1270.38176	-1.3416391	0.37177255	0.004364172
F25B5.3	1087.8376	1.26485026	0.35055279	0.004368399
clp-4	577.62534	1.30601321	0.36217649	0.004398687
ostd-1	1088.11324	1.30059686	0.36081525	0.004412816
mua-6	460.661252	1.39731842	0.38766194	0.004412816
ztf-22	208.488377	1.62297477	0.45045032	0.004431888
aqp-11	784.165228	1.33146949	0.36963872	0.004440729
eat-17	246.908781	1.64451838	0.45658418	0.004440729
cutl-26	105.778817	1.83362917	0.50928838	0.00445546
F46B6.12	696.60106	-1.2668168	0.35187156	0.00445546
T11F9.22	171.276513	-1.7532279	0.48783354	0.004558855
snf-1	220.138052	1.56952091	0.43685615	0.004566634
ketn-1	944.033032	1.3097674	0.36452473	0.004566634
F35E12.6	2713.97467	1.33564192	0.37196778	0.004595978
rpn-1	673.82339	1.27408212	0.35494091	0.004610756
clec-62	941.643042	1.3848222	0.38612065	0.004658954
phy-2	366.916577	-1.381226	0.38549081	0.004715004
unc-62	243.791181	1.47644275	0.41216919	0.00472507
txt-9	301.918865	-1.4113751	0.39411608	0.004737123

col-106	409412.737	-1.4007628	0.39125674	0.004742216
F46C3.6	682.611981	-1.4700481	0.41061174	0.004742216
W03G1.5	230.760567	2.23552178	0.62481666	0.00477702
T25G3.3	625.512991	-1.3287664	0.3717452	0.004834669
idhg-1	321.19898	1.45389745	0.4071076	0.004879663
Y43C5A.2	5856.04104	-1.1466171	0.32105123	0.004879663
spcs-2	1347.85606	1.26393699	0.35398026	0.004885219
C08E8.10	198.357407	1.87769003	0.52613182	0.004912138
hlh-33	141.454692	1.75453267	0.49169989	0.004916162
let-805	378.078955	1.56566936	0.4391585	0.004968916
elo-5	5124.98387	-1.2490958	0.35046256	0.004975292
R07B1.11	41.9686882	2.80946424	0.78820397	0.004975292
cyp-33C7	338.71058	-1.4428726	0.4049482	0.004988355
F53H1.3	82.5995847	2.00137118	0.56186726	0.00500171
Y50D4B.1	389.300571	1.57124954	0.44114934	0.00500171
vab-9	176.139796	1.73800551	0.4882708	0.005037363
npp-9	297.254027	1.44495598	0.40616042	0.005067575
daf-7	403.654671	1.638975	0.46076913	0.00507175
Y94H6A.8	2599.99821	1.19520167	0.33643764	0.005153024
vps-37	264.453067	1.44122783	0.40592269	0.00518606
cnt-1	321.646502	1.46302326	0.4124934	0.005253012
F36H5.19	576.759038	-1.6493927	0.46511691	0.005253421
sng-1	99.1994298	2.2997933	0.64854536	0.005253421
nspc-16	1295.85154	1.4525901	0.40992412	0.005297075
rbg-1	144.876502	1.70356285	0.48087272	0.005308561
hda-1	163.229085	1.62665905	0.45935438	0.005331226
tli-1	78.8804313	2.06054715	0.58212437	0.005347539
flp-26	1306.41486	1.19375426	0.33724133	0.005347539
C53B4.3	213.446213	-1.6771792	0.47387843	0.005349652
R08E5.3	346.187205	1.52122984	0.42986714	0.005351396
flp-19	1352.82437	1.21007243	0.34201161	0.005359445
T04A8.8	79.2571433	-2.0649369	0.58430343	0.00542919
nhr-143	335.477745	-1.419993	0.40178357	0.00542919
ril-2	920.19946	-1.258271	0.35624773	0.005463541
ZK154.6	340.231388	1.36495717	0.38649338	0.005464181
mtm-5	215.538006	-1.490161	0.42210808	0.005485413
math-26	202.641557	-1.7147541	0.48614332	0.0055414
Y18D10A.23	1507.97599	1.28433072	0.36424701	0.005561045

F47B10.5	2323.85948	-1.198763	0.34018507	0.005598923
rhi-1	886.772794	1.21518309	0.34520951	0.005670953
C36B1.6	653.210377	-1.2953352	0.36816141	0.005693973
zmp-3	492.183176	1.48086061	0.42087755	0.005693973
col-34	904.40911	1.38984687	0.39536144	0.005751593
lin-29	50.353232	2.46956996	0.70268927	0.005764479
Y47G6A.33	486.448658	1.44864738	0.41245896	0.005805855
Y17G7B.21	182.94434	1.547604	0.44140451	0.005933832
hil-3	991.3959	1.69162252	0.48259375	0.00594465
Y57A10A.26	629.824576	1.39545978	0.39816087	0.005948581
droe-4	552.218206	1.46204074	0.41763837	0.006031728
Y60A3A.19	587.480613	1.27832016	0.36539163	0.006075058
C18D11.3	268.935456	1.46225177	0.41811571	0.006080911
D1086.9	187.682633	1.88739895	0.53964218	0.006080911
cgr-1	665.329976	-1.5833504	0.45266636	0.006080911
F09G8.7	356.298351	1.37032339	0.39202898	0.006106401
Y7A9A.79	237.511217	-1.4881634	0.42570889	0.006106401
C17E4.11	154.419852	-1.6216774	0.46417889	0.00614051
K07D4.4	54.7463533	2.28410388	0.65396335	0.006154516
ent-7	725.14404	-1.3453303	0.38534298	0.006180504
fbp-1	3003.8159	1.19439761	0.34215317	0.006180934
F40D4.16	990.495469	-1.3724707	0.39319301	0.006180934
nspc-18	149.480015	1.95366675	0.55984316	0.006186788
phat-6	3219.89144	1.41756518	0.4062045	0.006186788
mec-5	450.774914	1.31372787	0.37655129	0.006198336
soem-1	87.2884604	2.03274089	0.58292496	0.006230281
Y11D7A.10	557.247958	1.31212626	0.37663385	0.00629256
sms-1	510.775637	1.30611625	0.37487355	0.00629256
F15E6.3	2066.04015	1.18615674	0.34051267	0.006293834
Y48G1C.8	100.512125	1.87424727	0.53811498	0.006296913
Y55B1BL.1	1067.44187	1.20555784	0.34616003	0.006296919
D1054.1	251.215724	-1.4494243	0.41641033	0.006334066
Y51A2D.13	413.518294	1.44985778	0.41673241	0.006365459
Y69A2AR.22	2670.60126	1.17085215	0.33664203	0.006383333
F58G6.7	161.18416	-1.6489856	0.47421429	0.006393054
tat-3	117.476644	1.86424462	0.53661577	0.006462268
C55A6.7	188.303734	-1.5300411	0.44045631	0.006462268
F54C9.3	3962.07403	-1.2420985	0.35797417	0.006550493

rsp-3	1126.98555	1.19870806	0.34550732	0.006551978
ZK688.11	943.921992	-1.2409492	0.35774453	0.006558734
gas-1	2301.04836	1.23815494	0.3571517	0.006601406
tsp-2	493.752217	-1.451754	0.41884768	0.006610212
T16G1.6	148.367491	-1.6750481	0.48362761	0.006665401
daf-28	541.138349	1.42069162	0.41026993	0.006674419
mec-7	298.518042	1.46089042	0.42192769	0.006676421
btb-17	836.118211	-1.3718344	0.39652741	0.006738124
bris-1	402.236351	1.52409113	0.44063716	0.006741702
kel-8	386.449817	1.51454894	0.43783803	0.006741702
pat-4	252.461381	1.56625468	0.45310976	0.006787788
grl-4	507.320272	1.33218262	0.38553469	0.006811551
rpn-7	414.42051	1.4008771	0.40554466	0.006831409
Y41E3.7	577.722883	1.31556337	0.38093598	0.006843775
copb-1	1103.42867	1.20606508	0.3493138	0.006856809
F15D3.6	319.570888	1.48859569	0.43143939	0.00689407
M01F1.4	538.499608	1.25542855	0.36382848	0.00689407
zyg-8	88.8621951	1.9390297	0.56199696	0.00689407
gcy-11	147.084597	1.64922108	0.47804746	0.006894584
ZK84.1	147.144391	1.85198509	0.53701474	0.006918256
Y54G2A.52	1233.59243	-1.2918753	0.37468016	0.006928708
akir-1	355.842185	1.33733528	0.38798384	0.00694771
nlp-51	1201.11193	1.22887346	0.35666517	0.006976376
rsr-1	148.520911	1.58310316	0.45981259	0.007025286
F57B7.2	61.0921754	2.19726034	0.63814799	0.007025286
F56A11.5	346.207889	1.40295111	0.40781135	0.007082964
T01C8.2	3260.28451	-1.1231048	0.32647575	0.007082964
fbxa-26	131.254014	-1.8355421	0.53369893	0.007094604
F52E1.2	135.24918	1.9100106	0.55539545	0.007094604
unc-84	145.881442	1.65539558	0.48176689	0.007163105
F32D1.5	3954.01665	1.31599522	0.38311154	0.007183192
Y14H12A.1	228.088637	-1.4991813	0.43672586	0.007234497
pcn-1	86.0535607	2.14227144	0.62491794	0.007343583
ife-2	787.306999	1.21504182	0.35441984	0.007343583
F28H1.4	65.2951265	2.26279194	0.66014029	0.007344285
ser-4	145.668638	1.74332972	0.50869536	0.007354288
jmjd-2	58.8927382	2.33175084	0.68048043	0.007357599
snb-1	6212.63098	1.13062239	0.33001055	0.007365515

rps-24	17990.0731	1.24797759	0.36441489	0.007395381
scav-6	231.773133	-1.4680716	0.4287482	0.007400974
best-22	186.617465	1.64855833	0.48187384	0.007473045
xpo-2	167.078171	1.52904588	0.44704181	0.007485808
clec-49	658.942505	1.39715342	0.40859176	0.007502781
prhg-1	100.333447	1.85756932	0.5435084	0.007541098
pqn-59	3674.05809	1.11975388	0.32776862	0.007560468
F59C6.11	211.280444	-1.5447297	0.45218412	0.007560468
acdh-7	369.282459	1.64853621	0.48257764	0.007560468
T05A8.3	1527.41575	1.1827712	0.34628155	0.007564926
Y77E11A.12	98.5928583	1.85093857	0.54196688	0.007567693
sodh-1	30525.4022	1.28744987	0.37706929	0.007583143
cpg-7	5230.96619	1.13819475	0.33357774	0.007638066
srx-125	144.169435	-1.644854	0.4822752	0.007670633
cox-15	180.665246	1.69804312	0.49792917	0.007673257
K08D12.6	2152.27328	1.43045054	0.41960021	0.007687694
dhs-13	1154.27713	1.15216469	0.33795987	0.007687694
bub-3	91.9458479	1.99723571	0.58606742	0.007713412
rpn-10	463.225255	1.26027544	0.37010162	0.007779736
K11E4.1	172.841243	1.59399926	0.46831504	0.007814461
kdp-1	7850.72072	1.19490011	0.35109833	0.007816232
atp-2	20273.3387	1.08856741	0.32020005	0.007913053
plin-1	956.625646	1.68734608	0.49660628	0.007942649
gldc-1	525.455634	1.39506406	0.41061237	0.007942649
F40H3.1	620.463294	1.28073851	0.37691282	0.007942649
Y38F1A.1	219.141641	1.46854392	0.4322554	0.007942649
cho-1	171.481323	1.96344442	0.57798648	0.007944109
nono-1	258.425198	1.41667843	0.4171405	0.007960672
tba-1	1416.47702	1.16304748	0.34262931	0.007992069
zipt-7.2	1648.57138	1.16779295	0.34402472	0.007992069
mak-2	946.362407	1.1766233	0.34685853	0.008048995
fust-1	744.020742	1.22120311	0.36003346	0.008049223
F13D12.3	1449.16356	1.19838374	0.35353556	0.008105182
twk-18	314.412746	-1.3822673	0.40791773	0.008129284
T28F4.4	257.129533	-1.4295851	0.42214841	0.008183926
Y52B11A.12	282.886439	-1.5371487	0.45429785	0.00826112
nlp-35	600.292457	1.22799172	0.36323489	0.008338363
try-10	583.969383	-1.5218478	0.45019862	0.008338784

C39D10.8	243.861962	1.61485812	0.47783136	0.008354937
pud-4	7631.35784	-1.1035456	0.32680286	0.008430025
usp-5	326.977576	1.34150596	0.39757311	0.008471357
F27D4.1	1113.19853	1.14931581	0.34054479	0.008471357
F28C6.5	116.523415	1.7957483	0.53217116	0.008471357
hid-1	753.21693	-1.2725555	0.37713882	0.008471357
srpr-1.1	63.8530975	-2.2263764	0.65999713	0.008490525
xpo-1	332.467631	1.3322319	0.3951548	0.008539769
oig-3	1088.2904	1.14920379	0.34098736	0.008567469
thn-2	8795.19582	1.17717112	0.34948084	0.008607326
cyp-34A8	815.372976	-1.2381385	0.36755266	0.008607326
max-2	211.761607	1.50304365	0.446324	0.008620916
nlp-18	2283.96117	1.36189746	0.40462869	0.008668258
prg-1	156.367118	1.63333451	0.48544837	0.008679418
gcy-21	133.242442	1.96300763	0.58344005	0.008679418
M04C3.5	91.1905282	-1.9711836	0.58583443	0.008679418
lipl-2	1278.72956	-1.2615771	0.37509877	0.008708436
sod-3	523.537025	1.23771995	0.36807356	0.008718641
fig-1	214.880852	1.45805999	0.43381059	0.008761246
nlp-67	127.786221	1.82403833	0.54299391	0.00880987
nhr-68	1142.07993	-1.1640281	0.34665761	0.008834328
E02A10.4	234.457281	1.55552572	0.46324506	0.008834328
snt-6	656.796157	1.28868547	0.38381658	0.008834569
mtx-1	161.029155	1.74331455	0.51958493	0.008900355
mys-2	42.5843828	2.43112327	0.724651	0.008901001
flp-2	1066.36587	1.31202849	0.39111862	0.008902198
T22B11.4	712.42215	1.60540796	0.47880726	0.008944935
spin-2	358.018887	1.58891911	0.47405792	0.008973878
vha-2	9552.93395	1.16768759	0.34870639	0.009065605
pnk-1	6335.34257	-1.4764479	0.44103121	0.009085672
pbs-5	2001.48656	1.109207	0.33154397	0.009114463
vgln-1	3335.18319	1.23693552	0.36972962	0.009114463
mmcm-1	2200.57844	1.14052618	0.34081328	0.009114463
F52E1.14	5932.60869	-1.1399182	0.34074587	0.009114463
tos-1	2389.8266	1.30738912	0.39070702	0.009114463
dhs-3	1774.61594	-1.2105764	0.36223337	0.00921646
clec-47	27174.2238	-1.4867177	0.44564294	0.009402983
E04F6.9	9000.40009	1.09596777	0.32872642	0.009465479

fos-1	92.2196547	1.80679063	0.54236181	0.0095457
pph-1	437.835507	1.29649378	0.38939132	0.009597407
zfp-3	501.422614	1.42764896	0.42887803	0.009612771
scpl-1	410.452632	1.24437558	0.37397496	0.009649934
lgc-33	55.7283548	2.24914796	0.67637062	0.009713059
K02E11.7	307.756384	1.90398869	0.57271674	0.009731855
H39E23.3	889.652724	1.37375261	0.41415267	0.009974665
C29F7.2	577.571259	-1.2865837	0.38787271	0.009974665
pck-1	29275.6595	1.23009932	0.37097012	0.010004246
hpo-26	229.813604	1.43444543	0.43263853	0.010005332
marb-1	501.64403	1.27432149	0.38471168	0.010108741
F09E10.1	2138.81837	-1.3740225	0.4149069	0.010125847
fbxa-6	175.72558	-1.5590946	0.47086367	0.010130358
C06H5.6	156.482941	1.50347155	0.45409336	0.010130358
B0205.12	460.363115	-1.5627872	0.47205289	0.01013106
ttr-42	112.090109	-1.6968212	0.51271088	0.010160705
csq-1	2912.59169	1.07406893	0.32476742	0.010234371
col-155	285.251337	1.38846545	0.4199746	0.010264829
ned-8	411.5915	1.33226229	0.40306621	0.010281689
clec-65	84.1424812	1.91791568	0.58038492	0.010288511
ZK1073.1	723.471782	1.28435204	0.38866162	0.010288511
Y51F10.3	510.732208	1.21396661	0.36755594	0.010341943
pnc-1	818.157104	1.23757848	0.37474537	0.010344361
Y43E12A.2	253.170169	1.47789263	0.44768114	0.010379245
pmp-4	263.433744	-1.3577788	0.41162183	0.010465392
W02B12.11	97.1821988	1.72422357	0.5227631	0.010466467
btbd-10	434.807677	1.25904206	0.38206754	0.010566054
F36H2.3	119.721382	1.72498845	0.5236088	0.010578955
F59F5.4	46.0088348	-2.3700179	0.71940428	0.010578955
C49F5.7	10254.157	-1.0487831	0.31854121	0.010642046
Y71F9B.9	352.843322	1.26340315	0.38394131	0.010700943
nemp-1	89.0523198	1.77229339	0.53899194	0.010778457
stt-3	1107.48699	1.17973986	0.35883195	0.010778457
F25B4.7	784.238307	-1.1606161	0.35301567	0.010778457
F11C1.1	173.908555	-1.4823616	0.45120054	0.010857514
T24C4.10	242.273201	-1.3720815	0.41778255	0.01088052
txt-17	10011.0321	1.25503212	0.38213936	0.01088052
acdh-3	970.658492	1.27985093	0.38979566	0.010900737

nrde-4	152.829423	-1.628202	0.49601343	0.010921083
linc-72	150.673998	-1.5920644	0.48529069	0.010985117
F46H5.3	73667.629	1.12383208	0.34261986	0.010994481
acaa-2	2600.43622	1.09291618	0.33329111	0.011009174
K02D3.1	106.225916	1.74916666	0.53338115	0.011009174
vit-5	150179.592	1.50112376	0.45826964	0.011136379
trpp-3	216.732783	1.39660274	0.4264679	0.011148549
acox-3	800.446805	-1.3975919	0.42677768	0.011148549
F13G3.6	108.33239	-1.7607506	0.53789268	0.011189847
K12B6.9	370.100533	-1.36527	0.41731057	0.011251215
madf-9	113.233079	1.66345302	0.50850677	0.011253462
valv-1	556.738626	1.25821687	0.38484113	0.011314124
unk-1	1570.82095	-1.1348129	0.34723194	0.011353787
cyp-36A1	91.0002443	1.85742464	0.5684654	0.011360381
F53A10.2	159.572801	1.48085703	0.45320978	0.011360381
K12H4.7	11505.3326	-1.5329672	0.46944629	0.011427708
scl-2	11545.0476	1.07819765	0.33026781	0.011451099
Y51H4A.5	170.857949	-1.5047709	0.4619386	0.011729842
skr-19	416.389535	1.58498262	0.48661475	0.011732645
bre-4	146.191929	1.52276394	0.46763479	0.011744375
M04F3.4	424.677228	1.26554309	0.38862197	0.011744375
Y47G6A.22	68.4303034	1.97035147	0.60534741	0.01177891
atgp-2	157.778991	1.68012681	0.51618126	0.01177891
tsp-13	49.4885764	2.18797273	0.67255663	0.011837534
smd-1	1949.20931	1.22791029	0.37770343	0.011911647
osta-2	269.588057	1.39202666	0.42820021	0.011911647
pcp-4	125.246177	1.64623153	0.50655605	0.011936821
lin-18	183.997712	1.42153885	0.43743513	0.011936821
ZK131.11	338.570258	1.39181325	0.42844105	0.011973774
calu-1	1646.00468	1.10185067	0.33924246	0.011986282
hmgr-1	379.708833	-1.2364775	0.38078176	0.01200672
C54E4.4	111.832725	1.82396426	0.5618369	0.012027684
cyld-1	409.115032	1.21794634	0.37523245	0.01204055
ZK550.3	53.7004965	2.13261067	0.65741988	0.012110713
F49H6.13	85.1155257	-1.8297765	0.56425587	0.01214544
ugt-58	3604.9518	-1.1081398	0.3420161	0.012252897
cand-1	376.430444	1.28697786	0.39749142	0.012338763
pan-1	150.119576	1.50119516	0.46389353	0.012363582

Y41C4A.17	495.623334	-1.2776096	0.39480402	0.012363582
aldo-1	10310.8476	1.20432233	0.37207403	0.012363582
ttr-45	10083.3453	1.07164207	0.33115669	0.012363582
T09B9.4	226.840935	1.44011471	0.44516064	0.012395378
acbp-6	1000.44103	-1.6360466	0.50595305	0.012446361
nhr-119	162.96294	1.50010324	0.46399234	0.012458588
par-1	317.859941	1.25825301	0.38972201	0.012641437
C01F1.6	158.876805	1.54662621	0.47931636	0.012662075
srr-6	241.878826	-1.6052172	0.49747422	0.012662075
zip-5	441.347244	-1.3497316	0.41819448	0.012662075
hsp-90	35.1457334	2.65208598	0.82167153	0.012662075
F47F2.1	101.490985	1.72785268	0.53545823	0.012662075
lact-4	499.005149	-1.2667678	0.39287307	0.012743705
T04C9.1	333.022858	1.27732662	0.39615141	0.012743705
met-2	98.2982468	-1.6975479	0.52659277	0.012762315
W10C4.1	53.2459108	2.30727201	0.71645413	0.012894987
Y97E10C.1	319.004679	1.40895464	0.43757763	0.012905387
far-7	2995.57958	1.28696126	0.3998707	0.012958439
rga-9	258.349857	1.3273618	0.41249752	0.012972042
mfb-1	470.803248	-1.1853803	0.36848314	0.013002431
K01A2.5	326.755584	1.53709071	0.47799235	0.013044191
Y54H5A.2	521.02154	-1.3134063	0.40851316	0.013060441
rad-23	966.25509	1.13778944	0.35399529	0.013074009
csn-5	116.448599	1.63519446	0.50877793	0.013074009
igcm-3	172.754539	1.50799722	0.46919535	0.013074009
rab-8	1172.53494	1.0843164	0.33750153	0.013113071
R05C11.4	128.564838	1.67017429	0.5199139	0.013113071
him-3	30.6104164	-2.828824	0.88062697	0.013113071
dnj-8	79.2872542	1.86719308	0.58158587	0.013181233
tth-1	1453.87569	1.07272427	0.33424409	0.0132199
arr-1	137.608175	1.51352292	0.47165268	0.013226905
gst-4	1154.20007	-1.1071626	0.34521288	0.013296812
K10C3.4	117.516595	1.57736428	0.49225296	0.013389091
C44B11.6	4393.84596	-1.2487243	0.38967945	0.013389091
flp-11	4174.08749	1.21693067	0.37977	0.013389091
mek-5	94.9360319	1.78366655	0.55724777	0.013541232
D2030.2	2558.61079	-1.0531326	0.32905234	0.013544763
atgl-1	274.927417	1.28095007	0.40027454	0.013547132

arf-3	5819.03128	1.13783344	0.35595001	0.013689928
nhr-232	150.300624	-1.5593516	0.48777724	0.013689928
B0457.6	283.825858	1.4564251	0.45602423	0.013813479
npp-3	81.1669574	1.96112998	0.61496877	0.01402943
kin-19	3464.71754	1.0554892	0.33108481	0.014052468
nhr-71	185.616422	1.49752042	0.46972529	0.014052468
lipl-5	10985.6093	1.08302425	0.33995377	0.014145167
nhr-126	105.672168	-1.6307622	0.51220546	0.014229582
klp-7	408.8786	1.25488354	0.39419424	0.014235426
unc-132	202.915814	1.74019114	0.54673941	0.014247886
Y44A6C.1	543.161342	1.18034294	0.37087168	0.014247886
acox-1.4	133.841916	-1.6693246	0.52459195	0.014258122
Y45F10D.2	37.4774103	2.4963674	0.78485219	0.014316498
tpp-2	696.0268	-1.1961043	0.37613777	0.014338788
C53B7.3	3868.53747	1.30744181	0.41119917	0.014344234
gst-20	791.727266	1.11910621	0.35200184	0.014346715
F22G12.4	157.073336	1.45198136	0.45683868	0.014353105
ntl-3	673.898343	1.16390459	0.36618108	0.014353105
R102.2	2833.20102	1.19671848	0.37646131	0.014353105
elo-3	423.353073	1.20116721	0.37802242	0.014380464
F21D5.5	189.346128	-1.4207373	0.44782537	0.014615691
igdb-2	748.95873	1.17977671	0.3719183	0.014621556
spop-1	202.571705	1.35793567	0.42813025	0.014626024
ins-6	318.807605	1.37059882	0.43244564	0.014732122
cox-6C	5103.65766	1.12217835	0.3540993	0.014734039
sem-4	139.660902	1.63677736	0.51659107	0.014755249
T01B10.5	51.7988346	-2.1701785	0.68517398	0.014796518
nhr-114	175.284203	1.54264712	0.48717662	0.014825366
clec-57	197.579337	-1.4649645	0.46277118	0.014856093
zyg-11	1047.89987	-1.1536457	0.36463325	0.014928133
C09H10.5	222.869985	1.37693466	0.43523037	0.014928133
pigu-1	128.643773	-1.6548354	0.52315884	0.014936688
sid-5	1265.0391	-1.0794249	0.34126723	0.014936688
T24D3.2	468.408506	-1.1984389	0.37897662	0.014958268
pgp-3	297.740249	-1.289104	0.40775461	0.014987364
C28C12.11	34.8951253	-2.6268343	0.8313738	0.015068493
ZK1290.14	713.445342	-1.2437058	0.39379899	0.015121658
ifc-1	169.729923	1.5881133	0.50287439	0.015121658

acs-4	307.102508	1.27641781	0.4042569	0.015140507
asb-2	15363.0371	1.02780967	0.32556125	0.015147623
Y43F8B.2	2377.0731	1.04328374	0.330491	0.015147863
ain-1	391.591164	1.28768628	0.4081059	0.015211808
tep-1	1529.70361	1.05843258	0.33575098	0.015346673
ogdh-1	3893.69152	1.04299112	0.33092793	0.015370409
nlp-77	29136.9561	1.21248221	0.38483676	0.015392628
ing-3	63.8562079	2.1146119	0.6711988	0.015392628
F26F2.8	208.217844	1.55956551	0.49499075	0.015392628
aman-3	133.800673	-1.5011305	0.47691052	0.015480435
puf-12	694.292588	-1.2667623	0.40246397	0.015480435
acl-8	111.46657	1.64932667	0.52392854	0.015480435
asp-13	5930.07277	-1.3597743	0.43200822	0.015480435
tre-3	1139.38029	-1.1706999	0.37188988	0.015480435
snx-17	452.566526	-1.1720447	0.37240369	0.015481036
F31C3.6	94.4787563	1.67955464	0.53373421	0.01549054
ras-1	156.310628	1.47166676	0.46772351	0.015495339
C18A11.1	2014.19614	-1.0663148	0.33905197	0.015544747
glo-1	185.357064	-1.5092612	0.47986598	0.015544747
F23C8.5	3886.84153	1.05756898	0.33631028	0.015550271
twk-8	165.484756	-1.4679524	0.46702193	0.015611025
rsp-1	819.340896	1.12872072	0.35917043	0.015617599
nhr-110	199.994071	-1.3940025	0.44358649	0.015617599
hrpk-1	107.358468	1.61438507	0.51381946	0.015637865
ZK863.8	738.499635	1.34743046	0.42896202	0.015666052
drd-10	198.345463	-1.5978124	0.50874114	0.01567474
C48E7.1	986.415589	1.12414401	0.35814492	0.015752912
fard-1	645.351898	-1.3840849	0.44096857	0.015752912
F45E1.4	902.129629	-1.0849304	0.34577964	0.015798227
lat-2	26.9322387	2.91305205	0.92860059	0.015816573
aars-2	564.224145	1.15447769	0.36812725	0.015840112
ell-1	239.055438	1.38571831	0.44186354	0.015840112
mrps-33	696.125872	-1.1254907	0.35899662	0.015878843
slc-17.1	229.693722	1.47280932	0.46983467	0.015884345
acs-22	1245.88094	-1.1581069	0.36949084	0.015892361
F53A9.9	859.237851	1.39146889	0.44399443	0.015897451
lbp-6	4014.12932	1.06583109	0.34012045	0.015899169
cpg-9	2106.42359	-1.2092032	0.38630599	0.016076603

tag-180	44.1851214	2.23416952	0.71393276	0.01610545
cnc-7	368.539399	-1.4183038	0.45329252	0.01611816
rps-7	28080.6478	1.40206555	0.44818879	0.016136916
F08G2.8	71.7022903	1.81042763	0.57913352	0.016243564
grh-1	122.07992	1.53092755	0.4898637	0.016278249
dhp-2	111.36556	1.88448215	0.6034895	0.016406545
rpn-11	1027.59901	1.07690049	0.34504277	0.016480306
F33H2.3	127.657485	1.52065099	0.48759573	0.01657107
nra-1	162.326681	1.45366438	0.46608923	0.01657107
W07B8.4	46.8351926	2.1730447	0.69672063	0.01657107
lim-8	114.822093	1.5932901	0.51118986	0.01666056
F43C11.7	1619.0218	-1.1797082	0.37867531	0.016700084
lbp-9	1847.70644	1.05962618	0.3400814	0.016700084
ldp-1	3532.84479	1.02520728	0.32906872	0.016700084
eif-3.D	581.900863	1.12910577	0.36253165	0.016733851
amx-3	157.624875	-1.5102354	0.48496531	0.016741541
oef-1	131.633695	-1.6057551	0.51575964	0.016768494
lmd-3	475.054431	1.15947175	0.37244932	0.016769795
Y57E12AL.1	1309.8378	1.06821706	0.34332392	0.01685214
F11G11.5	1231.07063	1.07326628	0.34497624	0.016852703
slc-17.3	80.4012786	-1.9670598	0.63247234	0.016881673
R102.11	306.998215	-1.641438	0.52774795	0.016881673
T12B5.15	5823.45112	-1.2652331	0.40690395	0.016906941
ekl-5	101.254266	-1.7354914	0.55826613	0.016932255
C24D10.4	114.405171	1.5425692	0.49628271	0.016944569
exos-7	167.390081	-1.544698	0.49722834	0.017023569
tes-1	411.673147	-1.1852226	0.38155903	0.017029284
flp-1	6064.66072	1.24611754	0.40123805	0.017048096
cct-8	206.702036	1.40358048	0.4520598	0.017081038
nlp-56	405.914589	1.25948078	0.40591382	0.017183715
pcca-1	7182.97827	1.04819146	0.33792707	0.017227085
cls-2	47.9026612	2.23620201	0.72106609	0.017231452
dbn-1	320.21753	1.30023288	0.41923335	0.017231452
rpl-7	36890.2179	1.30411756	0.4205689	0.017235701
H25K10.1	46.3077412	-2.2255175	0.71781129	0.017235701
pnk-4	284.922807	-1.3596731	0.43854618	0.017235701
F30F8.5	98.8909197	-1.6214869	0.52307129	0.017248638
W02D9.2	512.92489	1.15787703	0.37380506	0.017373624

rpl-24.2	2360.0463	1.18384223	0.38225565	0.017376308
C47D2.1	452.540491	1.26417672	0.40818462	0.017376308
B0035.13	7095.98459	-1.145422	0.37007569	0.017472447
C02D5.4	1640.28774	1.02634864	0.33165946	0.017473121
F38G1.3	88.2754461	1.69461328	0.54756853	0.017473121
K11D5.2	87.1376307	-1.7791609	0.57528005	0.017570378
ile-1	54.2631145	2.07421979	0.67127101	0.017640841
mat-3	32.5345172	2.55461694	0.82656096	0.017640841
T23B5.3	67.0751695	2.04435428	0.66157984	0.017640841
haly-1	207.978823	1.44588938	0.46779475	0.017640841
F23A7.4	2703.78758	-1.5371456	0.49745512	0.017640841
aak-2	291.570478	1.3254438	0.42889313	0.017640841
C33A11.2	248.86219	1.36635951	0.44240518	0.017715687
nsy-4	157.559564	1.62121192	0.52510613	0.017765258
dve-1	182.460715	-1.3471985	0.43677968	0.017930846
F22G12.5	105.479692	1.97304258	0.64015887	0.017983209
ZC239.16	345.066386	-1.3441654	0.43609101	0.017983209
Y53F4B.51	46.8840765	2.47031433	0.80145835	0.017983209
far-8	6350.82201	1.38322721	0.44876181	0.017983209
sca-1	8797.76274	0.9923144	0.32196887	0.017983209
eif-3.K	210.548898	1.36329086	0.44223846	0.017983209
H12I13.6	679.110138	-1.1609485	0.37672636	0.017988895
F40E10.6	1635.11694	1.03524038	0.33601775	0.01802014
F20G2.5	97.4477364	-1.6093914	0.52245869	0.018034789
ZC168.2	48.9649203	2.18489817	0.70942356	0.018040764
T20B3.14	323.725296	1.20407913	0.3909376	0.018040764
dmsr-2	114.694928	1.54587599	0.50215466	0.018055141
pry-1	189.501392	1.38039138	0.44845152	0.018055141
K01A2.10	238.589667	1.3217538	0.42937474	0.018055141
fbxa-59	320.048823	-1.2312636	0.39998797	0.018055141
tyr-1	232.897785	1.40784686	0.45737604	0.018055141
vab-2	46.9099031	2.15125012	0.69873899	0.018055141
F49E2.2	477.66277	-1.2494999	0.4059985	0.0180703
cpg-1	71.0777443	1.9168928	0.6230473	0.018113324
snn-1	65.0167347	1.92128856	0.62472028	0.018171459
C09B8.4	67.5272037	-2.1305459	0.6930879	0.018244715
C53B7.2	328.236415	1.33376755	0.43405622	0.018302569
R02E12.5	60.0386503	2.50603583	0.81580075	0.018344294

inx-17	452.309079	-1.2956157	0.42196039	0.018415577
rps-30	25698.0027	1.37500327	0.44818751	0.018557984
Mar-04	141.888028	1.64784101	0.53736273	0.018583168
vha-16	3797.9078	-1.0523125	0.34309167	0.018583168
gbh-2	384.519736	-1.1743398	0.38295411	0.018583168
C07H4.1	874.284506	-1.2242684	0.3991846	0.018583168
Y71H2AM.20	157.994166	1.43050999	0.46660467	0.018609994
C34F6.10	295.640789	-1.2636832	0.41221323	0.018609994
mafr-1	104.450213	1.65471832	0.53996988	0.018665822
T24A6.20	130.040117	1.60700325	0.52457664	0.018715157
dhs-15	170.083982	1.61073397	0.52611982	0.018818555
pcyt-2.1	456.101174	-1.1674996	0.38144632	0.01885449
ahcy-1	4841.76794	1.22137239	0.399128	0.018862417
C33A12.3	487.897755	-1.129013	0.3689369	0.018862417
cyp-34A5	28.124035	2.65356708	0.86766836	0.018962404
larp-5	322.27187	1.19431369	0.39073413	0.019016526
F27B10.1	406.647602	1.308214	0.42798501	0.019016526
dmd-10	34.6560756	2.45842103	0.80422148	0.019016526
cest-2.2	108.446665	-1.6087559	0.52634937	0.019016526
W05F2.7	224.125848	1.55758356	0.50982368	0.019028263
cox-5B	8958.36683	1.12467594	0.36810055	0.019028263
metl-6	49.0980473	-2.1374847	0.69964753	0.019028263
rpn-6.1	551.856952	1.10393561	0.36134924	0.019028263
swan-1	178.83725	-1.397627	0.45745816	0.019028263
act-1	4027.77488	1.01726743	0.33304465	0.019050297
ints-2	119.305967	-1.5507055	0.50809691	0.019191555
Y41D4A.5	265.723042	1.23899351	0.4062352	0.01930717
gst-36	910.095049	1.07797215	0.35347056	0.019308345
ugt-46	262.274672	-1.3224638	0.43369472	0.019317399
Y71F9AL.9	1284.40134	1.03500306	0.33949788	0.019344754
lars-1	2047.33827	-1.1289079	0.37038	0.01937145
pqn-35	229.113327	1.54004697	0.50548005	0.019437822
C07D10.7	70.5866643	-1.8552504	0.60924435	0.019521607
wip-1	113.41237	1.51658913	0.49816007	0.019556891
nlp-68	340.505093	1.33433743	0.438507	0.019636939
psd-1	509.148814	1.18996668	0.39122303	0.019702966
F10A3.4	71.5376602	1.83556984	0.6037367	0.019772976
set-30	552.644194	-1.1214403	0.3691323	0.019908798

pdi-6	3418.59827	0.98691603	0.32506945	0.020027167
emr-1	131.11105	1.45845719	0.48066077	0.020107887
ugt-43	154.228981	-1.4728142	0.48542385	0.020107887
lbp-7	263.614666	-1.3115974	0.43227139	0.020107887
math-22	227.080463	-1.5746085	0.51918996	0.020143788
ZK1128.7	340.173219	1.19220886	0.39309201	0.020143788
rad-50	126.789277	-1.5543965	0.51249472	0.020143788
tag-243	205.35092	1.33013115	0.43883874	0.020239618
crt-1	50078.9931	1.16545659	0.38455491	0.020239618
nlp-53	217.63905	1.47441037	0.48648956	0.020239618
Y32B12B.2	320.692249	-1.2123765	0.4001706	0.020291587
unc-43	847.408119	1.0953416	0.36160963	0.020314242
mbk-2	445.883084	1.12335741	0.37104115	0.020398474
ubc-8	264.727472	1.29412573	0.4274812	0.020399427
pcp-1	3382.25551	-1.3931467	0.46043752	0.020493177
flp-16	1932.77399	1.15492743	0.38183918	0.020535666
cpg-2	166.939088	1.71135818	0.56581369	0.020535666
W05G11.8	209.150714	1.32314819	0.43752489	0.020548617
F17E9.4	3562.51491	-1.1531892	0.38153003	0.020643168
T07A9.18	44.0940643	2.1431945	0.70944442	0.02073555
C31C9.7	517.691387	1.11904117	0.37066843	0.020854132
mnk-1	430.587512	1.60919416	0.53320995	0.020909642
linc-50	132.147791	-1.4646494	0.48568444	0.021052104
trap-4	2665.00365	1.02500912	0.33997166	0.021081092
sos-1	830.646268	1.13247297	0.37571591	0.021120874
sox-3	44.8094348	2.22166299	0.73749178	0.02122394
nac-1	113.09233	1.61331041	0.53597454	0.021376106
flp-33	901.306364	1.21433534	0.40397008	0.021645704
rimb-1	150.794152	1.55219981	0.51640843	0.021646042
F23F12.3	31.6561821	-2.511145	0.83569414	0.021693096
rpt-3	366.604456	1.1621313	0.38680323	0.021705392
ceh-45	45.5786401	2.54711727	0.84789071	0.021709942
lap-1	356.67935	1.233312	0.4105687	0.021709942
sacy-1	423.14738	-1.1283765	0.37583235	0.021784394
btb-16	456.291228	-1.1543064	0.38450129	0.021784394
prk-2	121.925038	1.52945623	0.50949269	0.021784394
ztf-29	139.682394	1.52718922	0.50871342	0.021784394
pgrn-1	1661.23891	1.03033577	0.34332404	0.021829066

zfh-2	91.1840303	1.78608525	0.5954906	0.021909438
tln-1	758.292909	1.06764185	0.35597204	0.021909438
F19C7.4	127.465492	-1.6887348	0.56297733	0.021909438
F22F7.7	1118.97624	1.14386313	0.38159453	0.022010702
lido-13	424.133147	1.31797471	0.43975223	0.022012907
ttr-25	5291.8425	0.96226051	0.32106165	0.022012907
B0303.7	518.431111	-1.108714	0.37006653	0.022075311
F35D11.1	27.6825763	2.66213795	0.88877787	0.022109382
T13C2.6	947.720849	1.07751356	0.35976813	0.022110921
apl-1	4324.9403	1.13953117	0.38068346	0.02221292
ufd-2	227.303864	-1.2438477	0.41569594	0.022241624
ZK673.2	507.993593	1.46817589	0.49058238	0.022241624
Y57G11B.5	4770.01297	-1.3399964	0.44783081	0.022241624
abcf-1	315.949462	-1.2250395	0.40943193	0.022241624
sup-36	401.577748	1.1511862	0.38478203	0.022243385
emb-9	3007.45411	1.02989405	0.34450937	0.022381164
nhr-286	59.8939974	-1.8575467	0.62137102	0.022381164
dnj-9	127.696103	-1.4399866	0.48183108	0.0224271
dim-1	1835.6033	1.01756989	0.34058057	0.022470154
pbs-2	760.615889	1.0839271	0.36309579	0.022638275
vha-14	1414.54772	1.06744762	0.35787069	0.022803739
ctnb-1	67.1725608	-1.9642395	0.65878	0.022836563
atg-4.1	253.847642	1.22844274	0.41199532	0.022836563
fubl-3	840.612275	1.12837843	0.37843264	0.022836563
dpf-2	408.753027	-1.1228064	0.3767025	0.022894786
ugt-18	91.0259843	-1.6030554	0.53791049	0.022912122
nhr-58	277.74751	1.22984041	0.41306766	0.023106227
C33G3.4	78.18963	-1.6875815	0.56738205	0.023315884
hpo-13	255.967378	-1.2365385	0.41576996	0.02331616
drd-50	154.499418	1.48434423	0.49919958	0.023347407
itr-1	1536.35946	-1.0124469	0.34060737	0.023403777
slc-30A9	83.0167435	1.6299886	0.54855115	0.023452997
atf-7	492.427432	1.12071843	0.37717309	0.023452997
madd-2	225.623538	1.25793584	0.42340118	0.023461015
unc-94	261.305911	1.27772703	0.43082724	0.023830884
W02D9.10	1810.6497	1.18989342	0.40118996	0.023830884
cpr-6	9405.73986	1.01150783	0.34109859	0.023836981
chtl-1	53.692362	2.06923074	0.69790469	0.023859449

vha-3	161.061226	1.50812282	0.50884383	0.023926523
mrpl-1	204.07209	-1.3323436	0.44963345	0.023940575
K04F1.9	493.980408	-1.2655482	0.42706285	0.023940575
ctg-1	746.351569	-1.0590333	0.35758182	0.02401641
mxt-1	191.673743	1.39418981	0.47071264	0.02401641
ave-1	98.7800927	1.55025283	0.52350066	0.02401641
B0238.12	151.148969	1.5801839	0.53361583	0.02401641
K07G5.5	164.942068	-1.3398648	0.45296941	0.024152478
drn-1	108.311293	1.80087454	0.6088101	0.024152478
Y51B9A.9	73.6119659	-1.7018272	0.57524935	0.024152478
ptp-3	242.84892	1.40638447	0.4754643	0.024152478
C49G7.3	33593.4106	1.18294235	0.39973919	0.024152478
clec-222	136.003794	-1.4020375	0.4739016	0.024152478
F47B7.1	4992.1	1.01038069	0.34148637	0.024152478
ntl-9	49.6177361	2.03107472	0.68736362	0.024373624
Y55F3AR.2	144.188543	1.39150322	0.47097298	0.024379938
hrpa-2	399.917704	1.16567796	0.39456514	0.024379938
F45E10.2	443.640574	-1.2070599	0.40865077	0.024382331
mxl-2	157.165147	1.40289172	0.47491126	0.024382331
F10D7.5	245.585145	1.31826734	0.44632328	0.024382331
ZC8.6	94.1793517	1.60179425	0.5423993	0.024399829
sel-12	36.4423157	2.25438763	0.76357761	0.024442011
C23H4.6	87.9141832	-1.6135246	0.54675289	0.02452668
T23F4.2	84.6416232	1.64049771	0.5560383	0.024569786
cgh-1	716.296681	1.21908885	0.41324942	0.024577384
col-124	24009.38	1.07218517	0.36352943	0.024609358
frm-8	90.1866963	1.77124547	0.60076409	0.024638747
cnk-1	110.834298	1.47384573	0.49988027	0.024638747
dkf-2	355.456487	1.3583749	0.46070301	0.024638747
hir-1	508.197571	-1.1316198	0.38398643	0.024705256
linc-15	797.270105	-1.1490099	0.38988349	0.024705256
grd-14	134.008961	1.42792809	0.48465199	0.024745766
F22F4.9	199.549786	1.36858956	0.46457411	0.024759055
Y57G7A.1	289.042438	1.25425067	0.42587302	0.024802725
C31C9.2	4047.17945	0.95627434	0.32482972	0.024881018
smg-1	92.78346	1.56206858	0.53073711	0.024883304
ngp-1	1266.42278	-1.1102784	0.37718079	0.024883304
Y48C3A.3	134.75735	1.40261497	0.47659584	0.024883304

C52B9.19	47.208734	-2.0405109	0.6932816	0.024883304
hmg-12	467.634486	1.27678261	0.43389462	0.024895286
npa-1	2612.19207	0.97733118	0.33218543	0.024915993
F10C1.9	92.6225221	-1.5730514	0.53491544	0.025008728
T27F6.6	255.079334	1.20572171	0.41006444	0.025024747
nhr-10	490.911147	-1.0844733	0.36893051	0.025054136
hlh-11	563.153292	1.05452541	0.35873845	0.025054136
F59A6.12	2161.07697	-0.9722591	0.33083264	0.025090908
BE0003N10.1	52.311591	1.93107342	0.65727515	0.025103086
fbxa-80	144.302131	-1.6844763	0.57333957	0.025103086
sqv-1	210.7387	-1.2607858	0.4291313	0.025103086
C15H9.11	934.766803	1.20423943	0.40998494	0.02514298
pdl-1	110.743212	1.55089763	0.52805993	0.025149365
tfg-1	902.400759	1.16847968	0.39809301	0.025275707
clh-1	510.056806	1.16447291	0.39689599	0.025358696
nlp-10	1608.16324	1.00939865	0.34461465	0.025741962
abhd-3.1	1718.99142	0.98698748	0.33726874	0.025943629
T23B7.3	149.851173	1.41245442	0.48284214	0.02599948
C34D4.4	198.045265	1.37345461	0.46950261	0.02599948
klp-15	37.9892527	2.2945129	0.78453881	0.026033112
nhr-6	101.239132	1.68598813	0.57655749	0.02605042
Y69A2AR.3	3203.01405	-1.02862	0.35192826	0.026142286
F40A3.6	273.769404	1.17764731	0.40293319	0.026142286
F49F1.7	112.719944	1.57623717	0.53962203	0.026265034
vav-1	194.838529	-1.2906996	0.44195672	0.026295107
madd-3	295.143806	-1.1512998	0.39429478	0.026320442
F17C11.11	2308.49605	-1.1249712	0.38544476	0.026408402
mrpl-4	91.1167177	-1.5801963	0.54155405	0.026452026
rme-1	1535.43352	0.99658083	0.34157866	0.026460028
F19B10.1	81.9989726	1.76866305	0.60633551	0.026492139
col-179	2345.99351	1.2189563	0.41793667	0.026504155
cnc-4	1001.23871	1.00766554	0.3456388	0.02659006
ech-3	181.908831	-1.2858342	0.44140358	0.026768659
eif-1	1150.10993	1.00565441	0.3456476	0.027057657
F01G4.6	38406.9698	0.98100605	0.33727555	0.027112756
W09C5.1	2522.90093	-1.0938677	0.3763565	0.027277116
ZK353.2	116.702547	-1.4456286	0.49741766	0.027277116
unc-96	160.511136	1.53323944	0.52760127	0.027277116

acl-7	264.169109	1.25139559	0.4308124	0.027357495
T07F12.2	99.9525269	1.62228151	0.55850434	0.027357495
sup-46	113.993646	1.61483237	0.55631565	0.02750985
C38H2.2	645.108684	1.04796105	0.36112547	0.027560215
zig-9	774.071204	-1.0860046	0.37441352	0.027662333
F32B4.5	123.111566	1.48025689	0.51059211	0.027760599
R07E4.3	6981.46948	-0.9964915	0.34373738	0.027760599
F23B12.4	1173.3802	1.0172349	0.35107595	0.027874982
pab-2	2079.27317	-0.9743751	0.33631828	0.02788154
T22C1.1	173.948532	-1.3797932	0.4763411	0.027909036
C18E9.9	871.851032	1.00137419	0.34594961	0.028022047
C24H11.5	88.0922221	1.6452038	0.56835365	0.028022047
T21B6.3	277.272039	1.25735895	0.43439718	0.028022047
F53H4.2	465.790128	-1.0963977	0.37877816	0.028022047
ptp-1	92.5007424	1.70730902	0.58993961	0.028042498
arx-7	298.947512	1.16938416	0.40414639	0.028073905
fbxa-165	36.6779106	2.35563931	0.8144632	0.028162079
F36D4.5	157.194029	1.39494777	0.48242215	0.028205867
T04H1.2	1003.52591	1.01166576	0.34990522	0.028212309
lgg-2	3056.39502	0.96354543	0.33330495	0.028226007
C05D2.10	451.912113	1.0646879	0.36853382	0.028377085
immt-1	985.919781	1.01086397	0.34993838	0.028383416
C49C3.9	356.00923	-1.1967382	0.41448254	0.028488586
clec-204	52.73549	-1.9895008	0.6893064	0.028565627
nlp-71	736.576216	1.24960679	0.43348262	0.028866561
pdp-1	105.930046	1.45451066	0.50465628	0.028874977
hyl-1	347.241771	-1.1518094	0.39962582	0.028874977
F25H5.8	1549.86854	-1.0068151	0.34961367	0.029053801
R02F2.8	326.844212	1.23098359	0.4274273	0.029053801
ife-5	35.6976594	2.6970219	0.93754173	0.029238157
mms-19	202.423059	-1.2684124	0.44079182	0.029238157
hsp-16.11	28.7068278	-2.5876333	0.89941654	0.029238157
B0222.1	92.8645505	1.81803342	0.63195308	0.029238157
ceh-93	74.547516	-1.705918	0.59300518	0.029238157
T22G5.3	113.478068	-1.4390202	0.50063989	0.029431218
ZK1073.2	112.276596	1.49939553	0.52167816	0.029431218
pqn-83	4913.40983	1.07489394	0.37416629	0.029541985
vps-4	906.688994	1.02399621	0.35650234	0.029561617

bath-45	28.7860737	-2.5548434	0.89037947	0.029818368
snt-4	1256.34468	1.27481688	0.44440714	0.02982456
uba-1	650.756509	1.04554263	0.36444585	0.02982456
dpy-11	538.081187	1.17967242	0.41125882	0.02982456
F52G3.8	51.8853671	-2.0972703	0.73098786	0.02982456
Y45F10C.4	554.940351	1.10078471	0.38388916	0.029897135
nhr-180	40.5577713	2.12244995	0.74037283	0.029944785
C18A11.3	71.081634	1.69185903	0.59030532	0.029986213
emre-1	989.217635	0.98240175	0.34286407	0.030040718
W08E12.7	886.026724	1.03837741	0.36253399	0.030099779
comt-5	97.8159794	1.68672681	0.58885588	0.030099779
F55G11.8	235.287745	1.36904653	0.47844492	0.030343123
F10E9.12	1162.18132	-1.0761709	0.37643443	0.030571542
moc-5	382.217609	-1.0801449	0.37791222	0.030614444
dmsr-16	34.2282802	-2.4913516	0.87231639	0.030803396
ugt-23	1574.39227	-0.9789082	0.342836	0.030849479
brap-2	210.212344	-1.25174	0.43846061	0.030874257
cul-1	103.003288	1.50179599	0.52624583	0.030956152
Y65A5A.1	72.305738	1.70023308	0.59583355	0.030959703
D1069.1	43.0425137	2.08914462	0.73258699	0.03107163
clec-60	2068.05481	1.11675078	0.39156247	0.03107163
hpo-6	561.443829	1.10677528	0.38807933	0.03107163
tag-267	280.574082	-1.2184311	0.42734009	0.031102954
B0334.3	3464.50942	0.93506461	0.32801531	0.031132934
lgc-22	1029.19029	1.14376122	0.40128925	0.031156401
rep-1	141.023413	1.42814193	0.50119084	0.031205583
npp-15	96.1643804	-1.5852301	0.55637679	0.031208038
W03F8.4	118.846153	1.4500748	0.50897004	0.031208038
dpm-1	404.840023	-1.1466834	0.40280699	0.03139213
C29F3.7	437.039352	-1.0719013	0.37651677	0.03139213
vab-19	183.769721	1.26463184	0.44430631	0.031412677
nhr-80	292.647482	1.33838858	0.47037408	0.031474411
pll-1	142.820447	1.56327726	0.54951819	0.031474411
ntc-1	378.322131	1.10831223	0.38957305	0.031474411
F23D12.11	32777.8701	-0.931339	0.32733731	0.031474411
pcaf-1	77.1935563	-1.7341637	0.61021158	0.031741456
cyp-29A4	184.435921	-1.3013518	0.45803845	0.03179608
tbcd-1	152.201743	-1.315631	0.46373377	0.032185582

pbs-7	646.613947	1.02239007	0.36043554	0.032214059
T02D1.8	1100.35398	-0.9778117	0.34481728	0.032273198
lfor-1	121.256697	-1.3950555	0.49202515	0.032292265
col-118	1430.32511	1.12005885	0.39554604	0.032641709
T10B10.8	160.561176	-1.3320538	0.4704751	0.032658693
ins-24	795.910108	1.07749216	0.38069996	0.032739116
mlst-8	89.9570059	-1.7046281	0.6025514	0.032847685
T03E6.9	78.8267771	-1.6316381	0.57682204	0.032861335
VM106R.1	161.29108	1.32325941	0.46813219	0.032971799
mlcd-1	523.051017	-1.03911	0.36759415	0.032971799
Y37E11B.1	223.589143	-1.2421211	0.43941122	0.032971799
C05D9.3	234.842435	1.17971487	0.41736863	0.032971799
cest-26	565.248377	-1.0232194	0.36200727	0.032971799
tmem-189	306.096021	1.13209671	0.4009023	0.033217007
gbf-1	250.377463	1.22023824	0.43216715	0.033217007
nhr-162	127.832182	-1.4560467	0.5156892	0.033217007
F46B6.6	169.429736	-1.4452694	0.51220327	0.033382249
pqn-94	2473.67616	1.1327607	0.40147812	0.033382249
crn-2	141.346845	1.39423537	0.49427021	0.033430663
vit-6	121089.607	1.17351427	0.41623516	0.033536329
Y113G7B.12	130.304932	-1.3643674	0.48392518	0.033536329
pho-1	254.514063	-1.5865253	0.56279003	0.033547161
praf-3	1041.70739	0.96497699	0.34235697	0.033567372
ZK688.5	296.508336	-1.1221673	0.3982494	0.033618315
K02A6.2	127.342796	1.41080029	0.50068986	0.033618315
F56D3.1	60.7634494	1.93062217	0.68585916	0.033891814
F42C5.9	532.04887	-1.0525486	0.37406033	0.033979937
C47B2.2	147.396988	-1.2955733	0.4604979	0.033994241
F32F2.2	50.2406328	-2.2243966	0.79073622	0.033994241
ifd-1	86.0475678	-1.7436219	0.61980001	0.033994241
dhs-20	268.656528	-1.1279889	0.40102682	0.034005334
tin-13	1578.67337	-1.0043596	0.35711544	0.034017547
C13C4.6	122.480826	-1.3819904	0.49184445	0.034271989
aat-4	92.5921751	-1.7684628	0.63003511	0.034557467
W02B12.1	608.228078	-1.199583	0.42751809	0.034604898
vha-17	1595.11469	0.96919071	0.34541841	0.034604898
asm-2	2061.40982	-1.5331275	0.54635948	0.034604898
sdhd-1	2195.18069	1.08030042	0.38508448	0.034634221

C41G7.9	1847.54293	1.00015122	0.35658237	0.034668775
Y62H9A.4	381.826802	-1.1770882	0.41993527	0.034840089
epg-9	556.334413	1.08030086	0.38553462	0.034918476
C27D6.12	1236.5903	1.01813022	0.36363561	0.035136485
srpa-72	89.4135739	1.5844473	0.5659806	0.035155898
mekk-3	520.4201	-1.0533159	0.37629836	0.035167804
rhgf-2	56.5656415	2.09519379	0.74865712	0.035204388
nhr-34	264.406262	-1.1346156	0.40566117	0.035361265
Y55D5A.3	171.531635	1.32828837	0.47497615	0.035383664
rpb-8	520.826842	-1.0652789	0.38098931	0.035409799
Y54G9A.7	245.573871	1.16227054	0.41582635	0.03549056
C56A3.5	135.912848	-1.3265809	0.47463906	0.03549056
perm-3	265.966112	1.22705173	0.43914075	0.035545819
nspc-3	29.2748675	2.36835657	0.8478968	0.035632257
atg-3	358.19291	1.11748979	0.40013561	0.035656917
spr-1	70.153153	-1.7234107	0.61726426	0.03571776
R06C1.6	727.210072	1.02593542	0.36758518	0.035804913
cerk-1	353.230821	-1.0994322	0.39410075	0.035913188
ears-2	158.982994	-1.3110684	0.46998205	0.035913188
ppm-2	1306.82716	-0.9469119	0.33957967	0.035968428
C35A5.3	518.422211	-1.2326192	0.4420166	0.035968428
F46G10.2	413.124639	-1.0602445	0.38022034	0.035968428
F08B4.7	264.802346	1.28784061	0.46189707	0.035981358
chd-7	300.56542	1.22539034	0.43966153	0.036072775
tns-1	283.360602	-1.1474411	0.41178356	0.036111016
R151.2	2677.61698	-1.1003556	0.39493816	0.036111016
ZK512.2	105.902209	-1.4177556	0.5088398	0.036111016
Y39F10A.1	185.689758	1.30133701	0.46751572	0.036381648
nhr-179	26.9298249	-2.4802225	0.89141737	0.036490432
pqn-88	249.96985	1.54695492	0.556061	0.036505913
F10C2.3	269.994092	-1.1534821	0.41487216	0.036668901
Y37A1A.2	324.672994	-1.1383947	0.40948195	0.036672968
F26F4.6	60.171519	-1.7159758	0.61752434	0.036794695
R13A5.7	121.11742	-1.3669805	0.49226309	0.036982895
K11H12.7	592.897831	0.98968155	0.35649498	0.03704851
eel-1	747.767812	0.99916607	0.36008954	0.037179013
R102.1	184.473833	-1.3729214	0.49482112	0.037179013
C01A2.2	451.687502	1.03961793	0.37492549	0.037327424

catp-1	195.111304	1.26498587	0.45618264	0.037327424
par-3	195.159393	1.25556374	0.45286372	0.037345533
hot-1	93.5534512	1.64726123	0.59419521	0.037349257
D1007.15	104.222895	-1.4999008	0.54132323	0.037467929
F16B4.4	1990.62569	0.92666118	0.33441388	0.037467929
eat-20	80.2240455	1.81149113	0.6538451	0.037476557
pdi-2	9191.00126	0.88713336	0.32025972	0.037507368
klp-16	71.6492264	1.75016975	0.63213025	0.037629586
bca-1	195.353521	1.36336303	0.49244379	0.037629586
gly-8	1299.00823	0.93946674	0.33940087	0.037644959
npp-22	70.620733	-1.6632456	0.60084613	0.037644959
kin-32	137.435232	-1.3481324	0.48717415	0.03770936
ufm-1	581.148072	1.0577392	0.38288713	0.038233798
Y42G9A.3	91.2061901	1.49976294	0.54310444	0.038335034
K07E3.4	3538.06218	0.93786947	0.33983005	0.038503882
pbs-3	551.825559	1.00332385	0.36370545	0.03862119
M6.4	65.9747054	2.28582297	0.82899445	0.038747081
T19C3.3	158.965792	1.47229205	0.53408488	0.038791439
cul-5	292.371269	-1.168657	0.4239559	0.038791439
F49C12.6	96.390482	-1.4617988	0.5304174	0.038839421
wdr-12	147.809604	-1.3614992	0.49432104	0.039012063
icd-2	18262.3907	1.1050801	0.40128896	0.039016702
skn-1	628.834048	1.00199149	0.36383886	0.039016702
col-50	1838.464	1.2330317	0.4479084	0.03910651
F44G4.3	70.6331487	-1.6000342	0.58149862	0.039236636
T08G11.4	400.514683	-1.0745426	0.39066311	0.039307838
T25G12.11	28.5484995	2.34290145	0.85176259	0.039307838
ZK262.2	251.279716	1.30084212	0.47300102	0.039327563
M57.2	281.019732	1.24758467	0.45394264	0.039526082
dnj-13	596.899953	-1.0620545	0.38670438	0.039731349
ech-5	37.9206292	2.14665033	0.78168103	0.039733796
glct-6	230.080987	1.13838524	0.41479481	0.039920226
ribo-1	414.402883	1.14188586	0.41619429	0.039989052
ifa-4	263.998008	1.25907778	0.45893557	0.039989052
C25H3.17	149.938213	-1.2789561	0.46632274	0.040007112
atg-13	297.545164	-1.1200458	0.40840027	0.040007112
sec-16A.1	342.47088	1.16160991	0.42355211	0.040007112
dct-8	10997.6083	-1.058635	0.38601123	0.040007112

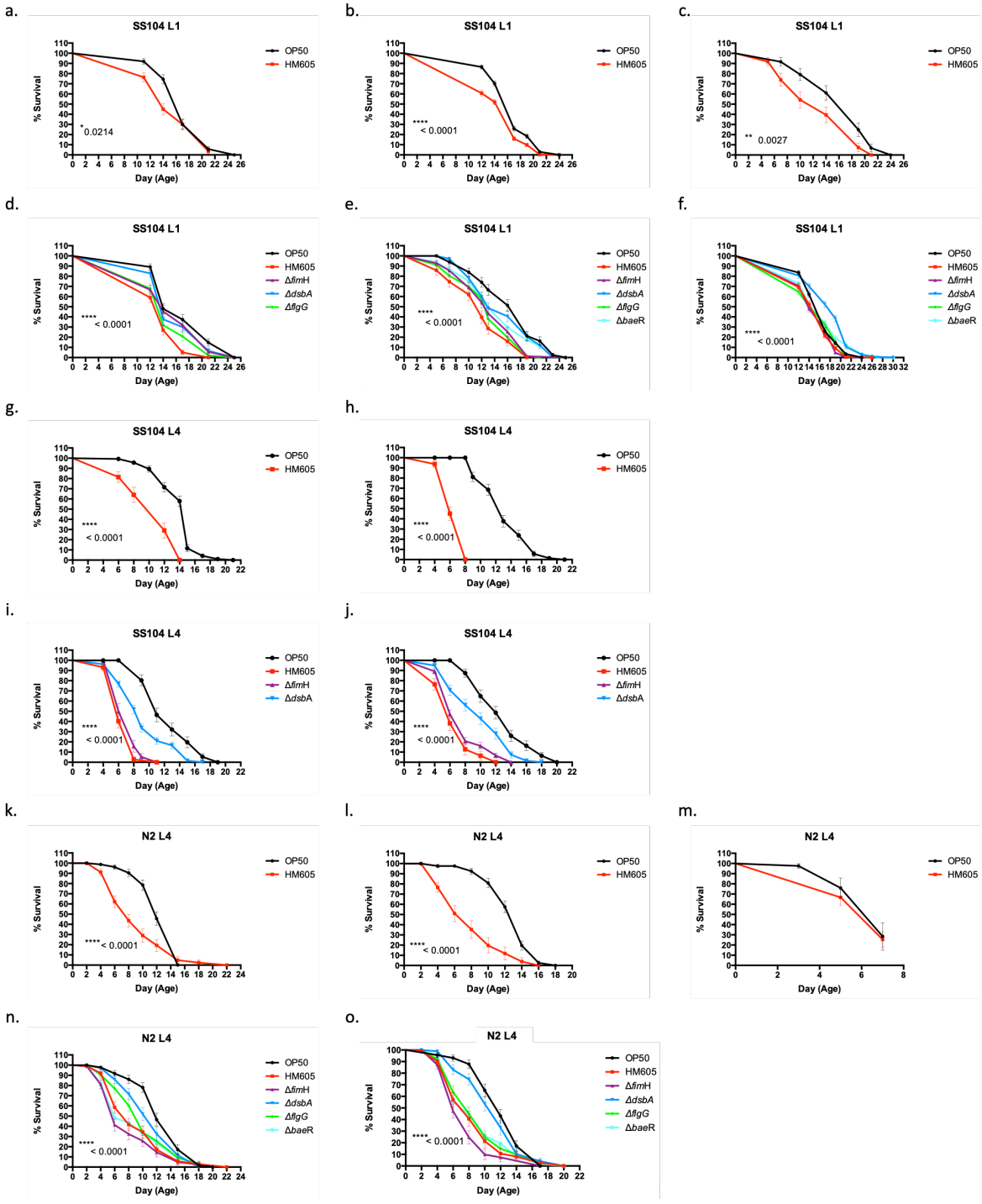
linc-21	1232.50038	-1.4222461	0.51869451	0.040020789
lbp-8	230.654455	-1.8163709	0.66241045	0.040020789
aagr-2	4898.19772	-0.978891	0.35710069	0.040076235
gei-4	131.633154	1.48676997	0.5426292	0.040076235
prk-1	299.756334	1.09683197	0.40026438	0.040076235
soap-1	265.84641	-1.1173089	0.40764482	0.040076235
B0024.11	93.2468892	-1.5244981	0.5563605	0.040076235
T16G1.9	380.626992	-1.1415734	0.41659413	0.040076235
txt-14	1273.89513	0.97940409	0.35732965	0.040076235
C26B9.1	119.72888	1.34037403	0.48921087	0.040076235
T28D9.1	1571.96818	0.96334111	0.351633	0.04008151
rga-4	157.928616	1.27290092	0.46480701	0.040161115
F45F2.9	374.958875	-1.1823813	0.43172111	0.040161115
ins-30	381.050904	1.19922009	0.43796618	0.040185041
rho-1	906.653302	1.01204119	0.36975954	0.04027329
tnt-4	370.101302	1.42133312	0.51929553	0.04027329
akap-1	811.384378	0.96705389	0.3533635	0.040286641
lido-8	819.12878	1.0390704	0.37978778	0.040358058
rab-5	489.755544	1.01351804	0.37064097	0.040507692
mev-1	3847.00225	0.99991097	0.36602577	0.040815254
atf-6	141.669852	-1.3253059	0.48536513	0.040947526
mccc-1	692.526886	-1.0397113	0.38081609	0.040961232
mlck-1	1110.21311	-1.0544619	0.38626521	0.040976565
cdc-48.2	593.717821	0.98301154	0.36018354	0.041037534
Y47G6A.21	124.813376	1.37634824	0.50466708	0.0412066
T28D6.6	160.19357	1.31358943	0.4816575	0.0412066
apm-3	118.675744	-1.3386806	0.49085096	0.0412066
moma-1	721.886928	0.95742525	0.35118113	0.041296937
hsp-4	235.278344	1.16407798	0.42703122	0.041311669
best-8	52.3351483	1.7608025	0.64652331	0.041597967
T19D12.2	64.0840741	1.63163458	0.59955351	0.041794756
oxy-4	117.513791	-1.3446168	0.49414108	0.041794756
dpf-4	272.431958	-1.1095286	0.40772114	0.041794756
F36H9.7	69.0113192	1.61924385	0.59501702	0.041794756
unc-33	367.193563	1.2874179	0.47324178	0.041857065
C45E1.4	175.004585	1.37844086	0.50693024	0.041909915
epg-6	201.202637	1.1944378	0.43916696	0.041909915
T07A9.12	188.478618	-1.1940377	0.43905747	0.041909915

nlp-25	116.866832	-1.3676454	0.50295667	0.041909915
nhr-18	255.059173	-1.1038102	0.40606658	0.041946012
sfxn-1.5	217.589239	1.17038875	0.43053734	0.041946012
nkat-3	380.914083	1.04352478	0.38383902	0.041946012
M04D5.3	453.599965	-1.1204646	0.41245554	0.042117879
C25H3.9	4790.94182	0.89431206	0.32920999	0.042117879
ZC250.4	1630.40706	-0.9922336	0.36545716	0.042282243
ncbp-2	85.6262692	-1.5938602	0.58722317	0.042346039
kel-3	467.82431	-1.0945974	0.4032939	0.042346039
R144.12	231.452695	-1.161684	0.42816354	0.042443589
W02H5.8	173.869519	1.20414479	0.44387107	0.042462852
plc-4	424.38389	-1.0155046	0.37447929	0.042571338
pyk-2	956.493834	-1.0254503	0.37831114	0.042696695
ZK742.4	61.1694377	1.844549	0.68094999	0.042904497
ptr-8	262.326009	-1.1449063	0.42276449	0.042960407
swt-7	1146.15341	0.95971721	0.3544071	0.042960407
ins-5	84.8393525	1.57534119	0.58187819	0.042987489
fut-1	293.911355	-1.2089827	0.44654449	0.042987489
sptf-1	74.4583002	-1.5767106	0.58269378	0.043148016
Y71G12B.10	270.267943	1.16261125	0.42998332	0.043309492
F19B6.1	769.31143	-1.1367891	0.4203797	0.043309492
let-413	259.846111	-1.1001733	0.40685439	0.043309492
Y43F8B.24	255.478366	-1.1588617	0.4285688	0.043309492
upp-1	216.355269	1.28922791	0.47707837	0.043480613
bud-31	105.1244	1.46882524	0.54366531	0.043536879
gst-33	38.0538913	2.29998612	0.85140398	0.043550413
bath-26	146.950336	-1.6029038	0.59350623	0.043611561
rsp-6	689.347516	0.95751061	0.35463337	0.043655213
Y105C5A.13	282.574927	-1.2950935	0.47966216	0.043655213
Y54G11A.11	149.359232	1.24932573	0.46325652	0.043993304
R102.4	704.718917	-1.1012898	0.40836439	0.043993304
T23F2.5	223.64997	1.11989088	0.41523628	0.043993304
F15B9.11	49.783439	-1.8211184	0.67533749	0.043996663
gst-40	97.0405961	1.71139003	0.63476687	0.044011418
C35A5.8	312.898456	-1.0818972	0.40127774	0.044011418
acp-7	84.7227527	1.58022508	0.58634022	0.044014904
R10H10.3	1567.0436	-0.9100685	0.33765479	0.044014904
frm-10	1106.19689	-0.9216595	0.3419293	0.044014904

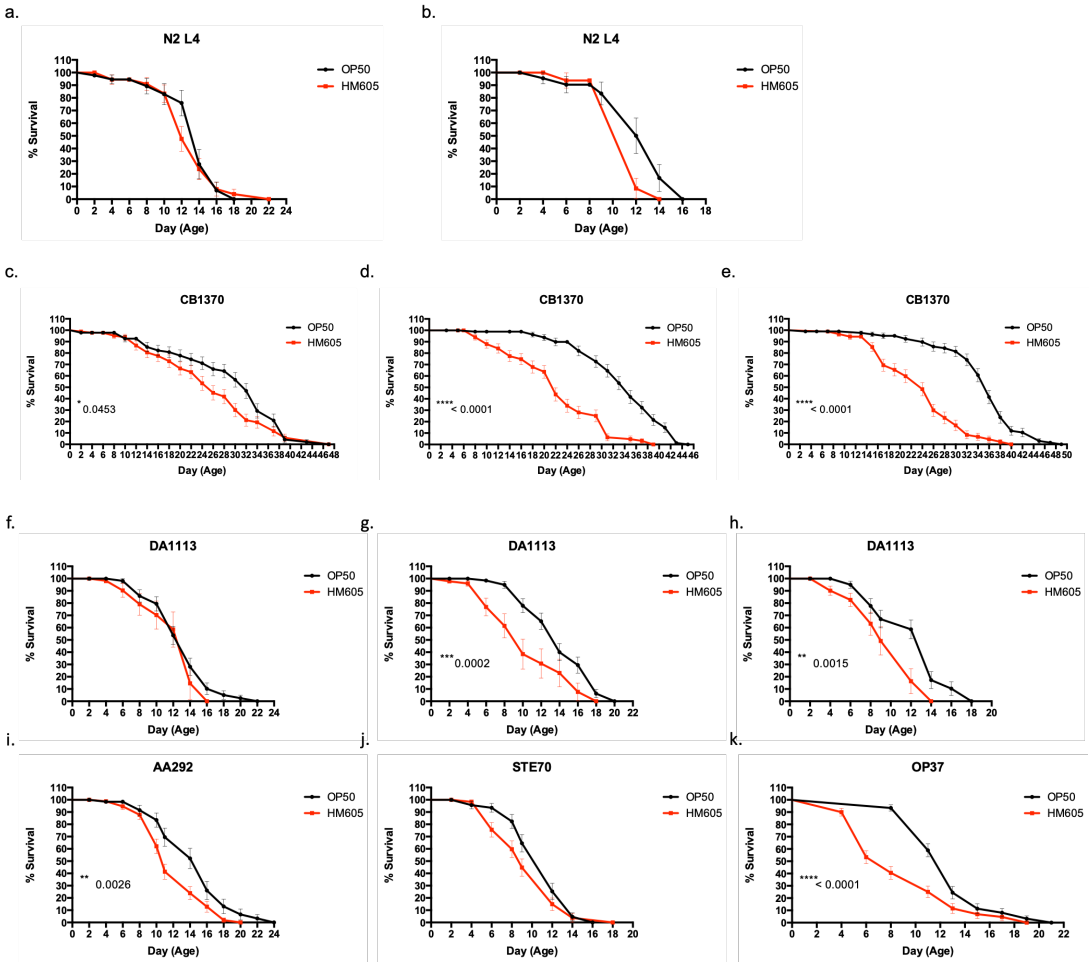
sptl-3	585.005043	-1.0077059	0.37385328	0.044014904
F23A7.8	347.191937	-1.4856502	0.55111242	0.044014904
R05D7.1	315.222641	1.20073075	0.44557649	0.044026134
Y41D4A.7	82.3930916	1.79900157	0.66817333	0.044312737
R10D12.6	29.4313015	-2.3035278	0.85565441	0.044325195
hmbx-1	90.2458945	1.44601093	0.53797157	0.044810033
clec-186	533.883658	1.02092897	0.37982185	0.044810033
hsp-1	10867.6632	0.85608185	0.31848733	0.044810033
alh-6	1702.87181	0.94072987	0.35005287	0.044850504
gly-19	347.807953	-1.0565586	0.39342918	0.045006242
rpl-6	26055.3526	1.18112514	0.43981765	0.045006242
T28D6.4	74.558602	1.53209327	0.57049369	0.045006242
nlp-33	5566.70272	-0.8795573	0.32752841	0.045006242
K11H12.11	233.593774	-1.2579735	0.46865208	0.045141304
rnh-1.2	114.178751	-1.4769133	0.55038142	0.045183672
nrfl-1	1000.96264	-1.0667587	0.39749474	0.045183672
cysl-3	704.266216	0.98139494	0.36579227	0.045183672
Y60C6A.3	50.5058231	1.93417259	0.72082307	0.045183672
col-150	213.017534	1.16859459	0.43555691	0.045183672
eef-2	68091.158	1.09143022	0.40688525	0.04520119
fah-1	2226.39055	0.9335632	0.34800869	0.04520119
sip-1	287.950204	1.27162385	0.47418537	0.045269156
vab-8	379.447981	-1.0659605	0.39758635	0.045326637
F53A9.8	15233.6971	-0.9996527	0.37304221	0.045482677
Y39B6A.3	1065.57891	-0.943699	0.35225736	0.045554469
mpc-2	1335.14892	0.97419102	0.36374911	0.045637719
T10C6.6	733.273362	1.03953002	0.38833142	0.045758368
ZC373.2	2241.46408	1.13598565	0.42436227	0.045758368
abl-1	201.993811	-1.1411937	0.42642792	0.045833045
sid-3	336.801764	1.08042019	0.40384152	0.045917298
nkcc-1	255.666301	1.09024449	0.40756583	0.045937116
C07B5.8	571.204879	-0.9629437	0.36035375	0.046294468
sma-2	229.328323	-1.1227239	0.42020337	0.046316795
Y44F5A.1	75.8416875	-1.5438246	0.57806518	0.046452922
C44B11.4	891.979609	1.12137968	0.41999758	0.046523693
ctn-1	369.004886	1.04541066	0.39169949	0.04658579
pat-12	748.284715	0.95473709	0.35769306	0.04658579
F57A8.1	137.025442	1.32019555	0.49468683	0.04658579

glt-4	205.697514	-1.1385729	0.42663478	0.04658579
R144.11	133.452782	-1.3009895	0.48763299	0.046636721
mrps-26	186.735694	-1.1747416	0.44030816	0.046636721
ctf-18	136.322294	-1.2544957	0.47034381	0.046690369
ceeh-2	324.628901	-1.0654097	0.39942601	0.046690369
nstp-5	119.010882	1.33413252	0.50028417	0.046724065
tpi-1	3455.47147	1.01837762	0.381985	0.046798929
nkb-1	658.222954	1.03785639	0.38948342	0.046954828
F16F9.4	137.48591	-1.4601064	0.5479897	0.046958395
Y38F1A.2	353.508634	1.04857831	0.39366744	0.047051561
T04C12.33	296.175426	-1.1672571	0.43841073	0.047183781
C05G5.2	70.506967	1.67420683	0.62901999	0.047277245
F26E4.3	294.239722	-1.0557758	0.39671325	0.047291877
unc-71	49.8326119	1.81585254	0.68236532	0.047291877
ZK250.13	30.5047502	-2.3298514	0.87580114	0.047385682
Y71G12B.25	305.652518	1.08700661	0.40866248	0.04740576
T20D4.12	127.815699	1.59802328	0.60099581	0.047512541
B0024.4	613.648389	-1.1529664	0.43369681	0.047555053
ZK836.3	61.0292988	1.71041996	0.64363541	0.04767232
D1086.6	805.578543	-1.0213789	0.38444769	0.047742629
pes-7	288.151279	1.06759191	0.40206207	0.047920866
C16C4.19	286.439369	-1.0913711	0.41119539	0.048056476
C09G1.5	419.567836	1.30929901	0.49360972	0.048263134
K12C11.7	125.032723	1.27301768	0.47996958	0.048265234
cdc-25.1	31.39515	2.31875152	0.87502082	0.048350203
hgo-1	2097.44204	-0.8870261	0.33459533	0.048350203
C04F12.5	146.729135	1.55270759	0.58582167	0.048350203
casc-3	160.56286	1.19836935	0.45220197	0.048350203
T20B12.3	158.283998	-1.2177846	0.45953598	0.048350203
unc-119	170.735044	1.38389589	0.52208947	0.048350203
tba-7	248.462354	1.14578437	0.43234232	0.048350203
dcap-1	104.539966	1.4383174	0.54268326	0.048350203
H28G03.2	174.301391	1.24720785	0.47064918	0.048350203
fbxa-156	305.921077	-1.0499723	0.39632716	0.048420018
eri-12	855.28175	0.95577903	0.36080484	0.048426132
ubc-26	345.425012	1.1862319	0.44788895	0.048473347
W09C5.7	136.364415	1.39941566	0.52855479	0.048523983
ctg-2	240.769465	-1.1817972	0.44647032	0.048523983

scp-1	322.22081	-1.1417876	0.43129987	0.048523983
C40H1.8	51.6252229	-1.7637846	0.66632617	0.048523983
sar-1	1411.09375	0.92011549	0.34757002	0.048523983
scl-3	245.243429	1.08929845	0.41146771	0.048523983
fozi-1	62.0780931	1.60692967	0.60713427	0.048529618
K08D8.6	434.527629	-1.0744437	0.40605723	0.048603049
E01G4.3	2480.69539	0.9257666	0.34993955	0.048641872
Y45G5AM.9	292.357243	1.15487076	0.43656092	0.048641872
cyp-37B1	1015.52099	-0.9761138	0.36918206	0.04881453
rpn-13	134.793062	1.38952268	0.52567252	0.048882803
K01C8.1	2431.15927	-0.9585082	0.36287345	0.049127534
F59A2.5	152.267308	-1.2061544	0.45701548	0.049425324
F11G11.15	216.761244	-1.5620388	0.59191064	0.049429287
bre-1	329.290785	-1.0484558	0.39762905	0.049723941
F09F7.6	2318.04893	0.90747111	0.34421025	0.049751688
cpg-8	2078.42219	0.86536363	0.32827232	0.049763105
cest-4	585.056064	-1.0206394	0.38730145	0.049849586
pqn-15	1640.0992	-1.0022522	0.38034118	0.049849586
T09B4.4	349.527664	-1.0446217	0.39657048	0.049912116
cnt-2	221.480092	1.11786143	0.42435982	0.049912116
K09G1.1	1318.97223	-0.8961021	0.34018828	0.049912116
lips-5	97.0244228	-1.457148	0.55332816	0.04998837

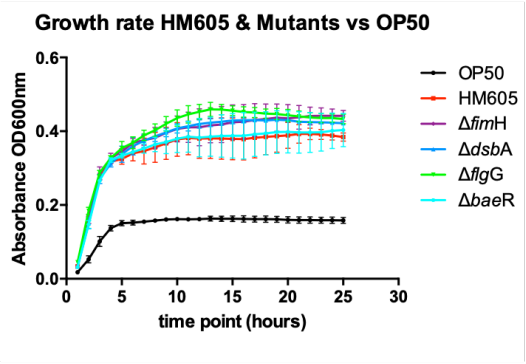


SI.5.1: Replicate lifespan *C. elegans* strain (a-f) SS104 L1 larvae, (g-j) SS104 L4 larvae and (k-o) N2 L4 larvae, when cultured with *E. coli* OP50, *E. coli* HM605 and deletion mutants: Δ*fim*H, Δ*dsb*A, Δ*flg*G and Δ*bae*R. Data was plotted using GraphPrism v6. Statistical analysis was performed through application of the log-rank test for survival curves (*= p<0.05; **=p<0.01; ***=p<0.001; ****=p<0.0001).

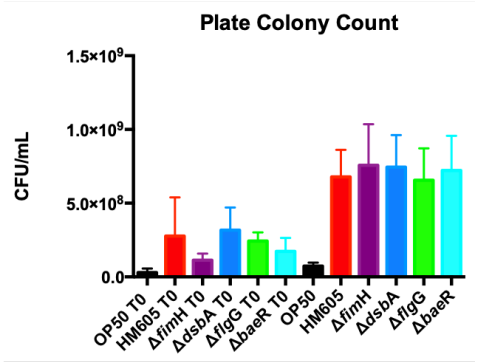


SI.5.2: Lifespan *C. elegans* strain (a and b) N2 L4 larvae when cultured with heat-killed *E. coli* OP50, *E. coli* HM605, (c-e) CB1370 (*daf-2* mutant), (f-h) DA1113 (*eat-2* mutant), (i) AA292 (*daf-36* mutant), (j) STE70 (*nhr-80* mutant) and (k) OP37 (*pha-4* mutant) L4 larvae cultured with live *E. coli* OP50, *E. coli* HM605. Data was plotted using GraphPrism v6. Statistical analysis was performed through application of the log-rank test for survival curves (*= p<0.05; **=p<0.01; ***=p<0.001; ****=p<0.0001).

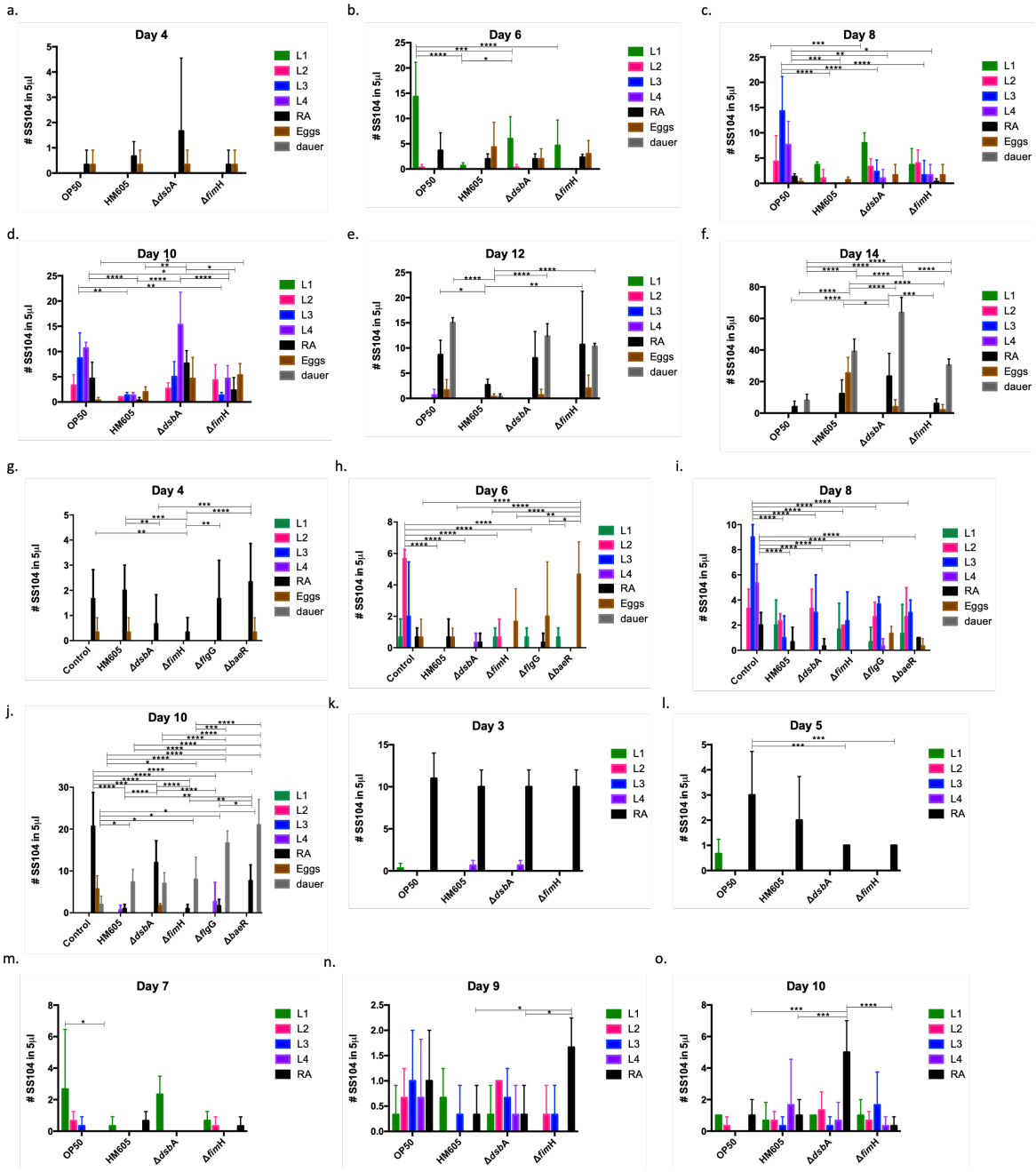
a.



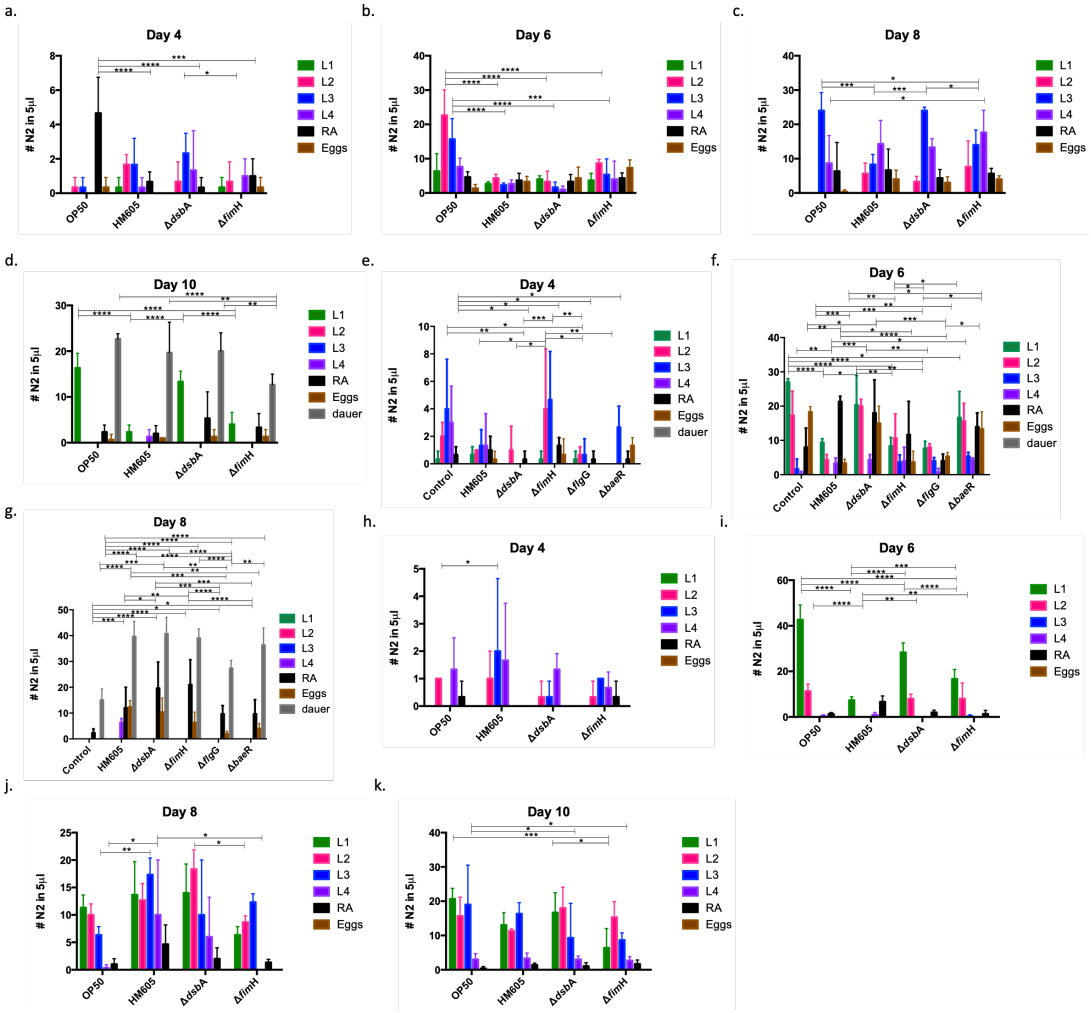
b.



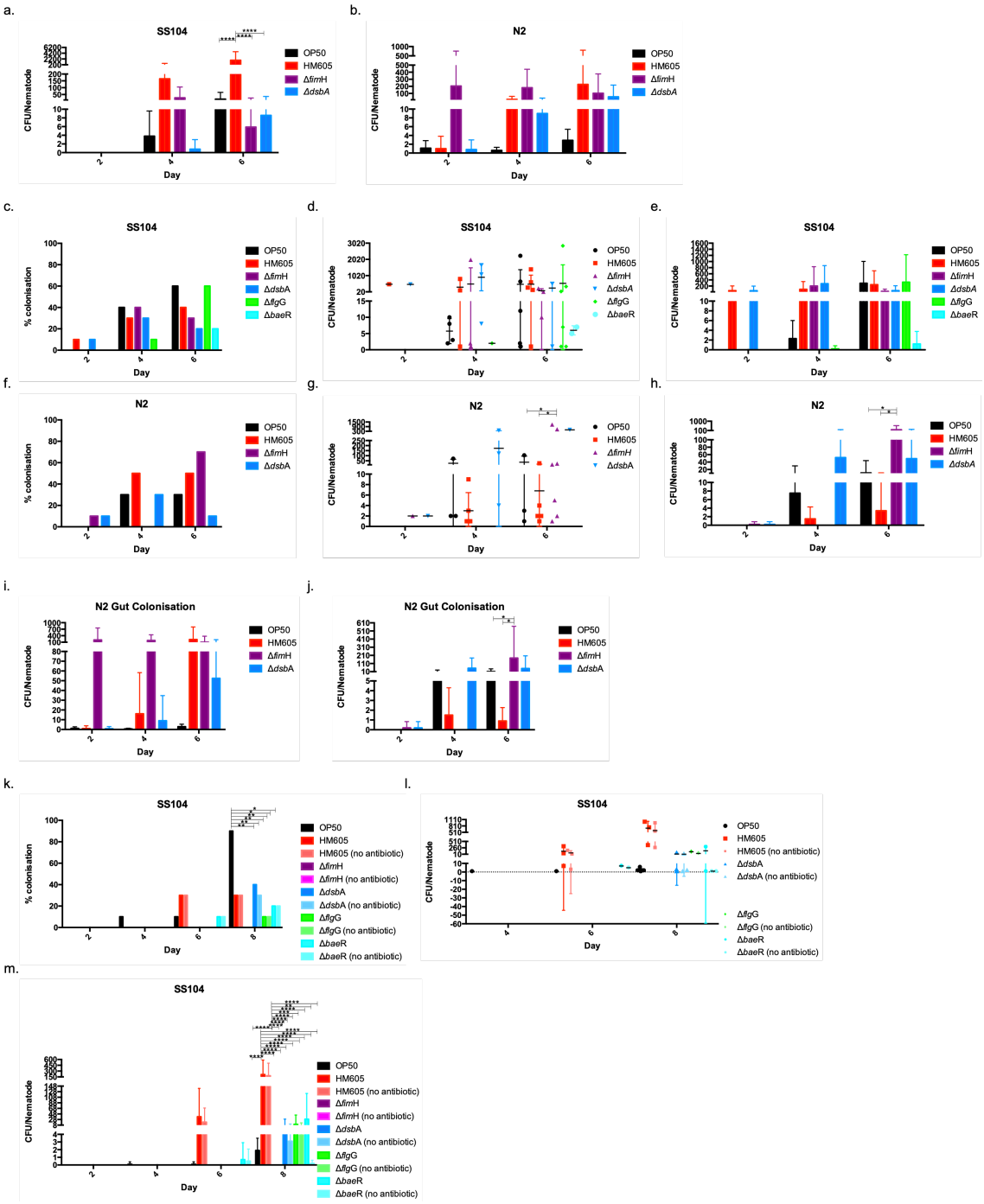
SI.5.3: Replicate growth rate of *E. coli* OP50, *E. coli* HM605 and deletion mutants: Δ*fim*H, Δ*dsb*A, Δ*flg*G and Δ*bae*R. GraphPrism v6. Statistics were carried out using one-way ANOVA, Tukey multiple comparison test (* = p<0.05; ** = p<0.01; *** = p<0.001; **** = p<0.0001).



SI.5.4: Development *C. elegans* strain SS104 L1 larvae, cultured with *E. coli* OP50, *E. coli* HM605 and deletion mutants: Δ*fim*H, Δ*dsb*A, Δ*flg*G and Δ*bae*R, from day 3 to day 14. Data was plotted using GraphPrism v6. Statistical significance is indicated and calculated using Kruskal-Wallis, Dunn's Multiple Comparison Test and Tukey's Multiple Comparison Test (*= p<0.05; **=p<0.01; ***=p<0.001; ****=p<0.0001).



SI.5.5: Development *C. elegans* strain N2 L1 larvae, cultured with *E. coli* OP50, *E. coli* HM605 and deletion mutants: Δ*fim*H, Δ*dsb*A, Δ*flg*G and Δ*bae*R, from day 4 to day 10. Data was plotted using GraphPrism v6. Statistical significance is indicated and calculated using Kruskal-Wallis, Dunn's Multiple Comparison Test and Tukey's Multiple Comparison Test (*= p<0.05; **=p<0.01; ***=p<0.001; ****=p<0.0001).



SI.5.6: Colonisation *C. elegans* strain SS104 L4 larvae (a) CFU/Nematode, (c-e) percent colonisation and CFU/Nematode; *C. elegans* strain N2 L4 larvae (b) CFU/Nematode, (f-j) percent colonisation and CFU/Nematode; (k-l) *C. elegans* strain SS104 L1 larvae percent colonisation and CFU/Nematode; when cultured on *E. coli* OP50, *E. coli* HM605 and deletion mutants: Δ*fim*H, Δ*dsb*A, Δ*flg*G and Δ*bae*R. Data was plotted using GraphPrism v6. Statistical significance indicated and calculated using Kruskal-Wallis, Dunn's Multiple Comparison Test and Tukey's Multiple Comparison Test (*= p<0.05; **=p<0.01; ***=p<0.001; ****=p<0.0001).

SI.5.7: Table of total differentially transcribed genes with adjusted p-value >0.05, in *C. elegans* strain SS104 cultured with *E. coli* HM605, compared to *E. coli* OP50. The base mean value, Log_2 Fold Change, Standard error and adjusted p-value are represented.

Gene name	Mean	Fold Change (log2)	Standard Error	adjusted p-value
clec-52	230.882287	-3.7916002	0.20614762	2.28E-71
asm-3	355.40074	-2.8344774	0.16937878	5.56E-59
pqn-60	243.127845	2.95878448	0.19608112	9.58E-48
acs-2	1750.24873	-2.0652449	0.14412906	5.45E-43
F53C11.1	725.128386	1.46875712	0.10317147	1.66E-42
F19B2.5	4289.74897	1.16231236	0.0821702	5.05E-42
tsp-1	732.13313	2.45620429	0.18858478	1.92E-35
K08D8.4	440.8491	2.67856732	0.20589547	2.05E-35
dct-17	1586.90915	2.35736304	0.18615792	1.43E-33
dhs-26	675.241552	-2.7454229	0.21673504	1.43E-33
cyp-35A3	65.206647	-4.5028727	0.35748564	3.06E-33
hsp-17	765.441734	1.73700395	0.14140974	1.40E-31
clx-1	778.631332	1.66923681	0.13745339	7.19E-31
dhs-2	348.365731	-1.743531	0.14544148	4.45E-30
ctsa-4.2	888.693449	1.40545935	0.11963915	7.35E-29
asp-13	3812.29209	-1.21718	0.10487403	3.63E-28
C49G7.7	594.461963	1.94275202	0.16977049	2.26E-27
Y37H2A.14	1494.47592	2.49704495	0.22185906	1.84E-26
C50F7.5	3925.70729	3.60151816	0.32539887	1.43E-25
C28C12.4	211.523745	2.67349971	0.2444478	5.82E-25
C17H12.6	393.428291	1.54018308	0.14089529	5.89E-25
T27C5.8	151.993895	5.1600611	0.47620967	1.61E-24
T24C4.4	993.667314	2.09474785	0.19474623	3.65E-24
F25A2.1	241.735913	2.55479531	0.24313854	5.03E-23
clec-218	118.664356	-2.960427	0.28551945	2.09E-22
clec-61	323.702468	-3.3571611	0.32598418	4.17E-22
VZK822L.2	98.6424924	2.66560683	0.26209952	1.51E-21
C01G10.4	76.0037918	3.73208299	0.3690287	2.61E-21
E02H4.7	532.010093	-2.429662	0.24299787	8.07E-21
srx-125	92.1410142	-1.9906498	0.19928799	8.62E-21

F49H6.13	122.895749	5.02649892	0.50413133	1.00E-20
F39G3.5	178.134774	1.76976466	0.18032683	4.63E-20
F55G11.4	11690.7796	2.07303859	0.21164181	5.43E-20
dhs-23	35.9993287	-3.5482354	0.36262997	5.84E-20
fipr-1	540.466569	-1.2732117	0.13032853	6.61E-20
clec-4	86.6248795	3.65675663	0.37451463	6.76E-20
gale-1	1196.21275	2.2458397	0.23224686	1.66E-19
ZK896.5	311.961517	2.08107328	0.21665987	3.03E-19
F20G2.5	443.127387	2.3537331	0.24513961	3.06E-19
F42A10.7	188.897685	-2.9151843	0.30451676	3.93E-19
tsp-2	858.090997	2.15126915	0.23186482	6.38E-18
cyp-35C1	459.554809	-1.7942411	0.19367368	7.09E-18
nspe-1	132.798204	7.00182894	0.75627146	7.32E-18
lips-11	92.4048164	2.36613111	0.25751701	1.38E-17
C01G10.17	101.326614	2.91037469	0.31858552	2.20E-17
ttm-5	329.620648	1.31637283	0.14562922	5.20E-17
skr-5	285.112191	1.44809197	0.16148388	9.79E-17
F33H12.7	1530.18033	3.11763317	0.34860981	1.20E-16
arf-1.1	160.33901	2.06146118	0.23058697	1.20E-16
ftn-1	739.926872	-1.6027506	0.18015311	1.75E-16
ZK6.11	15019.7658	2.08269689	0.23556121	2.81E-16
mtl-1	16541.8904	-2.3068196	0.26653738	1.44E-15
F35E8.10	236.918947	1.41354288	0.16660704	6.21E-15
F17B5.1	139.871888	-2.3758249	0.2830695	1.33E-14
K10D11.5	292.442035	1.76788085	0.21099677	1.47E-14
haf-7	88.9732095	1.91261163	0.23069179	3.04E-14
dod-22	1064.15658	1.3170716	0.15968024	4.28E-14
oac-31	154.154655	1.55441745	0.18888058	4.91E-14
fat-3	4139.70331	-1.3393399	0.16343677	6.44E-14
C49C3.9	1913.73913	2.26643073	0.27688682	6.85E-14
B0024.4	3595.80077	2.05551329	0.25134609	7.17E-14
clec-17	49.52039	3.49630902	0.42918339	9.02E-14
dod-21	71.3610999	2.34124013	0.28732913	9.02E-14
oac-6	287.081056	2.37574234	0.29260523	1.11E-13
F44E7.5	72.7589779	2.76330889	0.34254282	1.68E-13
asm-2	473.70305	-1.3383389	0.16650089	2.10E-13
cth-1	365.889209	0.99988258	0.12461235	2.32E-13
nep-22	246.848246	1.43330092	0.17876952	2.40E-13

daao-1	160.437658	-1.4917576	0.18958021	7.87E-13
srr-6	159.449584	1.94357729	0.24825395	1.06E-12
clec-166	240.976375	-1.3088851	0.16742925	1.15E-12
cyp-33C8	336.37761	1.98007611	0.25364954	1.24E-12
asns-2	2428.16845	-1.4712066	0.18940307	1.66E-12
C25H3.10	289.422272	-1.4288634	0.184347	1.87E-12
F53A9.8	7416.81575	-1.2035684	0.15602659	2.47E-12
T19D12.4	571.859576	1.59302851	0.20678022	2.63E-12
gst-6	618.424102	-1.1571341	0.15350739	9.39E-12
E02H4.4	42.2063145	-2.6427334	0.35137549	1.06E-11
ZK1320.9	484.03937	-0.8560804	0.11491952	1.80E-11
pqn-36	63.9437541	2.47856241	0.3342327	2.29E-11
clec-174	58.8549142	4.2539326	0.5739175	2.33E-11
F13A7.11	206.285125	1.59581233	0.21886891	5.68E-11
ZK1290.10	321.986266	1.83589986	0.25193529	5.78E-11
cpt-3	322.089589	2.55239735	0.35141886	6.82E-11
K09D9.1	371.095288	1.31684961	0.18175841	7.71E-11
C07E3.3	472.26038	1.49385349	0.20654107	8.34E-11
F23C8.14	77.2291625	-1.5051934	0.20823821	8.52E-11
skr-3	1157.1464	0.74199028	0.10320769	1.12E-10
C09B8.4	62.3336159	-3.3871556	0.47209185	1.23E-10
tsp-10	119.075602	-1.3337811	0.18690823	1.62E-10
dlhd-1	59.3427999	-1.9103767	0.27035146	2.65E-10
C32H11.9	69.239851	3.43739263	0.48839868	3.21E-10
nspe-2	61.82367	8.75026622	1.2455089	3.48E-10
T19H5.6	16.1182927	-3.1337447	0.44843513	4.49E-10
K10D11.2	54.0213125	2.02460497	0.29061789	5.18E-10
ttr-44	1044.53376	-1.3273606	0.19139485	6.40E-10
nspa-5	39.3739093	-1.9186193	0.27910151	9.73E-10
skr-4	693.92336	0.79696174	0.11640861	1.17E-09
col-138	42.3260708	3.39058216	0.49695828	1.37E-09
prx-2	212.088385	-0.9769498	0.1438672	1.69E-09
W02B12.1	395.853623	-0.8648012	0.12790361	2.05E-09
F49H6.3	61.9179782	2.51981153	0.37311283	2.14E-09
Y46G5A.20	927.277041	1.09916388	0.16289861	2.21E-09
T01D3.6	3975.37012	1.18254796	0.1765024	3.04E-09
fbxa-74	123.539451	1.56005555	0.23316273	3.20E-09
scl-20	663.56993	-2.3145766	0.34614135	3.26E-09

erfa-1	354.256575	1.26325994	0.1890555	3.34E-09
F41H10.1	333.57678	-1.5795989	0.23654281	3.40E-09
acox-1.2	171.457476	-1.626974	0.24607935	5.29E-09
M02E1.4	421.379739	-1.2611639	0.1913467	6.02E-09
pcp-1	860.2269	-1.450365	0.22017858	6.12E-09
oac-57	947.87508	1.48497642	0.22603267	6.82E-09
EEED8.2	78.7184345	-1.7808552	0.27249525	8.51E-09
hrg-7	5262.7865	1.75835913	0.26917296	8.60E-09
F23F1.2	186.862859	-1.2228086	0.18754032	9.25E-09
T16G1.4	19.7042841	-2.5095962	0.38500462	9.29E-09
clec-57	141.719556	-1.3857251	0.2138781	1.20E-08
F59A7.2	483.114348	-1.0407842	0.16166532	1.56E-08
R193.2	205.85632	2.53126782	0.39358767	1.61E-08
pgal-1	1445.47368	-0.5672279	0.08835564	1.70E-08
F27E5.9	391.535887	1.66942596	0.26003953	1.70E-08
folt-3	58.5070118	-1.7550186	0.27338936	1.70E-08
acox-1.4	241.723886	-1.171758	0.18356631	2.12E-08
ssp-10	260.970575	-1.0398174	0.16286888	2.12E-08
T26H5.8	28.3623284	-2.8266078	0.44301999	2.14E-08
dpy-13	56.2368951	2.96712576	0.46622629	2.36E-08
B0205.13	138.414477	1.21364748	0.19074929	2.37E-08
clec-47	19939.1492	-1.394415	0.22011892	2.81E-08
mtl-2	5442.68378	-1.3151181	0.20814105	3.10E-08
Y82E9BR.22	945.154471	-0.9366751	0.14851947	3.31E-08
oac-14	322.685737	1.01023658	0.16019739	3.31E-08
zipt-2.3	60.4944908	2.26191955	0.35934848	3.51E-08
rars-1	1668.07866	-0.5412989	0.08599156	3.51E-08
EGAP1.5	208.56293	-1.1878622	0.18920598	3.87E-08
K10D11.3	136.025552	1.46025645	0.23314143	4.23E-08
dhs-20	216.463937	-1.0149735	0.16213503	4.29E-08
D1022.3	22.3651152	-2.2501872	0.35978746	4.42E-08
Y51H4A.5	58.144599	-1.9157736	0.30699051	4.79E-08
fbxa-163	126.73603	-1.8990738	0.30444844	4.84E-08
clc-1	9821.10519	1.89696805	0.30429354	4.92E-08
lys-1	42413.2912	1.0264449	0.16558442	6.11E-08
cogc-3	104.879371	1.22680191	0.19805844	6.25E-08
F09F9.3	95.7589613	1.61364933	0.26229367	8.10E-08
R02C2.7	182.823438	-1.0349896	0.16978625	1.15E-07

Y39B6A.1	942.265513	1.98354413	0.32581992	1.20E-07
klf-3	183.274196	1.21142481	0.19947866	1.30E-07
scrm-4	220.989425	1.13528167	0.18725184	1.38E-07
F46B6.12	398.576459	-1.064929	0.17578235	1.41E-07
cyp-13A11	20.691916	-2.2132349	0.36643346	1.57E-07
ilys-3	409.454277	-2.3662363	0.39215842	1.62E-07
Y65B4A.6	204.779581	1.00731182	0.16729096	1.71E-07
F12E12.11	145.901518	-1.8060658	0.29990048	1.71E-07
W02D7.11	24.6992506	-3.5308783	0.5862412	1.71E-07
gck-2	61.8211544	1.64215633	0.27342092	1.87E-07
F31B9.2	62.0981275	1.66608832	0.27775399	1.95E-07
hrg-1	817.722856	2.93164122	0.4907492	2.25E-07
C05C10.3	712.931492	-1.1390809	0.19084873	2.31E-07
cri-1	102.885439	-2.2263717	0.37738054	3.49E-07
C14H10.3	466.024156	0.72379359	0.12269774	3.49E-07
F07C3.9	228.690955	-1.5549306	0.26452455	3.93E-07
ugt-1	54.282049	-1.4199125	0.24193887	4.13E-07
Y119C1B.12	11.462152	-3.4553477	0.58889795	4.14E-07
anmt-2	840.649072	-0.7625195	0.13008742	4.26E-07
F22H10.2	377.69776	3.2535861	0.55534983	4.31E-07
ZK673.1	103.580004	-1.5019031	0.25647972	4.36E-07
T16G1.7	30.4732211	-3.1972092	0.54774371	4.85E-07
sri-36	29.6873039	4.21417111	0.72338728	5.16E-07
kel-8	505.03944	0.872963	0.15126783	7.11E-07
cyp-35A5	32.5365343	-1.8522847	0.32180805	7.73E-07
F40B5.2	260.759672	0.81941472	0.1425687	8.07E-07
T23F11.6	174.113572	0.92753072	0.16158344	8.38E-07
B0238.12	156.466498	2.2615337	0.39425586	8.53E-07
C25F9.11	69.691314	2.1550014	0.37657206	9.18E-07
cyp-25A1	433.496082	-1.0301784	0.1808811	1.07E-06
Y75B8A.39	32.4151697	2.19790586	0.38601269	1.08E-06
taf-5	86.0018254	-1.1531264	0.20362594	1.28E-06
Y47H10A.5	2090.54761	2.67100531	0.4730343	1.39E-06
lipl-2	472.294333	-2.2012918	0.38987334	1.39E-06
cpt-5	227.090644	-1.5978468	0.28301595	1.39E-06
nhr-50	80.1655316	1.75515585	0.31152188	1.47E-06
gst-22	196.763116	1.40695687	0.24970601	1.47E-06
Y17G7B.8	246.150224	1.33868127	0.23773917	1.48E-06

cyp-34A9	753.732813	-1.1846625	0.21037426	1.48E-06
nmad-1	1159.62252	-0.8508761	0.15122293	1.51E-06
gst-41	112.182807	-0.9766062	0.17382272	1.58E-06
clec-71	21.0626418	-1.9810648	0.35523298	2.00E-06
cpr-3	1538.34475	2.23822777	0.40162528	2.03E-06
W01C8.5	358.267774	0.78792826	0.14156698	2.10E-06
kin-18	176.125165	0.96170161	0.17309312	2.21E-06
F21C10.11	824.47963	-1.0890889	0.19633492	2.32E-06
F57F4.4	2643.39947	1.46598601	0.26493754	2.49E-06
F14H12.3	854.211637	3.06415816	0.55388035	2.50E-06
txt-11	47.3978572	1.56604902	0.28331178	2.55E-06
act-5	3722.58557	1.13062669	0.20487377	2.67E-06
F48D6.4	7155.779	-0.6080647	0.11021751	2.68E-06
ttr-29	275.338116	1.78882906	0.32438091	2.69E-06
C30F2.3	45.7498399	2.55973452	0.46418327	2.69E-06
hyl-1	369.692278	0.68501315	0.12454222	2.90E-06
C55A6.6	207.744955	-1.138948	0.20714986	2.92E-06
ulp-3	266.170854	-0.7239103	0.13184597	3.04E-06
F55G11.8	483.342708	0.70687987	0.12889785	3.13E-06
T22F3.11	58.1368459	-2.645146	0.48282722	3.22E-06
dpy-4	77.2255694	2.01155897	0.36999486	4.05E-06
kreg-1	105.092207	3.82549368	0.70409283	4.11E-06
clec-55	56.2343897	-1.9108254	0.35234181	4.33E-06
col-63	45.3923522	3.55415888	0.65573105	4.38E-06
F31B9.4	28.942983	-1.5809287	0.29198244	4.50E-06
ugt-16	54.0540307	1.7330626	0.32043937	4.63E-06
linc-34	237.752195	-0.8209409	0.15201781	4.82E-06
F58A3.3	45.5906927	-1.634221	0.30286076	4.92E-06
fbxa-61	45.616686	-1.377111	0.25538283	4.99E-06
abf-5	552.33476	1.0955574	0.20328412	5.06E-06
lbp-8	169.662342	-1.0646562	0.1977862	5.22E-06
cpr-1	5402.96235	-1.6774999	0.31193936	5.34E-06
anr-46	5.27705673	-6.5612802	1.22208219	5.58E-06
C32F10.8	1268.0703	-0.4595148	0.08585447	6.09E-06
cest-12	45.6556358	2.16402632	0.40567387	6.69E-06
T19H12.15	126.73228	-1.4724608	0.27701672	7.40E-06
fipr-3	197.642713	-1.5040168	0.28313283	7.50E-06
ZK1055.7	942.092484	0.50642679	0.09535726	7.52E-06

W02A2.9	2761.12547	1.18212502	0.22267094	7.56E-06
cyp-33C4	74.7885845	-1.0460171	0.19712209	7.62E-06
oac-20	105.734789	1.5618953	0.29436489	7.62E-06
tth-1	1973.84786	1.59218407	0.3029154	9.95E-06
clec-186	1676.1065	1.45975435	0.27777291	9.96E-06
F19C6.5	84.3778796	-1.0853439	0.20663703	1.01E-05
fat-6	40455.8462	-1.0908239	0.20869724	1.15E-05
prx-3	146.214052	-1.0974455	0.2103404	1.21E-05
F42H10.6	603.62599	1.01852241	0.19588965	1.32E-05
mrpl-44	220.174501	-0.7789557	0.1500518	1.38E-05
F19C6.8	210.484593	-0.8229594	0.15889571	1.46E-05
Y57E12B.11	16.0369893	6.79052133	1.31484285	1.57E-05
fbxa-164	35.3551364	-1.9700714	0.38196273	1.63E-05
T22B7.7	13834.819	-1.2349713	0.23964436	1.66E-05
srh-2	68.4524897	-2.0706217	0.40240753	1.72E-05
spp-5	79453.1089	-0.7626412	0.1482532	1.73E-05
M02H5.8	7318.17641	1.08195104	0.21041461	1.74E-05
C56E6.4	5.33665377	-5.5708402	1.08401855	1.76E-05
C38H2.2	845.598934	1.24517213	0.24241294	1.77E-05
rgba-1	8.9370207	-4.0419009	0.78783663	1.83E-05
linc-46	546.323473	-0.7852037	0.15317692	1.86E-05
clec-227	40.4926132	-2.1841465	0.42722588	1.99E-05
lron-7	3811.85231	0.50763511	0.09941293	2.05E-05
F58G6.9	360.431822	0.92734525	0.18176229	2.09E-05
W07A12.8	76.1610933	-1.3415506	0.26402619	2.32E-05
F23H12.3	248.120998	0.85747626	0.16892613	2.37E-05
metl-18	95.573803	-0.9664592	0.19052048	2.40E-05
C16E9.1	27.108877	-1.6935183	0.33382988	2.40E-05
F49C12.7	475.414545	-0.7565853	0.14920528	2.41E-05
rgs-7	107.139489	1.37175916	0.27131984	2.60E-05
Y37A1A.4	91.9241434	1.4267192	0.28238215	2.63E-05
Y54G2A.48	58.5191105	-1.0962095	0.21750157	2.80E-05
tfg-1	773.169205	0.8078643	0.16096803	3.11E-05
Y26G10.7	91.4279759	-1.7075816	0.3407437	3.22E-05
C18D11.10	37.6797076	-1.9422019	0.38912888	3.57E-05
C46H11.2	83.7879784	-1.3097153	0.2625665	3.61E-05
ZK593.3	303.388351	-0.8172304	0.16437601	3.91E-05
cyp-35A1	9.34501129	-3.1170872	0.62872739	4.19E-05

F59C6.5	2550.21477	-0.458878	0.09261807	4.24E-05
ZK742.7	254.110517	-0.7478354	0.1510648	4.32E-05
EGAP9.3	44.3185737	-1.223426	0.2477009	4.56E-05
comt-3	688.13116	1.09513182	0.22210206	4.74E-05
T15B7.1	526.158208	-0.8736247	0.17724396	4.76E-05
bath-26	139.503628	-0.8690223	0.17665311	4.97E-05
tsp-9	102.025887	1.03960495	0.21134172	4.97E-05
spp-6	93.2425129	-0.9443805	0.1921237	5.05E-05
mboa-7	164.538848	-1.0464681	0.21328698	5.26E-05
ZK643.2	51.6494612	-1.3235585	0.27033707	5.53E-05
vit-1	8920.88852	-1.0002682	0.20438895	5.57E-05
col-14	50.4633728	1.92860647	0.39456511	5.72E-05
F19B10.13	175.105485	1.45287254	0.29850193	6.33E-05
F11E6.11	163.615269	-1.4927609	0.30691058	6.41E-05
hil-1	872.656672	-1.2048155	0.24847189	6.89E-05
tag-244	152.037246	1.82856184	0.37737159	6.98E-05
Y45G5AM.3	271.615762	0.87715487	0.18110604	7.03E-05
M03E7.2	13.3439216	-2.3741957	0.49026348	7.03E-05
cpt-4	70.5493142	-1.4467606	0.29907764	7.17E-05
H39E23.3	785.650239	-0.8903255	0.18404758	7.17E-05
C54C8.12	135.784804	-0.7588322	0.15727525	7.61E-05
C50B6.7	617.339263	-0.5697258	0.11818065	7.74E-05
F19B10.14	170.692987	1.49009594	0.30919337	7.77E-05
dod-17	196.285831	1.80466329	0.3749434	7.98E-05
clec-42	26.5031421	2.16898966	0.45076269	8.01E-05
slc-36.5	263.537549	-1.0019095	0.20874365	8.48E-05
trh-1	223.309849	-0.9618202	0.20069017	8.75E-05
ncx-9	19.7702979	2.492475	0.52024622	8.79E-05
rnh-1.0	388.327859	1.74788167	0.36492535	8.80E-05
pcm-1	316.502154	-0.5897459	0.12313398	8.80E-05
clec-72	37.8481208	1.78751439	0.37424082	9.36E-05
otub-2	25.7462779	2.22886841	0.46684106	9.38E-05
irld-11	6.54090365	-3.5540258	0.7444736	9.38E-05
C49G7.12	246.909565	1.03890662	0.21758152	9.38E-05
srr-4	132.357532	1.26195483	0.26469905	9.65E-05
F11D11.3	9.69080452	6.09262098	1.27985304	9.96E-05
ttr-33	290.525433	1.09060809	0.22928488	0.00010115
Y9C9A.16	132.210867	-1.2399713	0.2609219	0.00010297

ZK666.11	17.2511642	-2.1089914	0.44436269	0.0001058
lec-11	619.037024	1.97039055	0.41542272	0.00010702
F09F7.6	770.324671	-1.0037881	0.21175071	0.00010808
T06A1.5	134.334844	1.16322063	0.24627842	0.00011727
Y40H7A.10	2996.43965	-1.0607817	0.2246225	0.00011727
C17C3.1	1094.15043	-0.8882959	0.18838109	0.00012103
F44E7.3	34.8597494	-1.4558204	0.30898312	0.00012288
F22E5.1	96.5155981	1.06225257	0.22552144	0.00012335
cps-6	506.149776	-0.7305557	0.1551728	0.00012428
F13B6.2	189.154777	1.169242	0.24850085	0.0001256
ril-2	340.005105	-1.3481405	0.28660848	0.00012606
pud-3	2256.27051	1.55751872	0.33162848	0.00013016
F56D6.8	16991.6022	-0.6990382	0.14893297	0.00013161
C25D7.5	43.2204217	2.52622304	0.53923442	0.00013696
F01D5.5	1020.10054	1.60583951	0.34370452	0.00014521
T16G1.6	7.80467999	-3.2305207	0.69153681	0.00014521
ugt-31	77.1045556	-1.2090517	0.25887608	0.00014554
ugt-22	529.200103	-1.1233049	0.24077558	0.00014867
mig-1	102.683579	-0.93849	0.20157453	0.00015525
F53F10.1	78.8860807	-1.0081473	0.21677775	0.00015853
K08D8.12	107.076853	1.08811701	0.23399448	0.00015853
clec-265	271.293652	1.487625	0.32051045	0.00016488
valv-1	1097.48126	1.48507147	0.32024958	0.00016773
F43C11.7	308.332234	-1.9350476	0.41738455	0.0001681
ugt-53	91.8010132	-1.7849143	0.38537672	0.00017128
klp-7	220.152761	0.88586527	0.19164061	0.00017839
ZK856.5	128.992877	-1.1511837	0.24910719	0.00017895
dmsr-11	3.36712425	-5.926409	1.2832298	0.0001809
grsp-4	851.476646	-0.5247208	0.11368218	0.00018268
F49F1.7	534.186436	2.22825158	0.48287789	0.00018314
K11H12.4	256.748943	1.02046416	0.22120922	0.00018364
sox-4	200.502265	1.01676701	0.22042855	0.00018364
C41H7.2	17.5750427	2.50141915	0.5425047	0.00018468
nath-10	74.5610333	-0.8836969	0.19184306	0.00018817
uaf-1	84.3280533	1.73091977	0.37600585	0.00019025
F49E12.12	10.5700532	-2.3343975	0.50722482	0.00019072
F53H2.3	28.3169617	1.94053035	0.42213185	0.00019506
pcbd-1	3231.90179	-0.6809555	0.14833751	0.00020053

ZK1037.6	207.433826	0.84976398	0.18530235	0.00020437
C15B12.4	130.735753	-0.951471	0.20750132	0.00020437
mrpl-23	250.425298	-0.7216742	0.15766132	0.00021172
nhr-63	46.7045704	1.77089815	0.38698177	0.0002123
mnk-1	105.663529	1.09101756	0.23872859	0.00021725
C16D9.4	391.201613	1.28278736	0.28065428	0.00021725
nkb-3	1580.46344	0.52798609	0.11559872	0.00021943
W09G3.7	65.6609954	1.26799039	0.27786096	0.00022301
Y105E8A.21	46.2282423	-1.4001227	0.30697821	0.00022493
zip-5	327.388942	1.48793062	0.32634562	0.00022601
his-11	12.0464584	-2.2349482	0.49058586	0.00022928
F56A12.10	6.47705342	-3.128951	0.68690711	0.00022928
smgl-2	9.12934887	6.01006441	1.32002801	0.00023097
swt-6	4216.93832	0.77026032	0.16923724	0.00023208
col-166	621.677459	0.55289823	0.1215463	0.00023418
samt-1	290.954487	0.86967279	0.19137368	0.0002372
cest-10	62.7938725	-1.0703221	0.23548972	0.0002372
cest-1.1	209.390244	-1.5442151	0.33980014	0.0002372
gba-1	1096.02791	1.06095162	0.23385817	0.00024525
tatn-1	118.325797	0.86047985	0.1901792	0.00025904
irld-65	19.4326582	-1.8851536	0.41680029	0.00026034
F47D12.6	329.164266	1.13904346	0.25199931	0.00026319
C23H4.6	120.097188	1.80970174	0.4004433	0.00026342
R08C7.12	111.656932	1.09370007	0.24224122	0.0002681
yif-1	381.608337	-0.5012803	0.1111294	0.00027263
tin-10	482.620676	-0.8292126	0.18401122	0.00027765
C06G3.3	357.494121	-1.6942432	0.37628033	0.00028175
aat-1	312.593142	-0.6326315	0.1406048	0.00028531
C30G12.2	1476.59273	-1.7854232	0.39689172	0.00028565
nhx-6	20.4467732	1.96145871	0.4361567	0.00028671
tsp-13	52.6233105	1.55345192	0.34598153	0.0002957
ugt-8	313.642751	-0.5829177	0.13012976	0.00030974
C35E7.4	30.9647058	-1.3526732	0.30205953	0.00031085
Y37E11B.5	45.8191699	1.450589	0.32408407	0.00031237
glb-23	12.8792697	-1.9919628	0.44498486	0.00031237
ZK105.1	1952.71758	0.88502995	0.19801162	0.00032096
K08D8.6	1246.72204	1.13646817	0.25451466	0.00032667
nlp-29	533.560872	-0.6372664	0.14280147	0.00032982

F35E8.13	46.2974407	1.84223986	0.41333839	0.00033769
ZK470.14	18.4356982	-1.783168	0.40027378	0.00034011
ctsa-3.1	233.240024	-0.7415829	0.16656703	0.00034351
K05F1.10	155.933911	0.8025735	0.18035067	0.00034503
C49C8.5	237.901208	1.83233166	0.41174923	0.00034503
fil-1	64.955468	-2.5044131	0.56311368	0.00034836
tps-1	518.587051	-0.8261531	0.18588745	0.00035243
F14H3.12	488.946176	0.79784558	0.17957	0.0003528
ZK228.10	14.6948639	4.79742103	1.07976609	0.0003528
C39D10.11	173.685616	-1.1084334	0.24951295	0.00035291
gpx-7	23.4013404	-1.7081444	0.38499501	0.00036125
C23H5.8	15155.6355	-1.0340006	0.23314067	0.00036317
vnut-1	90.251601	1.2681248	0.28657431	0.00037839
ugt-23	884.755741	-0.7012261	0.15844677	0.00037839
poml-3	345.940768	-0.5847457	0.13242822	0.00039345
cutc-1	139.219142	0.84764678	0.19196118	0.00039345
cdd-1	70.5481882	1.50949212	0.34210932	0.00039839
fust-1	488.32368	0.59613436	0.13514545	0.00039968
Y105C5B.3	14.478819	3.85938089	0.87645842	0.00041303
pck-2	19764.4369	-0.4706479	0.10695388	0.00041704
R05H5.3	127.478825	1.38273214	0.31424439	0.00041704
F22H10.3	7425.63202	1.04657009	0.23790843	0.00041816
linc-27	23.168953	-1.5007165	0.34129553	0.00042082
K10D11.6	363.200419	1.35335273	0.30783864	0.00042123
spp-12	136.879864	-1.7187906	0.39100635	0.00042123
tba-7	420.086019	1.17211771	0.26669017	0.00042164
bgal-2	358.937858	-0.9301886	0.21206877	0.00043794
B0348.2	20.4735852	1.87958581	0.42888745	0.00044452
Y23H5B.6	66.7744773	0.99966607	0.22824673	0.00044801
dhhc-1	38.0590312	1.89846249	0.43347059	0.00044801
F46C5.1	173.302273	-1.2170173	0.27793232	0.00044865
let-805	137.212918	1.97374387	0.45109046	0.00045443
hpo-6	1987.63412	1.65507726	0.37895417	0.00046912
srbc-19	10.4897884	-2.5360256	0.58066211	0.00046912
T28F3.8	1356.46236	0.55075205	0.1261206	0.00046926
F44D12.6	13.8968643	-2.2236131	0.50956034	0.00047476
C15H11.16	30.9285726	1.60279529	0.36781461	0.00048714
Y51H4A.25	1064.06178	1.48321156	0.34043516	0.00048775

clec-125	15.4393918	4.87520827	1.11956037	0.00049155
C54C6.7	504.58174	0.62301768	0.14337567	0.00051142
Y17D7B.2	27.9869057	1.7605165	0.40541924	0.00051695
ugt-17	137.800698	-0.9363679	0.21576187	0.00052193
C14C11.7	61.7433685	1.91451668	0.44273393	0.0005587
R02F2.9	95.2385864	-1.1624268	0.26920819	0.00057365
try-9	237.672303	-0.6172366	0.14312161	0.00058611
Y60C6A.3	92.7303053	-1.3363153	0.30991154	0.00058669
srx-58	54.1343638	-0.9310796	0.2159941	0.00058862
K06G5.1	21540.539	0.46017341	0.10678182	0.0005904
nhr-112	72.147714	1.64610308	0.38214147	0.00059408
tps-2	18.1727067	5.09138479	1.18251097	0.00059806
skpo-3	537.143121	-0.8384892	0.19484256	0.00060247
mop-25.2	66.4039853	1.15502032	0.2685293	0.00060688
linc-107	7.44972519	-3.4618506	0.80508974	0.00060909
syx-2	128.168072	1.30974071	0.30496828	0.00062229
Y73B6BL.37	6.43444832	-5.0049341	1.16680149	0.00063564
ugt-52	68.5272982	-1.1199877	0.26126867	0.00064196
vhp-1	369.06776	1.80945018	0.42226951	0.00064529
Y57A10A.31	40.9898251	1.40741594	0.32849703	0.00064568
F28F9.2	31.7997351	-1.9876105	0.46412758	0.00064983
B0511.12	195.780945	0.87367401	0.20407275	0.00065206
F44A2.7	131.277889	-2.4526291	0.57308657	0.00065497
btb-17	370.676306	-0.972813	0.22743612	0.00066015
zip-11	192.998738	1.08602307	0.25394067	0.00066015
asp-12	200.742797	0.68718533	0.16069279	0.00066015
set-26	21.1447121	1.82205975	0.42619745	0.00066231
K06A9.1	83.3556517	1.09799226	0.25687693	0.00066307
F28A10.13	17.2159053	-1.6562998	0.38756387	0.00066386
F19C7.2	168.405072	0.64341711	0.15070938	0.00067543
C34C12.9	164.804537	0.68734347	0.16141158	0.00070769
lec-8	11120.4962	1.19561841	0.28098954	0.00071659
mrps-17	288.356494	-0.9219021	0.21672775	0.00071912
F16B4.7	279.188407	-1.4600053	0.34330981	0.00072071
str-7	8.52185242	5.91113438	1.39024184	0.00072186
T06E6.1	54.4075433	-1.3825856	0.32545284	0.00073218
C30G7.4	331.867329	-0.8257388	0.19465044	0.00074878
K09C8.7	139.331618	-0.9159086	0.21588345	0.00074878

vamp-7	119.629591	0.97298061	0.22958677	0.00076121
hpo-26	181.986822	1.46318229	0.34558787	0.00077341
rsr-1	68.1694048	0.99956143	0.23629465	0.00078465
Y102E9.3	4.60833067	-6.3907571	1.51208974	0.00079394
F25E5.1	57.1671502	1.29536902	0.30645266	0.00079394
acbp-3	414.933404	0.89899658	0.21272941	0.00079394
nhr-130	160.053921	-0.9001958	0.21304921	0.00079471
M199.8	4.91339531	-4.5522574	1.07808115	0.00080267
lys-5	6.63250098	-4.8987636	1.1612903	0.00081589
asah-1	1689.35998	-1.4410921	0.34175064	0.00081806
W03G1.5	29.3838471	1.69441378	0.40181264	0.00081806
oma-1	16.2975372	2.87631334	0.68233576	0.00082137
F54D1.6	620.856287	0.64677656	0.15345441	0.00082182
lgc-33	30.1363135	1.84929017	0.43951063	0.00084648
vwa-8	568.987481	-1.0430545	0.24806743	0.00085552
C07A9.13	14.166243	-2.3369483	0.55596897	0.00085876
acdh-2	51.526136	-1.0181028	0.24245181	0.00087289
clec-84	133.033129	1.61962054	0.38576467	0.00087382
nars-1	631.196253	0.7077085	0.16863571	0.00087702
dmd-8	25.9292028	-1.2971413	0.30906971	0.00087702
lec-7	100.69062	0.97900045	0.23344115	0.00088639
obr-2	489.768979	-0.9619816	0.23004196	0.00093257
T22C1.1	146.950319	-0.6863277	0.16432968	0.00095199
srbc-71	8.84319678	-2.4854652	0.59516266	0.00095199
trf-2	81.0211114	-0.895594	0.2147139	0.0009711
K09E9.4	23.2077968	1.89103007	0.45348047	0.0009736
abt-4	725.272801	1.06044386	0.25444027	0.00098134
T02E1.8	36.133331	-1.180642	0.28370485	0.00100641
aldo-2	37488.7228	-0.49767	0.11963017	0.00101067
M03B6.5	70.2257425	-1.0370325	0.24939278	0.00101672
D1086.10	2730.57876	-0.6572666	0.158417	0.00105654
ZK418.7	317.153287	0.99312861	0.23941196	0.00105787
C05B5.5	32.6359756	1.49116316	0.35960028	0.0010622
R08E3.1	3877.0704	0.60631593	0.1462302	0.0010622
K08F9.1	37.1958279	-1.2307597	0.29711322	0.00107828
deps-1	26.2771201	2.8478254	0.68810796	0.00109384
nhr-41	11.9742188	2.87483989	0.69471714	0.00109391
R02D5.8	40.069686	1.36735229	0.33052566	0.00109758

dlc-5	83.6587693	-0.7651261	0.18527465	0.00113028
bkip-1	79.876978	-0.9512858	0.23090618	0.0011775
C38D9.2	20.0129335	2.03686533	0.49490418	0.00119627
F28H1.1	52.5320188	2.36481026	0.5757847	0.00123897
spp-1	7724.9275	-1.2384126	0.30183201	0.00125869
nhr-22	61.0972014	-1.0151046	0.24781038	0.00129297
arrd-7	142.173815	0.97414285	0.23804337	0.00131284
K03H6.5	23.4171491	1.89200464	0.46276665	0.00133199
H14A12.5	54.4761425	1.26889693	0.31084338	0.00136551
nhr-263	17.2799932	-1.601821	0.39243445	0.00136551
T03E6.8	89.5104121	-1.190052	0.29159122	0.00136582
T07A9.15	319.079918	-0.6989722	0.17129489	0.00136727
Y6E2A.4	194.5916	-1.866726	0.45761504	0.00137201
cyp-35A4	3.87166843	-5.0758841	1.24475688	0.00137776
tag-175	89.029005	1.02804161	0.25224095	0.00138794
R08F11.4	123.739581	1.02345942	0.25123373	0.00139653
tbc-20	58.5730962	1.01720859	0.24973758	0.0013975
F40A3.2	1125.40097	-0.3993838	0.09821434	0.00143516
Y105E8A.14	13.2839199	4.0804792	1.00357114	0.00143534
atrn-1	235.709087	0.87990778	0.21643453	0.00143552
grd-4	486.494009	-0.4980465	0.12254297	0.00144013
K07H8.9	7.63708688	5.75139718	1.41743191	0.00147878
C16B8.3	1365.28136	1.46608257	0.36181732	0.0015118
F41G3.20	5.45936267	5.24097503	1.29450729	0.00153073
T18D3.5	16.9880183	-1.6579849	0.40962905	0.00153491
trxr-2	34.5520536	-1.4638339	0.36233543	0.00158195
zip-10	420.979144	1.51856354	0.37630156	0.00160944
F08A7.1	163.574002	-1.1449992	0.28422756	0.00165514
Y41D4B.14	106.698268	-0.7861436	0.19543155	0.00169356
Y48A5A.1	36.7272849	1.20307861	0.29916337	0.00169838
alh-1	2808.31874	-0.826073	0.20546457	0.00169888
F54E2.1	2178.49332	1.35969389	0.3381905	0.00169888
K02E10.7	12.3505395	-2.1330077	0.53091473	0.00171651
W04B5.3	415.451787	1.85300822	0.46146129	0.00172844
K09C8.8	6.0374135	-2.6941535	0.67104435	0.00172993
mbk-2	283.14005	0.64706764	0.16118742	0.00173017
F01D5.8	288.619378	1.07050351	0.26672319	0.00173305
arf-1.2	3703.18636	0.54275492	0.13524852	0.00173354

nxf-1	367.039152	0.79873211	0.19943487	0.00179017
Y71G10AR.4	135.963623	-0.7146238	0.17859288	0.00181391
Y43C5A.3	1061.73844	-0.9759845	0.24394934	0.00181541
F17B5.8	42.0283753	-1.4180138	0.35456103	0.00181941
gst-5	1468.164	-0.6943555	0.17361236	0.00181941
ins-8	3.79650633	-4.0708686	1.02072818	0.00190346
K11D2.1	23.9845763	1.53883857	0.38596803	0.00190984
nspa-8	165.367632	-1.5002624	0.37647623	0.00191834
linc-64	50.0920664	1.70054707	0.42671312	0.00191834
F41G3.21	105.266799	0.88788773	0.22303596	0.00194803
F26G1.5	42.8804858	-1.2123201	0.30519503	0.0020139
elt-2	149.920721	0.74652855	0.18794222	0.0020139
col-43	428.577952	1.19480653	0.30086453	0.00201753
mpk-2	89.2553635	0.84454577	0.21273539	0.00202487
ugt-18	84.8764208	1.58144215	0.39858958	0.00204106
C30G12.6	10.9657484	-2.0287549	0.51143212	0.00204398
C47F8.7	2.57933952	-5.5366217	1.39670077	0.00206378
dhc-1	610.670029	0.82853492	0.20941775	0.00212746
C11G10.1	251.934561	-0.9212551	0.23308159	0.00215822
Y58A7A.3	675.946759	0.81338876	0.20584131	0.00216298
arrd-24	20.4440023	2.129816	0.53933281	0.00218214
T23E7.6	899.954441	-1.3726338	0.34773973	0.00219349
C03A7.13	73.2933058	-1.2369017	0.31387565	0.00225027
clec-67	550.891715	1.23118165	0.31249799	0.0022549
ceh-62	96.3496915	1.25428909	0.31852501	0.00226142
Y60A3A.16	309.322273	0.89690807	0.22772051	0.00226142
C39B10.3	23.650285	-1.2606894	0.32014166	0.00226142
Y71F9AL.4	19.6058478	2.72220502	0.69181459	0.00228501
Y70C5A.3	31.3018468	-1.1465352	0.29170829	0.00232361
alx-1	1015.94067	0.5093919	0.1297063	0.00234994
T24B8.3	673.174952	0.7035065	0.17933104	0.00238821
K12G11.6	11.1749347	-1.8273049	0.46602125	0.00240252
ZK688.10	5.58447027	5.30424361	1.35356955	0.00241755
spl-2	114.123814	-1.3922822	0.35526935	0.00241755
sec-61.B	3098.78165	0.65654005	0.16758932	0.00242481
F55F3.4	4.10231686	-3.6218248	0.92557685	0.00246613
Y47D3A.21	42.4507248	1.32583063	0.33898843	0.00248126
hphd-1	1607.34628	-0.8683979	0.22214876	0.00249801

F59C6.8	12.9178424	-2.6559864	0.67961995	0.00250429
trpp-1	44.8629576	2.02503573	0.51849884	0.00252108
ttr-27	590.537419	0.76977183	0.19709546	0.00252108
Y75B8A.18	26.8146438	-1.405454	0.359953	0.00252732
F02A9.12	16.0156062	2.68678145	0.68843429	0.0025373
dod-20	10.0329874	4.24430485	1.08741332	0.0025373
T09A5.14	11.7446339	3.37191725	0.86421887	0.00254384
Y75B8A.28	469.842506	1.36446885	0.35023512	0.00260123
F25H5.2	20.8771817	-1.7396449	0.44697131	0.002633
Y52B11A.20	10.7774563	-1.9235947	0.49422542	0.002633
B0310.3	35.0552994	-1.3703822	0.35262608	0.00269257
nhr-97	434.845801	0.69397506	0.17880588	0.00274437
F07C3.3	13.7345693	-1.8582467	0.47934094	0.00279068
W10D9.3	28.966872	1.80159707	0.46499042	0.00281098
K04C2.2	28.396435	1.37210372	0.35464796	0.00286595
ugt-44	2266.52687	1.49283196	0.38583732	0.00286595
kin-29	218.775542	0.61910383	0.1600782	0.00287758
Y57A10A.27	61.1466929	-0.8615622	0.22279806	0.0028785
R02D5.7	25.8236321	2.42569044	0.62743327	0.00288483
col-17	11.7192351	4.57416294	1.18382636	0.00290563
clec-169	147.837769	-0.8832825	0.22869377	0.00291724
F25D1.5	31.5448401	-1.4269214	0.36947079	0.00291724
sma-1	855.832719	0.57618662	0.14922971	0.00292416
gpx-1	127.751912	0.79680447	0.20644077	0.00293531
Y105E8B.9	22.6012286	1.50641528	0.39034569	0.00293681
B0403.3	116.909206	1.84247707	0.47813461	0.00300111
let-526	277.754167	0.98893715	0.25677325	0.0030112
lig-4	70.8762871	0.96393465	0.2502407	0.0030112
T16G12.6	69.3978392	0.86129812	0.22361736	0.0030112
T03F1.12	64.1577848	0.9867099	0.25623685	0.00301385
qns-1	85.3231432	0.81151221	0.2107825	0.0030183
col-109	29.8064735	1.87768602	0.48784436	0.00302621
F44D12.19	20.3976885	-1.5832356	0.41142306	0.0030304
ZK1128.1	82.337167	-0.8030741	0.20889481	0.00307175
nhr-237	33.178185	-1.0798704	0.28092007	0.00307175
F46F5.16	24.487001	-1.9937295	0.5191543	0.00310648
phg-1	30.6506642	1.48992881	0.38799629	0.00310648
ekl-6	34.0213207	1.32735883	0.345625	0.00310648

svh-2	551.334975	0.67822681	0.17666065	0.00311281
lec-10	3201.96248	2.23868442	0.58373743	0.00315946
hrg-4	150.414308	1.51075691	0.39404588	0.0031687
C12D12.1	1990.03604	1.28573291	0.33540411	0.0031709
eak-4	4.63597208	5.00543193	1.3059731	0.00317419
gmps-1	443.917619	0.46928514	0.12252276	0.00320177
gpd-3	3394.12921	-0.451824	0.1179916	0.00320818
C45G9.12	91.4160074	-0.7303395	0.19078917	0.00321088
F26F2.1	6.26800247	-2.8686287	0.74934901	0.00321088
C07B5.2	49.8874534	-1.1834955	0.30917866	0.00321088
T03F1.11	725.262428	-0.5531395	0.14458371	0.00323348
wdr-46	50.8158641	-1.0393405	0.27170082	0.00323379
Y116A8C.29	233.551194	0.54238036	0.14184923	0.0032505
scl-2	3944.69183	-1.5032402	0.39343938	0.00328325
F58G6.7	403.851981	0.51904262	0.13596857	0.00332333
cyp-13A7	13.3084347	-2.3578451	0.61793012	0.00333487
exc-14	58.0311257	-1.03846	0.27212921	0.00333487
F10C1.9	61.1992917	-0.8328086	0.21845989	0.00337745
mrps-33	447.368271	-0.5647817	0.14817954	0.00338172
mccc-1	742.099011	-0.7046254	0.18491103	0.0033879
hach-1	648.602734	-0.7897772	0.20740067	0.00341876
srbc-61	3.4743144	-4.9103196	1.28967874	0.00342129
cfi-1	19.8184751	1.99667277	0.52547835	0.00352331
T03F6.9	40.5532568	-1.0356681	0.27271516	0.00354767
Y37F4.8	130.039371	-1.0131787	0.2669175	0.00356735
K08D8.1	72.4963685	-1.0068215	0.2656327	0.00364251
F07H5.10	9.9533884	3.24354456	0.85642572	0.00368048
K12B6.11	11.6267293	-1.9418268	0.513022	0.00370771
B0286.1	87.8969573	-0.8485053	0.22462055	0.00381613
nas-11	1154.01583	-0.5652797	0.14972976	0.00384343
ngp-1	370.248759	-0.9731343	0.25799312	0.00388992
aqp-2	186.004142	1.3401747	0.35552507	0.0039209
fbxa-19	41.1451177	1.51994181	0.40329019	0.00392587
drp-1	195.966459	0.80904153	0.2147424	0.00394102
C04F12.1	259.275115	1.02525876	0.27225647	0.00395337
clec-173	45.307923	2.43935542	0.64787815	0.00395337
dhs-24	11.4817118	4.42407824	1.17496749	0.00395337
dnj-25	56.4659104	1.02691077	0.27269175	0.00395337

math-10	5.64433473	-2.6269969	0.69788948	0.00396212
Y41E3.22	129.78506	-0.9260186	0.2461609	0.00398721
F59E11.7	308.037848	-0.8554327	0.22738357	0.00398721
K11H3.5	81.1598218	-1.2598836	0.33501533	0.00399963
nas-27	4.78457783	5.03933386	1.34053349	0.00401701
che-7	19.0613387	-1.6024402	0.42633062	0.00401913
cpz-2	2576.48878	-0.549182	0.14620114	0.00405049
decr-1.1	17.2737135	-1.6744304	0.44602197	0.00407994
plpp-1.2	341.605469	-0.6857156	0.18274857	0.00409491
R09E12.9	101.189885	-1.087951	0.28991559	0.00409491
nhr-173	169.600223	-0.9720034	0.25905828	0.00409491
msp-31	198.391199	-2.1606378	0.57624478	0.00411775
rab-6.1	310.152753	1.28232974	0.34198319	0.00411775
col-146	34.5047834	-1.4260979	0.38028885	0.00411775
C44E12.1	181.878083	-0.594082	0.15850721	0.00413665
C14A11.6	148.233027	-0.9637498	0.25725813	0.00415913
mus-101	68.438532	-1.0065789	0.26892642	0.00420745
kbp-4	24.0925715	-1.5763441	0.42130121	0.00422347
gtf-2F2	54.3997147	1.36461278	0.36474953	0.00422347
npr-28	35.8305279	1.56015287	0.41708264	0.00422713
col-74	17.2610342	-1.4017416	0.37490746	0.00424875
F35E12.10	1446.5237	0.90801026	0.24287527	0.00424875
K10D3.6	432.402173	-0.8638569	0.23132548	0.00431389
flap-1	92.1640204	-0.7108255	0.19040277	0.00431981
C14C10.2	18.5862076	-1.3270812	0.35543877	0.00431981
prdh-1	456.881909	-0.6609556	0.1771391	0.00434757
M28.8	306.43659	0.9828324	0.26364548	0.00439381
F19C7.1	10634.5788	0.94924549	0.25461756	0.00439381
H43E16.1	61.192212	1.10036306	0.29526081	0.00440335
R03D7.15	3.02936726	-4.7459724	1.27355534	0.00440335
vab-3	54.5672087	1.2221617	0.3281587	0.00443621
K01A2.10	115.067831	-0.7252954	0.19486827	0.00447055
mrpl-10	120.566428	-0.652398	0.17539985	0.00450138
daf-10	9.60169418	-2.2560977	0.60655277	0.00450138
B0228.7	125.885803	-0.7894556	0.21239366	0.00454019
Y9C9A.8	40.276167	2.20262895	0.59289576	0.00456782
wrk-1	156.232028	1.03433633	0.27847818	0.00457533
F13D11.3	138.980662	-0.8686028	0.23388168	0.00457561

sid-2	629.843161	1.08549602	0.2923303	0.00457977
ketn-1	552.452422	1.01790331	0.27420276	0.00458713
Y61A9LA.10	73.9034022	-0.9423064	0.25384732	0.00458713
sav-1	73.354713	0.87196573	0.23502617	0.00461708
fat-7	47.4949164	1.42291328	0.38391136	0.00467747
F41E6.15	1286.32483	-0.8761774	0.23641851	0.00467747
R05D3.3	3.70922702	-4.1443724	1.1188571	0.00470635
smc-6	18.3437177	2.08005617	0.56161825	0.00470743
fbxb-74	5.16661366	-2.7450163	0.74151974	0.00472722
C49G7.10	1165.84022	0.79263826	0.21411332	0.00472722
bcas-2	29.3449967	-1.2092211	0.32683676	0.00475332
tag-260	313.47933	0.65721991	0.17763933	0.00475332
bud-31	66.1757217	1.64827066	0.4455831	0.00475787
oac-5	28.1456518	1.88761971	0.51041933	0.00476893
mir-255	17.0516862	-1.6507904	0.44681609	0.00483021
F13B12.3	13.0476288	-2.2375653	0.60647651	0.00491409
pud-2.2	114.549761	0.83443846	0.22615724	0.00491409
T14B4.5	102.754224	-0.7321589	0.19853908	0.00494027
sri-40	13.9639509	2.5578138	0.69377475	0.00495111
nhr-143	180.394781	-0.7868093	0.21349885	0.00497317
gst-4	1265.98455	-0.8234588	0.22362543	0.00502479
W03F8.6	222.262684	-0.7672433	0.20874	0.00515153
K10C2.8	166.015442	0.68308162	0.18586502	0.00515312
ntc-1	177.765597	-0.5969902	0.16265132	0.00523549
mbr-1	88.0618498	0.80008554	0.21796546	0.00523549
F53B2.8	796.0947	1.8673017	0.50886895	0.00524553
F28B4.3	2979.50801	1.44276612	0.39321566	0.00524559
mzt-1	186.146599	-0.5904964	0.16111775	0.0053136
R166.3	103.04621	0.96988019	0.26467637	0.0053136
qui-1	19.6433367	1.98113327	0.54059271	0.0053136
C36B7.6	8.74484118	4.04131284	1.10258884	0.0053136
mrpl-38	226.21262	-0.5098004	0.13922845	0.00536421
linc-41	101.300459	-0.6728243	0.18387572	0.00540125
H25K10.1	52.8407923	-1.4630606	0.39980074	0.00540125
Y48C3A.5	77.997931	1.046427	0.28632457	0.00548323
Y41D4B.15	98.0479235	1.38757496	0.37968517	0.00548323
C15C6.2	4.10633425	4.84571541	1.3262653	0.00549448
linc-7	92.4436951	-0.9593266	0.26281421	0.00556093

W02D3.12	192.124635	-0.9075123	0.24870089	0.0055713
C06H5.8	100.629119	-0.8424211	0.23085714	0.0055713
R03G8.3	126.925717	1.07434638	0.29463594	0.00562139
Y75B8A.13	49.1980258	1.09228028	0.29963577	0.00563526
ZK384.7	1316.50172	0.9565528	0.26258033	0.00568159
golg-2	81.7675819	1.99770098	0.54862051	0.00570071
F32A5.8	31.2964681	1.82660895	0.50159977	0.00570071
hlh-31	15.0968294	-1.7316075	0.47615242	0.00579653
F01E11.3	4.92967634	5.09127702	1.400369	0.00581098
eif-3.C	739.255675	0.58769066	0.16170335	0.00582408
F41E6.5	311.961653	-0.6433632	0.17701666	0.00582408
ZK546.18	5.63314721	-2.3654189	0.65116304	0.00585609
Y52B11A.10	40.9143737	-0.9401648	0.25884586	0.00585858
K08H10.6	11.9446403	-2.2026998	0.60686507	0.00590759
F25B4.7	430.637077	-0.7965439	0.21964573	0.00597173
F15E6.10	231.526051	-1.352503	0.3730951	0.00598786
acp-5	109.600383	-0.912551	0.25171887	0.00598786
zig-3	51.6195373	-1.0243993	0.28272978	0.00602249
hrpk-1	92.4275974	1.39346663	0.38464636	0.00602646
F58B6.1	348.945694	-1.5899457	0.4392935	0.0060978
str-174	2.6561772	-5.5976491	1.5470897	0.00611388
Y34B4A.5	2735.40217	-0.8190045	0.22637324	0.00611388
K07H8.5	43.3843507	-0.9163812	0.25367565	0.00623722
ptr-22	30.4775529	-1.3246098	0.36695817	0.00629421
mat-3	20.3455038	2.57333953	0.71373244	0.00638909
trak-1	247.472245	0.93259728	0.2588392	0.00643271
F44G3.10	100.270318	1.61556361	0.44835741	0.00643271
C34E11.4	168.215828	-1.1489395	0.31905484	0.00647183
C13A2.12	33.4823606	-1.8231067	0.50650585	0.00650534
acs-17	606.314874	-0.3747768	0.10414529	0.00651621
bris-1	125.355827	1.11193001	0.30906364	0.00652894
B0198.3	15.2501744	2.53078571	0.70364039	0.00654617
hsp-4	690.380832	1.80790167	0.50290609	0.00656505
argk-1	37.5813132	1.71655825	0.47747117	0.00656505
Y34B4A.9	8949.84896	1.29640707	0.36057139	0.00656505
mtx-2	300.639691	-0.5966629	0.16601312	0.00657743
pud-2.1	110.545275	0.63630718	0.17707485	0.00658471
cgr-1	486.429961	-1.2681248	0.35305013	0.00661456

smn-1	46.2953255	1.1254692	0.31370893	0.00671536
slc-46A	182.263205	-0.8283369	0.23096337	0.00673684
cyp-35B1	420.119226	-0.9566109	0.26680098	0.00675267
T20D4.7	180.194028	0.72621793	0.20261225	0.00676968
ttr-23	1162.3468	0.70630602	0.19706442	0.00676968
cec-7	41.0742641	-0.9649333	0.26924934	0.00676974
Y110A7A.21	307.151443	-0.6043873	0.16878947	0.00684087
rga-9	125.438701	1.32113913	0.36912324	0.00687355
F38A5.2	494.713495	0.46668606	0.13050015	0.00694355
Y57G11C.1135	193.172064	-0.9707423	0.27150032	0.00695197
irg-7	7239.91204	1.18901027	0.33261476	0.00696244
sre-51	2.54825223	-4.4632199	1.24902213	0.00698057
stdh-4	2.54825223	-4.4632199	1.24902213	0.00698057
C15C8.5	7.80223785	-2.2628492	0.63339538	0.00699284
tsen-2	102.250203	-0.6519955	0.1826517	0.00706308
odc-1	559.436128	2.09127608	0.58605146	0.00708609
chaf-2	17.2405959	4.44384518	1.24571142	0.00710669
mrp-1	348.030802	0.46801514	0.13121228	0.00710994
fubl-1	224.46147	-0.524427	0.14706204	0.0071232
pigb-1	92.7952105	0.66839461	0.18757634	0.00718773
npr-29	63.5773106	-0.8518476	0.23914811	0.0072144
eat-17	122.034009	1.41774095	0.39820668	0.00725173
clec-134	5.02046289	5.10396657	1.43479112	0.0073068
pho-9	98.3510107	1.41765458	0.39854695	0.0073068
str-135	5.02046289	5.10396657	1.43479112	0.0073068
C15C8.6	22.8546032	-1.5322383	0.4307703	0.0073068
T25D3.4	38.0358587	2.59074903	0.72862123	0.00733321
F46E10.18	15.1759846	-2.960213	0.83304115	0.00738493
guk-1	161.92725	0.64552988	0.18185358	0.00742634
snrp-40.2	23.7907741	1.78266511	0.50211411	0.00742634
T05E7.1	39.2098424	-1.13091	0.3185532	0.00742634
F35C5.1	30.2409455	-1.0095789	0.28431686	0.00742634
Y20C6A.1	30.5448096	-1.2335971	0.34732987	0.00742634
nlp-42	917.81303	-0.7031832	0.1980977	0.00742634
C49F5.5	9.28495222	4.07543913	1.14770039	0.00742634
M57.2	247.273245	1.05794342	0.29861143	0.00761088
Y37E11B.10	4.39657978	4.96489443	1.40246741	0.00768125
F44A6.5	48.5546142	-0.8524678	0.24093905	0.00773012

Y24D9A.9	4.29932111	-3.2051207	0.90624962	0.00776195
slc-9B.2	118.704922	-0.5740432	0.16242347	0.00782432
smgl-1	64.9555568	1.11058662	0.3145874	0.00793182
clec-82	66.6927092	-1.8585503	0.52686032	0.00800307
ptb-1	64.705146	0.98163461	0.27840032	0.00803192
bre-3	381.338191	1.28256508	0.36374742	0.00803192
mpst-2	2.87482169	-4.6190346	1.31013297	0.00803258
W02D7.8	37.4010159	-2.0090321	0.56992736	0.00803937
F02C12.2	4.10282701	4.86156062	1.38031978	0.00812112
B0250.7	4.60405725	4.97350619	1.41263655	0.00815169
ppw-1	251.774821	0.6902663	0.19617324	0.00818182
W09G3.6	290.433228	1.10887673	0.31519242	0.00818182
srn-1	10.5055946	2.47638408	0.70382496	0.00818182
H02F09.2	4.63001012	4.98102243	1.41572106	0.00818182
hlh-29	4.09691356	4.84390713	1.37671599	0.00818182
nap-1	6024.75494	-0.768571	0.21849915	0.00818997
F36F2.8	21.6349609	-1.289704	0.36670828	0.00819603
clec-74	25.025994	1.85472575	0.52760092	0.00822458
F35E12.9	394.131395	1.10998158	0.31574298	0.00822458
F42G4.5	108.978177	0.82998539	0.23613672	0.00823127
K03H1.11	43.0751636	-1.192838	0.33955443	0.00826994
piit-1	130.217001	-0.5425174	0.15442171	0.00826994
F01D5.1	3655.35203	1.30986829	0.37295349	0.00827455
C07G1.15	41.1494347	-1.6167891	0.46030969	0.00827455
F17C8.3	49.7990691	-1.0044777	0.28604535	0.0082814
fmo-1	97.6266446	-1.0655096	0.30348772	0.00829371
mrp-7	66.207599	1.11714879	0.31826673	0.00830789
clec-240	4.32924287	4.90113807	1.39649518	0.00831346
nhr-31	120.776184	1.23320102	0.35148186	0.00833529
gpap-1	24.0965457	1.3850571	0.39497	0.00838279
him-3	13.7306375	1.99714173	0.56991644	0.00845059
slc-17.6	385.078276	0.51848464	0.14825342	0.00865391
pdi-6	4683.63836	0.93185334	0.26644408	0.00865391
set-25	3.71588148	4.70276613	1.34542	0.0087051
Y65B4A.2	110.292359	0.67896443	0.19434465	0.00875267
T25C12.3	4843.50183	1.24729544	0.35714928	0.00878295
F37C4.5	10236.6758	0.80763967	0.23134338	0.00881441
spp-4	1540.04288	-1.3484514	0.38649424	0.00887508

F41C3.7	142.631926	-1.2303152	0.35272537	0.0088837
C39B5.16	257.515316	-1.4012224	0.40169312	0.0088837
dod-19	9534.32657	1.82652398	0.52374659	0.00889315
W04D2.4	54.4057468	-0.8744376	0.25091098	0.00895069
fbxa-99	22.4189838	1.56312945	0.44849458	0.00895069
T28A11.17	13.8986657	-1.5614128	0.44842664	0.00904311
emb-4	20.0915674	2.96693486	0.85223616	0.00905347
F10B5.2	42.2296236	1.02875478	0.2961934	0.00929774
Y42G9A.3	37.7657273	1.38815902	0.3996423	0.00929774
R02D5.3	141.972151	1.12597208	0.32412534	0.00929774
btb-18	14.902173	1.8650993	0.53715321	0.00932345
pmp-5	621.933938	-0.7284053	0.20995311	0.0094107
K11E4.1	74.605696	1.21080178	0.34922468	0.0094788
nas-4	4.15468425	4.85585617	1.40137078	0.00953958
cyp-33E3	27.3383917	-1.012439	0.29242642	0.00963064
oac-22	9.98868247	-2.3486565	0.67850125	0.00964302
F44G4.1	258.851362	-1.023366	0.29568811	0.00964477
C10C5.3	123.202161	0.70922879	0.20493597	0.00964477
col-2	25.7277524	1.87963088	0.54316241	0.00964477
K08E4.2	15.7028224	1.72707516	0.49914186	0.00964927
grl-17	8.33793637	2.87871004	0.83214418	0.009663
cyp-35A2	212.603073	-1.3048058	0.37727889	0.00968478
F27C1.2	986.060606	-0.5948404	0.1720419	0.00969555
dhs-13	780.926729	0.52043312	0.15051623	0.00969555
F32H2.6	16.7214225	1.61477509	0.46714259	0.00971389
C54E4.4	29.6420425	1.39860783	0.40464981	0.00971569
ugt-66	177.531209	-0.6134247	0.17754688	0.00975269
K04F1.9	335.924947	-0.8345804	0.24165783	0.00979342
nlp-78	17.5954235	-1.4650003	0.42434693	0.00982551
T23G7.3	895.816816	-0.6827916	0.1978678	0.00987025
mix-1	116.866995	-0.6781568	0.19653814	0.00987025
cri-3	313.388239	0.51193666	0.14846336	0.00994216
asp-1	88476.8512	0.63497584	0.18416364	0.00994335
T05E11.2	76.6421154	-0.819104	0.23775484	0.01003256
F55G11.2	342.565953	0.81968763	0.23796932	0.01004516
F56B3.11	1069.02008	-0.5237695	0.15209257	0.01006158
trpp-11	59.6549118	-0.7602406	0.22092206	0.01013301
T05E12.3	327.124372	-1.0797604	0.31374838	0.01013301

nlp-62	151.843212	-1.0738493	0.31219099	0.01017747
pgs-1	62.7925496	-0.8188684	0.23819225	0.01022452
clec-8	153.274279	-0.9131551	0.26561058	0.01022452
set-17	275.510097	-0.5669872	0.16495987	0.01024012
F26A3.1	514.261272	-0.6806717	0.19805458	0.01024098
ZC395.5	2657.26279	-1.6459586	0.47903861	0.01026047
DH11.2	277.709055	-0.8929491	0.26000463	0.01030957
H40L08.1	166.815965	0.62042019	0.18069853	0.01033216
ztf-8	43.4956586	-1.0153563	0.29581585	0.01034282
egl-20	41.6064063	0.97481353	0.28401623	0.01034282
C50F4.4	43.390376	-1.0433001	0.30395089	0.01034282
C39B10.1	32.314357	-1.0390612	0.30276277	0.01034301
clec-66	1060.43656	0.91994675	0.26815973	0.01037382
C09E7.4	19.2249371	1.63106082	0.47549669	0.01037382
aagr-4	95.1049304	-0.6655949	0.1940397	0.01037382
H35N09.1	7.41180367	3.78034782	1.1023052	0.01038909
T12A7.6	102.830828	-0.8182296	0.23866036	0.01041817
crn-7	132.348663	0.55494625	0.16195215	0.01047639
sto-3	7.69782012	-2.1177966	0.61824386	0.01050712
R186.8	218.294306	-1.065396	0.31125849	0.01059764
itx-1	255.804647	1.52144703	0.44468304	0.01063018
mrps-24	416.859267	-0.6797457	0.19866783	0.01063018
sel-1	3.78071516	4.6959991	1.37289137	0.01065348
app-1	727.186752	0.58483023	0.17118619	0.01079399
del-1	12.6902913	-1.6000248	0.46832955	0.01079399
lact-6	7.82812015	-2.6977604	0.78995683	0.01083216
F21C10.18	24.8068328	1.31631325	0.38553464	0.01084048
nhr-208	25.7203841	-1.0426155	0.30536835	0.01084048
srw-91	2.2657465	-5.3669717	1.57236432	0.01086583
ubc-18	900.011128	0.5417918	0.15896611	0.01105825
nlt-1	3720.87491	0.62051329	0.18211825	0.01108737
ugt-6	173.532109	-0.9021704	0.26484222	0.0111057
Y38H6C.20	12.3127923	2.1860734	0.64184174	0.01111395
M03A1.8	64.3219983	0.94719773	0.27849706	0.01129977
clec-264	121.672932	-0.7500097	0.22054608	0.01130421
K02E11.7	127.046571	0.97032313	0.28573207	0.01149049
F10C1.t1	8.54962781	-2.1026567	0.61942745	0.01153674
comt-2	24.7625301	2.33319257	0.68826124	0.01171633

sas-4	10.3923514	2.1523494	0.63497174	0.01171635
F47B8.10	3.68418176	-4.0084836	1.18270928	0.01172218
ace-1	120.029538	-0.6713701	0.19813933	0.01174624
Y116A8C.25	18.0057223	-1.3440868	0.39703668	0.01186565
math-8	2.79532488	-5.642772	1.66708197	0.01187319
E01G4.6	9.34939919	3.14726677	0.9299862	0.0118866
C35D10.17	931.89493	-0.8159277	0.24113682	0.01189679
Y32H12A.1	4.07815289	-3.1422119	0.92916576	0.01195547
sprr-1	10.7404887	-1.5445239	0.45672768	0.01195547
ZK896.1	32.9630049	1.0076593	0.29802123	0.01196637
C31H5.4	2774.63329	-0.7484892	0.22166681	0.01213328
ZK822.5	399.367737	-0.4751256	0.14071721	0.01213328
F11A5.13	13.3139273	-1.4342779	0.42471885	0.01213328
D2023.4	83.9280838	-1.0122965	0.29988379	0.01215658
T20G5.9	101.158646	0.66559218	0.19720148	0.01216282
Y54E5A.2	49.0576956	0.93672374	0.2776806	0.01222903
rpn-3	812.486265	-0.3485549	0.10333384	0.01222903
mab-10	30.3775755	1.77354861	0.52603764	0.01228568
ent-6	197.729008	-0.5115816	0.15176397	0.01230009
T16G12.8	2.35908998	-4.3433189	1.28863911	0.0123061
VW02B12L.2	15.4141355	-1.337033	0.39685673	0.01234262
lys-3	192.814014	0.61669823	0.18303793	0.01234262
ugt-58	2530.06136	-0.8682553	0.25782932	0.01239652
Y43F8A.1	230.965825	-1.3260984	0.39394805	0.0124454
Y47H9C.1	245.246797	1.60110356	0.47589037	0.01251057
T05H4.10	90.8792359	-0.7505046	0.2231338	0.01254087
Y81G3A.1	6.03741356	-2.8320332	0.84213583	0.01255265
Y45F10C.2	557.675798	-0.4438583	0.13200024	0.01255555
ZK1307.9	58.9290699	-0.7919955	0.23572167	0.01265039
drd-50	786.827854	1.72893701	0.51467245	0.01265039
F20A1.8	8.67058681	4.00220347	1.19135571	0.01265039
C17H11.5	17.4407978	-1.2918466	0.38454035	0.01265039
H10D18.1	7.68129027	3.95403541	1.17722455	0.01266061
R17.3	36.4695509	1.26891407	0.3782175	0.01282177
F28C6.10	43.7155919	2.06063552	0.61466386	0.01292556
F53A9.6	531.594685	0.95574906	0.28527307	0.01301311
Y7A9A.79	237.875788	-0.8179403	0.24421899	0.01304655
rrc-1	30.0397571	-1.0335606	0.30861806	0.01304655

lact-5	48.2608985	-0.9804683	0.292793	0.01304786
W02F12.8	62.2365306	-1.673758	0.49998169	0.01308282
gsnl-1	354.762921	-0.6055793	0.18093252	0.01309962
clec-83	1180.8635	1.55894803	0.46583042	0.01310417
ins-19	1892.00141	-1.0829077	0.3236901	0.013142
K10G6.9	104.989603	-1.4375023	0.42988545	0.01318961
adah-1	398.725982	-0.8455346	0.25283853	0.01318961
F25B5.6	243.470271	-0.6162899	0.1843964	0.01325757
twk-14	25.6633108	-1.1257114	0.33688629	0.0132763
slc-17.5	55.1292633	0.98315972	0.29438187	0.01334738
yars-1	220.574983	0.51735302	0.15507065	0.01350248
pals-26	114.643918	-0.9892159	0.29658346	0.0135306
fmo-2	47.2030313	-1.5715582	0.47123938	0.01353706
T20D3.2	28764.5986	0.76947031	0.23078242	0.01356019
rme-8	217.626374	0.53148057	0.1595738	0.01372021
hipr-1	77.1918737	1.08252502	0.32518756	0.01378984
W07G1.25	66.2707449	1.75332423	0.52745012	0.01401343
unc-86	37.6905039	-0.8592841	0.25855773	0.01403792
T09E11.8	21.9467165	-1.3803303	0.41559215	0.01412502
gras-1	77.3638844	-0.6613473	0.19914204	0.01412931
acds-10	275.206449	-0.5852233	0.17636261	0.01425114
T03D8.8	3.66440633	-3.2514898	0.98034941	0.01431975
pud-1.1	99.0530801	0.8461112	0.25521151	0.0143732
sre-1	3.65801377	4.64024541	1.3999001	0.01439101
K07C11.14	17.4355222	-1.5367225	0.46365469	0.01439306
ubc-22	14.6339979	-1.4334032	0.43257594	0.01441543
cgt-3	1603.53232	0.64354436	0.19422809	0.0144161
aqp-4	146.651697	0.98472652	0.29723342	0.01442029
C16C10.8	300.69586	-1.0256645	0.30963351	0.01442928
dhs-30	608.728073	-0.3947371	0.11934673	0.01467579
C23H5.11	15.4229052	1.60087818	0.4840688	0.01467915
col-97	42.9837765	1.82203066	0.55099046	0.01467987
col-49	16.9918388	1.96210864	0.59386294	0.0147915
such-1	44.6440229	1.20876344	0.36586588	0.0147915
kqt-2	86.4731289	1.04380985	0.31592029	0.0147915
B0334.6	4.21118258	-2.7652533	0.83711363	0.01480402
Y40B1B.7	1474.5342	-0.7243242	0.21934954	0.01485089
Y47G7B.2	27.5973309	-1.5302274	0.46383484	0.01499883

Y26D4A.3	39.1419769	0.99336122	0.30120567	0.01504387
D1007.19	29.2190465	1.37614234	0.41744092	0.01510011
F49F1.2	4.16370281	-2.7759019	0.84218849	0.01511475
ung-1	11.8747252	2.62029212	0.79527446	0.01514178
ech-9	1029.01159	1.06936464	0.32456978	0.01514178
cah-4	940.589282	2.10969304	0.64032942	0.01514178
str-245	67.7605097	1.23186025	0.37403495	0.01518635
W06B4.2	81.4095809	-0.7272911	0.22086203	0.01518635
arl-5	115.081725	-0.5943233	0.18049407	0.01518635
F53H1.3	40.9083166	0.96384055	0.2927173	0.01518635
ZK863.8	294.321739	0.51329226	0.15595925	0.01525435
col-162	31.2197663	2.28470627	0.6944743	0.01531277
T04C12.32	37.0181877	-1.1319027	0.34411795	0.01532719
Y54F10AL.1	219.211009	0.71549171	0.21756421	0.01533125
scl-3	172.888115	0.9616685	0.29241924	0.01533125
R05H5.7	6.88735978	3.7781183	1.15018887	0.01549641
B0244.4	9.55435723	2.26054359	0.68817672	0.01549641
epg-6	167.797518	0.65131038	0.19826835	0.01549641
C37C3.11	17.3872	-1.2615992	0.38451552	0.01568936
cyp-14A2	27.6683176	-1.044172	0.31828226	0.01569381
ubc-13	128.445074	1.335083	0.40704863	0.01570348
ttll-11	7.14666641	-2.1728071	0.66241928	0.01570348
nep-11	120.561148	0.87683867	0.26739331	0.01572684
hmr-1	83.7286106	1.3841111	0.42233657	0.01581948
clec-53	56.0732974	-1.5997701	0.48837947	0.01589355
hda-2	39.1193381	-0.8561282	0.26142424	0.01592326
F13E9.11	62.6863377	-0.80179	0.24488045	0.01594417
fbxc-58	481.924898	0.90026845	0.27505791	0.01599591
F54F11.1	10.5098162	2.13364952	0.65210972	0.01604214
T08B1.1	157.777159	1.12939429	0.34553259	0.0162176
F49C12.14	1132.42049	-0.755041	0.23112462	0.0163019
F56C3.9	377.527873	0.69248197	0.21208613	0.01638475
C14C10.9	21.3929521	-1.3874998	0.42501014	0.01639577
sri-16	8.25086142	4.03337001	1.23568026	0.01641078
C04E12.2	225.641062	1.25846973	0.38561462	0.01642625
ZK287.9	454.979943	0.50520426	0.15498153	0.01662986
C01F6.14	74.0432818	-0.8469973	0.25988842	0.01665398
F13G3.12	64.8421827	-0.8674761	0.26636237	0.01675825

sgk-1	257.962746	0.664303	0.20396162	0.01675825
mapk-15	27.0377957	-1.157027	0.3553323	0.01677541
gln-6	39.4742214	1.43045927	0.43938028	0.01679169
egl-13	67.3035423	1.12549617	0.34601974	0.01693296
F13D11.4	274.836573	-0.8150736	0.25058289	0.01693296
Y94H6A.2	7.98988852	3.87245965	1.19113119	0.01701288
Y56A3A.41	15.2223563	1.7745181	0.54613645	0.01710619
mrp-4	63.2807267	1.40760106	0.43324572	0.01710619
lgc-28	148.813575	-0.5089252	0.15667009	0.01711462
mett-10	44.2812951	-1.0804505	0.33262309	0.01711462
srh-39	3.89072004	-3.4444871	1.06068916	0.01715022
epg-4	404.207722	-0.4542744	0.14001276	0.017308
pbrm-1	76.8600853	0.82693455	0.25509048	0.0174445
B0462.5	213.003253	0.96095599	0.29642382	0.0174445
cyp-33A1	566.236002	-0.9414444	0.29046327	0.01746116
akt-2	392.997253	-0.539094	0.16652134	0.01767799
gcy-8	6.89190246	-2.0703752	0.63963837	0.01769787
bed-1	38.9855291	0.94836692	0.29314986	0.01778625
F53A9.1	506.86905	1.96481948	0.60754435	0.01783504
C04F12.16	76.246117	-0.7506669	0.23216172	0.01784588
elc-1	349.016634	-0.7465828	0.2309035	0.01784588
F58D5.5	683.369128	-0.510666	0.15812169	0.01806324
K12C11.7	190.339362	0.78726112	0.24388382	0.0181094
fbxa-21	47.8112162	-1.1281888	0.34953152	0.0181094
C45G9.2	6.58573337	4.56002045	1.41311543	0.0181094
mul-1	151.517957	1.95275605	0.60492243	0.0181094
nlp-20	3037.41319	-0.5004288	0.15507152	0.0181094
cbd-1	44.977583	1.53415673	0.47536742	0.0181094
Y51H4A.24	304.091394	-0.4783693	0.14817166	0.0181094
acr-18	67.6042855	0.92615489	0.28723001	0.01825024
iglr-3	21.3831901	1.29460779	0.40155901	0.01825647
Y82E9BL.18	48.542788	1.47899426	0.45877462	0.01825647
scl-11	7.57057278	-3.2650525	1.01292121	0.01826399
Y53C12A.3	119.56314	-0.6476938	0.20098117	0.01826772
Y58A7A.5	231.956573	0.83042998	0.25765448	0.01826772
C30G7.2	79.0688145	1.47495645	0.45770179	0.01826772
fbxa-60	1369.48941	0.84864646	0.26339741	0.01827297
ZC196.4	8.3492891	-1.7929579	0.55649055	0.01827297

C18G1.6	12.6609313	1.80974609	0.5619487	0.0183463
Y62F5A.10	18.3146779	-2.0916302	0.64955653	0.01835412
F41C3.1	26.1219524	-1.3687386	0.4252444	0.01839455
nhr-232	119.146976	-0.6538453	0.20315006	0.01839455
tmem-135	127.416206	0.54688989	0.16992726	0.01839455
C18B12.6	100.723745	1.06042944	0.32944887	0.01839455
T25B9.8	62.8811364	-1.0021754	0.31162692	0.01853359
lin-29	23.0574189	1.94344487	0.6044184	0.01855166
clec-40	17.4912691	1.64452087	0.51150998	0.01855781
F01D5.6	14.5799236	2.95214217	0.91853195	0.01860853
Y34F4.6	165.384821	-0.6959468	0.21657358	0.01861203
fbxa-88	9.53004841	2.5198054	0.78415884	0.01861203
Y71G12B.2	16.5779512	1.48963984	0.46368591	0.01862103
T19C9.8	213.045398	0.7641602	0.23785174	0.01862103
nhr-45	88.4565689	1.24542402	0.38768763	0.01862103
C14B9.3	86.2109074	-0.713991	0.22232767	0.01865153
scl-18	3.65834222	-4.0694175	1.26708155	0.01865153
elt-1	22.956547	-1.1392319	0.3548091	0.01867345
col-73	38.3294774	1.56266976	0.48683815	0.01870576
samp-1	86.8461595	0.81053849	0.25254102	0.01870576
F32E10.9	44.8023851	1.44422217	0.44995103	0.01870576
F13B6.1	28.8439655	1.25716398	0.3917698	0.01872723
nmgp-1	88.7872441	0.74489497	0.23222943	0.01879813
tbc-17	144.11042	1.23778105	0.38594373	0.01879913
rcs-1	217.337264	0.81714273	0.25479702	0.01879913
F45E1.1	38.7765132	1.47840941	0.46107864	0.01880943
lep-5	10313.3485	-0.4091544	0.12760773	0.01880943
acs-19	1350.59235	-0.7054953	0.22008112	0.01882807
W09G12.7	1586.53134	0.87590657	0.27324871	0.01882807
hsd-2	16.8370072	1.52907199	0.47710352	0.01885147
C08F11.12	764.709354	-0.8540142	0.26654433	0.01889197
mks-3	4.8746498	-2.8589371	0.89264705	0.01895738
dop-5	28.1453301	-0.9849141	0.30757318	0.01897635
taf-11.1	34.0564048	1.35933823	0.42454518	0.01898141
Y104H12D.10	3.08002594	4.40754172	1.37674342	0.01899324
21ur-8756	2.15782153	-4.1905644	1.30972406	0.01908043
R160.10	23.3910635	-1.1330667	0.35411593	0.01908043
chn-1	185.404396	-0.720954	0.22534975	0.01908357

Y87G2A.16	42.8609135	-1.2050404	0.37680585	0.01914742
glb-2	13.5868021	-1.5693548	0.49077208	0.0191508
abf-2	3393.50366	-0.5630816	0.17618954	0.01925582
exos-7	74.1818274	-0.8488465	0.26566617	0.01928659
F57B9.3	39.4534247	1.54854015	0.48474609	0.0193107
F26E4.2	435.429006	-0.4586241	0.14360272	0.01934544
ZK1236.9	9.59407867	-2.1059499	0.6594499	0.01934544
taf-2	25.6474339	1.79838077	0.56351599	0.01947149
B0238.9	11.8102621	2.33947806	0.73337237	0.01954356
F13D12.5	47.3195774	1.14871322	0.36019683	0.01958682
mrps-18B	234.036287	-0.5627239	0.17649159	0.01961906
istr-1	415.995865	0.89045902	0.2794074	0.01969873
T13F3.7	11.5637362	1.73587677	0.54485294	0.01974916
hrpu-2	5.05517038	-2.4944436	0.78365908	0.01991085
ugt-61	103.967583	-0.5781328	0.18162316	0.01991085
W09C5.1	1186.78901	-0.6777908	0.21302418	0.01995358
patr-1	209.291765	0.58689858	0.18446247	0.01995358
Y71H2AM.3	77.1600036	-0.7076984	0.22241943	0.01995358
C31H5.7	63.7843862	-0.8034105	0.25257781	0.01999255
Y75B8A.31	108.132474	-0.5980094	0.18807195	0.02003671
ipla-6	178.189595	-0.5866316	0.18448849	0.02003671
atg-16.2	343.910707	-0.7979067	0.25099734	0.02005279
best-17	206.226506	0.46960822	0.14773307	0.02005279
Y48G9A.7	2.46449122	-4.3866498	1.38002562	0.02005279
sop-3	196.232219	0.59257209	0.18648126	0.02008775
ets-4	118.24325	0.63540438	0.19994825	0.02008775
ceh-45	12.6496842	1.82738879	0.57531119	0.02015918
copa-1	774.059035	0.88593328	0.27893938	0.02015918
C06E1.7	19.6999147	2.37673646	0.74837943	0.02015918
C14B9.10	8763.00451	-0.5457639	0.17187301	0.02017279
ceeh-1	629.570163	-0.530609	0.16712263	0.02018419
F39G3.4	7.94052863	3.44047989	1.08394338	0.02023085
F42A8.1	1587.15459	0.5596033	0.17633922	0.02023624
F08G2.8	97.2986183	1.2080015	0.38062986	0.02023624
dhhc-14	149.129833	0.65196779	0.20550437	0.02028267
npr-1	5.63752468	-2.4622713	0.77627902	0.02030912
trx-3	32.4518587	1.79912657	0.56728954	0.02032237
cdc-48.2	723.800534	0.41330099	0.13033857	0.02033683

thn-5	36.5916927	-0.8865119	0.27981705	0.02051531
pgl-1	73.1506187	0.90741597	0.28644338	0.02051923
Y32H12A.6	28.7207593	1.48293379	0.4681711	0.02052712
Y41C4A.32	128.963226	1.47426459	0.46574515	0.02065873
col-139	2239.35882	-1.1297021	0.3569647	0.02068633
ubr-1	194.626469	0.69263531	0.21909601	0.02091183
clk-1	126.913635	-0.5194108	0.16438707	0.02100028
sql-1	34.7141553	0.98840368	0.31282644	0.02100028
gst-31	22.3225937	-1.162455	0.3682805	0.02119373
Y38A10A.7	87.5676403	-0.93772	0.2970846	0.02119373
Y71G12B.23	34.2312087	1.09572628	0.34727747	0.02124044
C32D5.7	48.9534085	1.14555472	0.36309948	0.02124044
clec-6	31.3499648	-1.4081785	0.44628473	0.02124044
C49C8.8	10.2496295	-1.7419794	0.55222211	0.02124044
glr-5	35.0172861	1.02837032	0.32598947	0.02124044
daf-18	71.636261	-0.8185621	0.25958842	0.02130813
spr-5	51.0647287	1.10757981	0.35153459	0.02145764
Y17G7B.21	201.631724	0.92889328	0.29482067	0.02145764
tag-153	126.985701	1.16940707	0.37118097	0.02145764
Y37H2A.10	3.12837594	4.42395033	1.40438768	0.02146926
Y54G9A.9	173.95406	-0.6820476	0.21655004	0.02148625
twk-26	25.4732093	-0.999344	0.31760752	0.02169893
best-1	69.0218858	-0.6882121	0.21879225	0.02172488
T19F4.8	1.78463147	-5.007052	1.59200428	0.02172488
F35E12.2	29.3861623	1.9274753	0.61282729	0.02172488
F09A5.3	3.6510478	4.69498842	1.49278843	0.02172488
prp-18	58.4145689	-0.7691026	0.24456162	0.0217278
drd-1	262.07946	-0.8036799	0.2555889	0.02173857
nep-17	2475.91639	1.00296507	0.31901782	0.02175761
K09C4.5	218.079794	-0.7649499	0.24334372	0.02177011
C36B1.9	15.1034666	-1.935175	0.61567659	0.02177574
Y51H4A.15	265.066163	-0.8154685	0.25947051	0.02178231
Y62H9A.10	2.70205192	-3.5100363	1.11692935	0.02178231
hum-1	189.439712	0.89373219	0.28444397	0.02180413
C49A9.9	161.068981	0.93702673	0.29827174	0.02182359
col-71	147.158519	0.7333885	0.23361428	0.02196979
enu-3.2	23.913727	1.45729174	0.46438809	0.02203643
Y43F8B.3	3.09300238	4.41428332	1.40675248	0.02203643

F54D5.2	12.3929285	2.61381859	0.83306793	0.02204339
maph-1.3	26.6761785	1.34288136	0.42810671	0.02208404
F58A4.6	37.8869443	1.1933541	0.38063607	0.02218845
nhr-42	52.9164678	-0.776131	0.24766122	0.02226925
eif-2Bbeta	40.1741191	1.10438213	0.35252383	0.02233035
ced-7	375.60284	-0.6693253	0.21375404	0.02242563
nlp-32	11.5309732	2.11863048	0.67682413	0.02248567
ugt-27	58.0055779	-0.8935407	0.28553434	0.02249648
hal-3	18.3495876	-1.1384247	0.36373017	0.02249648
cyp-14A5	243.967019	0.9864419	0.31519765	0.02249648
cyp-37B1	545.614145	-1.4682258	0.46935155	0.02256656
apy-1	1838.34881	-0.335994	0.10749143	0.02273425
F44F4.3	33.481476	-1.1171434	0.35777542	0.02297156
Y67H2A.2	102.35478	-0.5615488	0.17989682	0.02302759
mis-12	6.58499698	3.09393165	0.9919383	0.02316801
dcn-1	61.6333259	1.74466831	0.559449	0.02316801
ugt-7	154.620037	0.57651533	0.18487104	0.02316801
add-2	419.640047	-0.6439394	0.20646078	0.02316801
nfya-1	26.8312642	-1.0221635	0.32775143	0.02316801
cdc-37	378.801727	0.75155432	0.24105064	0.02317197
C33A12.19	263.40098	-0.7801069	0.25019688	0.02317197
ZK154.6	238.688986	1.22306381	0.39229935	0.02317197
bath-42	179.378022	0.55484435	0.17807187	0.02329709
sek-6	39.7440599	-0.7895958	0.25345653	0.0233198
F30A10.9	557.757061	-0.9539524	0.30627693	0.02335073
popl-4	17.4491082	2.18147784	0.70069116	0.02343818
Y75B12B.1	8.75956758	2.34048954	0.75186299	0.02345057
klp-15	18.7436844	2.95931038	0.95104434	0.02353261
ugt-62	1619.07676	0.64809158	0.20832021	0.02354176
Y43F8C.13	1185.81297	0.71770361	0.23069035	0.02354176
srw-86	16.130367	1.60269533	0.51529659	0.02358573
E02H1.1	125.923955	-0.8398108	0.27016686	0.02370605
fbxa-9	12.0941124	-1.415604	0.45561812	0.02380627
ttr-36	3246.51258	-0.6667735	0.21465771	0.02384929
C29E4.9	2.95381732	4.36606324	1.40594793	0.02389358
srh-10	4.56285675	-2.2063153	0.71062102	0.02392649
trap-3	1752.36002	0.72722862	0.23425642	0.02392955
Y15E3A.4	440.778921	-0.4822659	0.15535701	0.02392955

ing-3	37.4103357	1.21009993	0.39058076	0.02440217
T05B11.1	75.9391674	0.82302772	0.26569652	0.02443005
bath-36	15.9814649	-1.8730154	0.60486868	0.02449714
Y56A3A.6	133.14435	0.74258524	0.23983659	0.02450601
bcmo-1	6.49082419	-3.1796342	1.02762291	0.02463524
his-74	60.59532	0.7668602	0.24782577	0.02463524
spr-2	176.696399	-0.6179559	0.19974407	0.02465033
jmjd-2	20.8454809	1.73579397	0.56144044	0.02480151
C41G11.1	253.949945	-0.774337	0.25048441	0.024808
dbr-1	30.0189071	-1.041948	0.33725493	0.02494346
T04B8.5	602.330288	1.00853394	0.32660956	0.02502111
Y53F4B.1	17.6026749	1.65022991	0.53447027	0.02502111
flp-14	3815.3768	-0.5090495	0.16486626	0.02502111
ZK792.7	161.792837	-0.7090477	0.22961057	0.02502111
cutl-20	38.4098563	0.94469742	0.30619253	0.02519429
fbxa-105	150.17472	0.72275937	0.2343234	0.02524599
ceh-83	11.2467402	-1.8113282	0.58743805	0.02531163
lmn-1	387.409164	0.7596724	0.24648597	0.02541247
D2045.7	22.0612087	1.45462013	0.47209386	0.02546019
snf-9	50.8916552	0.76802479	0.24944308	0.02563249
fbxa-30	27.0089665	1.10776071	0.35991932	0.02571113
F58H1.5	42.2341406	1.0479912	0.34054132	0.02572261
F41E6.12	99.289786	0.73163997	0.2378312	0.02579915
T05E12.8	18.0471639	-1.7547548	0.57070481	0.02591551
B0457.6	201.740069	1.17721384	0.38290464	0.0259192
M03F8.1	17.9940464	1.78409133	0.58040626	0.02592623
Y57E12B.10	21.400909	-1.0610491	0.34515739	0.02592623
F36D1.12	53.8511535	-1.551756	0.50494507	0.02597029
C17E4.11	107.609647	-0.7644432	0.24878584	0.02598606
exo-3	28.3374141	1.67936068	0.54670207	0.02604291
icd-1	504.270621	-0.6006212	0.19596241	0.02662274
htp-2	27.5999307	1.14635892	0.3740726	0.02664093
C23H4.8	61.3260822	0.88065877	0.28751024	0.02675184
C34C12.2	46.5895754	-0.7263639	0.23736344	0.02699213
sri-5	3.97541079	-2.6754504	0.87453472	0.027047
otpl-1	14.3758806	1.4764825	0.48277993	0.02711483
Y76B12C.8	135.67408	-0.7666715	0.25085056	0.02727491
W03A5.2	4.61298466	-2.2473465	0.73547944	0.02731369

linc-125	4.87897351	-2.621083	0.85791663	0.02733267
atn-1	959.736182	0.36851684	0.12065659	0.02737184
R04E5.7	8.30952878	2.81557085	0.92181288	0.02737184
ubc-1	282.664444	-0.7151851	0.23432489	0.02754687
tra-2	74.8738854	0.670154	0.21960847	0.02757292
acaa-2	1239.63823	-0.5354925	0.17559354	0.02773237
chil-15	2.05934363	-4.1364418	1.35696907	0.02778652
nhr-142	75.4539754	-0.7642896	0.25074545	0.02778652
Y102A5C.4	2.05934363	-4.1364418	1.35696907	0.02778652
linc-43	2.05934363	-4.1364418	1.35696907	0.02778652
nlp-17	804.25424	-0.8302962	0.27245199	0.02781751
cel-1	93.6180757	-0.960264	0.31513926	0.02783106
R10E4.3	7.1899415	-1.6841029	0.55287919	0.02789532
F08F1.3	119.077514	1.46331936	0.48041647	0.02789532
F20G2.6	30.6047094	1.38521758	0.4548191	0.02790047
nas-28	15.0520902	-1.2784054	0.41979898	0.02791223
pnk-1	4163.28772	-0.8028318	0.26372368	0.02798899
rfip-2	87.4419707	0.98301688	0.32295971	0.02800779
ech-3	136.131035	-0.9093396	0.29880305	0.02803233
gsp-4	2.78276594	4.27575801	1.40545161	0.02810416
C03B1.14	346.657308	0.62638468	0.20599937	0.02822737
tba-6	36.5441202	-0.9964388	0.32800997	0.02843536
Y37D8A.6	1265.30694	0.7028211	0.23135952	0.02843536
srm-3	53.9480598	0.9851839	0.32428502	0.02843536
T28B8.4	4.03909436	4.81351415	1.58618717	0.02871075
poml-2	181.612639	-0.7473641	0.24633415	0.02873226
nduf-2.2	28.804041	1.03707718	0.34182284	0.02873226
Y106G6H.1	152.291514	0.73481079	0.24227252	0.02877378
aars-1	24.7864138	-1.3012789	0.42906613	0.02877378
Y66H1A.4	220.779762	0.44891481	0.14802	0.02877378
vab-1	51.4792497	1.07836096	0.35564719	0.028817
nob-1	49.2080402	0.81153816	0.26774322	0.02887479
trx-2	1346.29987	-0.3858269	0.12728648	0.02887479
Y43C5A.4	10.67816	1.74786743	0.57671521	0.02888117
abts-1	337.273427	0.38673026	0.12774848	0.02919008
C10C5.5	13.124173	2.60894516	0.86213795	0.02927795
C04C3.14	9.67341172	2.4282264	0.80264411	0.0293375
akt-1	513.194101	-0.3443896	0.11384794	0.02934253

Y45F10D.15	1.68702379	-4.9231954	1.62801085	0.02935565
clec-34	3.04460387	4.37193559	1.44578392	0.02935565
F57C12.2	49.7867688	0.73559019	0.2432079	0.02935565
phf-33	1.68702379	-4.9231954	1.62801085	0.02935565
Y41D4B.17	130.140361	0.8862336	0.29314443	0.02940302
ent-7	722.511964	-1.0513771	0.34781711	0.02942011
axl-1	15.5929377	-1.1454333	0.37907258	0.02945525
T23D8.3	522.638008	-1.0995535	0.36386991	0.02945525
Y53F4B.13	12.3834819	-1.5225917	0.50392102	0.02945525
puf-3	5.65531441	5.31379528	1.75850654	0.02945525
clec-224	20.1641917	1.57642013	0.52194657	0.0295511
fbxa-13	21.9200567	-1.0450336	0.3460544	0.02956904
magu-2	98.0540183	0.80199686	0.26570751	0.02969376
Y47G6A.25	7.49565588	2.68225758	0.88881417	0.02970489
Y82E9BR.18	62.8593152	0.94966384	0.31470156	0.02970489
F52H2.7	35.0258271	1.18872754	0.39394046	0.02970489
W04C9.8	12.9745858	-1.4118074	0.4680062	0.02976918
cdk-5	194.523734	0.75192467	0.24934156	0.02984472
Y40C5A.4	180.088987	-0.7378918	0.2447124	0.02985117
T24C4.10	296.974911	1.11976835	0.37146444	0.02991426
ppk-2	177.940562	1.17540335	0.39015263	0.02997672
Y55D5A.4	36.3142306	1.11700786	0.37076015	0.02997672
lgc-50	92.5547268	0.60063799	0.19935025	0.02997672
ttm-1	528.889065	0.64352935	0.21358337	0.02997672
set-12	9.75476651	1.99460219	0.66204808	0.02997672
cest-2.3	4.93338768	-2.3898673	0.79352375	0.03004879
fos-1	45.8165158	2.19886593	0.73032141	0.03011456
C06A6.4	593.298099	-0.3133547	0.10410238	0.03016666
tsp-19	2.9232312	-3.0315315	1.00757231	0.03027441
W06F12.2	218.08373	0.72202008	0.24006941	0.03037118
F43C9.1	69.707274	-0.6111586	0.20325136	0.03037508
nhr-14	192.071986	0.66788374	0.22213411	0.03037508
K01A12.3	5.01440459	4.15490954	1.38193687	0.03037508
M153.1	209.94214	-0.5466555	0.18180267	0.03037508
T24B8.4	242.435123	0.8159802	0.2714754	0.03043801
jph-1	129.3527	0.57583051	0.19168482	0.03056636
lron-5	19.9174936	-1.1533595	0.38394336	0.03056636
ifd-2	127.57844	1.23712402	0.41194536	0.03062939

C56G2.3	12.9189242	-1.7315116	0.57671317	0.03068148
srd-64	28.9971736	1.22757333	0.40894795	0.03071833
Y73C8B.9	6.4643203	-1.8933524	0.6309571	0.03078588
Y6G8.2	71.8692382	-1.1205706	0.37344197	0.03078588
arx-5	539.900083	0.48210039	0.16076681	0.03094245
fbxa-18	58.2875977	0.95494634	0.31845865	0.03094245
pph-4.2	52.9173461	1.2708895	0.4239073	0.03098159
col-38	27.6487657	1.48908882	0.49686224	0.03104189
mir-239.1	2.64713662	4.22948323	1.41118947	0.03104189
slc-17.9	15.0166086	-1.4165234	0.47273794	0.03107571
fndc-1	2.03603883	-4.0576145	1.35446803	0.03112364
C50E3.6	30.4396126	1.07926037	0.36036743	0.03118575
W08F4.11	68.5819755	-1.0318823	0.34462002	0.03120322
F35C5.14	4.70102092	-2.3984593	0.80098059	0.03120322
lin-11	47.3957845	0.95566366	0.31921239	0.03122522
chup-1	88.5674763	-0.8513316	0.28438711	0.03122763
eif-3.J	247.477485	1.08037831	0.36102713	0.03131217
laf-1	42.9633482	1.51445862	0.50618045	0.03134816
T16G12.1	134.031235	-0.6927049	0.23157977	0.03136286
Y41C4A.11	77.3606093	-0.5737031	0.19181742	0.03136286
pph-4.1	69.3491594	1.48192968	0.49542155	0.03136286
cdf-1	177.103568	0.59718166	0.1996622	0.03136286
B0272.4	160.131926	-0.7781556	0.26020101	0.03136899
spc-1	729.273745	0.57560756	0.19252953	0.0314365
T23F11.11	11.3244274	-1.4104353	0.47220273	0.03170054
W03F8.3	18.3184673	-1.3353285	0.4471989	0.03177498
T24E12.5	130.927186	0.77552692	0.25975452	0.03178974
marc-3	9.1005862	3.11677976	1.04416653	0.03183581
EGAP5.1	38.8964629	1.13524494	0.3808194	0.03221878
C39H7.4	408.206521	0.79576725	0.26717057	0.03245461
rsd-2	202.921017	0.51089754	0.17153589	0.03245461
zmp-4	1244.91141	-0.3649754	0.1225706	0.03250443
mig-32	14.5709267	-1.2400841	0.41675696	0.03265735
D1086.9	43.8207708	-0.7068104	0.2375254	0.03265735
nlp-67	46.1575787	0.88689035	0.29805601	0.03265735
lpd-7	701.179047	-0.5404509	0.18171535	0.03278198
ile-1	40.4677329	2.27257344	0.76424397	0.03279136
skpt-1	13.0089386	-1.5693114	0.52772003	0.03279136

Y51B9A.8	101.797514	-0.801877	0.26973547	0.03285231
linc-55	17.9351526	1.48636696	0.5001492	0.03293319
F53F1.6	126.345696	1.31888653	0.44403243	0.03308082
apg-1	521.649828	0.59463028	0.2002624	0.03316352
F35G2.1	484.226896	0.56967277	0.19189384	0.0332006
F53A9.7	251.937544	1.07155224	0.3610155	0.0332331
math-38	36.9817837	-1.0537865	0.35510227	0.03327406
clec-89	22.8622236	1.73913719	0.58636368	0.03341134
srv-34	7.56385532	-2.1165115	0.71362915	0.03341134
F53C11.9	1537.17913	-0.7923084	0.26716827	0.03341561
nlp-76	47.0534331	-0.8330255	0.28095652	0.03343379
olrn-1	12.0518135	2.02315295	0.68233446	0.03343379
nspf-3	3.52829791	4.6221782	1.55917558	0.03343518
F07A11.5	357.531839	0.93626011	0.31582058	0.03343518
col-51	16.3216929	-1.9161709	0.64667934	0.03354362
nhr-25	2.921951	4.33020512	1.4613977	0.03354362
R02E4.3	10.9787876	1.86577186	0.62995845	0.03366321
pals-22	33.3778609	-0.8107098	0.27379193	0.03369029
irk-2	43.9356008	-0.9462969	0.3195587	0.03369029
aff-1	10.8338287	1.75267628	0.59202847	0.03372109
lsm-5	440.455676	-0.3932236	0.13283166	0.03372109
Y47H9C.9	3.29720991	-5.8857243	1.98891324	0.03376276
T28A8.3	8.0651469	3.82608341	1.29282932	0.03376276
C10F3.15	3.29720991	-5.8857243	1.98891324	0.03376276
panl-2	81.5929669	-0.5743438	0.19410455	0.0337741
ell-1	63.7657964	1.57674139	0.53336107	0.03404706
gpx-5	1456.53949	1.00667623	0.34068151	0.03417138
lin-8	23.5940723	-1.1204809	0.37939675	0.0342963
ugt-51	231.722849	-1.1861191	0.40162245	0.0342963
klo-1	742.694334	-0.4483562	0.1518845	0.03442335
fld-1	58.8441975	0.82665025	0.28006193	0.03442673
F25E5.3	6.44922802	3.54654448	1.20161531	0.03442673
col-72	10.8769883	-1.5735985	0.53340469	0.03453712
F52F10.2	5.2677397	-2.8684245	0.97233134	0.03453712
dnc-6	152.711411	0.63715316	0.21608793	0.03467643
hsr-9	85.6235039	0.59447209	0.20164615	0.03470627
mrp-5	748.889902	0.43648576	0.14807551	0.0347231
elo-4	23.9700986	-1.0997112	0.37316777	0.03472337

C48B4.12	21.6102791	1.75342909	0.59501652	0.03472337
F41E6.8	15.9820943	1.61190173	0.54689253	0.03472337
lig-1	23.621948	-1.1506401	0.39046604	0.03472337
F26G1.15	12.0433298	-1.3552436	0.46003618	0.03479834
F36A2.12	3.02461296	4.41286009	1.4981253	0.03481034
K06B9.6	85.8218339	-0.7942815	0.26966826	0.03481034
nhr-19	45.7273356	-0.8000895	0.27167462	0.03482764
arrd-18	117.34928	0.63695108	0.21630232	0.03483689
Y39B6A.8	3.05412158	4.4265955	1.50343644	0.03485803
Y38H6C.24	62.584057	0.68354013	0.23218515	0.0348754
M02D8.3	141.741059	-0.4636961	0.1575288	0.03489347
dma-1	15.1255651	1.80826489	0.61446553	0.03495202
Y47D9A.1	310.03896	0.50454694	0.17146812	0.03496268
inf-1	26.2911953	7.51951137	2.55723117	0.03516678
ccf-1	341.317298	0.95129661	0.32358781	0.03521555
F41C6.6	3.16858546	-2.5786712	0.87727906	0.03524111
his-25	51.1440876	-0.7282094	0.24776719	0.03525139
T24C4.8	160.916624	0.81489078	0.2772893	0.03526203
alkb-7	36.7781367	0.96806369	0.32953776	0.03536622
W05F2.7	71.9200901	0.64603824	0.21998629	0.03544636
fahd-1	301.170868	-0.5611899	0.1911461	0.03551277
hot-1	65.7970626	0.9901994	0.33754752	0.03576446
wts-1	107.945026	0.7400918	0.2523754	0.03583355
insc-1	24.7073876	1.27903615	0.43616268	0.03583355
slcr-46.2	21.5662882	1.15461983	0.39390472	0.03595381
mef-2	148.597947	0.70426152	0.24031347	0.03600042
H20J04.4	18.423664	-1.2878149	0.43961017	0.0361083
21ur-15576	3.49336601	-3.2565023	1.11211458	0.03617781
W06E11.1	12.1709591	2.04144606	0.69713994	0.03617781
F31F4.1	23.3706487	-1.1248252	0.38413593	0.03617781
algn-5	322.296071	0.42357357	0.14468848	0.03623507
mrpl-1	123.12801	-0.8567747	0.29281637	0.03638559
F14F9.8	83.463561	-0.9475022	0.32399141	0.03653733
unc-104	154.959179	-0.5130672	0.17545581	0.03654359
best-20	90.9201555	1.60356811	0.5484546	0.03656534
F47H4.2	27.0677531	-1.3517412	0.46247942	0.03664437
F46G11.4	62.236538	-0.6671384	0.22826199	0.03664437
K07E8.7	42.0608764	-0.7300127	0.24985858	0.03673468

ltah-1.2	303.874943	1.04528939	0.35781271	0.03675306
F59F5.4	21.6824834	-1.3462071	0.46088677	0.03677761
F11E6.6	53.6311908	0.93256564	0.3194808	0.03697711
pkc-3	236.32125	0.73527997	0.2519192	0.03698585
F45D3.4	4721.41125	-0.9079954	0.31116636	0.0370403
clec-5	343.335815	-0.57711	0.19780335	0.03706734
Y75B8A.16	55.5663658	-0.6280183	0.21528285	0.03709121
ZK1010.8	31.5340864	1.6378439	0.56164989	0.03719025
rer-1	916.351072	0.5175771	0.17752546	0.0372385
csn-2	393.945215	-0.5438732	0.18657772	0.03724601
ZK822.8	2520.32478	-1.1369304	0.39005448	0.03724601
R193.6	77.5253106	1.60554245	0.55078367	0.03724601
alkb-8	71.7686329	-0.6212384	0.21320668	0.03734138
irg-4	288.038474	-0.5883573	0.20193862	0.03734432
clec-86	826.275934	-0.6327969	0.21721345	0.03735397
C18B2.4	941.895627	0.8777335	0.30136764	0.03741782
ZK84.2	130.315876	-0.5601951	0.19236891	0.03744156
fnta-1	107.0866	0.75032414	0.25768325	0.03744933
T05F1.8	2.52443524	4.14648916	1.42427881	0.0374599
F46G11.2	29.6328537	-0.9342499	0.32090461	0.0374599
ssb-1	421.215706	0.3861859	0.13270346	0.03757202
C02D5.2	34.4198032	-0.8282857	0.2848172	0.03778857
acs-9	8.00968369	-1.9774469	0.68006575	0.03781123
Y67D2.2	69.7294373	0.88861439	0.30569581	0.03789065
gst-38	333.979543	0.50204412	0.17273079	0.03790665
rsd-6	143.755342	0.53583346	0.18438888	0.03794317
F14D7.6	117.201873	-0.5306504	0.18265175	0.03800691
linc-142	3.6687411	-2.5414026	0.8748322	0.0380101
rlbp-1	134.430985	0.54130665	0.18639111	0.03808135
nspb-10	3.33489791	4.55827211	1.56978059	0.03808135
nhr-37	2.72875067	-4.5844624	1.57876097	0.03808135
F46G10.4	222.185757	0.51093009	0.17596576	0.03808135
Y51A2A.4	2.45363961	4.08008294	1.40545698	0.03812201
C06E2.9	7.28466531	2.426182	0.83601341	0.03821111
ent-4	162.530282	0.88313372	0.3046099	0.03853478
dbn-1	231.499438	0.56285446	0.19421429	0.03864212
Y97E10AR.1	38.1838274	-0.8909201	0.30743324	0.03864212
ZK673.11	2.87355249	4.28504169	1.4790686	0.03865651

cku-70	103.219612	0.5449629	0.18810998	0.03865651
Y69A2AR.31	46.1954327	0.83161546	0.28705598	0.03865651
F15A8.12	4.30532577	-3.7649344	1.29970964	0.03865651
mig-2	410.242564	0.74494236	0.2571536	0.03865651
cest-24	425.242437	0.57863089	0.19984835	0.03880317
F08G2.5	661.57885	0.54245728	0.18738021	0.03882577
sdha-2	155.746232	-0.5578775	0.19274572	0.03887189
unc-29	33.2017553	-0.8739358	0.30203304	0.03895215
F40A3.7	59.684008	-0.9867033	0.34107506	0.038999
cest-3	23.5853712	-1.1732332	0.40559131	0.03900655
F58F9.1	176.128106	-0.5560875	0.19226122	0.03901691
scav-5	80.9706257	0.59279005	0.20498466	0.03905009
col-180	62.9040496	-0.6727166	0.23267108	0.03909817
wht-7	81.3244033	0.79278352	0.27423717	0.03912277
sra-25	1.58941612	-4.8342366	1.67385304	0.03944361
F31C3.14	3.18242106	-2.9659249	1.02744154	0.03959041
C49A1.10	186.588686	0.73330606	0.25427803	0.03992167
fbxa-77	2.70811608	-2.9257542	1.01468511	0.03995373
cgt-1	57.2470046	1.08605958	0.37674851	0.04001495
twk-9	12.437982	-1.4103128	0.48928261	0.0400273
prx-10	76.9212103	-0.8104756	0.28128049	0.04013159
magu-3	11.7754632	2.11705251	0.73487734	0.0401594
F23B2.10	9.84892065	2.11549922	0.7343599	0.0401594
dct-18	1751.06413	1.55124174	0.53855672	0.0401798
B0393.6	3.95858766	3.80298361	1.3204482	0.04019099
Y34F4.2	1094.07665	-0.4979667	0.17291608	0.04019645
R01H2.8	1.58249278	-4.8406358	1.68132807	0.0402669
cyp-13A6	5.75669669	-2.5578793	0.8885838	0.04029789
crls-1	431.114173	0.42076903	0.14622149	0.04039741
del-6	1505.56594	-0.3381331	0.11767434	0.04090463
VF15C11L.2	2.52794248	4.11044735	1.43085752	0.0409511
T26A5.6	13.0583689	-1.2637442	0.43991717	0.0409511
ZK669.2	133.877295	0.75836942	0.26409545	0.04106836
Y105C5A.1270	58.5098106	-1.2509963	0.43589852	0.0412556
T19B10.5	243.284241	-0.5567516	0.19401671	0.04126988
mlt-8	39.0490147	0.91326177	0.31848853	0.04151979
F56H9.9	45.5416297	-1.4240314	0.49685725	0.04167752
stn-2	43.4925522	-0.7521466	0.26257312	0.04185502

T05H4.11	47.0074686	-0.7157276	0.24989825	0.04185869
C07A4.3	12.9754244	-1.1662811	0.40719401	0.04185869
C09G9.1	479.090233	0.60309091	0.21067555	0.04201941
ribo-1	439.001556	1.28354955	0.44855533	0.04211635
Y102A11A.3	58.5545149	1.86013987	0.65005668	0.04211635
K04H4.2	3.2191625	4.45006163	1.55662908	0.04245159
srv-7	23.6289793	-1.0641636	0.37250719	0.0426947
spe-48	59.8599538	1.0821211	0.37894184	0.04270513
cytb-5.2	6024.86678	-0.4946892	0.17319493	0.04270513
ncs-2	982.821655	1.51490931	0.53046446	0.04270513
oxa-1	2.70119275	-2.943041	1.03048777	0.04270513
Y41D4A.7	20.9317613	1.87575425	0.65669169	0.04270513
col-39	88.6749402	-0.6443646	0.2256677	0.04271343
fubl-2	4.74815174	5.06373886	1.77376242	0.042761
unc-30	7.37902448	3.35612945	1.17584064	0.042761
hpo-9	31.5469817	1.26386064	0.44280988	0.042761
utx-1	32.231672	-0.7932147	0.2778855	0.042761
mtm-9	57.1994508	0.70230987	0.24610731	0.04280172
R160.12	2.68606593	4.2413077	1.48651738	0.04283968
oig-4	23.5841691	1.02247167	0.35846028	0.04288964
F54H12.5	23.6366927	-0.9466228	0.33185176	0.04288964
T01D1.3	256.347972	0.6010643	0.21075948	0.04292942
fbxa-182	115.712457	0.86415401	0.30304605	0.04294693
F58E6.13	11.6055179	2.30724686	0.8094977	0.04310017
Y73E7A.3	120.018612	0.96547634	0.33901138	0.04332869
M110.13	4.11963907	-2.4518513	0.86091208	0.04332869
hsp-3	1489.54964	1.50133161	0.52715101	0.04332869
dut-1	21.8070989	1.36892517	0.48094487	0.04345696
T10B9.14	1.69394713	-4.9190657	1.72837323	0.04345696
pqn-75	1117.9136	0.87129718	0.30608754	0.04345696
F10D2.10	32.7745402	0.90589347	0.31831041	0.04345696
nhx-4	161.59661	0.77294843	0.2715254	0.04345696
smg-4	89.4314858	-1.1223688	0.39446135	0.04351395
txt-18	90.462029	-0.7749677	0.27245085	0.0436073
lys-2	26334.6438	0.51802445	0.18213438	0.04361238
bath-38	165.20896	-0.5446055	0.19151416	0.04365338
F26G1.11	2.53365967	-3.3253007	1.17032948	0.0439474
pid-1	18.2615397	1.47570015	0.51946582	0.04399266

F53B3.3	2.52408826	-3.524262	1.24067974	0.04399373
B0563.9	199.329058	-1.1568201	0.4072916	0.0440088
Y48G10A.1	283.020541	0.55746817	0.19657326	0.04455896
egl-9	180.22864	1.00346714	0.35384452	0.04455896
pdi-1	1176.32479	0.75199999	0.26529157	0.04470929
F09C6.14	28.1440965	0.932718	0.32911607	0.04474649
C16B8.t3	84.3365427	0.84468227	0.29805927	0.04474649
Y105C5B.5	4656.26465	-0.5022476	0.17736548	0.04503088
C17H12.8	16953.3856	0.67430561	0.23836069	0.04539482
F13E9.19	4.86261418	-2.1145681	0.74771738	0.04546408
Y57G11C.51	14.5494669	1.30686396	0.46209716	0.04546408
atfs-1	323.09803	0.64932416	0.2296393	0.04549865
F22B7.9	1226.14308	-0.6684041	0.23647582	0.04559126
C35B1.8	6.52461484	-2.3590889	0.83459887	0.04559126
rsp-7	82.6409108	0.65759578	0.23269829	0.04564232
Y50D7A.10	168.177295	0.41024604	0.14524835	0.04579987
Y57G11C.40	94.7141967	0.80880089	0.28634238	0.04579987
eif-2D	90.4641675	-0.8057282	0.285383	0.04593133
pef-1	51.9191622	-0.8595352	0.3045002	0.04598067
fkh-6	15.8366944	1.36968665	0.48544967	0.04608612
rhy-1	425.207683	0.86017276	0.30484363	0.04608612
clec-41	26640.7315	0.95486449	0.3384577	0.04608612
fis-2	1054.22658	0.56973794	0.20194362	0.04608612
bli-6	95.6399224	0.76581241	0.27148302	0.04611062
nlp-47	584.681061	-0.3643959	0.12923253	0.04624775
npp-22	67.2177135	-0.6716034	0.23825109	0.04633408
spp-17	19655.6151	-0.7810769	0.27732997	0.04665571
R102.4	745.612203	-0.3680748	0.13069627	0.04665571
C36B7.5	2.29205742	4.01766631	1.42685203	0.04669955
rom-2	51.9124788	-1.0086211	0.35826558	0.04673781
Y106G6A.4	13.1930854	-1.182516	0.42009063	0.04676381
cct-8	150.402877	0.82212351	0.29234399	0.04713251
vps-34	74.0063804	0.85388926	0.30369301	0.04717499
ifg-1	509.363665	0.87801532	0.31234578	0.04724046
F54B11.8	43.1461852	-0.7303592	0.25991076	0.0473573
F29F11.10	1.76652061	-3.883583	1.38233721	0.04738672
Y7A5A.22	1.76652061	-3.883583	1.38233721	0.04738672
col-111	147.199848	-0.7763417	0.27639834	0.04745316

sri-74	9.10603675	2.1743075	0.77440353	0.04755992
F09C6.12	56.9646934	-0.9137583	0.3254531	0.04755992
imp-2	361.502099	1.13754017	0.40520833	0.04758208
C36B1.14	99.5376205	-0.7380749	0.26306447	0.04770145
sgn-1	63.9803188	-0.6564557	0.23396488	0.04770145
fbxa-28	1.77344394	-3.8680781	1.37842507	0.04770145
pnc-2	12.3076189	1.54662011	0.55118177	0.04770145
W04H10.2	17.7235117	1.1670806	0.41608657	0.04778742
ubxn-4	247.587994	0.6319314	0.22541136	0.04797129
T28A11.25	59.8468606	0.74443493	0.26557308	0.04799065
K12H6.10	1.7604675	-3.8681214	1.38031284	0.04800578
ZK637.12	11.7080725	1.90694286	0.68050959	0.04800578
srd-26	2.93137169	4.33599237	1.54703638	0.04800578
ZK813.1	8190.99561	-0.3875916	0.13831599	0.04800578
Y6B3B.4	10.5609054	2.24957089	0.80289022	0.04803197
C39F7.5	24.6449204	-1.1714013	0.41813616	0.04805536
aat-9	20.4420929	1.1647269	0.41578689	0.04805871
K11G9.5	79.6409616	0.57722588	0.20608816	0.04808696
F53A2.11	2.86876859	-4.6274559	1.6524788	0.04811008
C06B8.3	2.86876859	-4.6274559	1.6524788	0.04811008
F22D6.19	2.5114588	4.13928339	1.47873842	0.04815639
cblc-1	152.291903	-0.6329205	0.22608857	0.04815639
Y56A3A.31	53.2706643	0.92009375	0.32867722	0.04815639
Y40A1A.3	5.21929843	-2.3202946	0.8288392	0.04815639
R11G10.4	4.59383077	-2.6911873	0.96166446	0.04823561
clec-258	16.7766479	1.62070988	0.57931478	0.04833059
srj-32	2.27908098	4.0113308	1.43431954	0.0484435
D2096.13	177.225653	-0.5776525	0.20662832	0.04857361
pdi-2	10010.604	0.53844624	0.19265878	0.0486629
C32D5.11	112.057198	1.2768439	0.45707416	0.04881063
C49C3.11	12.9622842	1.96032044	0.70175903	0.04881063
tag-229	193.821048	0.88321955	0.3162965	0.04894055
ttr-34	998.252788	-0.5249616	0.18805015	0.04902754
clh-3	130.692957	0.58347667	0.20906729	0.04909564
Y54G11A.14	75.1826527	-1.2319109	0.44142554	0.04909564
nrf-5	1539.505	0.56929748	0.2040091	0.04909671
C44E4.5	36.9273002	0.87008946	0.31188237	0.04917718
ncx-3	34.7619104	-0.9438161	0.33833133	0.04917718

Y94H6A.10	1513.85856	0.91344821	0.32754698	0.04927855
Y60A9.1	3.3344319	-3.2647299	1.17107285	0.04939196
T03E6.9	25.1224893	-1.4058659	0.50435731	0.04941815
F14B6.6	52.5755698	-0.6953662	0.24952496	0.0494827
F07F6.2	6.11855464	2.86491786	1.02809786	0.0494827
ZC434.3	2.88307019	4.34038319	1.55847083	0.04951394
unc-43	718.406538	0.80460128	0.28886979	0.04951394
cdr-7	171.036441	-0.6544652	0.23497892	0.04951394
srr-1	24.2414168	-1.0086792	0.36211296	0.04951394
T27A10.2	48.8580197	0.6771022	0.24302795	0.04951394
mig-15	133.075234	1.12348636	0.40333157	0.04951394
F52D10.2	210.589838	-0.5408165	0.1941201	0.04951394
damt-1	20.4256304	-1.3111162	0.47104815	0.04973232
M88.4	2.70495582	4.26825463	1.53375726	0.04977356
K07C5.2	132.191606	-0.7009599	0.25189584	0.04977356
col-58	11.6657698	1.74720805	0.62814219	0.04983469
pno-1	2416.87211	-0.3569927	0.12833667	0.04983469
C29E4.13	27.2206797	-1.005903	0.36158437	0.04983469
C50C3.1	6.50017239	3.16019132	1.13600814	0.04983469

SI.5.8: Table of total differentially transcribed genes with adjusted p-value >0.05, in *C. elegans* strain SS104 cultured with Δ*fim*H, compared to *E. coli* HM605. The base mean value, Log_2 Fold Change, Standard error and adjusted p-value are represented.

Gene name	Mean	Fold Change (log2)	Standard Error	adjusted p-value
pud-3	1985.63317	-2.5355138	0.29179428	5.68E-14
col-166	625.997259	-0.8891748	0.10681233	6.59E-13
rpl-5	25243.5129	-0.7174243	0.09559026	3.19E-10
nspe-1	147.130729	-1.8968904	0.26243403	1.53E-09
F19B2.5	4821.48329	-0.8226089	0.11334154	1.53E-09
C45B2.8	87.4702471	3.08416275	0.45193142	2.29E-08
D1086.9	80.4722616	1.500173	0.22234655	3.36E-08
adah-1	537.141077	0.93155548	0.1471625	4.77E-07
rpl-4	25116.6857	-0.844196	0.13395807	5.09E-07
dpy-4	79.0521027	-1.6875329	0.26863178	5.21E-07
Y47G6A.9	96.0890878	1.09532522	0.17581531	6.61E-07
atg-16.2	423.328494	0.69169757	0.11214944	9.00E-07
nmad-1	1398.50167	0.6855747	0.11411822	2.26E-06
rla-0	46925.5427	-0.751402	0.12767021	4.12E-06
pud-2.1	105.692141	-1.2042581	0.20422475	4.12E-06
Y41G9A.5	27.0531373	1.51104987	0.25859223	4.98E-06
rmd-1	428.51734	-1.1701546	0.20133599	5.66E-06
unc-93	37.6958712	1.45102031	0.25056856	6.06E-06
nspe-2	71.0569737	-1.7023228	0.29599088	7.26E-06
ksr-1	114.283263	0.99182508	0.1736816	8.77E-06
col-138	44.9354445	-1.9834446	0.34901723	9.38E-06
srh-276	4.58330848	-5.7497527	1.01103244	9.38E-06
rpl-7A	23770.6249	-0.7404938	0.13266966	1.62E-05
fbxa-163	118.96529	1.03710319	0.18630866	1.64E-05
fat-3	3937.6483	0.53876835	0.09683429	1.64E-05
rpl-18	26603.2729	-0.840304	0.15201385	1.94E-05
C34F11.8	358.3238	0.68236599	0.12580191	3.36E-05
oac-54	12.5764585	2.87560671	0.53662248	4.66E-05
exos-9	92.4027798	1.13997261	0.21524555	6.14E-05
exos-7	103.911754	1.02106371	0.19264871	6.14E-05
rrn-1.1	42.99106	-3.6915682	0.704159	7.96E-05

rpl-9	17095.2994	-0.8108356	0.15619538	0.00010175
cpin-1	215.456728	0.81062825	0.15649607	0.00010483
asps-1	77.9458575	0.96021496	0.18670949	0.00012401
F48C1.11	47.8653632	2.41112101	0.46994242	0.00012852
F53F10.7	6.8654206	-4.006401	0.78185153	0.00012928
C46H11.2	104.815475	1.13841434	0.22317198	0.00013368
pho-4	401.861254	0.7151875	0.14054107	0.00013368
tba-7	489.985427	-0.6823017	0.13407951	0.00013368
svh-1	7.93158201	3.82069994	0.74905347	0.00013368
T25B9.11	40.9703781	-1.6218679	0.31830808	0.00013368
C39D10.11	220.790146	1.00741056	0.19706105	0.00013368
tfg-1	835.179893	-0.7866504	0.15585824	0.00015874
F13H8.1	43.9076614	1.24676193	0.24691876	0.00015874
gst-29	323.707281	0.62201588	0.12355588	0.00016606
pud-4	8001.94199	-2.0214391	0.40428422	0.00019413
Y22D7AL.10	440.482591	-0.8024088	0.16091103	0.00020364
sgo-1	13.1011556	2.33553533	0.46894566	0.00020596
nep-18	62.0573542	-0.8866345	0.17944205	0.00024705
T28A11.18	9.406446	6.60429389	1.33918311	0.00025416
F13E9.9	14.7330657	5.42124296	1.10756919	0.00030074
T19H5.6	12.7330307	1.97043951	0.40402769	0.00032273
dnj-13	635.608691	-0.6550005	0.13518118	0.00037153
catp-2	15.9734954	2.01974043	0.41728566	0.00037426
Y54G2A.18	2499.52404	-0.6812289	0.14142508	0.00041305
F47B8.10	13.0298216	5.14452369	1.06888318	0.00041367
F40G12.5	39.7459711	3.97155376	0.82939105	0.00045925
rpl-1	28353.3528	-0.8088833	0.16906984	0.00046049
glb-2	26.16502	2.12075774	0.44357587	0.00046049
col-109	31.1491969	-1.4936889	0.31309204	0.00047656
math-38	51.8802588	1.15889181	0.24346872	0.00048752
ZK1248.15	32.1204567	1.47759829	0.31044795	0.00048752
emr-1	118.213205	-0.8910731	0.18763884	0.00050586
math-37	6.85273278	3.6784929	0.77754114	0.00053039
clec-52	132.382186	2.07254738	0.43769805	0.00053039
B0507.9	17.6436495	1.68190429	0.35559339	0.00053039
fbxa-141	15.4253011	2.131421	0.45094394	0.00053097
C16A3.4	359.102542	0.56541308	0.12002176	0.000565
lec-1	6015.8919	-0.8609055	0.18313778	0.00058496

dhs-26	568.268184	1.66851403	0.35620221	0.00062562
gakh-1	55.7535983	0.85941682	0.18401948	0.00066014
sdhd-1	1164.59964	-1.0184361	0.21896053	0.00071399
col-159	439.684062	-1.7191651	0.3700265	0.00072209
dnj-18	47.9893425	1.06233808	0.22925802	0.00075583
rrc-1	44.1230116	1.23843518	0.26801872	0.00079446
F52H2.5	37.3832564	1.41711846	0.30810395	0.00086826
mpc-2	626.950178	-0.9100595	0.19889842	0.00096128
npr-34	20.604057	-2.2285574	0.48776176	0.00097904
F15B9.8	12.6205725	-1.7210365	0.37707339	0.00097904
K09E9.1	331.42737	0.60522025	0.13261759	0.00097904
clec-61	166.426404	1.37324627	0.30200486	0.00103341
sde-2	86.2947554	1.57727479	0.34683191	0.00103341
Y65B4A.6	224.749865	-0.8269292	0.18199495	0.00103761
pud-1.2	105.67918	-1.1213644	0.24717555	0.00105977
C01B10.11	824.959955	-0.6659258	0.14691802	0.00106773
mec-10	19.5817833	-1.3755973	0.30374397	0.00107462
vps-22	369.609091	0.69299376	0.15320977	0.00107868
F10E9.7	35.91307	1.55794889	0.34443911	0.00107868
enu-3.2	23.2780613	-1.6097941	0.35637715	0.0010955
pud-1.1	101.067565	-1.0941158	0.24232302	0.0010955
crld-1	159.080608	0.66657706	0.14843209	0.0012149
R105.1	2.78274513	4.81307799	1.07507627	0.00128217
ugt-24	29.7684982	1.99539667	0.44632691	0.00130607
ZK1058.3	42.2922173	-0.9784238	0.21949998	0.0013743
ran-2	206.509557	0.58034562	0.13042174	0.00140984
clec-57	150.843653	0.84898924	0.19109619	0.00144153
F53G12.9	71.9387114	-0.8560605	0.1944024	0.00171049
pals-26	175.661134	1.30398638	0.29643222	0.00171196
pptr-2	332.377236	0.49807691	0.11320795	0.00171196
clec-34	2.67422338	-4.9464555	1.12902685	0.00183914
atl-1	47.5781579	0.82139352	0.18785537	0.00189496
frpr-14	14.0229331	-1.6984825	0.39062976	0.00209789
Y67D8B.1	2.9184748	4.95421426	1.14182003	0.00209882
C25G4.17	24.0855595	1.89521629	0.43662139	0.00209882
syp-2	13.4885711	1.66958725	0.38437303	0.00209882
col-143	73163.0315	-1.5746711	0.36251332	0.00209882
clec-264	213.955549	1.42277962	0.32802176	0.00209882

C35E7.4	38.0621112	1.16759363	0.27032123	0.00215124
acox-1.4	289.31374	0.92700017	0.21434769	0.00215124
cki-1	107.646034	-0.8384196	0.1940829	0.00215124
F37H8.6	15.0684018	2.28966207	0.529489	0.00215124
madf-11	9.15605017	-2.1153358	0.49010014	0.00215124
srsx-27	12.8652665	-1.7059079	0.39522301	0.00215124
T16G1.6	8.75435376	2.66151962	0.61483599	0.00215124
cest-1.1	358.744564	1.92200942	0.44467329	0.00215124
nhr-62	110.386442	0.71133611	0.16495098	0.00216675
ubl-1	14923.1857	-0.7333862	0.17013032	0.00216675
cyp-14A3	12.4213383	4.02587136	0.9350779	0.00220094
tag-52	38.1338118	-0.9851685	0.22954802	0.00232064
tps-1	614.550918	0.62593637	0.14624808	0.0024269
fbxc-52	79.8462135	0.72750739	0.17005887	0.00242845
polq-1	32.7741442	1.20439297	0.28203128	0.00249155
col-80	33484.4627	-1.699458	0.39837706	0.00250097
T28B11.19	2.96691005	-5.0960914	1.19429962	0.00250097
cyp-32A1	117.390914	0.89857527	0.21109877	0.00256582
fubl-1	275.412093	0.48488787	0.11390107	0.00256582
vnut-1	98.6092808	-0.990115	0.23311202	0.00263261
cyp-35B1	570.110051	1.03131975	0.24274111	0.00263261
chil-17	4.13159421	5.36919505	1.26524682	0.00265666
cpr-5	3224.08333	-0.8997908	0.21223978	0.00268476
T27D12.6	67.1937552	0.8040132	0.18994113	0.00273859
C09G1.5	137.033287	-1.3564129	0.32054299	0.00273859
C02B8.6	80.7138815	0.68464357	0.16231679	0.00288801
scl-25	39.5568058	2.39760262	0.56882169	0.0029037
glr-6	23.0920334	1.24800652	0.29692497	0.00303844
let-391	38.7906954	0.96530868	0.23000325	0.00305449
T23G7.3	1278.9544	0.94771897	0.22571791	0.00305449
col-103	10120.5457	-1.2601242	0.30023218	0.00305449
F17C8.3	75.3425167	1.28111452	0.30546046	0.00307145
C27H6.9	23.3981034	1.92575881	0.45959575	0.0031028
T28A11.3	6.7166746	3.65172033	0.87227193	0.00313097
alg-5	3.84065537	4.23920168	1.01428289	0.00320534
F49C12.7	522.261803	0.3939569	0.09430818	0.00321345
bath-38	222.447509	0.72490042	0.17365464	0.00323284
F52H2.3	53.0356536	0.9648461	0.23133037	0.00326057

nas-27	4.58019661	-3.2887468	0.78948055	0.00331219
F23C8.13	44.9158458	-1.0099804	0.242948	0.00341477
scl-19	38.2445097	5.3695308	1.29378343	0.00349608
asp-1	91165.6643	-0.860225	0.20849215	0.00386083
srw-68	3.07632069	4.92184159	1.19404925	0.00390162
rgs-6	48.1328615	-1.0229273	0.24832732	0.00392156
cpz-2	3673.58531	0.85603011	0.2081124	0.00399783
nhr-38	11.6154696	1.88278803	0.45799828	0.00400701
lys-5	5.53011154	3.79349651	0.92338171	0.00400701
rpl-2	25599.5417	-0.8995513	0.21888205	0.00400701
F28C1.1	53.6013574	0.93619453	0.22818833	0.00407785
fbxa-61	48.6961623	0.84630532	0.20686217	0.00425948
C44F1.1	63.2299554	-0.9032165	0.2212816	0.00440752
C07C7.1	7.64459753	2.26316544	0.55566345	0.00454956
irld-6	24.2329154	2.42903546	0.59674343	0.00456837
T16G12.8	3.40882357	4.06467783	1.00083472	0.00472265
F22D6.9	17.9610457	1.31961867	0.32519343	0.00476107
clec-167	15.9682805	-1.5902219	0.3922416	0.00477929
nhr-152	51.8996827	0.96672789	0.23839382	0.00477929
T10B9.14	2.81523376	4.79383586	1.18521527	0.00494698
wdr-83	47.7152677	1.40179878	0.3468331	0.00498024
mop-25.3	9.0774385	2.15780904	0.53421533	0.00500342
Y47G6A.14	16.8464838	1.33414618	0.33047438	0.00501939
cyp-35A1	11.5267281	2.7209642	0.6743085	0.00502964
F48G7.7	2.19109426	4.52684449	1.12277473	0.00504233
linc-100	2.19109426	4.52684449	1.12277473	0.00504233
C26C6.4	18.523804	1.40640252	0.3496466	0.00512742
T12G3.6	9.79147058	2.13913018	0.53173782	0.00512742
W02F12.4	141.504939	0.62031961	0.15426539	0.00512742
F10C2.7	55.6449658	1.2845765	0.31914301	0.00512742
scav-4	110.843237	-0.9549969	0.23742048	0.00512742
F44G4.1	321.674267	0.88821215	0.22135047	0.00528393
lpd-7	842.647873	0.44444416	0.11080342	0.00528978
mks-3	8.86017648	3.07403177	0.76671049	0.00529886
ZK185.5	294.476336	0.54290208	0.13548633	0.00532133
teg-4	66.542808	0.67479562	0.16858177	0.00535896
mrpl-10	157.760194	0.73237888	0.18303524	0.00535896
F56A8.5	125.776545	0.66382048	0.16583066	0.00535896

nas-10	9.41698146	2.27893325	0.56970502	0.00535896
R10D12.19	4.97082405	2.66243749	0.66611469	0.00540328
Y39G10AR.32	103.154578	0.58114301	0.14562877	0.00548513
col-86	4.30397261	-3.305381	0.82848698	0.00548513
Y102E9.3	2.04374099	4.37785198	1.09731881	0.00548513
Y37E11AL.1	6.03891263	-2.2019803	0.55261177	0.00554087
Y43F8C.11	48.6941426	-0.9382813	0.23539944	0.00554087
alh-8	23687.7332	-0.8118145	0.20410091	0.00564784
ddr-2	26.1466986	1.05690924	0.26564793	0.00564784
T14G8.2	18.6339075	1.59175743	0.40030019	0.00564784
Y44F5A.1	53.2987496	1.16323332	0.29283427	0.00571594
dlhd-1	54.6387324	1.03355825	0.26052093	0.00576942
Y46G5A.20	1065.77375	-0.7045671	0.17763165	0.00576942
abu-10	7.12427369	-2.69105	0.67839635	0.00576942
T05E7.4	124.030095	1.41775653	0.35786962	0.00585679
npr-23	47.4785009	-1.2552837	0.3171462	0.00586928
cup-14	233.738232	-0.646037	0.16328734	0.00586928
Y54G2A.57	136.746315	1.77805372	0.44914367	0.00586928
F26D10.13	2.12414382	4.45895958	1.12703293	0.00586928
pud-2.2	115.399775	-1.1168475	0.2824416	0.00589215
dex-1	9.48880182	1.82588202	0.46197973	0.00591154
T28A11.4	5.17582171	5.75269857	1.45635531	0.00593787
M04C9.2	7.85124961	3.45041364	0.87409454	0.00597483
D2023.4	106.496395	0.91717435	0.23262915	0.00606548
Y119C1B.12	10.4372512	2.45460393	0.62313206	0.00609591
C37A5.3	117.505719	1.5068469	0.38249246	0.00609591
F26A3.1	686.173279	0.79552575	0.20235488	0.00618522
nhr-101	185.071238	0.95633908	0.24330527	0.00618522
F53F4.1	5.67547653	2.47540731	0.62940926	0.00618522
C54D2.2	130.69088	-0.5658473	0.14398269	0.00618522
cnnm-2	130.025804	0.69898915	0.17769053	0.00618522
twk-14	33.708106	1.07738542	0.27430505	0.006215
C41H7.2	19.5000207	-1.4527209	0.370102	0.00622024
T26H5.8	21.9673347	1.60257299	0.40815798	0.00622024
T21B6.15	2.10060781	4.37775518	1.11559236	0.00622024
aldo-1	4296.96469	-0.8494651	0.21657519	0.00623928
col-34	314.602784	-0.8401181	0.21424931	0.00623928
tbb-1	1556.98078	-0.8202611	0.20935284	0.00629243

del-2	5.13405694	3.0733521	0.78523857	0.00637334
lips-17	97.9869746	1.13163688	0.28942829	0.00640854
hlh-3	4.80077251	-2.5828551	0.66067977	0.00640854
H35N09.1	7.6108427	-2.0393227	0.52165426	0.00640854
F32A11.3	2.42850081	-4.838374	1.23888199	0.00648402
bath-23	1.95339894	4.3405569	1.11244326	0.00649536
rps-3	33556.2259	-0.7530935	0.19299194	0.00649536
cpr-2	30.4823855	1.89652986	0.48580465	0.00649536
klu-2	153.936384	0.66960182	0.17170293	0.00652222
sri-39	13.0868551	2.19355616	0.56274505	0.00653282
D1022.3	22.6412931	1.55212256	0.39847066	0.00653282
F26C11.4	4.97808577	3.0488972	0.78248729	0.00653282
C05B5.1	14.2926747	-1.6511702	0.42378841	0.00653282
Y48G8AL.12	10.3512851	-2.7396857	0.70415203	0.00659854
H41C03.2	9.02922734	2.17053052	0.55787546	0.00659854
mev-1	1809.28847	-0.7326924	0.18840325	0.00661824
C54G4.5	79.3539432	0.70376839	0.18128925	0.0067814
ceh-45	11.531491	-2.3264072	0.59948541	0.0067905
K09C8.8	6.98083022	2.15174267	0.55463425	0.00679295
anr-32	13.5724614	1.73473745	0.44748549	0.00684689
F23C8.5	3254.95044	-0.7485281	0.19338242	0.00688418
cox-4	8893.54029	-0.8682053	0.22427327	0.00688418
T22F7.3	4.57528522	-2.8549907	0.73723169	0.00688418
T24C4.5	4.79358311	-3.0575241	0.78999488	0.00688418
hsp-12.6	535.409564	3.37842998	0.87245141	0.00688418
F48E8.8	41.383226	0.92757735	0.23985057	0.00694104
maa-1	131.612397	0.83061536	0.21513308	0.00709573
21ur-6778	6.51458697	-2.7683585	0.71719818	0.00709573
fndc-1	4.87041348	4.55264073	1.18005215	0.00709597
dhs-23	23.8977309	2.11335092	0.54764745	0.00709597
T01B7.5	268.315859	0.67060251	0.17389662	0.00711627
hda-2	48.2055118	0.73173202	0.18986937	0.00715971
cln-3.2	93.0803662	0.60884395	0.15809991	0.00721543
C55B7.11	16.4354786	1.38271667	0.35917956	0.007227
mut-14	89.9843848	0.90491616	0.23547318	0.00739775
F16C3.2	160.94308	1.54532576	0.40247983	0.00747352
C44B11.4	386.219973	-0.5816972	0.15165421	0.00756154
txt-11	51.8007192	-1.1438044	0.29835464	0.00759307

T28A11.13	4.47109569	2.93037004	0.76482364	0.00763416
dpyd-1	482.041956	-0.5552946	0.14501779	0.00767585
vrk-1	32.8515992	1.25820617	0.32877115	0.00771366
prx-6	125.78281	0.64041641	0.16750866	0.00780419
fbxa-143	21.3160717	1.43872784	0.37663972	0.00787871
dsbn-1	373.635121	0.72344727	0.18963581	0.0079787
sqst-2	256.303741	0.55772912	0.14617817	0.0079787
Y38A10A.7	111.298101	0.86536217	0.22703276	0.00805609
tag-63	14.0773888	1.38420755	0.36343409	0.00806152
ugt-66	340.648971	1.51865429	0.39868349	0.00806152
K08F11.1	26.4928501	-0.9497893	0.24930404	0.00806152
K06A4.15	31.3068366	1.77549617	0.46638177	0.00808816
xpa-1	79.6044691	1.08269732	0.28493887	0.00829637
F43C11.7	280.980558	1.01730765	0.26856251	0.00866779
slc-17.9	23.8995864	1.68856305	0.44590365	0.00867584
col-96	417.055881	-0.8986819	0.23782803	0.00892747
nlp-30	98.8319506	1.13951298	0.30162526	0.00892747
K03H6.1	21.155237	-1.1035531	0.29220305	0.00893978
F14F9.4	95.8515073	0.69187394	0.18332038	0.00899888
Y47D3A.14	78.0412637	-1.0525402	0.27904448	0.00904537
col-142	1534.42117	-1.3913264	0.36958693	0.00928418
T28B8.1	2620.23563	-0.5074976	0.1348438	0.00928631
F10E7.5	484.460139	1.00559556	0.26739888	0.00932969
W02D7.11	19.2950486	2.33190807	0.62002344	0.00932969
Y47D3A.20	71.9669033	-0.70253	0.18691406	0.00937464
dhhc-12	4.83345047	3.07962426	0.8201681	0.00948094
him-10	21.1362333	1.39810036	0.37315439	0.00976042
hal-3	23.9663981	1.10074138	0.29442145	0.01004311
B0334.6	6.39174716	2.74348332	0.73421121	0.01005736
spe-26	13.2337109	1.53680039	0.41128797	0.01005736
T20D3.6	691.640345	-0.5299764	0.14187648	0.01006574
ptr-22	91.3365728	2.73227542	0.73163479	0.01007097
bcas-2	61.563582	2.06036898	0.55196916	0.01010524
F49D11.2	5.09401825	3.88400903	1.04142688	0.01020169
Y69A2AR.31	45.5557116	-1.1976399	0.32166534	0.01042249
C11D2.3	2.86446958	3.83071304	1.03024516	0.01055885
H12D21.11	2.86446958	3.83071304	1.03024516	0.01055885
T27E4.5	4.06246957	-2.7167005	0.73122412	0.01064795

C30H6.9	86.1581993	-0.6850625	0.18460287	0.01079288
EEED8.2	81.9823822	1.15783722	0.31225902	0.01088033
nlp-81	85.4970688	-1.0008808	0.26997786	0.01088033
VW02B12L.2	20.3058233	1.29720991	0.35011554	0.01093783
B0361.9	626.100363	0.46860893	0.12654858	0.01099205
C54F6.18	98.4229009	2.84785252	0.76972715	0.01109377
capg-1	93.6393116	-0.798431	0.21612883	0.01128427
Y110A2AR.1	33.8551291	-0.957267	0.25915326	0.01128427
prx-14	199.138302	0.69873486	0.18949113	0.01149738
T22F3.12	10.8831866	-1.5260536	0.41385577	0.01149738
F14H12.2	4.66523217	2.99240635	0.81247876	0.01165732
T05A12.3	328.680259	0.44183524	0.12000074	0.01167078
C26D10.4	36.7792787	1.095984	0.29799795	0.01175146
F52F10.2	5.71426567	2.23541725	0.60782744	0.01175146
ugt-1	61.7576394	1.01412747	0.2756517	0.01175146
C30F12.3	438.697148	2.02607878	0.55154406	0.01185007
W04H10.5	1.80520347	4.18429596	1.13916023	0.01185007
srt-14	3.15573693	4.96011015	1.35033593	0.01185007
sel-13	74.951981	1.28495031	0.35002307	0.01190988
sqv-3	42.4355781	-0.7921438	0.2160102	0.01205411
syp-5	20.0840339	1.43370564	0.39114524	0.01209888
col-69	9.54611138	-2.3354098	0.63823488	0.01231958
adm-4	65.3551932	-0.9812152	0.26809449	0.01231958
C05E4.12	2.45133899	4.66730532	1.27639874	0.01240395
nath-10	84.4709206	0.55555491	0.15214906	0.01254234
F10E9.1	24.3267031	1.44227195	0.3949818	0.01254234
rack-1	26173.0945	-0.7286839	0.19948915	0.01254234
chil-11	6.05424923	1.96753268	0.53923067	0.01263137
C50F2.4	287.001997	-0.7086888	0.19436809	0.01272363
F59B10.3	10.5556974	-1.8434036	0.50636609	0.01296692
cyp-35A4	4.69129979	4.61053841	1.26705992	0.01297281
col-43	407.781712	-1.647231	0.45263125	0.01297281
syx-6	84.030747	0.73129218	0.20102396	0.01298043
T07G12.5	31.7408869	1.36891187	0.37641765	0.01299922
C12D12.1	2192.10028	-0.9676237	0.2662332	0.01307049
C44H4.4	129.001562	0.6104417	0.16815478	0.0132482
E02D9.3	75.8436032	0.91769232	0.25287067	0.01326247
F46F2.3	5978.17604	-1.3637406	0.3758504	0.01326247

sre-9	3.05303301	3.92630665	1.08254937	0.0133003
rps-11	28239.601	-0.8375243	0.23106131	0.01337543
F08H9.4	6.77721658	-1.9968395	0.551163	0.01342531
magu-2	177.1923	0.71758145	0.19814413	0.01346064
npr-32	14.5496728	-2.3430674	0.64729577	0.01351131
F56D5.6	429.342169	0.74714038	0.20651016	0.01356798
ech-3	222.777325	1.38515233	0.38388929	0.01404567
gpd-1	47.9181175	-0.9901434	0.27452519	0.01408367
lido-13	172.999057	-0.6239607	0.17307011	0.01412413
C45B2.3	50.3528123	1.54078411	0.42766605	0.01418407
E02H4.4	31.5794176	1.34424367	0.37312719	0.01418407
F23D12.3	181.144139	0.85789728	0.23857301	0.01451169
col-63	53.8484314	-1.3732844	0.38262743	0.01481368
sec-61.B	3198.35312	-0.8686529	0.2420051	0.01481368
rps-22	16362.0166	-0.7448489	0.20777106	0.01496814
E02H9.7	136.126708	-1.0561385	0.29471576	0.01496814
col-101	66596.3699	-1.3197579	0.36847675	0.01496814
ilys-3	547.278089	2.15116928	0.60024278	0.01496814
T05E11.2	104.164364	0.92848001	0.25915029	0.01496814
F11A5.13	16.6807278	1.18556999	0.33105379	0.01496814
T27A10.2	52.3189894	-0.7517384	0.20982999	0.01496814
F20B6.4	15.5556012	-1.3234625	0.36969798	0.01500369
M03F4.6	53.7695778	-0.8950221	0.25029784	0.01519357
T16G1.5	22.7453998	1.50810484	0.42202984	0.01528928
aph-1	75.3331225	0.91391848	0.25617455	0.01559379
fut-1	378.535987	0.55778036	0.15642736	0.01565861
col-48	45.4127991	-0.9130559	0.25632025	0.0158298
rnp-8	65.2258845	-0.8142388	0.22881329	0.01599126
K08D12.4	16.5010934	-1.3813466	0.38832868	0.01599126
mrpl-48	217.61316	0.76692934	0.2156345	0.01599126
M03B6.4	33.6385643	0.99393058	0.27935055	0.01599126
map-2	759.210115	-0.6159924	0.17335239	0.01607018
lys-3	420.456496	1.19759155	0.33704818	0.01607018
npr-18	22.2959085	1.10842519	0.31183874	0.01607018
F13C5.1	28.741548	1.94007294	0.54652121	0.01623008
bub-1	22.6222549	-1.163719	0.32796882	0.01628482
glb-12	8.62029914	1.67286156	0.47192392	0.01645769
mec-5	438.546854	-0.9097374	0.25677707	0.01652991

F41F3.3	120.539315	-1.2909478	0.36472855	0.01670156
hira-1	26.2500576	-0.979333	0.27691846	0.01684328
serp-1.1	5101.4599	-0.6567582	0.18614078	0.01733099
srg-10	7.74635622	-2.2527039	0.63892002	0.01744821
ZC204.12	2091.6758	0.78101017	0.22155864	0.01744991
klc-1	43.5496395	0.98124093	0.27842535	0.01745787
swt-3	1524.26764	0.86959353	0.24700192	0.01756139
cpt-4	114.560544	1.75592214	0.49868942	0.01756139
T21E8.7	1.86197466	-4.4350868	1.25949227	0.01756139
ram-2	156.095194	-0.9379527	0.26666181	0.01759494
B0464.6	50.0764983	1.0036649	0.28540471	0.01759494
W05B10.6	21.7675805	1.21949385	0.3467693	0.01759494
F53F1.4	186.903719	-1.4865862	0.42263401	0.01759494
C25F9.16	32.0572132	2.1434994	0.60944983	0.01759494
nhr-22	67.9931179	0.63569041	0.18091204	0.0176919
linc-107	5.64563085	2.22189206	0.63221849	0.0176919
M04G7.1	469.026015	-0.8799129	0.25057053	0.01779135
K08H2.10	2.09976562	4.40619958	1.25725093	0.01821951
cyp-35A5	40.0438777	1.58554139	0.45331675	0.01864287
R10E8.3	18.3846449	-1.1521485	0.3294537	0.01864287
R06C1.6	189.16759	-0.5743464	0.16451313	0.01884456
clx-1	1975.83723	1.23008526	0.35230826	0.01884456
T24A6.7	34.6923435	2.27254911	0.6509466	0.01884456
rpl-28	14249.3421	-0.7100544	0.20340148	0.01884456
arrd-28	3.32163192	3.18862229	0.91329316	0.01884456
Y102A11A.7	12.3500743	-1.3952727	0.39992617	0.01894384
R02F2.1	10980.3711	-0.6826103	0.19576293	0.01901055
F22B3.8	2.28657659	-4.7157711	1.3525613	0.01901055
pax-3	2.3667627	-3.7152223	1.0659165	0.01903974
Y17D7B.3	16.8344224	3.09369936	0.88811945	0.01913819
abch-1	6.30103536	2.03149261	0.58336336	0.01916128
ftn-1	920.463219	1.36194485	0.39116352	0.01916128
H17B01.5	61.5223863	-1.0380068	0.29825352	0.01922109
F59B2.8	1.82775288	4.16835683	1.19807307	0.0192503
T16G1.7	29.7285169	2.3720778	0.68226057	0.01937771
C29E4.13	33.7064673	0.84431633	0.2429543	0.0193975
rpm-1	48.0199857	0.74755957	0.21508401	0.0193975
acc-1	18.5823574	1.34242423	0.38645004	0.01940964

far-4	148.621784	1.33329212	0.38379258	0.01940964
F44E5.5	134.684348	-1.6813994	0.48457169	0.0195137
rpc-2	128.769373	0.49234402	0.14184948	0.0195137
B0024.3	33.3399636	1.50497094	0.43374628	0.0195137
slcf-2	72.6318501	0.97052477	0.27961479	0.0195137
C26B9.3	84.0072554	1.16813308	0.33707755	0.01977577
Y105E8A.21	47.7801023	0.79107996	0.22851776	0.02000056
cest-6	31.4904205	1.64810732	0.47625539	0.0200445
atrn-1	268.746288	-0.6145871	0.17765842	0.0200845
pid-5	13.4294692	1.43917555	0.41647685	0.02031982
oaz-1	12145.7109	-0.7374181	0.21343798	0.02032006
F26G1.5	26.3484341	-0.974293	0.2820704	0.02033794
dna-2	20.5527063	1.53684443	0.44515817	0.02041987
ZK792.1	237.606293	0.77836838	0.22566335	0.02060792
F53F8.3	3.54975731	3.31761009	0.96239442	0.02071237
psr-1	53.6741489	0.77576756	0.22537103	0.02102531
his-17	2.39840292	-3.7649276	1.09384334	0.02102531
T14B4.8	24.1914464	-0.9854567	0.28646744	0.02107463
M199.2	27.7073162	1.06827651	0.31050252	0.02107463
ZK1240.9	3.70668052	3.3898159	0.98560245	0.0210799
ham-3	60.979582	0.74203473	0.21590842	0.02120457
F37C4.5	11397.1354	-0.6682544	0.19445877	0.02120457
dhs-2	308.321548	0.76009037	0.22138627	0.02135475
phat-4	8.88363339	-1.7529196	0.51050226	0.02135475
F27C1.3	2.66996382	3.79065895	1.10503353	0.02154002
ZK512.7	4302.82929	-0.7490076	0.21842335	0.02158609
W09C5.1	1349.69967	0.41164185	0.12006996	0.02160079
H06H21.11	79.5269213	0.57662933	0.16823107	0.02161095
ins-18	180.974373	-0.573096	0.16728465	0.02169966
dph-1	85.5042117	0.83824843	0.24501043	0.02196989
Y60C6A.3	156.519847	1.73596108	0.50740016	0.02196989
arrd-8	10.1282411	2.80375704	0.82046222	0.02219458
C23H5.11	17.691552	-1.0326958	0.30219821	0.02219458
ZK1290.13	356.791031	0.41374796	0.12110523	0.02221363
F52C9.5	3.85131726	-3.729061	1.09241932	0.02225241
dpy-20	1.66877601	4.06641816	1.19147957	0.02225241
nhr-103	73.5919388	1.0614659	0.31079969	0.02225241
nlp-31	1251.90112	1.34480145	0.39400762	0.02225241

asp-18	42.6418058	5.7821489	1.69331973	0.02225241
mel-26	380.631954	0.67976612	0.19942409	0.0225534
clec-199	80.4828112	-0.9572378	0.28118232	0.02277301
ZK380.t2	116.932565	1.80832919	0.53125962	0.02277301
hlh-13	116.016359	0.87163158	0.25609184	0.02277301
aqp-8	413.759599	-0.6113785	0.17959807	0.02277301
Y71A12C.2	34.7934175	-0.8528019	0.25062136	0.02279301
ZK688.9	73.659618	0.83538163	0.24570415	0.02297738
klf-1	95.9435391	-0.9586654	0.28226993	0.02321994
C04B4.1	2.73966572	3.69176236	1.08712924	0.02321994
skpt-1	15.2790161	1.23349052	0.36364919	0.02350199
gtf-2H1	75.1403349	0.90187761	0.26603107	0.02355942
cfz-2	19.6426135	-1.2535533	0.36974333	0.02355942
ZC155.2	5.60244129	2.15016256	0.63452071	0.02359833
col-95	73026.5929	-1.2469852	0.36800677	0.02359833
oac-29	7.19773018	1.78764679	0.52774805	0.02364854
nlp-18	829.69346	-0.8209121	0.24268996	0.02401024
ZC581.3	285.649898	0.61050667	0.18061622	0.02417102
F35C5.12	19.9362133	-1.478646	0.43765665	0.02420663
spp-9	31.3515141	5.18984441	1.53598274	0.02420663
Y73B6BL.37	3.84226579	3.44631466	1.0203449	0.02423915
ztf-8	52.0926967	0.79189991	0.23464132	0.02441733
F17A9.4	200.434705	0.98688418	0.29246087	0.02441733
F44E5.4	91.0377201	-1.6145899	0.47908718	0.02469406
F57H12.6	385.608033	1.64713533	0.4886927	0.02469406
Y105C5B.8	12.6246095	1.4056485	0.41716015	0.02469406
rab-30	87.0662315	0.82787375	0.24576491	0.02473228
B0228.7	172.535994	0.93944473	0.27935801	0.025116
ZC477.3	115.100353	0.83414499	0.24803613	0.025116
Y62H9A.16	4.97273332	2.57428092	0.76556739	0.025116
ZK470.14	23.4089548	1.51382548	0.45035614	0.02517126
C45G9.10	3.09387582	3.00598997	0.89545618	0.02548571
F48E3.2	64.0287138	0.62929019	0.18746636	0.02548571
C35B1.4	2599.38428	-0.6570858	0.19581261	0.02553705
tbc-14	252.65529	0.35625606	0.10625496	0.0257477
F53F10.1	106.844971	1.06386772	0.31778214	0.02616761
F11A5.9	2177.1418	-0.5004853	0.14961217	0.02635712
ZK742.4	26.7530445	0.92218157	0.27573153	0.02637203

M70.4	85.892869	0.56978968	0.17049243	0.02655307
rps-10	24106.8018	-0.7563537	0.22671949	0.02707211
col-181	56060.6918	-1.1905992	0.3569713	0.02709445
T10E10.3	8.11012945	2.37809466	0.71325483	0.02714988
gnrr-7	8.67040113	-1.5431808	0.46302526	0.02722381
acs-17	846.2926	0.69646118	0.20912092	0.02740375
cbn-1	21.8856795	1.365727	0.41028416	0.02745906
ZK697.8	2.38823675	3.50456766	1.0527602	0.02745906
T24A11.7	2.6904299	4.72317721	1.42064882	0.02775114
ptd-2	7.94387927	1.5504345	0.46634276	0.02775114
F55H2.7	61.8107425	0.93193282	0.28042045	0.02777113
Y113G7B.15	1.88461971	4.18919591	1.26049346	0.02777113
F54H5.3	9.65290422	1.68331406	0.50707361	0.02804759
aldo-2	30554.2752	-0.7782553	0.23445232	0.02804759
R07B7.2	13.8806898	1.39729312	0.42124957	0.02823741
Y55H10A.2	1.62451937	4.09043375	1.23451648	0.02849303
arrd-24	23.5195837	-1.1296626	0.34089237	0.02849303
pigo-1	63.9737144	0.83052497	0.25140782	0.02935024
clec-246	9.00106197	-2.1982412	0.66524219	0.02935024
C24H10.2	130.23675	0.53527124	0.16203512	0.02935024
W01A11.7	25.8008321	2.14163958	0.64884137	0.02957723
ttm-2	247.736284	0.60350301	0.18302293	0.02986779
rps-8	53220.7983	-0.7073919	0.21466244	0.02996867
comt-3	785.761083	-0.7287964	0.2211214	0.02996867
cdh-3	5.57930882	2.47815746	0.75229614	0.03004281
C49F5.6	4.60022065	2.56489657	0.77916216	0.03022624
fbxa-206	6.33269308	3.57288133	1.08619576	0.03043798
oac-42	1.56666596	3.96289359	1.20507891	0.03047184
acds-10	353.949958	0.64391442	0.1958443	0.03047805
str-116	1.39894665	-4.0416574	1.23029983	0.03072193
sru-40	6.53120133	-1.9351458	0.58941278	0.03087265
Y48B6A.1	205.824263	-0.7013014	0.21367063	0.03092426
ZK177.14	18.9539661	1.13109491	0.34490087	0.03115976
fbxa-52	17.9185744	1.25047705	0.38138503	0.03117717
ZC443.1	106.32895	1.11706004	0.3407546	0.03118184
zig-6	177.399105	1.1835568	0.36118532	0.03126881
W02D9.7	1715.00175	-0.6683661	0.20425112	0.03167539
eif-2Bepsilon	111.264248	0.44905583	0.1372587	0.03167539

F54C4.4	52.0158799	1.00601508	0.30745656	0.03167539
ZC443.3	7.27909117	2.95130294	0.90263822	0.03183525
T24C4.3	16.9962708	1.33206832	0.40750782	0.03186767
pals-3	3.34249695	3.19512347	0.97880938	0.03225256
ipla-7	3615.27881	0.60116656	0.1841605	0.03225256
M03F8.3	98.6102473	0.77872101	0.23859241	0.03225256
T05H4.10	109.693855	0.60959414	0.18683676	0.03225687
F08B12.4	19062.1372	-0.4038362	0.12375355	0.03225687
nlp-68	145.470872	-0.6301159	0.19338093	0.03268509
F32H5.1	791.063149	0.83836704	0.25733298	0.03268509
pals-2	2.33826266	3.47528469	1.06717803	0.03278418
ZK666.11	21.1796132	1.77019228	0.544035	0.03297412
F08G2.8	116.483737	-0.6125337	0.18827547	0.03297412
dhc-4	13.5665699	-1.838405	0.56509064	0.03297412
pho-11	9418.15985	0.44839372	0.13791436	0.03315071
W03G9.9	3.58323173	-3.5208022	1.083791	0.03330096
F38B7.2	131.581442	0.5442169	0.16753456	0.03330096
C11G10.1	336.320161	0.97303504	0.29953264	0.03330096
ptp-4	27.484903	0.96457072	0.29714079	0.03349909
E02H1.1	146.488621	0.58666995	0.18081565	0.03354583
ceh-23	9.38023575	1.75633853	0.54133638	0.03354583
T23B12.11	348.777525	0.67589546	0.20833893	0.03354583
ule-1	36281.7306	-0.6075432	0.18741489	0.03376083
T14B4.5	128.764556	0.69610876	0.21475885	0.03376083
klp-7	238.548576	-0.8198606	0.2531421	0.03400983
T05H4.15	134.840255	0.68665129	0.21213106	0.03416494
F08F8.9	201.245111	0.64279933	0.19874172	0.03441205
C28G1.10	109.60336	0.45459937	0.14066505	0.03465888
T04D3.8	3.73630754	4.27587615	1.32431725	0.03496694
ZK688.7	102.476123	0.89688312	0.27785481	0.03499444
rrbs-1	210.648723	0.8371609	0.25938496	0.03499444
F02E11.2	144.365906	-0.8912015	0.27680409	0.03587286
cyn-17	1.78181187	4.21556072	1.30944252	0.03587286
Y11D7A.7	9.2212685	2.34578139	0.72915781	0.03609003
npp-2	89.1386458	0.66352222	0.2065247	0.03657087
Y48A6B.9	82.7001004	0.93514984	0.29120264	0.03669183
C50E3.6	56.3711568	0.65217567	0.20315447	0.03676595
srh-78	2.99939678	3.81898705	1.18993162	0.03680653

K03H6.5	25.3468759	-1.360724	0.42415883	0.036916
Y6B3B.9	32.2147452	0.78380289	0.24437619	0.0369393
lin-56	22.5060721	1.37026539	0.4273937	0.03703661
K02E2.7	9.26738272	1.58622696	0.49492098	0.03711105
pfn-2	3723.79545	-0.639992	0.19978523	0.03725355
cogc-5	344.535177	0.5957985	0.18608247	0.03725864
cyp-13A5	714.531502	0.56601793	0.17673332	0.03725864
fkh-5	1.49887332	3.88007205	1.21201529	0.03725864
spe-49	1.49887332	3.88007205	1.21201529	0.03725864
W06B4.1	6.97766307	-1.8573055	0.5803513	0.03729523
acs-7	96.1931038	1.52242371	0.47574989	0.03729523
C01G5.5	38.7565128	0.71216532	0.22264836	0.03735189
ddo-2	346.79657	0.54855785	0.17148128	0.03735189
ZK262.2	83.273452	-0.5271482	0.16484919	0.03739724
pir-1	183.670599	1.11641873	0.34933928	0.03758698
nhr-232	153.087818	0.68543301	0.21467229	0.03789746
tkr-3	23.9171887	0.91060923	0.28533914	0.03799541
srd-17	1.95325454	4.25489627	1.33332772	0.03799541
his-40	302.135261	-0.8315539	0.26062819	0.03801033
cyp-13B1	64.5301622	1.62199812	0.50863918	0.03816608
his-61	25.0648653	-1.0749386	0.33743786	0.03840741
frk-1	6.55211075	2.05434924	0.64484201	0.03840741
ugt-33	37.9436444	2.20088625	0.69074441	0.03840741
F55C12.4	66.1961659	0.89433634	0.2808719	0.03847457
mans-4	20.0312513	1.23884075	0.38907114	0.03847457
fbxa-15	27.2811247	0.90245279	0.28360797	0.03867415
F35A5.2	511.582639	-0.4185717	0.13155943	0.03867415
R03H10.6	20.2865359	1.50802017	0.4744153	0.03875144
clhm-1	53.7855911	0.80564435	0.25358063	0.03875144
F45E12.6	31.5795339	2.06376595	0.64996754	0.03875144
ctsa-1.2	12060.284	-0.9766416	0.30746318	0.03875144
rei-1	350.662755	1.22861599	0.38678425	0.03875144
M01A8.1	75.6999785	-0.686102	0.21608948	0.03875144
clp-6	3.29718495	-2.4234778	0.76278421	0.03875144
gst-41	118.464566	0.4760309	0.14994425	0.03875144
C24B5.4	140.768251	0.69701213	0.21920229	0.03875144
T13F3.7	11.8780916	-1.4721172	0.46349219	0.03875144
ZK228.13	2.83257479	-4.019278	1.26575303	0.03875144

K02E10.7	14.1212023	1.69098292	0.53174799	0.03875144
cah-4	968.518524	-1.7019658	0.53609299	0.03875144
F45D3.4	7126.46262	1.22109404	0.38477989	0.03885187
EGAP9.3	54.6730239	1.04642149	0.32984881	0.03891131
sdf-9	1.6578502	4.0063837	1.26301334	0.03891131
smf-3	52.9131667	1.16773519	0.36828522	0.03902784
srab-13	3.11459023	2.89392948	0.91335296	0.03920447
phy-3	63.9742483	-1.0661816	0.33647676	0.03920447
atp-4	6848.06628	-0.8357059	0.26381052	0.03922671
F20C5.6	25.6884239	1.35412233	0.42776212	0.03946387
grl-16	20.9579459	-1.9211836	0.60727675	0.03954078
ech-8	276.937455	1.15144408	0.36391536	0.03954078
F23H12.3	430.547852	0.61229122	0.19350077	0.03954078
cdk-5	212.936658	-0.7066092	0.22342083	0.03960174
emb-27	38.3647458	1.31662246	0.41639549	0.03963682
R13H4.6	19.3177478	1.12120843	0.35519753	0.04030917
K02C4.5	169.101367	0.55460925	0.17587291	0.04062294
rpt-6	555.437217	-0.7786266	0.24691881	0.04062294
col-73	40.2947384	-1.3886184	0.44079539	0.04066438
F19C7.1	12067.2898	-0.6735073	0.213641	0.04066438
T21H3.1	42406.6999	-0.7375989	0.23401737	0.04066438
tofu-1	43.8656174	0.79855029	0.25343635	0.04066438
hpx-2	1.40768908	3.85173656	1.22253583	0.04066438
C15H11.11	72.6809586	0.75054518	0.23822079	0.04066438
efhd-1	263.453823	0.69161898	0.21961875	0.04074925
R03H10.1	264.951011	0.71100383	0.22588601	0.04078388
pbs-6	665.192173	-0.5153521	0.16375615	0.04078388
faah-6	118.694781	-0.625974	0.19890314	0.04078388
R04F11.3	42.7625804	1.0333463	0.32827364	0.04078388
F49E12.10	27.5039804	1.94952676	0.62029212	0.04123601
Y37A1A.3	51.7941105	1.18342372	0.37652177	0.04123601
ipla-4	2.56983967	-4.9042882	1.56129884	0.04138089
rtel-1	49.6672303	1.05575066	0.33617242	0.04138089
Y105E8A.11	204.415035	-0.6791556	0.21624352	0.04138089
K09E3.7	6.36706179	-2.1296651	0.67831773	0.04143955
rps-1	31986.0764	-0.8130324	0.25954074	0.04238067
rpl-43	32849.6007	-0.7898598	0.25221358	0.04243996
F49E12.12	9.84994038	1.39869972	0.44672574	0.04247568

R11G10.4	5.54762813	2.14140123	0.68449427	0.04278053
skr-12	915.67794	0.81841781	0.26182664	0.04303232
M6.4	22.8084923	1.40334102	0.4488992	0.04303232
twk-7	220.263669	0.82070717	0.26269194	0.04319698
glb-23	13.4196421	1.31292277	0.42032944	0.04322713
ugt-59	12.8373419	1.55734272	0.49907405	0.04361584
slc-25A18.1	806.531554	-0.4075336	0.13062193	0.04362477
C53D5.1	101.538707	0.56248939	0.18032634	0.0436553
F17B5.1	90.0941866	0.7049848	0.22609704	0.04375527
nlp-29	658.980827	0.58644688	0.18810227	0.04375527
srsx-16	2.96701829	2.92810494	0.94065586	0.04440007
C54F6.3	2.35189992	4.62311526	1.4853479	0.04440007
pqn-94	547.493257	-0.6154825	0.19778215	0.04441592
asm-3	171.886586	0.6071922	0.19520848	0.04449666
tra-3	89.9040363	0.92204529	0.29642022	0.04449666
col-85	35.5607913	-1.4074724	0.45268208	0.0445595
T05E11.8	31.3889049	1.09383918	0.3518116	0.0445595
str-261	4.68462659	2.60001891	0.83654164	0.0445905
pho-6	70.7397847	1.22144279	0.39293765	0.0445905
folt-2	790.740963	-0.8944712	0.28791187	0.04471959
C36B1.11	29.9197286	0.99602472	0.32068371	0.04476476
T06E4.9	2.44793336	-4.8675145	1.56735541	0.04476476
nlf-1	40.8129801	-0.7579991	0.24420207	0.04493592
ZK682.7	4.25403573	-3.086134	0.99482092	0.04513918
ins-8	5.51859262	3.8620235	1.24558547	0.04532028
F41E7.2	123.754455	0.91199909	0.29428701	0.04549054
sti-1	303.788947	-0.7171398	0.23145505	0.04551655
W05F2.6	43.6220448	-0.6673202	0.21548136	0.04554484
T15B7.1	619.061852	0.65328706	0.21094926	0.04554484
mlc-2	18680.5112	-0.825664	0.26653888	0.04554484
unc-64	563.135623	0.77909963	0.2517625	0.04579796
trap-3	1939.4375	-0.6435326	0.20797	0.04579796
K03B4.4	174.681924	-0.6582556	0.21276924	0.04582225
ngp-1	411.577837	0.59412281	0.19220587	0.04611627
thn-5	46.5095539	0.81457322	0.26356014	0.04611627
nlp-71	266.881623	-0.4661005	0.15081557	0.04611627
flp-8	776.59254	-0.5383365	0.17430148	0.04635851
C02B4.8	16.4879528	-2.3520801	0.76166413	0.04636118

dhs-20	322.309322	1.26639754	0.41029143	0.04646655
vap-1	82.6290753	-0.9867431	0.31969345	0.04646655
hda-3	61.985582	0.5917487	0.19180206	0.04650026
W04A8.6	14.192182	1.17525951	0.38110163	0.04650026
C14C6.13	3.11647058	-2.7136526	0.87992464	0.04650026
flp-11	1489.055	-0.6565919	0.21291082	0.04650026
C03B1.6	7.69950005	2.97865745	0.96581949	0.04650026
tbb-4	50.3093932	-0.8505683	0.27582748	0.04650026
W03A5.1	2.91220513	2.85859136	0.92769195	0.04679192
gst-23	24.0547972	0.97501403	0.31649149	0.04679357
F31E9.3	46.6119534	1.17291782	0.38075267	0.04679357
ppm-1.A	685.655877	0.51897752	0.1685021	0.04681631
T05H4.11	76.8942082	1.26927381	0.4121702	0.04682031
K10H10.13	3.20357716	4.04935399	1.31538681	0.04691579
Y43D4A.2	2.30358914	-3.7039016	1.20662121	0.04825109
sqt-2	19.792564	-1.2408314	0.404313	0.04828807
bli-6	98.7841494	-0.9478836	0.30896759	0.04839325
Y116A8C.25	23.1501502	1.23045604	0.40130923	0.04854592
fbxa-90	61.7775921	1.43049648	0.46652494	0.04854592
cpn-3	13254.0389	-0.5803099	0.18933061	0.04864568
C25H3.7	274.29719	0.73234545	0.2390129	0.04874188
W02H3.3	8.73058472	1.38294397	0.45144983	0.04878652
lect-2	99.9621828	0.57890846	0.18901035	0.04879817
ZK643.5	106.991489	0.77420581	0.2528522	0.04888335
C39E9.8	3484.21716	0.86836727	0.28372626	0.04902769
R11D1.2	3.79115643	2.71115361	0.88605351	0.04908452
fbxa-155	3.60816917	5.23253363	1.71112516	0.04931987
chil-18	6.14870412	3.56500022	1.16612031	0.04932343
eef-1A.1	50888.3723	-0.8200321	0.26824056	0.04932343
C15C6.2	4.41708514	-2.2485679	0.73605399	0.04942504
ant-1.3	3.69542544	2.49057411	0.81521014	0.04942504
arrd-18	131.026284	-0.5726462	0.18738257	0.04942504
srr-4	260.88758	0.78039756	0.25550415	0.04942504
hum-10	3.50026155	-4.3035391	1.40893897	0.04942504
C56A3.5	116.672485	0.71602635	0.23448881	0.04948429
exc-6	53.0935788	-1.2941659	0.42390907	0.04951877
R03H10.7	25.1131121	0.94505701	0.30966972	0.04956326
R05D3.8	14.0698979	1.29997119	0.42596282	0.04956326

ptr-12	265.943917	-0.665194	0.21801856	0.04959728
fipr-19	2.38703845	-3.6372711	1.19240741	0.04959728
F18G5.6	1735.02343	0.27628306	0.09057332	0.04959728
col-118	531.492577	-0.8453203	0.27731283	0.04987643

SI.5.9: Table of total differentially transcribed genes with adjusted p-value >0.05, in *C. elegans* strain SS104 cultured with Δ*dsb*A, compared to *E. coli* HM605. The base mean value, Log_2 Fold Change, Standard error and adjusted p-value are represented.

Gene name	Mean	Fold Change (log2)	Standard Error	adjusted p-value
H39E23.3	1205.94103	1.4229348	0.09748981	4.82E-44
D1086.9	127.157064	2.48308256	0.17143486	1.23E-43
pqn-60	267.980785	-1.1142485	0.09413927	1.36E-28
ftn-1	815.235038	1.29927264	0.11294049	5.08E-27
dhs-2	329.948106	1.10725246	0.09852239	8.50E-26
dhs-26	580.56175	1.87333473	0.16849566	2.76E-25
clx-1	1460.74015	0.76881488	0.07308956	1.63E-22
cyp-35A3	33.11717	2.75903188	0.27106352	4.98E-21
C01G10.4	74.2422261	-1.9143471	0.19249014	4.74E-20
hsp-17	851.086285	-0.7502195	0.07909577	3.91E-18
K08D8.4	475.174121	-1.1684642	0.12748759	7.24E-17
E02H4.7	498.997178	1.72630906	0.19073826	1.91E-16
F25A2.1	273.991424	-0.899093	0.10045181	4.39E-16
gst-29	316.460572	0.77903325	0.0875292	6.42E-16
ugt-8	371.169215	0.65720129	0.07753168	2.49E-14
cyp-35C1	454.108436	1.24081225	0.14666938	2.70E-14
F49C12.7	555.394685	0.75670892	0.09209958	1.99E-13
dod-22	1101.82094	-0.8697588	0.10635834	2.59E-13
clec-61	193.663447	1.83178727	0.23034676	1.55E-12
clec-17	51.4420454	-1.4651218	0.18472999	1.75E-12
fat-6	38925.3304	0.55905618	0.07074812	2.11E-12
F53C11.1	815.201774	-0.6179046	0.07828913	2.11E-12
scl-20	738.224063	1.93783403	0.24558783	2.11E-12
ttr-29	290.305983	-0.9999236	0.12820385	4.18E-12
cyp-35A5	43.7337872	1.87409649	0.24094516	4.75E-12
fbxa-163	113.753833	1.12662238	0.14540539	5.78E-12
try-9	294.594849	0.79252815	0.10247464	6.23E-12
col-43	382.577738	-1.4890475	0.19327171	7.57E-12
dhs-23	23.8183492	2.22881584	0.29053891	9.47E-12
C50B6.7	690.419445	0.51466837	0.06718308	9.94E-12
F55G11.4	11574.3975	-1.3983638	0.1845331	1.83E-11

F22E5.1	84.8432652	-1.4604207	0.19344788	2.20E-11
VZK822L.2	109.54532	-1.0305585	0.13743847	3.16E-11
ugt-66	252.125761	1.08455773	0.14586261	4.94E-11
dod-21	75.0767294	-1.2135415	0.16421452	6.58E-11
C25F9.11	75.0495798	-1.0035997	0.13579429	6.58E-11
C54C8.12	188.370322	1.13285914	0.15338653	6.61E-11
pbo-1	554.49522	-0.4571003	0.0634383	2.46E-10
cyp-13A11	25.049396	1.98996507	0.28267606	7.96E-10
dlhd-1	74.4573112	1.81194155	0.25887713	1.04E-09
clec-218	63.0336167	1.16727499	0.16771205	1.34E-09
M02E1.4	471.837892	1.04588074	0.15060374	1.46E-09
slc-17.9	27.3915018	2.09150814	0.30738412	3.81E-09
folt-2	752.640563	-0.736628	0.10899405	5.11E-09
C28C12.4	236.392932	-0.9978266	0.14893045	7.47E-09
clec-57	132.819281	0.74563064	0.11152891	8.07E-09
gale-1	1294.01622	-1.0318208	0.15494517	9.44E-09
asp-13	3302.51363	0.41251575	0.06250915	1.39E-08
gst-5	1731.78481	0.72957441	0.11097156	1.61E-08
ZK899.2	1608.92647	0.43018837	0.06557916	1.74E-08
dct-17	1815.16566	-0.8291824	0.12688498	2.01E-08
F19B2.5	4365.06984	-0.8624195	0.13320464	2.95E-08
cyp-33E1	169.784043	0.73069428	0.11313041	3.21E-08
clec-52	99.3322392	1.70746752	0.2675407	5.22E-08
C01G10.17	103.2677	-1.477289	0.2322379	5.87E-08
poml-3	384.455165	0.50941568	0.08133204	1.08E-07
Y53G8B.2	1739.38986	1.06718426	0.17084109	1.17E-07
B0024.4	3569.14051	-1.3782542	0.22058932	1.17E-07
sec-61.B	3075.34583	-0.6709602	0.10945328	2.40E-07
nep-22	271.150785	-0.6885516	0.11291559	2.89E-07
hil-1	885.856076	0.78232974	0.12845546	2.98E-07
F12E12.11	128.830306	1.02049558	0.1677	3.03E-07
F44E5.5	120.516347	-1.8186548	0.29963926	3.23E-07
asm-3	216.202316	1.30444365	0.21484159	3.23E-07
nspa-5	38.3481445	1.33660433	0.2229343	5.03E-07
F49H6.13	135.286027	-1.3628973	0.2277022	5.19E-07
F19C6.5	90.2193811	0.81313985	0.13584511	5.19E-07
clec-42	25.6706918	-1.5725185	0.26382917	5.97E-07
ZK593.3	332.061325	0.64781633	0.10880056	6.11E-07

col-50	621.268156	0.96000842	0.16154116	6.46E-07
cdr-3	19.370901	2.80058279	0.47239406	6.94E-07
Y51H4A.5	64.8674981	1.59662556	0.2715153	9.17E-07
T15B7.1	521.646296	0.44954231	0.07659308	9.67E-07
spp-12	168.098472	1.61041561	0.27497057	1.03E-06
clec-197	77.8431745	0.94379102	0.16180322	1.17E-06
EEED8.2	72.9975604	1.08008919	0.18612433	1.38E-06
skr-3	1242.05547	-0.4435451	0.07679318	1.60E-06
clec-71	22.50531	1.58789458	0.27544269	1.67E-06
gst-3	105.079501	0.89122646	0.15458586	1.67E-06
fat-3	3624.32295	0.55424548	0.09715026	2.35E-06
Y26D4A.3	35.2579376	-1.2952814	0.22749701	2.48E-06
cyp-34A9	760.576116	0.75061713	0.13189745	2.49E-06
mop-25.2	66.8183654	-0.8866763	0.15598447	2.55E-06
W02D7.11	14.4446896	1.96863996	0.35165673	4.16E-06
C17H11.5	24.003258	1.49894385	0.26824628	4.36E-06
cyp-14A3	7.85464944	3.45058607	0.6202076	4.96E-06
E04D5.2	16.6596425	-1.7535906	0.31543707	5.02E-06
F13B6.2	196.425118	-0.7877859	0.14224281	5.60E-06
ZK550.6	1940.13806	0.44771596	0.08128794	6.59E-06
R07E3.2	348.45205	1.09186124	0.19979143	8.30E-06
K10D11.5	309.772892	-0.963853	0.17659307	8.53E-06
F09F9.3	100.190277	-0.942537	0.17364508	9.99E-06
F49E12.12	13.2439261	2.14108104	0.39459841	1.00E-05
ZK596.1	206.457471	-0.5487795	0.10122074	1.01E-05
hrg-2	46.5796667	-0.9130864	0.1685746	1.03E-05
ttr-44	987.420941	0.72437637	0.1339615	1.07E-05
cth-1	396.195984	-0.5413076	0.10028625	1.12E-05
T14B4.5	114.804461	0.62095886	0.1153028	1.19E-05
dhs-20	238.542491	0.8118221	0.15091433	1.22E-05
Y54G2A.7	83.9928988	0.76081679	0.14149454	1.22E-05
T27C5.8	168.977146	-1.3091192	0.24395533	1.28E-05
ifb-2	615.48677	-0.5704968	0.10639189	1.29E-05
C05B5.5	31.0316598	-1.3243368	0.24689747	1.29E-05
F22B5.4	205.219796	0.80558706	0.15037204	1.31E-05
F17B5.1	97.9790876	1.09426561	0.20536139	1.52E-05
stg-2	18.5531923	-1.5001484	0.28205872	1.59E-05
Y65B4A.6	204.311733	-0.8454759	0.16030162	2.01E-05

F23B2.10	7.39954428	-4.4521996	0.84748513	2.23E-05
clec-86	996.148994	0.73513942	0.14097512	2.72E-05
C32H11.9	73.9821443	-1.3767863	0.26482957	2.94E-05
cdf-1	179.323283	-0.5736484	0.11090941	3.36E-05
spp-2	10948.6456	0.78961755	0.15374895	4.05E-05
B0563.10	13.537478	-1.7514887	0.3418749	4.29E-05
gck-1	271.326799	-0.5353537	0.10462013	4.39E-05
T19H5.6	16.4975507	2.5164455	0.49234161	4.49E-05
F23F1.2	201.248868	0.9229324	0.18348205	6.82E-05
pho-11	9359.19128	0.64920652	0.12917455	6.91E-05
chil-15	4.49369629	4.62647667	0.92534789	7.85E-05
F09C6.1	7.52770933	-3.0589077	0.61223516	7.92E-05
nspe-1	162.802383	-0.9081631	0.1820894	8.22E-05
ptr-22	36.3535384	1.21766018	0.24473993	8.68E-05
cyp-33C9	354.495661	0.51807985	0.10423884	8.85E-05
acr-18	66.500762	-0.8619827	0.17411783	9.70E-05
prx-2	213.526341	0.56274275	0.113731	9.75E-05
K11G9.5	122.386588	0.64412818	0.13033208	9.97E-05
rlbp-1	134.990618	-0.5692975	0.11526972	0.0001006
nhr-13	69.9736914	-0.8220997	0.16810572	0.00012781
ugt-1	54.6107528	0.9207382	0.18865076	0.00013323
clec-222	142.881965	-0.5603312	0.11554391	0.00015474
aat-1	328.332308	0.40202637	0.08303427	0.00015971
mtss-1	117.294188	0.72037942	0.14948091	0.00017744
gst-38	328.095358	-0.6074936	0.12650803	0.00019192
lips-11	106.199074	-0.7993075	0.16675624	0.00019603
his-11	13.741103	1.87960908	0.39202949	0.00019603
Y73F4A.3	436.369183	-0.4388216	0.09151589	0.00019603
sma-1	900.297097	-0.4177202	0.08731627	0.00020379
R11G10.4	8.48919167	3.02762057	0.6341468	0.00021227
btb-18	13.7965996	-1.7296275	0.36246864	0.00021339
rme-8	223.592798	-0.4707265	0.09881222	0.0002188
wdr-83	34.8571948	0.91974212	0.19305335	0.0002188
T22B7.7	14544.5448	0.88763138	0.18646225	0.00022102
pck-2	20511.8899	0.24719011	0.05200616	0.00022753
catp-5	84.6808511	-0.620442	0.13089806	0.00024117
F59G1.8	14.6852436	-1.4460537	0.3055746	0.00024698
C32D5.10	80.7862057	-1.0208772	0.21572467	0.00024698

sre-15	2.88792606	5.00198316	1.05777441	0.00024951
spp-23	2267.3343	0.76983272	0.16302259	0.00025591
cpz-2	2736.20494	0.36503546	0.07746157	0.00026669
ast-1	26.7477316	-1.151005	0.24444132	0.00026983
C11G10.1	272.489146	0.70562258	0.14992967	0.00027115
ascc-1	143.194977	0.58171266	0.12368503	0.00027189
F10C1.8	27.8487617	-1.1355395	0.24144506	0.00027189
wdr-46	60.3152754	0.96950385	0.20629438	0.00027476
cyp-35B1	468.436675	0.79089972	0.1693148	0.00031363
cest-1.1	222.286623	1.16943481	0.25096254	0.00032934
gss-1	319.203529	-0.3303204	0.07099296	0.00033725
T05B4.13	2.53238054	-4.7655497	1.02434906	0.00033725
T16G1.6	7.03833662	2.39589231	0.51527415	0.00033925
F37B12.1	242.859296	-0.5353441	0.11587927	0.00038954
Y51B9A.8	122.745956	0.86347346	0.18699607	0.00039131
tsp-10	105.614753	0.58016917	0.12588453	0.00040582
pmt-1	8390.52187	0.31319419	0.06801212	0.00041068
K04A8.19	19.1351554	1.52196943	0.33119894	0.0004275
cyp-35A1	9.23943438	2.46000613	0.53635855	0.00044327
Y47G6A.9	76.4477267	0.77405161	0.16899257	0.00045365
F56D6.8	19580.4629	0.67753081	0.14874807	0.00050618
pepm-1	6.01956782	2.78359168	0.6110617	0.00050618
F48D6.4	7561.45543	0.39808959	0.08760877	0.00053002
ctsa-4.2	1089.72028	-0.2956035	0.0651526	0.00053754
C14B9.3	96.5874295	0.62930975	0.13872198	0.00053754
C39E9.8	2541.25714	0.32554	0.07172119	0.00053754
spp-6	98.4405643	0.65922285	0.1453308	0.00053754
poml-2	229.160281	0.9176364	0.202481	0.00053857
taap-1	952.434104	0.31906323	0.07039245	0.00053857
mtl-1	10702.8261	0.84727804	0.18687896	0.00053857
C55A1.6	22.7189321	1.43841726	0.31813706	0.000563
ugt-14	131.736102	0.65262555	0.14494248	0.00060816
F41E6.5	345.187486	0.53856919	0.11961241	0.00060816
srh-32	3.60280345	4.26113359	0.95324917	0.00070438
calm-1	38.0429087	-1.2216336	0.27403877	0.00074164
F12A10.8	7.71125484	2.78113206	0.62472996	0.00075795
T28A11.18	3.64193162	5.34603564	1.20112797	0.00075795
pid-5	12.4003536	1.50682342	0.3386534	0.0007587

twk-16	93.7343148	-0.7667469	0.17308294	0.00082621
C04C3.14	8.61814474	-2.1430422	0.48458801	0.00084638
F31B9.4	27.3271662	0.94814447	0.21436377	0.00084638
stdh-1	3947.31118	0.6502911	0.14709634	0.00084791
C54F6.6	10.3214351	1.92540194	0.43606021	0.00086016
T26H5.8	18.2565691	1.3866841	0.3139925	0.00086016
fmo-1	115.296843	0.99169922	0.22489062	0.00087869
col-33	3.35021022	4.21356818	0.95609971	0.00088487
F35E8.13	51.8023046	-0.7941625	0.1805113	0.00091134
T22F3.11	34.2922782	0.98634266	0.22455091	0.0009315
dpyd-1	461.40321	-0.3918097	0.08919151	0.0009315
C43D7.7	37.9039769	-0.8632796	0.19670171	0.00094279
vha-15	1504.80952	-0.2792716	0.06366368	0.0009471
Y71F9AM.8	6.08755777	-2.7466696	0.62730321	0.00097815
W09D10.4	124.311845	0.65646398	0.14999808	0.00098242
srbc-71	11.2414352	2.27960593	0.52171991	0.0010097
vmo-1	7.54453258	3.92894365	0.89953806	0.00101237
srh-195	6.88169882	2.11133575	0.4843438	0.00104758
arrd-7	153.303463	-0.5347937	0.12308469	0.00111238
R03H10.4	11.918329	1.72114936	0.39673331	0.00114077
F02A9.1	32.0029428	1.02211096	0.23651513	0.00122494
T03G6.1	4.22924724	4.51808231	1.04743888	0.00126445
C01G5.5	39.2879064	0.93980726	0.21795788	0.00126734
F21C10.11	845.770032	0.70905513	0.16467068	0.00129577
gst-6	602.071067	0.64211033	0.14953472	0.00135234
T19D12.4	633.047516	-0.7212585	0.16805751	0.00135234
cku-70	104.632843	-0.5290537	0.12325668	0.00135234
fmo-2	45.1626802	0.94518043	0.22006563	0.00135234
Y26G10.7	83.8693642	1.00294459	0.2337248	0.00135234
C14E2.7	2.00754955	4.47391661	1.04651373	0.00144682
F31B12.3	12.2225931	1.74957595	0.41067342	0.00153885
abu-10	6.09351266	-3.5961184	0.84483009	0.00155686
egrh-2	4.13449013	3.58324339	0.84457361	0.00164924
ceh-23	9.27789455	1.875086	0.44228135	0.0016602
clec-72	41.8647503	-0.7890825	0.18618857	0.0016602
F57F4.4	2811.43084	-0.8280353	0.19536271	0.0016602
slc-9B.2	129.318561	0.45535845	0.10748561	0.00166464
ZK666.11	16.0014548	1.40131772	0.33109682	0.00168769

Y43C5A.4	30.7227506	1.61749565	0.38261692	0.00171705
ptb-1	66.7217876	-0.7184045	0.1700315	0.00172712
F48C1.11	29.3419963	1.67285728	0.39662467	0.00177674
ilys-2	217.787105	-0.6977639	0.16551328	0.00178441
cyp-35A4	4.28740628	4.59982712	1.09209976	0.00180704
pcp-3	724.676421	-0.3745221	0.08894905	0.00181017
otpl-1	12.8873821	-1.6045904	0.38241021	0.00192177
jac-1	170.745092	-0.3908423	0.09325435	0.00195475
F35F10.5	210.506735	0.77690058	0.18564983	0.00199638
C49G7.12	251.754865	-0.796756	0.19041177	0.00199638
VF15C11L.2	2.0293807	-4.4444857	1.06507836	0.00209054
btb-17	355.106594	0.43763975	0.10501064	0.00213095
pcbd-1	3356.89243	0.41146991	0.09890036	0.00218915
akt-1	565.79962	0.31370272	0.07547436	0.00221867
gpx-7	22.7441512	1.13322803	0.27330373	0.00230805
F13B12.4	14.0449657	2.21515291	0.53624553	0.00245945
T16G1.7	17.7753947	1.61865805	0.39196369	0.0024624
F44A6.5	53.3096635	0.654766	0.15920235	0.00263787
set-22	1.87418226	4.3655583	1.06284572	0.00267749
pqn-36	74.5732428	-0.766228	0.18653866	0.00267749
gnrr-3	22.0024154	-1.0020863	0.24416146	0.00270394
F49H6.5	11.629161	-1.4254864	0.34748867	0.00270439
ptrn-1	175.602623	-0.5306295	0.12934084	0.00270439
M6.4	17.8569327	1.09863436	0.26787788	0.00270505
pdfr-1	77.0615889	-0.8633917	0.21066662	0.00272769
gpdh-2	2632.75607	0.24039553	0.05871369	0.00276409
C44C10.3	8.49011504	-1.9100175	0.46779953	0.00289142
T24C4.4	1223.10294	-0.4891139	0.11985241	0.00290488
nhr-50	87.7508274	-0.8261668	0.20252342	0.0029133
pqn-98	4.80832628	-3.1445835	0.77131763	0.00293263
mans-2	730.048016	-0.2500868	0.06159272	0.00313621
F19C7.2	180.774702	-0.3897537	0.09609509	0.00318341
dhs-30	659.164815	0.30082592	0.0742001	0.00319353
nit-1	442.980348	0.58532702	0.14463413	0.00327034
F08H9.4	6.13331067	-2.3118342	0.57126679	0.00327034
mom-4	36.3271317	-1.0067884	0.24928132	0.00337205
lec-4	4392.74484	0.27456232	0.06801491	0.00338727
C04F12.16	85.4359089	0.64449493	0.15975818	0.00341184

nas-27	4.15067257	-3.5475125	0.88057598	0.00346681
R05D8.9	6.98912129	2.22963302	0.55336081	0.00346681
clk-1	142.959681	0.48425233	0.1204078	0.00354829
H40L08.3	18.9489946	-1.6513553	0.4106456	0.00354829
nlp-42	683.310529	-0.5514801	0.13720291	0.0035637
grl-2	8.58421009	-1.9672278	0.48976264	0.00359196
cdt-1	2.01779124	-4.4756765	1.11723	0.00372957
srh-182	2.01779124	-4.4756765	1.11723	0.00372957
C49C3.9	2124.93705	-0.9251067	0.23103248	0.00374436
R09E12.9	109.510571	0.8345666	0.20886361	0.00386652
cutl-3	55.5936621	1.06406342	0.26719782	0.00407679
F21D5.1	105.518057	-0.5425161	0.13651707	0.00420646
C53D5.1	91.068667	0.51210543	0.12912764	0.00427412
math-45	68.2567583	0.70156405	0.17696891	0.00427412
F41G3.21	111.740757	-0.5605714	0.14134249	0.00427412
ZK688.7	88.8817616	0.77667882	0.19592818	0.00427412
glb-23	12.9989075	1.43543197	0.36203643	0.00427412
CD4.11	8.78921667	-2.0334127	0.512878	0.00427412
srh-276	4.58487421	-3.1631689	0.79777063	0.00427412
dlc-3	82.9042508	0.58318839	0.14720053	0.0042989
eri-5	21.8895925	1.15690127	0.29208916	0.004303
lbp-8	162.938976	0.53624359	0.13550865	0.00435129
kbrl-1	111.801493	-0.5417988	0.13696309	0.00436248
F08G2.5	865.751219	0.25261853	0.06388032	0.00436971
F40G12.5	10.1282886	1.81089522	0.45814927	0.00438957
M04C9.2	5.62381418	2.98669286	0.75594364	0.00440508
F52G2.3	34.7453541	-1.1414282	0.28904114	0.00442522
linc-57	5.23964747	2.2325213	0.56568802	0.00445528
T03F6.9	47.4572106	0.97286193	0.24670813	0.00449926
K04C2.3	538.926186	0.41323742	0.10499832	0.00461724
nlf-1	37.0097718	-0.7572114	0.19240535	0.00461724
T28F2.1	3.09918962	5.08923435	1.29367708	0.0046175
T06G6.3	5.61154164	2.64627749	0.67269628	0.0046175
K09E9.1	273.14315	0.34913297	0.08889234	0.00472282
fbxa-106	3.66313634	-3.3173112	0.8456058	0.00479744
F09C6.11	5.69513261	-2.0262876	0.5175636	0.00494147
rrc-1	33.5163292	0.83453653	0.21340394	0.00501651
srg-69	5.1563883	-2.4689258	0.63291153	0.00519562

dpf-6	416.685727	0.58352569	0.14962057	0.00519562
scl-3	172.493952	-0.834232	0.21392356	0.00519562
coa-7	81.2976446	-0.6662099	0.17089754	0.00520774
ZK105.1	2111.62365	-0.4920927	0.1262637	0.00521103
F33H12.7	1737.82231	-1.0154193	0.26088949	0.00526598
spd-3	20.0591579	-1.5022537	0.38584707	0.00526598
catp-6	151.499297	-0.4808294	0.12355577	0.00526598
F14F9.6	25.3033955	-1.2441299	0.31965609	0.00526598
C45B2.8	44.8368317	2.09811711	0.53967975	0.00533359
pnp-1	1230.39099	0.34919842	0.0899383	0.00542818
elt-2	158.49177	-0.4926896	0.12704236	0.00551142
kgb-1	391.537225	-0.3386286	0.08738041	0.00555748
B0281.3	372.69076	-0.500793	0.12946226	0.00570292
F44E5.4	85.9304529	-1.4548227	0.37638097	0.00575401
vrk-1	30.0271036	1.2431376	0.3219486	0.00583032
C24H10.1	51.0474901	0.86763599	0.22508794	0.00597167
mpz-5	4.91570107	-2.315443	0.6022227	0.00618567
lec-7	107.840206	-0.5898858	0.15343754	0.00618567
ZC239.4	3.81826126	4.36277145	1.13716564	0.00634865
hsp-16.11	31.4117629	-0.8640386	0.22517838	0.00634865
B0416.2	9.98044408	-2.857032	0.74494316	0.00636216
T27E4.7	1339.65523	0.45915419	0.11987332	0.00647003
grd-13	195.670562	-0.4168888	0.10892861	0.00653299
C44F1.1	59.512314	-0.8119388	0.21229255	0.00653941
adah-1	412.269689	0.52221935	0.13656821	0.00653941
T01C3.11	440.078225	0.72364791	0.18913957	0.00653941
F14H3.12	529.336938	-0.4414701	0.1154269	0.00653941
hsp-70	140.30082	-0.6240691	0.16344166	0.0066683
M6.11	4.60564464	3.1303013	0.82189052	0.00691239
Y54F10BM.3	1.76210155	4.26756174	1.12229076	0.00706362
C39B10.1	35.8488956	0.82114726	0.21600299	0.0070703
C46F9.5	8.72207451	1.76498285	0.46497166	0.00721165
Y48G8AL.13	1666.18204	0.25351942	0.06683837	0.00727348
W04A4.2	332.933239	-0.4830945	0.12755697	0.00742098
nath-10	77.3531241	0.55232394	0.1459498	0.00743698
Y102E9.3	3.00839549	5.04431813	1.33282772	0.00743698
K09C8.7	145.943112	0.61899211	0.16355119	0.00743698
K06G5.1	23471.4639	-0.2352147	0.06216425	0.00743698

C30G12.2	1489.78883	1.27451762	0.3369244	0.00744355
F35E8.10	264.722962	-0.6296706	0.16649924	0.00745068
swt-2	2.54525182	3.79603489	1.00473765	0.00751722
F53F1.4	184.848611	-1.0790041	0.28558678	0.00751722
C03B1.6	4.81936724	2.36908259	0.62740471	0.0075595
cpr-1	5696.70884	1.26919068	0.3362817	0.00759109
srxa-12	2.82897369	3.93459128	1.04268951	0.00759109
F02E11.3	2.441626	4.74027697	1.25709118	0.0076158
linc-158	4.88421363	3.94052014	1.04508862	0.0076158
egrh-1	146.317091	-0.5952256	0.15782008	0.0076158
hrg-3	19.924753	-1.1869628	0.31615456	0.0081001
K06A9.1	92.2030201	-0.5480996	0.14610663	0.00817429
gly-2	85.5427707	-0.6666126	0.17788576	0.00828011
T28A11.19	184.914928	0.55342459	0.14777885	0.00829047
R07B7.2	12.9273559	1.46104708	0.39009051	0.00829047
abf-4	4.43079716	-3.652669	0.97502956	0.00829047
H23N18.6	9.77599985	1.75154851	0.46790214	0.00831789
C09B7.2	470.48542	0.29575593	0.0790354	0.00833865
Y67A10A.2	6.50478995	2.75991003	0.73830519	0.0084451
Y106G6A.4	16.2447065	1.17281959	0.31393312	0.00847411
B0464.6	41.8134444	0.75914616	0.20317569	0.00847411
col-51	22.0093087	1.93192001	0.51738281	0.00851325
K08H2.10	2.32954529	4.66350497	1.24929961	0.00852762
gst-23	21.4282512	0.90968254	0.24400057	0.00864071
cyp-13B1	44.1290212	1.03155995	0.27669317	0.00864071
ttr-36	3503.51791	0.49612367	0.13312237	0.00866299
T16G12.8	3.62103423	4.28186549	1.15053451	0.00881871
C31A11.13	7.28243212	-2.1172266	0.57083527	0.00924501
clec-68	31.4246125	1.42835889	0.38524819	0.00926942
clec-73	2.58352569	3.77475408	1.01984595	0.00947128
linc-55	18.528049	-1.0230688	0.27644665	0.00947128
T06E6.1	62.1352108	1.16780158	0.31594729	0.00961784
gpd-4	10.7062237	1.37939823	0.37373424	0.00979527
K09C8.8	5.61598837	2.00300307	0.54311436	0.00987908
far-3	20644.3069	0.43076111	0.11710171	0.0102256
B0252.5	10.14973	-1.783028	0.48483195	0.0102341
F32H2.6	14.5296691	-1.8633311	0.50755576	0.01041112
ugt-52	72.6899551	0.82076326	0.22356328	0.01041112

C14A11.5	2.63074503	-4.8193651	1.31275324	0.01041112
F47G4.5	12.6997068	-1.4227466	0.38785728	0.01049979
K07F5.12	43.5350858	0.80535974	0.21962516	0.01049979
cat-4	1893.04705	0.54918628	0.1497428	0.01049979
C02B4.8	17.0913593	-1.4599676	0.39826136	0.010518
fbxa-164	33.8649785	1.32440829	0.36178766	0.01069008
F41C3.7	156.208091	0.96947373	0.26503963	0.01069008
lin-56	19.0799513	1.16778679	0.319267	0.01069008
R166.3	116.014674	-0.402839	0.11013562	0.01069008
T07G12.5	27.6166834	1.25582437	0.34314493	0.01069008
chup-1	112.15951	0.98831592	0.27011495	0.01069008
F42A10.7	120.845174	1.49405007	0.40873082	0.01073145
hrg-7	5806.63516	-0.7955886	0.21762586	0.01073145
K08D12.4	15.0905101	-1.3637111	0.37379506	0.01100189
unc-83	242.187045	-0.5036499	0.1381503	0.01108591
Y67A10A.11	2.00738877	-4.4668157	1.22775429	0.01138289
bnc-1	7.26456719	1.77073186	0.48800949	0.01178984
ZK858.7	54.949556	0.64612707	0.17838997	0.01196677
ubc-25	415.013363	0.46844378	0.12928969	0.01196677
T03F6.3	1697.56212	0.36841842	0.10169902	0.01196677
Y57G11C.46	58.8869791	-0.7836253	0.21626489	0.01196677
Y37H2A.14	1852.33816	-0.558566	0.15429133	0.01201931
C25F9.14	134.052406	-0.5082014	0.14045827	0.01205325
pes-8	37.5483175	-0.7940018	0.2194181	0.01205325
acox-1.6	156.178015	0.48503852	0.1341019	0.01208005
C33F10.8	1.5861611	4.11148207	1.13731827	0.01210036
C06E1.1	43.2197988	-0.8930589	0.24707265	0.01210036
srh-83	7.83213361	2.01653704	0.55774788	0.01210036
F10C1.t1	10.6050744	1.91881873	0.53101923	0.01212142
Y44F5A.1	45.7526048	1.0109319	0.27993389	0.01219157
srg-34	9.04643919	2.03443674	0.56374623	0.0122812
sodh-1	599.162377	0.65272317	0.1812071	0.01257094
acox-1.4	243.200503	0.73242178	0.20350481	0.0126255
pho-5	304.035512	-0.3177137	0.08825336	0.0126255
gcy-6	6.26295815	2.58337088	0.71769993	0.0126255
ZK1127.5	54.5182528	0.56134344	0.15605979	0.01266391
W07A12.8	67.3093864	0.60575778	0.16838799	0.01266391
ZK1240.9	3.93954863	3.51595383	0.97872314	0.01282649

gst-2	3.93954863	3.51595383	0.97872314	0.01282649
lonp-1	107.549198	-0.7050568	0.19663381	0.013001
F14B6.6	62.2947675	0.72031381	0.20093921	0.013001
C34F11.8	294.674802	0.41983106	0.1170487	0.013001
act-5	4166.10337	-0.4917416	0.13718664	0.013001
linc-94	1.41880088	-3.964697	1.10552443	0.013001
acr-3	38.1393054	0.78003753	0.2174584	0.013001
mfsd-10	158.176818	-0.523305	0.1459632	0.013001
R07B7.10	291.768235	0.27462416	0.07676321	0.01331074
R10D12.19	4.41683616	2.52233712	0.70513935	0.01331074
21ur-15001	1.46738964	-3.9933925	1.11750882	0.01346312
cyp-25A1	406.430932	0.43963612	0.12310669	0.01352547
glb-2	14.7838331	1.22349068	0.34261564	0.01352547
pgp-12	17.8515678	-1.0075337	0.28242807	0.01368193
shpk-1	16.7844202	-1.6652614	0.46714842	0.0137848
ZK697.8	2.26152995	3.64882926	1.02374312	0.0137848
nhx-6	21.1805012	-1.1895572	0.3344393	0.01414115
K06A4.10	32.91652	0.74261395	0.20881792	0.01414115
K09F6.3	1.53678333	-4.0392482	1.13654929	0.01423315
T24E12.12	2.23756178	-4.5811119	1.29049084	0.01440121
F08F8.7	715.586853	0.34621462	0.09753492	0.01440121
K03H6.5	24.3237875	-1.0753184	0.30310083	0.01440671
F35E12.2	32.2345765	-0.8851373	0.24948175	0.01440671
prx-3	145.157742	0.62605908	0.17641553	0.01440671
nlp-24	715.112153	-0.4281848	0.1209062	0.01471921
mfb-1	506.315922	0.50532095	0.14292676	0.01482115
cri-1	75.4231306	1.04204462	0.29467303	0.01482115
pde-12	41.375855	-0.8619244	0.24379583	0.01482115
daao-1	131.716911	0.55746224	0.15761742	0.01482115
R13A1.17	6.68908638	2.18933699	0.61863902	0.01482115
fem-3	3.81853139	2.81944097	0.79737936	0.01482115
C30F2.3	56.2969948	-0.6228218	0.17605667	0.01482115
ZC487.2	2.08907084	4.50926184	1.27583761	0.01484841
ugt-27	71.6761893	0.95705275	0.27097157	0.0149389
T01B7.8	3.07703418	-3.1438362	0.89021188	0.0149389
T07A5.9	7.22716903	1.82689103	0.51766411	0.01504441
cnep-1	198.231417	-0.484341	0.13742884	0.01528548
acox-1.2	136.952679	0.61417444	0.17436561	0.01529692

lgc-20	11.5669109	-1.1618698	0.32975509	0.01529692
mrps-31	6.24583474	2.50141503	0.7100883	0.01529692
clec-169	154.678218	0.59991288	0.17057266	0.01557026
enri-1	32.4927915	-0.7779041	0.2212214	0.01557377
K05F1.10	170.822437	-0.398427	0.11351691	0.01592778
ztf-8	53.4116479	1.03043209	0.29364885	0.01592903
ent-4	161.717777	-0.7896745	0.22506457	0.01592903
F43C11.12	3.06212288	3.10381567	0.88511805	0.01601344
Y71H2AM.14	3.99749781	3.53765175	1.01086965	0.01640744
npr-18	19.9360579	1.04625636	0.29916348	0.01651593
F19B10.14	178.32278	-0.9102651	0.26046812	0.01663799
ant-1.2	2.176839	3.51875028	1.00740142	0.01669971
col-183	24985.0606	0.88500896	0.25339686	0.01669971
Y52B11A.10	45.5406814	0.76158617	0.21816804	0.0167736
ttr-5	3014.39399	0.43763563	0.1256415	0.01722085
ngp-1	362.216337	0.49565354	0.14240015	0.01734498
ZK228.13	2.49314463	-4.7406024	1.36226698	0.01735777
slc-46A	203.893505	0.69875116	0.20117784	0.01767886
C06G3.3	263.540305	0.48486048	0.13957565	0.01767886
F10D7.10	56.7178102	-0.598671	0.17232481	0.01767886
clec-174	64.2549037	-1.3362544	0.38503281	0.0178266
M01G12.14	24.2025721	1.14837792	0.33128152	0.01795873
Y49E10.18	436.130609	-0.2744572	0.07916152	0.01795873
Y39H10A.1	84.0274191	0.82998268	0.23944801	0.01795873
T21E8.7	1.70559115	-4.2008541	1.21149428	0.01795873
unc-34	99.0019379	-0.4917941	0.14192792	0.01799678
sqv-3	40.5296029	-0.6292851	0.18167598	0.01804737
let-391	31.7964971	0.69521233	0.20074294	0.01804841
Y34F4.2	1205.13216	0.42165769	0.12184134	0.01817775
M28.8	315.723991	-0.7218021	0.20873782	0.01832766
F36F2.12	2.241373	3.54792237	1.02809407	0.01857462
mut-16	86.9198829	-0.4857231	0.14064979	0.01857462
F13A2.1	1.42920336	-3.9717244	1.15087579	0.01857462
srx-117	1.42920336	-3.9717244	1.15087579	0.01857462
nas-21	2.11297225	-3.504857	1.01525925	0.01857462
nhr-63	49.2669736	-0.9859415	0.28555452	0.01857462
srz-4	1.30243922	3.86628298	1.12148292	0.01877801
ZK742.7	260.272379	0.43017839	0.124879	0.01892849

AH9.1	5.56276403	2.19245285	0.63674489	0.0189977
T10B11.8	8.56333855	-1.6261356	0.47236482	0.01900603
F39G3.5	212.363202	-0.5070065	0.14730824	0.01900603
ugt-48	294.736198	-0.5072222	0.14738645	0.01900603
C18E9.7	2.65701398	-3.7726096	1.09690291	0.01907746
C18B2.2	2.37406603	3.65744256	1.06329569	0.01907746
T09B4.5	11.6803214	-1.1488757	0.33430999	0.01923462
W02B12.1	391.536738	0.44056803	0.12830358	0.0193926
C14H10.3	530.357904	-0.2461302	0.071691	0.01939529
F53F10.8	4.04195237	2.43287748	0.70934893	0.01960313
mab-9	9.11302098	-1.4537091	0.42392503	0.01960313
fbxc-19	6.36474414	2.00315255	0.58434429	0.01960313
nspb-10	2.81480033	-3.9364513	1.14845841	0.01960313
T05B11.1	77.1123875	-0.6878109	0.2006596	0.01960313
F20G2.5	502.539069	-0.8643024	0.25222414	0.01962702
spp-5	82840.1847	0.48415925	0.14133388	0.01966618
rsa-2	5.00989559	2.37505165	0.69366173	0.01975095
lin-1	170.798067	-0.4877047	0.14246784	0.01976062
vps-8	76.6518523	-0.5215124	0.15245789	0.0199084
F28G4.3	2.28615053	-4.6130889	1.35056238	0.02023888
C06E2.5	27.9287369	-0.83332	0.24411879	0.02035504
lipl-2	332.232839	0.91667015	0.26861622	0.02039121
icmt-1	18.8704993	1.45136064	0.42544244	0.02043724
cyd-1	3.0787028	-3.0874918	0.90525203	0.02045504
R08E3.1	4343.85086	-0.2303664	0.06756527	0.02049793
T05A10.6	63.118699	0.54701334	0.16061176	0.02073934
nfm-1	141.888625	-0.5740702	0.16860691	0.02077695
C17G1.13	3.14307495	3.07532379	0.90348357	0.02080759
mlt-3	185.500212	0.4804484	0.14138759	0.02120925
F41D9.t2	9.52246976	1.49859047	0.44178005	0.02163176
K11H12.t1	1.80897399	4.34262344	1.28168421	0.02190318
K09E3.7	5.79627186	-2.1506509	0.6355584	0.02220948
Y57G11B.6	3.19618135	-3.0234673	0.89375498	0.02224719
nhr-235	14.3509476	-2.0092746	0.59437786	0.02240053
cln-3.3	33.0060482	0.67920202	0.20103792	0.02252003
gei-8	135.801124	0.44793463	0.13263205	0.02257561
Y46G5A.20	1051.0604	-0.4317599	0.12787986	0.02261294
anr-46	1.28115264	3.84968811	1.14089123	0.02269224

T10B10.8	106.489564	-0.633129	0.18760502	0.02269224
F13C5.1	16.0149873	0.9416686	0.27914677	0.02272332
F07E5.9	1.32978923	-3.8410609	1.13903481	0.02277727
gst-9	103.513903	0.45884839	0.13612585	0.02285344
tbc-9	181.4891	-0.3698683	0.10980627	0.02300937
srf-3	125.20695	-0.4667311	0.13863384	0.02302345
F44A2.7	106.540081	1.47599377	0.4383569	0.02302345
C14F11.6	62.0003781	0.65561067	0.19471232	0.02302345
scav-5	81.5414139	-0.5822311	0.17297132	0.02302961
clec-55	44.8264645	0.87387406	0.25971744	0.02309889
skr-5	350.879522	-0.305606	0.09086414	0.02317148
npr-1	5.3776856	1.83425462	0.54551108	0.02320199
T20D4.11	286.168444	0.42142629	0.12539693	0.02330298
W02F12.8	64.229655	1.22788984	0.3654628	0.02333707
Y53G8AM.8	226.306977	0.28785144	0.08572921	0.02343148
oac-57	1022.08929	-0.7797996	0.23223112	0.02343148
cyp-29A2	198.690574	0.47200619	0.14081261	0.02387218
F48A11.4	12.3153001	-1.2110906	0.36150774	0.02399288
F22B3.8	2.08955891	-4.4803109	1.33951667	0.02441882
C15C7.6	5.75757494	-1.8004054	0.53842444	0.02445161
ugt-41	1558.91048	0.75226026	0.22519856	0.02470847
ugt-17	136.923796	0.50309699	0.15066539	0.02477575
R03H10.1	226.097825	0.54610358	0.1636165	0.02486108
E02H4.4	26.7494333	1.18006864	0.35388965	0.02509752
alh-2	8.88558464	1.51193985	0.45384418	0.02533798
W03A5.1	3.06279715	3.11728116	0.93759839	0.0259036
hpx-2	1.95570355	4.41040035	1.32772457	0.02613415
bath-46	4.85993766	-3.3326294	1.00369136	0.02621816
wts-1	116.807451	-0.4179555	0.12593637	0.02632026
F53G12.19	4.53452833	1.92360302	0.57990469	0.02642796
F31D5.6	5.10945176	-2.8082527	0.84671723	0.02642796
Y47G6A.13	17.1715592	0.95487496	0.28796487	0.02644605
F17C11.13	193.607829	0.58245242	0.17601444	0.02705071
col-156	16.187963	1.36758715	0.41334424	0.02705309
ZK353.11	4.27629532	-5.5393547	1.67561161	0.02726839
K03A11.5	224.536919	0.36168098	0.10943168	0.02729618
fipr-24	119.258321	0.61300548	0.18551538	0.02732034
F22D6.19	2.17244511	-3.5158566	1.06425769	0.02734597

C55A6.6	196.687093	0.55661941	0.16869762	0.0276961
F16B4.7	283.006738	0.99441728	0.30159119	0.02787189
dct-19	4.32249377	-2.2082035	0.66992654	0.02792668
acc-1	15.4312782	1.16746519	0.35432036	0.02800123
vps-53	52.9267429	-0.5014954	0.15232736	0.02812476
fat-7	48.8704665	-0.948391	0.28801669	0.02812476
F07C3.3	12.3056781	1.1137603	0.33825476	0.02812476
F28F9.2	29.1756097	1.26167306	0.38341369	0.02818534
srv-24	8.85577093	1.87678307	0.57033444	0.02818534
Y39B6A.1	980.902949	-1.1219063	0.34107351	0.02826569
exos-7	91.9591388	0.93254965	0.28360654	0.02833273
clec-141	6.5940442	1.74261428	0.53016141	0.02840734
Y57G11C.14	13.027051	-1.7602848	0.53584728	0.02855006
clec-166	222.908988	0.6546355	0.19938552	0.0286816
sym-4	106.63523	-0.7630655	0.23281279	0.02921355
fbxc-23	60.9291482	-0.4844322	0.1478391	0.02924999
srz-85	7.84286214	-1.3440973	0.41069267	0.02961547
K01C8.2	65.6650115	-0.6464181	0.19763414	0.02977178
atn-1	1017.97042	-0.2645157	0.08094451	0.03002857
poml-1	3.73918177	2.69527178	0.82499855	0.03006862
C14A11.2	5.23055159	-1.8024305	0.5521593	0.0303016
nhr-260	11.5967437	1.36840459	0.41933496	0.0303367
hsp-16.41	1053.58294	-0.6661135	0.20413932	0.0303367
M01A8.1	71.8810336	-0.5683721	0.17423063	0.03037612
hsp-16.2	1054.94206	-0.5730207	0.17571717	0.03044693
R05A10.4	65.639496	0.55041264	0.16886346	0.03055933
cysl-1	461.727081	0.29193579	0.08958974	0.03060747
F52F10.2	5.20156623	2.24601581	0.68955792	0.0307071
tofu-4	5.00568034	2.84668523	0.87519389	0.03099307
taf-5	96.6010711	0.95197772	0.29266098	0.03099307
Y43F4B.5	888.28466	-0.2722253	0.08368182	0.03099307
Y38H6C.8	16.1670521	-0.920248	0.28281736	0.03099307
bli-3	273.56005	0.31139678	0.09576043	0.03102855
ilc-17.1	2.89852924	-3.0577294	0.9406145	0.03109151
pho-8	33.9968925	-0.9457637	0.29098919	0.03110625
C18D11.10	36.42093	1.30036564	0.40022975	0.03117684
pals-10	3.53490519	-2.5992312	0.80045381	0.03131576
cpin-1	167.467947	0.41827461	0.12882536	0.03131576

C26C6.4	16.0117639	1.249147	0.38521148	0.03171466
F09F7.6	802.870766	0.67694005	0.20884708	0.03182214
C35E7.8	3.60640998	2.76195301	0.85265878	0.03196795
K08F11.1	25.6625691	-0.7280223	0.22482366	0.03196795
T09F5.12	68.6303594	-0.7789938	0.24056902	0.03196795
asns-2	2126.6805	0.67965188	0.20983301	0.03196795
aexr-2	4.60392202	1.89635515	0.5858679	0.03206107
gls-1	84.674739	-0.4900552	0.1514224	0.03206288
B0416.7	20.6419578	-0.8119449	0.25111008	0.03233973
cest-10	66.4748934	0.75442609	0.2334297	0.03245701
inx-19	3.04880506	-2.3797354	0.73653758	0.03251115
T06G6.6	3.15104694	2.56623017	0.79472598	0.03262141
fbxa-157	47.8157792	-0.6145988	0.19031662	0.03262141
gst-4	1352.67218	0.59230941	0.18347486	0.03265834
ZK228.10	16.9129821	-1.1708812	0.36283515	0.03274841
gmps-1	484.514612	-0.2355568	0.07301935	0.03280317
cest-12	52.5494268	-0.7873314	0.24408623	0.03280317
ran-5	134.590933	-0.3470785	0.10766258	0.03288066
nmad-1	1173.59829	0.47921319	0.1486284	0.03288066
F55D10.4	32.934498	0.87361898	0.27101013	0.03288066
Y58A7A.1	341.439974	-0.2669527	0.08286656	0.03306801
Y55H10A.2	1.41384567	4.00362072	1.24329104	0.03311156
twk-46	91.0591841	0.46733369	0.1451089	0.03311156
nspd-2	2.48010973	4.81442781	1.49545791	0.03315245
gei-6	70.9402234	-0.6645622	0.20646108	0.03316207
Y32H12A.1	3.66859227	2.289889	0.7115821	0.0332017
T12G3.6	6.7109447	1.60157087	0.49844381	0.0337176
B0272.4	176.649697	0.62914513	0.19584983	0.03375282
srd-48	1.47408039	4.00078793	1.24696874	0.03416851
nmr-1	9.11777775	-1.3551614	0.42266094	0.03436966
aqp-8	395.480698	-0.4593022	0.1432718	0.03436966
trap-2	2506.64296	-0.2682387	0.08380847	0.03493998
E02H9.1	10.1080634	-2.3712986	0.74148188	0.03519636
K01A2.10	123.40448	0.51210045	0.16031489	0.03548423
bbs-5	35.460266	1.06666127	0.33386625	0.03548423
col-176	172.839805	-1.2407689	0.38837416	0.03548423
rig-6	101.44268	-1.0164026	0.31849153	0.03580348
tig-3	44.4310944	-0.6039657	0.18930398	0.03585243

kmo-2	16.6725009	1.19881186	0.37596603	0.03602463
F40A3.3	1497.24897	0.24834041	0.0778971	0.03603819
pup-3	3.24532242	3.2288522	1.0134319	0.03623172
nhr-237	37.7976643	0.90759073	0.28493132	0.03627063
vap-2	46.3428831	0.63190965	0.19846342	0.03637555
F18E3.12	1864.89983	0.386894	0.12155678	0.03646818
pgp-2	433.730338	-0.2804163	0.08829305	0.03728295
acs-2	1066.23161	0.4287658	0.13504414	0.03734966
fbxc-52	65.0792426	0.4640148	0.14643856	0.03800286
EGAP2.2	1.16907193	3.69734459	1.16751775	0.03800286
F54H5.5	1.14778535	3.67835901	1.16054537	0.03800286
col-2	26.1728478	-1.1561799	0.36507377	0.03800286
F36G9.7	281.03042	0.53580901	0.16916294	0.03800286
srh-154	1.67557072	-4.1555999	1.31186281	0.03800286
ZK154.1	2.80092226	2.86789792	0.90541345	0.03800286
C28H8.14	441.689774	-0.6132176	0.19374019	0.03810748
epg-7	234.604268	0.50053341	0.15812701	0.03810748
ttll-11	7.03319436	1.57266962	0.49701678	0.03817207
famh-161	5.94267814	-2.1917394	0.69339113	0.03855106
gst-7	1620.10412	0.59447553	0.18819221	0.03870227
gfat-2	7.17050789	2.35378294	0.74510097	0.03870227
C32H11.5	3.38291149	5.2304299	1.65606953	0.03871467
F41H10.1	286.195849	0.73669989	0.23331565	0.03876441
sru-40	6.19901907	-1.7139992	0.54291304	0.03877008
C23H5.12	4.67875346	1.91277353	0.60598711	0.03878913
H21P03.2	12.7261287	1.11506506	0.35378067	0.03934682
hus-1	11.877602	-1.2490678	0.3964266	0.03937618
clec-210	11.6288791	1.51327512	0.48028904	0.03937618
Y37F4.5	1.4095854	-3.9106451	1.24146885	0.03941757
fbl-1	97.2590727	-0.6108423	0.19416957	0.0399136
C35E7.4	28.9036022	0.70420555	0.2239244	0.04000222
nhr-62	91.225925	0.45902715	0.14604775	0.04019488
K03B8.8	86.3697392	-0.7017616	0.22334874	0.04027159
hsp-16.48	32.6597164	-0.8665424	0.27600382	0.04054214
linc-19	31.793087	1.14401046	0.36456109	0.04069726
ccm-3	127.819817	-0.354237	0.11291762	0.04076481
Y14H12A.5	254.731019	-0.8198084	0.26144951	0.04091325
del-6	1379.63346	-0.2145381	0.06845803	0.04109932

R13H4.5	221.723067	0.40553167	0.12951475	0.04141805
cyk-3	71.943686	-0.5612605	0.17934384	0.04158864
bath-26	145.664895	0.55880833	0.17868537	0.04178011
Y41D4B.14	120.224524	0.67544913	0.21598423	0.04178011
anmt-2	796.333924	0.23636974	0.07564943	0.04205152
W02F12.2	284.054028	0.47649144	0.15249845	0.04205152
cyp-35A2	237.002023	1.07452998	0.3439766	0.04208931
dhc-3	10.4206454	-1.4866697	0.47632236	0.04241575
F26E4.5	2.89554336	-4.9753977	1.59471448	0.04252854
H39E23.2	19.3486183	0.87385624	0.28045091	0.04305169
sri-40	15.3170347	-1.0134221	0.32528787	0.04305257
lec-8	12108.9655	-0.6194525	0.19887705	0.04309388
F10G8.1	1.51732781	4.03746824	1.297244	0.04325864
T19D12.1	72.6665523	-0.8366327	0.2687915	0.04325864
C03B1.5	1.51732781	4.03746824	1.297244	0.04325864
ZK1236.12	15.3715014	0.94407951	0.30338867	0.04327832
ehs-1	104.643845	-0.4132083	0.13282597	0.04334533
ZC581.7	1.25986606	3.8299491	1.23214657	0.04362648
srh-10	1.12279514	-3.6160269	1.16387388	0.04362648
obr-2	550.22639	0.81375392	0.26192095	0.04362648
Y51A2D.8	14.1377878	1.16134523	0.37377355	0.04362648
F59D12.3	8.77583175	-1.3510837	0.43478552	0.04362648
smu-2	81.4365471	0.51571015	0.16609446	0.0438372
mltn-9	151.42523	-0.4344837	0.13994844	0.0438372
col-46	11.0463284	1.44940739	0.46724355	0.04415514
C09B8.4	28.3641694	1.32402952	0.42739213	0.04470865
F38B6.3	12.0613222	1.39715945	0.45107771	0.04472745
unc-29	20.813259	-1.0521511	0.34002196	0.04502634
fbxa-169	2.55995916	-2.7606371	0.89221327	0.04502634
str-177	2.33589719	3.65694046	1.18167832	0.04502634
col-52	2.38181318	-3.5983936	1.16426096	0.04545836
JC8.7	44.6650103	0.74046833	0.23959717	0.04545836
B0310.3	33.7934299	0.80492093	0.26049564	0.04547276
T24D1.3	7.92651136	1.39565561	0.45194384	0.04562704
spp-13	114.508989	0.53391512	0.17289082	0.04562704
rev-3	31.3511248	0.78579422	0.25461149	0.04585049
C18F10.2	18.2641973	1.44043959	0.46694532	0.04588163
ZC132.3	11.5020966	-1.1320504	0.36697199	0.04588163

D2021.4	59.180886	0.60196437	0.19513902	0.04588163
C40H1.7	58.3285423	-0.7304284	0.2369684	0.0461567
T14G8.2	14.2588188	1.20344891	0.39045266	0.0461567
C09E7.4	19.0925157	-1.1470056	0.37259218	0.04666054
pgp-5	90.1001286	-0.833592	0.27081142	0.04666054
F48G7.10	13.5122293	-1.4184064	0.46087034	0.0466675
gei-13	12.5842538	1.69032957	0.55035206	0.04759898
srw-140	5.18169956	2.78151523	0.90602085	0.0477447
Y54G11A.19	13.9960634	1.12952589	0.3682548	0.04812677
rpl-43	32343.2023	-0.514707	0.16789979	0.04826451
F47E1.1	14.8408118	0.9105601	0.29701209	0.04826451
aph-1	58.8072571	0.54598218	0.17819617	0.0483763
clec-8	165.506332	0.69475703	0.22677536	0.0483763
clec-263	1.71717668	3.19589984	1.04291345	0.0483763
ZK1010.8	30.6425269	-1.2726719	0.41562283	0.04856118
arf-1.1	190.965454	-0.5874041	0.19214406	0.04930793
nos-2	7.12777506	1.54400491	0.50513623	0.04932142
K02A2.5	39.3933946	-1.3902348	0.45491013	0.04934393
Y62H9A.4	1021.02301	-0.3181315	0.10411807	0.04937159
R12B2.3	3.44779312	2.24940408	0.73697521	0.04980632
T28C6.10	87.2801232	0.53904763	0.17661871	0.04980632
F01F1.14	161.20721	0.41369316	0.13560483	0.04995718